Detrital zircon provenance of the Bremnes Migmatite Complex on Bømlo, SW Norway

Master of Science thesis

Matz Sagebakken Slotnes

Department of Earth Science
University of Bergen
August 2021

Abstract

Detrital zircon provenance, geochemistry, and field descriptions from the Bremnes Migmatite Complex provide new insights in the origin and evolution of the Early Ordovician ophiolitic terrane of SW Norway. The Bremnes Migmatite Complex developed as the Laurentian continental margin was subducted sufficiently below the ophiolitic terrane to commence partial melting of the sedimentary protolith. The migmatization of the complex at 477 ± 7 Ma, occurred prior to the intrusion of the Vardafjell Gabbro (472 ± 2 Ma), and simultaneously to the intrusion of the S-type granitoids of the West Karmøy Igneous Complex (474 +3/-2 Ma). Appinites related to an early volatile-rich phase of the Vardafjell Gabbro intruded the migmatite complex, and most likely marks the cessation in subduction of the Laurentian continental margin.

Zircons of the Bremnes Migmatite Complex are dominated by Archean (~2700 Ma), Paleoproterozoic (~1800 Ma), and Mesoproterozoic (~1100 Ma) ages, and show major similarities with the provenance signatures of the S-type granitoids of the West Karmøy Igneous Complex, the Vikafjord Group, and the Mundheim Group of the Early Ordovician ophiolitic terrane. Combined, the provenance signature of the Bremnes Migmatite Complex, and the other units of the ophiolitic terrane, resemble sedimentary successions that accumulated at the Laurentian margin in Mid Neoproterozoic (*c.* 700 Ma) to Early Paleozoic (*c.* 520 Ma). Our results constrain the continental component of the Early Ordovician ophiolitic terrane to be sourced in a sedimentary succession best described by the Dalradian Supergroup of the Scottish Caledonides. Major- and trace-element composition of the Bremnes Migmatite Complex indicates that the complex primarily developed from fine-grained sedimentary rocks sourced in the Dalradian Supergroup. This is consistent with the formation of time-equivalent migmatites and granitoids exposed within the Scottish Caledonides, that have inherited their continental component from the Dalradian Supergroup, suggesting that the Early Ordovician ophiolitic terrane of SW Norway and time-equivalent units exposed in the Scottish Caledonides were closely related both temporally and spatially.

These findings reveal that the continental component present within the Bremnes Migmatite Complex, and several other units of the Early Ordovician ophiolitic terrane, were derived from the Laurentian continental margin, and provides new insights into key parts of the tectono-magmatic evolution of the ophiolitic terrane of SW Norway.

Acknowledgments

First, I would like to thank my supervisor Professor Rolf B. Pedersen for allowing me to work with such an interesting project, for scientific advice during the last two years and for excellent feedback in the last period of writing this thesis. I also wish to thank my co-supervisor Håvard H. Stubseid for feedback on the thesis, and for help with practicalities during the last two years.

Furthermore, I would like to thank everyone that has taken part in the lab work that is behind this thesis. Thank you to Ida M. Gabrielsen for help in preparing the samples for major- and trace-element analyses, and detrital zircon provenance. I am grateful to Leif E. Rydland Pedersen for help during all steps in preparing and analyzing the samples for detrital zircon provenance.

In addition, I would like to thank Ingvild Aarrestad, Andreas L. Viken, and Andreas H. Liland for feedback on the thesis. Especially I would like to thank Simen, Trond and Frida for being excellent field companions during the two periods of fieldwork. I would like to thank Øystein and the rest on "Black Smoker" for making the last two years unforgettable!

Finally, I would like to thank my girlfriend, Ingvild, and my family for support and non-scientific advice during the last two years.

Bergen, 20.08.2021

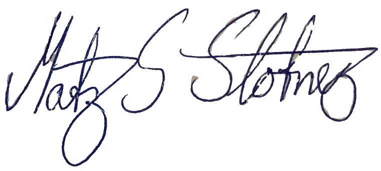

Matz Sagebakken Slotnes

Table of Contents

1 Introduction

The Bremnes Migmatite Complex on Bømlo, SW Norway, is exposed together with island arc lithologies and magmatic suites related to the Early Ordovician ophiolitic terrane that formed in the Iapetus Ocean between Baltica and Laurentia. Fragments of this ophiolitic terrane are preserved within the Upper Allochthon of the SW Norway tectonostratigraphy and are exposed at several locations in SW Norway (Figure 1.1). Whether this ophiolitic terrane formed adjacent to the Baltic or Laurentian continental margin has been a matter of debate for almost half a century. Based on U-Pb radiometric dating of detrital and inherited zircons a Laurentian provenance was suggested (Pedersen *et al.*, 1992; Pedersen and Dunning, 1997). The U-Pb ages presented at the time were scarce, and no data constrained the provenance of the rocks. The application of LA-ICP-MS on single zircon U-Pb dating allowed for more extensive dating and a potential Laurentian provenance became more evident and well documented (Fonneland, 2002). Following the introduction of this new analytical approach more studies on the provenance of sedimentary sequences associated with the Lower Ordovician ophiolitic terrane of SW Norway were conducted (Stubseid, 2017; Viken, 2017).

This thesis presents a comprehensive study of inherited and detrital zircon geochronology and geochemistry of the Bremnes Migmatite Complex. These new analyses are compared and evaluated in the light of previous data and studies (e.g. Pedersen and Dunning, 1997; Hamnes, 1998; Fonneland, 2002; Cawood *et al.*, 2003, 2007, 2014; Bingen *et al.*, 2005B; Slama *et al.*, 2011; Slama and Pedersen, 2015; Stubseid, 2017; Viken, 2017). Through this approach, the provenance of the continental component present within the Bremnes Migmatite Complex and several other units of the ophiolitic terrane are carefully constrained. Additionally, a source for the continental component is suggested, and the evolution of the Bremnes Migmatite Complex better understood.

The detrital zircon provenance studies on the Bremnes Migmatite Complex enables us to deduct the origin of the detritus involved in the formation of the continental component of the complex. Since the Laurentian inheritance first was suggested (Pedersen *et al.*, 1992; Pedersen and Dunning, 1997; Fonneland, 2002) the amount of published data on the provenance of sedimentary successions associated with the Laurentian and Baltic margin has greatly increased (e.g. Cawood *et al.*, 2003; Bingen *et al.*, 2005B; Cawood *et al.*, 2007; Slama and Pedersen, 2015). This enables the present study to properly constrain the origin of the continental component, which earlier was not possible. In addition to provenance analyses, several samples from the Bremnes Migmatite Complex are analyzed for major- and trace-elements. The geochemical analyses increases our knowledge about the environment in which the migmatite complex formed and help constrain the composition and origin of the continental component.

This study combines geochemical analyses, detrital zircon provenance, and field descriptions from the Bremnes Migmatite Complex, and expand our knowledge about the evolution, origin, and provenance of the Early Ordovician Ophiolitic terrane of SW Norway.

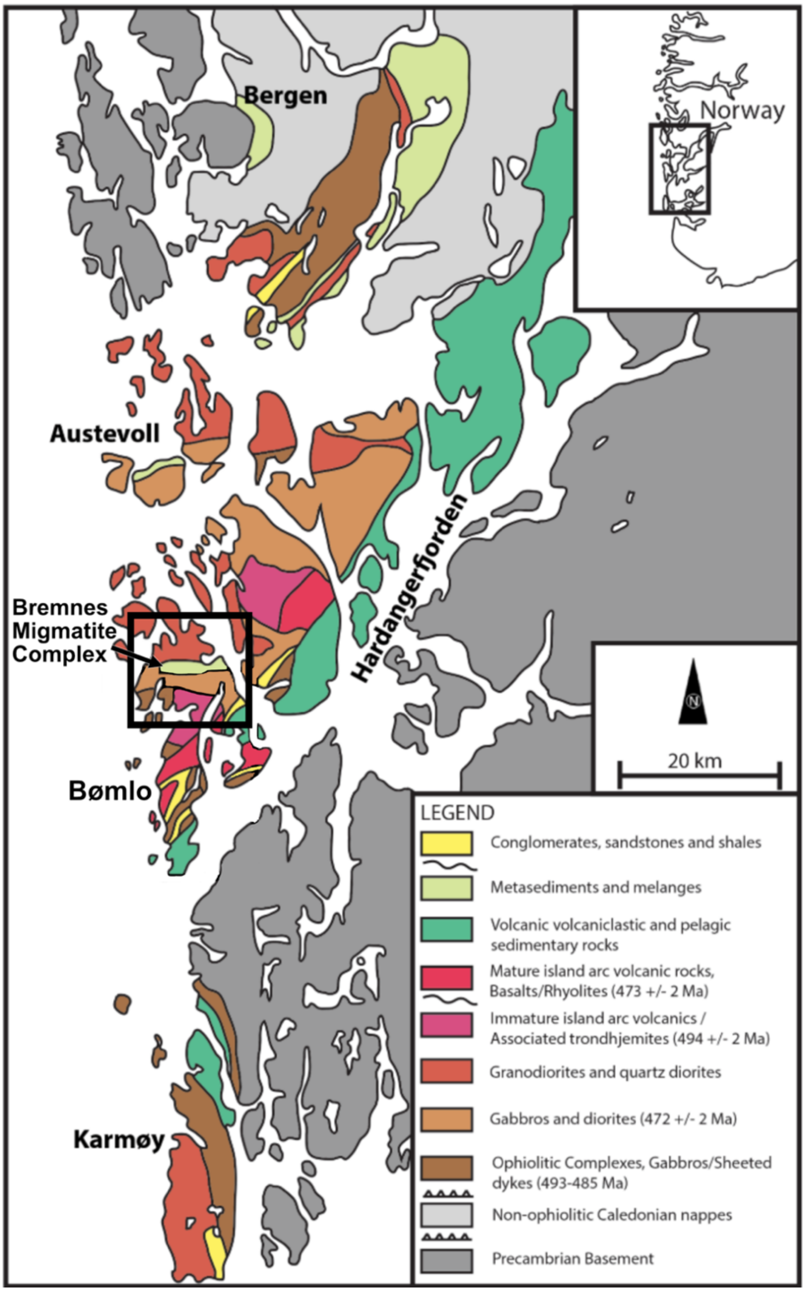

Figure 1.1: Simplified geological map of the ophiolitic terrane of SW Norway. Redrawn from Pedersen and Dunning (1997) and modified from Viken (2017).

2 Regional Geology

2.1 The Scandinavian Caledonides

The Caledonian orogeny in SW Norway form a part of the Scandinavian Caledonides representing the remains of an Early Paleozoic orogenic event, that stretched from the high arctic southwards on both sides of the North Atlantic through Greenland, Newfoundland, Scandinavia, the British Isles and southeastern USA (Slagstad *et al.,* 2011).

The evolution of the Scandinavian Caledonides begins with the opening of the Iapetus Ocean in the Neoproterozoic (*c.* 600 Ma), and ends with the collision (Scandian Event) between Laurentia, Baltica, and Avalonia in Ordovician-Silurian time (*c.* 430 Ma) (Van Staal *et al.*, 1998; Corfu *et al.*, 2007). During the Scandian Event several thrust nappes derived from the Iapetus Ocean, the Laurentian-, and the Baltic continental margins, were emplaced onto the Fennoscandian Shield (Roberts and Gee, 1985). These thrust nappes constitute the exposed section of the Caledonian Orogeny in SW Norway and have been divided into the following five units: The Autochthon-Parautochthon, Lower, Middle, Upper and the Uppermost Allochthons.

The Autochthon-Parautochthon constitutes the Fennoscandian basement which the nappe stack was thrusted on top of. It consists of the Precambrian crystalline basement and black shales deposited on the Baltic margin in the Late Proterozoic to Early Paleozoic (Roberts and Gee, 1985). The Lower Allochthon consists of sedimentary successions deposited in the Late Proterozoic to Early Paleozoic related to the Baltic margin, interpreted to be distal shelf equivalents to the (para-) autochthonous rocks (Roberts and Gee, 1985; Fonneland, 2002). The Middle Allochthon are made up of Precambrian crystalline rocks and unfossiliferous metasandstones of Late Proterozoic to Early Paleozoic age locally cross cut by mafic intrusions (Roberts and Gee, 1985; Corfu *et al.*, 2007). The Upper Allochthon consists of ophiolite and island arc complexes formed in the Iapetus Ocean, and the Upper Ordovician-Silurian transgressive sedimentary sequences (Gale and Roberts, 1974; Roberts and Gee, 1985; Pedersen *et al.*, 1988, 1991; Andersen and Andresen, 1994). The Uppermost Allochthon is mostly preserved in northern Norway, and consists of intrusive and sedimentary rocks (Roberts and Gee, 1985). This study will further focus on the Upper Allochthon, which contain the Early

Ordovician ophiolitic terrane and the Bremnes Migmatite Complex, and consequently the Upper Allochthon are explained further.

2.2 The Upper Allochthon

The Upper Allochthon of the SW Norway tectonostratigraphy contains the Lower Ordovician ophiolite complexes, island arcs and associated sedimentary sequences, represented by the Karmøy Ophiolite Complex (493 +7/-4 Ma; Dunning and Pedersen, 1988), Gullfjellet Ophiolite Complex (489 ± 3 Ma; Dunning and Pedersen, 1988) and the Lykling Ophiolite. The Upper Allochthon also contain the Upper Ordovician ophiolitic terranes, represented by the Solund-Stavfjord Ophiolite Complex (443 ± 3 Ma; Dunning and Pedersen, 1988), and the transgressive Ordovician-Silurian sedimentary sequences that lie unconformably on the Lower Ordovician outboard terranes. Following is a description of the Early Ordovician ophiolite and arc complexes exposed at Bømlo and Karmøy, as these are of particular interest for this study.

Karmøy Ophiolite Complex and West Karmøy Igneous Complex

Karmøy Ophiolite Complex and related magmatic suites formed during a period of *c.* 25 Myr, from the Late Cambrian (*c.* 495 Ma) to the Early Ordovician (*c.* 470 Ma) (Dunning and Pedersen, 1988; Pedersen and Hertogen, 1990). The ophiolite complex is exposed at Karmøy and Feøy together with two other related units, the West Karmøy Igneous Complex and the Torvastad Group (Figure 1.1 and Figure 2.1) (Sturt et al., 1979; Pedersen and Hertogen, 1990).

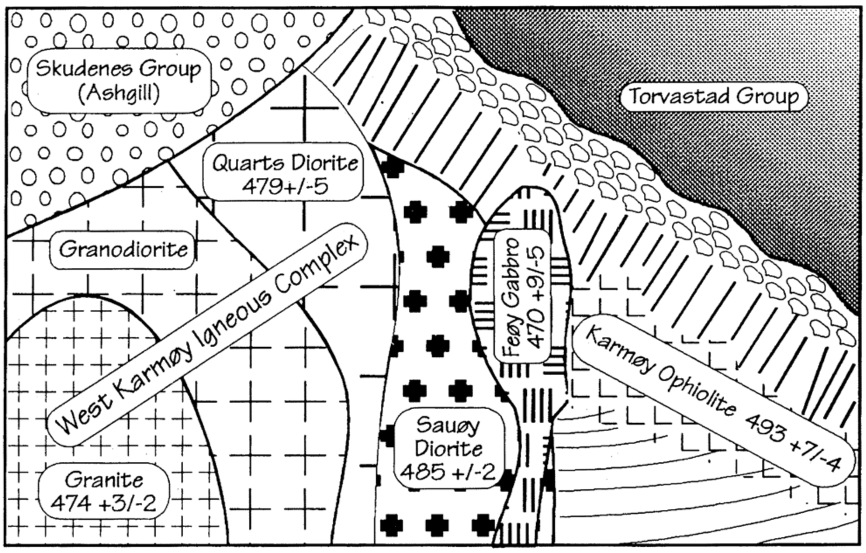

Figure 2.1: Illustration of the intrusive relations of the units found at Karmøy. The Skudenes Group is not mentioned in the text, but represents the Upper Ordovician transgressive sedimentary sequence exposed at Karmøy. From Pedersen and Dunning (1997).

The Karmøy Axis Sequences (KAS) is the principal and oldest unit of Karmøy Ophiolite Complex. The unit consists of layered gabbro that gradually evolved to textured gabbro, followed by the sheeted dykes of the Feøy Gabbro (Figure 2.1) (Pedersen and Hertogen, 1990). Dunning and Pedersen (1988) reported an age of 493 +7/-4 Ma from a plagiogranite associated with the KAS and suggested that this represents the age of the complex. The KAS is intruded by a sequence of boninitic intrusions from the Sauøy Diorite (485 ± 2 Ma) (Dunning and Pedersen, 1988). Several dyke swarms crosscut both the KAS and the Sauøy diorite. These younger dykes are all cut by the Feøy Gabbros (470 +9/-5 Ma; Dunning and Pedersen, 1988) constraining the period in which the dyke swarms intrude (Pedersen and Hertogen, 1990).

The West Karmøy Igneous Complex (WKIC) is a granitic intrusion that intersects the plutonic part of the ophiolite and crosscut the dyke swarms (Figure 2.1) (Pedersen and Dunning, 1997). The WKIC constitute an I-type and S-type complex made up of quartz diorites, granites and granodiorites, respectively (Hamnes, 1998). Pedersen and Dunning (1997) suggest a crystallization age of 479 ± 5 Ma for the quartz diorite, and 474 +3/-2 Ma for the granites and granodiorites. The I- and S-type type granitoids of the WKIC contain a significant amount of enclave material suggested to be inherited from their protoliths (Hamnes, 1998). The I-type suite is dominated by mafic to ultramafic enclaves, while the S-type mostly contain mafic and metasedimentary enclaves (Hamnes, 1998). The Sm-Nd isotope systematics of the granitoids, combined with the presence of inherited zircon grains of Precambrian age and metasedimentary enclaves suggest that a continental component was present at the time when the WKIC developed (Pedersen and Dunning, 1997). The S-type granitoids are suggested to have formed primarily from partial melting of the continental component with minor input from the mantle source (Pedersen and Dunning, 1997; Hamnes, 1998), while the I-type granitoids formed by mixing between a mantle and continental sources (Pedersen and Dunning, 1997; Hamnes, 1998).

Extrusive rocks at Karmøy are mostly confined within the Torvastad Group, a volcano-sedimentary sequences that contains extrusive equivalents to the intrusive rocks found at Karmøy (Figure 2.1) (Pedersen and Hertogen, 1990). Sivertsen (1992) suggested that the Torvastad Group was deposited in a back-arc basin in Early Ordovician time. Similar deposits are also found at Bømlo and at other locations in SW Norway (Andersen and Andresen, 1994; Pedersen and Dunning, 1997).

Geology of Bømlo

Bømlo is located at the mouth of the Hardanger Fjord, between Bergen and Karmøy in SW Norway (Figure 1.1). The geology of Bømlo is dominated by rocks of Cambrian to Silurian age mostly restricted within the Upper Allochthon of the Caledonian nappe pile. Brekke *et al.* (1984) suggested that the units found at Bømlo represents an almost complete succession of old oceanic crust, related island arcs and marginal basins sequences, and divided the lithostratigraphy of Bømlo into the five following units: the Lykling Ophiolite, the Geitung Unit, the Siggjo Complex, the Vikafjord Group, and the Langevåg Group (Figure 2.2 and Figure 2.3).

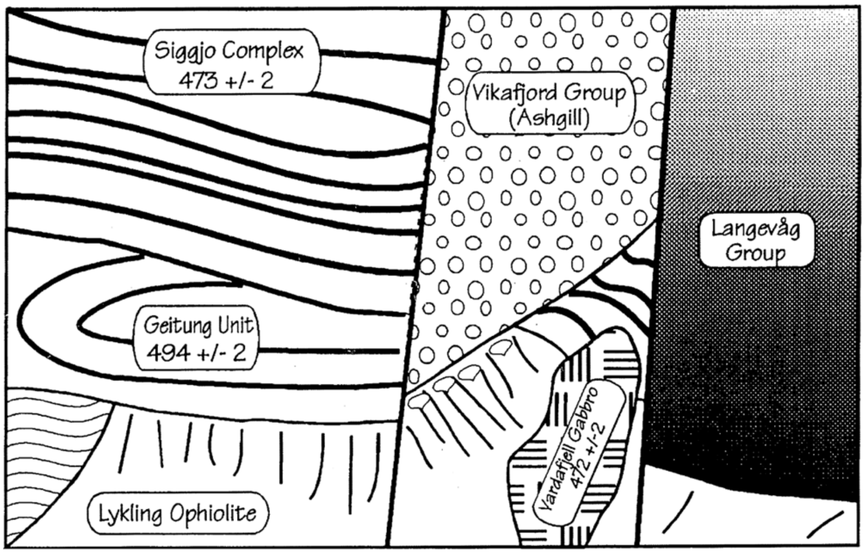

Figure 2.2: Illustration of the intrusive relations of the units found at Bømlo. From Pedersen and Dunning (1997).

The Lykling Ophiolite represents the oldest unit on Bømlo and crop out north of Lykling (Brekke *et al.*, 1984). Pedersen and Dunning (1997) suggested based on structural and geochemical evidence that the Lykling Ophiolite formed because of supra-subduction magmatism. The absolute age of the Lykling Ophiolite is not known, but the unconformably overlying Geitung Unit has been dated to 494 ± 2 Ma (Pedersen and Dunning, 1997) suggesting that the Lykling Ophiolite have a similar age as the other Early Ordovician ophiolite complexes found at Karmøy (493 +7/-4 Ma) and Gullfjellet (489 ± 3 Ma) (Dunning and Pedersen, 1988).

The Geitung Unit represents the extrusive to sedimentary zone of the ophiolite complex (Figure 2.2) (Nordås *et al.*, 1985). The trace-element patterns exhibited by the Geitung Unit resemble an immature island arc, and similar trace-element patterns have been reported from the axis sequence of the Karmøy Ophiolite Complex (Brekke *et al.*, 1984; Pedersen and Dunning, 1997; Viken, 2017). Based on the similarities in trace-element patterns and U-Pb ages it is suggested that the Geitung Unit (494 ± 2 Ma) and the KAS (493 +7/-4 Ma) developed at the same time and in similar environments (Dunning and Pedersen, 1988; Pedersen and Dunning, 1997).

The Siggjo Complex represents a mature island arc sequences and lies unconformably over both the Lykling Ophiolite and Geitung Unit (Figure 2.2) (Brekke *et al.*, 1984; Pedersen and Dunning, 1997). The subaerial alkaline to sub-alkaline volcanics of the Siggjo Complex have yielded an age of 473 ± 2 Ma (Pedersen and Dunning, 1997). The Kattnakken volcanics on the neighboring island of Stord show a similar age (476 ± 4 Ma), suggesting that these represent the same volcanic sequence (Pedersen and Dunning, 1997). Rhyolites of the Huglo Formation, in the Hardanger Fjord area, reveal U-Pb age of 474 ± 2 Ma and are correlated with the Siggjo Complex (Stubseid, 2017). The absolute ages reported from these volcanic sequences correlates with the high-K calc-alkaline Feøy Gabbro related to the Karmøy Ophiolite Complex (470 +9/-5 Ma, Dunning and Pedersen, 1988).

Resting unconformably on the ophiolite complex is the sedimentary rocks and subaerial volcanics of the Vikafjord Group (Figure 2.2) (Nordås *et al.*, 1985). The Vikafjord Group has been correlated with the Mundheim Group located further east in the outer Hardanger Fjord (Stubseid, 2017). There has not been reported an absolute age for the Vikafjord Group, but Stubseid (2017) suggested an Upper Ordovician age (Sr-isotopes, 445-460 Ma) for limestones related to the Mundheim Group. This age correlates well with Late Ordovician to Early Silurian age suggested based on faunal evidence (Brekke *et al.,* 1984). The Vikafjord Group and the Mundheim Group are interpreted to be deposited in transgressive basin that probably developed into the Late Ordovician Solund-Stavfjord Ophiolite Complex (Stubseid, 2017; Viken, 2017). The presence of a significant Archean detrital zircon population within sandstones associated with both the Vikafjord Group and the Mundheim Group, suggest that the basin developed close to the Laurentian continental margin (Stubseid, 2017; Viken, 2017).

The volcanics and fine-grained sedimentary rocks of the Langevåg Group are suggested to represent the formation and deepening of a back-arc basin (Figure 2.2) (Brekke *et al.,* 1984). These rocks have a primary depositional contact with the Lykling Ophiolite, however no such contact is recognized with the Geitung Unit or Siggjo Complex (Brekke *et al.*, 1984; Nordås *et al.*, 1985). It has been suggested that the Langevåg Group and Torvastad Group on Karmøy represent comparable back-arc deposits, based on similarities in trace-element patterns and lithostratigraphy (Pedersen and Dunning, 1997).

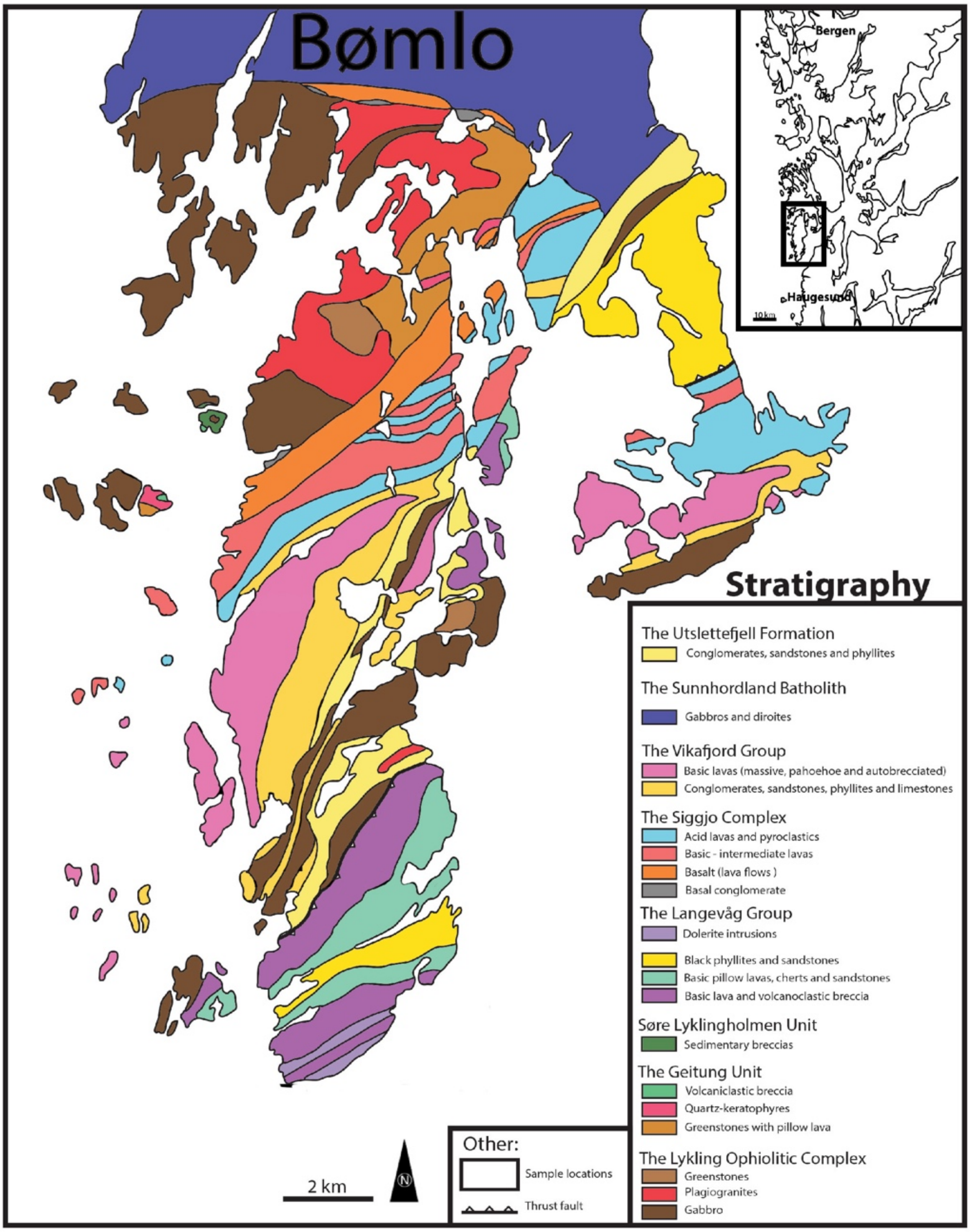

Figure 2.3: Geological map of central and southern Bømlo. Modified after Brekke *et al.* (1984), from Viken (2017).

2.3 Sunnhordland Batholith

The Sunnhordland Batholith is an intrusive magmatic body that intruded into the Early Ordovician ophiolitic terrain. The batholith is exposed on Bømlo, Stord, Tysnesøy, Rekstern, Austevoll and several smaller islands in the Sunnhordland area. The batholith is classified as an I-type complex that became more acidic as the magma chamber evolved (Andersen and Jansen, 1987). Based on relative age and composition the batholith has been divided into three different units; Unit I, II & III (Andersen *et al.*, 1991). Unit I is the oldest and includes mostly diorites and gabbros. The best studied parts of Unit I is the Vardafjell Gabbro and the Stolmen Gabbro (Andersen and Jansen, 1987). Unit II compromises the Rekstern Granodiorite, exposed at Austevoll, Rekstern, and Tysnesøy (Andersen and Jansen, 1987). Unit III is composed of three plutons, the Håkre and Drøni monzogranites and the Rolvsnes Granite (Andersen and Jansen, 1987). Andersen and Jansen (1987) suggested that the Sunnhordland batholith formed as a resulted of convergence in the Late Ordovician to Early Silurian. This was correlated with an Rb-Sr age of 430 ± 6 Ma for the Krossnes Granite of Unit III (Fossen and Austrheim, 1988), however recent discoveries indicate that this age most likely represents the metamorphic overprint of the Scandian event, and that a U-Pb age of 468 ± 3 Ma represents the actual age (Scheiber *et al.*, 2016). This suggests that the Sunnhordland Batholith formed in relation the Early Ordovician ophiolite and island arc complexes, similar to the Vardafjell Gabbro (472 ± 2 Ma), which intrude into the Early Ordovician ophiolitic terrane (Pedersen and Dunning, 1997).

2.4 The Early Ordovician ophiolitic terrane

Origin of the Early Ordovician ophiolitic terrane

Early research on the Caledonian nappe pile in Norway suggested that the Early Ordovician outboard terranes formed adjacent to the Baltic margin (e.g. Gee, 1975; Sturt *et al.*, 1980; Brekke *et al.*, 1984; Roberts *et al.*, 1984). This was suggested despite the presence of Laurentian associated fauna within several of the units associated with the ophiolitic terrane, as a Laurentian inheritance did not provide a satisfactory model combined with the available paleontological, geochemical and sedimentological data (e.g. Gee, 1975; Roberts *et al.*, 1984). First when the units related to the Early Ordovician ophiolitic terrane units were radiometrically dated with the use of U-Pb in detrital zircons the formation at the Laurentian margin was suggested (Pedersen *et al.*, 1992; Pedersen and Dunning, 1997; Fonneland, 2002). The presence of a significant Archean detrital zircon population within several of the units related to the ophiolitic terrane combined with faunal evidence, suggested that the Early Ordovician ophiolite complexes and island arc sequences formed close to the Laurentian rather than the Baltic margin. Dunning and Pedersen (1988) noted that the Early Ordovician outboard terranes located in the Upper Allochthon show geochronological similarities with ophiolites and island arc sequences associated with the Laurentian margin. They suggested that these ophiolites and associated island arc sequences formed a part of an extensive Early Ordovician ophiolitic terrane that developed close to the Laurentian margin. This was later confirmed by Pedersen and Dunning (1997) who argued based on geochemistry and geochronology that the ophiolite and arc complexes within the Upper Allochthon of SW Norway were closely related and provided a combined evolutionary model for the ophiolitic terrane.

Evolution of the Early Ordovician ophiolitic terrane

Seafloor spreading, island arc magmatism and subsequent spreading-related magmatism are characteristic for the evolution of the Early Ordovician ophiolitic terrane (Figure 2.4). Based on U-Pb geochronology, the evolution of this terrain can been constrained within the Late Cambrian (*c.* 495 Ma) to Early Ordovician (*c.* 470 Ma), over a period of *c.* 25 Myr, and are summarized in the following three steps (Pedersen and Dunning, 1997):

I. The main crust forming stage. Tholeiitic magmas formed ophiolitic axis sequences and volcanic bodies that possibly formed island arcs.
II. Dominated by boninitic magmas with minor amounts tholeiitic magma. Boninitic magmas influenced by a continental component intrude into the newly formed tholeiitic crust. This marks the start of a period (*c.* 10-15 Myr) where the continental component was present within the mantle derived melts.
III. Formation of calc-alkaline and alkaline magmas which evolved into highly alkaline, shoshonitic magmas. Eruption of oceanic island basalts (OIB) marks the end of magmatism.

The first stage initiates with the eruption of marine to subaerial volcanics upon oceanic crust of unknown age (Figure 2.4). This occurs at 494 ± 2 Ma and is represented by the basaltic to tholeiitic lavas of the Geitung Unit (Pedersen and Dunning, 1997). This happens more or less simultaneously with the formation of ophiolitic crust of the Karmøy Axis Sequence (493 +7/-

4 Ma) and the Gullfjellet Ophiolite Complex (489 ± 3 Ma) (Dunning and Pedersen, 1988; Pedersen and Hertogen, 1990).

The intrusion of boninitic dykes of the second stage, that both pre- and postdates the Sauøy Diorite (485 ± 2 Ma), marks the end of the first stage (Figure 2.4) (Dunning and Pedersen, 1988; Pedersen and Hertogen, 1990). The second stage is further characterized by tonalitic, quartz dioritic, and granitic intrusions that contain inherited zircons. These rocks intrude to form the Sauøy Diorite (485 ± 2 Ma), an arc-related tonalite of the Gullfjellet Ophiolite Complex (482 +6/-4 Ma), and several dykes that predate the WKIC (479 ± 5 Ma) (Dunning and Pedersen, 1988; Pedersen and Hertogen, 1990).

The third stage is dominated by the eruption of high-K calc-alkaline volcanics of the Siggjo Complex (473 ± 2 Ma), intrusion of calc-alkaline plutons on both Bømlo (Vardafjell Gabbro 472 ± 2 Ma) and Karmøy (Feøy Gabbros 470 +9/-5 Ma), and the intrusion of S-type granites (474 +3/-2 Ma) of the WKIC (Figure 2.4) (Pedersen and Hertogen, 1990; Pedersen and

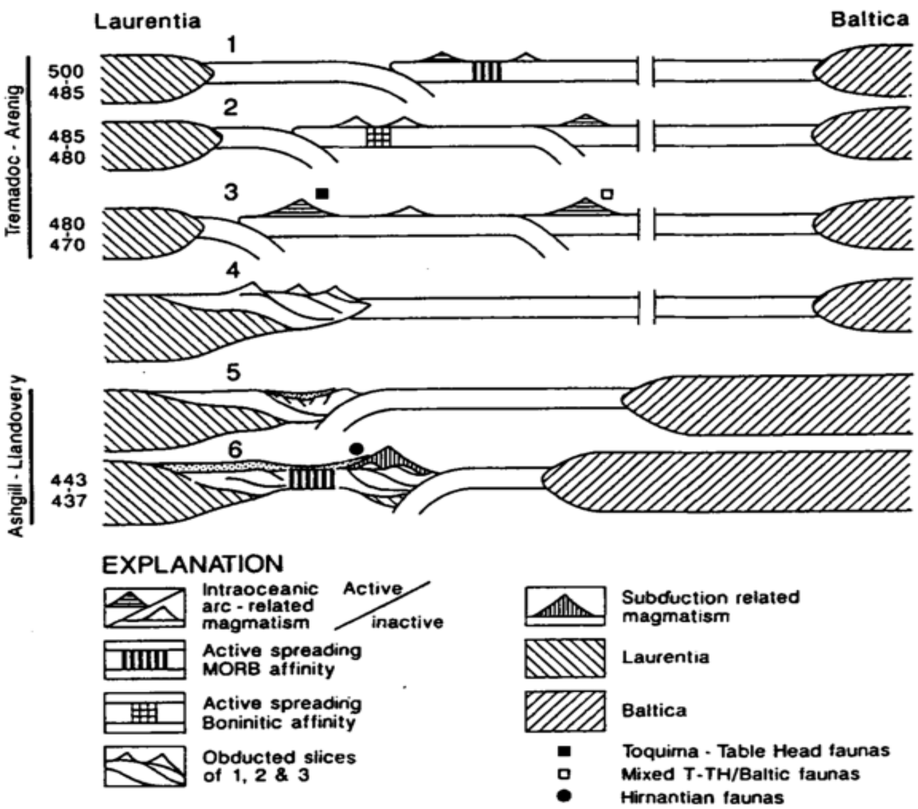

Figure 2.4: Evolution of the Early and Late Ordovician ophiolite complexes. Step 1 and 2 shows the initiated of subduction and formation of an immature island arc. Step 3 shows the development of a mature island arc and continued formation. Step 4 shows the emplacement of the island arc onto the Laurentian continental margin. Further the development of the Upper Ordovician ophiolite is seen in steps 5 and 6. From Pedersen *et al.* (1992).

Dunning, 1997). The third stage ends with the eruption of shoshonites and OIB-like lavas which also marks an end to the magmatism.

2.5 The geology of the study area: Bremnes Migmatite Complex

The Bremnes Migmatite Complex (BMC) make up a central part of the geology on Bømlo and is situated in the northern part between the Rolvsnes Granite (468 ± 3 Ma; Scheiber *et al.*, 2016) and the Vardafjell Gabbro (472 ± 2 Ma; Pedersen and Dunning, 1997) (Figure 2.5). The migmatite complex is made up of dia- and metatexites that formed from near complete anatexis of sedimentary rocks (Andersen *et al.*, 1991). The sedimentary component of the BMC consists of sandstones, schists, and calcareous sediments, now visible as xenoliths (restites) within the complex (Nordås *et al.*, 1985). Andersen *et al.* (1991) correlated restites from the BMC with fine-grained sedimentary rocks of the Siggjo Complex and suggested that the sedimentary component of the BMC was < 5 million years old at the time of migmatization. Andersen *et al. (1991)* suggested that the migmatization was initiated at the time when the Vardafjell Gabbro intruded, and that heat from the gabbroic body was the main factor in partial melting of the protoliths. Fonneland (2002) contradicted this and suggested that the BMC was accreted to the ophiolitic terrain prior to the intrusion of the Vardafjell Gabbro. This was suggested based on tectonic relations between the BMC and the Lykling Ophiolite, and similarities with the S-type granitoids of the WKIC. The sedimentary protolith of the migmatite complex was suggested based on lithological, geochemical, and geochronological similarities between the restites of the BMC and the enclaves of the S-type granitoids to be derived from the same continental source as the S-type granitoids (Fonneland, 2002).

Prior to this study there have been two other major studies on the BMC (Nielsen, 1990; Fonneland, 2002). The work done by Nielsen (1990) is reproduced in Andersen *et al.* (1991), and focused on the structural relationship between the BMC and the Sunnhordland Batholith, and the P-T conditions of the migmatite complex. Fonneland (2002) presented U-Pb detrital zircon ages, and Sm-Nd model ages and isotope systematics from the BMC, combined with data from several other units of the Early Ordovician ophiolitic terrane to further constrain the provenance of the ophiolitic terrane

Andersen *et al*. (1991) described biotite-cordierite-sillimanite bearing, locally garnetiferous, irregularly banded dia- and metatexites from the BMC. The diatexites were limited to areas of the migmatite complex that are close to the Vardafjell Gabbro, and the metatexites mostly appeared in areas far from the contact zone. Andersen *et al.* (1991) noted that in areas with abundant amounts of metasedimentary inclusions, the restites were often dominated by one lithology, reflecting a ghost stratigraphy – indicating limited exchange of material vertically. Andersen *et al.* (1991) suggested that several sedimentary successions within the Sunnhordland area were partially melted and migmatized as consequence of the intruding Sunnhordland Batholith. This interpretation was suggested for the formation of BMC, and the extraction of melt and partial migmatization of metasedimentary succession in the Møkster area.

From the BMC, Fonneland (2002) reported U-Pb detrital zircon provenance from one

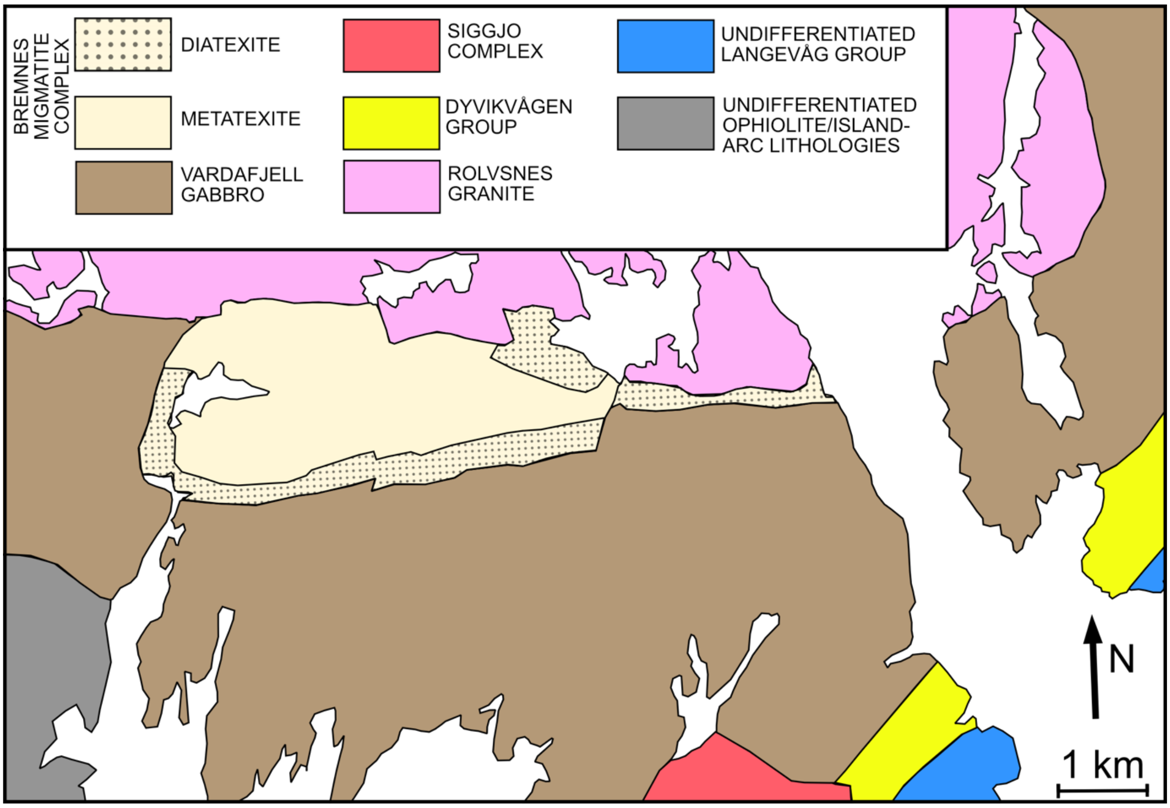

Figure 2.5: Simplified geological map of the Bremnes Migmatite Complex, and the surrounding Sunnhordland Batholith and other and other units of the Early Ordovician ophiolitic terrane of SW Norway, located in northern to central part of Bømlo. Modified after Andersen *et al*. (1991).

metasandstone restite, and Sm-Nd model ages and isotope systematics from 19 samples of diatexites and metatexites. The data from the BMC was presented together with data from several other units of the Early Ordovician ophiolitic terrane and compared to sedimentary successions associated with the Baltic and Laurentian margin. The provenance of the Early Ordovician units showed similarities with Laurentian derived sediments, and no major similarities with sedimentary succession associated with Baltic margin. Comparably, the Sm-Nd model ages from the BMC were significantly older than model ages from the Baltic margin.

A Laurentian affiliation was further supported by the Sm-Nd isotope systematics, which were comparable with sedimentary successions deposited on the Laurentian margin and not the Baltic. Combined this led Fonneland (2002) to suggested that the Early Ordovician ophiolite and arc complexes formed adjacent to the Laurentian margin, rather than the Baltic.

3 Analytical methods

3.1 Sampling and Fieldwork

A total of 67 samples were collected during two periods of fieldwork in June and August 2020. Samples were mostly collected from areas accessible by car, but the overall goal, getting a representative number of samples of the Bremnes Migmatite Complex was achieved. Samples of restites and dia- and metatexites were used for both geochemistry and geochronology, while appinites and gabbroic samples were analyzed for geochemistry. A total of 40 samples were prepared for geochemical analyses, and 10 samples for provenance/geochronology. Both samples for geochemistry and geochronology were selected depending on their position within the complex and their petrology. All samples were prepared and analyzed at the University of Bergen.

3.2 Geochronology

All samples for geochronology were cut with a diamond saw, crushed in a jaw crusher and subsequently pulverized (< 315 µm, common size for zircons) using a Fritsch Pulverisette 13 disc mill. The pulverized samples were regularly sieved using a Retsch Vibratory Sieve Shaker AS 200 to ensure that only the sample fraction < 315 µm was collected for mineral separation.

Mineral separation

The first separation was conducted on a Holman-Wilfley shaking-table. The sample was separated into three different fractions depending on mineral density. Only the heaviest fraction was processed further. A handheld magnet was used to remove ferromagnetic minerals before processing through a Franz Magnetic Separator (15-degree tilt and plunge). To allow for a good magnetic separation, the sample was processed with an increasing current in five steps (0.3, 0.5, 0.7, 1.0, and 1.2 amperes), removing the magnetic fraction from the sample for each step.

Next, the remaining minerals were then separated by density using heavy liquids. Diiodomethane (MI) with a density of ± 3.325 g/ml was used to separate minerals with a density ≥ 3.325 g/ml (i.e. zircon, 3.9 – 4.7 g/ml) from lighter minerals. The sample was placed in a falcon tube containing an appropriate amount of MI. The MI and sample were mixed to allow the minerals to separate, before the bottom of the falcon tube was frozen solid in liquid nitrogen. The lighter minerals and liquid MI were then poured out of the tube and into a 12-15 μm filter to separate the light fraction and liquid MI, the heaviest fraction remained frozen in the falcon tube. The tube was washed with acetone to ensure that only the heaviest fraction remained when the frozen MI melted. When melted, the heaviest fraction was poured into a separate filter. Both fractions were washed with acetone to ensure that all MI was removed from the samples before it was left to dry. The heaviest fraction was processed further. Every sample that contained a significant amount of sulfides was placed in a solution of Aqua Regia (3:1 concentrated HCl + HNO_3) on a heating plate for 30-60 minutes to dissolve the sulfides.

Selection of zircons and mounting

The zircons were picked using a pipette and a light microscope. For each sample between 600-1000 zircons were selected at random to get a representative subset of the total population. The sample was further mounted in epoxy-filled blocks. To properly expose the zircons for analyses, the epoxy mounts were grinded with 15 μm silicon carbide powder and 6 μm diamond paste, and further polished with 0.05 μm silicon carbide powder before analyses.

Scanning electron microscope

Image mosaics of all 10 mounts were collected using Zeiss Atlas (version 3.0) connected to a Zeiss Supra 55 VP Scanning Electron Microscope (SEM) equipped with a CENTAURUS CL detector and associated BS detector. Cathodoluminescence (CL) and backscatter (BS) provides detailed images of the zonation and inclusions within the zircon grains and help choose areas for analyzing. All images were collected with an energy of 15.00 kV and a working distance of 15 mm and 9 mm for CL and BS respectively. All mounts were coated with carbon prior to analysis in SEM, and subsequently removed before further analysis with 0.05 μm silicon carbide powder polish.

Laser Ablated Inductively Coupled Plasma Mass Spectrometer (LA-ICP-MS)

Before analyses, all 10 mounts were immersed in 2% HNO_3 and washed with deionized water to remove any surface contaminants that could affect the results. U-Pb analysis of zircon was conducted using a 193 mm ArF excimer laser ablation system (RESOlution M-50 LR) coupled to an HR-SC-ICP-MS (Nu Instruments Attom ES) using parameters found in Appendixes 3 – LA-ICP-MS. Following 15 s of blank measurement the zircons were ablated for 30 s using

19/26 µm spot size, 5Hz, and fluence between 2 – 2.5 J/cm^2. The data was acquired in time-resolved peak-jumping pulse-counting mode with 1 point measured per peak for masses ^{202}Hg + ^{204}Pb + ^{204}Hg, ^{206}Pb, ^{207}Pb, ^{208}Pb, ^{232}Th, ^{235}U, and ^{238}U. Due to the non-linear transition between the two detector modes in the ICP-MS, ^{238}U was calculated from ^{235}U when measured in attenuated mode (> 2 000 000 counts, ^{238}U = ^{235}U counts x 137.818) using a purpose-made python script. If measured in counting mode, the data was left unchanged.

Data reduction was done using Iolite 4 (v. 4.4.5) with the VizualAge UComPbine33 data reduction scheme (Chew *et al.*, 2014). The method of data reduction follows Paton (Paton *et al.*, 2010), and includes a correction for gas blank, laser-induced elemental fractionation of Pb and U, and instrument mass bias. Blank counts and instrumental bias were corrected with an automatic spline function, while down-hole element fractionation was corrected using an exponential or exponential + line function. Common Pb was only monitored. Zircons with significant amounts of common lead were excluded. The remaining element fractionation and instrumental mass bias were corrected by normalization to the natural zircon reference material 91500 (1065 Ma - Wiedenbeck *et al.*, 1995), while GJ-1 (609 - Jackson *et al.*, 2004) and Plešovice (337 Ma - Sláma *et al.*, 2008) was used for quality control. With mean ages of 1066.5 ± 27.8, 604.4 ± 13.7 and 344.8 ± 9.9 Ma, respectively.

Isoplot (9.0) and detritalPy (1.3) were used to present the data. IsoplotR is built on the Isoplot platform developed by Ludwig (1994) and allows to plot concordia, probability density and weighted mean (Vermeesch, 2018). DetritalPy is developed by Sharman *et al.* (2018) and allows processing/comparison of large datasets.
All detrital zircon U-Pb ages are presented as ^{238}U/^{206}Pb ages below 1550 Ma, and ^{207}Pb/^{206}Pb ages above 1550 Ma. The 1550 Ma threshold was selected due to having the overall least effect on the dataset.

3.3 Geochemistry (major- and trace-elements)

The samples were cut clean of weathering skin, veins, and inclusions using a diamond saw. Then crushed to fine gravel (< 0.5 cm) using a hammer and pulverized in an agate ring or ball mill depending on the sample amount. The pulverized samples were then exposed to 1000 ºC for two hours to remove volatiles and organics, and subsequently the loss on ignition (L.O.I.) was calculated based on the weight loss.

X-ray fluorescence

Glass beads for XRF were prepared with 0.9600 ± 0.0002 g sample and 6.7200 ± 0.0002 g flux agent (Spectromelt A10 di-lithium tetraborate) and was heated to ~1100 ºC and melted using a fusion furnace in which the samples were constantly stirred to obtain a homogenous melt. After melting and stirring for 20 minutes the solutions were poured into mounts and solidified into glass beads. The glass tablets were analyzed for Silicon (Si) using an X-ray fluorescence spectrometer (Bruker S4 PIONEER). The reference material USGS CRM BCR-2 (Columbia River basalt) was used for quality control.

ICP-MS and ICP-AES

The abundance of a selection of trace-elements (Li, Sc, Ti, V, Cr, Mn, Co, Ni, Cu, Zn, Rb, Sr, Y, Zr, Nb, Cs, Ba, Hf, Ta, Pb, Th, and U) and REE were analyzed using a high-resolution Inductively Coupled Plasma Mass Spectrometer (ICP-MS) (Thermo Scientific ELEMENT XR). Indium (In) was used for internal standardization and BCR-2 for calibration. To control the calibration curve and to monitor the performance during analytical runs, the synthetic water CRM SPS-SW-2 (sea water, Spectrapure Standards) was analyzed repeatedly throughout the run.

The concentration of most major- and a selection of trace-elements (Al, B, Ba, Ca, Co, Cr, Cu, Fe, K, Li, Mg, Na Mn, Ni, P, Pb, S, Sr, Ti, V, Y, Zn, Zr) were measured using an ICP Atomic Emission Spectrometer (ICP-AES) (Thermo Scientific ICap 7600). Quantification was done utilizing external calibration curves that were defined by multi-element standard solutions prepared from certified single elements solutions (Spectrapure). Scandium (Sc) was used for internal standardization. Prior to instrumental analysis the samples were diluted to an appropriate level by 2% HNO_3. USGS CRM BCR-2 was used for quality control.

Before the ICP-MS/AES analysis, 0.10 g of dried sample was dissolved in 3 ml concentrated HF using 25 ml PFA Savillex beakers. The solution was kept at 135 ºC for 48 hours for the solution to evaporate. The solutions were then hydrolyzed by adding a weak solution of HNO_3 and left at sub-boiling temperature on a heating plate to evaporate. The nitrates were further dissolved in ~ 2 ml 2N HNO_3 before being diluted with 2% HNO_3 to 50 ml. If some of the samples did not completely dissolve, it was redissolved in ~ 1 ml Aqua Regia on a heating plate.

4 Results

The data presented here is derived from 40 geochemical (major- and trace element analyses) and 10 provenance (detrital zircon) analyses of metatexites, diatexites, gabbros, appinites, and restites (metasediments) from the Bremnes Migmatite Complex and the adjacent Vardafjell Gabbro. A total number of 3538 detrital zircons were analyzed. To follow is a description of the area, with special emphasis on the BMC and the Vardafjell Gabbro, as the Rolvsnes Granite intruded at a later stage.

To better describe the migmatites a key set of expressions are used; paleosome, neosome, melanosome, leucosome, diatexite, metatexite and restite (Maxeiner *et al.*, 2017). Paleosome represents the part of the migmatite that did not undergo partial melting and in which structures as foliation, folding and layering, therefore, are preserved. The new material formed during melting is the neosome and is subdivided into leucosome (melt fraction) and melanosome, which represents the modified residue from the partial melting. Dia- and metatexite is a classification of the amount of neosome present in a rock. Rocks that have lost structural cohesion and typically consist of >60% neosome are diatexitic whereas metatexites contain between 26 and 60% neosome. A restite is a rock unit that had its appearance altered due to partial melting.

4.1 Description of the study area

The BMC compromises diatexites, metatexites and appinites which a cut by basaltic dykes, pegmatites and granitic to granodioritic intrusions (Figure 4.1).
The diatexites appear adjacent to the contact with the Vardafjell gabbro and are defined by an irregular banding of melanosome and leucosome (Figure 4.2). The melanosome is biotite-cordierite-sillimanite bearing and the leucosome is characterized by quartz and felspathic minerals. In the diatexites the melanosome is the most prominent part of the neosome while the leucosome appears to be mobilized into the adjacent metatexites, gabbros, or concentrated within certain areas. The diatexites contain restites/enclaves of sandstones, mica schist, quartzites, and marbles which form an E-W trend together with the irregular banding of melanosome and leucosome (Figure 4.2). The metatexites are located further from the gabbros and contain a minor amount of neosome compared to the diatexites. These rocks locally exhibit an irregular layering of quartzite and mica schist which together with the neosome and restites

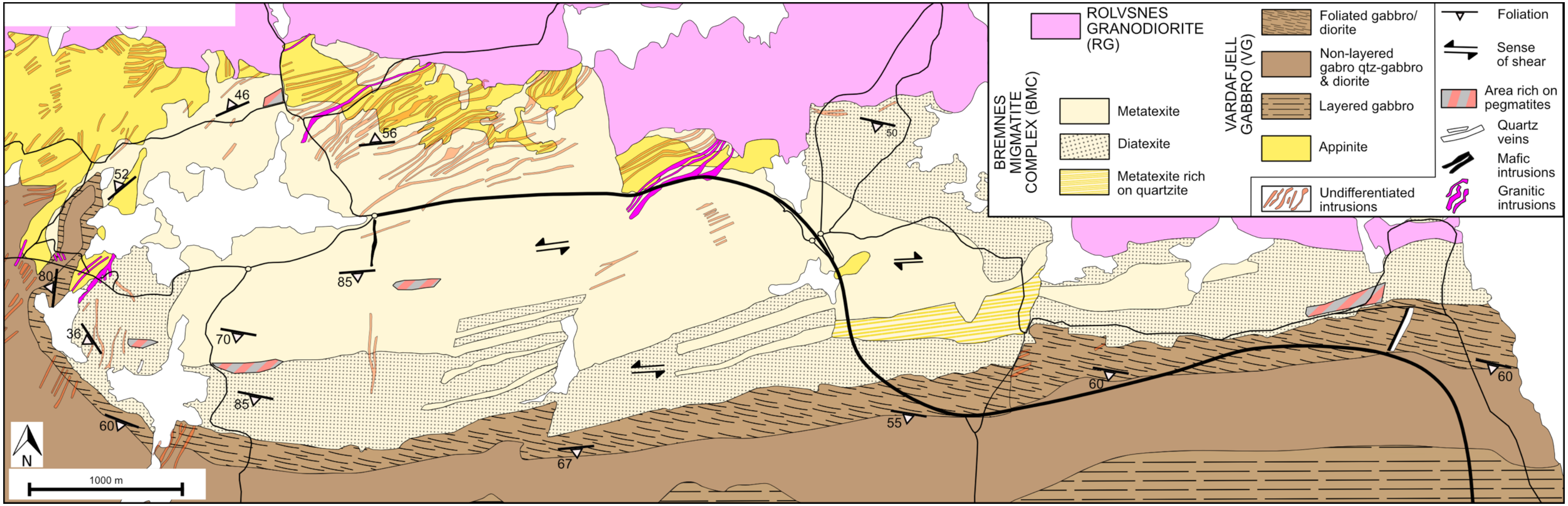

Figure 4.1: Geological map of the Bremnes Migmatite Complex. Redrawn after Nielsen (1990), with data from Andersen (1991) and this study. The undifferentiated intrusions are redrawn after Nielsen (1990), and are made up of granitic, basaltic, and pegmatitic intrusions.

exhibit an E-W trend (Figure 4.2). There is a significantly more restite material present in the metatexites compared to the diatexites.

The restites are mainly composed of sandstones, mica schists, and quartzite, with minor amounts of marble and amphibolite. Leucosome found in the metatexites and diatexite both exhibit in-situ, in-source, and injection features, with the latter occurring more frequent in the metatexites (Figure 4.2). The paleosome are mostly concentrated within enclaves and in some areas as partly melted inclusions of a larger size (restites). Outcrops dominated by paleosome are rare in the study area. The foliation and lineation of the paleosome are preserved in certain restites.

The northern part of the BMC is characterized by both fine- and coarse-grained appinites (Figure 4.1 and Figure 4.4). The coarse-grained appinites exhibit well-developed (≤ 25 cm) hornblende crystals in a fine-grained matrix of plagioclase with coherent sulfide-mineralization. The appinites have an intrusive contact with adjacent metatexites (Figure 4.4).

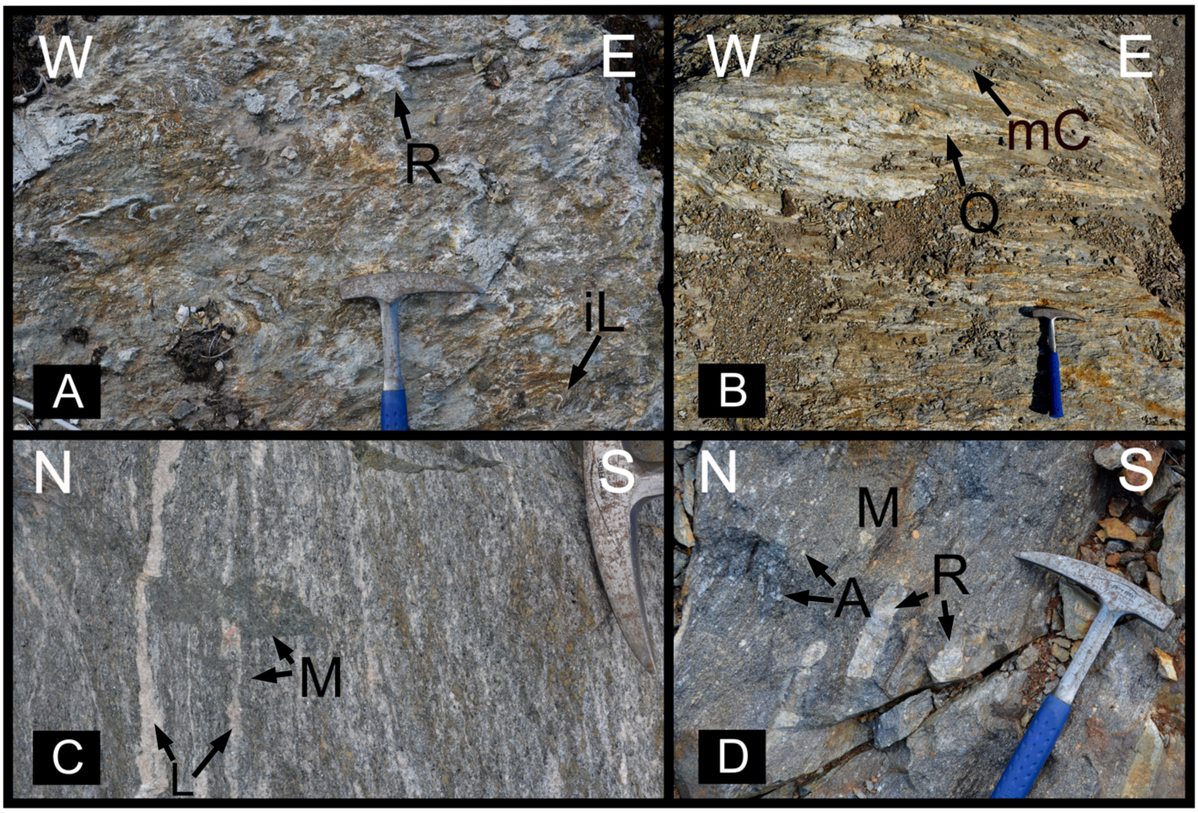

Figure 4.2: A) Leucosomal material with small restites (R) and coherent melanosome, indicating in-situ leucosome (iL). B) Leucosome and melanosome with banding of quartzites (Q) and mica schist (mC). C) Leucosome (L) and melansome (M) banding in metatexite. D) Melanosome rich outcrop, with aggregates (A) and restites of quartzite and sandstone. Hammer for scale.

There is an intrusive contact between the migmatite and the Vardafjell Gabbro. Within a 50-200 m wide zone adjacent to the BMC, the Vardafjell Gabbro is net-veined by leucocratic material, which represents mobilized leucosome from the migmatite (Figure 4.3). Mixing of the gabbroic and granitic material has led to the formation of quartz-rich gabbros, and in areas with no mixing to formation of a distinctive gneissic banding. Adjacent to the migmatite the granitic and gabbroic material define an E-W orientation similar to the migmatite. Further into the Vardafjell gabbro the trend becomes less apparent, and the leucocratic material appears

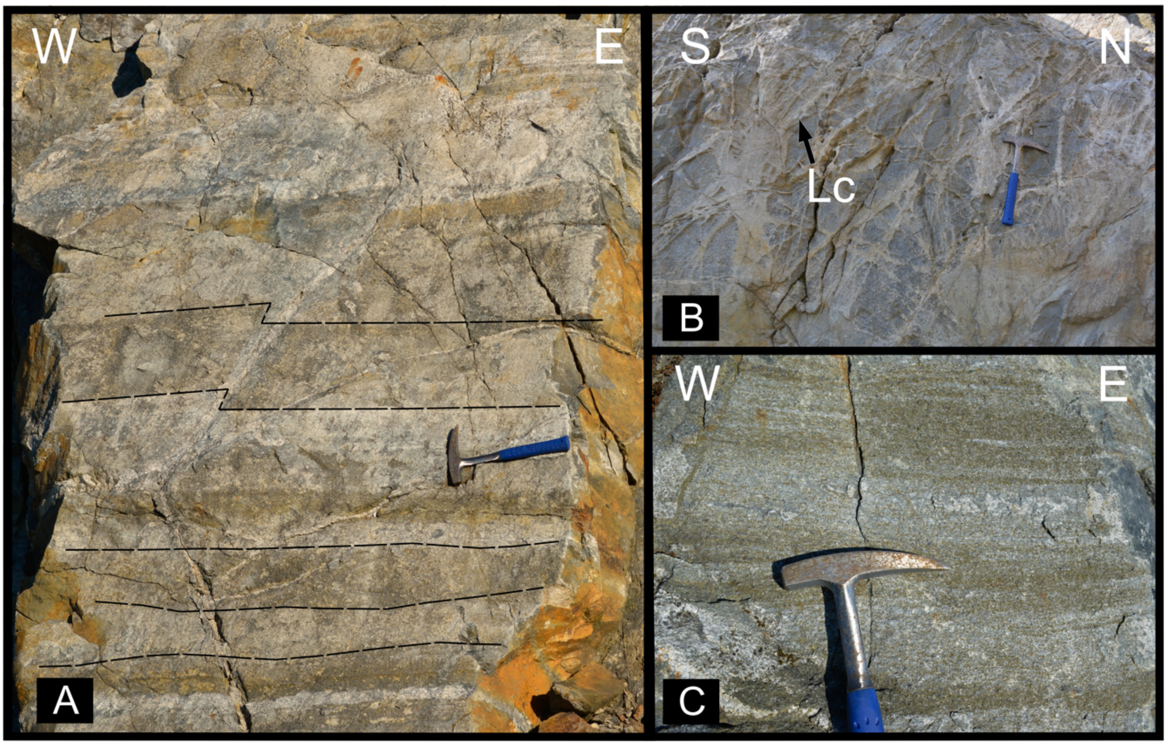

Figure 4.3: A) Layered gabbro with distinctive layers of plagioclase (light) and ferromagnesian minerals (dark), located 1-2 km from the Bremnes Migmatite Complex. B) A gabbroic/diorittic matrix net-veined of leucocractic (Lc) material from the migmatite complex, near the contact zone with the Vardafjell Gabbro. C) Irregular layered gabbro, layers of ferromagnesian minerals and plagioclase, approximately 1-2 km from the migmatite complex.

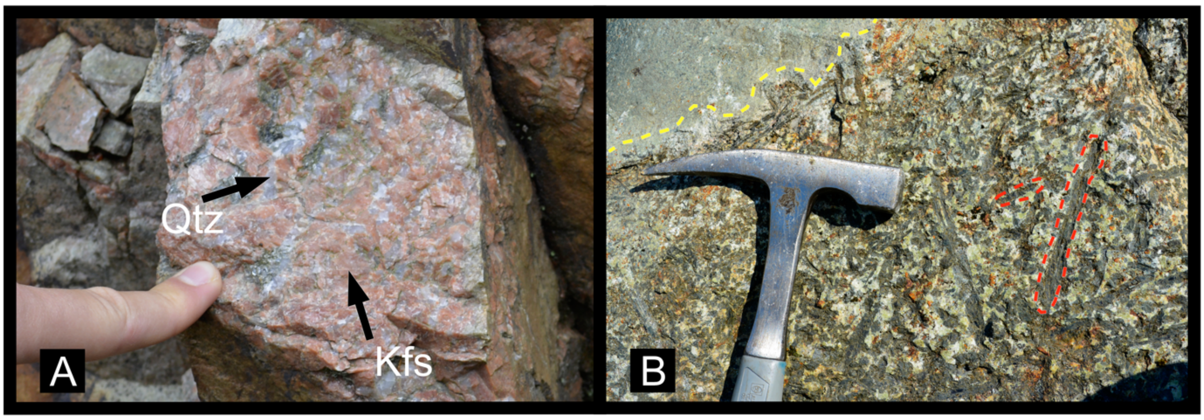

Figure 4.4: A) Typical exposure of the Rolvnes Granite, qtz = quartz, kfs = k-feldspar. B) Coarse-grained appinite, with large amphibole crystals in a fine-grained matrix of plagioclase. The appinite exhibits an intrusive relation to the surrounding migmatite (yellow).

randomly orientated (net-veined). In areas ~1000 m from the contact the Vardafjell Gabbro exhibits irregular layering (Figure 4.3).

In the north, there is an intrusive contact between the migmatite and the Rolvsnes Granite (Figure 4.1). The contact zone is characterized by dykes of K-felspathic granitic material orientated NE-SW (Figure 4.4 and Figure 4.5). The dykes are concentrated within an area of 0–200 m into the migmatite (Figure 4.1). Adjacent to or in the proximity of the granitic intrusions there are mafic and pegmatitic intrusions with similar orientation (NE-SW). The intrusions from Rolvsnes Granite crosscut granitic veins in the appinites (Figure 4.5). Mafic dykes, pegmatitic and quarzitic veins occur regularly across the BMC, and exhibit similar NNE-SSW orientation as the granitic intrusions from the Rolvsnes Granite. Some of the mafic dykes show N-S orientation. The intrusion ranges from 20–200 cm in width.

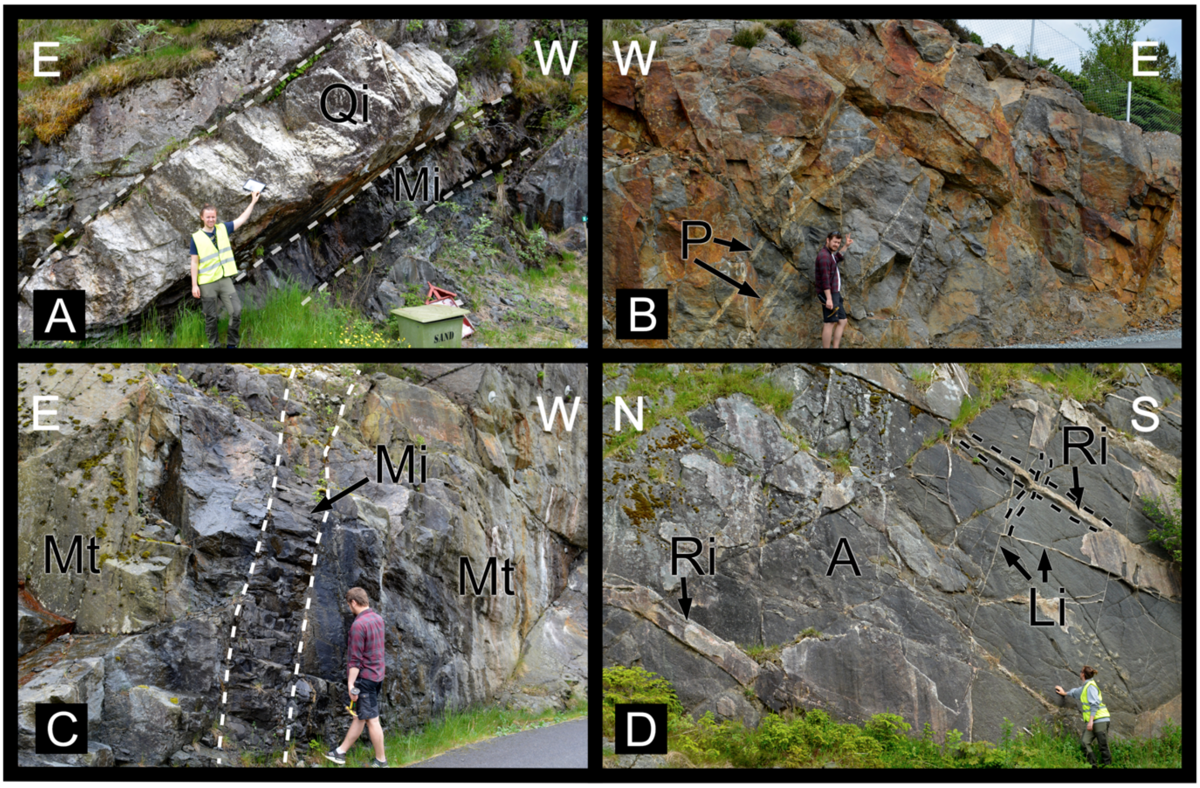

Figure 4.5: A) Quartz intrusion (Qi) with an adjacent mafic intrusion (Mi) with NNE-SSW orientation, located within the diatexites of the Bremnes Migmatite Complex B) Pegmatites (P) intruding metatexites in an NNE-SSW direction. C) Mafic intrusion cross-cutting metatexite (Mt) in N-S direction. D) Granitic intrusion (Ri) from Rolvnes Granite cross-cutting minor leucocratic intrusions (Li) in a fine-grained appinite (A).

Classification of the restite material

The metasedimentary restites within the metatexites and diatexites consist of sandstones, quartzites, and mica schist, with minor amounts of amphibole and marble. They vary in size and lithology, from aggregates (2 cm) to enclaves (50 cm). The different lithologies are restricted to certain areas of the dia- and metatexites, and one outcrop rarely shows more than one lithology. The amphibolitic restites are typically confined close to the gabbros, whereas the quartzites, sandstones, marbles, and mica schists appear more evenly across the BMC. Due to their partially melted nature, it can be difficult to distinguish the different lithologies from each other at most outcrops. Restites that do not exhibit any characteristics of melt extraction are rare (Figure 4.6). In areas with distinctive neosomal E-W banding, the restites show similar orientation. If there is no neosomal banding, the restites appear randomly orientated (Figure 4.8). The metasedimentary restites are elongated, rounded, chubby, and angular. A leucocratic

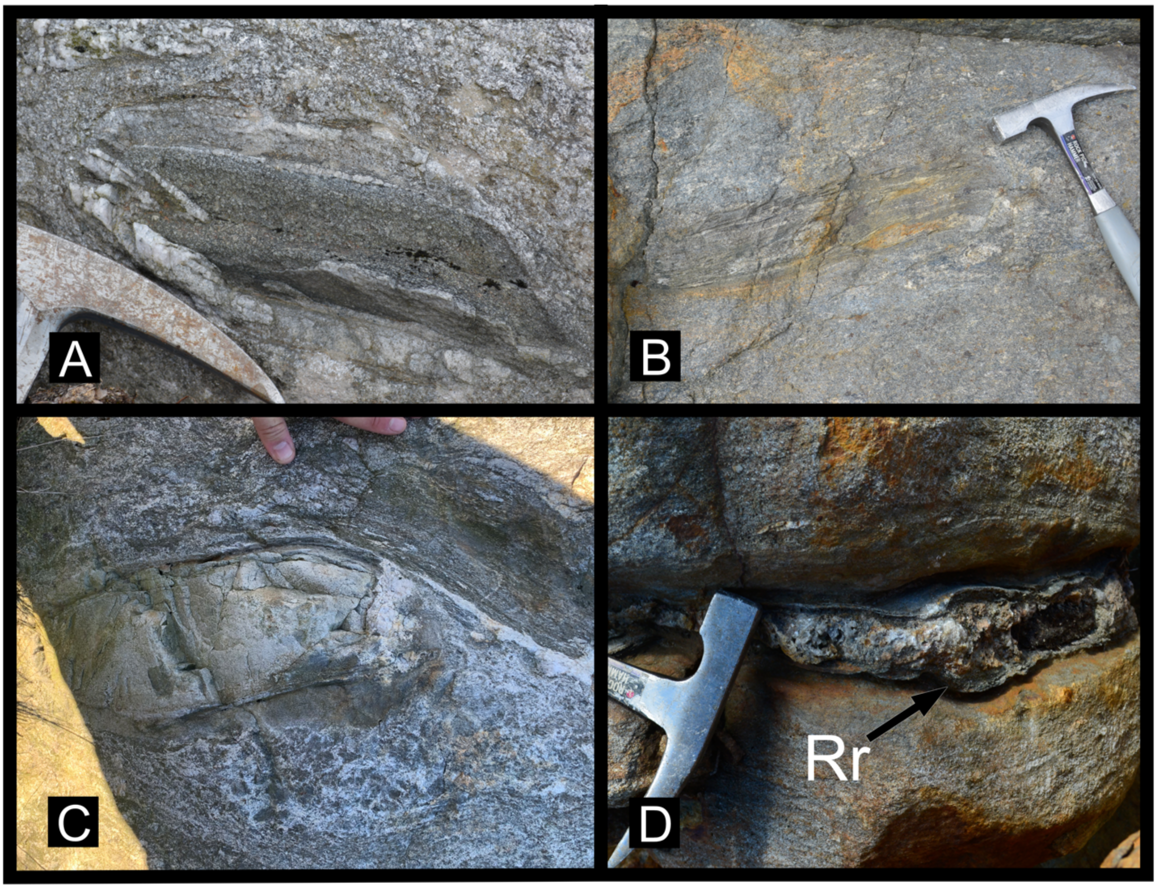

Figure 4.6: A) Quartz-felspathic restite with leucosome aggregates. Notice the leucosome rich rim around the restite. B) Partly melted restite of quartz-felspathic or mica schist composition, with distinctive segregation of leucosome and melanosome, indicative of partial melting. Notice the apparent foliation/layering preserved by the leucosome/melanosome. C) Massive quartz-felspathic restite/enclave, with the apparent extraction of leucosome. D) Restite of unknown composition, with a prominent reaction rim (Rr) of a fine-grained material.

band of 2-5 mm thickness incapsulates 40% of the restites. Some restites have reaction zones, where leucosomal material show flow structures around the restite (Figure 4.6).

Quartz felspathic restites are common across the migmatite. Structures such as foliation and bonding are often preserved in the quartz felspathic restites. They appear elongated or as partly melted imprints in which the melanosome and leucosomal material are visible (Figure 4.6 and Figure 4.7).

Restites of mica schists appear as elongated and rounded xenoliths. In areas dominated by melanosome, the mica schists appear as aggregates. Structures as foliation and bonding are preserved in certain restites (Figure 4.6 and Figure 4.7).

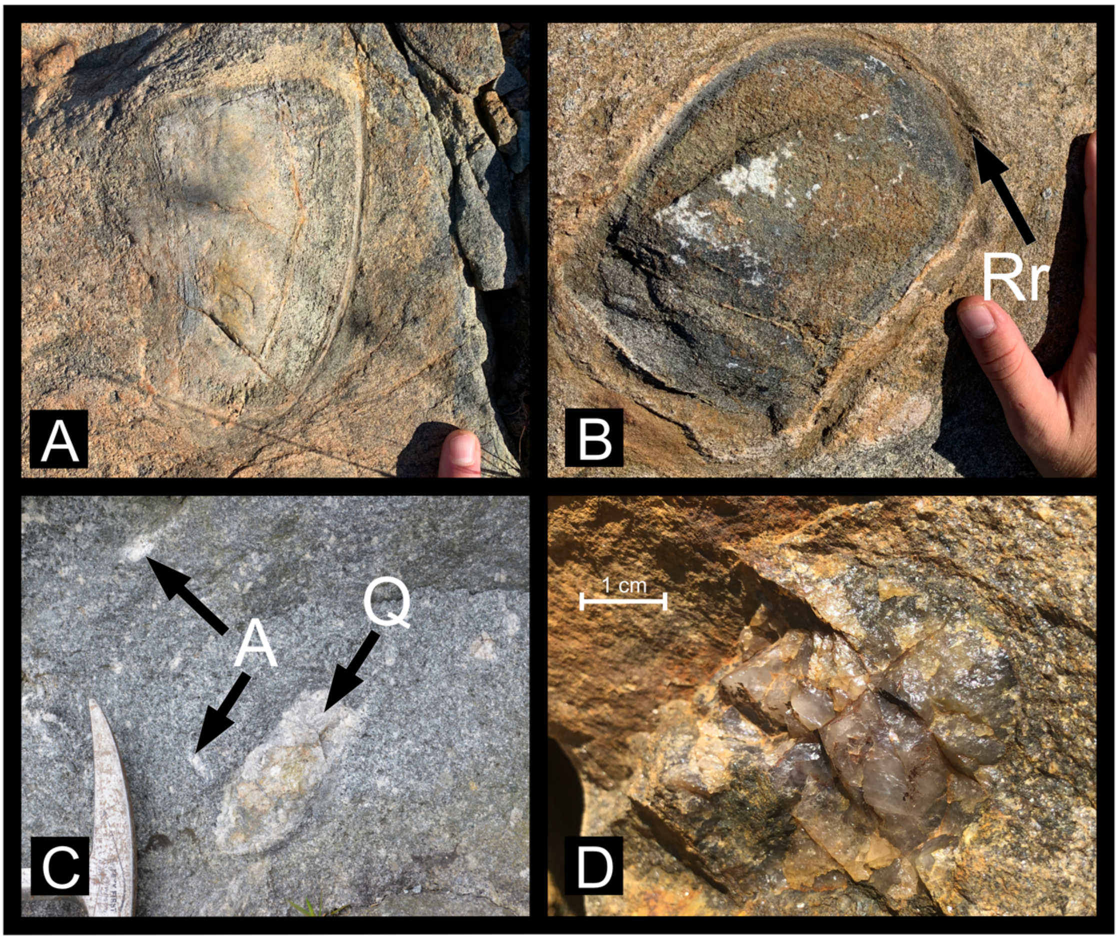

Figure 4.7: A) Quartz-felspathic restite with a leucosome rich rim. B) Mica schist restite with an apparent reaction rim (Rr). Notice the veins of leucosomal material in the restite, indicative of the extraction of melt. C) Quarzitic aggregates (A) and quartzite (Q) restites in a massive matrix of leucosome and melanosome. D) “Quartz-lump” with an “smokey quartz” appearance. Notice the difference in appearance between the quartzite in C and D.

Quarzitic restites appear mostly as aggregates with no apparent layering or foliation. At certain outcrops the quartzites appear as "quartz lumps" and differ significantly in size and color compared to the other quarzitic restites (Figure 4.7).

The distribution, orientation, and number of restites present at outcrop depend on the amount of leucosome/melanosome. Restites in melanosome-rich outcrops appear mostly as aggregates, and rarely with a length > 3 cm. Outcrops rich in leucosome often exhibit neosomal banding

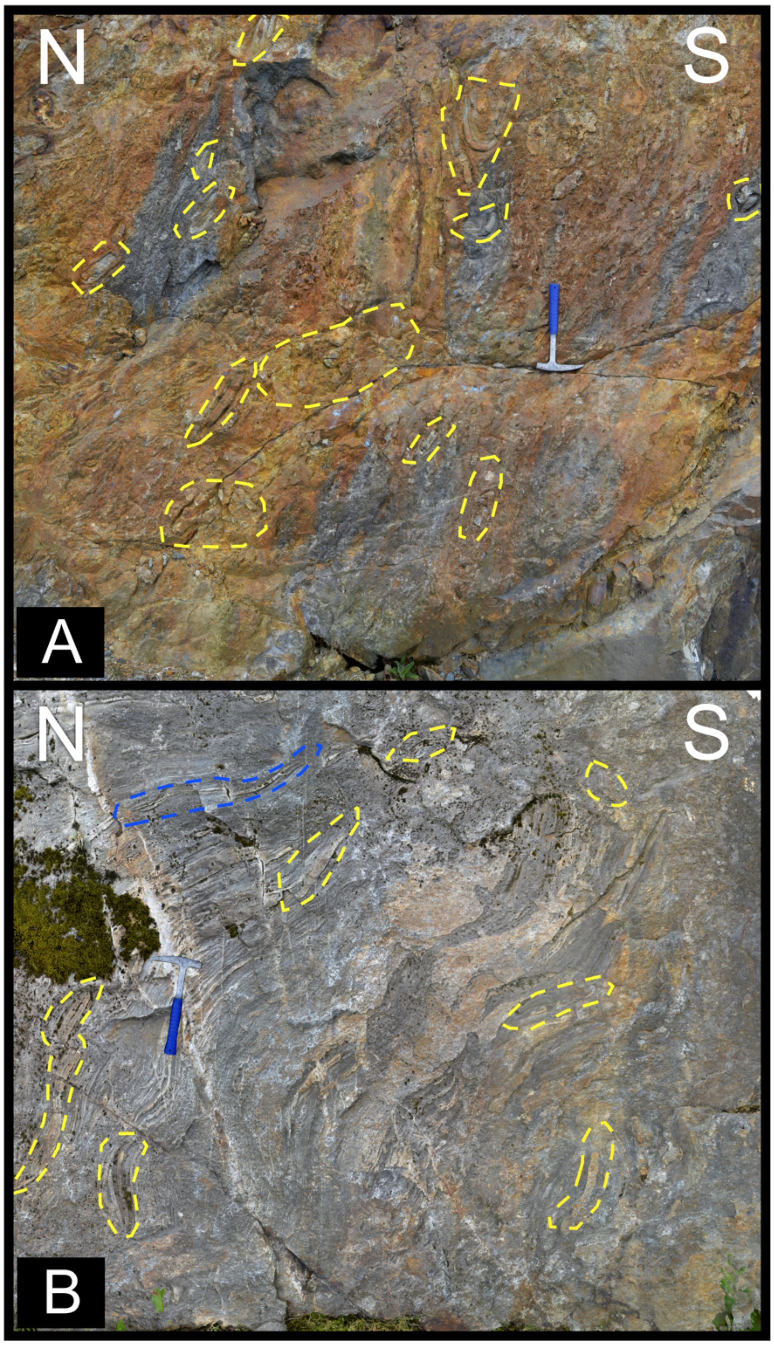

Figure 4.8: A) Restites in melanosome rich metatexite, with no apparent orientation of quartz-felspathic restites (yellow). B) Neosomal banding of leucosome and melanosome (blue) in metatexite. Notice orientation of restites (yellow) parallel to the banding.

that the restites orientate relative to (Figure 4.8). At outcrops rich in melanosome the restites orientate randomly, and these outcrops often lack the neosomal banding found in leucosome rich outcrops (Figure 4.8). Certain areas contain a significantly higher number of restites, these are mostly confined to metatexitic outcrops.

4.2 Sample description and major-element geochemistry

The description of the samples collected in the area are grouped according to their affiliation, i.e. Vardafjell Gabbro, and restites, diatexites and metatexites of the BMC. Following is a general description of the different categories of samples, this includes field and thin section description, and major element composition (Appendixes 1 – Sample descriptions and locations and Appendixes 2 – Major- and trace-elements analysis). All sampling locations can be seen in Figure 4.9.

Diatexites and metatexites

A total of 17 samples (6 diatexites and 11 metatexites) were analyzed for major- and trace-elements from the BMC (Figure 4.9). All 17 samples show similar appearance at outcrop and differ mainly in the amount of leucosomal material present. Biotite-cordierite-sillimanite banding is characteristic for 6 of the samples, while in the other 11 samples this is not a defining feature. On average the major-element composition of the dia- and metatexites is characterized by 17.44% Al_2O_3, 60.13% SiO_2 and 8.34% Fe_2O_3. Most diatexites and metatexites have a high content of Al_2O_3 and show a peraluminous character (Figure 4.10 and Figure 4.11). Thin-sections of dia- and metatexites are dominated by quartz, plagioclase/saussurite, biotite, muscovite, sillimanite, chlorite, and garnet, with minor variations them between. Certain areas within the thin section are dominated by quartz or chlorite, indicating small-scale restites or melanosome rich sections. The biotite-sillimanite banding is clearly visible in certain thin sections. The dia- and metatexites plots primarily as diorites after the classification of Middlemost (1994) (Figure 4.11).

Restites

Eight samples of restites were collected and analyzed for major- and trace-elements (Figure 4.9). During sample preparation it was hard to properly separate the restite from their surrounding neosome due to their partial melted nature. Therefore, the results do not reflect a

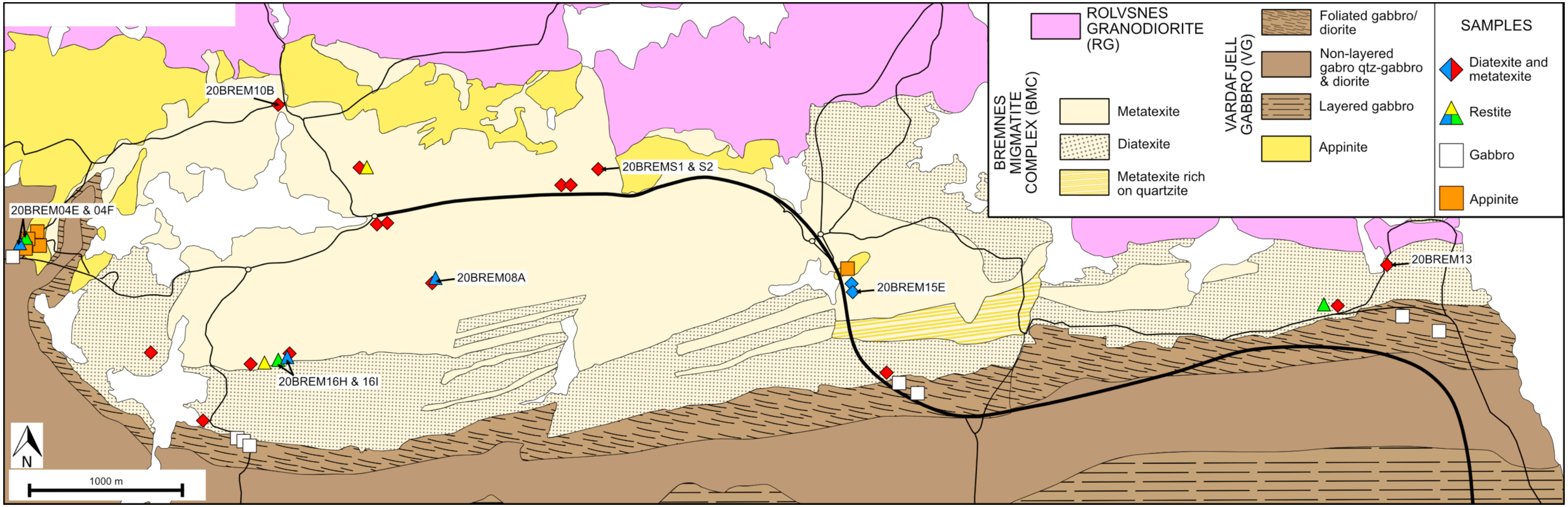

Figure 4.9: Simplified geological map of Bremnes Migmatite Complex and the adjacent Vardafjell gabbro and Rolvsnes granodiorite, modified after Nielsen (1990). Sampling locations for samples collected and analyzed for major- and trace-elements and geochronology in this study, 8/10 samples collected for geochronology was also analyzed for major- and trace-elements. Only samples collected for geochronology are shown here, see Appendix 1 for all sampling locations. Diatexites and metatexites are divided according to two trends shown within the REE-patterns. The restite samples are divided according to their affiliation, yellow = quartzite, blue = mica schists, green = quartz-felspathic material.

clean analyses of a restite, and their composition may be altered due to the neosomal material. Of the eight samples collected, there were three samples of quartzites, three of quartz-felspathic material, and two mica-schists (Figure 4.9). At outcrop, they differ in their appearance, i.e., foliation/layering and composition. All the restites contain varying amounts of quartz, plagioclase, mica (biotite and muscovite), chlorite, and sillimanite. In areas with significant neosomal component plagioclase appears to be recrystallized into saussurite. The foliation of sillimanite and biotite is visible in restites that exhibit such textures at outcrop. Garnet appears in some of the quartz-felspathic restites. The major-element analyses shows that the restites greatly varies in chemical composition (Figure 4.10 and Figure 4.11). The quartzites show an average composition of 72.80% SiO_2, 13.92% Al_2O_3, and 2.08% Fe_2O_3. The high SiO_2 and low Fe_2O_3 content reflects their felsic origin. The two samples of mica schists contain an average of 54.63% SiO_2, 17.91 % Al_2O_3, and 10.70% Fe_2O_3 and may indicate that the samples contain a considerable amount of melanosome (ferromagnesian minerals) (Figure 4.10). The three samples of quartz-felspathic material are characterized by a high average CaO of 15.3% compared to the quartzites and mica schists (5.67% and 5.29% respectively). The high CaO can indicate that the restites contains a significant amount of plagioclase, as no calcite was recognized in thin-section nor at outcrop. Further, the quartz-felspathic material has an average SiO_2 of 53.08%, 6.66% Fe_2O_3 and Al_2O_3 content of 16.32%. The Al_2O_3 content resembles that of the quartzites and mica-schists. Only two of eight restites show a peraluminous character (Figure 4.11).

Vardafjell Gabbro

From the Vardafjell Gabbro nine samples of gabbros and five of appinites were collected and analyzed for REE, major- and trace-elements (Figure 4.9). One sample of the Vardafjell Gabbro collected approximately 2 km from the BMC is included for comparison (data from Saltvedt, in prep.). The gabbroic samples collected furthest from the migmatite contain the least amount of leucocratic material. One of the nine collected samples of the Vardafjell Gabbro contains leucocratic material from the migmatite. In thin-section the gabbro is characterized by amphibole, pyroxene (recrystallized), and plagioclase (saussurite), with minor amounts of quartz, chlorite, and titanite. At outcrops 100 m from the BMC, the gabbroic samples show a mineralogy dominated by fine-grained plagioclase and pyroxene/amphibole. Closer to the contact zone with the BMC quartz and mica appear. Major-element analyses of the gabbroic samples show an average composition of 52.98% SiO_2, 9.03% Fe_2O_3, and 5.55% MgO, reflecting the mafic origin of the gabbroic body (Figure 4.10). The relatively high content of SiO_2 can be influenced by the presence of quartz in samples taken close to the migmatite (Figure 4.10 and Figure 4.11).

The appinite samples are both fine- and coarse-grained, with small (< 1 cm) and large (10 cm) crystals of amphibole within a fine-grained matrix of plagioclase. The average composition of the appinites is 63.24% SiO_2, 3.46% Fe_2O_3, and 1.45% MgO (Figure 4.10). The similarities in major-element composition between the appinites, restites, metatexites, and diatexites could be related to the unsuccessful separation of appinite and leucocratic material. Both the appinites and the gabbros show a metaluminous character (Figure 4.11).

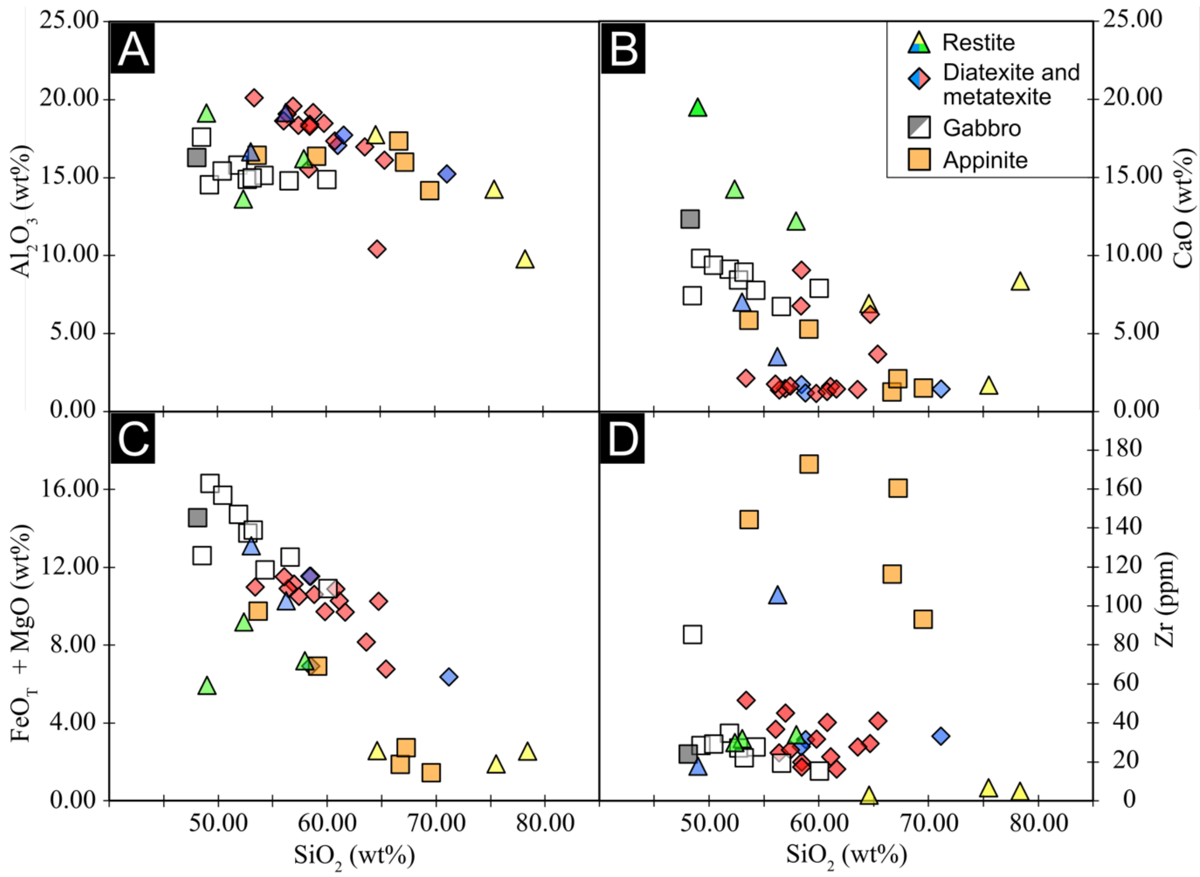

Figure 4.10: Harker diagrams of SiO_2 against Al_2O_3 (A), CaO (B), FeO_T + MgO (C) and Zr (D). A) Show the evenly high content of Al_2O_3 across all samples of the Bremnes Migmatite Complex, with a prominent decreasing trend as the SiO_2 content increases. B) The quartz-felspathic restites contain a high amount of CaO, resembling a high content of plagioclase. Notice the uniformly low content of CaO in the dia- and metatexites. C) Illustrates that the FeO_T and MgO content are high in the mantle derived magmas of the Vardafjell Gabbro, the intermediate composition of the partial melted constituents (dia- and metatexites), and the varying composition of the restites. D) Illustrates the analytical error during sample preparation, in which Zr is not completely dissolved and continental derived rocks consequently exhibit a Zr content of 10 ppm. Gabbroic samples are color coded according to their affiliation, grey = reference material collected the furthest from the contact zone with BMC (Saltvedt, in prep.), white = all other samples collected within ~200 m of the contact zone. Diatexites are divided according to two trends seen in the REE-patterns. Restites are color coded according to their affiliation, yellow = quartzite, blue = mica schist, green = quartz-felspathic material.

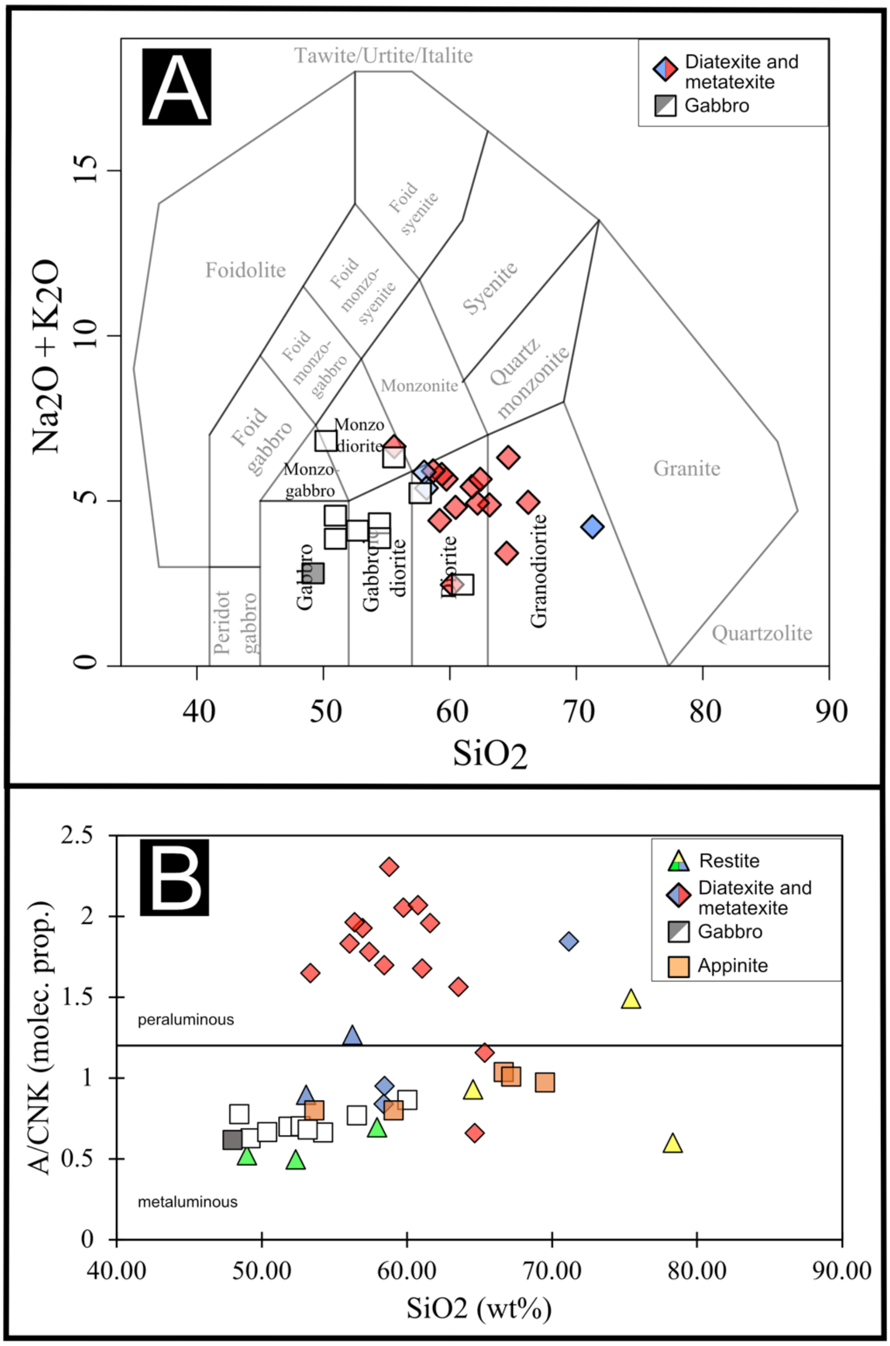

Figure 4.11: A) Classification of the dia- and metatexites from the BMC, and gabbros from the Vardafjell Gabbro, after Middlemost 1994. B) Plot of A/CNK, showing the peraluminous origin for most of the dia- and metatexites, and metaluminous orogin of the appinites and gabbros. Gabbroic samples are color coded according to their affiliation, grey = reference material collected the furthest from the BMC (Saltvedt, in prep.) white = all other samples collected within 200m of the contact zone with BMC. Diatexites are divided according to two trends seen in the REE-patterns. Restites are color coded according to their affiliation, yellow = quartzite, blue = mica schist, green = quartz-felspathic material.

Trace-element compositions

The trace-element patterns are grouped according to their lithologies, i.e. dia- and metatexites, restites, gabbros, and appinites (Figure 4.12 and Figure 4.13). The spider-diagrams are normalized against primitive mantle values from Sun and McDonough (1989), and REE to the chondritic values from Taylor and McLennan (1985). Negative anomalies for Zr, Hf, and Ti are present in all analyses and represent an analytical error due to the incomplete dissolvement of Zr, Hf, and Ti during sample preparation (Figure 4.12 and Figure 4.13). The analytical error is prominent in Figure 4.10, where remains of continental derived rocks plots with a Zr content of *c.* 10 ppm.

Diatexites and metatexites – Bremnes Migmatite Complex

The diatexites and metatexites show two trends, both enriched in the light-REE (LREE) relative to heavy-REE (HREE) (Figure 4.12). The difference is prominent, with trend 1 being two-three times as enriched in LREE and HREE relative to second trend (Figure 4.12). Despite the difference in enrichment, all analyzed dia- and metatexites show the same trends (Figure 4.12). There is no apparent difference between the dia- and metatexites that constitutes the first and the second trend, suggesting that the difference could be related to the sampling location. The samples of the second trend were collected in proximity of an appinite exposure (Figure 4.9). Almost all analyzed dia- and metatexites show positive Eu anomalies.

The spider-diagrams for the dia- and metatexites exhibit the same two trends as seen in the REE plots (Figure 4.13). The dia- and metatexites are enriched in the incompatible mobile elements (Th, U, La, Pb) and HFSE (high field strength elements), and slightly less enriched in the more compatible elements (Hf – Yb). There is prominent negative anomaly for Ta-Nb, Zr-Hf and Ti. The depletion of Ta-Nb is characteristic of subduction zone derived magmas (White, 2013), and are present within all analyzed samples (Figure 4.13).

Restites – Bremnes Migmatite Complex

The REE-patterns for the restites show two trends enriched in LREE relative to HREE (Figure 4.12). The first trend (mica schists and quartz-felspathic restites) are four to five times as enriched in LREE and HREE compared to the second trend (quartzites and quartz-felspathic restites) (Figure 4.12). The second trend are not as enriched in LREE relative to HREE, and consequently show a less steep curve. Restites collected in proximity of each other exhibit different trace-element trends, suggesting that the trace-element patterns are not restricted to certain areas of the BMC (Figure 4.9). The enriched trend shows negative Eu anomalies, and the second less enriched trend shows positive Eu anomalies (Figure 4.12).

In the spider-diagram, the restites form the same two trends as seen in the REE patterns (Figure 4.12 and Figure 4.13). Both trends are enriched in the incompatible mobile elements and HFSE, and are slightly less enriched in the more compatible elements. The difference in the enrichment of the incompatible mobile elements and the more compatible elements are not that pronounced, giving rise to a flat trend in the spider-diagram (Figure 4.13). The quartzites are less enriched in Th relative to U, opposite of the mica schists that are more enriched in Th relative to U. There are prominent negative anomalies for Ta-Nb, Zr-Hf and Ti.

Gabbros – Vardafjell Gabbro

The gabbroic rocks of the Vardafjell Gabbro show an enriched trend similar to the other units of the study area (Figure 4.12). One of the nine analyzed gabbroic samples, exhibit a very enriched trend resembling the appinitic samples (Figure 4.12). The other eight samples show a pattern resembling the less enriched trend of the dia- and metatexites, but with a slightly less steep curve (Figure 4.12). The gabbroic rocks show a slight negative Eu anomaly. The reference sample from the Vardafjell Gabbro show comparable trends with the gabbroic samples collected in proximity of the BMC, and a positive Eu anomaly (Saltvedt, in prep.).

In the spider-diagram the gabbroic samples are enriched in the incompatible mobile elements (Th, U, La, Pb) and HFSE, and less enriched in the compatible elements. The trend showed by the reference samples exhibit similarities with the other gabbroic rocks, enriched in La and Pb, but less enriched in Th, U, Ta, and Nb (Figure 4.13).

Appinites – Sunnhordland Batholith

The appinites are heavily enriched in LREE (200 – 600 times that of a chondrite) and depleted in HREE (< 10 times the reported value for a chondrite) (Figure 4.12). The analyzed appinites show no similarities with the other rocks of the study area, suggesting that they were derived from a completely different source.

In the spider-diagram the appinites are highly enriched (1100 times that of primitive mantle) in the incompatible mobile elements and HFSE and depleted in the more compatible elements (Figure 4.13). The high content of the incompatible mobile elements combined with relatively low concentrations of the more compatible elements, leads to the formation of a steep curve in the spider-diagram which are not recognize elsewhere within the BMC (Figure 4.13).

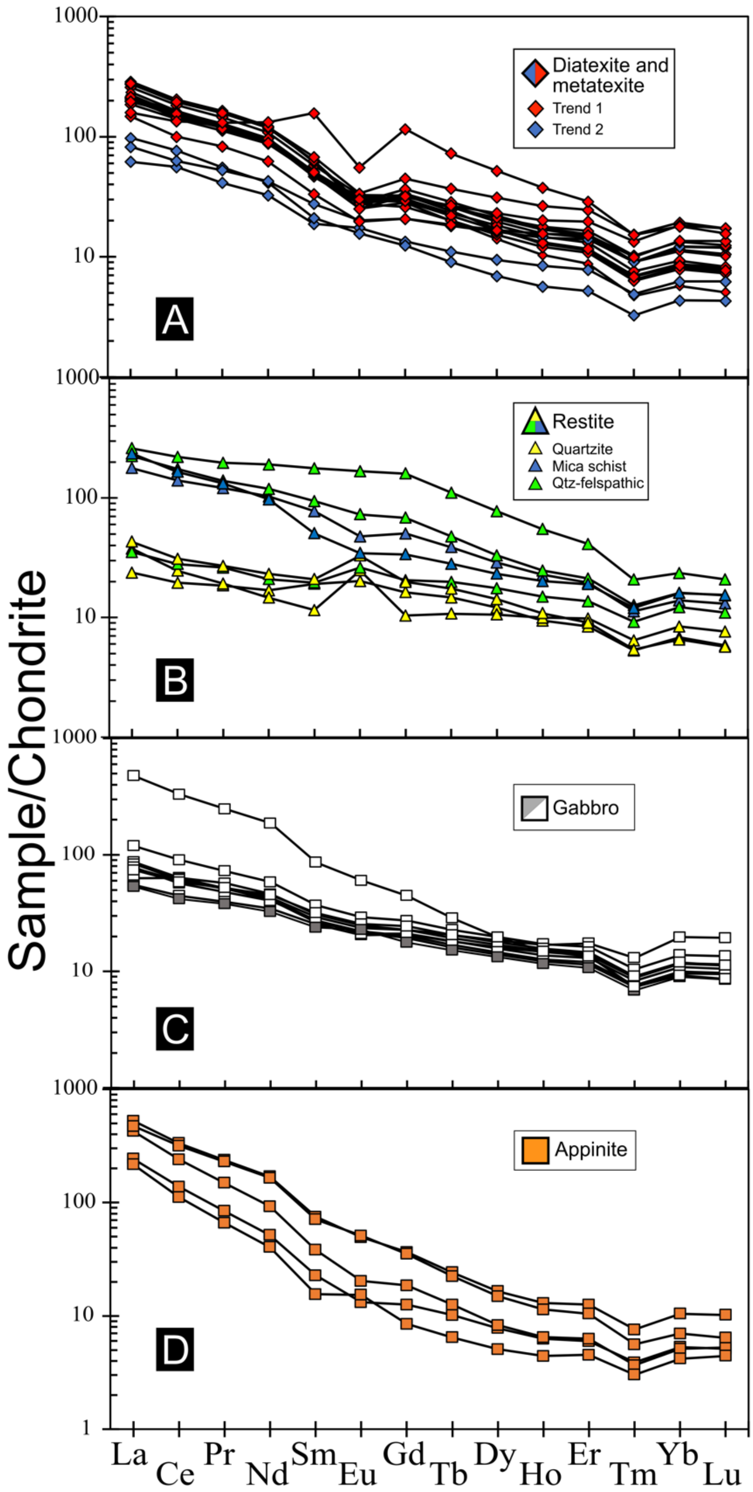

Figure 4.12: Chondrite normalized rare earth element (REE) plots for all analyzed samples, notice the enriched trend exhibited by all analyzed samples A) Dia- and metatexites form two trends related to their sampling location. Notice the distinct negative Eu anomalies. B) The two trends exhibited by the restites are related to lithological difference. Notice that the restites show both positive and negative Eu anomalies. C) The gabbros show a flat enriched trend, enriched in LREE relative to HREE. D) The appinites are significantly enriched in LREE and depleted in HREE, and show no major similarities with the other units. Gabbroic samples are color coded according to their affiliation, grey = reference material collected the furthest from the contact zone with BMC (Saltvedt, in prep.), white = all other samples collected within ~200m of the contact zone. See text for further explanation.

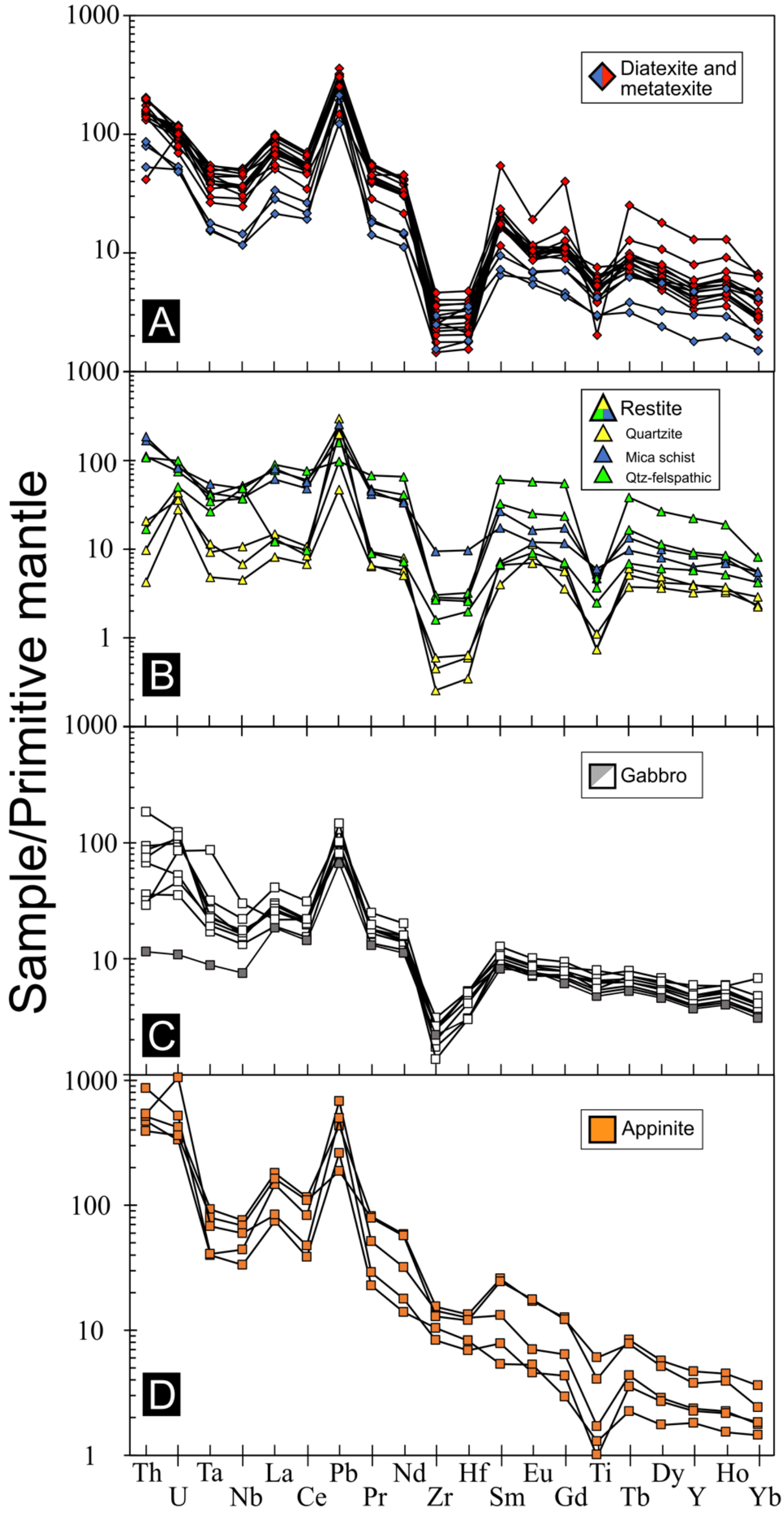

Figure 4.13: Primitive mantle normalized spider-diagrams for the dia- and metatexites, and restites of the Bremnes Migmatite Complex, gabbroic samples from the Vardafjell Gabbro, and appinites found in relation to the migmatite complex. All samples show Ta-Nb anomalies, suggesting that the rocks developed in a subduction zone system, and are enriched in the incompatible mobile elements (Th, U, La, Pb) and HFSE relative to the more compatible elements (Tb, Dy, Y, Ho, Yb) A) The two trends seen in the REE plots for the dia- and metatexites are not as prominent in the spider-diagram plots. B) The restites show the same distinction in the spider-diagram as the REE plots, forming two relatively flat trends. C) The Vardafjell Gabbro (white from this study, grey from Saltvedt, in prep.) show a trend different from the other rock units analyzed here, indicative of their calc-alkaline origin. D) The appinites are very enriched in the incompatible mobile elements relative to the more compatible elements, indicating that these rocks developed from a distinctively different source.

4.3 Geochronology – detrital zircon provenance

Mean age of migmatization

From all the Caledonian zircons (500 – 460 Ma) that have a discordance of ≤ 5 % there is calculated a weighted mean of 477 ± 7 Ma. This weighted mean age is interpreted to represent the metamorphic overgrowths on the zircons that occurred at the time of migmatization. There was a total of 16 zircons from 7 of 10 analyzed samples that had a discordance (≤ 5 %) and age (500 – 460 Ma) within the filter.

Detrital zircon in restites

The analyzed zircon grains from five restites, collected within different parts of the BMC (Figure 4.9), range in size from 40-300 µm. About 90% are confined as subangular to rounded, with minor amounts of angular grains (Figure 4.15). Most grains are confined within the size range of 80-170 µm, the smallest (< 50 µm) and largest (> 200 µm) grains make up < 5% of the sample. The zircons appear as elongated and stubby crystals, most of the largest grains are appear as elongated crystals, while the smaller grains appear as both elongated and stubby. Around 70% of the grains exhibits sector or oscillatory zonation, and *c.* 50% contain xenocrystic cores. The xenocrystic cores vary in size and show contrasting ages, with light banded overgrowths present around 50% of the grains. Fractures are common in grains that contain xenocrystic cores, and less apparent in other grains. Inclusions are present in 40% of grains with no apparent distribution in size, shape, or form (Figure 4.15). A minor population of grains exhibits neither inclusion nor fractures.

The different types of restites contain zircon grains of contrasting size but show the same cumulative age distribution (Figure 4.16). The grain size difference can either reflect the degree of melting or the protolith. From cathodoluminescence and back-scatter imaging the grain size difference appears to be coupled with the degree of melting. Samples of well-preserved restites contain the largest grains, and the more reworked/partial melted restites exhibit smaller grain sizes.

The cumulative age distribution and probability density plots (PDP) for the five analyzed restite samples plot similarly and show that 40-60% of the zircons have a Mesoproterozoic age, with significant Archean (10%), Paleoproterozoic (10%), Neoproterozoic (10-30%) and Early

Paleozoic (0-10%) populations (Figure 4.16). A discordance filter of 10/-15% is set to ensure that all age groups were included, and a total of 1310/1729 analyses had a discordance within this filter (Figure 4.16).

Sample 20BREM08A was analyzed with a smaller spot size (19 µm vs. 26 µm) due to grain size and have therefore yielded a more inaccurate analysis compared to the other samples. The analytical difference has led to sample 20BREM08A showing a zircon age distribution that differs from the other samples (Figure 4.16). Where the Late Neoproterozoic zircons is completely absent from the analyses. However, if the analyses is presented with the 2S error instead of the 2SE, the age distribution resembles that of the other samples (Figure 4.14 and Figure 4.16). The difference between 2SE and 2S error are not as prominent on Mesoproterozoic and Archean zircons, as it is on the Neoproterozoic population (Figure 4.14). There is no apparent reason for the grain size difference, it could possibly be related to either lithological difference between the restites, degree of melting, or represent a sampling error during the selection of zircons.

Concordant analyses for all 5 restite samples is plotted in Figure 4.17 and show similar age distributions as the cumulative plots (Figure 4.16). There are three significant discordant trends all with a lower intercept at 480 ± 55 Ma, and upper intercepts at 1875 ± 100 Ma, 2707 ± 44 Ma, and 3202 ± 340 Ma (Figure 4.17).

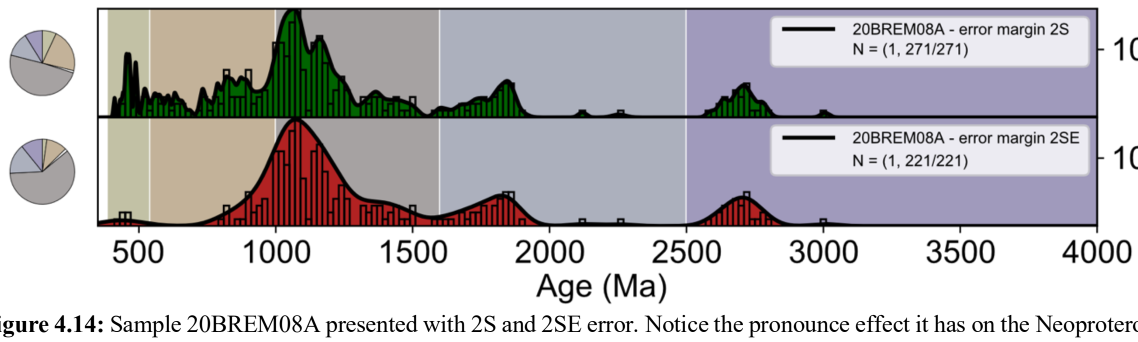

Figure 4.14: Sample 20BREM08A presented with 2S and 2SE error. Notice the pronounce effect it has on the Neoproterozoic population. The difference is not as apparent in Mesoproterozoic grains or older. Sample 20BREM08A were the only sample shot with 19 µm spot size.

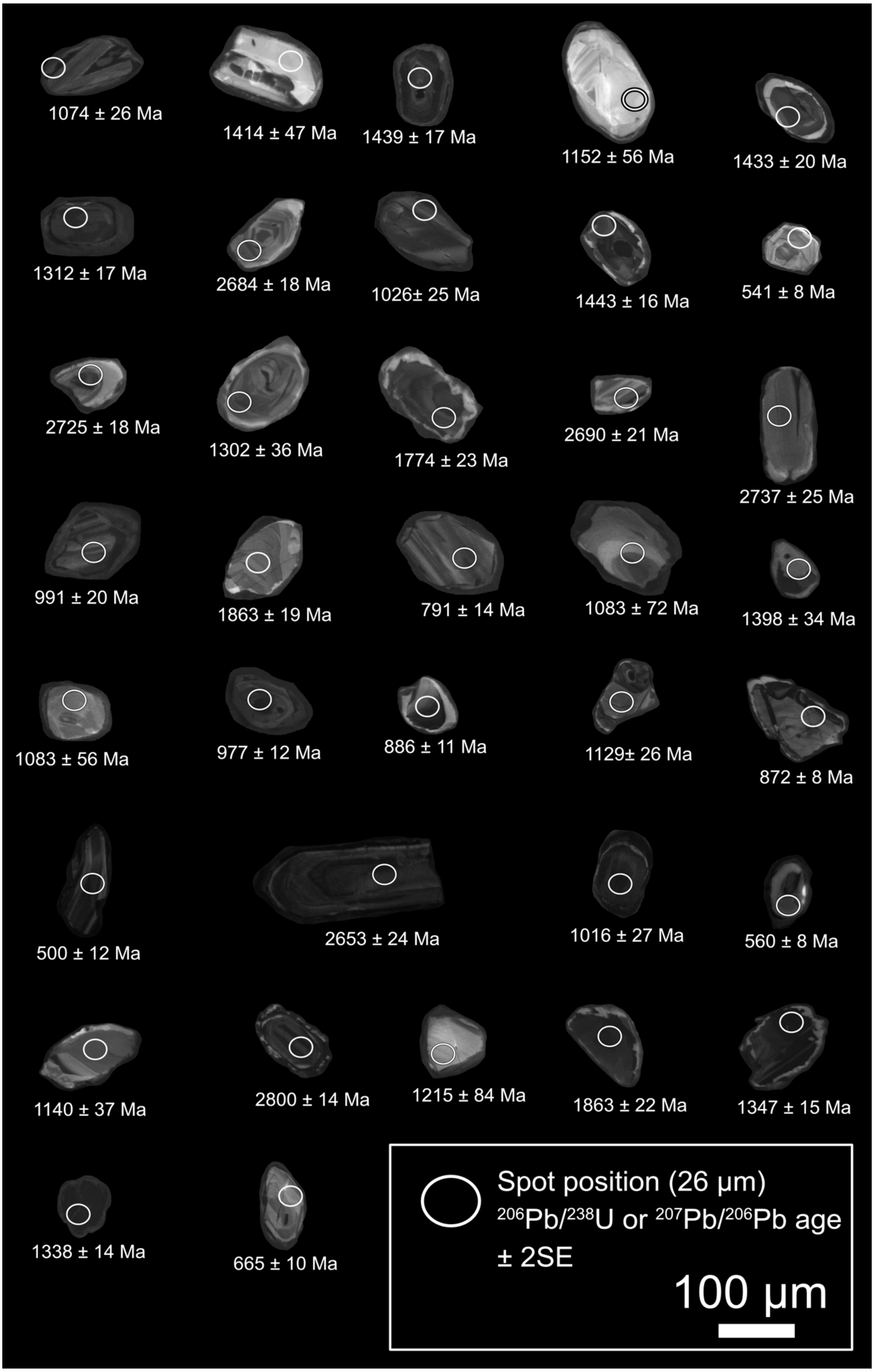

Figure 4.15: A representative selection of zircon grains from the analyzed restite samples shown in Figure 4.16, with coherent age and spot position.

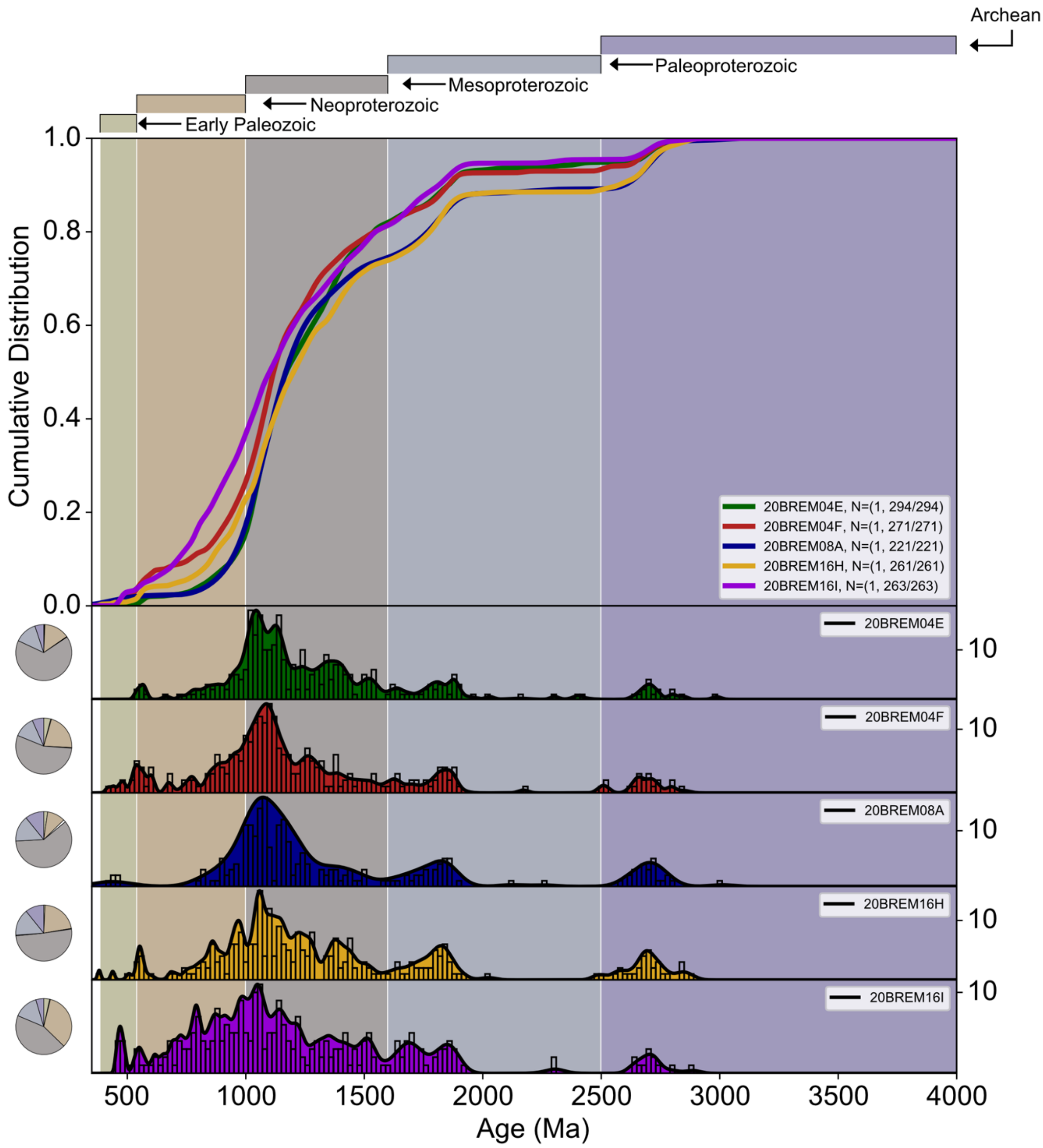

Figure 4.16: Cumulative distribution, probability density plots and associated pie charts shows the age distribution of restites 20BREM04E (green), 20BREM04F (red), 20BREM08A (blue), 20BREM16H (yellow) and 20BREM16I (purple). Notice the similarity between restites despite of different protolith, mica schist/sandstone (20BREM04E, 20BREM04F, 20BREM16I) and quartzite (20BREM08A, 20BREM16H). The apparent difference between the Neoproterozoic population of 20BREM08A and the other restites are related to analytical differences, see text for further explanation. Background coloring according to the chronostratigraphic table. Discordance is set to 10/-15 %. N = 1310.

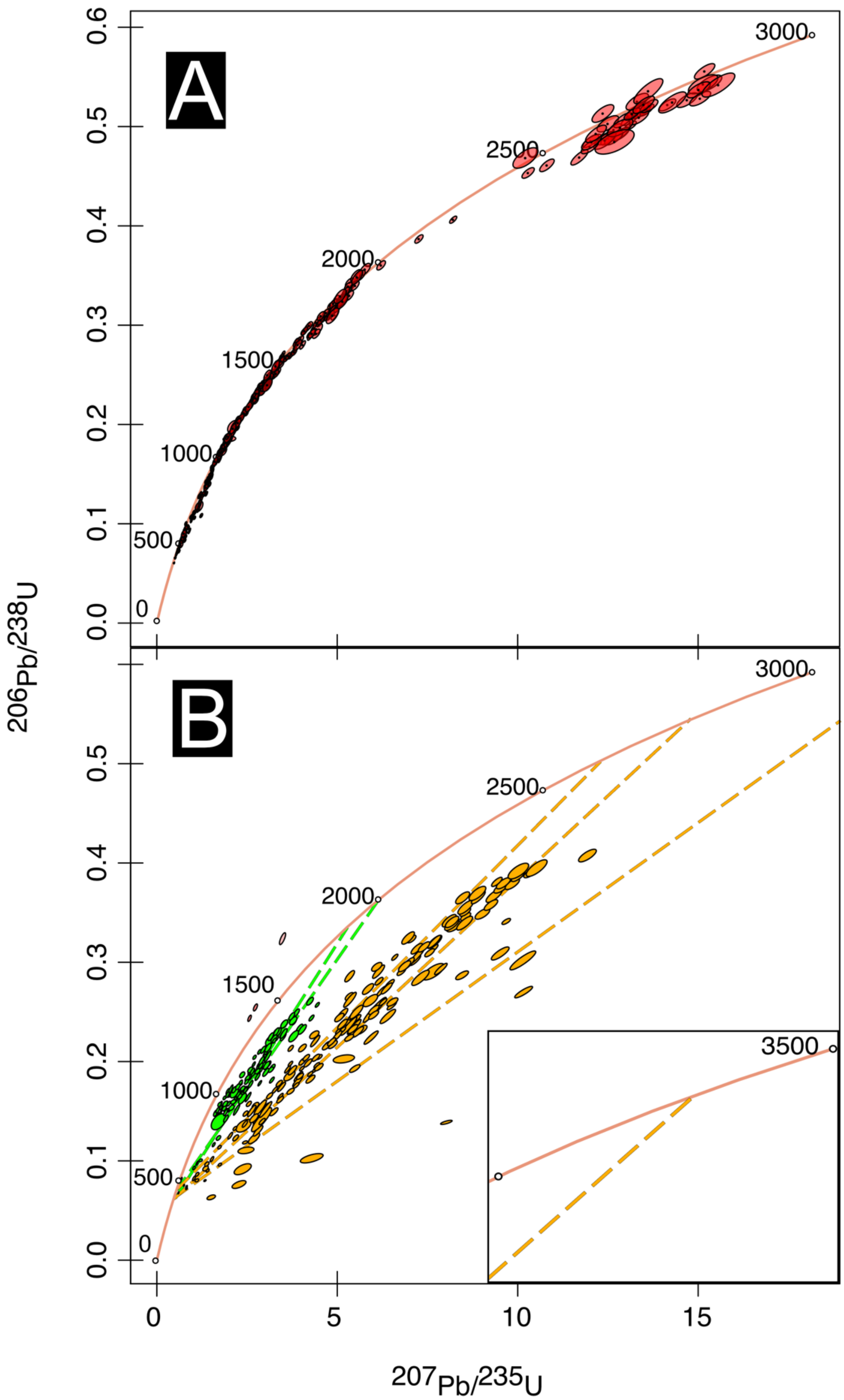

Figure 4.17: A) Concordant analyses from five analyzed restite samples (20BREM04E, 20BREM04F, 20BREM08A, 20BREM16H & 20BREM16I). All analyses ≤ 5 % discordant, and a total of 650/1226 analyses plot as concordant, according to the total amount of analyses shown in Figure 4.16. B) Analyses with a discordance ≥ 20%, N = 334. Three discordant trends with upper intercepts at 1875 ± 100 Ma, 2707 ± 44 Ma and 3220 ± 340 Ma, and lower intersecpt at 480 ± 55 Ma.

Detrital zircons in diatexites and metatexites

Detrital zircons from five dia- and metatexites from the BMC were analyzed (Figure 4.9). The zircons vary in size from 40-400 μm with most grains confined within 120-200 μm range (Figure 4.18). The largest (> 250 μm) and smallest (< 90 μm) grains constitute < 5% of the total zircon population. The shape of the crystals is mostly elongated or stubby, with the largest grains preferentially being elongated (Figure 4.18). Approximately 80% of the analyzed zircons are subangular to rounded, with minor amounts of angular grains. Oscillatory or sector zoning is present in *c.* 85% of the grains and 30% contain xenocrystic cores of varying size and age (Figure 4.18). There are overgrowths present at 40% of the grains. Most grains contain inclusions, while fracturing is mostly confined within the crystals that contain xenocrystic cores. A minor population of grains exhibit neither inclusion nor fractures.

The cumulative age distribution and PDP for the five analyzed dia- and metatexites show two different trends (Figure 4.19). The main trend, exhibited by 20BREM10B, 20BREM13, 20BREMS1, 20BREMS2, contain early Paleozoic zircons (2-5%), and significant Neoproterozoic (10-20%), Mesoproterozoic (40-60%), Paleoproterozoic (20-30%) and Archean (~20%) zircon populations (Figure 4.19). 20BREM15E contains major Archean (50%) and Paleo-proterozoic (40%) zircon populations, with the Mesoproterozoic only constituting ~10% of the analyzed grains. Neoproterozoic and early Paleozoic grains are absent from 20BREM15E, only constituting ~2% of the analyzed grains (Figure 4.19).

There is no apparent difference in grain size, shape, or form between the five analyzed samples. The difference in age distribution could be related to either sampling location, the ratio of melanosome/leucosome, or reflect a high content of paleosome, in which old undifferentiated sediments are preserved.

A discordance filter of 10/-15% is set to ensure that all age groups were included, and a total of 1514/1809 analyses had a discordance within this filter (Figure 4.19). Concordant analyses (discordance ≤ 5%) show similar age distributions as the cumulative plots (Figure 4.20). There are three significant discordant trends, all with a lower intercept at 480 ± 55 Ma, and upper intercepts at *c.* 3700 Ma, 3220 ± 340 Ma, 2769 ± 44, and 1875 ± 100 Ma (Figure 4.20). A concordant population of Archean age (~3700 Ma) is not present, however, 5 discordant grains of Eoarchean age are reported, with the oldest yielding an age of 3966 ± 43 Ma.

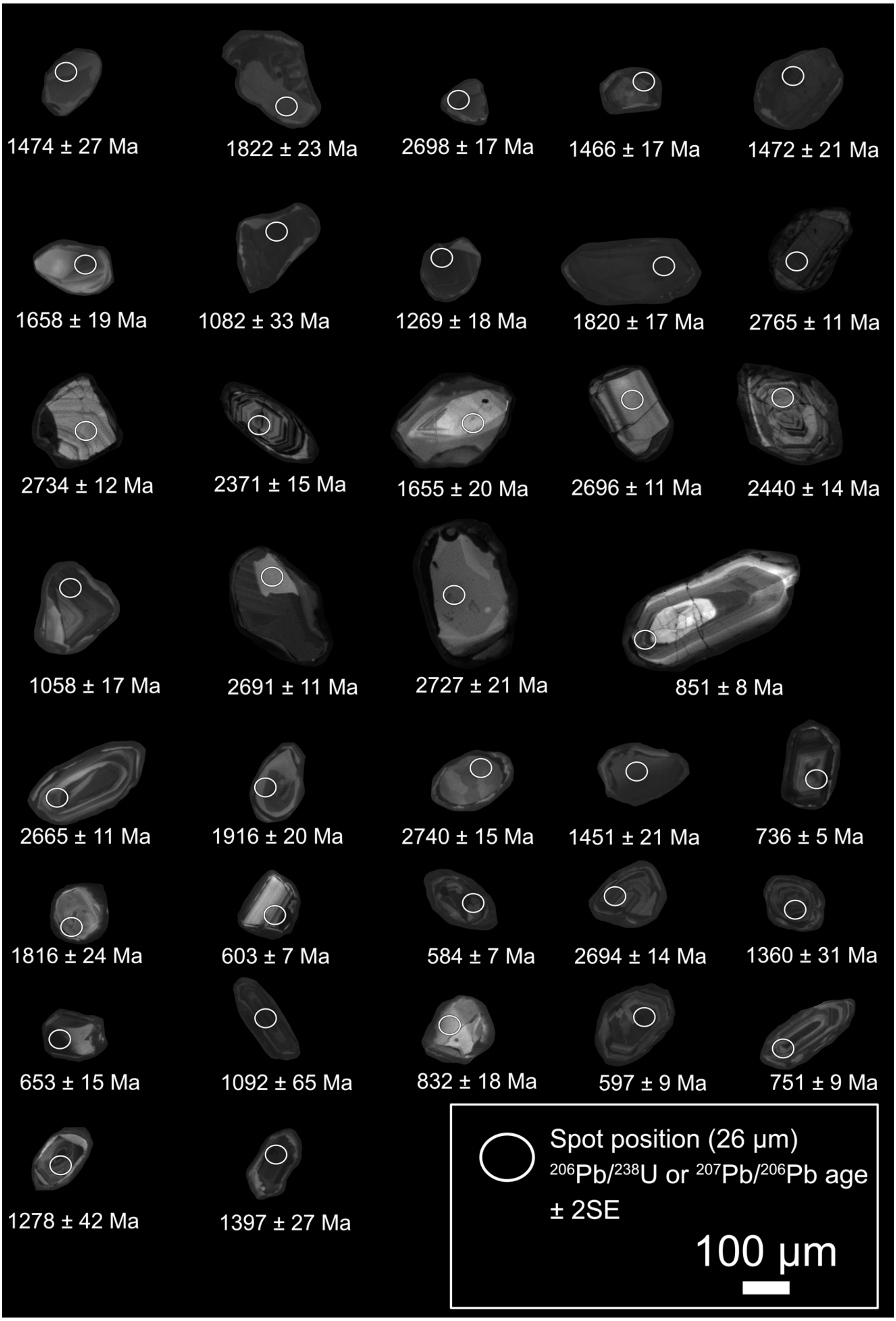

Figure 4.18: A representative selection of zircon grains from the analyzed diatexites and metatexites shown in Figure 4.19, with coherent age and spot position.

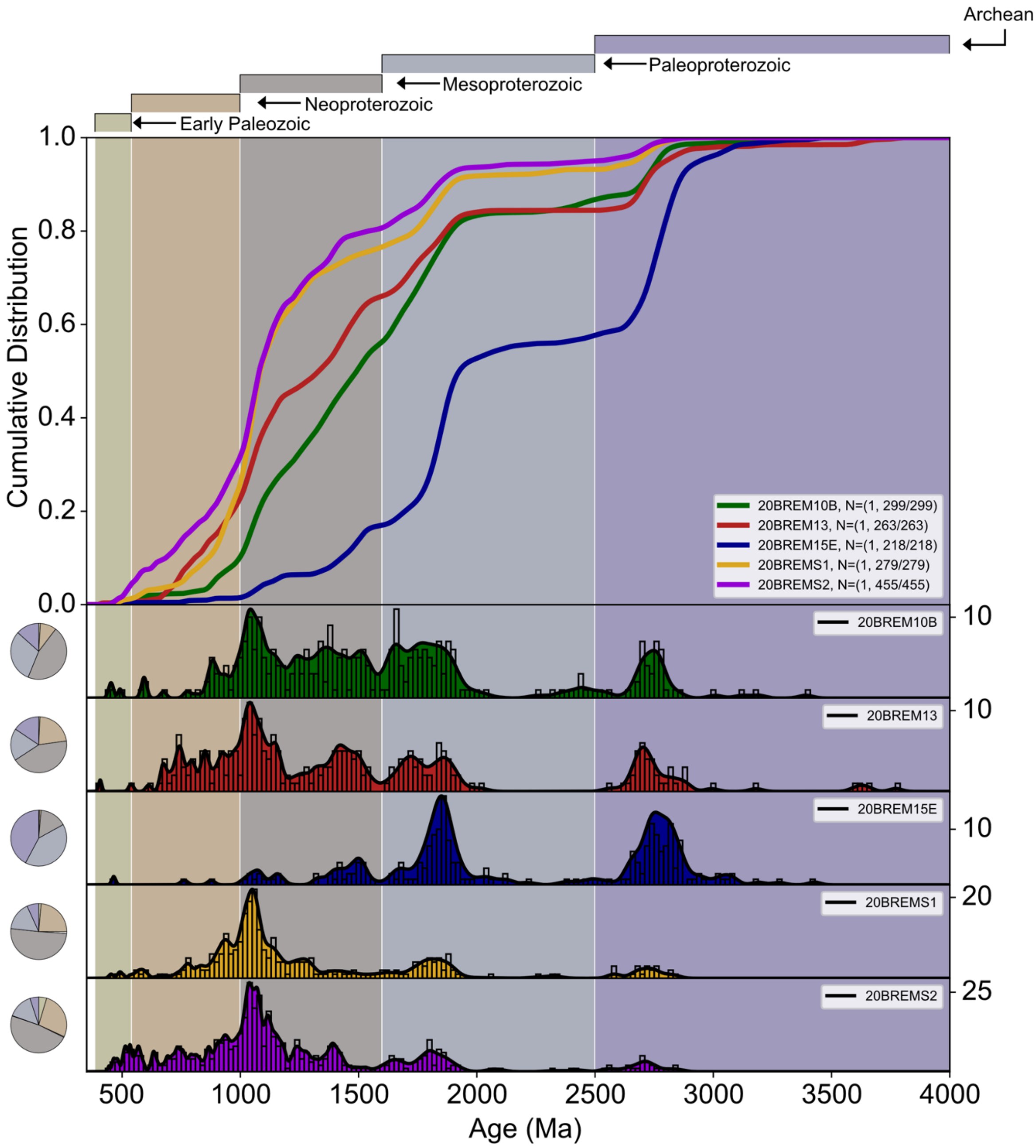

Figure 4.19: Cumulative distribution, probability density plots and associated pie charts shows the age distribution of diatexites and metatexites from within the Bremnes Migmatite Complex, samples: 20BREM10B (green), 20BREM13 (red), 20BREM15E (blue), 20BREMS1 (yellow) and 20BREMS2 (purple). Notice that 20BREM15E (blue) exhibits different age distribution related to sampling location, see text for further explanation. Divisions according to the chronostratigraphic table. Discordance filter is set to 10/-15 %. N = 1514.

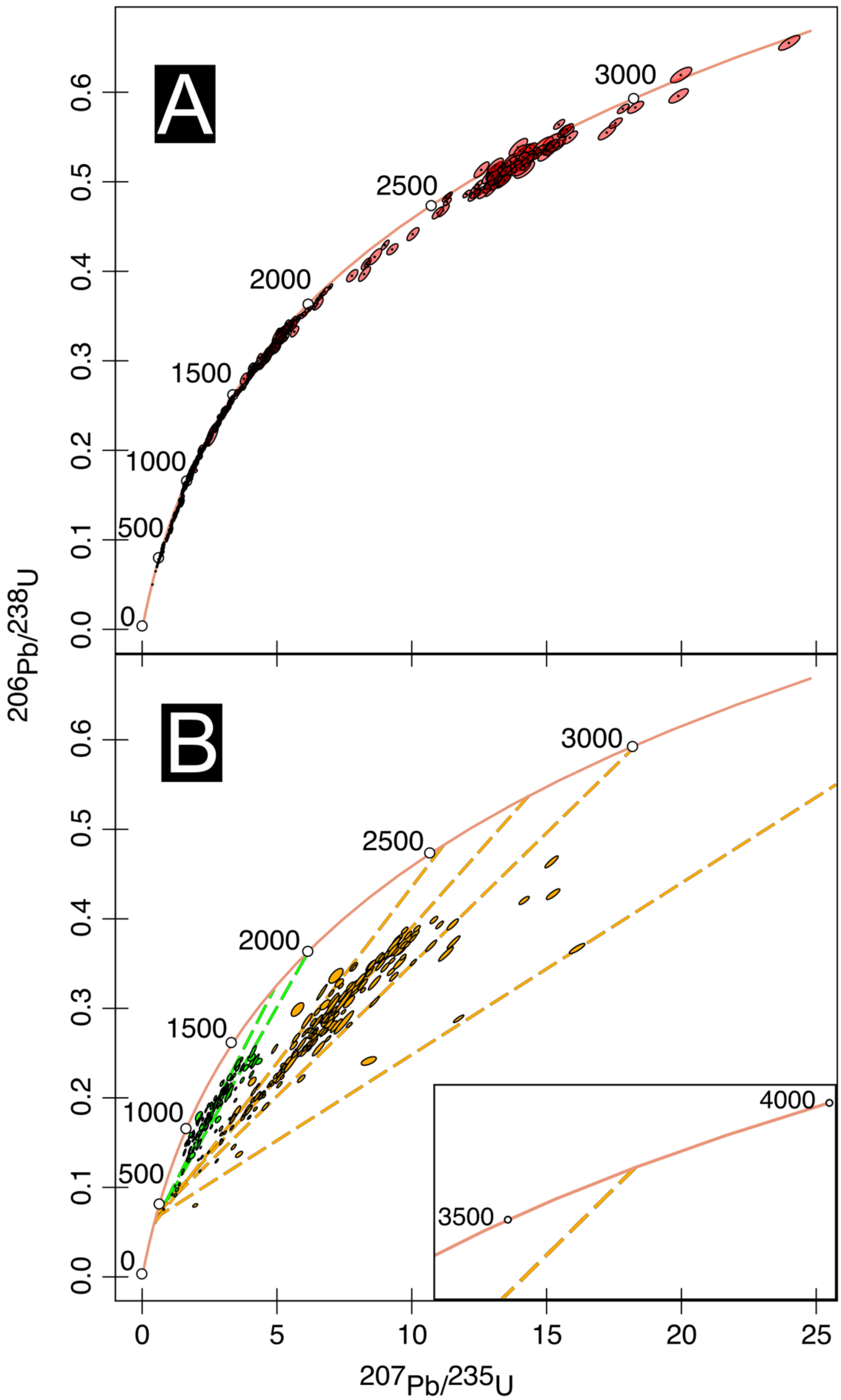

Figure 4.20: A) Concordant analyses from five analyzed dia- and metatexite samples (20BREM10B, 20BREM13, 20BREM15E, 20BREMS1 & 20BREMS2). All analyses ≤ 5 % discordant, and a total of 769/1349 analyses plot as concordant, according to the total amount of analyses shown in Figure 5.19. B) Several discordant trends with upper intercepts at 1875 ± 100 Ma, 2769 ± 44 Ma, 3220 ± 340 Ma and ~3700 Ma, with lower intercept at 480 ± 55 Ma. A total of 258 grains plots with a discordance of ≥ 20%.

5 Discussion

Following is a description of the trace-element patterns exhibited by the diatexites, metatexites, and restites of the BMC, and the adjacent appinites and gabbros of the Vardafjell Gabbro. Based on the geochemistry, geochronology, and relative age between the units, a temporal evolution of the study area is suggested. The detrital zircon data from the BMC and other units of the Lower Ordovician ophiolitic terrane (the WKIC, the Vikafjord Group, and the Mundheim Group) is compared with sedimentary successions associated with both the Laurentian and Baltic margin. By comparing the provenance data and geochemical analyses from the BMC with possible source regions, the origin for the continental component is properly constrained. Combined from this an evolutionary model for the migmatite complex is suggested.

5.1 Trace-element patterns and temporal evolution

Diatexites and migmatites

The trace-element patterns for the diatexites and metatexites form two trends (Figure 4.12 and Figure 4.13). The enriched trend is made up of samples collected evenly across the BMC, while the second less enriched trend is constituted by three samples collected adjacent to an appinite exposure (Figure 4.9). The samples collected in proximity of the appinite differ significantly in their major-element composition, suggesting that the trace-element geochemistry was not inherited from their source, but rather altered at a later stage. This is supported by the other samples of dia- and metatexites, which show the same trends regardless of major-element composition. The trace-element patterns of the dia- and metatexites resemble that of the average shale, with slightly lower values for the HREE (Figure 5.1) (Piper, 1974; Gromet *et al.*, 1984). The lower HREE values could be related to the partial melted nature of the migmatite in which the compatible HREE prefer to accumulate in the material that did not melt (restites). This combined with the presence of garnet within both the partial melted material and the restites could explain the lower content of HREE in the dia- and metatexites and the higher HREE content in the restites (Figure 4.12). Garnet are in areas of high-grade metamorphism and anatexis interpreted to act as a sink for the HREE (Taylor *et al.*, 2015), and are recognized within several of the restites, and samples of dia- and metatexites. The similarities between the trace-element patterns of the average shale and the BMC, suggest that the continental component of the migmatite complex had a composition close to that of the average shale (Figure 5.1).

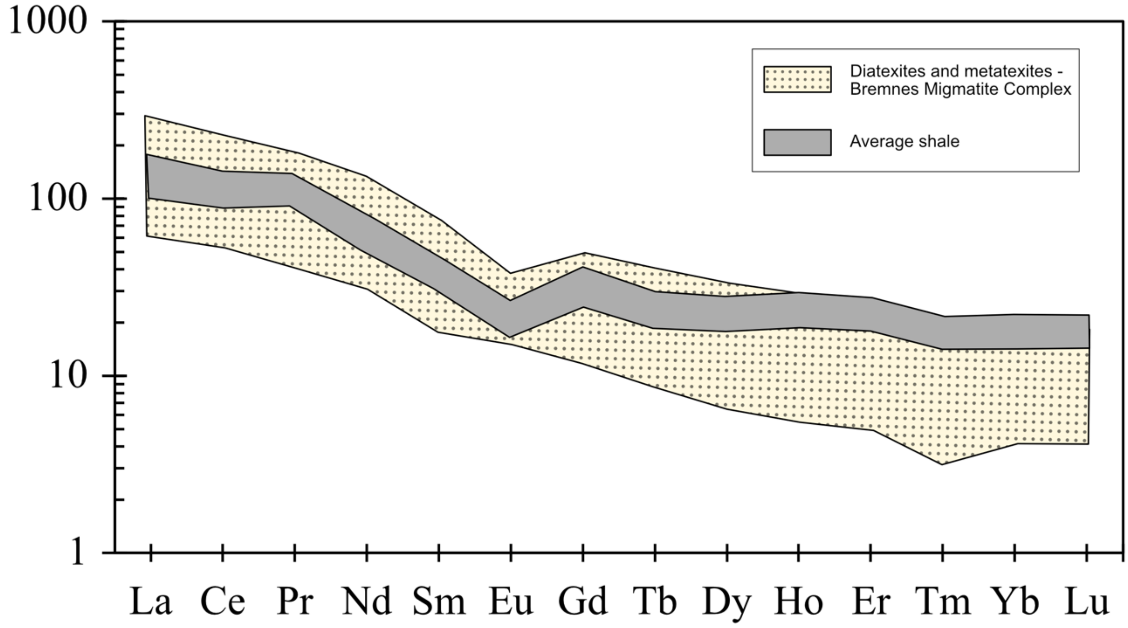

Figure 5.1: Chondrite normalized REE-patterns for the Bremnes Migmatite Complex and the average shale. The analyses from the migmatite complex overlaps with that of the average shale, suggesting that the sedimentary component of the BMC had a composition close to that of the average shale. The difference in HREE is most likely related to the partial melted nature of the migmatite complex, see text for further explanation. Normalized to the chondritic values presented by Taylor and McLennan (1985). Average shale values from Piper (1974) and Gromet *et al.* (1984).

Restites

The trace-element patterns for restites collected within the BMC show two distinctive trends (Figure 4.12 and Figure 4.13). The variation in the trace-element pattern is apparent in restites collected adjacent to each other, suggesting that the trace-element composition was inherited from the source and not altered at a later stage (Figure 4.9). The quartzites and quartz-felspathic restites that constitutes the less enriched trend all show positive Eu anomalies, while the mica-schists and quartz-felspathic restite of the enriched trend show negative Eu anomalies. It seems reasonable to suggest that the Eu anomalies exhibited by the restites are related to the maturity of the source (sediments). The immature sediments contain plagioclase and therefore show positive Eu anomalies, while in the mature sediments the plagioclase is weathered and consequently show negative Eu anomalies.

Vardafjell Gabbro

The Vardafjell Gabbro shows trace-element patterns that are indicate of their calc-alkaline origin (Figure 4.12). The trends shown by these gabbroic rocks are comparable to the calc-alkaline Siggjo Complex on Bømlo, and similar calc-alkaline gabbros found on Karmøy (Pedersen and Dunning, 1997). The difference between the trace-elements patterns from the Vardafjell Gabbro, the BMC, and the appinites suggest that the units developed from distinctively different sources.

Appinites

The level of enrichment seen in the appinites suggest that these rocks cannot have been derived from the exact same melts as the other rocks exposed in relation to the BMC (Figure 4.12 and Figure 4.13). In general terms appinites are suggested to develop whenever mafic magma becomes anomalously enriched in water, mostly in relation with subduction zone environments (Murphy, 2013). In regions were the tectonic setting is well constrained, appinites are believed to develop very soon after the cessation of subduction, either by terrane or continental collision, or by ridge-trench collision (Murphy, 2013, and the references therein). According to Murphy (2013), several textures within appinites indicates that the magma had a high volatile content. The appearance of amphibole as both phenocrysts and in matrix, are one of these textures, and are recognized within the BMC (section 4.1). The presence of amphibole suggests that the appinites formed from a magma that had a sufficiently high content of water and could explain the high level of enrichment seen in the trace-element patterns. Based on the intrusive relations between the different rocks associated with the BMC, it is reasonable to suggest that the appinites developed in relation to the Early Ordovician ophiolitic terrane of SW Norway. Appinites have not been reported from other localities within the ophiolitic terrane, but major appinitic bodies are associated with the Bindal Batholith (Barnes *et al.*, 2003), located further north in the Scandinavian Caledonides, and the Scottish Caledonides (Murphy, 2013). The appinites in these areas are somewhat younger than those associated with the BMC; 456 ± 8 Ma (Bindal Batholith; Barnes *et al.*, 2003), 422 ± 3 Ma and 429 ± 3 Ma (Scottish Caledonides; Rogers and Dunning, 1991).

Appinites in general have compositions ranging from high-K calc-alkalic, shoshonitic, to low-K calc-alkalic (Murphy, 2013). The appinites at Bømlo show trace-element patterns that are similar to the calc-alkaline magmas of the Siggjo Complex and the Vardafjell Gabbro. In the

Caledonian Orogen, appinites are often recognized in relation with mafic shoshonitic magmas (Murphy, 2013, and references therein). No shoshonitic magmas have been reported from the Bømlo area, but have been recognized in relation to the Karmøy Ophiolite Complex (Sivertsen, 1992; Pedersen and Dunning, 1997). Pedersen and Dunning (1997) described a complex interrelation between the calc-alkaline and alkaline magmas, and the highly alkaline shoshonitic magmas, of the SW Norway ophiolitic terrane. Considering the close relation between the Karmøy Ophiolite Complex and the ophiolite and island arc sequences on Bømlo, it seems reasonable to suggest that the appinites may be related to the shoshonites. However, it was suggested that the shoshonites represent the last stage in the development of the ophiolitic terrane, and post-date both the calc-alkaline magmas and the development of the BMC. This contradicts the relative age of the appinites, which suggest that the appinites intrude prior to the intrusion of the Vardafjell Gabbro (472 ± 2 Ma; Pedersen and Dunning, 1997).

Temporal evolution

There are intrusive contacts between all rock units adjacent to the BMC (Figure 5.2). The Rolvsnes Granite (468 ± 3 Ma; Scheiber *et al.*, 2016) are the youngest unit within the area and represent the latest stage of the Sunnhordland Batholith (Andersen and Jansen, 1987). The granitoids from the Rolvsnes Granite intrude both the BMC (477 ± 7 Ma), the appinites, and the Vardafjell Gabbro (472 ± 2 Ma), suggesting that it post-dates all other units (Figure 5.2). From the age relations it is clear that the intrusion of the Vardafjell Gabbro post-date the migmatization of the BMC, and based on previous mapping the gabbroic body appear to crosscut the appinites, suggesting that the Vardafjell Gabbro post-dates both (Figure 4.1) (Nielsen, 1990). The appinites are mostly located in the boundary between the BMC and the adjacent rock units and show an intrusive relation with the migmatite complex (section 4.1) (Figure 4.4). The age relations of the study area suggests that the appinites intrude in between the migmatization of the BMC (477 ± 7 Ma) and the intrusion of the Vardafjell Gabbro (472 ± 2 Ma). This documents that the BMC (477 ± 7 Ma) are the oldest unit within the area, and that the other units intrude accordingly, appinites (of unknown age), Vardafjell Gabbro (472 ± 2 Ma; Pedersen and Dunning, 1997), and Rolvsnes Granite (468 ± 3 Ma; Scheiber *et al.*, 2016) (Figure 5.2).

The similarities in geochemistry and the age relations between the appinites and the Vardafjell Gabbro, combined with the complex interrelation between the calc-alkaline, alkaline magmas and the highly alkaline shoshonitic magmas of the Early Ordovician ophiolitic terrane of SW Norway, suggests that the appinites may be related to an early stage in the development of the Vardafjell Gabbro. It seems likely that the appinites developed at a time when sufficient amounts of water were present within the mantle derived melts.

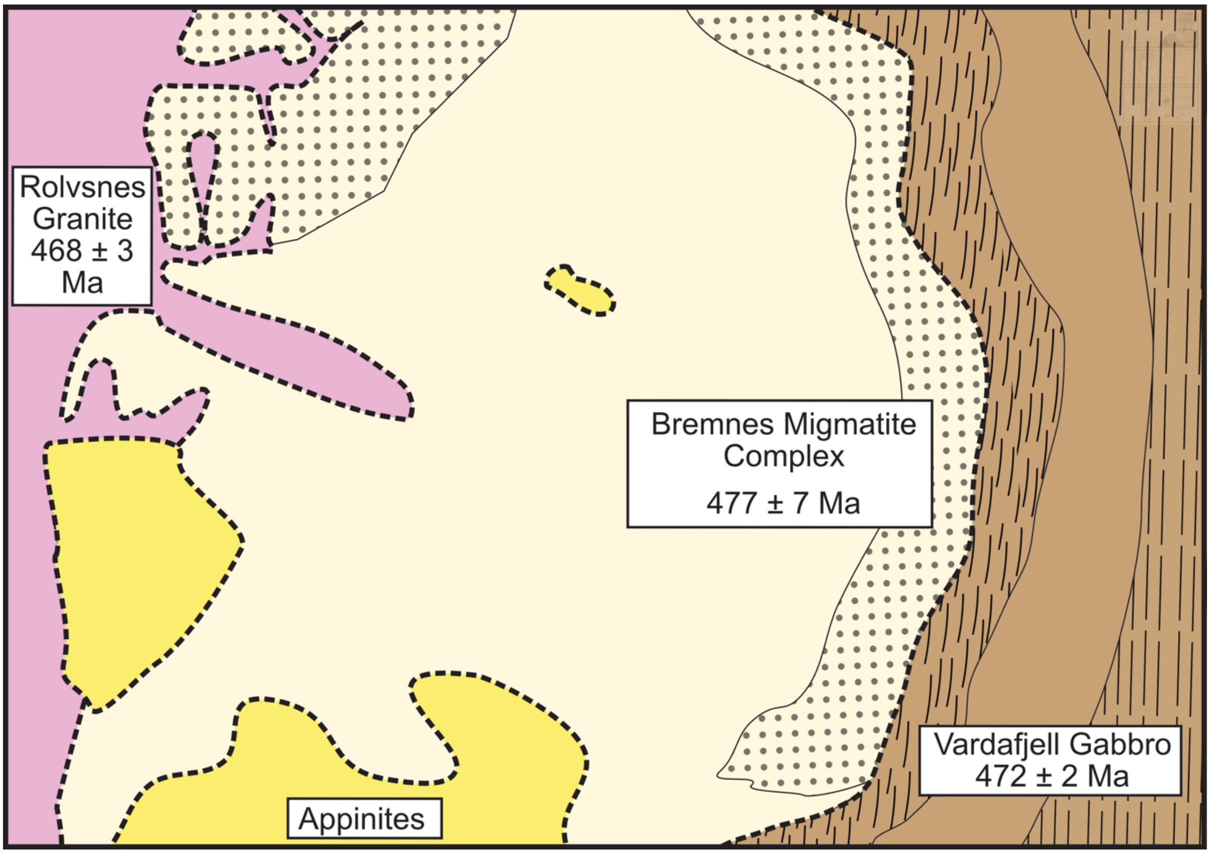

Figure 5.2: Schematic illustration of the age relations within the Bremnes Migmatite Complex. The migmatite complex was migmatized at 477 ± 7 Ma, intruded by appinites related to an early phase of the Vardafjell Gabbro, which intruded at 472 ± 2 Ma. Further, as the Sunnhordland Batholith evolved, the Rolvsnes Granite intrude at 468 ± 3 Ma. See text for further explanation.

5.2 Geochronology

Provenance of the Baltic margin

Shelf and distal shelf sedimentary sequences that were deposited on the pre-Caledonian passive continental margin of Baltica are today exposed within the Lower Allochthons and the (para-) autochthon of the Caledonides of SW Norway (Fonneland, 2002; Bingen *et al.*, 2005B; Slama and Pedersen, 2015). The (para-) autochthonous successions (Hardangervidda Group) comprise Cambrian to Lower Ordovician sandstones and phyllites (Figure 5.3). The Lower Allochthon contains Ordovician to Lower Silurian sandstones and phyllites, and phyllites also predominate within the décollement zone. Sandstones form a part of the Sundvollen Formation and represent the Caledonian foreland. The Sundvollen Formation is suggested to be derived almost exclusively from detritus related to the Jotun Nappe Complex of the Lower Allochthon (Slama and Pedersen, 2015, and references therein).

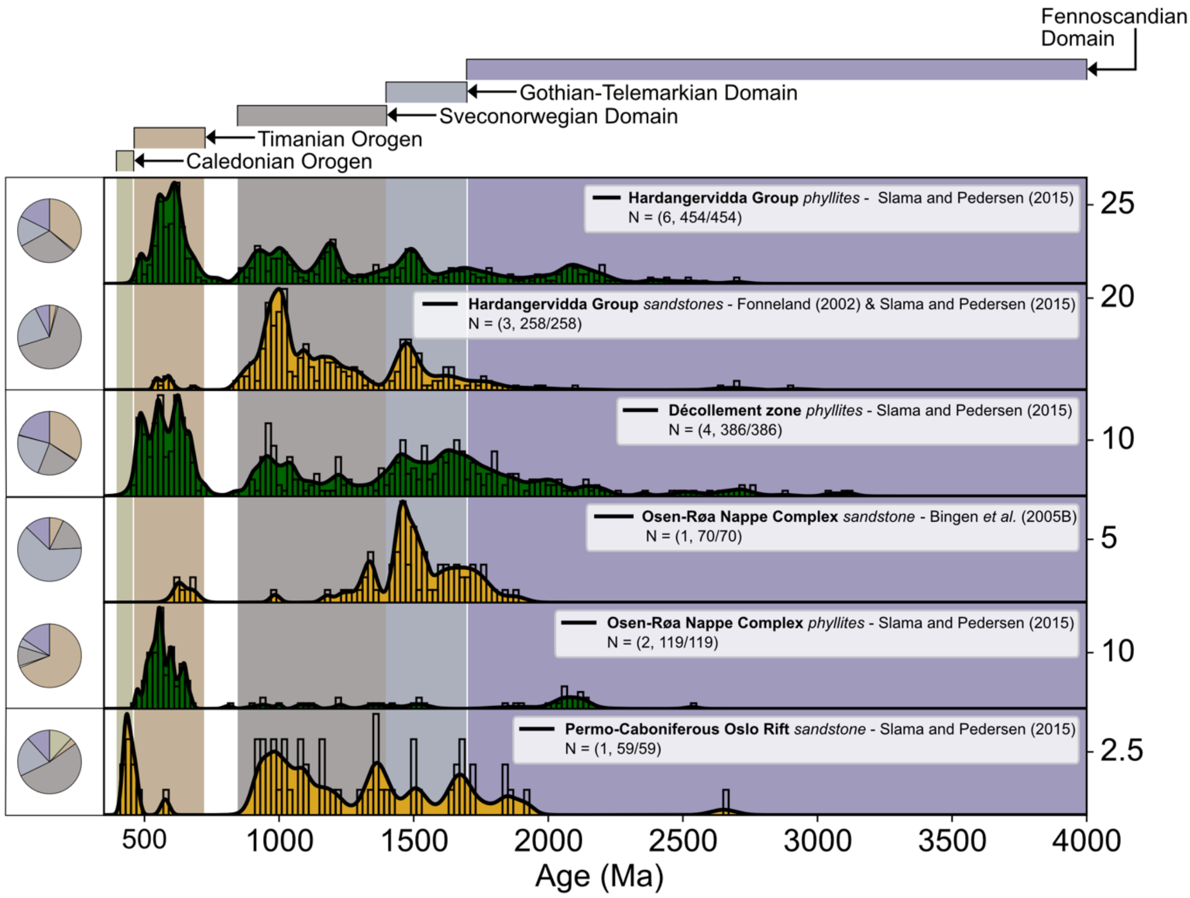

Figure 5.3: The provenance signature of (para-) autochthonous and allochthonous sedimentary successions (green = phyllites, yellow = sandstones) associated with the Baltic margin. Notice, that the sandstones contain similarly aged zircons despite being sampled at several locations. The same is applicable for the phyllites, which contain similarly aged zircons regardless of sampling location. This is related that they probably formed with input from the same sources. All presented ages are derived from U-Pb analyses (zircons), either as 207/206 Pb or 238 U /206 Pb, with a discordance filter of 10/-15%. Background coloring according to source region.

A late Neoproterozoic to Early Paleozoic zircon population (800-500 Ma) that are present in these shelf deposits likely represents remnant detritus from the Timanian orogeny (Figure 5.3) (Slama and Pedersen, 2015). Mesoproterozoic zircons are related to the Sveconorwegian domain, which represents one of many orogens at this time, an equivalent to the Grenville orogen in Laurentia (Bingen *et al.*, 2005A). Late Paleoproterozoic to Early Mesoproterozoic zircons (1700-1400 Ma) are related to the Gothian and Telemarkian orogenic events, with arc magmatism, sedimentation and accretion in an subduction zone environment on the accretionary margin of Fennoscandia (Bingen *et al.*, 2005A; Roberts and Slagstad, 2015; Wiest *et al.*, 2018). Zircons of Proterozoic to Archean age do most likely represent detritus from the Fennoscandian domain (Slama and Pedersen, 2015). The Early Paleozoic population, which is particularly distinct in the Silurian sandstone, is clearly derived from the Caledonian orogen (Figure 5.3).

The difference in age distribution of zircons between the fine-grained phyllites and coarse-grained sandstones, of the (para-) autochthonous and allochthonous rocks, indicates that the sandstones were derived from a local source within the Sveconorwegian and/or Gothian-Telemarkian domain, with minor input from Timanian and Fennoscandian sources (Figure 5.3) (Slama and Pedersen, 2015). The phyllites exhibit major input from Timanian and Fennoscandian domains, which at that time were located *c.* 2000 km from the Baltic continental margin. Slama and Pedersen (2015) suggested an extensive drainage pattern across the whole northeastern fringe of Baltica to the southwestern passive margin as the potential source for these zircons.

Provenance of the Laurentian margin

The sedimentary sequences associated with the Laurentian margin represents time-equivalent successions deposited from Mid-Neoproterozoic (*c.* 700 Ma) to Early Paleozoic (*c.* 490 Ma) during the breakup of the Rodinian Supercontinent and the subsequent opening of the Iapetus Ocean. These sequences are now exposed in Scotland, Greenland, and Newfoundland (Figure 5.4) (Cawood and Nemchin, 2001; Cawood *et al.*, 2003, 2007, 2014; Slama *et al.*, 2011).

The Dalradian Supergroup is exposed in Scotland, Ireland and Shetland, and consists of marine siliciclastic deposits with varying proportions of carbonate and volcanic rocks, with an upper depositional age at *c.* 520 Ma that is constrained by Early Cambrian fauna (Figure 5.4) (Cawood *et al.*, 2003, and references therein). The Ardvreck Group is time-equivalent to the Dalradian Supergroup of quartzites and sandstones, suggested to represent respectively shallower and deeper parts of the same passive-margin basin (Cawood *et al.*, 2007, and references therein). The Moine Supergroup is a clastic-dominated sequence that accumulated

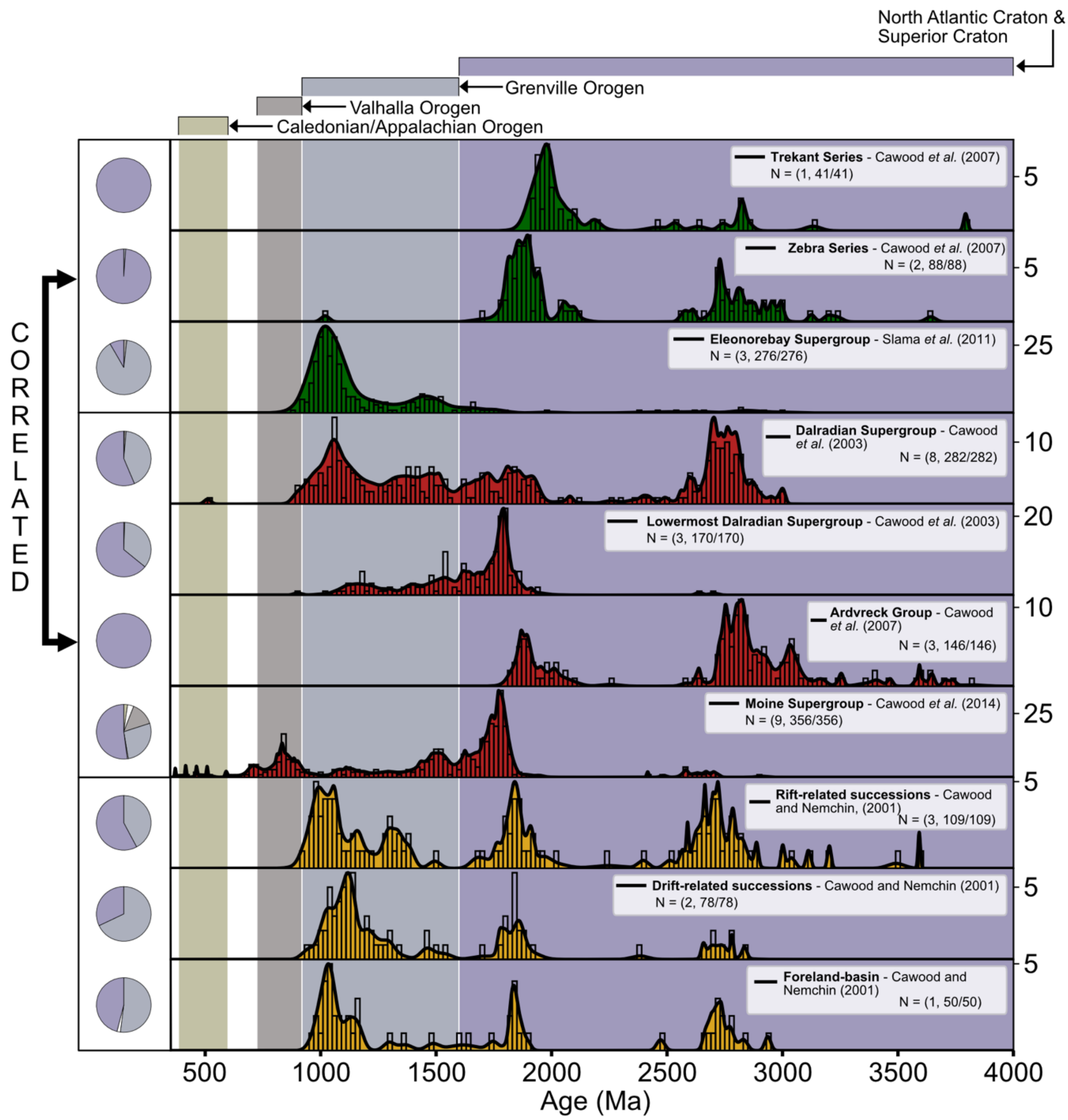

Figure 5.4: The provenance signature of sedimentary successions associated with the Laurentian margin. All presented sedimentary successions were deposited at or peripheral to the Laurentian continental margin in Mid-Neoproterozoic (*c.* 700 Ma) to Early Paleozoic (*c.* 520 Ma). Coloring according to area of origin, green = Greenland, red = Scotland, yellow = Newfoundland. All presented ages are derived from U-Pb analyses (zircons), either as 207/206 Pb or 238 U/206 Pb, with a discordance filter of 10/-15%. Background coloring according to source region.

early in the development of the Laurentian margin (Early Neoproterozoic) (Figure 5.4). This is unconformably overlain by the Dalradian Supergroup (Cawood *et al.*, 2014).

The East-Greenland Neoproterozoic sandstones of the Eleonore Bay Supergroup represent Neoproterozoic cover sequences deposited between 840-540 Ma in a marginal basin, possibly time-equivalent to the Dalradian Supergroup in Scotland (Figure 5.4) (Sønderholm and Tirsgaard, 1993; Slama *et al.*, 2011). The Trekant Series represents Mesoproterozoic successions of sandstones, siltstones and conglomerates, unconformably overlain by the quartzites, mudstones and sandstones of the Zebra Series (Cawood *et al*, 2007). The shallow-marine deposits from the Zebra Series are correlated with the Ardvreck Group in the Scottish Caledonides (Figure 5.4) (Higgins *et al.*, 2004).

The sedimentary sequences presented from the Newfoundland Appalachians are foreland-basin and rift-drift-related sequences deposited in the Neoproterozoic to early Paleozoic time and are representative for the upper Laurentian margin at that time (Figure 5.4) (Cawood and Nemchin, 2001). These rift-drift and foreland basin successions consist of quartzite, arkosic sandstone, siltstone, and shales, deposited in relation to the opening and closing of the Iapetus Ocean. These are compared with time-equivalent strata from Scotland and Greenland (Cawood *et al.*, 2003, 2007).

The Archean zircon populations are probably derived from the Superior and/or North Atlantic craton. The distinctive 2900-2600 Ma population relates to the main accretional event between the two cratons (Hoffman, 1988; Hoffman *et al.*, 1989; Cawood *et al.*, 2007). The Paleoproterozoic zircons (2100-1800 Ma) are probably related to the assembly of the North Atlantic and Superior craton, and the subsequent formation of the New Quebec and Torngat orogen, Nagssugtoqidian belt and Ketilidian-Makkovik province (Cawood *et al.*, 2007, and references therein). Zircons of Paleo- and Eoarchean ages are suggested to be derived from the West-Greenland to easterly Labrador part of the North Atlantic craton (Nutman *et al*., 2002). Zircon populations between 1650-1500 Ma could be derived from the Labrador region, possibly the Trans-Labradorian batholith, the Pinware arc, and/or Mesoproterozoic Grenville (Figure 5.4) (Gower, 1996). Mesoproterozoic to earliest Neoproterozoic grains represents detritus from the Grenville orogen, and the final assembly of the Rodinian Supercontinent (Rivers, 1997; Cawood *et al.*, 2003). Neoproterozoic zircons are related to the Valhalla orogen, which developed along the margin of an assembled Rodinia, and to the Knoydartian tectonothermal events (Cawood *et al.*, 2014). Early Paleozoic grains are almost absent indicating little input from the Appalachian/Caledonian orogen, except for certain zircons at *c.* 550 Ma, which suggests input from magmatic activity related to the opening of the Iapetus Ocean (Cawood *et al*., 2007).

Laurentian or Baltic affinity in the provenance of the Bremnes Migmatite Complex

The BMC show an age distribution dominated by Archean (*c.* 2700 Ma), Paleoproterozoic (*c.* 1800), and Mesoproterozoic (*c.* 1100) zircons, with minor Neoproterozoic (900-600 Ma) and Early Paleozoic (*c.* 550 Ma) populations. Of the ten analyzed samples, one exhibit a significantly different age distribution and are not presented together with the other nine samples, which are combined and exhibits the average age distribution of the migmatite complex (section 4.3 for individual analyses). The BMC lacks the prominent Neoproterozoic zircon population of the (para-) autochthonous and allochthonous phyllites associated with the Baltic margin but compares well with the Mesoproterozoic population in the sandstones derived from the same stratigraphic sequence (Figure 5.5). The BMC exhibits prominent Paleoproterozoic (1900-1800 Ma) and Archean (2800-2600 Ma) zircon populations, which is

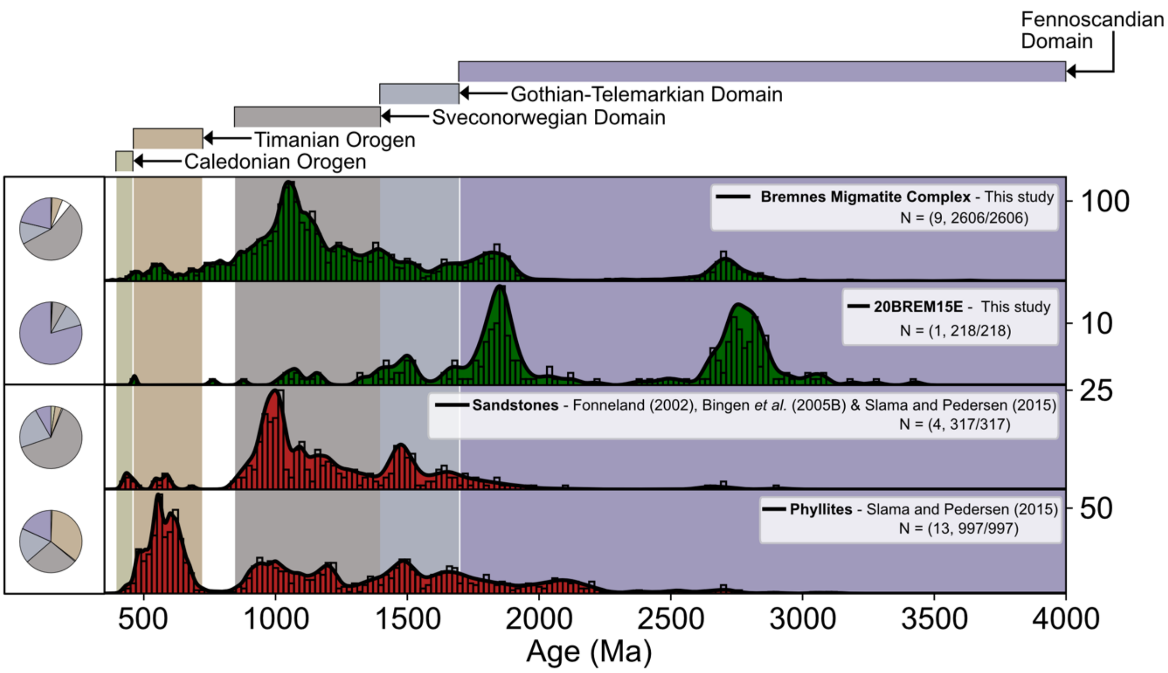

Figure 5.5: Comparison of the zircon provenance exhibited by the Bremnes Migmatite Complex (green) and sedimentary sequences associated with the Baltic margin (red). The sedimentary succession associated with the Baltic margin are plotted individually in Figure 5.3. In this plot, the successions are grouped according to their lithology. One sample from the BMC exhibits a significantly different zircon age distribution compared to the other samples, and therefore plotted separately. All presented ages are derived from U-Pb analyses (zircons), either as 207/206 Pb or 238 U/206 Pb, with a discordance filter of 10/-15%. Background coloring according to source region for successions associated with the Baltic margin.

completely absent from the analyzed (para-) autochthonous and allochthonous units of Baltic origin but fits well with the sedimentary sequences associated with the Laurentian margin (Figure 5.6). The overall provenance of the BMC show similarities with sedimentary successions from both Scotland, Greenland, and Newfoundland, with prominent peaks in the Archean (2800-2600 Ma), Paleoproterozoic (1900-1800 Ma), and Mesoproterozoic (1200-1000 Ma). The Neoproterozoic to Early Paleozoic (> 900 Ma) zircon populations present in the BMC are not characteristic of the associated successions, with only the Moine Supergroup exhibiting similar zircon populations (Figure 5.6). With 80% of the analyzed zircons exhibiting

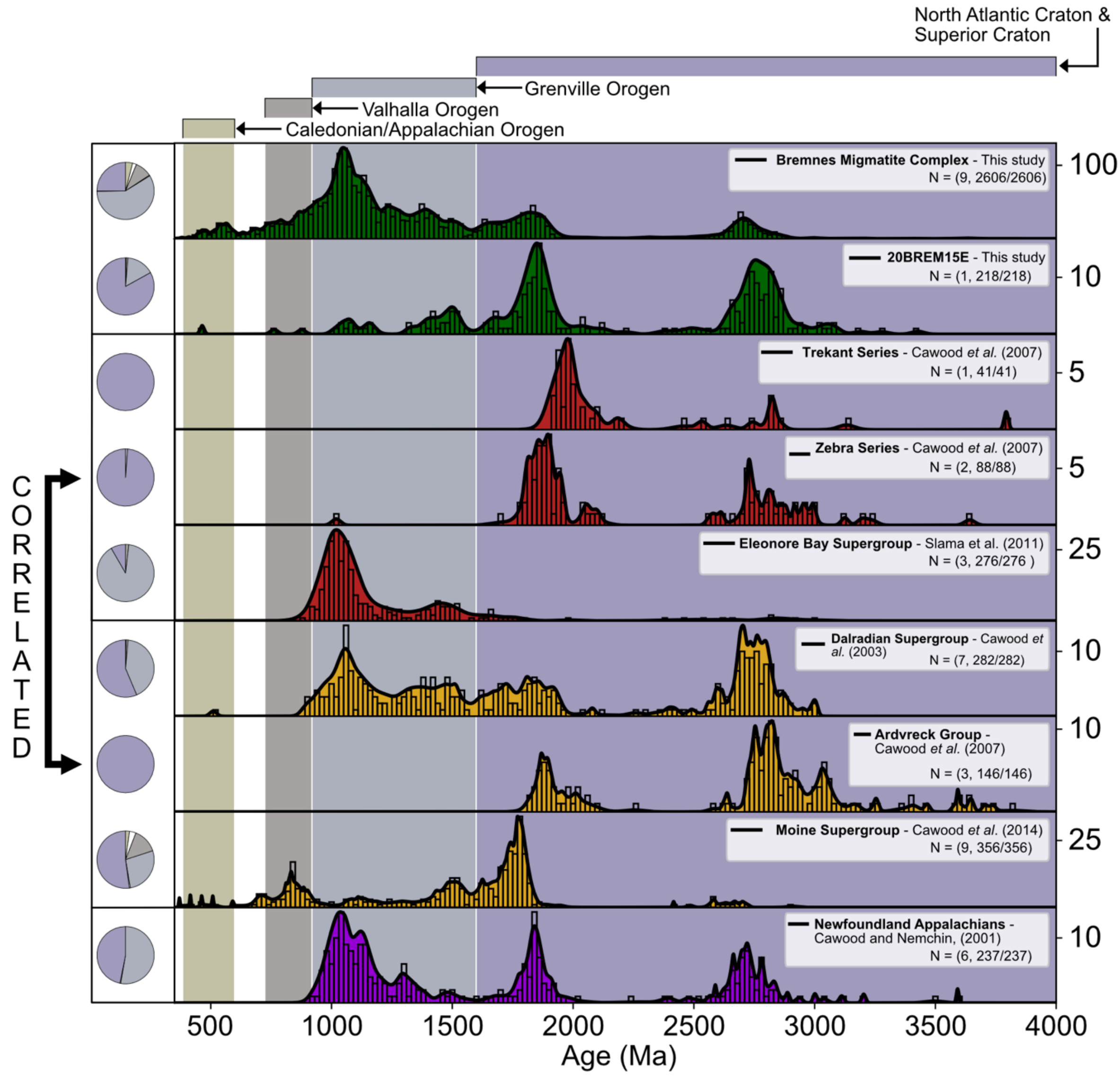

Figure 5.6: Comparison of the zircon age distribution exhibited by the Bremnes Migmatite Complex (green) and sedimentary sequences associated with the Laurentian margin. The migmatite complex show major similarities with the detrital zircon age distribution exhibited by the sedimentary successions associated with the Laurentian margin. Samples from Greenland (red), Scotland (yellow) and Newfoundland (purple). One sample (20BREM15E) from the BMC exhibits a significantly different provenance compared to the other samples, and therefore presented separately. All presented ages are derived from U-Pb analyses (zircons), either as 207/206 Pb or 238 U/206 Pb, with a discordance filter of 10/-15%. Background coloring according to the probable source region of the detrital zircons for the sedimentary succession associated with the Laurentian margin.

Paleoproterozoic ages or older ages, one of the analyzed samples (20BREM15E) shows no similarities with the presented sedimentary sequences from the Baltic margin (Figure 5.5). This sample exhibits striking similarities with the Zebra Series and Ardvreck Group from Greenland and Scotland, respectively (Figure 5.6). The data presented here indicates that the sediments involved in the formation of the BMC accumulated at or peripheral to the Laurentian margin, with limited to no input from the Baltic margin. Both the lack of Neoproterozoic populations in the BMC and the prominent Paleoproterozoic and Archean zircon populations are consistent with the derivation of the detritus from the Laurentian margin.

The Laurentian margin deposits in Greenland, Newfoundland, and Scotland

The comparison of detrital zircon data from the Laurentian margin indicates that the continental component involved in the formation of the BMC was sourced from or similarly as Mid-Neoproterozoic to Early Paleozoic sedimentary successions now exposed in Scotland, East Greenland, and Newfoundland rather than similar sedimentary succession from the Baltic margin. It seems most likely that the continental component was sourced from a sedimentary succession now exposed in Scotland, rather than Greenland or Newfoundland, as there has not been reported any Early Ordovician ophiolites and island arc complexes from the East Greenland Caledonides (Kalsbeek *et al.*, 2001, and the references therein). It seems reasonable to assume that if the BMC formed from a continental component sourced mainly in a sedimentary succession exposed in the East Greenland Caledonides, that similarly aged migmatites, ophiolites, and arc complexes would be present within the East Greenland Caledonides. In the Newfoundland Appalachians there are ophiolite complexes and island arc sequences of Early Ordovician age, similar to what is reported from the Early Ordovician ophiolitic terrane of SW Norway (Dunning and Krogh, 1986; Dunning and Pedersen, 1988). The detrital zircon age distribution exhibited by the adjacent rift-drift successions show similarities with the main trend of the BMC (Figure 5.6). There has, however, not been reported any succession from the Newfoundland Appalachians that are dominated by Archean and Paleoproterozoic zircons, similar to what is reported from the BMC. The lack of such sedimentary successions is suggested to be related to contrasting drainage patterns on the Laurentian margin at the time of deposition for these Neoproterozoic to Early Paleozoic successions (Cawood *et al.*, 2007). Therefore, it seems reasonable to suggest that the continental component of BMC cannot have been primarily sourced from the Newfoundland rift-drift sedimentary successions.

From the British Caledonides there is reported granitoids, migmatites and island arc lithologies of a Early Ordovician age, similar to the granitoids, migmatites, ophiolites and island arc complexes of the Early Ordovician ophiolitic terrane of SW Norway (Palin *et al.*, 2018, and references therein). The presence of time-equivalent units within the Scottish Caledonides combined with similarities in the geological history between the two terranes, make it reasonable to suggest that the continental component of the BMC, and several other units of the Early Ordovician ophiolitic terrane of SW Norway, could be sourced within a sedimentary succession now exposed in the British Caledonides.

The evolution of the Early Ordovician units within the British Caledonides

The Early Ordovician migmatites, S- and I-type granitoids exposed in the British Isles formed in relation to emplacement of an island arc on to the Laurentian continental margin, known as the Grampian Event (*c.* 490 – 465 Ma) (e.g. Chew *et al.*, 2007; Appleby *et al.*, 2010; Johnson *et al.*, 2015; Palin *et al.*, 2018). The magmatic history of the Grampian Event, with intrusions of boninitic lavas related to an immature island arc, formation of plagiogranites with influence of supracrustal material at 490 ± 3 Ma and 488 ± 2 Ma, and intrusion granitic and gabbroic rocks between 473 – 465 Ma and 475 – 470 Ma respectively (Chew *et al.,* 2007; Palin *et al.*, 2018, and references therein), fits well with the recorded history from the SW Norway ophiolite and island arc complexes (Dunning and Pedersen, 1988; Pedersen and Dunning, 1997). This may suggest that ophiolite and island arc sequences of the British Caledonides developed in the same island arc system as the time-equivalent sequence found in SW Norway. This is supported by similarities in isotope systematics (ε_{Nd}, $^{87}Sr/^{86}Sr$) and geochronology between S- and I-type granitoids, sedimentary successions, and migmatites exposed in SW Norway and on the British Isles (Hamnes, 1998; Kinny *et al.*, 1999; Fonneland, 2002; Chew *et al.*, 2007; Appleby *et al.*, 2010; Johnson *et al.*, 2015; Viken, 2017). The continental component involved in the formation of the Grampian migmatites and granitoids (S- and I-type) are widely accepted to be sourced from the Dalradian Supergroup (e.g. Pidgeon and Aftalion, 1978; Johnson *et al.*, 2003; Steinhoefel *et al.*, 2008; Weinberg and Geordie, 2008). This is based on stratigraphic relations, similarities in geochronology, and isotope systematics between the Dalradian successions and the Grampian granitoids and migmatites.

5.3 Comparison with units of the Early Ordovician ophiolitic terrane, SW Norway

Time-equivalent granitoids and sedimentary sequences that also form a part of the Lower Ordovician ophiolitic terrane of SW Norway exhibit similar inherited or detrital zircon age distribution as the BMC, with prominent Archean and Paleoproterozoic populations (Figure 5.7). South of the study area, Fonneland (2002) reported detrital zircon data from the S- and I-type granitoids of the WKIC. The granitoids exhibit prominent Archean, Paleo- and Mesoproterozoic zircon populations that resemble the age distribution shown by the BMC (Figure 5.7). In the same study, Fonneland (2002) reported detrital zircon data from the BMC with age distributions dominated by Archean and Paleoproterozoic zircons, similar to sample 20BREM15E (Figure 5.7). Fonneland (2002) argued that the Archean and Paleoproterozoic zircons and isotope systematics seen in the granitoids of WKIC and at the BMC were sourced

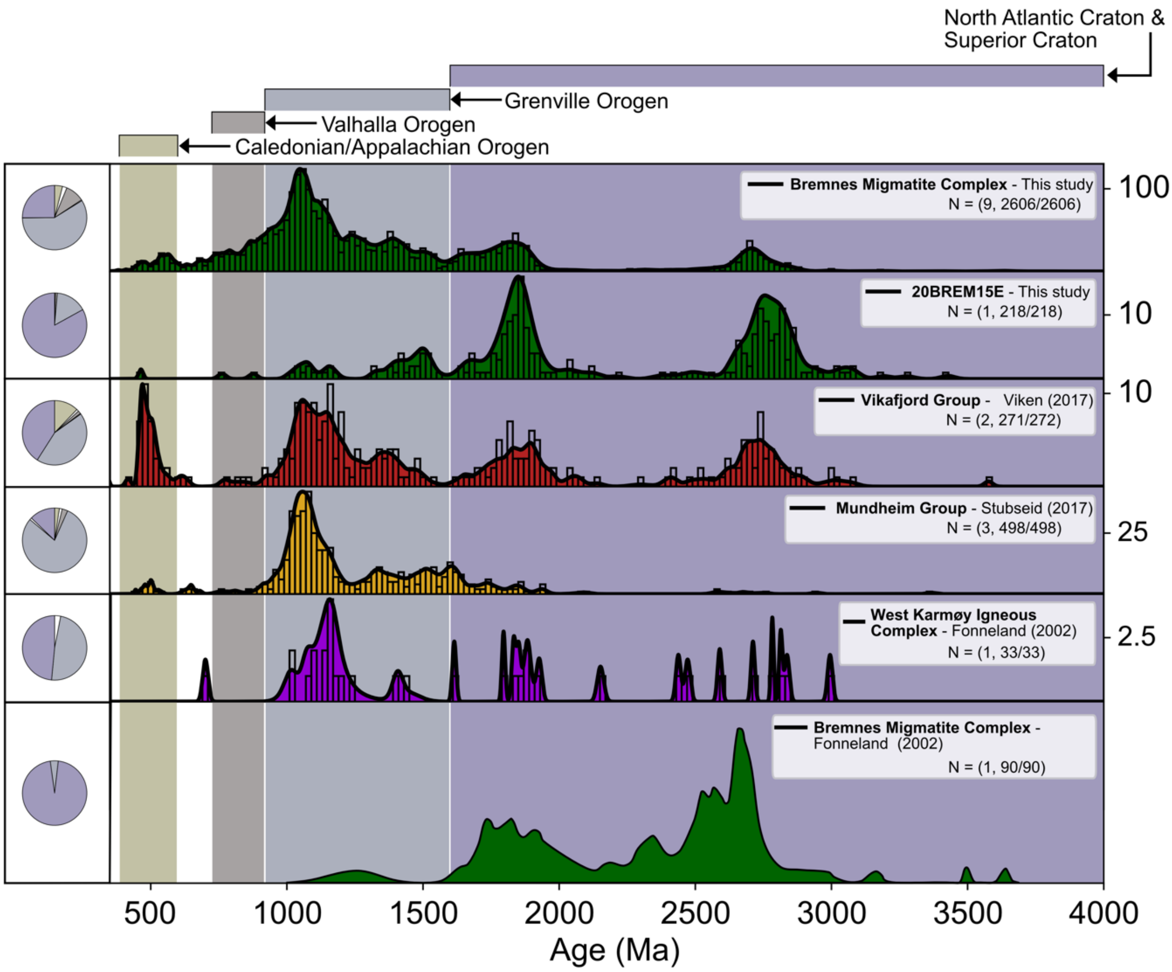

Figure 5.7: Comparison of detrital zircon age distribution between the Bremnes Migmatite Complex and associated sedimentary successions and granitoids of the Early Ordovician ophiolitic terrane of SW Norway. The similarities between the migmatite complex and the other units of the ophiolitic terrane, suggest that these sedimentary sequences and granitoids developed with input from similar sources as the migmatite complex. All presented ages are derived from U-Pb analyses (zircons), either as 207/206 Pb or 238 U/206 Pb, with a discordance filter of 10/-15%. Background coloring according to source region. No discordance filtering was applied on the data presented by Fonneland (2002), as the data was not available.

from the Laurentian margin, as detrital zircon data and isotope systematics from the Baltic margin differ significantly from the WKIC and the BMC. This interpretation has previously been suggested based on isotope systematics, faunal evidence, and U-Pb data (Pedersen *et al.*,1992; Pedersen and Dunning, 1997; Hamnes, 1998). More recent studies on sedimentary sequences located on Bømlo supports derivation from the Laurentian rather than the Baltic margin. Viken (2017) presented detrital zircon data from the Vikafjord Group dominated by Archean, Paleo- and Mesoproterozoic grains (Figure 5.7). Both the reported age distribution and discordant trends exhibit similarities with the BMC, and it was suggested that the two rock units were sourced similarly. The Vikafjord Group was correlated with sedimentary succession located further east in the outer Hardanger Fjord area (Figure 5.7) (Stubseid, 2017). This suggests that the sediment source involved in the formation of the WKIC, and the BMC also influenced many sedimentary sequences that are present within the Early Ordovician terrane of SW Norway.

Sedimentary source for the Early Ordovician ophiolitic terrane of SW Norway

The data that is presented here, indicates that continental component involved in the formation of the BMC, and consequently the WKIC, the Vikafjord Group and other units of the Lower Ordovician terrane, accumulated at the Laurentian rather than the Baltic margin as previously suggested (e.g. Gee, 1975; Sturt *et al.*, 1980; Brekke *et al.*, 1984; Roberts *et al.*, 1984). Based on detrital zircon data, Sm-Nd, and Sr isotope systematics Hamnes (1998) suggested that the Dalradian Supergroup or a sedimentary sequence with similar characteristics as the most likely source for the continental component. Sm-Nd isotope systematics (ε_{Nd}) from the granitoids (-17 to -20.9) overlapped with that of the Dalradian (-9.4 to -28.1) (O'Nions *et al.*, 1983; Frost and O'Nions, 1985) and showed no major similarities with isotopic data from the Baltic margin (17.4 to -12.6) (Figure 5.8) (Kullerud and Dahlgren, 1993; Fonneland, 2002). Similar isotope systematics were also reported for a meta-sedimentary restite from the BMC, with ε_{Nd} values between -14.5 and -29.6 (Figure 5.8) (Fonneland, 2002). However, Fonneland (2002) argued based on the detrital zircon data that the Archean and Paleoproterozoic dominated age distribution exhibited by the BMC resembled that of the Torridonian succession in the Scottish Caledonides (Rainbird *et al.,* 2001), but noted that the Sm-Nd isotope data from both the WKIC and BMC showed prominent similarities with the Dalradian succession. One of ten samples presented here exhibit an age distribution similar to the data presented by Fonneland (2002), while the other nine samples are dominated by Mesoproterozoic zircons that are absent from the Archean and Paleoproterozoic dominated sample (Figure 5.7).

Located just north of the study area on the island of Møkster a metasedimentary sequence exhibit ε_{Nd} values between -11.76 and -21.01 (Figure 5.8) (unpublished data, R.B. Pedersen). This sequence shows similar Sm-Nd isotope systematics as the BMC, the WKIC, and the Dalradian Supergroup (Figure 5.8). Rykkelid (1987) described ophiolites, metasediments with depositional contact to the ophiolite, intrusive rocks and migmatites from the Møkster area. The depositional age of the metasedimentary succession on Møkster have not been constrained, but a monazite U-Pb (SIMS) age of 462 ± 5 Ma have been suggested to represent the prograde metamorphism of the area (Hordvik, 2015), and provides a relative age for the time of deposition. The recorded prograde metamorphic history from Møkster (462 ± 5 Ma) correlates well with the Barrovian metamorphism (*c.* 473-465 Ma) from the Scottish Caledonides (Johnson *et al.*, 2015, and references therein), and suggests that they formed in similar environments. There are no major similarities between the Sm-Nd data from Møkster and isotopic data reported from sedimentary sequences deposited at the Baltic margin. A

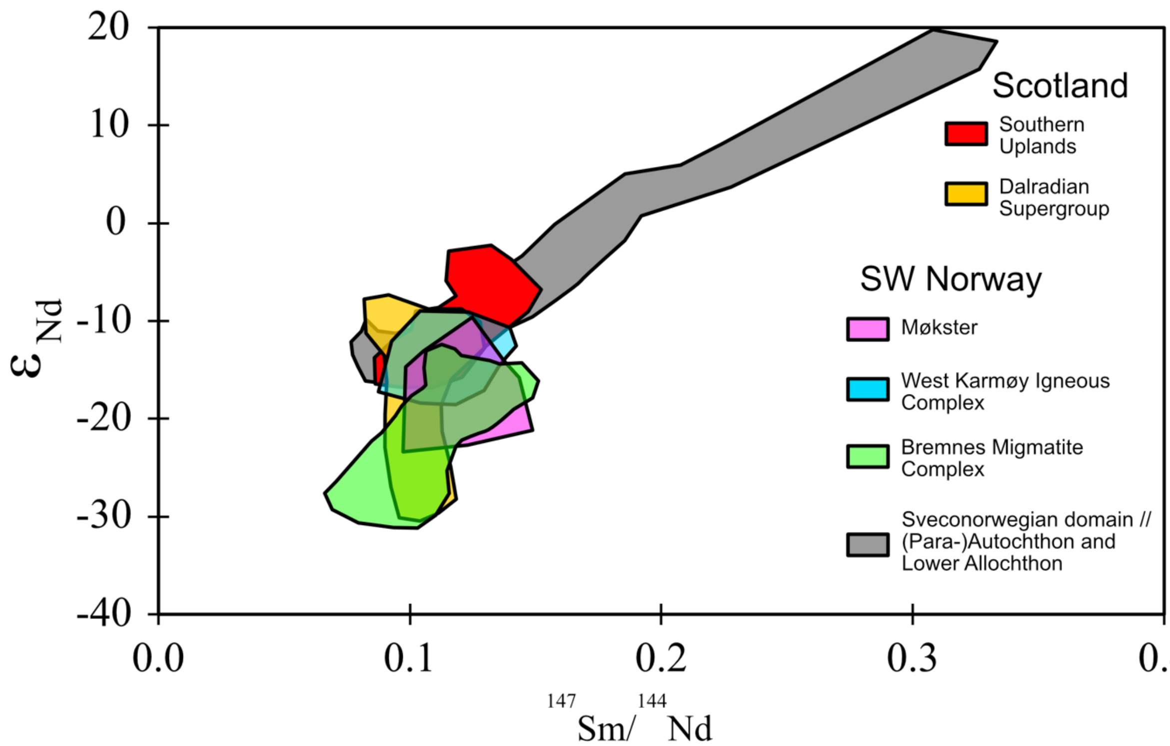

Figure 5.8: The Sm-Nd data of the Bremnes Migmatite Complex overlaps with that of the Dalradian Supergroup, the metasedimentary succession exposed at Møkster, and the S-type granitoids of the WKIC. Sm-Nd data from Scotland, Dalradian: O'Nions et al. (1983) and Frost & O'Nions (1985), Southern Uplands: O'Nions et al. (1983). Data from SW Norway, WKIC: Hamnes (1998), BMC: Fonneland (2002), Sveconorwegian domain, (para-) autochthon and Lower Allochthon: Kullerud & Dahlgren (1993) and Fonneland (2002), Møkster: R. B. Pedersen, unpublished data.

combination of the depositional constraints, lithological and isotopic similarities, suggest that the rocks on Møkster are closely related to the BMC.

To further constrain the origin of the I- and S-type granitoids of the WKIC, Hamnes (1998) compared Sm-Nd and Sr isotope systematics from the WKIC with comparable granitoids of supposed Laurentian and Baltic affinity. The I- and S-type granites exhibited ε_{Nd} values of -12.7 and -12.8, and $^{87}Sr/^{86}Sr$ values of 0.7139 and 0.7201, respectively. These isotope systematics resembles data reported from the Early Ordovician S-type granitoids Aberdeen, Longmannhill, and Strichen from the British Isles, with ε_{Nd} between -11 and -12.7, $^{87}Sr/^{86}Sr$ between 0.7115 and 0.7161 (Hamilton *et al.*, 1980; Kneller and Aftalion, 1987). On the other hand, the I- and S-type granites of the Ordovician-Silurian Bindal Batholith associated with the Baltic margin show no major similarities with the granitoids of the WKIC, with ε_{Nd} between -3 and -9, $^{87}Sr/^{86}Sr$ between 0.704 and 0.710. Hamnes (1998) suggested that the granitoids of the WKIC, had been influenced by a continental component similar to that of the Aberdeen, Longmannhill, and Strichen granitoids, with minor influence from the Baltic margin.

Constraining the origin of the continental component

The similarities seen in geology, geochronology and isotope systematics between the time-equivalent units found within the Early Ordovician ophiolitic terrane of SW Norway and the British Caledonides suggest that their environment of formation was similar and possibly that both terranes were associated with the same island arc complex. The sedimentary component of the time-equivalent units found within the British Caledonides is widely accepted (e.g. Pidgeon and Aftalion, 1978; Johnson *et al.*, 2003; Steinhoefel *et al.*, 2008; Weinberg and Geordie, 2008) to be derived from the Dalradian Supergroup, and it seems reasonable to suggest based on the data presented here that the continental component of the BMC was sourced either directly from or similarly to the Dalradian Supergroup. This is consistent with lithological similarities between the Dalradian (shales, quartzites, sandstones, limestones, greywackes, and volcaniclastics) and the metasedimentary restites, enclaves, and greywackes found in the BMC, the WKIC and on Møkster.

The presence of Archean and Paleoproterozoic dominated detritus within the BMC suggests that the continental component was not uniform. Considering the data presented here it seems reasonable to suggest that the detritus dominated by Archean and Paleoproterozoic zircons are sourced within the Dalradian Supergroup, rather than other succession associated with the Laurentian margin (section 5.3) (Figure 5.9). The source for the samples dominated by Archean and Paleoproterozoic aged zircons could be the Appin Group, which form a part of the Upper Dalradian succession and exhibit age distributions similar to sample 20BREM15E and to the detrital zircon data reported by Fonneland (2002) (Figure 5.9). Based on the sampling location of 20BREM15E, it seems reasonable to suggest that the difference in detrital zircon age distribution is related to an area within the metatexites that are dominated by quartzites (Figure 4.9). However, Fonneland (2002) reported similar age distribution from a restite of unknown origin within the BMC, which could indicate that similar sediments are found within several locations of the migmatite complex.

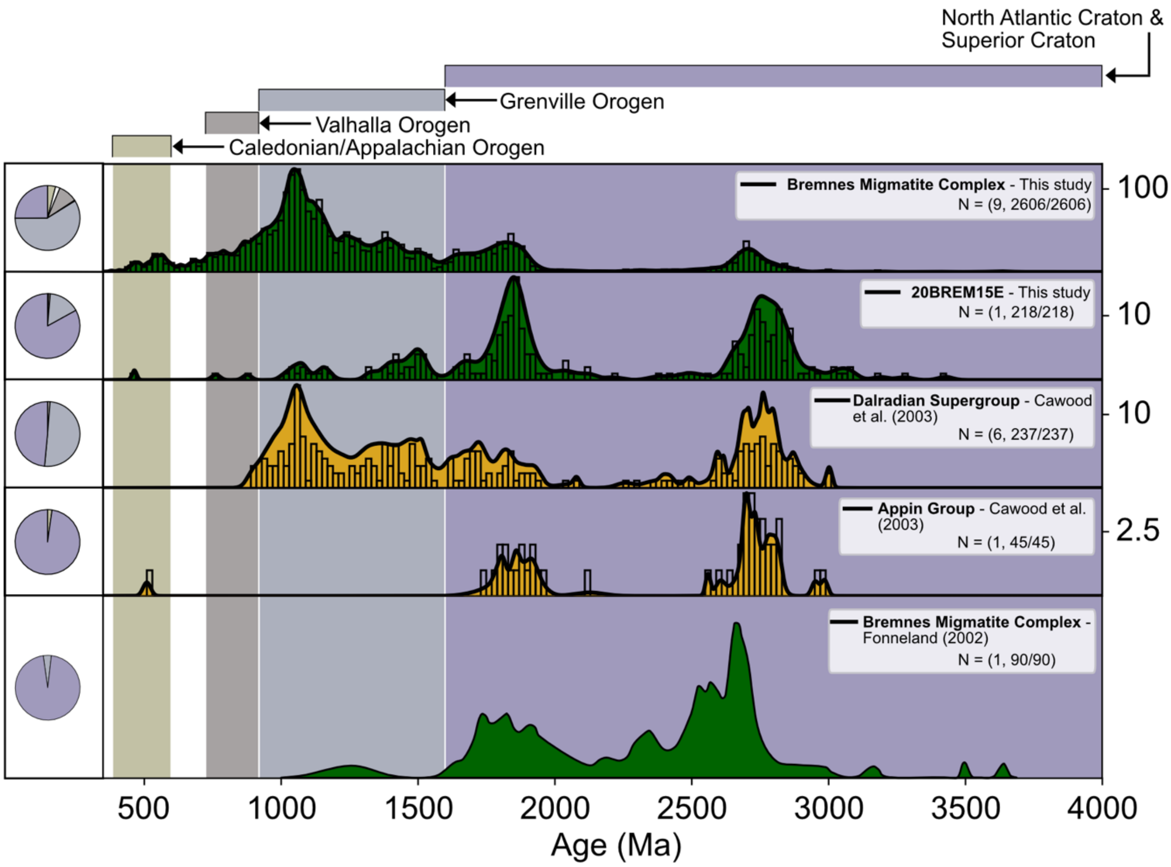

Figure 5.9: Comparison detrital zircon data from the BMC with the Dalradian Supergroup from NW Scotland. The main trend of the migmatite complex resemble that of the Dalradian Supergroup. The sample dominated by Archean and Paleoproterozoic aged zircons (20BREM15E) show prominent similarities with the Appin Group of the Dalradian succession. Combined the data presented in this study suggest that the continental component of the Bremnes Migmatite Complex, and several other units of the Early Ordovician ophiolitic terrane of SW Norway, is best described by the Dalradian Supergroup. See text for further details. All presented ages are derived from U-Pb analyses (zircons), either as 207/206 Pb or 238 U/206 Pb, with a discordance filter of 10/-15%.

5.4 The development of the Bremnes Migmatite Complex

Fonneland (2002) suggested that the BMC developed at the same time and from the same continental component as the S-type granitoids of the WKIC. This was proposed based on the similarities in isotope systematics and zircon provenance between the two complexes, and the presence of xenoliths (restites/enclaves) of the same lithologies within both the BMC and the S-type granitoids. The data presented in this study supports this interpretation and constrain the time of formation of the BMC to 477 ± 7 Ma which overlaps with the formation of the S-type granitoids of the WKIC (473 +3/-2 Ma; Pedersen and Dunning, 1997). Formation models for the WKIC suggests that the S-type granitoids developed exclusively from melts derived from a continental component, with little to no input from mantle derived melts (Hamnes, 1998). It seems reasonable, based on the similarities between the two complexes, to suggest a similar formation model for the BMC and consequently that the migmatite complex formed primarily by partial melting of a continental component. Further, to properly understand the evolution of the BMC it is crucial to know the origin and composition of the protolith (the continental component).

The protolith of the BMC and its composition.

All the data presented here implies that the continental component of the BMC, and consequently several other units of the Early Ordovician ophiolitic terrane of SW Norway, is best represented by the Dalradian Supergroup of the Scottish Caledonides (section 5.3). Geochemical analyses of the BMC show that the migmatite complex has major-element (i.e. Al_2O_3, MgO, NaO, K_2O) compositions similar to the Dalradian Shales (Figure 5.10) (Atherton and Brotherton, 1982, and references therein). The intermediate composition of the BMC (SiO_2 average of 60.13%) are comparable to the fine-grained sedimentary rocks (pelites/shales) of the Dalradian Supergroup (SiO_2 average of 59.88%). The partial melted constituent of the BMC (diatexites and metatexites) completely overlaps with the reported major-element compositions of the Dalradian shales, while the remains of the continental component (restites) only partly overlap (Figure 5.10). This suggests that fine-grained sedimentary rocks of the Dalradian Supergroup were the first to melt, and make up a major part of the BMC, while the restites (quartzites, mica schists, and quartz-felspathic material) represents a section of the continental component that did not completely melt and are consequently preserved as xenoliths within the migmatite complex. This interpretation is consistent with the trace-element compositions of the BMC, which resemble that of the average shale, implying that the migmatite complex formed from a source similar in composition to the average shale (section 5.1) (Figure 5.1). The resemblance between the BMC and the average shale, and the similarities in major-element composition with the fine-grained sedimentary rocks of the Dalradian Supergroup, suggest that the migmatite complex developed primarily from partial melting of a fine-grained sedimentary protolith sourced in the Dalradian Supergroup.

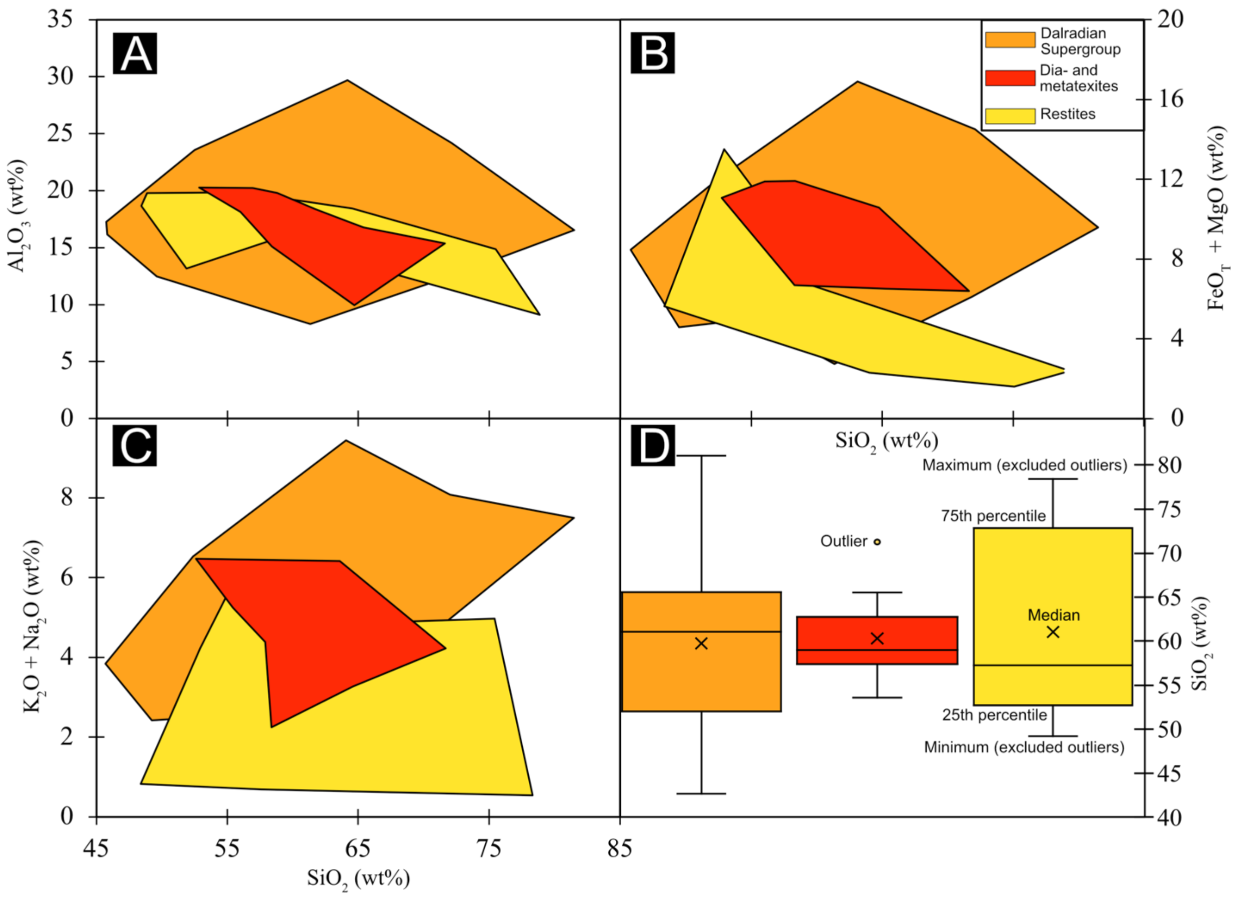

Figure 5.10: Major-element comparison between the samples of diatexites (red), metatexites (red), and restites (yellow) collected from the Bremnes Migmatite Complex, with the pelites of the Dalradian Supergroup (orange). A,B, and C, show Harker diagrams of Al_2O_3, FeO_T + MgO, and alkali ($K_2O + Na_2O$) plotted against SiO_2. The Harker diagrams show that the major-element composition of the fine-grained sedimentary rocks of the Dalradian Supergroup completely overlaps with the partial melted constituents (dia- and metatexites) of the migmatite complex, and partly with the restites. See text for further explanation D) A box plot of the SiO_2 content of the respective units, notice the similarities in the median value across the units of the BMC (diatexites, metatexites, and restites) and the pelites of the Dalradian Supergroup. The data presented here from the BMC, are based on 8 analyses of restites, and 17 analyses of dia- and metatexites. From the Dalradian Supergroup, the dataset contains 230 analyses of pelites collected within several locations of the Dalradian Supergroup (Atherton and Brotherton, 1982, and references therein).

The timing of migmatization

The timing of the migmatization can be constrained by a mean age of 477 ± 7 Ma, calculated from the overgrowths on the Caledonian zircons from 7 of 10 samples (500-460 Ma, discordance of ≤ 5 %, n = 16). This age fits well with the intrusion of the S-type granitoids of the WKIC at 474 +3/-2 Ma (Pedersen and Dunning, 1997). The presented ages combined with the temporal evolution of the study area, indicates that the BMC was migmatized prior to the intrusion of the Vardafjell Gabbro at 472 ± 2 Ma (Pedersen and Dunning, 1997) (section 5.1).

Andersen *et al.* (1991) suggested that the BMC formed in the roof of the Vardafjell Gabbro, and that heat from the gabbroic body represented the main factor in the initiation of migmatization. This seems unlikely, considering the radiometric ages, the uniform geochemical composition of the BMC, and the age relations between the gabbroic rocks and the migmatite complex. It seems more likely that the migmatization occurred prior to the intrusion of the Vardafjell Gabbro and that the migmatization was caused by crustal thickening and radiometric heating. However, the presence of mobilized leucosome within the parts of the Vardafjell Gabbro that are closest to the BMC suggest that the heat from the intrusion led to some degree of melting. This contribution from the Vardafjell Gabbro could explain why the diatexites (higher degree of melting) occur close to the contact with the gabbroic rocks (Figure 4.1).

In Scotland, Grampian migmatites yield similar ages for migmatization as the BMC with zircon overgrowths dated to 461 ± 13 Ma and 467 ± 10 Ma (Kinny *et al.*, 1999). These migmatites occur together with Grampian age S-type granitoids and gabbroic rocks with ages between 473-465 Ma and 475-470 Ma, respectively (Appleby *et al.*, 2010; Palin *et al.*, 2018). The source of partial melting and migmatization in the area is suggested to be related to crustal thickening and radiogenic heating following arc-continent collision, with local contribution from the intruding gabbroic rocks (Appleby *et al.*, 2010, and the references therein). The evolution of the Grampian migmatites and granitoids correlates with the proposed evolution for the BMC; main migmatization (477 ± 7 Ma) was initiated during arc-continent collision prior to the intrusion of the Vardafjell Gabbro (472 ± 2 Ma).

Evolutionary model for the BMC

Based on the detrital zircon data and geochemical analyses presented here, combined with the work of others (Pedersen and Dunning, 1997; Hamnes, 1998; Fonneland, 2002), an evolutionary model for the BMC and associated units of the Early Ordovician ophiolitic terrane (S-type granitoids of the WKIC, and the appinite and gabbroic rocks of the Vardafjell Gabbro) is suggested (Figure 5.11). The evolution of the Early Ordovician ophiolite complexes and island arc sequences of SW Norway begins with the formation of an immature island arc (494

± 2 Ma) with subduction zone affinity (Pedersen and Dunning, 1997). The immature island arc shows no sign of continental input, which indicate that the island arc at the time was located sufficiently far from the Laurentian continental margin. At 485 ± 2 Ma boninitic dyke swarms intrude into the ophiolitic terrane. These rocks exhibit ε_{Nd} values (between -8.1 and 1.3) influenced by a continental component and marks the beginning of a period (10-15 Myr) where the continental component was present within the mantle derived melts (Figure 5.11) (Pedersen and Dunning, 1997). The sedimentary protolith of the BMC, and the continental component of other units in the Early Ordovician ophiolitic terrane, is best described by the fine-grained sedimentary rocks of the Dalradian Supergroup, which were deposited on the Laurentian margin in the mid-Neoproterozoic (*c.* 700 Ma) to Early Paleozoic (*c.* 520 Ma) (Cawood *et al.*, 2003). The Dalradian shales was first introduced to the mantle derived melts by the subduction of continental derived deposits (485 ± 2 Ma). Further, as the subduction continued, the Laurentian continental margin was subducted (Figure 5.11). The BMC (477 ± 7 Ma) and the S-type granitoids (474 +3/-2 Ma) developed as the Laurentian margin was subducted sufficiently to commence partial melting of the Dalradian shales (Figure 5.11). Shortly after the partial melting, and subsequent formation of the BMC and the S-type granitoids, appinites related to an early phase of the Vardafjell Gabbro (472 ± 2 Ma) intrude the migmatite complex (section 5.1) (Figure 5.11). Appinites present in areas where the tectonic evolution is properly constrained, are suggested to intrude as the subduction ceases (Murphy, 2013, and references therein). It seems reasonable based on the data presented here to suggest that the appinites found in relation to the BMC intrude between the migmatization of the BMC (*c.* 477) and the intrusion of the Vardafjell Gabbro (*c.* 472), and that the intrusion mark the cessation in the subduction of the Laurentian continental margin.

A modern analog to the plate-tectonic situation seen at the Laurentian margin in Early Ordovician has been suggested to be the ongoing subduction of the Australian continental margin beneath the Banda-arc (Snyder and Barber, 1997). This ongoing collision has led to the obduction of ophiolites, island arcs and changes in polarity similar to what is recorded within the Caledonian Orogeny (Vroon *et al.*, 1993; Snyder and Barber, 1997). Island arcs related to this system show comparable trace-element patterns to the Siggjo Complex (Stolz *et al.*, 1990; Viken, 2017) and isotope systematics thought to be altered due to contamination by a continental component (Stolz *et al.*, 1990). Another modern analogue for the plate-tectonic situation at the Laurentian margin in the Early Ordovician could be the ongoing arc-continent collision recorded in Taiwan (Huang *et al.*, 2006), which feature obduction of island arcs, opening of arc-basins, and changes in polarity recorded over the last 15-16 Myr similar to what is described from the Laurentian margin in Early Ordovician (Snyder and Barber, 1997).

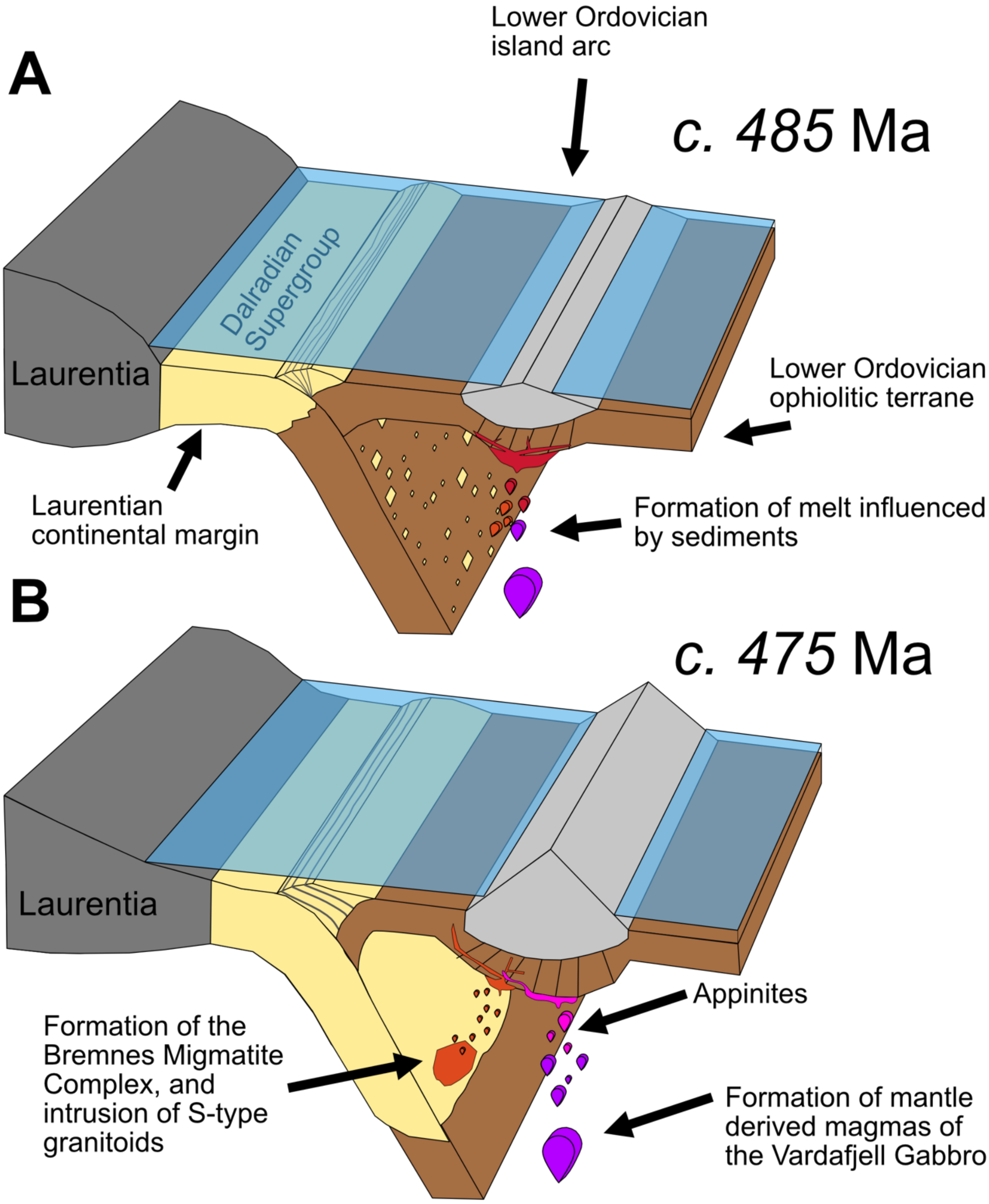

Figure 5.11: Evolutionary model for the formation of the Bremnes Migmatite Complex. The Dalradian Supergroup accumulated at the Laurentian continental margin in the Mid-Neoproterozoic (*c.* 700 Ma) to Early Paleozoic (*c.* 520 Ma), prior to onset of the subduction. A) Intrusion of boninitic magmas influenced by a continental component (Dalradian Supergroup) at *c.* 485 Ma. This indicates that the Eraly Ordovician ophiolitic terrane of SW Norway was close to the Laurentian margin. B) The subduction of the Laurentian continental margin, and the formation of the BMC and S-type granitoids of the WKIC by anatexis in the Dalradian Supergroup at *c.* 475 Ma. The intrusion of appinites, related to an early volatile rich phase of the mantle derived calc-alkaline magmas of the Vardafjell Gabbro. The appinites intrude prior to the Vardafjell Gabbro (472 ± 2 Ma).

6 Conclusion

Based on major- and trace-element geochemical and detrital zircon U-Pb provenance data, the present study provides new insights into the evolution and origin of the BMC and the Early Ordovician ophiolitic terrane of SW Norway. From the present study the following conclusion can be made:

- The detrital zircon populations of the BMC, indicates that the continental component of the complex was derived from within the Laurentian paleocontinent, confirming that the Early Ordovician ophiolitic terrane developed adjacent to the Laurentian continental margin.
- The results of the present study indicates that the BMC and the S-type granitoids of the WKIC developed primarily from a fine-grained continental component sourced in the Dalradian Supergroup. This is consistent with the development of time-equivalent migmatites and granitoids in the Scottish Caledonides, interpreted to have their sedimentary component from the Dalradian Supergroup, and suggest that the Early Ordovician ophiolitic terrane of SW Norway may be closely related in both time and space to the time-equivalent units of the Scottish Caledonides.
- It has previously been suggested that the BMC (477 ± 7 Ma) developed at the same time, and from the same continental component as the S-type granitoids of the WKIC (474 +3/-2 Ma). This is consistent with the findings presented in this study. The BMC developed as the Laurentian continental margin was subducted sufficiently beneath the Early Ordovician ophiolitic terrane to commence partial melting of the continental component.
- The BMC was migmatized (477 ± 7 Ma) prior to the intrusion of the Vardafjell Gabbro (472 ± 2 Ma), and at the same time as the S-type granitoids of the WKIC intruded the ophiolitic terrane (474 +3/-2 Ma). Appinites found in relation to the BMC, represents an early volatile-rich phase of the Vardafjell Gabbro, that intruded the migmatite complex prior to the intrusion of the Vardafjell Gabbro (472 ± 2 Ma). This event may mark the termination of the arc-continent collision and the subduction of the Laurentian continental margin below the arc complex.

7 Future work

Sm-Nd data from the metasedimentary succession exposed at Møkster, overlaps with isotope systematics from the BMC, the granitoids of the WKIC, and the Dalradian Supergroup, suggesting that these units are somehow related. It would be interesting with a provenance study on the metasedimentary succession found at Møkster, to properly constrain the origin of these sediments and its relation to the other rocks of the Lower Ordovician ophiolitic terrane of SW Norway.

From the results presented in the study, it is suggested that the appinites found in relation to the BMC were derived from an early volatile-rich phase of the Vardafjell Gabbro. A comprehensive study on the origin, age, and composition of the appinites, would be interesting to further understand it in relation to the BMC, Vardafjell Gabbro (Sunnhordland Batholith), and other magmatic suites found within the Early Ordovician ophiolitic terrane.

The findings presented here, suggest that the Early Ordovician ophiolitic terrane of SW Norway may be closely related to the time-equivalent rocks of the Scottish Caledonides, and that these systems once represented an extensive island arc complexes that developed adjacent to the Laurentian continental margin. It would be interesting with a study that further investigates these findings.

References

Andersen, T. B., Nielsen, P., Rykkelid, E. and Sølna, H. (1991) 'Melt-enhanced deformation during emplacement of gabbro and granodiorite in the Sunnhordland Batholith, west Norway', *Geological Magazine*, 128(3), pp. 207–226.

Andersen, T. B. and Andresen, A. (1994) 'Stratigraphy, tectonostratigraphy and the accretion of outboard terranes in the Caledonides of Sunnhordland, W. Norway', *Tectonophysics*, 231(1–3), pp. 71–84.

Andersen, T. B. and Jansen, Ø. J. (1987) 'The Sunnhordland Batholith, W. Norway: regional setting and internal structure, with emphasis on the granitoid plutons.', *Norsk Geologisk Tidsskrift*, 67(3), pp. 159–183.

Appleby, S. K., Gillespie, M. R., Graham, C. M., Hinton, R. W., Oliver, G. J. H. and Kelly, N. M. (2010) 'Do S-type granites commonly sample infracrustal sources? New results from an integrated O, U-Pb and Hf isotope study of zircon', *Contributions to Mineralogy and Petrology*, 160(1), pp. 115–132.

Atherton, M. P. and Brotherton, M. S. (1982) 'Major element composition of the pelites of the Scottish Dalradian', *Geological Journal*, 17(3), pp. 185–221.

Barnes, C. G. Prestvik, T., Barnes, M. A. W., Anthony, E. Y. and Allen, C. M. (2003) 'Geology of a magma transfer zone: The Hortavær Igneous Complex, north-central Norway', *Norsk Geologisk Tidsskrift*, 83(3), pp. 187–208.

Bingen, B., Skår, Ø., Marker, M., Sigmond, E. M. O., Nordgulen, Ø., Ragnhildstveit, J., Mansfeld, J., Tucker, R. D. and Liegeois, J-P. (2005A) 'Timing of continental building in the Sveconorwegian orogen, SW Scandinavia', *Norsk Geologisk Tidsskrift*, 85(1–2), pp. 87–105.

Bingen, B., Griffin, W. L., Torsvik, T. H. and Saeed, A. (2005B) 'Timing of Late Neoproterozoic glaciation in Baltica constrained by detrital zircon geochronology in the Hedmark Group, south-east Norway', *Terra Nova*, 17(3), pp. 250–258.

Brekke, H., Furned, H., Nordås, J. and Hertogen, J. (1984) 'Lower Palaeozoic convergent plate margin volcanism on Bømlo', *Journal of the Geological Society*, 141, pp. 1015–1032.

Cawood, P. A., Nemchin, A. A., Smith, M. and Loewy, S. (2003) 'Source of the Dalradian Supergroup constrained by U-Pb dating of detrital zircon and implications for the East Laurentian margin', *Journal of the Geological Society*, 160(2), pp. 231–246.

Cawood, P. A. Strachan, R. A., Merle, R. E., Millar, I. L., Loewy, S. L., Dalziel, I. W. D., Kinny, P. D., Jourdan, F., Nemchin, A. A. and Connelly, J. N. (2014) 'Neoproterozoic to early Paleozoic extensional and compressional history of East Laurentian margin sequences: The Moine Supergroup, Scottish Caledonides', *Bulletin of the Geological Society of America*, 127(3–4), pp. 349–371.

Cawood, P. A. and Nemchin, A. A. (2001) 'Paleogeographic development of the East Laurentian margin: Constraints from U-Pb dating of detrital zircons in the Newfoundland Appalachians', *Bulletin of the Geological Society of America*, 113(9), pp. 1234–1246.

Cawood, P. A., Nemchin, A. A. and Strachan, R. (2007) 'Provenance record of Laurentian passive-margin strata in the northern Caledonides: Implication for plaeodrainage and paleogeography', *Bulletin of Geological Society of America,* 119(7-8), pp. 993-1003

Chew, D. M., Graham, J. R. and Whitehouse, M. J. (2007) 'U-Pb zircon geochronology of plagiogranites from the Lough Nafooey (= Midland Valley) arc in western Ireland: Constraints on the onset of the Grampian orogeny', *Journal of the Geological Society*, 164(4), pp. 747–750.

Chew, D. M., Petrus, J. A. and Kamber, B. S. (2014) ‘U-Pb LA-ICPMS dating using accessory mineral standards with variable common Pb’, *Chemical Geology*, 363, pp. 185–199.

Corfu, F., Roberts, J. R., Torsvik, T. H., Ashwal, L. D. and Ramsay, D. M. (2007) ‘Peri-Gondwanan elements in the Caledonian Nappes of Finnmark, Northern Norway: Implications for the paleogeographic framework of the Scandinavian Caledonides’, *American Journal of Science*, 307(2), pp. 434–458.

Dunning, G. R. and Krogh, T. E. (1986) ‘Geochronology of ophiolites of the Newfoundland Appalachians’, *Canadian Journal of Earth Sciences*, 22, pp. 1659–1670.

Dunning, G. R. and Pedersen, R. B. (1988) ‘U/Pb ages of ophiolites and arc-related plutons of the Norwegian Caledonides: implications for the development of Iapetus’, *Contributions to Mineralogy and Petrology*, 98(1), pp. 13–23.

Fonneland, H. C. (2002) *Radiogenic Isotope Systematics of Clastic Sedimentary rock - with Emphasis on Detrital Zircon Geochronology*. PhD thesis. Bergen: University of Bergen.

Fossen, H. and Austrheim, H. (1988) ‘Age of the Krossnes Granite, West Norway’, *Bulletin - Norges geologiske undersokelse*, pp. 61–65.

Frost, C. D. and O'Nions, R. K. O. (1985) ‘Caledonian magma genesis and crustal recycling’, *Journal of Petrology*, 26(2), pp. 515–544.

Gale, G. H. and Roberts, D. (1974) ‘Trace element geochemistry of Norwegian Lower Palaeozoic basic volcanics and its tectonic implications’, *Earth and Planetary Science Letters*, 22(4), pp. 380–390.

Gee, D. (1975) ‘A tectonic model for the central part of the Scandinavian Caledonides’, *American Journal of Science*, pp. 468–515.

Gower, C. F. (1996) ‘The evolution of the Grenville Province in eastern Labrador, Canada’, *Precambrian crustal evolution in the North Atlantic region*, (112), pp. 197–218.

Gromet, L. P., Dymek E. R., Haskin, L. A. and Korotev, R. L. (1984) ‘The “North American shale composite”: Its compilation, major and trace element characteristics’, *Geochimica et Cosmochimica Acta*, 48(12), pp. 2469–2482.

Hamilton, P. J., O’Nions, R. K. and Pankhurst, R. J. (1980) ‘Isotopic evidence for the provenance of some caledonian granites’, *Nature*, 287(5780), pp. 279–284.

Hamnes, G. M. (1998) *Petrografi, geokjemi og petrogenese til Vest-Karmøy Intrusiv Kompleks*. Cand. Scient thesis. Bergen: University of Bergen.

Higgins, A. K. Elvevold, S., Escher, J. C., Frederiksen, K. S., Gilotti, J. A., Henriken, N., Jepsen, H. F., Jones, K. A., Kalsbeek, F., Kinny, P.D., Leslie, A.G., Smith, M. P., Thrane, K. and Watt, G. R. (2004) ‘The foreland-propagating thrust architecture of the East Greenland Caledonides 72°-75°N’, *Journal of the Geological Society*, 161(6), pp. 1009–1026.

Hoffman, P. F. (1988) ‘UNITED PLATES OF AMERICA , THE BIRTH OF A CRATON : Early Proterozoic Assembly and Growth of Laurentia’, *Annual Review of Earth and Planetary Sciences*, 16, pp. 543–603.

Hoffman, P. F., Bally, A. W. and Palmer, A. R. (1989) ‘Precambrian geology and tectonic history of North America’, *The geology of North America—an overview*, pp. 447–512.

Hordvik, Ø. (2015) *Comparison of metamorphic evolution and tectonic position of metasediments of the Austevoll islands with rocks from the Samnanger Complex (Major Bergen Arc, Norwegian Caledonides*. Master thesis. Bergen: University of Bergen.

Huang, C. Y., Yuan, P. B. and Tsao, S. J. (2006) ‘Temporal and spatial records of active arc-continent collision in Taiwan: A synthesis’, *Bulletin of the Geological Society of America*, 118(3–4), pp. 274–288.

Jackson, S. E., Pearson, N. J., Griffin, W. L. and Belousova, E. A. (2004) 'The application of laser ablation-inductively coupled plasma-mass spectrometry to in situ U-Pb zircon geochronology', *Chemical Geology*, 211(1–2), pp. 47–69.
Johnson, T. E., Kirkland, C. L., Reddy, S. M. and Fischer, S. (2015) 'Grampian migmatites in the Buchan Block, NE Scotland', *Journal of Metamorphic Geology*, 33(7), pp. 695–709.
Johnson, T. E., Hudson, N. F. C. and Droop, G. T. R. (2003) 'Evidence for a genetic granite-migmatite link of the Dalradian of NE Scotland', *Journal of the Geological Society*, 160(3), pp. 447–457.
Kalsbeek, F., Jepsen, H. F. and Nutman, A. P. (2001) 'From source migmatites to plutons: Tracking the origin of ca. 435 Ma S-type granites in the East Greenland Caledonian orogen', *Lithos*, 57(1), pp. 1–21.
Kinny, P. D., Friend, C. R. L., Strachan, R. A., Watt, G. R. and Burns, I. M. (1999) 'U-Pb geochronology of regional migmatites in East Sutherland, Scotland: Evidence for crustal melting during the Caledonian orogeny', *Journal of the Geological Society*, 156(6), pp. 1143–1152.
Kneller, B. C. and Aftalion, M. (1987) 'The isotopic and structural age of the Aberdeen Granite', *Journal of the Geological Society, London*, 144, pp. 717–721.
Kullerud, L. and Dahlgren, S. H. (1993) 'Sm-Nd geochronology of Sveconorwegian granulite facies mineral assemblages in the Bamble Shear Belt, South Norway', *Precambrian Research*, 64(1–4), pp. 389–402.
Ludwig, K. R. (1994) 'A plotting and regression program for radiogenic isotope data, version 2.75', *US Geol. Surv., Open-file Report*, pp. 91–445.
Maxeiner, R. O., Ashton, K., Card, C. D., Morelli, R. M. and Knox B. (2017) 'A Field Guide to Naming Migmatites and Their Textures, with Saskatchewan Examples', *Summary of Investigations 2017, Volume 2, Saskatchewan Geological Survey, Saskatchewan Ministry of the Economy, Miscellaneous Report 2017-4.2, Paper A-2*, (December), pp. 1–21.
Middlemost, E. A. K. (1994) 'Naming materials in the magma/igneous rock system', *Earth Science Reviews*, 37(3–4), pp. 215–224.
Murphy, J. B. (2013) 'Appinite suites: A record of the role of water in the genesis, Transport, Emplacement and crystallization of magma', *Earth-Science Reviews*, 119, pp. 35–59.
Nielsen, P. E. (1990) *Geologiske relasjoner mellom Bremneskomplekset og Sunnhordlandsbatholitten, Bømlo, Vest Norge*. Oslo: University of Oslo.
Nordås, J., Amaliksen, K., Brekke, H., Suthren R. J., Furnes, H., Sturt, B. A. and Robins, B. (1985) 'Lithostratigraphy and petrochemistry of Caledonian rocks on Bømlo, southwest Norway', in Gee, D. G. and Sturt, B. A. (eds) *The Caledonide orogen - Scandinavia and related areas*. New York: John Wiley & Sons Ltd, pp. 679–692.
Nutman, A. P., Friend, C. R. L. and Bennett, V. C. (2002) 'Evidence for 3650-3600 Ma assembly of the northern end of the Itsaq Gneiss Complex, Greenland: Implication for early Archaean tectonics', *Tectonics*, 21(1), pp. 5-1-5–28.
O'Nions, R. K., Hamilton, P. J. and Hooker, P. J. (1983) 'A Nd isotope investigation of sediments related to crustal development in the British Isles', *Earth and Planetary Science Letters*, 63(2), pp. 229–240.
Palin, R. M., Sayed, A. B., White, R. W. and Mertz-Kraus, R. (2018) 'Origin, age, and significance of deep-seated granulite-facies migmatites in the Barrow zones of Scotland, Cairn Leuchan, Glen Muick area', *Journal of Metamorphic Geology*, 36(8), pp. 1071–1096.
Paton, C., Woodhead, J. D., Hellstrom, J. C., Hergt, J. M., Greig, A. and Maas, R. (2010) 'Improved laser ablation U-Pb zircon geochronology through robust downhole

fractionation correction', *Geochemistry, Geophysics, Geosystems*, 11(3).
Pedersen, R. B., Bruton, D. L. and Furnes, H. (1992) 'Ordovician faunas, island arcs and ophiolites in the Scandinavian Caledonides', *Terra Nova*, 4(2), pp. 217–222.
Pedersen, R. B. and Dunning, G. R. (1997) 'Evolution of arc crust and relations between contrasting sources: U-Pb (age), Nd and Sr isotope systematics of the ophiolitic terrain of SW Norway', *Contributions to Mineralogy and Petrology*, 128(1), pp. 1–15.
Pedersen, R. B., Furnes, H. and Dunning, G. (1991) 'A U/Pb age for the Sulitjelma Gabbro, North Norway: Further evidence for the development of a Caledonian marginal basin in Ashgill–Llandovery time', *Geological Magazine*, 128(2), pp. 141–153.
Pedersen, R. B., Furnes, H. and Dunning, G. R. (1988) 'Some Norwegian ophiolite complexes reconsidered', *Nor. Geol. Unders. Spec. Publ*, 3, pp. 80–85.
Pedersen, R. B. and Hertogen, J. (1990) 'Magmatic evolution of the Karmøy Ophiolite Complex, SW Norway: relationships between MORB-IAT-boninitic-calc-alkaline and alkaline magmatism', *Contributions to Mineralogy and Petrology*, 104(3), pp. 277–293.
Pidgeon, R. T. and Aftalion, M. (1978) 'Cogenetic and inherited zircon U-Pb systems in granites: Palaeozoic granites of Scotland and England', *Crustal Evolution in Northwestern Britain and Adjacent Regions*, pp. 183–220.
Piper, D. Z. (1974) 'Rare earth elements in the sedimentary cycle: A summary', *Chemical Geology*, 14(4), pp. 285–304.
Rainbird, R. H., Hamilton, M. A. and Young, G. M. (2001) 'Detrital zircon geochronology and provenance of the Torridonian, NW Scotland', *Journal of the Geological Society*, 158(1), pp. 15–27.
Rivers, T. (1997) 'Lithotectonic elements of the Grenville Province: Review and tectonic implications', *Precambrian Research*, 86(3–4), pp. 117–154.
Roberts, D. and Gee, D. G. (1985) 'An introduction to the structure of the Scandinavian Caledonides', in *The Caledonide orogen - Scandinavia and related areas*. 1st edn, pp. 55–68.
Roberts, D., Grenne, T. and Ryan, P. D. (1984) 'Ordovician marginal basin development in the central Norwegian Caledonides', *Geological Society Special Publication*, 16, pp. 233–244.
Roberts, N. M. W. and Slagstad, T. (2015) 'Continental growth and reworking on the edge of the Columbia and Rodinia supercontinents; 1.86-0.9 Ga accretionary orogeny in southwest Fennoscandia', *International Geology Review*, 57(11–12), pp. 1582–1606.
Rogers, G. and Dunning, G. R. (1991) 'Geochronology of appinitic and related granitic magmatism in the W Highlands of Scotland: Constraints on the timing of transcurrent fault movement', *Journal of the Geological Society*, 148(1), pp. 17–27.
Rykkelid, E. (1987) *Geologisk utvikling i Møkster/Selbjørn-området i Sunnhordland*. Bergen: University of Bergen.
Saltvedt, S. (in prep.) (The formation of the ophiolitic terrane of SW Norway - relationships between immature island arc sequences and trondhjemitic complexes on Bømlo) Master thesis. Bergen: University of Bergen.
Scheiber, T., Viola, G., Wilkinson, C. M., Ganerød, M., Skår, Ø. and Gasser, D. (2016) 'Direct 40Ar/39Ar dating of Late Ordovician and Silurian brittle faulting in the southwestern Norwegian Caledonides', *Terra Nova*, 28(5), pp. 374–382.
Sharman, G. R., Sharman, J. P. and Sylvester, Z. (2018) 'detritalPy: A Python-based toolset for visualizing and analysing detrital geo-thermochronologic data', *The Depositional Record*, 4(2), pp. 202–215.
Sivertsen, J.-E. (1992) *Stratigraphy and geochemistry of the extrusives of the Torvastad group: marginal basin deposits associated with the Karmøy ophiolite complex, SW*

Norway. Master thesis. Bergen: University of Bergen.
Slagstad, T., Davidsen, B. and Stephen Daly, J. (2011) 'Age and composition of crystalline basement rocks on the norwegian continental margin: Offshore extension and continuity of the Caledonian-Appalachian orogenic belt', *Journal of the Geological Society*, 168(5), pp. 1167–1185.
Sláma, J., Walderhaug, O., Fonneland, H., Kosler, J. and Pedersen, R. B. (2011) 'Provenance of Neoproterozoic to upper Cretaceous sedimentary rocks, eastern Greenland: Implications for recognizing the sources of sediments in the Norwegian Sea', *Sedimentary Geology*, 238(3–4), pp. 254–267.
Sláma, J., Kosler, J., Condon, D. J., Crowely, J. L., Gerdes, A., Hanchar, J. M., Hortswood, M. S. A., Morris, G. A., Nasdala, L., Norberg, N., Schaltegger, U., Schoene, B., Tubrett, M. N. and Whitehouse, M. J. (2008) 'Plešovice zircon - A new natural reference material for U-Pb and Hf isotopic microanalysis', *Chemical Geology*, 249(1–2), pp. 1–35.
Sláma, J. and Pedersen, R. B. (2015) 'Zircon provenance of SW caledonian phyllites reveals a distant timanian sediment source', *Journal of the Geological Society*, 172(4), pp. 465–478.
Snyder, D. B. and Barber, A. J. (1997) 'Australia-Banda Arc collision as an analogue for early stages in Iapetus closure', *Journal of the Geological Society*, 154(4), pp. 589–592.
Van Staal, C. R., Dewey, J. F., Niocaill C. M. and Mckerrow, W. S. (1998) 'The Cambrian-Silurian tectonic evolution of the northern Appalachians and British Caledonides: history of a complex, west and southwest Pacific- type segment of Iapetus', *Geological Society Special Publication*, 143, pp. 199–242.
Steinhoefel, G., Hegner, E. and Oliver, G. J. H. (2008) 'Chemical and Nd isotope constraints on granitoid sources involved in the Caledonian Orogeny in Scotland', *Journal of the Geological Society*, 165(4), pp. 817–827.
Stolz, A. J., Varne, R., Davies, G. R., Wheller, G. E. and Foden, J. D. (1990) 'Magma source components in an arc-continent collision zone: the Flores-Lembata sector, Sunda arc, Indonesia', *Contributions to Mineralogy and Petrology*, 105(5), pp. 585–601.
Stubseid, H. H. (2017) *Geological evolution and stratigraphic relationships of the ophiolitic terrane in the outer Hardangerfjord area: evidence from geochronology and geochemistry*. Master thesis. Bergen: University of Bergen.
Sturt, B. A., Thon, A. and Furnes, H. (1979) 'The Karmøy ophiolite, southwest Norway', *Geology*, 7(6), pp. 316–320.
Sturt, B. A., Thon, A. and Furnes, H. (1980) 'The geology and preliminary geochemistry of the Karmøy ophiolite, SW Norway', *Ophiolites*, pp. 438–554.
Sun, S. S. and McDonough, W. F. (1989) 'Chemical and isotopic systematics of oceanic basalts: Implications for mantle composition and processes', *Geological Society Special Publication*, 42(1), pp. 313–345.
Sønderholm, M. and Tirsgaard, H. (1993) 'Lithostratigraphic framework of the Upper Proterozoic Eleonore Bay Supergroup of East and North-East Greenland', *Bulletin Grønlands Geologiske Undersøgelse*, 167, pp. 1–38.
Taylor, R. J. M., Harley, S. L., Hinton, R. W., Elphick, S., Clark, C. and Kelly, M. (2015) 'Experimental determination of REE partition coefficients between zircon, garnet and melt: A key to understanding high-T crustal processes', *Journal of Metamorphic Geology*, 33(3), pp. 231–248.
Taylor, S. R. and McLennan, S. M. (1985) 'The continental crust: its composition and evolution'. United States: N.p.
Vermeesch, P. (2018) 'IsoplotR: A free and open toolbox for geochronology', *Geoscience*

Frontiers, 9(5), pp. 1479–1493.
Viken, A. L. (2017) *Accretionary history of Lower Ordovician island arc complexes on Bømlo: evidence from detrital zircon dating and geochemical data*. Master thesis. Bergen: University of Bergen.
Vroon, P. Z., van Bergen, M. J., White, W. M., Varekamp, J. C. (1993) 'Sr-Nd-Pb isotope systematics of the Banda Arc, Indonesia: combined subduction and assimilation of continental material', *Journal of Geophysical Research*, 98(B12).
Weinberg, R. F. and Geordie, M. (2008) 'Magma migration, folding, and disaggregation of migmatites in the Karakoram Shear Zone, Ladakh, NW India', *Bulletin of the Geological Society of America*, 120(7–8), pp. 994–1009.
White, W. M. (2013) *Geochemistry*. Itacha, New York: Wiley-Blackwell - A John Wiley & Son, Ltd., Publication.
Wiedenbeck, M., Corfu F., Griffin, W. L., Meier, M., Oberli, F., von Quadt, A., Roddick, J. C. and Spiegel, W. (1995) 'Three natural zircon standards for U-Th-Pb, Lu-Hf, trace element and REE analyses', *Geostandards Newsletter*, 19(1), pp. 1–23.
Wiest, J. D., Jacobs, J., Ksienzyk, A. K. and Fossen, H. (2018) 'Sveconorwegian vs. Caledonian orogenesis in the eastern Øygarden Complex, SW Norway – Geochronology, structural constraints and tectonic implications', *Precambrian Research*, 305(April 2017), pp. 1–18.

Appendixes

Appendix 1 – Sample description and sampling location

Appendix 2 – Major- and trace-elements analysis

Appendix 3 – LA-ICP-MS

Appendixes 1 – Sample descriptions and locations

Sample	Locality	Lithology	Analysis	Longitude	Latitude
20BREM01	Bremnes Migmatite Complex	Metatexite	Geochemistry	5.185	59.80027778
20BREM02	Bremnes Migmatite Complex	Restite	Geochemistry	5.185	59.80027778
20BREM04A	Sunnhordland Batholith	Appinite	Geochemistry	5.251111111	59.80111111
20BREM04B	Sunnhordland Batholith	Appinite	Geochemistry	5.15	59.795
20BREM04C	Sunnhordland Batholith	Appinite	Geochemistry	5.15	59.795
20BREM04D	Sunnhordland Batholith	Appinite	Geochemistry	5.148333333	59.79472222
20BREM04E	Bremnes Migmatite Complex	Restite	Geochemistry & Geochronology	5.15	59.795
20BREM04F	Bremnes Migmatite Complex	Restite	Geochemistry & Geochronology	5.148611111	59.79472222
20BREM05	Bremnes Migmatite Complex	Diatexite	Geochemistry	5.163333333	59.78861111
20BREM06B	Bremnes Migmatite Complex	Metatexite	Geochemistry	5.187222222	59.79694444
20BREM06C	Bremnes Migmatite Complex	Metatexite	Geochemistry	5.187222222	59.79694444
20BREM08A	Bremnes Migmatite Complex	Restite	Geochemistry & Geochronology	5.187777778	59.79694444
20BREM08B	Bremnes Migmatite Complex	Metatexite	Geochemistry	5.191388889	59.79277778
20BREM09D	Bremnes Migmatite Complex	Metatexite	Geochemistry	5.191388889	59.79333333
20BREM09E	Bremnes Migmatite Complex	Metatexite	Geochemistry	5.191388889	59.79333333
20BREM10B	Bremnes Migmatite Complex	Metatexie	Geochemistry & Geochronology	5.208055556	59.79888889
20BREM11B(1)	Vardafjell Gabbro	Gabbro	Geochemistry	5.2075	59.79916667
20BREM12(1)	Bremnes Migmatite Complex	Diatexite	Geochemistry	5.207222222	59.79916667
20BREM12(2)	Bremnes Migmatite Complex	Restite	Geochemistry	5.206944444	59.79916667
20BREM13	Bremnes Migmatite Complex	Diatexite	Geochemistry & Geochronology	5.206944444	59.79916667
20BREM14	Rolvsnes Granite	Granite	Geochemistry	5.175	59.80305556
20BREM15D	Sunnhordland Batholith	Appinite	Geochemistry	5.175	59.80333333
20BREM15E(1)	Bremnes Migmatite Complex	Metatexite	Geochemistry & Geochronology	5.298611111	59.79472222
20BREM15E(2)	Bremnes Migmatite Complex	Metatexite	Geochemistry & Geochronology	5.298611111	59.79472222
20BREM15K	Bremnes Migmatite Complex	Metatexite	Geochemistry	5.298888889	59.79472222
20BREM16A	Bremnes Migmatite Complex	Restite	Geochemistry	5.298888889	59.79472222

20BREM16B	Bremnes Migmatite Complex	Metatexite	Geochemistry	5.298611111	59.79444444
20BREM16E	Bremnes Migmatite Complex	Metatexite	Geochemistry	5.294166667	59.79388889
20BREM16H	Bremnes Migmatite Complex	Restite	Geochemistry & Geochronology	5.294166667	59.79388889
20BREM16I	Bremnes Migmatite Complex	Restite	Geochemistry & Geochronology	5.297222222	59.79611111
20BREM17	Vardafjell Gabbro	Gabbro	Geochemistry	5.297777778	59.79805556
20BREM18	Vardafjell Gabbro	Gabbro	Geochemistry	5.238055556	59.79555556
20BREM19	Vardafjell Gabbro	Gabbro	Geochemistry	5.238888889	59.79472222
20BREM21	Bremnes Migmatite Complex	Diatexite	Geochemistry	5.238888889	59.79472222
20BREM22	Vardafjell Gabbro	Gabbro	Geochemistry	5.238888889	59.79472222
20BREM23	Vardafjell Gabbro	Gabbro	Geochemistry	5.238888889	59.79472222
20BREM24A	Bremnes Migmatite Complex	Diatexite	Geochemistry	5.239166667	59.79472222
20BREM24B	Vardafjell Gabbro	Gabbro	Geochemistry	5.239444444	59.79388889
20BREM24C	Vardafjell Gabbro	Gabbro	Geochemistry	5.239722222	59.79388889
20BREM24D	Vardafjell Gabbro	Gabbro	Geochemistry	5.238888889	59.79472222
20BREMS1	Bremnes Migmatite Complex	Metatexite	Geochronology	5.2115863	59.7999675
20BREMS2	Bremnes Migmatite Complex	Metatexite	Geochronology	5.2115863	59.7999675

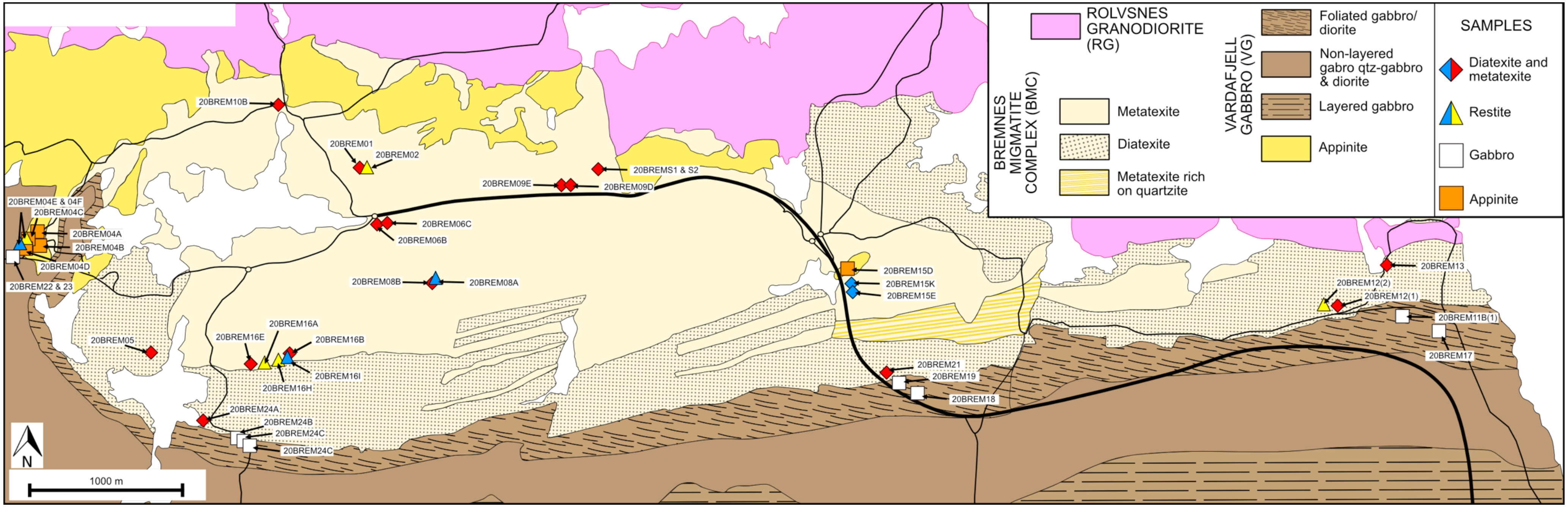
ROLVSNES GRANODIORITE (RG)
BREMNES MIGMATITE COMPLEX (BMC)
Metatexite
Diatexite
Metatexite rich on quartzite
VARDAFJELL GABBRO (VG)
Foliated gabbro/ diorite
Non-layered gabbro qtz-gabbro & diorite
Layered gabbro
Appinite
SAMPLES
Diatexite and metatexite
Restite
Gabbro
Appinite
20BREM10B
20BREM01
20BREM02
20BREMS1 & S2
20BREM09E
20BREM09D
20BREM04E & 04F
20BREM04C
20BREM04A
20BREM04B
20BREM04D
20BREM22 & 23
20BREM06C
20BREM06B
20BREM08B
20BREM08A
20BREM05
20BREM16A
20BREM16E
20BREM16B
20BREM16I
20BREM16H
20BREM24A
20BREM24B
20BREM24C
20BREM24C
20BREM15D
20BREM15K
20BREM15E
20BREM21
20BREM19
20BREM18
20BREM13
20BREM12(2)
20BREM12(1)
20BREM11B(1)
20BREM17
N
1000 m

Appendixes 2 – Major- and trace-elements analysis

Major-element analysis

Sample ID	Na_2O	MgO	Al_2O_3	SiO_2	P_2O_5	K_2O	CaO	TiO_2	MnO	Fe_2O_3	% LOI	SUM
20BREM01	2.53	1.75	16.64	53.03	1.42	1.49	7.03	1.13	0.31	12.76	0.97	99.07
20BREM02	2.60	2.32	18.28	58.45	0.21	3.08	1.73	1.28	0.23	10.34	1.01	99.52
20BREM04A	5.50	0.57	17.33	66.69	0.17	4.97	1.27	0.28	0.06	1.46	0.83	99.11
20BREM04B	3.50	0.39	14.15	69.53	0.10	5.57	1.52	0.21	0.06	1.17	0.57	96.77
20BREM04C	3.94	0.63	15.98	67.22	0.14	5.07	2.13	0.38	0.07	2.34	0.57	98.47
20BREM04D	3.45	2.52	16.35	59.12	0.45	4.78	5.31	0.94	0.13	4.94	0.57	98.54
20BREM04E	0.48	0.39	9.77	78.35	0.40	0.20	8.39	0.16	0.29	2.43	1.13	101.99
20BREM04F	0.38	1.73	16.20	57.93	1.15	0.45	12.20	1.01	0.41	6.13	2.21	99.80
20BREM05	1.90	2.21	19.16	58.80	0.18	2.77	1.20	1.41	0.15	9.43	2.49	99.69
20BREM06B	1.30	2.18	10.40	64.69	3.49	2.11	6.24	0.44	0.44	9.05	0.46	100.82
20BREM06C	2.21	2.61	19.58	56.95	0.22	3.51	1.50	1.28	0.24	9.58	2.09	99.77
20BREM08A	2.28	0.46	14.24	75.48	0.41	2.49	1.70	0.24	0.06	1.61	1.72	100.68
20BREM08B	1.90	2.90	19.06	56.40	0.30	3.75	1.39	1.34	0.16	8.99	3.34	99.53
20BREM09D	2.71	2.08	16.95	63.55	0.31	3.50	1.42	0.85	0.14	6.83	1.45	99.79
20BREM09E	2.18	2.79	17.06	61.07	0.21	3.35	1.63	1.12	0.20	8.39	2.03	100.03
20BREM10B	3.34	1.92	16.11	65.38	0.21	1.56	3.70	0.83	0.33	5.43	0.82	99.63
20BREM11B(1)	0.47	4.24	14.88	60.06	0.17	1.97	7.89	1.19	0.14	7.49	2.49	101.00
20BREM12(1)	2.04	2.16	18.48	59.78	0.22	3.23	1.18	1.08	0.12	8.50	2.98	99.76
20BREM12(2)	0.26	0.68	19.13	48.97	0.40	0.70	19.49	0.54	0.89	5.89	3.00	99.95
20BREM13	2.29	2.50	18.63	56.05	0.28	2.92	1.78	1.64	0.13	10.12	2.60	98.96
20BREM14	4.19	1.34	17.38	65.42	0.18	1.88	4.61	0.52	0.10	3.16	0.78	99.56
20BREM15D	4.30	3.15	16.41	53.64	0.72	2.58	5.86	1.31	0.14	7.40	1.60	97.10
20BREM15E(1)	0.50	1.61	18.42	58.45	0.26	1.89	9.07	0.63	0.26	5.97	2.68	99.75
20BREM15E(2)	1.88	1.53	15.24	71.14	0.09	2.32	1.46	0.65	0.09	5.41	0.89	100.71
20BREM15K	2.57	5.10	15.53	58.40	0.14	1.77	6.78	0.92	0.14	7.24	1.49	100.07

20BREM16A	3.55	2.59	19.17	56.23	0.18	2.60	3.55	1.30	0.22	8.63	1.38	99.42
20BREM16B	2.48	2.73	20.10	53.36	0.53	3.88	2.15	1.23	0.16	9.26	3.57	99.45
20BREM16E	1.40	2.36	17.35	60.78	0.41	3.43	1.30	0.98	0.14	9.58	2.13	99.87
20BREM16H	0.54	2.12	13.63	52.33	5.03	0.55	14.25	0.80	0.41	7.95	1.86	99.48
20BREM16I	2.60	0.61	17.76	64.56	1.45	2.07	6.92	0.16	0.14	2.21	1.38	99.86
20BREM17	2.41	7.43	14.53	49.24	0.18	1.28	9.82	1.39	0.16	9.98	1.97	98.40
20BREM18	2.89	6.15	15.78	51.85	0.19	1.14	9.12	1.41	0.15	9.63	1.75	100.07
20BREM19	2.66	5.66	14.89	52.71	0.22	1.46	8.43	1.56	0.15	9.10	3.08	99.92
20BREM21	2.22	2.24	17.72	61.62	0.17	2.55	1.45	1.13	0.14	8.37	2.73	100.34
20BREM22	2.62	5.29	14.79	56.59	0.16	2.53	6.73	1.10	0.14	8.12	1.91	99.99
20BREM23	3.65	4.09	17.58	48.48	0.80	2.95	7.43	1.69	0.13	9.54	2.06	98.41
20BREM24A	2.43	2.26	18.34	57.41	0.38	3.04	1.66	1.15	0.28	9.25	2.84	99.04
20BREM24B	3.57	4.88	15.14	54.26	0.16	2.62	7.78	1.16	0.14	7.83	1.59	99.13
20BREM24C	2.74	5.85	14.97	53.18	0.18	1.10	8.96	1.40	0.16	9.05	1.19	98.79
20BREM24D	2.28	6.34	15.42	50.41	0.21	2.24	9.37	1.72	0.18	10.51	1.31	99.99

Trace-element analysis (REE)

Sample ID	**La**	**Ce**	**Pr**	**Nd**	**Sm**	**Eu**	**Gd**	**Tb**	**Dy**	**Ho**	**Er**	**Tm**	**Yb**	**Lu**
Diatexites and metatexites (Bremnes Migmatite Complex)														
20BREM02	61.10	112.1	13.82	50.76	8.86	1.89	6.63	0.909	4.31	0.722	1.87	0.232	1.39	0.190
20BREM05	47.48	90.60	11.25	42.30	7.51	1.69	5.96	0.823	4.25	0.746	1.93	0.249	1.48	0.206
20BREM06B	37.71	82.04	12.46	61.63	24.07	3.22	23.80	2.72	13.20	2.13	4.78	0.548	3.05	0.398
20BREM06C	68.28	124.9	15.62	57.12	9.42	1.60	6.87	0.971	4.98	0.886	2.40	0.326	2.07	0.304
20BREM08B	65.10	119.2	14.94	55.20	9.70	1.65	7.53	1.07	5.58	0.977	2.54	0.328	1.95	0.268
20BREM09D	52.62	95.01	11.55	42.72	7.71	1.57	6.63	0.978	5.29	0.950	2.48	0.325	1.89	0.257
20BREM09E	55.81	99.96	12.07	44.48	7.38	1.46	5.79	0.747	3.58	0.587	1.45	0.170	0.973	0.129
20BREM10B	35.06	61.28	7.89	29.10	5.10	1.14	4.27	0.693	4.24	0.881	2.51	0.359	2.31	0.343
20BREM12(1)	50.27	92.92	11.66	42.77	7.14	1.60	5.34	0.751	3.89	0.682	1.79	0.227	1.34	0.185

20BREM13	44.17	85.78	10.69	40.94	7.45	1.84	6.24	0.866	4.65	0.833	2.17	0.274	1.58	0.210
20BREM15E(1)	14.68	34.30	3.93	15.18	2.88	1.01	2.75	0.414	2.40	0.478	1.29	0.176	1.06	0.158
20BREM15E(2)	23.17	46.94	5.27	19.37	3.22	0.906	2.55	0.339	1.76	0.320	0.860	0.117	0.738	0.109
20BREM15K	19.52	38.45	5.00	19.94	4.23	1.17	4.27	0.676	4.10	0.820	2.31	0.327	2.06	0.303
20BREM16B	66.15	119.1	15.08	56.43	10.40	1.95	9.22	1.38	7.91	1.50	4.06	0.551	3.28	0.438
20BREM16E	48.99	87.79	11.36	42.28	7.50	1.59	6.51	0.962	5.38	1.01	2.71	0.368	2.26	0.317
20BREM21	51.12	98.69	12.22	45.26	7.84	1.76	6.03	0.825	4.23	0.742	1.93	0.246	1.44	0.196
20BREM24A	46.45	94.95	11.15	41.67	7.77	1.46	6.57	1.00	5.88	1.14	3.26	0.483	3.11	0.439
Restites (Bremnes Migmatite Complex)														
20BREM01	42.19	85.54	11.52	48.19	11.86	2.76	10.37	1.45	7.31	1.29	3.24	0.405	2.36	0.332
20BREM04E	5.63	11.99	1.76	7.90	2.93	1.17	3.35	0.551	3.08	0.534	1.39	0.191	1.16	0.148
20BREM04F	53.11	107.0	13.24	55.71	14.43	4.23	14.05	1.78	8.40	1.40	3.50	0.456	2.74	0.389
20BREM08A	8.93	15.05	1.83	6.85	1.77	1.44	2.13	0.403	2.69	0.563	1.62	0.232	1.43	0.194
20BREM12(2)	8.37	17.17	2.48	9.78	3.00	1.52	4.22	0.744	4.47	0.845	2.27	0.331	2.08	0.279
20BREM16A	55.80	101.3	12.56	45.46	7.74	2.01	6.95	1.05	5.91	1.14	3.14	0.433	2.72	0.393
20BREM16H	61.78	134.9	18.67	88.93	27.06	9.70	32.94	4.14	19.64	3.11	6.83	0.748	4.01	0.530
20BREM16I	10.20	19.01	2.57	10.81	3.20	1.91	4.08	0.653	3.62	0.615	1.50	0.194	1.11	0.145
Gabbro (Vardafjell Gabbro)														
20BREM11B(1)	14.94	38.88	5.42	21.49	4.70	1.44	4.65	0.763	4.69	0.954	2.88	0.469	3.34	0.493
20BREM17	13.06	27.25	3.76	16.13	3.89	1.19	4.27	0.675	4.11	0.827	2.27	0.317	1.98	0.285
20BREM18	18.26	36.48	4.85	20.03	4.46	1.37	4.65	0.721	4.30	0.851	2.36	0.326	2.00	0.291
20BREM19	28.23	55.31	6.89	27.32	5.65	1.69	5.59	0.850	5.00	0.970	2.69	0.375	2.35	0.344
20BREM22	20.55	38.84	4.91	19.15	4.01	1.27	3.97	0.600	3.53	0.687	1.89	0.264	1.63	0.241
20BREM23	112.8	202.3	23.49	87.25	13.16	3.49	9.17	1.07	4.97	0.839	2.22	0.266	1.57	0.219
20BREM24B	19.75	37.46	4.87	19.46	4.19	1.28	4.15	0.631	3.69	0.717	1.98	0.273	1.69	0.246
20BREM24C	18.51	34.85	4.56	18.84	4.21	1.22	4.32	0.677	3.97	0.777	2.15	0.299	1.85	0.266
20BREM24D	17.57	35.76	4.95	21.12	4.85	1.48	5.01	0.767	4.52	0.888	2.41	0.327	2.03	0.286
Appinite (Sunnhordland Batholith)														
20BREM04A	51.37	68.47	6.28	18.89	2.38	0.890	1.75	0.242	1.29	0.251	0.750	0.109	0.714	0.113
20BREM04B	57.52	84.39	8.00	24.14	3.48	0.766	2.58	0.381	1.98	0.355	0.992	0.140	0.903	0.130

20BREM04C	101.0	146.9	14.16	43.12	5.84	1.18	3.82	0.469	2.11	0.368	1.04	0.132	0.871	0.134
20BREM04D	124.4	204.8	22.50	79.40	11.46	2.87	7.51	0.906	4.19	0.735	2.08	0.273	1.78	0.259
20BREM15D	112.1	194.2	21.78	77.02	10.87	2.96	7.25	0.838	3.79	0.644	1.73	0.202	1.19	0.163

Trace-element analysis (Spider-diagrams)

Sample ID	Th	U	Ta	Nb	La	Ce	Pb	Pr	Nd	Zr	Hf	Sm	Eu	Gd	Ti	Tb	Dy	Y	Ho	Yb
Diatexites and metatexites (Bremnes Migmatite Complex)																				
20BREM02	14.87	1.81	2.01	36.82	61.10	112.1	22.64	13.82	50.76	19.77	0.549	8.86	1.89	6.63	7673.60	0.909	4.31	19.48	0.722	1.39
20BREM05	12.49	2.49	1.87	24.15	47.48	90.60	18.16	11.25	42.30	31.29	0.877	7.51	1.69	5.96	8452.95	0.823	4.25	19.00	0.746	1.48
20BREM06B	3.54	2.11	1.43	26.14	37.71	82.04	10.49	12.46	61.63	29.42	0.647	24.07	3.22	23.80	2637.80	2.72	13.20	59.12	2.13	3.05
20BREM06C	17.37	2.16	2.21	36.24	68.28	124.9	25.50	15.62	57.12	44.99	1.24	9.42	1.60	6.87	7673.60	0.971	4.98	22.35	0.886	2.07
20BREM08B	16.39	2.45	2.24	34.85	65.10	119.2	18.38	14.94	55.20	24.51	0.697	9.70	1.65	7.53	8033.30	1.07	5.58	23.60	0.977	1.95
20BREM09D	13.40	2.08	1.68	26.31	52.62	95.01	21.79	11.55	42.72	27.55	0.795	7.71	1.57	6.63	5095.75	0.978	5.29	24.50	0.950	1.89
20BREM09E	12.02	2.07	1.80	31.43	55.81	99.96	19.27	12.07	44.48	22.64	0.630	7.38	1.46	5.79	6714.40	0.747	3.58	15.17	0.587	0.973
20BREM10B	11.23	1.99	1.21	20.36	35.06	61.28	15.23	7.89	29.10	40.92	1.15	5.10	1.14	4.27	4975.85	0.693	4.24	23.60	0.881	2.31
20BREM12(1)	12.78	2.33	1.56	26.27	50.27	92.92	18.31	11.66	42.77	31.67	0.913	7.14	1.60	5.34	6474.60	0.751	3.89	16.78	0.682	1.34
20BREM13	11.93	1.46	1.09	17.56	44.17	85.78	22.95	10.69	40.94	36.66	1.02	7.45	1.84	6.24	9831.80	0.866	4.65	21.13	0.833	1.58
20BREM15E(1)	4.49	1.06	0.629	8.31	14.68	34.30	13.68	3.93	15.18	17.25	0.561	2.88	1.01	2.75	3776.85	0.414	2.40	13.67	0.478	1.06
20BREM15E(2)	6.76	1.12	0.644	8.31	23.17	46.94	15.11	5.27	19.37	33.06	1.01	3.22	0.906	2.55	3896.75	0.339	1.76	8.18	0.320	0.738
20BREM15K	7.34	1.02	0.731	10.29	19.52	38.45	8.72	5.00	19.94	27.88	1.10	4.23	1.17	4.27	5515.40	0.676	4.10	21.51	0.820	2.06
20BREM16B	16.79	2.43	1.91	31.40	66.15	119.1	21.83	15.08	56.43	51.61	1.47	10.40	1.95	9.22	7373.85	1.38	7.91	36.29	1.50	3.28
20BREM16E	13.19	2.18	1.61	21.72	48.99	87.79	21.94	11.36	42.28	40.11	1.16	7.50	1.59	6.51	5875.10	0.962	5.38	24.21	1.01	2.26
20BREM21	13.73	1.67	1.57	25.04	51.12	98.69	21.66	12.22	45.26	16.24	0.477	7.84	1.76	6.03	6774.35	0.825	4.23	17.80	0.742	1.44
20BREM24A	17.01	2.20	2.11	33.01	46.45	94.95	18.01	11.15	41.67	26.03	0.733	7.77	1.46	6.57	6894.25	1.00	5.88	26.86	1.14	3.11
Restites (Bremnes Migmatite Complex)																				
20BREM01	14.23	1.80	1.75	26.95	42.19	85.54	14.89	11.52	48.19	31.92	0.855	11.86	2.76	10.37	6774.35	1.45	7.31	39.29	1.29	2.36
20BREM04E	0.360	0.587	0.198	3.20	5.63	11.99	3.34	1.76	7.90	5.03	0.185	2.93	1.17	3.35	959.20	0.551	3.08	18.19	0.534	1.16
20BREM04F	9.46	1.58	1.66	37.01	53.11	107.0	11.34	13.24	55.71	33.99	0.990	14.43	4.23	14.05	6054.95	1.78	8.40	41.98	1.40	2.74

20BREM08A	1.76	0.753	0.471	4.85	8.93	15.05	21.08	1.83	6.85	6.69	0.198	1.77	1.44	2.13	1438.80	0.403	2.69	14.73	0.563	1.43
20BREM12(2)	1.43	1.06	1.09	34.53	8.37	17.17	6.90	2.48	9.78	17.86	0.610	3.00	1.52	4.22	3237.30	0.744	4.47	26.33	0.845	2.08
20BREM16A	15.76	1.73	2.22	34.30	55.80	101.3	18.01	12.56	45.46	105.8	3.00	7.74	2.01	6.95	7793.50	1.05	5.91	28.83	1.14	2.72
20BREM16H	9.16	2.09	1.42	26.36	61.78	134.9	6.94	18.67	88.93	29.99	0.801	27.06	9.70	32.94	4796.00	4.14	19.64	101.3	3.11	4.01
20BREM16I	0.831	0.915	0.379	7.67	10.20	19.01	14.00	2.57	10.81	2.86	0.107	3.20	1.91	4.08	959.20	0.653	3.62	17.72	0.615	1.11
Gabbro (Vardafjell Gabbro)																				
20BREM11B(1)	2.47	1.79	3.54	21.40	14.94	38.88	5.74	5.42	21.49	15.21	0.927	4.70	1.44	4.65	7134.05	0.763	4.69	26.82	0.954	3.34
20BREM17	3.04	0.742	0.700	9.50	13.06	27.25	7.35	3.76	16.13	28.48	1.60	3.89	1.19	4.27	8333.05	0.675	4.11	21.00	0.827	1.98
20BREM18	5.73	1.10	0.863	11.52	18.26	36.48	7.08	4.85	20.03	34.68	1.62	4.46	1.37	4.65	8452.95	0.721	4.30	22.04	0.851	2.00
20BREM19	7.97	2.08	1.30	15.66	28.23	55.31	8.11	6.89	27.32	27.24	1.59	5.65	1.69	5.59	9352.20	0.850	5.00	24.95	0.970	2.35
20BREM22	15.75	2.59	0.789	10.89	20.55	38.84	9.24	4.91	19.15	19.43	0.948	4.01	1.27	3.97	6594.50	0.600	3.53	17.58	0.687	1.63
20BREM23	25.84	5.26	2.49	41.38	112.8	202.3	12.97	23.49	87.25	85.21	2.58	13.16	3.49	9.17	10131.55	1.07	4.97	21.48	0.839	1.57
20BREM24B	7.37	2.28	1.07	11.1	19.75	37.46	7.21	4.87	19.46	27.72	1.37	4.19	1.28	4.15	6954.20	0.631	3.69	18.10	0.717	1.69
20BREM24C	6.32	2.39	0.948	11.92	18.51	34.85	10.42	4.56	18.84	22.07	1.27	4.21	1.22	4.32	8033.30	0.677	3.97	19.68	0.777	1.85
20BREM24D	2.69	0.972	0.917	12.53	17.57	35.76	7.24	4.95	21.12	29.19	1.58	4.85	1.48	5.01	10311.40	0.767	4.52	21.98	0.888	2.03
Appinite (Sunnhordland Batholith)																				
20BREM04A	39.99	6.99	1.63	23.73	51.37	68.47	18.50	6.28	18.89	116.2	2.55	2.38	0.890	1.75	1678.60	0.242	1.29	8.23	0.251	0.714
20BREM04B	45.75	22.06	2.78	42.43	57.52	84.39	35.17	8.00	24.14	93.06	2.13	3.48	0.766	2.58	1258.95	0.381	1.98	10.29	0.355	0.903
20BREM04C	73.40	10.91	1.67	31.52	101.0	146.9	48.17	14.16	43.12	160.5	3.88	5.84	1.18	3.82	2218.15	0.469	2.11	10.74	0.368	0.871
20BREM04D	43.66	8.82	3.80	53.94	124.4	204.8	30.64	22.50	79.40	172.7	4.13	11.46	2.87	7.51	5275.60	0.906	4.19	21.34	0.735	1.78
20BREM15D	33.24	7.58	3.26	48.83	112.1	194.2	13.30	21.78	77.02	144.4	3.71	10.87	2.96	7.25	7853.45	0.838	3.79	17.13	0.644	1.19

Appendixes 3 – LA-ICP-MS

Laboratory & Sample Preparation	
Laboratory name	Department of Earth Science, University of Bergen
Sample type/mineral	Zircon
Sample preparation	Conventional mineral separation, 2.5 cm resin mount, 0.025 m polish to finish
Imaging	CL, Zeiss Supra55 VP, 15 kV, 1 nA, 15mm working distance
Laser ablation system	
Make, Model & type	RESOlution M-50 LR with a Coherent COMPexPRO® 110 193 nm ArF excimer laser
Ablation cell & volume	Two volume
Laser wavelength	193 nm
Pulse duration	20 ns
Fluence	2.2 - 2.5 $J.cm^{-2}$
Repetition rate	5 Hz
Ablation duration	30 secs
Spot diameter	19 and 26 µm
Sampling mode / pattern	Static spot ablation/circular
Carrier gas	He (0.75 l/min) with small amounts of N2 (0.004 ml/min) mixed in before entering the ICP-MS to increase sensitivity.
Signal smoothing device	"Squid" connected between the laser and the ICP-MS
ICP-MS Instrument	
Make, Model & type	Nu Instruments, Nu Attom HR, SC-ICP-MS
Sample introduction	Ablation aerosol from laser ablation
RF power	1300W
Cool gas	Ar 13 l/min
Aux gas	Ar 0.7 l/min
Make-up gas flow	Ar 0.49 l/min
Detection system	MasCom Electron Multiplier
Masses measured	^{202}Hg, ^{204}(Hg + Pb), ^{206}Pb, ^{207}Pb, ^{208}Pb, ^{232}Th, ^{238}U
Integration time per peak/dwell times	200µs for ^{202}Hg, ^{204}(Hg + Pb), ^{206}Pb, ^{208}Pb, ^{232}Th, ^{238}U 800 µs for ^{207}Pb and ^{235}U
Number of sweeps per cycle	10
Total time per cycle	0.0493 s
Analysis method	Deflector jump
IC Dead time	14 ns
Detection Mode	Ion counting mode and ion-attenuated mode
Data Processing	
Gas blank	15 s

Calibration strategy	91500 (Wiedenbeck et al., 1995) used as primary reference material, while Plesovice (Sláma et al., 2008), Mud Tank (Horstwood et al., 2016), & GJ1 (nr. 63; Jackson et al., 2004) are used as secondaries.
Data processing package used / Correction for LIEF	Iolite4 (v. 4.4.5) for data normalization, uncertainty propagation and age calculation. LIEF correction assumes reference material and samples behave identically.
Common-Pb correction	No common-Pb correction applied to the data. Analysis that are marked or cleared contain a significant amount of common lead, see table below.
Data reduction	VizualAge UComPbine (Chew et al. 2014)
Down-hole correction model	Exponential or Exponential + linear
Uncertainty level & propagation	Ages are quoted at 2*s* absolute, propagation is by quadratic addition.
Quality control / Validation	**<u>Run 1 – LAS393 and LAS394</u>** *Plêsovice* – Wtd ave $^{206}Pb/^{238}U$ age = 334.83 ± 0.72 Ma (1*s*, MSWD = 6.28, n = 89/90) *GJ-1* – Wtd ave $^{206}Pb/^{238}U$ age = 589.44 ± 1.49 Ma (1*s*, MSWD = 21.6, n = 87/90) *91500* – Wtd ave $^{206}Pb/^{238}U$ age = 1045.40 ± 3.43 Ma (1*s*, MSWD = 14.3, n = 88/90) Systematic uncertainty for propagation is 1% (1*s*). **<u>Run 2 – LAS396, LAS397 and LAS398:</u>** *Plêsovice* – Wtd ave $^{206}Pb/^{238}U$ age = 345.02 ± 0.691 Ma (1*s*, MSWD = 21.4, n = 141/144) *GJ-1* – Wtd ave $^{206}Pb/^{238}U$ age = 598.17 ± 1.17 Ma (1*s*, MSWD = 24.5, n = 142/144) *91500* – Wtd ave $^{206}Pb/^{238}U$ age = 1053.90 ± 1.56 Ma (1*s*, MSWD = 4.49, n = 144/144) Systematic uncertainty for propagation is 1% (1*s*). **<u>Run 3 – LAS399, LAS400 and LAS401:</u>** *Plêsovice* – Wtd ave $^{206}Pb/^{238}U$ age = 340.06 ± 1.19 Ma (1*s*, MSWD = 22.6, n = 150/150) *GJ-1* – Wtd ave $^{206}Pb/^{238}U$ age = 595.52 ± 1.40 Ma (1*s*, MSWD = 11.9, n = 150/150)

	91500 – Wtd ave $^{206}Pb/^{238}U$ age = 1051.40 ± 2.31 Ma (1*s*, MSWD = 3.10, n = 149/149) Systematic uncertainty for propagation is 1% (1*s*). **Run 4 – LAS395 and LAS402:** **LAS402 (*26 µm*)** *Plêsovice* – Wtd ave $^{206}Pb/^{238}U$ age = 348.25 ± 1.74 Ma (1*s*, MSWD = 29.8, n = 74/76) *GJ-1* – Wtd ave $^{206}Pb/^{238}U$ age = 612.89 ± 4.93 Ma (1*s*, MSWD = 270, n = 75/76) *91500* – Wtd ave $^{206}Pb/^{238}U$ age = 1046.95 ± 1.98 Ma (1*s*, MSWD = 3.47, n = 78/78) **LAS395 (*19 µm*)** *Plêsovice* – Wtd ave $^{206}Pb/^{238}U$ age = 343.73 ± 5.05 Ma (1*s*, MSWD = 503, n = 62/64) *GJ-1* – Wtd ave $^{206}Pb/^{238}U$ age = 611.36 ± 5.85 Ma (1*s*, MSWD = 236, n = 64/64) *91500* – Wtd ave $^{206}Pb/^{238}U$ age = 1025.87 ± 2.85 Ma (1*s*, MSWD = 1.82, n = 62/64) Systematic uncertainty for propagation is 1% (1*s*).
Data reporting	Reported in the format of the plasmage.org data reporting template (http://www.plasmage.org/recommendations/home.html) using a python script made by Joe Petrus (https://github.com/iolite-LA-ICP-MS/iolite4-python-examples/blob/master/export/PlasmAge.py).
Data visualization	Plotting of KDE using IsoplotR (Vermesch, 2018).

LAS393 (20BREM04E)														
	Isotopic Ratios							Calculated ages (Ma)						
ID	$^{207}Pb/^{235}U$	2σ	$^{206}Pb/^{238}U$	2σ	Rho	$^{207/206}Pb$	2σ	$^{207/206}Pb$	2σ	$^{206}Pb/^{238}U$	2σ	$^{207}Pb/^{235}U$	2σ	%conc
LAS393_Shot_7_Grain_1	2.0908	0.5	0.19286	0.5	0.64	0.08030	0.44	1196	22	1136	23	1145	19	99.3
LAS393_Shot_8_Grain_2	1.5688	0.5	0.15947	0.5	0.73	0.07263	0.37	997	21	954	20	956	17	99.8
LAS393_Shot_9_Grain_3	2.1795	0.4	0.19816	0.4	0.74	0.08133	0.31	1226	19	1165	23	1174	19	99.2
LAS393_Shot_10_Grain_4	0.6963	2.0	0.08604	1.1	0.17	0.06087	2.12	897	68	531	15	528	19	100.7
LAS393_Shot_11_Grain_5	4.5307	0.5	0.30104	0.4	0.63	0.11092	0.37	1808	19	1697	33	1735	22	97.8
LAS393_Shot_12_Grain_6	2.0914	0.5	0.19382	0.4	0.51	0.07948	0.42	1177	22	1141	23	1144	18	99.8
LAS393_Shot_13_Grain_7	1.2281	0.8	0.13080	0.7	0.89	0.06896	0.35	892	21	792	18	810	16	97.7
LAS393_Shot_14_Grain_8	2.7798	0.5	0.22275	0.4	0.59	0.09167	0.45	1453	22	1297	25	1347	20	96.2
LAS393_Shot_15_Grain_9	2.5834	0.5	0.21895	0.4	0.31	0.08682	0.55	1346	26	1276	25	1294	20	98.6
LAS393_Shot_16_Grain_10	1.7196	0.8	0.16202	0.6	0.25	0.07800	0.88	1119	38	969	21	1012	19	95.8
LAS393_Shot_17_Grain_11	1.3354	0.9	0.13922	0.6	0.39	0.07055	0.83	921	37	841	19	858	17	98.1
LAS393_Shot_18_Grain_12	2.6397	0.5	0.22921	0.5	0.02	0.08446	0.48	1294	23	1330	26	1310	19	101.5
LAS393_Shot_19_Grain_13	1.8536	0.7	0.18224	0.5	0.22	0.07483	0.78	1040	35	1078	22	1062	19	101.5
LAS393_Shot_20_Grain_14	7.9277	0.4	0.37358	0.4	0.56	0.15545	0.40	2401	18	2045	38	2221	24	92.1
LAS393_Shot_27_Grain_15	4.4757	0.4	0.29454	0.4	0.65	0.11113	0.32	1814	18	1663	31	1725	22	96.4
LAS393_Shot_28_Grain_16	3.0810	0.5	0.22155	0.4	0.33	0.10184	0.51	1650	23	1289	25	1426	21	90.4
LAS393_Shot_29_Grain_17	2.8995	0.5	0.24304	0.5	0.62	0.08721	0.33	1360	19	1401	28	1379	20	101.6
LAS393_Shot_30_Grain_18	2.3767	0.5	0.20740	0.5	0.70	0.08351	0.37	1278	21	1216	25	1233	19	98.6
LAS393_Shot_31_Grain_19	2.1577	0.5	0.19155	0.4	0.58	0.08243	0.42	1248	22	1129	22	1166	19	96.8
LAS393_Shot_32_Grain_20	0.7073	1.1	0.08770	0.6	0.15	0.05950	1.21	681	45	542	12	541	14	100.0
LAS393_Shot_33_Grain_21	1.8892	0.9	0.18407	0.5	0.11	0.07525	0.97	1040	42	1089	22	1072	20	101.6
LAS393_Shot_34_Grain_22	4.1950	0.4	0.28765	0.3	0.45	0.10668	0.39	1737	19	1630	30	1671	21	97.5
LAS393_Shot_35_Grain_23	1.5900	0.5	0.15844	0.4	0.33	0.07348	0.40	1019	22	948	19	965	17	98.2
LAS393_Shot_36_Grain_24	11.8748	0.4	0.47702	0.4	0.55	0.18239	0.38	2670	17	2512	44	2593	25	96.9
LAS393_Shot_37_Grain_25	1.9317	0.5	0.18752	0.5	0.36	0.07547	0.57	1069	27	1107	22	1090	18	101.5
LAS393_Shot_39_Grain_27	1.8077	0.8	0.17670	0.5	0.22	0.07524	0.84	1046	38	1048	22	1044	19	100.4
LAS393_Shot_40_Grain_28	2.8390	0.7	0.22941	0.5	0.33	0.09094	0.69	1424	30	1330	27	1362	22	97.7
LAS393_Shot_47_Grain_29	6.3170	1.0	0.27733	0.9	0.93	0.16664	0.39	2519	18	1574	36	2009	27	78.4
LAS393_Shot_48_Grain_30	4.5466	0.4	0.32091	0.4	0.54	0.10399	0.40	1692	20	1793	33	1738	22	103.2
LAS393_Shot_49_Grain_31	2.7861	0.5	0.23377	0.5	0.42	0.08801	0.54	1370	25	1353	27	1351	20	100.2
LAS393_Shot_50_Grain_32	1.5992	0.4	0.15851	0.4	0.67	0.07405	0.34	1039	21	948	19	969	17	97.8
LAS393_Shot_51_Grain_33	4.9729	0.7	0.31287	0.6	0.38	0.11701	0.73	1896	29	1754	36	1811	24	96.9

LAS393_Shot_52_Grain_34	3.4308	0.6	0.26961	0.4	0.28	0.09365	0.62	1492	27	1538	30	1508	22	102.0
LAS393_Shot_53_Grain_35	2.9067	0.5	0.24225	0.4	0.47	0.08823	0.51	1377	25	1398	27	1381	21	101.2
LAS393_Shot_54_Grain_36	4.1421	0.4	0.27089	0.4	0.64	0.11220	0.36	1830	19	1544	29	1661	22	93.0
LAS393_Shot_55_Grain_37	3.0475	0.5	0.24143	0.4	0.30	0.09279	0.53	1472	25	1394	27	1418	21	98.3
LAS393_Shot_56_Grain_38	1.8924	0.7	0.18735	0.5	0.30	0.07453	0.70	1037	31	1106	23	1076	19	102.8
LAS393_Shot_57_Grain_39	7.1657	0.8	0.30466	0.7	0.78	0.17190	0.49	2569	21	1713	37	2126	27	80.6
LAS393_Shot_58_Grain_40	1.9559	0.6	0.18916	0.4	0.25	0.07589	0.63	1076	30	1116	22	1098	19	101.7
LAS393_Shot_59_Grain_41	1.8143	0.8	0.17474	0.6	0.04	0.07644	0.87	1082	35	1037	22	1045	20	99.2
LAS393_Shot_60_Grain_42	2.4476	0.5	0.21171	0.4	0.44	0.08453	0.48	1294	24	1237	24	1255	19	98.6
LAS393_Shot_67_Grain_43	2.2805	0.5	0.20386	0.4	0.34	0.08215	0.48	1238	24	1196	23	1204	19	99.3
LAS393_Shot_68_Grain_44	1.3235	0.4	0.13574	0.4	0.65	0.07145	0.33	965	21	821	17	855	15	95.9
LAS393_Shot_69_Grain_45	2.7641	0.5	0.23141	0.4	0.28	0.08785	0.49	1368	24	1341	26	1345	20	99.7
LAS393_Shot_70_Grain_46	1.7840	0.5	0.17366	0.5	0.73	0.07535	0.38	1073	21	1032	21	1039	18	99.3
LAS393_Shot_71_Grain_47	1.8337	0.7	0.18198	0.5	0.18	0.07419	0.76	1019	34	1077	22	1054	19	102.2
LAS393_Shot_72_Grain_48	7.1303	0.4	0.33361	0.4	0.62	0.15691	0.36	2418	17	1855	35	2126	23	87.2
LAS393_Shot_73_Grain_49	1.7002	0.8	0.16592	0.5	0.21	0.07545	0.78	1051	35	989	21	1004	19	98.5
LAS393_Shot_74_Grain_50	2.1798	0.7	0.19711	0.5	0.48	0.08098	0.63	1212	29	1159	24	1171	20	98.9
LAS393_Shot_75_Grain_51	1.6344	1.3	0.16107	0.8	0.16	0.07590	1.41	1092	54	961	23	976	22	98.5
LAS393_Shot_76_Grain_52	4.7432	0.5	0.31068	0.5	0.59	0.11243	0.45	1830	21	1743	33	1772	22	98.3
LAS393_Shot_77_Grain_53	2.1497	0.5	0.19350	0.5	0.47	0.08132	0.51	1220	25	1140	23	1163	19	98.0
LAS393_Shot_78_Grain_54	13.2217	0.6	0.52237	0.6	0.40	0.18749	0.69	2705	26	2704	52	2689	27	100.5
LAS393_Shot_80_Grain_56	4.5823	0.4	0.30814	0.5	0.52	0.10936	0.44	1783	21	1730	33	1744	22	99.2
LAS393_Shot_87_Grain_57	1.6804	0.6	0.16786	0.4	0.27	0.07399	0.63	1026	29	1000	20	999	18	100.1
LAS393_Shot_88_Grain_58	9.5580	0.3	0.34230	0.4	0.25	0.20591	0.35	2869	16	1897	35	2391	24	79.3
LAS393_Shot_89_Grain_59	2.9117	0.7	0.24080	0.5	0.32	0.08945	0.69	1397	30	1390	28	1382	21	100.5
LAS393_Shot_90_Grain_60	1.8166	0.5	0.17764	0.4	0.43	0.07552	0.52	1071	25	1054	21	1050	18	100.3
LAS393_Shot_91_Grain_61	2.2689	0.5	0.20559	0.5	0.76	0.08142	0.37	1226	21	1205	25	1201	19	100.4
LAS393_Shot_92_Grain_62	5.3159	0.4	0.33886	0.3	0.39	0.11567	0.41	1883	20	1880	34	1870	22	100.6
LAS393_Shot_93_Grain_63	10.2087	1.0	0.47969	0.9	0.42	0.15827	1.06	2413	39	2516	55	2442	31	103.0
LAS393_Shot_94_Grain_64	1.8511	1.0	0.17709	0.6	0.10	0.07755	1.10	1104	47	1052	23	1058	22	99.4
LAS393_Shot_95_Grain_65	0.7500	2.1	0.08550	1.0	0.03	0.06627	2.34	1034	77	528	15	554	21	95.3
LAS393_Shot_96_Grain_66	4.3889	0.4	0.28191	0.4	0.68	0.11498	0.33	1875	18	1600	30	1709	22	93.6
LAS393_Shot_97_Grain_67	3.6295	0.4	0.26945	0.4	0.49	0.09933	0.39	1606	20	1537	29	1555	21	98.9
LAS393_Shot_98_Grain_68	1.9494	0.6	0.18894	0.5	0.50	0.07608	0.49	1088	25	1117	22	1096	18	101.9
LAS393_Shot_99_Grain_69	12.3103	0.6	0.49198	0.6	0.51	0.18505	0.62	2688	24	2575	49	2624	26	98.1

LAS393_Shot_100_Grain_70	2.4796	0.5	0.20930	0.4	0.49	0.08730	0.44	1359	22	1224	24	1265	19	96.8
LAS393_Shot_107_Grain_71	3.0825	0.5	0.24482	0.4	0.34	0.09241	0.51	1471	24	1411	27	1426	21	99.0
LAS393_Shot_108_Grain_72	3.6488	0.4	0.26775	0.3	0.46	0.10016	0.35	1623	19	1529	28	1559	21	98.1
LAS393_Shot_109_Grain_73	1.8454	1.0	0.17855	0.6	-0.05	0.07651	1.09	1068	45	1058	23	1054	21	100.4
LAS393_Shot_110_Grain_74	1.7457	0.4	0.17171	0.3	0.39	0.07451	0.44	1047	23	1021	20	1024	17	99.7
LAS393_Shot_111_Grain_75	2.6464	0.5	0.22168	0.4	0.41	0.08787	0.51	1368	24	1290	25	1312	20	98.3
LAS393_Shot_112_Grain_76	3.0331	1.0	0.24669	0.8	0.14	0.09195	1.23	1414	49	1418	33	1410	25	100.6
LAS393_Shot_113_Grain_77	1.4528	0.6	0.14995	0.4	0.24	0.07121	0.61	944	30	901	18	909	17	99.2
LAS393_Shot_114_Grain_78	3.4753	0.4	0.27279	0.4	0.54	0.09371	0.40	1496	20	1554	29	1521	21	102.2
LAS393_Shot_115_Grain_79	1.7734	0.8	0.17189	0.6	0.44	0.07584	0.77	1070	34	1022	22	1033	19	98.9
LAS393_Shot_116_Grain_80	1.5216	0.8	0.15617	0.5	0.21	0.07140	0.87	953	38	935	20	936	18	99.8
LAS393_Shot_117_Grain_81	2.8572	0.7	0.23748	0.5	0.04	0.08831	0.74	1373	31	1373	27	1366	22	100.6
LAS393_Shot_118_Grain_82	1.7810	0.6	0.18123	0.4	0.23	0.07223	0.68	975	31	1073	21	1036	18	103.5
LAS393_Shot_119_Grain_83	2.0755	0.5	0.19507	0.5	0.72	0.07796	0.38	1138	21	1149	24	1140	19	100.7
LAS393_Shot_120_Grain_84	11.8256	0.4	0.46571	0.4	0.56	0.18598	0.39	2701	18	2463	44	2588	25	95.2
LAS393_Shot_127_Grain_85	1.2106	0.6	0.12534	0.5	0.58	0.07003	0.48	921	25	762	16	804	15	94.8
LAS393_Shot_128_Grain_86	13.1025	0.5	0.50996	0.5	0.52	0.18747	0.50	2712	21	2653	48	2684	26	98.9
LAS393_Shot_129_Grain_87	2.6080	0.6	0.22460	0.4	0.35	0.08465	0.57	1292	27	1305	25	1300	20	100.4
LAS393_Shot_130_Grain_88	1.8303	0.7	0.17786	0.5	0.33	0.07503	0.68	1051	32	1055	21	1054	19	100.0
LAS393_Shot_131_Grain_89	1.8406	0.5	0.17962	0.4	0.41	0.07492	0.51	1054	25	1064	21	1059	18	100.5
LAS393_Shot_132_Grain_90	5.2192	0.5	0.32938	0.4	0.29	0.11563	0.56	1882	23	1834	34	1854	23	98.9
LAS393_Shot_133_Grain_91	2.4912	0.4	0.21319	0.4	0.21	0.08525	0.44	1312	22	1245	24	1268	19	98.2
LAS393_Shot_134_Grain_92	6.5944	1.0	0.35555	0.8	0.23	0.13639	1.10	2151	43	1958	44	2050	29	95.5
LAS393_Shot_135_Grain_93	4.9466	0.4	0.31299	0.4	0.54	0.11527	0.36	1878	18	1755	32	1809	22	97.0
LAS393_Shot_136_Grain_94	4.5466	0.4	0.29404	0.4	0.14	0.11279	0.42	1840	20	1661	31	1737	22	95.6
LAS393_Shot_137_Grain_95	1.7660	0.5	0.16992	0.4	0.46	0.07585	0.44	1083	23	1011	20	1032	17	98.0
LAS393_Shot_138_Grain_96	14.1287	0.5	0.52481	0.5	0.51	0.19680	0.46	2793	19	2716	49	2756	25	98.6
LAS393_Shot_139_Grain_97	1.1548	0.6	0.11951	0.4	0.20	0.07073	0.65	931	30	728	15	778	15	93.5
LAS393_Shot_140_Grain_98	1.9477	0.8	0.17357	0.7	0.74	0.08223	0.75	1233	30	1033	21	1095	19	94.4
LAS393_Shot_147_Grain_99	2.7947	0.4	0.22465	0.4	0.35	0.09105	0.45	1439	22	1306	25	1352	20	96.6
LAS393_Shot_148_Grain_100	2.6816	0.7	0.19885	0.6	0.80	0.09876	0.41	1593	21	1168	24	1320	21	88.5
LAS393_Shot_149_Grain_101	2.2409	0.9	0.21401	0.7	0.37	0.07697	0.89	1085	40	1249	27	1188	22	105.1
LAS393_Shot_150_Grain_102	2.3827	0.6	0.21043	0.5	0.23	0.08312	0.70	1253	31	1230	25	1234	20	99.7
LAS393_Shot_151_Grain_103	3.8618	0.5	0.28260	0.4	0.26	0.10003	0.54	1612	24	1604	30	1603	22	100.0
LAS393_Shot_152_Grain_104	1.8504	0.5	0.17908	0.4	0.67	0.07565	0.40	1079	22	1061	21	1063	18	99.9

LAS393_Shot_153_Grain_105	2.8219	0.7	0.19334	0.5	0.37	0.10704	0.67	1731	28	1139	23	1359	21	83.8
LAS393_Shot_154_Grain_106	3.6864	1.1	0.19670	0.8	0.91	0.13677	0.48	2178	21	1155	27	1557	26	74.2
LAS393_Shot_155_Grain_107	8.1576	0.4	0.40754	0.4	0.56	0.14671	0.34	2303	17	2204	39	2247	24	98.1
LAS393_Shot_156_Grain_108	1.7820	0.7	0.17315	0.5	0.22	0.07561	0.76	1063	34	1029	21	1035	19	99.4
LAS393_Shot_157_Grain_109	1.4896	1.0	0.14422	0.9	0.88	0.07537	0.45	1070	23	867	21	921	19	94.2
LAS393_Shot_158_Grain_110	2.0044	0.7	0.18924	0.5	0.27	0.07793	0.71	1128	32	1117	22	1114	19	100.2
LAS393_Shot_159_Grain_111	9.9317	0.4	0.40479	0.4	0.66	0.18036	0.34	2653	16	2189	40	2427	25	90.2
LAS393_Shot_160_Grain_112	1.9439	0.6	0.18481	0.5	0.36	0.07732	0.59	1115	28	1093	22	1094	18	99.9
LAS393_Shot_167_Grain_113	1.8945	0.5	0.18700	0.4	0.46	0.07438	0.49	1044	25	1105	22	1078	18	102.5
LAS393_Shot_168_Grain_114	1.7791	0.8	0.17225	0.5	0.17	0.07603	0.82	1071	37	1024	21	1034	19	99.1
LAS393_Shot_169_Grain_115	2.3141	0.6	0.18991	0.5	0.73	0.08950	0.38	1409	20	1120	23	1215	19	92.2
LAS393_Shot_170_Grain_116	2.2671	0.8	0.21866	0.8	0.62	0.07644	0.68	1088	31	1273	29	1198	21	106.3
LAS393_Shot_171_Grain_117	1.5662	0.5	0.15506	0.4	0.71	0.07424	0.34	1044	20	929	19	956	16	97.2
LAS393_Shot_172_Grain_118	3.8876	0.4	0.27572	0.4	0.60	0.10361	0.39	1683	20	1570	30	1609	21	97.6
LAS393_Shot_173_Grain_119	3.1622	0.8	0.25067	0.6	0.25	0.09317	0.84	1469	35	1440	29	1443	23	99.8
LAS393_Shot_174_Grain_120	9.9526	0.4	0.39807	0.4	0.41	0.18398	0.44	2683	19	2160	40	2428	24	89.0
LAS393_Shot_175_Grain_121	1.3616	1.2	0.13782	1.0	0.91	0.07237	0.48	988	25	831	22	864	21	96.1
LAS393_Shot_176_Grain_122	3.0798	1.0	0.15824	0.7	0.87	0.14213	0.56	2244	23	946	22	1416	26	66.8
LAS393_Shot_177_Grain_123	1.9728	0.6	0.19376	0.5	0.82	0.07468	0.32	1055	20	1141	23	1104	19	103.3
LAS393_Shot_178_Grain_124	2.2272	1.0	0.20599	0.7	0.19	0.08014	1.11	1161	46	1206	27	1183	22	101.9
LAS393_Shot_179_Grain_125	2.4514	0.5	0.21091	0.5	0.49	0.08579	0.49	1324	24	1234	25	1256	19	98.2
LAS393_Shot_180_Grain_126	1.7750	0.7	0.17543	0.7	0.69	0.07486	0.57	1050	27	1041	23	1033	19	100.7
LAS393_Shot_187_Grain_127	4.7579	0.5	0.32127	0.4	0.38	0.10921	0.49	1778	22	1795	33	1775	23	101.1
LAS393_Shot_188_Grain_128	2.0605	0.6	0.18700	0.4	0.23	0.08118	0.61	1215	29	1105	22	1134	19	97.4
LAS393_Shot_189_Grain_129	1.8028	0.9	0.17710	0.5	0.17	0.07523	0.97	1046	41	1051	22	1041	20	100.9
LAS393_Shot_190_Grain_130	2.1996	0.9	0.21392	0.6	0.21	0.07613	0.90	1071	41	1248	26	1175	21	106.3
LAS393_Shot_191_Grain_131	2.0657	0.5	0.19544	0.5	0.74	0.07794	0.35	1139	20	1150	23	1136	18	101.3
LAS393_Shot_192_Grain_132	1.6494	0.7	0.16347	0.5	0.25	0.07470	0.75	1036	34	975	20	986	18	98.9
LAS393_Shot_193_Grain_133	1.8017	0.5	0.17434	0.4	0.44	0.07623	0.47	1093	24	1036	20	1045	17	99.1
LAS393_Shot_194_Grain_134	3.6643	0.5	0.25003	0.4	0.39	0.10815	0.51	1760	23	1438	28	1562	21	92.0
LAS393_Shot_195_Grain_135	8.3857	0.3	0.35627	0.4	0.66	0.17356	0.33	2588	17	1963	36	2272	24	86.4
LAS393_Shot_196_Grain_136	2.4079	0.8	0.21938	0.6	0.25	0.08057	0.85	1197	37	1277	27	1239	22	103.1
LAS393_Shot_197_Grain_137	1.7832	0.5	0.17807	0.4	0.28	0.07400	0.52	1029	27	1056	21	1039	17	101.7
LAS393_Shot_198_Grain_138	2.7878	0.4	0.23186	0.4	0.39	0.08872	0.46	1391	22	1344	26	1350	20	99.5
LAS393_Shot_199_Grain_139	1.6110	0.4	0.16096	0.4	0.68	0.07392	0.35	1035	21	962	19	974	17	98.7

LAS393_Shot_200_ Grain_140	2.1143	0.8	0.20536	0.7	0.62	0.07616	0.68	1079	31	1202	26	1148	21	104.8
LAS393_Shot_207_ Grain_141	1.7968	0.8	0.17660	0.5	0.21	0.07542	0.89	1055	39	1048	22	1040	20	100.7
LAS393_Shot_208_ Grain_142	2.0803	0.5	0.19877	0.4	0.35	0.07711	0.54	1115	26	1168	23	1141	19	102.4
LAS393_Shot_209_ Grain_143	0.8674	0.9	0.09199	0.5	0.27	0.06920	0.88	877	40	567	12	631	14	89.9
LAS393_Shot_210_ Grain_144	1.2787	0.5	0.13100	0.4	0.68	0.07178	0.38	972	22	794	16	835	15	95.1
LAS393_Shot_211_ Grain_145	2.1132	0.7	0.19603	0.5	0.12	0.07957	0.83	1159	37	1153	23	1149	20	100.4
LAS393_Shot_212_ Grain_146	2.1746	0.9	0.19424	0.6	0.34	0.08276	0.87	1244	36	1143	24	1168	21	97.8
LAS393_Shot_213_ Grain_147	2.8159	0.5	0.23154	0.4	0.26	0.08940	0.59	1400	27	1342	26	1357	20	98.9
LAS393_Shot_214_ Grain_148	2.1489	0.8	0.19135	0.5	0.25	0.08250	0.85	1232	36	1130	23	1160	21	97.4
LAS393_Shot_215_ Grain_149	1.9494	0.8	0.18093	0.5	0.27	0.07910	0.83	1155	37	1071	22	1093	20	98.0
LAS393_Shot_216_ Grain_150	5.1624	0.5	0.32587	0.4	0.36	0.11637	0.51	1890	23	1817	34	1844	23	98.5
LAS393_Shot_217_ Grain_151	1.5771	1.0	0.15662	0.8	0.78	0.07354	0.61	1015	29	937	22	955	20	98.1
LAS393_Shot_218_ Grain_152	1.8514	0.6	0.17152	0.6	0.59	0.07921	0.53	1167	26	1020	21	1061	18	96.1
LAS393_Shot_219_ Grain_153	15.6780	0.4	0.51682	0.5	0.53	0.22202	0.46	2988	19	2683	48	2856	25	93.9
LAS393_Shot_220_ Grain_154	1.7250	0.5	0.17000	0.4	0.49	0.07411	0.45	1035	24	1012	20	1016	17	99.6
LAS393_Shot_227_ Grain_155	1.6872	0.5	0.16756	0.4	0.44	0.07320	0.49	1009	25	998	20	1002	17	99.6
LAS393_Shot_228_ Grain_156	2.3912	0.6	0.17250	0.5	0.77	0.10049	0.42	1627	20	1025	21	1236	20	82.9
LAS393_Shot_229_ Grain_157	1.8165	1.1	0.15852	0.9	0.77	0.08320	0.70	1252	31	947	24	1043	21	90.8
LAS393_Shot_230_ Grain_158	2.1353	0.4	0.19599	0.4	0.38	0.07913	0.47	1166	24	1153	23	1159	18	99.5
LAS393_Shot_231_ Grain_159	5.3821	0.5	0.32531	0.4	0.32	0.12029	0.53	1952	23	1814	34	1882	23	96.4
LAS393_Shot_232_ Grain_160	1.6238	0.8	0.16678	0.5	0.22	0.07089	0.91	929	40	994	21	976	19	101.9
LAS393_Shot_233_ Grain_161	3.8809	0.4	0.25736	0.4	0.40	0.10937	0.45	1782	21	1476	28	1608	22	91.7
LAS393_Shot_234_ Grain_162	2.8615	0.5	0.23860	0.5	0.48	0.08670	0.50	1344	25	1378	27	1370	20	100.6
LAS393_Shot_235_ Grain_163	13.2294	0.4	0.50233	0.4	0.53	0.19016	0.36	2739	17	2622	45	2694	25	97.3
LAS393_Shot_236_ Grain_164	2.1650	0.4	0.19878	0.4	0.39	0.07858	0.45	1155	23	1169	23	1168	18	100.1
LAS393_Shot_237_ Grain_165	13.9411	0.4	0.43760	0.4	0.58	0.23032	0.35	3051	16	2338	42	2744	25	85.2
LAS393_Shot_238_ Grain_166	3.4346	0.7	0.23344	0.6	0.80	0.10592	0.44	1726	21	1351	29	1506	23	89.7
LAS393_Shot_239_ Grain_167	3.2427	0.4	0.25207	0.4	0.75	0.09276	0.32	1478	18	1449	28	1466	20	98.8
LAS393_Shot_240_ Grain_168	1.3447	0.5	0.12630	0.5	0.49	0.07691	0.47	1108	23	766	16	864	16	88.7
LAS393_Shot_247_ Grain_169	7.7979	0.6	0.31667	0.5	0.80	0.17735	0.34	2624	17	1772	35	2204	25	80.4
LAS393_Shot_248_ Grain_170	4.6659	0.4	0.30359	0.4	0.59	0.11116	0.33	1813	18	1708	32	1760	22	97.1
LAS393_Shot_249_ Grain_171	3.0894	0.5	0.24546	0.4	0.00	0.09091	0.54	1433	25	1414	27	1427	20	99.1
LAS393_Shot_250_ Grain_172	1.8410	0.5	0.17552	0.4	0.64	0.07585	0.39	1084	21	1042	21	1059	18	98.4
LAS393_Shot_251_ Grain_173	3.8503	0.4	0.27795	0.3	0.39	0.10026	0.40	1623	20	1580	29	1602	21	98.6
LAS393_Shot_252_ Grain_174	2.8319	0.5	0.23570	0.5	0.74	0.08698	0.37	1355	20	1364	27	1362	21	100.2

LAS393_Shot_253_ Grain_175	1.7691	0.7	0.17189	0.4	0.23	0.07438	0.71	1033	33	1022	20	1032	18	99.1
LAS393_Shot_254_ Grain_176	1.8601	0.6	0.17144	0.4	0.33	0.07860	0.58	1148	28	1020	21	1066	19	95.7
LAS393_Shot_255_ Grain_177	4.4749	0.4	0.25817	0.4	0.64	0.12546	0.35	2030	18	1480	28	1724	22	85.8
LAS393_Shot_256_ Grain_178	2.7937	0.7	0.23365	0.5	0.25	0.08685	0.79	1338	34	1352	27	1349	22	100.2
LAS393_Shot_257_ Grain_179	4.6690	0.4	0.30855	0.4	0.39	0.10992	0.41	1791	20	1733	32	1760	22	98.4
LAS393_Shot_258_ Grain_180	5.5068	0.6	0.24926	0.5	0.84	0.16035	0.31	2455	16	1433	29	1897	24	75.5
LAS393_Shot_259_ Grain_181	2.2886	0.7	0.21178	0.5	0.13	0.07927	0.82	1148	36	1237	25	1206	21	102.6
LAS393_Shot_260_ Grain_182	2.9570	0.4	0.24142	0.4	0.43	0.08945	0.47	1404	23	1393	27	1396	20	99.8
LAS393_Shot_267_ Grain_183	2.8130	0.5	0.23791	0.5	0.74	0.08644	0.35	1343	20	1375	27	1357	20	101.3
LAS393_Shot_268_ Grain_184	13.7111	0.4	0.50581	0.4	0.57	0.19823	0.37	2806	17	2637	46	2728	24	96.7
LAS393_Shot_269_ Grain_185	11.7830	0.3	0.47359	0.4	0.48	0.18228	0.34	2668	16	2499	43	2586	24	96.6
LAS393_Shot_270_ Grain_186	6.8444	0.5	0.34225	0.4	0.53	0.14585	0.40	2296	19	1897	34	2089	23	90.8
LAS393_Shot_271_ Grain_187	1.9621	0.5	0.18870	0.4	0.38	0.07632	0.55	1093	26	1114	22	1101	19	101.2
LAS393_Shot_272_ Grain_188	1.4303	0.8	0.14595	0.5	0.26	0.07205	0.79	962	35	878	18	899	17	97.6
LAS393_Shot_273_ Grain_189	2.6741	0.4	0.22733	0.4	0.43	0.08611	0.42	1336	22	1320	25	1320	20	100.0
LAS393_Shot_274_ Grain_190	1.8418	0.5	0.17806	0.4	0.28	0.07574	0.55	1078	27	1056	21	1058	18	99.8
LAS393_Shot_275_ Grain_191	14.0708	0.4	0.50649	0.4	0.59	0.20315	0.35	2848	17	2642	47	2752	25	96.0
LAS393_Shot_276_ Grain_192	3.8714	0.5	0.26756	0.5	0.65	0.10576	0.41	1720	20	1528	30	1605	22	95.2
LAS393_Shot_277_ Grain_193	3.6211	0.5	0.26609	0.4	0.44	0.09998	0.47	1614	22	1520	29	1553	21	97.9
LAS393_Shot_278_ Grain_194	3.1294	0.5	0.24859	0.4	0.40	0.09240	0.51	1465	24	1431	28	1439	21	99.5
LAS393_Shot_279_ Grain_195	3.9346	0.4	0.27028	0.4	0.46	0.10682	0.40	1741	20	1542	29	1620	21	95.1
LAS393_Shot_280_ Grain_196	2.8671	0.5	0.23449	0.4	0.46	0.08952	0.47	1407	22	1358	26	1372	20	99.0
LAS393_Shot_287_ Grain_197	7.3232	0.3	0.35373	0.3	0.52	0.15147	0.32	2359	16	1951	35	2151	23	90.7
LAS393_Shot_288_ Grain_198	2.8328	0.6	0.24091	0.4	0.29	0.08625	0.60	1329	28	1391	27	1362	20	102.1
LAS393_Shot_289_ Grain_199	2.1045	0.6	0.19217	0.4	0.02	0.08040	0.72	1179	27	1133	22	1147	19	98.7
LAS393_Shot_290_ Grain_200	12.0354	0.5	0.47397	0.5	0.75	0.18582	0.36	2700	17	2498	46	2603	25	96.0
LAS393_Shot_291_ Grain_201	10.9030	0.4	0.44580	0.4	0.38	0.17895	0.40	2637	18	2377	42	2514	24	94.5
LAS393_Shot_292_ Grain_202	1.7843	0.5	0.17287	0.4	0.34	0.07553	0.55	1068	26	1027	20	1038	18	99.0
LAS393_Shot_293_ Grain_203	0.8066	0.8	0.09362	0.6	0.38	0.06321	0.76	706	34	577	13	599	13	96.3
LAS393_Shot_294_ Grain_204	2.0789	0.4	0.18674	0.4	0.47	0.08166	0.45	1229	22	1103	22	1140	18	96.7
LAS393_Shot_295_ Grain_205	2.4144	0.6	0.21302	0.4	0.35	0.08310	0.57	1258	27	1245	24	1244	19	100.1
LAS393_Shot_296_ Grain_206	2.0625	0.7	0.19482	0.5	0.24	0.07777	0.79	1117	35	1147	23	1133	20	101.2
LAS393_Shot_297_ Grain_207	1.7957	1.0	0.17102	0.6	0.27	0.07703	1.03	1100	44	1017	22	1038	22	97.9
LAS393_Shot_298_ Grain_208	0.7436	1.8	0.09013	0.8	0.07	0.06134	1.92	864	61	556	14	554	19	100.3
LAS393_Shot_299_ Grain_209	4.9997	0.6	0.31488	0.5	0.71	0.11621	0.42	1894	20	1763	34	1819	23	96.9

LAS393_Shot_300_ Grain_210	2.2351	0.5	0.19293	0.5	0.76	0.08462	0.36	1301	20	1137	23	1190	19	95.5
LAS393_Shot_307_ Grain_211	1.7635	0.5	0.16781	0.5	0.50	0.07702	0.48	1112	25	1000	20	1031	18	97.0
LAS393_Shot_308_ Grain_212	2.2342	0.6	0.20581	0.4	0.25	0.07958	0.65	1171	29	1206	24	1190	20	101.4
LAS393_Shot_309_ Grain_213	3.0656	0.6	0.24882	0.4	0.39	0.09018	0.59	1417	27	1431	28	1421	22	100.7
LAS393_Shot_310_ Grain_214	2.1064	0.5	0.19306	0.4	0.38	0.07983	0.48	1181	24	1137	22	1149	18	99.0
LAS393_Shot_311_ Grain_215	2.1174	0.9	0.18874	0.5	0.14	0.08225	0.98	1216	40	1115	23	1149	21	97.0
LAS393_Shot_312_ Grain_216	1.8387	0.7	0.17765	0.5	0.17	0.07578	0.77	1066	34	1054	21	1056	19	99.7
LAS393_Shot_313_ Grain_217	0.7632	1.6	0.09166	0.9	0.15	0.06194	1.71	824	59	566	15	570	18	99.3
LAS393_Shot_314_ Grain_218	0.7388	0.9	0.09136	0.5	0.16	0.05920	0.94	622	38	563	12	560	13	100.6
LAS393_Shot_315_ Grain_219	1.8422	0.7	0.16713	0.6	0.52	0.08057	0.64	1193	30	996	21	1059	19	94.1
LAS393_Shot_316_ Grain_220	1.6777	0.4	0.16746	0.4	0.64	0.07292	0.34	1005	20	998	20	999	17	99.9
LAS393_Shot_317_ Grain_221	2.0585	0.7	0.18987	0.5	0.34	0.07881	0.66	1153	31	1120	23	1132	19	99.0
LAS393_Shot_318_ Grain_222	2.1178	0.9	0.19455	0.6	0.18	0.07958	1.00	1162	43	1146	25	1150	22	99.7
LAS393_Shot_319_ Grain_223	2.3110	0.8	0.17869	0.4	0.23	0.09456	0.83	1503	35	1059	21	1212	20	87.4
LAS393_Shot_320_ Grain_224	5.3937	0.7	0.34634	0.6	0.28	0.11318	0.73	1835	31	1915	38	1878	25	102.0
LAS393_Shot_327_ Grain_225	3.0077	0.5	0.24608	0.4	0.41	0.08878	0.50	1391	24	1417	27	1408	21	100.7
LAS393_Shot_328_ Grain_226	1.8313	0.6	0.17817	0.5	0.21	0.07479	0.70	1039	32	1056	21	1054	18	100.3
LAS393_Shot_329_ Grain_227	2.1850	0.5	0.20583	0.4	0.50	0.07702	0.46	1111	23	1206	23	1174	19	102.7
LAS393_Shot_330_ Grain_228	1.9790	0.6	0.18737	0.4	0.21	0.07679	0.67	1098	31	1107	22	1105	19	100.1
LAS393_Shot_331_ Grain_229	2.8865	0.4	0.23882	0.4	0.51	0.08781	0.37	1371	20	1380	26	1377	20	100.2
LAS393_Shot_332_ Grain_230	2.0895	0.6	0.19358	0.5	0.32	0.07866	0.62	1149	29	1140	23	1145	18	99.6
LAS393_Shot_333_ Grain_231	2.2875	0.8	0.21354	0.7	0.54	0.07805	0.72	1128	33	1246	27	1205	21	103.4
LAS393_Shot_334_ Grain_232	2.1258	0.7	0.19505	0.5	0.20	0.07937	0.73	1166	33	1149	24	1154	20	99.6
LAS393_Shot_335_ Grain_233	3.8077	0.8	0.24631	0.6	0.62	0.11271	0.61	1828	26	1418	29	1588	23	89.3
LAS393_Shot_336_ Grain_234	6.5964	0.4	0.30589	0.4	0.68	0.15684	0.33	2417	17	1720	33	2058	23	83.6
LAS393_Shot_337_ Grain_235	3.8167	0.6	0.24168	0.5	0.64	0.11497	0.46	1872	21	1394	28	1593	22	87.5
LAS393_Shot_338_ Grain_236	1.9570	1.0	0.18267	0.6	0.19	0.07857	1.05	1123	45	1081	23	1094	21	98.7
LAS393_Shot_339_ Grain_237	1.9650	0.6	0.18383	0.5	0.42	0.07784	0.61	1127	29	1087	22	1101	19	98.8
LAS393_Shot_340_ Grain_238	1.8206	0.5	0.17809	0.5	0.72	0.07459	0.39	1055	21	1056	22	1051	18	100.5
LAS393_Shot_347_ Grain_239	13.2211	0.5	0.51985	0.5	0.46	0.18674	0.51	2706	21	2695	49	2694	26	100.1
LAS393_Shot_348_ Grain_240	12.5412	0.4	0.48397	0.5	0.52	0.18964	0.44	2733	19	2544	46	2643	25	96.2
LAS393_Shot_349_ Grain_241	3.3571	0.4	0.26246	0.4	0.15	0.09360	0.44	1497	20	1502	28	1492	21	100.6
LAS393_Shot_350_ Grain_242	2.7332	0.5	0.22867	0.4	0.68	0.08729	0.38	1362	20	1328	26	1335	20	99.4
LAS393_Shot_351_ Grain_243	3.6048	0.8	0.26253	0.6	0.25	0.10076	0.81	1620	34	1501	31	1544	23	97.2
LAS393_Shot_352_ Grain_244	2.2471	0.6	0.20306	0.4	0.34	0.08103	0.61	1212	27	1191	24	1193	19	99.8

LAS393_Shot_353_ Grain_245	0.7428	2.1	0.09079	1.1	0.18	0.06145	2.19	939	69	559	16	554	22	101.0
LAS393_Shot_354_ Grain_246	2.3901	1.2	0.19421	1.1	0.92	0.08954	0.47	1408	24	1141	31	1226	25	93.0
LAS393_Shot_355_ Grain_247	1.8336	0.6	0.17674	0.5	0.34	0.07588	0.63	1074	30	1049	21	1055	18	99.5
LAS393_Shot_356_ Grain_248	1.2340	0.6	0.12770	0.4	0.51	0.07058	0.52	931	26	774	16	815	16	95.1
LAS393_Shot_357_ Grain_249	2.0525	0.6	0.19876	0.5	0.35	0.07571	0.61	1071	29	1168	23	1132	19	103.2
LAS393_Shot_358_ Grain_250	1.6417	0.5	0.16470	0.4	0.70	0.07275	0.38	1001	22	982	20	985	17	99.7
LAS393_Shot_359_ Grain_251	2.6871	0.4	0.21976	0.4	0.61	0.08923	0.37	1404	20	1280	25	1324	19	96.7
LAS393_Shot_360_ Grain_252	2.7640	0.8	0.22911	0.6	0.48	0.08851	0.71	1374	31	1329	27	1341	22	99.1
LAS393_Shot_367_ Grain_253	1.7316	0.5	0.17321	0.5	0.68	0.07339	0.39	1018	21	1029	21	1020	17	100.9
LAS393_Shot_368_ Grain_254	1.7868	0.7	0.17159	0.6	0.62	0.07635	0.58	1093	27	1020	22	1037	18	98.3
LAS393_Shot_369_ Grain_255	1.7527	1.5	0.17537	1.0	0.11	0.07398	1.66	1112	63	1039	27	1012	26	102.7
LAS393_Shot_370_ Grain_256	1.8890	0.5	0.18015	0.4	0.35	0.07668	0.47	1103	24	1067	21	1076	18	99.2
LAS393_Shot_371_ Grain_257	2.2540	0.5	0.20102	0.4	0.42	0.08194	0.47	1236	23	1180	23	1197	19	98.6
LAS393_Shot_372_ Grain_258	1.8515	0.4	0.18073	0.4	0.43	0.07488	0.43	1057	23	1071	21	1063	17	100.8
LAS393_Shot_373_ Grain_259	2.1257	0.4	0.19447	0.3	0.46	0.07983	0.39	1187	21	1146	22	1156	18	99.1
LAS393_Shot_374_ Grain_260	3.0572	0.5	0.25622	0.4	0.34	0.08723	0.55	1359	25	1470	28	1419	21	103.5
LAS393_Shot_375_ Grain_261	3.3778	0.4	0.26056	0.4	0.67	0.09455	0.30	1515	18	1493	29	1498	20	99.7
LAS393_Shot_376_ Grain_262	3.6336	0.5	0.26419	0.4	0.47	0.10065	0.49	1631	22	1510	29	1555	21	97.1
LAS393_Shot_377_ Grain_263	8.3054	0.6	0.35485	0.5	0.63	0.17135	0.46	2565	20	1956	38	2261	25	86.5
LAS393_Shot_378_ Grain_264	1.5651	1.6	0.15401	1.0	0.43	0.07509	1.51	1066	58	921	25	942	26	97.8
LAS393_Shot_379_ Grain_265	1.7529	0.5	0.17229	0.5	0.49	0.07467	0.51	1047	25	1025	21	1027	18	99.8
LAS393_Shot_380_ Grain_266	4.4694	0.5	0.30350	0.4	0.23	0.10846	0.48	1764	22	1707	32	1724	21	99.0
LAS393_Shot_387_ Grain_267	2.0226	1.1	0.18207	0.8	0.00	0.08223	1.35	1198	54	1078	25	1115	22	96.7
LAS393_Shot_388_ Grain_268	3.1947	0.8	0.24658	0.6	0.33	0.09485	0.76	1504	32	1419	29	1450	23	97.9
LAS393_Shot_389_ Grain_269	2.5445	0.5	0.21722	0.4	0.39	0.08590	0.48	1325	23	1267	25	1283	20	98.7
LAS393_Shot_390_ Grain_270	3.8390	0.5	0.27514	0.4	0.56	0.10196	0.41	1655	20	1566	30	1599	21	97.9
LAS393_Shot_391_ Grain_271	1.7750	0.5	0.17212	0.5	0.71	0.07533	0.41	1071	22	1023	21	1035	17	98.9
LAS393_Shot_392_ Grain_272	2.8020	0.6	0.23287	0.6	0.73	0.08780	0.40	1372	21	1348	28	1353	20	99.6
LAS393_Shot_393_ Grain_273	10.1698	0.5	0.38636	0.5	-0.02	0.19270	0.45	2758	19	2104	39	2449	23	85.9
LAS393_Shot_394_ Grain_274	1.8175	0.9	0.17739	0.6	0.24	0.07499	0.93	1046	40	1053	23	1047	20	100.6
LAS393_Shot_395_ Grain_275	1.8739	0.5	0.18016	0.4	0.29	0.07590	0.59	1080	27	1067	21	1071	18	99.7
LAS393_Shot_396_ Grain_276	4.8216	0.4	0.30875	0.4	0.53	0.11392	0.41	1858	20	1733	33	1786	22	97.0
LAS393_Shot_397_ Grain_277	2.1163	0.5	0.20059	0.4	0.40	0.07681	0.53	1104	26	1178	23	1152	19	102.3
LAS393_Shot_398_ Grain_278	2.8343	0.5	0.23718	0.4	0.71	0.08687	0.34	1353	19	1371	27	1363	20	100.6
LAS393_Shot_399_ Grain_279	1.7779	0.5	0.17280	0.4	0.39	0.07506	0.54	1059	26	1027	20	1035	18	99.2

LAS393_Shot_400_ Grain_280	1.6749	0.6	0.16030	0.5	0.75	0.07624	0.50	1089	25	958	20	997	17	96.1
LAS393_Shot_407_ Grain_281	1.3839	1.4	0.14433	0.8	0.15	0.07046	1.48	928	54	870	21	871	22	99.9
LAS393_Shot_408_ Grain_282	3.6201	0.4	0.24899	0.4	0.54	0.10598	0.38	1725	19	1433	27	1553	21	92.2
LAS393_Shot_409_ Grain_283	0.8367	0.8	0.09184	0.6	0.75	0.06611	0.53	797	27	566	13	615	13	92.0
LAS393_Shot_410_ Grain_284	2.2850	0.5	0.21242	0.4	0.61	0.07839	0.49	1150	24	1241	24	1206	19	102.9
LAS393_Shot_411_ Grain_285	1.8245	1.0	0.17650	0.7	0.26	0.07585	1.05	1064	44	1048	23	1047	21	100.1
LAS393_Shot_412_ Grain_286	3.0780	0.5	0.22120	0.5	0.70	0.10132	0.39	1643	20	1287	26	1427	21	90.2
LAS393_Shot_413_ Grain_287	1.8541	1.4	0.17627	0.9	0.13	0.07794	1.54	1137	57	1045	26	1054	24	99.1
LAS393_Shot_414_ Grain_288	3.6797	0.4	0.26914	0.4	0.46	0.09980	0.42	1614	21	1536	29	1566	21	98.1
LAS393_Shot_415_ Grain_289	0.7055	1.4	0.08761	0.7	0.10	0.05904	1.49	733	54	541	13	537	16	100.7
LAS393_Shot_416_ Grain_290	1.8574	1.0	0.17983	0.7	0.03	0.07608	1.17	1068	49	1065	23	1063	22	100.2
LAS393_Shot_417_ Grain_291	1.9496	0.7	0.18758	0.6	0.08	0.07870	3.53	1071	28	1108	24	1094	19	101.3
LAS393_Shot_418_ Grain_292	2.6650	0.5	0.22527	0.5	0.69	0.08624	0.36	1338	20	1309	26	1317	19	99.3
LAS393_Shot_419_ Grain_293	1.9175	0.9	0.18378	0.7	0.19	0.07667	0.99	1082	43	1086	24	1083	21	100.3
LAS393_Shot_420_ Grain_294	11.3988	0.4	0.42463	0.4	0.63	0.19546	0.35	2786	17	2280	41	2554	24	89.3
LAS393_Shot_427_ Grain_295	1.6814	0.5	0.16433	0.4	0.47	0.07472	0.44	1054	23	980	19	1001	17	98.0
LAS393_Shot_428_ Grain_296	2.0302	0.5	0.18921	0.4	0.33	0.07830	0.51	1143	25	1117	22	1124	18	99.4
LAS393_Shot_429_ Grain_297	1.9165	1.4	0.18630	0.8	0.10	0.07604	1.52	1119	57	1100	26	1075	25	102.3
LAS393_Shot_430_ Grain_298	0.6984	2.9	0.08729	1.3	0.02	0.06080	3.20	1106	89	542	18	516	27	105.0
LAS393_Shot_431_ Grain_299	1.8152	1.3	0.17884	0.7	0.15	0.07471	1.34	1048	52	1059	24	1041	23	101.8
LAS393_Shot_432_ Grain_300	1.3777	0.5	0.14044	0.5	0.65	0.07151	0.42	963	23	847	17	878	16	96.4
LAS393_Shot_433_ Grain_301	2.3797	0.8	0.22063	0.6	0.45	0.07871	0.77	1141	35	1284	27	1232	22	104.2
LAS393_Shot_434_ Grain_302	2.7729	0.5	0.24466	0.5	0.41	0.08301	0.57	1260	26	1410	28	1345	20	104.8
LAS393_Shot_435_ Grain_303	2.7305	0.5	0.23130	0.4	0.48	0.08619	0.44	1334	23	1341	26	1335	19	100.4
LAS393_Shot_436_ Grain_304	2.9561	0.8	0.24109	0.6	0.31	0.09002	0.81	1402	35	1391	29	1392	23	99.9
LAS393_Shot_437_ Grain_305	1.7419	0.6	0.17325	0.4	0.32	0.07351	0.59	1012	29	1030	20	1022	18	100.7
LAS393_Shot_438_ Grain_306	1.7771	0.8	0.15025	0.7	0.79	0.08621	0.51	1332	25	901	21	1034	19	87.2
LAS393_Shot_439_ Grain_307	2.6187	0.5	0.22378	0.5	0.64	0.08542	0.42	1317	22	1301	26	1304	20	99.8
LAS393_Shot_440_ Grain_308	2.0711	0.7	0.19232	0.5	0.23	0.07874	0.74	1151	33	1133	23	1138	20	99.6
LAS393_Shot_447_ Grain_309	4.0581	0.5	0.29424	0.4	0.43	0.10043	0.50	1629	22	1662	32	1644	21	101.0
LAS393_Shot_448_ Grain_310	3.0399	0.5	0.23985	0.5	0.47	0.09248	0.55	1464	25	1385	28	1415	20	97.8
LAS393_Shot_449_ Grain_311	2.0911	0.6	0.19211	0.5	0.38	0.07905	0.62	1165	29	1132	23	1143	19	99.1
LAS393_Shot_450_ Grain_312	2.5153	0.7	0.17430	0.6	0.70	0.10495	0.47	1709	22	1035	22	1273	20	81.3
LAS393_Shot_451_ Grain_313	1.2970	0.6	0.11265	0.6	0.63	0.08353	0.52	1274	25	688	15	842	16	81.7
LAS393_Shot_452_ Grain_314	0.9521	1.5	0.10860	0.8	0.12	0.06487	1.63	861	57	665	16	671	20	99.1

LAS393_Shot_453_Grain_315	3.7061	0.5	0.27112	0.4	0.41	0.09956	0.47	1609	22	1546	29	1571	21	98.4
LAS393_Shot_454_Grain_316	5.3549	0.6	0.22508	0.6	0.81	0.17274	0.37	2580	18	1307	27	1874	24	69.8
LAS393_Shot_457_Grain_319	1.7427	1.4	0.17015	0.8	0.17	0.07498	1.48	1068	57	1011	24	1013	24	99.8
LAS393_Shot_458_Grain_320	2.0547	0.5	0.18955	0.4	0.33	0.07896	0.58	1157	27	1118	22	1131	19	98.8
LAS393_Shot_459_Grain_321	3.0640	0.6	0.23012	0.5	0.42	0.09718	0.58	1556	26	1335	28	1421	21	94.0
LAS393_Shot_460_Grain_322	1.5256	0.4	0.14829	0.4	0.68	0.07465	0.31	1055	20	891	17	940	16	94.8

LAS394 (20BREM04F)														
Isotopic Ratios								Calculated ages (Ma)						
ID	^{207}Pb/^{235}U	2σ	^{206}Pb/^{238}U	2σ	Rho	$^{207/206}$Pb	2σ	$^{207/206}$Pb	2σ	^{206}Pb/^{238}U	2σ	^{207}Pb/^{235}U	2σ	%conc
LAS394_Shot_467_Grain_323	0.5144	1.5	0.06714	0.8	0.09	0.05652	1.57	688	51	419	10	417	13	100.4
LAS394_Shot_468_Grain_324	2.4805	1.8	0.17128	1.4	0.67	0.10586	1.36	1669	52	1017	32	1239	32	82.0
LAS394_Shot_469_Grain_325	3.8190	0.4	0.27575	0.4	0.52	0.10089	0.43	1635	21	1569	30	1596	22	98.3
LAS394_Shot_470_Grain_326	1.2372	0.4	0.12682	0.4	0.64	0.07116	0.37	955	21	769	16	817	15	94.2
LAS394_Shot_471_Grain_327	1.1185	0.6	0.10413	0.5	0.40	0.07829	0.64	1143	30	638	13	761	15	83.9
LAS394_Shot_472_Grain_328	1.5780	0.5	0.14026	0.4	0.46	0.08199	0.52	1234	25	846	17	960	17	88.1
LAS394_Shot_473_Grain_329	6.1795	0.6	0.28299	0.6	0.66	0.15899	0.47	2436	20	1605	32	1998	24	80.3
LAS394_Shot_474_Grain_330	0.7494	2.2	0.09169	1.1	0.05	0.06048	2.34	1025	73	565	16	553	22	102.1
LAS394_Shot_475_Grain_331	2.1887	0.7	0.19653	0.5	0.38	0.08128	0.68	1211	30	1157	24	1175	20	98.4
LAS394_Shot_476_Grain_332	1.9784	0.6	0.18645	0.5	0.46	0.07757	0.56	1123	27	1101	22	1107	18	99.5
LAS394_Shot_477_Grain_333	1.9361	0.5	0.18434	0.5	0.73	0.07678	0.37	1109	21	1090	22	1093	18	99.7
LAS394_Shot_478_Grain_334	2.3160	0.5	0.19924	0.5	0.55	0.08500	0.49	1304	23	1171	23	1215	19	96.4
LAS394_Shot_479_Grain_335	1.9111	0.6	0.18838	0.5	0.39	0.07385	0.64	1026	30	1112	23	1083	18	102.6
LAS394_Shot_480_Grain_336	1.9409	1.4	0.19113	0.9	0.17	0.07524	1.53	1081	57	1125	27	1086	25	103.6
LAS394_Shot_487_Grain_337	2.1906	0.6	0.19334	0.5	0.45	0.08285	0.55	1255	26	1139	23	1175	19	96.9
LAS394_Shot_488_Grain_338	3.1285	0.6	0.23667	0.5	0.35	0.09668	0.61	1545	27	1368	27	1436	21	95.3
LAS394_Shot_489_Grain_339	1.7327	3.5	0.16169	2.3	0.01	0.08893	4.22	1664	108	948	40	965	51	98.2
LAS394_Shot_490_Grain_340	3.3252	0.9	0.17486	0.8	0.83	0.13843	0.53	2199	23	1039	24	1477	25	70.3
LAS394_Shot_491_Grain_341	3.3589	0.7	0.25650	0.6	0.45	0.09610	0.69	1532	29	1470	31	1491	22	98.6
LAS394_Shot_492_Grain_342	2.1246	0.5	0.19275	0.5	0.61	0.08083	0.47	1211	23	1135	24	1155	19	98.3
LAS394_Shot_493_Grain_343	14.1322	0.5	0.57189	0.6	0.64	0.18130	0.51	2655	21	2913	54	2754	26	105.8
LAS394_Shot_494_Grain_344	0.9839	0.7	0.10973	0.5	0.38	0.06581	0.73	778	34	671	15	693	15	96.9
LAS394_Shot_495_Grain_345	9.6630	0.6	0.42384	0.6	0.66	0.16717	0.48	2522	20	2274	44	2398	25	94.8
LAS394_Shot_496_Grain_346	12.0242	0.5	0.49011	0.5	0.61	0.17976	0.49	2642	20	2567	48	2602	26	98.7

LAS394_Shot_497_Grain_347	0.7592	2.5	0.09215	1.2	0.06	0.06261	2.68	1088	80	567	17	559	25	101.4
LAS394_Shot_498_Grain_348	1.9656	0.6	0.18535	0.5	0.33	0.07797	0.64	1129	29	1095	22	1102	19	99.4
LAS394_Shot_499_Grain_349	4.9010	0.4	0.31749	0.4	0.55	0.11318	0.40	1845	19	1776	33	1800	22	98.7
LAS394_Shot_500_Grain_350	1.6493	0.5	0.16400	0.5	0.51	0.07380	0.49	1025	25	978	20	987	17	99.1
LAS394_Shot_507_Grain_351	2.8674	0.5	0.24481	0.5	0.40	0.08596	0.56	1324	26	1411	28	1370	20	102.9
LAS394_Shot_508_Grain_352	1.8699	0.6	0.18349	0.5	0.42	0.07476	0.58	1049	28	1085	22	1068	18	101.6
LAS394_Shot_509_Grain_353	2.0034	0.6	0.18680	0.5	0.40	0.07880	0.63	1151	29	1103	23	1114	19	99.0
LAS394_Shot_510_Grain_354	2.4549	0.8	0.21486	0.7	0.76	0.08372	0.54	1272	26	1253	27	1254	22	100.0
LAS394_Shot_511_Grain_355	1.8608	0.6	0.18088	0.6	0.40	0.07567	0.70	1063	32	1071	23	1065	19	100.6
LAS394_Shot_512_Grain_356	2.6000	0.6	0.18552	0.5	0.65	0.10230	0.46	1661	22	1096	23	1297	20	84.5
LAS394_Shot_513_Grain_357	1.3983	0.6	0.13808	0.5	0.43	0.07423	0.56	1038	26	833	17	886	16	94.0
LAS394_Shot_514_Grain_358	1.4693	0.9	0.14754	0.6	0.23	0.07346	0.97	998	41	886	20	915	18	96.9
LAS394_Shot_515_Grain_359	2.0143	0.7	0.19041	0.5	0.36	0.07778	0.71	1120	32	1123	23	1117	19	100.5
LAS394_Shot_516_Grain_360	1.9779	0.5	0.18461	0.5	0.38	0.07845	0.56	1147	27	1091	22	1106	18	98.7
LAS394_Shot_517_Grain_361	2.6131	0.5	0.21870	0.5	0.69	0.08769	0.43	1370	21	1274	26	1303	20	97.8
LAS394_Shot_518_Grain_362	3.1329	0.8	0.25241	0.6	-0.03	0.09059	0.78	1424	31	1449	30	1434	23	101.1
LAS394_Shot_519_Grain_363	13.3216	0.6	0.53116	0.6	0.41	0.18398	0.69	2674	26	2743	53	2698	26	101.7
LAS394_Shot_520_Grain_364	1.6296	0.9	0.15651	0.6	0.67	0.07577	0.66	1072	31	937	20	977	19	95.9
LAS394_Shot_527_Grain_365	1.8930	0.8	0.17644	0.6	0.37	0.07829	0.83	1132	37	1047	22	1073	20	97.5
LAS394_Shot_528_Grain_366	1.5999	0.9	0.15861	0.6	0.22	0.07382	0.96	1012	44	948	20	965	20	98.2
LAS394_Shot_529_Grain_367	2.1959	0.6	0.19624	0.5	0.35	0.08197	0.61	1229	28	1154	23	1177	19	98.1
LAS394_Shot_530_Grain_368	2.5002	0.7	0.20757	0.6	0.78	0.08799	0.46	1372	23	1215	26	1268	21	95.8
LAS394_Shot_531_Grain_369	0.6830	1.6	0.08703	1.0	0.24	0.05817	1.64	711	56	537	15	522	17	102.9
LAS394_Shot_532_Grain_370	1.7528	0.5	0.17429	0.5	0.67	0.07380	0.46	1026	24	1035	22	1027	18	100.8
LAS394_Shot_533_Grain_371	2.1272	0.6	0.19464	0.5	0.60	0.08006	0.51	1189	25	1146	24	1155	19	99.1
LAS394_Shot_534_Grain_372	1.8034	1.0	0.17280	0.6	0.21	0.07635	1.05	1083	45	1027	22	1040	21	98.7
LAS394_Shot_535_Grain_373	1.4880	0.7	0.15184	0.5	0.34	0.07184	0.69	965	32	911	19	924	17	98.6
LAS394_Shot_536_Grain_374	2.2367	0.5	0.20240	0.5	0.28	0.08112	0.51	1210	24	1188	24	1190	19	99.8
LAS394_Shot_537_Grain_375	3.0280	0.9	0.23875	0.7	0.22	0.09374	1.05	1461	43	1378	31	1406	24	98.0
LAS394_Shot_538_Grain_376	2.1047	0.7	0.19572	0.6	0.10	0.07882	0.82	1147	30	1151	25	1146	19	100.4
LAS394_Shot_539_Grain_377	1.9178	0.7	0.18495	0.6	0.37	0.07644	0.72	1082	32	1094	23	1084	19	101.0
LAS394_Shot_540_Grain_378	1.6256	0.6	0.15790	0.5	0.32	0.07598	0.68	1075	31	945	20	979	18	96.5
LAS394_Shot_547_Grain_379	1.8813	0.8	0.18061	0.7	0.66	0.07659	0.58	1098	28	1069	24	1070	19	99.9
LAS394_Shot_548_Grain_380	3.0169	0.6	0.22398	0.5	0.40	0.09977	0.61	1606	26	1302	26	1410	21	92.3
LAS394_Shot_549_Grain_381	1.2830	0.5	0.12628	0.5	0.63	0.07507	0.40	1069	21	766	16	837	15	91.5

LAS394_Shot_550_Grain_382	3.2809	0.7	0.25615	0.6	0.42	0.09460	0.69	1504	30	1469	30	1471	22	99.8
LAS394_Shot_551_Grain_383	0.8999	0.7	0.09820	0.5	0.56	0.06768	0.60	843	29	604	13	651	14	92.7
LAS394_Shot_552_Grain_384	2.9908	0.4	0.22470	0.4	0.63	0.09840	0.39	1589	20	1306	26	1404	21	93.0
LAS394_Shot_553_Grain_385	2.6073	0.5	0.22003	0.4	0.47	0.08758	0.47	1363	23	1281	25	1300	20	98.5
LAS394_Shot_554_Grain_386	1.9037	0.5	0.17758	0.5	0.62	0.07908	0.43	1165	23	1053	21	1080	18	97.5
LAS394_Shot_555_Grain_387	1.6931	1.0	0.16885	0.6	0.25	0.07438	0.99	1021	43	1005	21	1000	21	100.5
LAS394_Shot_556_Grain_388	10.4952	0.4	0.43094	0.4	0.56	0.18033	0.36	2652	17	2308	41	2478	24	93.2
LAS394_Shot_557_Grain_389	8.3308	0.4	0.35574	0.4	0.55	0.17350	0.39	2586	18	1962	36	2265	24	86.6
LAS394_Shot_558_Grain_390	2.1757	0.7	0.18677	0.6	0.52	0.08654	0.68	1332	30	1103	24	1170	20	94.3
LAS394_Shot_559_Grain_391	2.0617	0.5	0.19639	0.4	0.46	0.07782	0.49	1132	24	1155	23	1135	18	101.7
LAS394_Shot_560_Grain_392	2.5814	0.5	0.22459	0.4	0.40	0.08521	0.51	1310	24	1306	25	1293	20	101.0
LAS394_Shot_567_Grain_393	2.0745	0.7	0.18281	0.5	0.70	0.08386	0.48	1280	24	1082	23	1138	19	95.1
LAS394_Shot_568_Grain_394	1.8543	0.5	0.18427	0.5	0.62	0.07478	0.44	1054	23	1090	22	1064	18	102.4
LAS394_Shot_569_Grain_395	1.4670	0.5	0.15048	0.5	0.58	0.07223	0.48	981	25	903	18	915	16	98.7
LAS394_Shot_570_Grain_396	1.6992	1.5	0.17289	0.9	0.17	0.07421	1.63	1061	60	1026	26	995	25	103.1
LAS394_Shot_571_Grain_397	4.6551	0.5	0.30416	0.4	0.46	0.11308	0.48	1840	22	1712	33	1757	22	97.4
LAS394_Shot_572_Grain_398	1.3868	0.8	0.14280	0.7	0.76	0.07121	0.48	957	26	860	19	880	17	97.7
LAS394_Shot_573_Grain_399	4.2413	0.5	0.28970	0.4	0.26	0.10825	0.47	1761	21	1639	31	1679	22	97.6
LAS394_Shot_574_Grain_400	1.5059	0.6	0.14793	0.5	0.61	0.07522	0.49	1063	24	889	19	931	17	95.5
LAS394_Shot_575_Grain_401	0.7520	1.0	0.09443	0.6	0.05	0.05903	1.13	643	43	581	13	568	14	102.4
LAS394_Shot_576_Grain_402	0.8814	0.7	0.09798	0.5	0.35	0.06619	0.74	794	35	602	13	640	14	94.2
LAS394_Shot_577_Grain_403	1.6909	0.5	0.16568	0.5	0.49	0.07522	0.52	1064	26	988	21	1005	17	98.3
LAS394_Shot_578_Grain_404	1.8151	0.4	0.17955	0.5	0.65	0.07465	0.39	1054	22	1064	22	1050	17	101.4
LAS394_Shot_579_Grain_405	1.8401	0.9	0.17607	0.6	0.30	0.07671	0.89	1085	38	1046	22	1054	20	99.2
LAS394_Shot_580_Grain_406	1.9567	0.6	0.18441	0.6	0.47	0.07795	0.58	1131	28	1091	23	1098	19	99.4
LAS394_Shot_587_Grain_407	3.7369	0.5	0.27364	0.5	0.46	0.10035	0.55	1618	25	1558	31	1578	22	98.7
LAS394_Shot_588_Grain_408	1.8900	1.0	0.18322	0.7	0.27	0.07592	1.03	1063	43	1083	24	1071	21	101.1
LAS394_Shot_589_Grain_409	1.8868	0.7	0.17978	0.5	0.27	0.07767	1.28	1092	25	1065	22	1073	18	99.3
LAS394_Shot_590_Grain_410	1.1018	1.0	0.10471	0.9	0.86	0.07674	0.50	1105	25	642	16	751	17	85.4
LAS394_Shot_591_Grain_411	0.7031	1.0	0.08727	0.6	0.15	0.05931	1.12	659	42	539	12	538	13	100.3
LAS394_Shot_592_Grain_412	2.2202	0.6	0.19977	0.5	0.46	0.08119	0.57	1216	27	1173	24	1184	19	99.1
LAS394_Shot_593_Grain_413	0.5918	1.0	0.07478	0.6	0.37	0.05803	0.95	574	40	465	11	470	12	99.0
LAS394_Shot_594_Grain_414	0.7186	2.0	0.08959	1.0	0.19	0.05939	2.06	871	70	552	15	540	20	102.3
LAS394_Shot_595_Grain_415	3.9718	0.9	0.26799	0.8	0.85	0.10834	0.44	1766	21	1527	35	1619	25	94.3
LAS394_Shot_596_Grain_416	0.7133	2.0	0.08918	0.9	0.08	0.05953	2.17	894	69	550	14	538	20	102.2

LAS394_Shot_597_Grain_417	10.2111	0.5	0.41119	0.5	0.63	0.18149	0.39	2661	18	2218	41	2451	25	90.5
LAS394_Shot_598_Grain_418	2.2856	0.8	0.20496	0.6	0.29	0.08190	0.83	1211	36	1201	25	1202	21	99.9
LAS394_Shot_599_Grain_419	0.7593	1.4	0.09068	0.9	0.13	0.06188	1.50	790	54	559	14	568	16	98.4
LAS394_Shot_600_Grain_420	4.7348	0.6	0.30235	0.6	0.63	0.11454	0.52	1863	23	1701	34	1769	23	96.1
LAS394_Shot_607_Grain_421	15.2056	0.6	0.54999	0.6	0.42	0.20440	0.67	2850	25	2820	53	2823	27	99.9
LAS394_Shot_608_Grain_422	3.3991	0.8	0.26281	0.6	0.35	0.09563	0.84	1510	35	1505	32	1499	23	100.4
LAS394_Shot_609_Grain_423	2.0009	0.6	0.18557	0.5	0.38	0.07969	0.63	1175	29	1097	23	1114	19	98.5
LAS394_Shot_610_Grain_424	1.6895	0.7	0.15985	0.6	0.40	0.07797	0.70	1123	31	955	20	1002	18	95.3
LAS394_Shot_611_Grain_425	3.2476	0.7	0.25013	0.6	0.41	0.09595	0.69	1530	30	1439	30	1467	22	98.1
LAS394_Shot_612_Grain_426	1.0628	1.0	0.11268	0.6	0.20	0.06985	1.06	905	44	688	15	731	16	94.1
LAS394_Shot_613_Grain_427	1.9248	0.7	0.18498	0.6	0.21	0.07692	0.75	1093	33	1093	23	1086	19	100.7
LAS394_Shot_614_Grain_428	2.0705	0.6	0.19491	0.5	0.40	0.07837	0.65	1141	30	1147	23	1137	20	100.9
LAS394_Shot_615_Grain_429	3.9333	0.5	0.25935	0.4	0.57	0.11169	0.42	1819	20	1486	29	1618	22	91.8
LAS394_Shot_616_Grain_430	1.6185	0.6	0.15992	0.6	0.69	0.07464	0.46	1048	24	956	20	975	17	98.0
LAS394_Shot_617_Grain_431	2.0355	0.5	0.19944	0.5	0.42	0.07542	0.51	1070	26	1172	23	1125	18	104.1
LAS394_Shot_618_Grain_432	4.0371	0.5	0.27359	0.5	0.47	0.10902	0.49	1774	23	1558	30	1640	21	95.0
LAS394_Shot_619_Grain_433	4.9160	0.5	0.32839	0.5	0.38	0.11056	0.49	1800	22	1829	35	1802	23	101.5
LAS394_Shot_620_Grain_434	4.7150	0.4	0.31302	0.4	0.54	0.11106	0.39	1811	20	1754	33	1768	22	99.2
LAS394_Shot_627_Grain_435	1.7369	0.5	0.16073	0.5	0.73	0.07982	0.40	1186	22	960	20	1021	18	94.1
LAS394_Shot_628_Grain_436	1.9870	0.5	0.18911	0.5	0.32	0.07736	0.59	1122	27	1117	23	1109	18	100.7
LAS394_Shot_629_Grain_437	1.1435	0.7	0.12116	0.6	0.51	0.06965	0.65	901	31	737	16	772	16	95.5
LAS394_Shot_630_Grain_438	1.7549	0.8	0.17450	0.5	0.25	0.07448	0.82	1025	37	1036	22	1026	19	101.0
LAS394_Shot_631_Grain_439	1.7295	0.5	0.16854	0.5	0.56	0.07557	0.44	1074	23	1004	20	1019	18	98.5
LAS394_Shot_632_Grain_440	1.7608	0.5	0.17237	0.5	0.49	0.07536	0.51	1066	25	1025	21	1030	18	99.5
LAS394_Shot_633_Grain_441	4.6926	0.5	0.30796	0.5	0.50	0.11235	0.50	1829	23	1730	34	1764	23	98.1
LAS394_Shot_634_Grain_442	0.8160	0.8	0.09193	0.5	0.28	0.06545	0.84	772	38	567	12	604	14	93.8
LAS394_Shot_635_Grain_443	1.6896	0.9	0.16642	0.7	0.35	0.07466	0.86	1043	37	991	22	1000	19	99.1
LAS394_Shot_636_Grain_444	1.3766	0.6	0.14220	0.6	0.66	0.07120	0.50	952	25	857	19	876	17	97.8
LAS394_Shot_637_Grain_445	2.9872	0.5	0.23729	0.5	0.74	0.09259	0.36	1473	20	1372	27	1402	20	97.8
LAS394_Shot_638_Grain_446	0.5502	1.0	0.07082	0.5	-0.09	0.05743	1.09	574	41	441	10	443	11	99.5
LAS394_Shot_639_Grain_447	1.9823	1.3	0.18756	1.0	0.15	0.07834	1.46	1152	58	1107	28	1100	25	100.7
LAS394_Shot_640_Grain_448	2.9610	0.5	0.23812	0.5	0.66	0.09102	0.39	1443	21	1376	27	1395	20	98.6
LAS394_Shot_647_Grain_449	1.4887	0.5	0.14613	0.5	0.60	0.07456	0.44	1048	23	879	18	924	16	95.1
LAS394_Shot_648_Grain_450	1.8814	0.5	0.17899	0.5	0.48	0.07659	0.49	1105	25	1061	21	1073	18	98.9
LAS394_Shot_649_Grain_451	1.1661	1.5	0.12241	1.3	0.18	0.06920	0.64	894	30	742	23	773	21	96.0

LAS394_Shot_650_Grain_452	0.6255	1.3	0.07780	0.7	0.01	0.05908	1.45	737	52	483	11	490	14	98.4
LAS394_Shot_651_Grain_453	1.0569	1.9	0.09913	1.2	0.76	0.07750	1.20	1102	48	608	18	718	22	84.6
LAS394_Shot_652_Grain_454	1.5153	0.6	0.15152	0.6	0.54	0.07302	0.54	1003	27	909	19	936	17	97.1
LAS394_Shot_653_Grain_455	13.1368	0.6	0.49020	0.6	0.68	0.19655	0.49	2792	20	2569	50	2686	26	95.6
LAS394_Shot_654_Grain_456	2.2558	0.6	0.19648	0.5	0.58	0.08387	0.50	1280	24	1156	23	1196	20	96.7
LAS394_Shot_655_Grain_457	2.9202	0.6	0.23893	0.5	0.42	0.08956	0.64	1399	29	1380	28	1384	21	99.7
LAS394_Shot_656_Grain_458	2.4185	0.7	0.21615	0.6	0.37	0.08221	0.71	1229	32	1261	26	1246	21	101.3
LAS394_Shot_657_Grain_459	2.8122	0.6	0.22299	0.5	0.44	0.09261	0.62	1463	27	1298	26	1355	21	95.8
LAS394_Shot_658_Grain_460	1.8238	0.9	0.13470	0.8	0.76	0.09917	0.58	1599	25	814	20	1049	20	77.6
LAS394_Shot_659_Grain_461	0.7330	0.8	0.09141	0.5	0.19	0.05912	0.89	605	37	564	12	557	13	101.1
LAS394_Shot_660_Grain_462	1.8726	0.5	0.18158	0.4	0.30	0.07566	0.54	1075	26	1076	21	1070	18	100.6
LAS394_Shot_667_Grain_463	4.9854	0.4	0.31781	0.5	0.55	0.11518	0.42	1876	20	1778	34	1815	22	98.0
LAS394_Shot_668_Grain_464	2.0006	0.9	0.18676	0.6	0.33	0.07895	0.89	1139	39	1103	23	1111	21	99.3
LAS394_Shot_669_Grain_465	0.6837	1.3	0.08445	0.9	0.20	0.06024	1.41	737	52	522	13	526	16	99.2
LAS394_Shot_670_Grain_466	2.1875	0.5	0.18445	0.5	0.56	0.08756	0.53	1360	25	1090	23	1175	19	92.8
LAS394_Shot_671_Grain_467	2.0201	0.5	0.19290	0.5	0.50	0.07703	0.53	1113	26	1136	23	1122	19	101.3
LAS394_Shot_672_Grain_468	12.6929	0.6	0.49115	0.6	0.52	0.19001	0.58	2732	23	2572	48	2652	26	97.0
LAS394_Shot_673_Grain_469	11.7987	0.5	0.43344	0.5	0.59	0.20025	0.47	2821	19	2318	44	2586	25	89.6
LAS394_Shot_674_Grain_470	1.7295	1.5	0.17164	0.9	0.17	0.07548	1.68	1104	60	1020	26	1005	25	101.5
LAS394_Shot_675_Grain_471	10.1437	0.5	0.42053	0.5	0.53	0.17762	0.45	2623	19	2260	42	2445	25	92.5
LAS394_Shot_676_Grain_472	1.7716	0.6	0.17353	0.5	0.31	0.07550	0.69	1061	32	1032	21	1033	18	100.0
LAS394_Shot_677_Grain_473	7.1946	0.5	0.38902	0.5	0.52	0.13628	0.46	2172	21	2116	39	2133	24	99.2
LAS394_Shot_678_Grain_474	0.7900	1.4	0.09741	0.9	0.23	0.06033	1.55	751	57	599	15	587	17	102.0
LAS394_Shot_679_Grain_475	1.9248	0.6	0.18294	0.5	0.27	0.07789	0.71	1128	31	1082	22	1089	19	99.4
LAS394_Shot_680_Grain_476	1.9458	1.1	0.16141	0.9	0.93	0.08834	0.64	1376	28	963	24	1087	22	88.6
LAS394_Shot_687_Grain_477	0.6734	1.2	0.08400	0.8	0.11	0.05948	1.26	701	46	520	13	519	14	100.0
LAS394_Shot_688_Grain_478	2.8194	1.0	0.18827	0.8	0.84	0.10957	0.57	1782	24	1113	27	1351	25	82.3
LAS394_Shot_689_Grain_479	4.1931	0.5	0.29166	0.5	0.47	0.10577	0.49	1719	23	1649	32	1670	22	98.7
LAS394_Shot_690_Grain_480	2.8570	0.5	0.21707	0.4	0.48	0.09675	0.45	1554	22	1266	24	1370	20	92.5
LAS394_Shot_691_Grain_481	4.6027	0.6	0.30044	0.6	0.41	0.11304	0.62	1841	26	1693	35	1746	23	96.9
LAS394_Shot_692_Grain_482	2.0128	0.4	0.18914	0.4	0.49	0.07844	0.43	1150	22	1116	22	1119	18	99.8
LAS394_Shot_693_Grain_483	5.0227	0.5	0.32112	0.5	0.45	0.11502	0.50	1874	23	1794	34	1821	23	98.5
LAS394_Shot_694_Grain_484	2.1323	0.5	0.18947	0.4	0.40	0.08282	0.55	1251	26	1119	22	1157	19	96.8
LAS394_Shot_695_Grain_485	1.6253	0.8	0.16083	0.6	0.36	0.07439	0.81	1026	36	961	21	976	19	98.4
LAS394_Shot_696_Grain_486	0.7795	1.1	0.08753	0.7	0.23	0.06539	1.17	809	46	541	13	583	15	92.8

LAS394_Shot_697_Grain_487	1.7395	1.2	0.16495	0.8	0.21	0.07897	1.29	1155	50	985	24	1019	23	96.6
LAS394_Shot_698_Grain_488	2.4970	0.4	0.20885	0.4	0.60	0.08783	0.40	1371	21	1222	24	1269	19	96.3
LAS394_Shot_699_Grain_489	1.3682	0.5	0.14016	0.5	0.69	0.07162	0.38	971	21	845	17	874	16	96.7
LAS394_Shot_700_Grain_490	1.8666	0.7	0.17631	0.6	0.43	0.07750	0.65	1124	31	1047	22	1066	19	98.2
LAS394_Shot_707_Grain_491	12.7292	0.5	0.47207	0.5	0.61	0.19740	0.41	2798	18	2492	46	2657	25	93.8
LAS394_Shot_708_Grain_492	1.4130	0.7	0.14732	0.5	0.28	0.07048	0.77	920	36	885	19	893	17	99.2
LAS394_Shot_709_Grain_493	1.4710	0.7	0.14860	0.5	0.29	0.07261	0.71	990	33	893	19	916	17	97.5
LAS394_Shot_710_Grain_494	1.7477	0.8	0.17047	0.6	0.27	0.07541	0.85	1047	39	1014	21	1022	19	99.2
LAS394_Shot_711_Grain_495	2.0387	0.5	0.18876	0.5	0.48	0.07938	0.53	1172	25	1114	23	1127	19	98.9
LAS394_Shot_712_Grain_496	1.0032	0.6	0.10965	0.5	0.19	0.06707	0.60	822	29	670	14	704	14	95.3
LAS394_Shot_713_Grain_497	1.8532	1.0	0.17824	0.7	0.29	0.07652	1.03	1072	44	1056	24	1058	21	99.8
LAS394_Shot_714_Grain_498	1.6081	0.6	0.16171	0.5	0.37	0.07297	0.62	993	30	967	20	971	17	99.6
LAS394_Shot_715_Grain_499	8.4365	0.4	0.38242	0.5	0.61	0.16185	0.39	2469	18	2086	39	2277	24	91.6
LAS394_Shot_716_Grain_500	2.6535	1.4	0.17215	1.2	0.92	0.11162	0.56	1814	24	1021	29	1296	28	78.7
LAS394_Shot_717_Grain_501	4.4026	1.1	0.30349	0.9	0.28	0.10848	1.26	1722	48	1704	39	1705	28	99.9
LAS394_Shot_718_Grain_502	2.9527	0.8	0.24019	0.6	0.32	0.09049	0.81	1416	35	1386	29	1391	22	99.6
LAS394_Shot_719_Grain_503	1.8196	0.7	0.17672	0.5	0.24	0.07588	0.79	1064	36	1048	22	1048	19	100.0
LAS394_Shot_720_Grain_504	1.7300	0.7	0.16911	0.5	0.23	0.07533	0.76	1056	35	1007	21	1017	18	99.0
LAS394_Shot_727_Grain_505	1.8061	0.6	0.17644	0.6	0.51	0.07527	0.58	1069	28	1047	22	1046	19	100.0
LAS394_Shot_728_Grain_506	5.7661	0.8	0.36190	0.7	0.41	0.11755	0.80	1903	32	1987	41	1933	26	102.8
LAS394_Shot_729_Grain_507	2.2242	0.5	0.20364	0.5	0.63	0.08043	0.46	1198	24	1194	24	1186	19	100.6
LAS394_Shot_730_Grain_508	1.2680	0.7	0.11209	0.6	0.65	0.08342	0.56	1270	26	684	15	829	16	82.5
LAS394_Shot_731_Grain_509	2.4744	0.5	0.21506	0.5	0.53	0.08479	0.48	1300	24	1256	25	1263	20	99.4
LAS394_Shot_732_Grain_510	2.2117	0.8	0.19873	0.6	0.23	0.08229	0.88	1221	39	1168	25	1180	21	99.0
LAS394_Shot_733_Grain_511	3.1772	0.6	0.22798	0.6	0.72	0.10268	0.44	1666	21	1323	27	1448	21	91.3
LAS394_Shot_734_Grain_512	2.4689	0.6	0.21321	0.5	0.36	0.08528	0.69	1307	31	1245	25	1260	21	98.8
LAS394_Shot_735_Grain_513	3.4986	0.5	0.26648	0.4	0.46	0.09660	0.51	1551	24	1522	29	1524	22	99.9
LAS394_Shot_736_Grain_514	1.1862	2.7	0.12648	1.4	0.45	0.07244	3.23	1176	86	765	25	758	33	100.9
LAS394_Shot_737_Grain_515	2.0398	0.7	0.19118	0.5	0.43	0.07838	0.65	1139	30	1127	23	1126	19	100.1
LAS394_Shot_738_Grain_516	9.6658	0.4	0.42762	0.4	0.59	0.16618	0.41	2513	18	2293	42	2402	25	95.4
LAS394_Shot_739_Grain_517	1.2693	0.9	0.13054	0.6	0.26	0.07176	0.90	951	40	790	17	828	17	95.5
LAS394_Shot_740_Grain_518	3.9186	0.5	0.27062	0.5	0.52	0.10632	0.46	1732	22	1543	30	1616	21	95.5
LAS394_Shot_747_Grain_519	2.7375	0.8	0.22781	0.7	0.10	0.08873	0.89	1378	36	1321	29	1332	22	99.2
LAS394_Shot_748_Grain_520	11.5271	0.6	0.46441	0.6	0.52	0.18239	0.58	2663	23	2455	47	2562	26	95.8
LAS394_Shot_749_Grain_521	1.6795	0.6	0.16716	0.6	0.65	0.07368	0.46	1023	24	996	21	999	17	99.7

LAS394_Shot_750_ Grain_522	2.7251	0.7	0.21744	0.6	0.57	0.09181	0.58	1455	27	1268	26	1332	21	95.2
LAS394_Shot_751_ Grain_523	3.7293	0.5	0.27305	0.5	0.47	0.10018	0.49	1619	22	1555	31	1576	21	98.7
LAS394_Shot_752_ Grain_524	5.2009	0.8	0.33443	0.7	0.40	0.11439	0.82	1848	33	1856	40	1846	25	100.5
LAS394_Shot_753_ Grain_525	2.2655	0.9	0.21281	0.6	0.31	0.07828	0.93	1123	39	1242	26	1198	22	103.7
LAS394_Shot_754_ Grain_526	12.5461	1.0	0.48824	0.6	0.91	0.18645	0.59	2699	23	2563	47	2632	18	97.4
LAS394_Shot_755_ Grain_527	0.8761	1.4	0.09803	0.9	0.20	0.06549	1.54	864	56	602	15	632	18	95.3
LAS394_Shot_756_ Grain_528	1.7960	0.7	0.17293	0.6	0.35	0.07587	0.75	1072	34	1027	22	1041	19	98.7
LAS394_Shot_757_ Grain_529	1.5116	0.5	0.14495	0.5	0.46	0.07626	0.56	1091	27	872	18	933	17	93.5
LAS394_Shot_758_ Grain_530	1.4924	0.6	0.12032	0.5	0.60	0.09061	0.51	1428	24	732	15	925	17	79.1
LAS394_Shot_759_ Grain_531	1.7115	0.5	0.16015	0.4	0.39	0.07796	0.53	1132	26	957	19	1011	17	94.7
LAS394_Shot_760_ Grain_532	2.0415	0.5	0.18811	0.5	0.65	0.07895	0.40	1164	21	1110	22	1128	18	98.5
LAS394_Shot_767_ Grain_533	5.5189	1.2	0.23276	1.1	0.87	0.17255	0.58	2576	24	1347	35	1893	29	71.2
LAS394_Shot_768_ Grain_534	3.1463	0.6	0.24589	0.5	0.38	0.09343	0.59	1487	26	1416	28	1442	21	98.2
LAS394_Shot_769_ Grain_535	1.6507	0.8	0.16466	0.6	0.24	0.07310	0.80	1004	36	982	21	986	19	99.6
LAS394_Shot_770_ Grain_536	4.5435	0.5	0.29025	0.5	0.64	0.11428	0.41	1861	20	1643	32	1736	22	94.6
LAS394_Shot_771_ Grain_537	2.8823	0.6	0.21839	0.5	0.55	0.09653	0.55	1547	25	1273	26	1376	22	92.5
LAS394_Shot_772_ Grain_538	2.7596	0.5	0.21952	0.5	0.41	0.09161	0.40	1452	21	1278	26	1342	19	95.2
LAS394_Shot_773_ Grain_539	3.8039	0.6	0.27505	0.5	0.40	0.10115	0.61	1631	26	1566	31	1590	22	98.5
LAS394_Shot_774_ Grain_540	0.7146	1.4	0.09100	0.8	0.05	0.05851	1.62	745	56	561	14	545	17	102.9
LAS394_Shot_775_ Grain_541	12.5064	0.5	0.49088	0.5	0.49	0.18631	0.50	2705	21	2573	48	2640	25	97.5
LAS394_Shot_776_ Grain_542	2.7631	0.5	0.22522	0.4	0.59	0.08968	0.43	1410	22	1309	26	1344	20	97.4
LAS394_Shot_777_ Grain_543														
LAS394_Shot_778_ Grain_544	1.8850	1.1	0.15951	0.7	0.14	0.08732	1.19	1321	49	953	22	1069	22	89.1
LAS394_Shot_779_ Grain_545	7.5058	0.4	0.34442	0.5	0.69	0.15963	0.35	2448	17	1906	36	2172	24	87.8
LAS394_Shot_780_ Grain_546	2.5323	0.5	0.21633	0.5	0.42	0.08570	0.54	1320	26	1262	25	1279	20	98.7
LAS394_Shot_787_ Grain_547	1.7538	0.6	0.16970	0.5	0.34	0.07584	0.64	1071	30	1010	21	1026	18	98.4
LAS394_Shot_788_ Grain_548	5.2122	0.5	0.33071	0.4	0.53	0.11535	0.46	1879	21	1840	35	1852	23	99.4
LAS394_Shot_789_ Grain_549	1.5971	0.8	0.15688	0.7	0.05	0.07483	0.73	1039	32	939	21	964	19	97.3
LAS394_Shot_790_ Grain_550	1.8391	0.8	0.17941	0.6	0.29	0.07553	0.83	1061	36	1063	23	1057	20	100.5
LAS394_Shot_791_ Grain_551	1.7017	0.4	0.16674	0.4	0.67	0.07478	0.35	1056	20	994	20	1008	17	98.6
LAS394_Shot_792_ Grain_552	1.2816	0.7	0.12808	0.6	0.44	0.07358	0.74	1013	33	776	17	835	17	93.0
LAS394_Shot_793_ Grain_553	3.6956	0.4	0.26054	0.4	0.54	0.10364	0.42	1682	21	1492	28	1569	22	95.1
LAS394_Shot_794_ Grain_554	2.6014	0.5	0.21913	0.5	0.69	0.08671	0.38	1347	20	1277	25	1301	20	98.1
LAS394_Shot_795_ Grain_555	3.3079	0.7	0.24306	0.6	0.26	0.09971	0.74	1597	31	1401	29	1478	22	94.8
LAS394_Shot_796_ Grain_556	12.8398	0.5	0.49583	0.5	0.53	0.18895	0.52	2726	21	2592	48	2665	25	97.3

LAS394_Shot_797_ Grain_557	1.8101	0.6	0.17527	0.5	0.32	0.07558	0.61	1070	29	1040	21	1048	18	99.3
LAS394_Shot_798_ Grain_558	12.4467	0.4	0.48634	0.5	0.58	0.18659	0.43	2708	19	2552	47	2636	25	96.8
LAS394_Shot_799_ Grain_559	3.3144	0.8	0.24883	0.7	0.56	0.09713	0.67	1556	29	1430	31	1478	23	96.8
LAS394_Shot_800_ Grain_560	2.0631	0.7	0.18185	0.5	0.56	0.08236	0.57	1244	27	1076	22	1135	20	94.9
LAS394_Shot_807_ Grain_561	4.9543	0.7	0.31194	0.7	0.39	0.11599	0.81	1871	33	1747	37	1805	25	96.8
LAS394_Shot_808_ Grain_562	4.0197	0.6	0.28778	0.6	0.55	0.10150	0.58	1641	25	1628	33	1635	23	99.6
LAS394_Shot_809_ Grain_563	11.5141	0.4	0.45712	0.5	0.61	0.18278	0.39	2672	18	2426	45	2563	25	94.7
LAS394_Shot_810_ Grain_564	1.4154	0.7	0.13952	0.6	0.27	0.07411	0.73	1024	33	841	18	894	17	94.2
LAS394_Shot_811_ Grain_565	2.0516	0.6	0.18940	0.5	0.35	0.07894	0.61	1153	28	1117	23	1131	19	98.8
LAS394_Shot_812_ Grain_566	1.7709	0.6	0.16913	0.6	0.37	0.07600	0.66	1087	30	1007	21	1032	18	97.6
LAS394_Shot_813_ Grain_567	11.0912	0.8	0.40717	0.7	0.83	0.19750	0.44	2800	19	2198	45	2522	28	87.2
LAS394_Shot_814_ Grain_568	2.0944	0.7	0.19429	0.5	0.40	0.07882	0.63	1151	29	1145	23	1143	20	100.1
LAS394_Shot_815_ Grain_569	2.6576	1.5	0.14412	1.1	0.86	0.13361	0.83	2125	31	866	23	1301	28	66.5
LAS394_Shot_816_ Grain_570	3.9133	0.6	0.27245	0.6	0.70	0.10428	0.45	1694	22	1553	32	1612	23	96.3
LAS394_Shot_817_ Grain_571	1.9792	0.7	0.18855	0.5	0.31	0.07635	0.71	1085	32	1113	23	1105	19	100.7
LAS394_Shot_818_ Grain_572	1.4482	1.4	0.14218	0.8	0.21	0.07490	1.46	1083	55	856	20	898	23	95.3
LAS394_Shot_819_ Grain_573	2.7711	0.5	0.22952	0.4	0.34	0.08804	0.53	1372	25	1332	26	1345	20	99.0
LAS394_Shot_820_ Grain_574	2.0778	0.9	0.19302	0.6	0.18	0.07898	0.94	1140	40	1137	24	1137	21	100.0
LAS394_Shot_827_ Grain_575	0.6314	1.4	0.07778	0.7	0.07	0.06058	1.52	763	53	483	11	494	15	97.7
LAS394_Shot_828_ Grain_576	3.2663	0.6	0.25705	0.6	0.44	0.09353	0.61	1484	27	1473	30	1471	22	100.2
LAS394_Shot_829_ Grain_577	1.8327	0.8	0.17771	0.7	0.25	0.07621	0.92	1075	41	1053	23	1055	21	99.9
LAS394_Shot_830_ Grain_578	1.2602	0.6	0.12598	0.5	0.41	0.07383	0.60	1025	28	765	16	826	16	92.6
LAS394_Shot_831_ Grain_579	1.9695	0.6	0.17575	0.5	0.35	0.08225	0.65	1240	30	1043	21	1103	19	94.5
LAS394_Shot_832_ Grain_580	1.7959	1.9	0.17358	1.2	0.14	0.07746	2.09	1221	71	1030	29	1020	31	101.0
LAS394_Shot_833_ Grain_581	1.7078	0.5	0.17007	0.5	0.38	0.07414	0.58	1032	28	1012	21	1011	18	100.1
LAS394_Shot_834_ Grain_582	1.8200	0.6	0.17764	0.6	0.36	0.07588	0.69	1074	31	1053	22	1052	18	100.1
LAS394_Shot_835_ Grain_583	12.7654	0.5	0.49475	0.6	0.46	0.19054	0.56	2736	22	2587	48	2658	26	97.3
LAS394_Shot_836_ Grain_584	2.1418	1.5	0.20365	1.0	0.15	0.07890	1.66	1158	61	1194	31	1145	28	104.2
LAS394_Shot_837_ Grain_585	1.7920	0.5	0.16918	0.5	0.44	0.07864	0.52	1150	25	1007	21	1042	17	96.6
LAS394_Shot_838_ Grain_586	1.8236	0.5	0.18043	0.5	0.47	0.07469	0.44	1055	22	1069	22	1052	18	101.6
LAS394_Shot_839_ Grain_587	1.6081	0.6	0.15314	0.5	0.56	0.07751	0.54	1125	26	919	19	972	17	94.6
LAS394_Shot_840_ Grain_588	0.6936	1.0	0.08748	0.7	0.16	0.05892	1.10	636	43	540	12	532	13	101.6
LAS394_Shot_847_ Grain_589	4.7037	0.5	0.31462	0.5	0.11	0.11087	0.50	1803	23	1762	34	1765	22	99.8
LAS394_Shot_848_ Grain_590	1.5596	0.5	0.15621	0.6	0.73	0.07407	0.44	1036	24	935	20	952	17	98.2
LAS394_Shot_849_ Grain_591	2.4179	0.8	0.21459	0.7	0.37	0.08415	0.85	1266	37	1253	27	1244	22	100.7

LAS394_Shot_850_Grain_592	2.2852	0.6	0.20802	0.5	0.56	0.08161	0.51	1225	25	1217	25	1206	19	101.0
LAS394_Shot_851_Grain_593	8.4347	0.4	0.36974	0.5	0.63	0.16950	0.40	2547	19	2026	38	2277	25	89.0
LAS394_Shot_852_Grain_594	0.7171	2.0	0.08571	1.1	0.06	0.06372	2.31	980	74	529	15	537	21	98.6
LAS394_Shot_853_Grain_595	1.4107	0.7	0.13477	0.5	0.34	0.07742	0.71	1117	32	815	17	891	17	91.5
LAS394_Shot_854_Grain_596	2.5915	0.4	0.22624	0.5	0.54	0.08468	0.44	1300	22	1316	27	1297	20	101.5
LAS394_Shot_855_Grain_597	0.6995	1.5	0.08622	0.8	0.02	0.06067	1.66	773	56	533	13	532	16	100.2
LAS394_Shot_856_Grain_598	1.7665	1.2	0.17745	0.8	0.29	0.07444	1.22	1012	51	1051	25	1026	22	102.5
LAS394_Shot_857_Grain_599	2.6223	0.7	0.21136	0.6	0.30	0.09204	0.82	1444	35	1235	26	1302	22	94.9
LAS394_Shot_858_Grain_600	2.1496	1.2	0.20083	0.8	0.27	0.07930	1.22	1138	50	1178	27	1156	24	101.9
LAS394_Shot_859_Grain_601	4.3112	0.6	0.29414	0.5	0.38	0.10862	0.63	1764	26	1662	33	1695	23	98.1
LAS394_Shot_860_Grain_602	9.8504	0.4	0.44248	0.4	0.57	0.16405	0.38	2493	18	2360	43	2418	24	97.6
LAS394_Shot_867_Grain_603	1.6125	0.9	0.15744	0.8	0.63	0.07541	0.70	1068	32	944	22	971	19	97.1
LAS394_Shot_868_Grain_604	1.2526	1.4	0.12892	1.0	0.78	0.07115	0.88	932	39	780	21	815	21	95.7
LAS394_Shot_869_Grain_605	2.8464	0.6	0.22851	0.5	0.43	0.09154	0.62	1443	27	1328	28	1364	21	97.3
LAS394_Shot_870_Grain_606	3.5590	0.7	0.26924	0.6	0.34	0.09724	0.71	1554	30	1535	31	1536	23	99.9
LAS394_Shot_871_Grain_607	3.0274	0.8	0.21134	0.7	0.73	0.10486	0.54	1703	24	1234	27	1408	22	87.6
LAS394_Shot_872_Grain_608	4.1543	0.6	0.27346	0.6	0.59	0.11139	0.55	1811	24	1559	33	1660	23	93.9
LAS394_Shot_873_Grain_609	1.9048	1.0	0.18103	0.7	0.06	0.07763	1.06	1108	43	1072	24	1075	21	99.7
LAS394_Shot_874_Grain_610	2.7983	0.4	0.20883	0.5	0.65	0.09834	0.40	1588	20	1222	25	1353	20	90.3
LAS394_Shot_875_Grain_611	2.3137	0.8	0.20036	0.6	0.33	0.08467	0.77	1289	33	1177	24	1212	21	97.1
LAS394_Shot_876_Grain_612	3.6327	0.5	0.27112	0.5	0.53	0.09832	0.51	1583	23	1545	31	1554	22	99.4
LAS394_Shot_877_Grain_613	1.5542	0.9	0.15300	0.6	0.13	0.07503	1.04	1034	45	917	20	949	19	96.7
LAS394_Shot_878_Grain_614	2.7589	0.5	0.22657	0.5	0.44	0.08940	0.51	1401	24	1316	26	1343	20	98.0
LAS394_Shot_879_Grain_615	2.5494	0.5	0.21123	0.5	0.63	0.08847	0.44	1386	22	1235	25	1284	20	96.1
LAS394_Shot_880_Grain_616	2.0998	0.8	0.18577	0.6	0.41	0.08313	0.77	1250	33	1097	24	1145	20	95.9

LAS395 (20BREM08A)														
Isotopic Ratios								Calculated ages (Ma)						
ID	$^{207}Pb/^{235}U$	2σ	$^{206}Pb/^{238}U$	2σ	Rho	$^{207/206}Pb$	2σ	$^{207/206}Pb$	2σ	$^{206}Pb/^{238}U$	2σ	$^{207}Pb/^{235}U$	2σ	%conc
LAS395_shot_793_grain_547	1.9093	1.0	0.18597	0.7	0.34	0.08961	0.94	1366	64	1096	185	1071	130	80
LAS395_shot_794_grain_548	0.7193	1.0	0.10835	0.7	0.28	0.06006	1.00	761	55	662	115	545	82	121
LAS395_shot_795_grain_549	1.5283	0.7	0.18871	0.6	0.33	0.07489	0.64	1032	57	1112	187	935	120	108
LAS395_shot_796_grain_550	1.3623	1.9	0.16168	1.4	0.16	0.07610	0.87	1090	56	956	161	825	108	88
LAS395_shot_797_grain_551	1.6158	2.3	0.21918	1.2	0.18	0.07744	2.56	1326	77	1272	212	928	123	96

LAS395_shot_798_grain_552	2.0454	0.6	0.25928	0.6	0.38	0.07785	0.64	1117	58	1483	242	1124	133	133
LAS395_shot_799_grain_553	1.8945	0.6	0.24728	0.5	0.48	0.07650	0.56	1082	57	1422	232	1075	129	131
LAS395_shot_800_grain_554	1.8128	1.5	0.22893	1.1	0.58	0.07762	0.61	1103	57	1317	214	1023	121	119
LAS395_shot_801_grain_555	1.3853	1.8	0.18086	1.3	0.86	0.07251	0.90	1012	59	1066	181	844	110	105
LAS395_shot_802_grain_556	1.5455	0.7	0.20367	0.7	0.53	0.07367	0.57	1011	56	1191	199	944	119	118
LAS395_shot_803_grain_557	4.1850	0.8	0.36589	0.8	0.69	0.10762	0.61	1733	55	2002	319	1653	160	116
LAS395_shot_804_grain_558	1.4485	0.6	0.17583	0.6	0.63	0.07487	0.53	1045	56	1042	178	904	117	100
LAS395_shot_805_grain_559	3.0466	0.6	0.30136	0.5	0.49	0.08803	0.56	1356	56	1694	272	1414	149	125
LAS395_shot_806_grain_560	1.4957	0.5	0.16863	0.5	0.53	0.07327	0.48	999	57	1004	169	925	118	100
LAS395_shot_813_grain_561	9.6703	1.7	0.32185	1.5	0.94	0.17373	0.68	2571	51	1763	294	2268	229	69
LAS395_shot_814_grain_562	0.9244	1.2	0.08489	0.9	0.51	0.06607	1.12	923	59	524	92	654	95	80
LAS395_shot_815_grain_563	2.6789	0.4	0.19097	0.4	0.57	0.08338	0.38	1266	52	1126	189	1321	142	89
LAS395_shot_816_grain_564	2.1902	0.6	0.17127	0.5	0.38	0.07598	0.62	1065	57	1018	172	1173	139	96
LAS395_shot_817_grain_565	1.0451	0.8	0.09169	0.7	0.69	0.06745	0.57	830	60	565	99	720	99	78
LAS395_shot_818_grain_566	1.0205	1.0	0.09505	0.8	0.20	0.06413	0.76	782	56	584	101	704	99	83
LAS395_shot_819_grain_567	0.9273	1.7	0.08863	0.8	0.18	0.06370	1.68	1066	66	547	96	642	95	85
LAS395_shot_820_grain_568	3.9906	0.8	0.23807	0.9	0.71	0.10434	0.63	1678	53	1372	227	1621	161	82
LAS395_shot_821_grain_569	0.8734	1.7	0.09103	0.8	0.14	0.06156	1.73	1009	66	561	99	618	93	91
LAS395_shot_822_grain_570	1.4215	0.6	0.12986	0.5	0.37	0.07060	0.63	915	59	786	136	893	115	88
LAS395_shot_823_grain_571	4.4011	0.6	0.29042	0.6	0.61	0.10011	0.50	1610	52	1640	264	1703	160	102
LAS395_shot_824_grain_572	1.9220	0.6	0.16208	0.5	0.41	0.08064	0.57	1192	57	967	163	1084	129	81
LAS395_shot_825_grain_573	1.9674	0.8	0.18483	0.6	0.33	0.07450	0.78	1019	59	1092	183	1096	128	107
LAS395_shot_826_grain_574	0.6095	0.5	0.07446	0.4	0.51	0.05837	0.46	554	56	463	82	482	74	96
LAS395_shot_833_grain_575	2.5280	1.0	0.18674	0.8	0.77	0.10631	0.59	1715	53	1099	185	1263	139	64
LAS395_shot_834_grain_576	1.8070	0.5	0.17907	0.5	0.52	0.07969	0.47	1174	54	1061	179	1045	123	90
LAS395_shot_835_grain_577	7.3862	0.9	0.33650	0.8	0.74	0.17421	0.63	2570	49	1860	296	2136	174	72
LAS395_shot_836_grain_578	2.8398	0.7	0.24437	0.6	0.43	0.09224	0.71	1437	59	1408	232	1358	146	98
LAS395_shot_837_grain_579	1.9111	0.6	0.19251	0.5	0.44	0.07879	0.57	1142	58	1134	191	1082	127	99
LAS395_shot_838_grain_580	1.6282	0.6	0.16330	0.5	0.53	0.07890	0.53	1147	57	975	165	976	120	85
LAS395_shot_839_grain_581	4.4837	0.5	0.31008	0.5	0.57	0.11343	0.50	1835	51	1741	283	1723	161	95
LAS395_shot_840_grain_582	0.8327	1.3	0.08615	0.9	0.74	0.07452	0.83	1042	60	531	93	605	88	88
LAS395_shot_841_grain_583	1.7105	1.9	0.16076	1.5	0.56	0.07900	0.94	1150	58	952	165	951	128	83
LAS395_shot_842_grain_584	0.9963	0.7	0.08997	0.5	0.56	0.08560	0.57	1307	56	555	97	698	98	80
LAS395_shot_843_grain_585	1.0649	0.6	0.10842	0.5	0.36	0.07538	0.63	1057	59	663	115	734	101	90
LAS395_shot_844_grain_586	2.0560	1.0	0.19815	0.7	0.31	0.08015	1.01	1181	61	1163	195	1119	133	98

LAS395_shot_845_grain_587	1.7466	1.3	0.09899	0.6	0.60	0.13160	0.95	2075	55	608	106	1008	114	60
LAS395_shot_846_grain_588	12.5832	0.5	0.49990	0.6	0.63	0.18948	0.47	2723	45	2608	397	2641	179	96
LAS395_shot_853_grain_589	0.6173	0.5	0.07881	0.5	0.51	0.05743	0.46	524	55	489	86	487	74	100
LAS395_shot_854_grain_590	0.6410	0.9	0.07841	0.6	0.28	0.05989	0.88	726	56	486	85	499	76	98
LAS395_shot_855_grain_591	1.4953	0.9	0.13767	0.7	0.66	0.07918	0.66	1144	59	830	142	919	117	90
LAS395_shot_856_grain_592	0.7190	1.0	0.08536	0.7	0.29	0.06201	1.03	806	56	528	93	544	82	97
LAS395_shot_857_grain_593	0.5794	0.8	0.07344	0.7	0.46	0.05791	0.76	606	53	456	80	462	71	99
LAS395_shot_858_grain_594	2.9144	0.7	0.23208	0.7	0.68	0.09191	0.54	1443	55	1343	224	1376	148	93
LAS395_shot_859_grain_595	9.2069	0.6	0.37318	0.6	0.70	0.18053	0.43	2647	46	2038	319	2350	177	77
LAS395_shot_860_grain_596	1.5370	0.7	0.15247	0.6	0.59	0.07361	0.58	1001	59	914	156	938	118	91
LAS395_shot_861_grain_597	4.7174	0.5	0.30472	0.5	0.46	0.11369	0.51	1844	51	1712	272	1766	161	93
LAS395_shot_862_grain_598	1.4632	0.7	0.13342	0.5	0.35	0.08005	0.68	1168	59	808	141	911	115	89
LAS395_shot_863_grain_599	1.6115	0.9	0.15985	0.8	0.78	0.07396	0.56	1012	58	953	163	962	125	94
LAS395_shot_864_grain_600	0.9489	1.1	0.10375	0.8	0.75	0.06716	0.74	848	57	635	111	670	96	95
LAS395_shot_865_grain_601	1.6301	1.6	0.15879	1.1	0.47	0.07697	1.35	1164	64	944	161	953	123	81
LAS395_shot_866_grain_602	1.7299	0.8	0.15282	0.7	0.84	0.08288	0.45	1248	55	914	156	1008	128	73
LAS395_shot_873_grain_603	0.6027	1.4	0.07364	0.6	0.12	0.06157	1.43	943	61	458	81	469	74	98
LAS395_shot_874_grain_604	3.9175	0.7	0.23877	0.7	0.68	0.12277	0.59	1980	51	1378	228	1611	158	70
LAS395_shot_875_grain_605	0.6015	0.6	0.07851	0.5	0.43	0.05751	0.56	552	55	487	86	477	73	102
LAS395_shot_876_grain_606	1.1739	0.8	0.12445	0.5	0.49	0.07030	0.69	928	59	756	131	783	106	97
LAS395_shot_877_grain_607	2.8158	0.8	0.20211	0.7	0.67	0.10469	0.62	1683	54	1184	198	1350	144	70
LAS395_shot_878_grain_608	1.7173	0.4	0.17236	0.5	0.57	0.07446	0.41	1043	56	1025	173	1012	122	98
LAS395_shot_879_grain_609	13.2550	0.6	0.52650	0.6	0.60	0.18886	0.55	2718	47	2717	409	2691	184	100
LAS395_shot_880_grain_610	1.7475	0.8	0.17216	0.8	0.67	0.07603	0.62	1067	57	1021	173	1017	127	96
LAS395_shot_881_grain_611	2.2892	0.6	0.17510	0.6	0.50	0.09850	0.60	1569	54	1038	175	1203	137	66
LAS395_shot_882_grain_612	0.7163	1.3	0.09087	0.7	0.13	0.05995	1.34	865	61	560	98	540	83	104
LAS395_shot_883_grain_613	1.6766	1.2	0.16961	0.9	0.49	0.07492	1.09	1076	62	1006	171	978	123	93
LAS395_shot_884_grain_614	0.7154	1.3	0.08876	0.7	0.18	0.06098	1.36	905	61	548	96	538	84	102
LAS395_shot_885_grain_615	4.3643	0.8	0.29911	0.7	0.46	0.11007	0.74	1758	56	1684	273	1696	161	96
LAS395_shot_886_grain_616	1.8930	1.1	0.18308	0.8	0.39	0.07781	1.07	1146	62	1079	182	1058	130	94
LAS395_shot_893_grain_617	2.2300	1.3	0.20744	0.8	0.18	0.08035	1.39	1239	65	1211	202	1168	141	98
LAS395_shot_894_grain_618	1.3846	0.8	0.13540	0.7	0.64	0.07425	0.65	1018	57	817	140	874	114	93
LAS395_shot_895_grain_619	1.7023	1.0	0.15527	0.6	0.33	0.07977	0.98	1143	62	929	159	1001	123	81
LAS395_shot_896_grain_620	2.2982	0.8	0.20788	0.6	0.27	0.08010	0.87	1167	61	1216	204	1202	139	104
LAS395_shot_897_grain_621	2.1386	0.8	0.19001	0.6	0.52	0.08030	0.69	1164	60	1119	189	1151	133	96

LAS395_shot_898_grain_622	1.1477	1.6	0.08349	0.7	0.10	0.10015	1.72	1474	74	516	91	756	101	68
LAS395_shot_899_grain_623	1.6727	1.4	0.13233	1.0	0.88	0.08696	0.74	1351	55	797	138	968	132	82
LAS395_shot_900_grain_624	1.2314	2.3	0.09139	1.4	0.91	0.09067	1.14	1395	64	562	99	780	103	72
LAS395_shot_901_grain_625	5.2214	0.7	0.31929	0.6	0.74	0.11533	0.48	1868	50	1780	284	1843	167	95
LAS395_shot_902_grain_626	7.2392	0.5	0.33077	0.5	0.49	0.15501	0.55	2384	48	1839	292	2132	171	77
LAS395_shot_903_grain_627	2.7664	0.5	0.22871	0.5	0.26	0.08567	0.45	1312	53	1326	220	1341	143	101
LAS395_shot_904_grain_628	1.8490	0.5	0.17427	0.5	0.53	0.07546	0.52	1059	56	1035	174	1059	128	98
LAS395_shot_905_grain_629	1.9874	0.6	0.16640	0.6	0.65	0.08548	0.49	1310	54	992	170	1105	129	76
LAS395_shot_906_grain_630	1.8194	0.7	0.17210	0.6	0.26	0.07663	0.80	1086	61	1022	173	1044	127	94
LAS395_shot_913_grain_631	3.0334	0.8	0.20315	0.7	0.54	0.11345	0.73	1819	55	1190	198	1405	148	65
LAS395_shot_914_grain_632	1.0153	1.2	0.10878	0.7	0.21	0.07122	1.22	1045	60	665	116	699	100	95
LAS395_shot_915_grain_633	2.9131	0.5	0.20804	0.5	0.60	0.10559	0.46	1708	50	1218	199	1381	145	71
LAS395_shot_916_grain_634	0.9391	1.4	0.08669	0.7	0.11	0.08273	1.46	1313	67	535	94	658	97	81
LAS395_shot_917_grain_635	1.9575	0.7	0.16928	0.7	0.80	0.08629	0.44	1328	53	1006	172	1094	131	76
LAS395_shot_918_grain_636	0.5062	1.5	0.05865	0.9	0.42	0.06404	1.38	882	65	367	65	409	66	74
LAS395_shot_919_grain_637	3.3500	1.2	0.22592	1.1	0.88	0.10865	0.57	1753	53	1302	216	1455	151	96
LAS395_shot_920_grain_638	0.9768	1.1	0.10732	0.8	0.57	0.06731	0.91	896	55	656	114	683	98	98
LAS395_shot_921_grain_639	1.3096	1.5	0.13466	1.1	0.61	0.07111	1.07	999	62	811	140	827	110	88
LAS395_shot_922_grain_640	1.5960	0.7	0.14048	0.6	0.51	0.08304	0.68	1228	59	846	145	962	121	91
LAS395_shot_923_grain_641	12.8023	0.5	0.47731	0.5	0.57	0.19451	0.46	2769	46	2511	381	2658	181	99
LAS395_shot_924_grain_642	0.5890	0.5	0.07426	0.5	0.42	0.05744	0.53	535	55	462	82	469	72	86
LAS395_shot_925_grain_643	2.4302	0.9	0.20035	0.8	0.78	0.08773	0.59	1356	55	1172	197	1234	147	115
LAS395_shot_926_grain_644	2.2056	0.9	0.21356	0.7	0.43	0.07557	0.90	1084	58	1244	208	1169	136	97
LAS395_shot_933_grain_645	3.9687	0.6	0.29729	0.6	0.55	0.10684	0.55	1724	53	1674	267	1621	158	93
LAS395_shot_934_grain_646	4.2987	0.7	0.30796	0.6	0.65	0.11431	0.53	1858	50	1728	274	1684	161	96
LAS395_shot_935_grain_647	3.6077	0.6	0.28697	0.6	0.69	0.10469	0.50	1691	51	1622	263	1543	156	106
LAS395_shot_936_grain_648	0.6936	1.3	0.09021	1.0	0.86	0.06424	0.67	764	56	555	97	525	78	97
LAS395_shot_937_grain_649	1.5314	0.6	0.17410	0.6	0.39	0.07597	0.66	1069	59	1033	174	939	119	97
LAS395_shot_938_grain_650	1.7961	0.5	0.19491	0.5	0.54	0.08041	0.50	1185	57	1146	191	1041	126	84
LAS395_shot_939_grain_651	8.7909	0.5	0.41650	0.5	0.66	0.18445	0.39	2684	46	2243	342	2313	174	80
LAS395_shot_940_grain_652	1.5372	0.7	0.16396	0.6	0.70	0.08204	0.53	1222	55	977	166	938	121	73
LAS395_shot_941_grain_653	2.5154	0.9	0.21039	0.8	0.71	0.10478	0.63	1682	54	1226	205	1262	144	101
LAS395_shot_942_grain_654	0.7448	0.6	0.09225	0.5	0.31	0.07022	0.65	910	59	568	99	563	83	82
LAS395_shot_943_grain_655	6.4958	0.7	0.35872	0.8	0.75	0.15572	0.51	2398	49	1967	312	2034	173	76
LAS395_shot_944_grain_656	7.9248	0.9	0.36717	0.8	0.80	0.17929	0.49	2632	47	2011	318	2201	171	101

LAS395_shot_945_grain_657	1.2731	0.6	0.13906	0.5	0.52	0.07461	0.59	1033	60	838	143	830	111	79
LAS395_shot_946_grain_658	1.6612	1.7	0.16333	1.3	0.58	0.07981	1.30	1233	63	969	168	952	129	92
LAS395_shot_953_grain_659	17.3622	0.7	0.47448	0.7	0.51	0.18856	0.70	2702	48	2491	376	2941	186	74
LAS395_shot_954_grain_660	1.0139	0.9	0.08416	0.6	0.48	0.06048	0.76	684	57	520	91	705	97	107
LAS395_shot_955_grain_661	2.7862	0.6	0.18592	0.6	0.56	0.07378	0.53	1025	57	1098	184	1347	144	105
LAS395_shot_956_grain_662	6.2253	0.7	0.30386	0.6	0.40	0.10184	0.66	1626	56	1707	274	1996	170	82
LAS395_shot_957_grain_663	3.4372	0.8	0.19126	0.6	-0.08	0.09167	1.14	1381	60	1127	191	1501	146	68
LAS395_shot_958_grain_664	0.8747	1.0	0.06950	0.7	0.59	0.06404	0.81	794	55	433	77	632	91	94
LAS395_shot_959_grain_665	2.6954	0.9	0.18112	0.7	0.37	0.07903	0.90	1141	59	1070	180	1313	144	89
LAS395_shot_960_grain_666	15.2529	0.7	0.45033	0.7	0.79	0.18309	0.45	2675	46	2389	369	2817	189	93
LAS395_shot_961_grain_667	6.1992	0.6	0.30582	0.6	0.58	0.11434	0.55	1849	52	1718	271	1998	169	83
LAS395_shot_962_grain_668	1.0376	1.5	0.09403	0.8	0.15	0.06615	1.59	1061	63	578	101	700	102	73
LAS395_shot_963_grain_669	0.9149	0.8	0.07667	0.5	0.34	0.07223	0.79	967	60	476	84	653	93	93
LAS395_shot_964_grain_670	2.8236	0.9	0.21046	0.6	0.23	0.08628	0.99	1315	61	1229	205	1346	145	80
LAS395_shot_965_grain_671	14.1013	0.9	0.43767	0.8	0.81	0.21312	0.47	2918	45	2324	362	2733	198	64
LAS395_shot_966_grain_672	6.9639	0.7	0.28742	0.7	0.78	0.16824	0.47	2526	47	1624	263	2092	174	120
LAS395_shot_973_grain_673	2.6352	0.8	0.27358	0.6	0.40	0.08588	0.76	1300	61	1554	253	1300	143	77
LAS395_shot_974_grain_674	4.2422	1.0	0.28686	0.9	0.82	0.13251	0.59	2109	50	1614	262	1653	165	76
LAS395_shot_975_grain_675	2.1864	1.4	0.14445	0.9	0.86	0.13299	0.70	2100	51	868	149	1146	129	98
LAS395_shot_976_grain_676	3.5620	0.9	0.30201	0.8	0.81	0.10678	0.52	1730	51	1692	276	1521	163	110
LAS395_shot_977_grain_677	1.6465	0.5	0.19797	0.5	0.26	0.07574	0.58	1058	57	1164	196	984	121	97
LAS395_shot_978_grain_678	1.0259	1.2	0.11171	0.8	0.51	0.08255	1.06	1242	61	681	118	705	100	83
LAS395_shot_979_grain_679	1.5125	0.5	0.16728	0.4	0.43	0.08124	0.50	1204	56	997	168	933	119	112
LAS395_shot_980_grain_680	1.2957	1.8	0.15051	1.3	0.91	0.07301	0.87	1044	56	896	154	802	114	99
LAS395_shot_981_grain_681	11.4665	0.5	0.52289	0.5	0.70	0.19081	0.34	2745	44	2706	403	2556	181	101
LAS395_shot_982_grain_682	2.4893	0.8	0.24042	0.7	0.74	0.08857	0.54	1377	54	1387	228	1258	144	78
LAS395_shot_983_grain_683	7.5913	1.0	0.36685	0.9	0.84	0.17238	0.48	2567	46	2004	316	2160	174	111
LAS395_shot_984_grain_684	0.6925	1.7	0.09420	0.8	0.17	0.06160	1.71	993	62	580	102	523	81	89
LAS395_shot_985_grain_685	3.4234	1.5	0.25798	1.2	0.84	0.10350	0.79	1647	58	1462	241	1454	159	85
LAS395_shot_986_grain_686	1.9657	0.9	0.18221	0.9	0.75	0.08350	0.67	1258	56	1074	181	1089	132	89
LAS395_shot_993_grain_687	0.8734	1.1	0.09066	0.8	0.68	0.06383	0.80	781	56	558	98	629	90	62
LAS395_shot_994_grain_688	7.3718	1.9	0.27747	1.6	0.95	0.16890	0.56	2524	48	1554	252	2052	163	105
LAS395_shot_995_grain_689	2.8714	0.7	0.22797	0.6	0.54	0.08366	0.61	1258	56	1322	217	1364	147	60
LAS395_shot_996_grain_690	2.2255	0.7	0.15410	0.6	0.63	0.09616	0.57	1527	54	923	156	1184	133	93
LAS395_shot_997_grain_691	2.1912	0.6	0.18453	0.6	0.55	0.07983	0.56	1172	55	1091	182	1173	134	42

LAS395_shot_998_grain_692	3.3389	0.6	0.15699	0.6	0.64	0.14325	0.51	2250	49	938	159	1482	152	74
LAS395_shot_999_grain_693	3.7515	0.5	0.22928	0.5	0.63	0.11098	0.44	1799	51	1331	219	1580	153	90
LAS395_shot_1000_grain_694	2.1459	0.5	0.18236	0.5	0.63	0.08092	0.47	1199	55	1078	182	1161	135	91
LAS395_shot_1001_grain_695	3.9813	0.5	0.26582	0.5	0.55	0.10382	0.50	1676	52	1517	247	1625	157	85
LAS395_shot_1002_grain_696	1.6257	0.9	0.15145	0.8	0.62	0.07543	0.73	1062	58	907	155	970	126	97
LAS395_shot_1003_grain_697	1.8412	0.6	0.17268	0.5	0.44	0.07580	0.59	1057	58	1026	172	1056	129	102
LAS395_shot_1004_grain_698	1.9133	0.7	0.18239	0.6	0.35	0.07565	0.72	1061	58	1079	181	1080	129	104
LAS395_shot_1005_grain_699	2.0336	1.0	0.19475	0.7	0.30	0.07632	1.04	1100	62	1145	191	1112	134	102
LAS395_shot_1006_grain_700	0.9086	1.0	0.08277	0.7	0.59	0.07962	0.82	1167	61	512	90	653	92	102
LAS395_shot_1013_grain_701	4.3419	0.8	0.31306	0.7	0.82	0.10603	0.44	1717	51	1748	281	1688	167	103
LAS395_shot_1014_grain_702	3.6813	0.5	0.28675	0.5	0.60	0.09883	0.42	1589	52	1624	261	1563	153	96
LAS395_shot_1015_grain_703	0.7968	0.8	0.09938	0.6	0.36	0.06289	0.84	763	57	610	106	591	85	101
LAS395_shot_1016_grain_704	0.9366	1.3	0.10288	1.2	0.86	0.07095	0.70	944	57	629	110	657	93	60
LAS395_shot_1017_grain_705	0.7704	1.2	0.09407	0.8	0.51	0.06433	1.12	832	60	579	101	575	87	90
LAS395_shot_1018_grain_706	5.3164	1.1	0.25807	0.9	0.86	0.16050	0.55	2443	48	1471	242	1837	175	105
LAS395_shot_1019_grain_707	1.4671	0.7	0.15542	0.6	0.71	0.07416	0.50	1027	57	929	158	910	116	110
LAS395_shot_1020_grain_708	1.2279	1.0	0.14016	0.8	0.61	0.06906	0.82	914	58	844	145	802	108	79
LAS395_shot_1021_grain_709	2.2616	0.6	0.22193	0.5	0.46	0.08040	0.60	1178	57	1291	215	1194	136	92
LAS395_shot_1022_grain_710	5.3982	1.6	0.30379	1.3	0.93	0.13451	0.55	2136	50	1689	275	1811	170	95
LAS395_shot_1023_grain_711	1.4671	0.6	0.13984	0.4	0.50	0.08168	0.51	1219	55	843	144	913	116	62
LAS395_shot_1024_grain_712	11.2382	0.7	0.48036	0.7	0.73	0.18124	0.49	2649	46	2518	387	2529	186	86
LAS395_shot_1025_grain_713	2.0426	1.6	0.15454	1.0	0.71	0.09746	0.93	1495	62	922	158	1083	131	102
LAS395_shot_1026_grain_714	1.7160	1.2	0.16716	0.7	0.32	0.07870	1.14	1157	62	993	168	1000	125	89
LAS395_shot_1033_grain_715	12.9977	0.7	0.51714	0.7	0.45	0.18040	0.72	2629	50	2675	397	2665	180	58
LAS395_shot_1034_grain_716	1.2454	0.6	0.11987	0.5	0.50	0.07432	0.58	1022	59	729	126	818	108	97
LAS395_shot_1035_grain_717	2.5065	1.5	0.16663	1.3	0.91	0.10580	0.67	1706	54	989	171	1238	153	98
LAS395_shot_1036_grain_718	0.5627	0.4	0.07090	0.4	0.48	0.05723	0.43	507	55	441	78	453	71	89
LAS395_shot_1037_grain_719	3.3573	0.8	0.25723	0.6	0.45	0.09508	0.73	1496	58	1472	240	1485	150	90
LAS395_shot_1038_grain_720	0.8215	1.1	0.08654	0.7	0.49	0.06973	0.98	961	59	535	94	601	89	97
LAS395_shot_1039_grain_721	0.8562	0.9	0.09046	0.7	0.64	0.06940	0.66	923	53	557	98	622	92	93
LAS395_shot_1040_grain_722	3.2429	0.6	0.25418	0.5	0.46	0.09499	0.60	1505	54	1457	238	1462	150	98
LAS395_shot_1041_grain_723	1.5408	0.7	0.15648	0.6	0.43	0.07359	0.69	1009	59	937	160	941	118	96
LAS395_shot_1042_grain_724	0.7870	1.4	0.09125	0.8	0.15	0.06625	1.54	1066	65	562	98	575	88	100
LAS395_shot_1043_grain_725	12.3986	0.6	0.49684	0.6	0.50	0.18811	0.57	2707	47	2595	397	2625	183	98
LAS395_shot_1044_grain_726	1.6599	0.6	0.16882	0.5	0.46	0.07392	0.62	1010	59	1005	169	988	124	96

LAS395_shot_1045_grain_727	4.4083	0.5	0.30721	0.5	0.60	0.10777	0.43	1751	51	1724	275	1711	157	101
LAS395_shot_1046_grain_728	1.7227	0.4	0.17136	0.4	0.53	0.07523	0.41	1060	55	1018	172	1015	122	86
LAS395_shot_1053_grain_729	0.6975	1.3	0.08660	0.9	0.37	0.05696	1.27	779	61	535	94	529	81	103
LAS395_shot_1054_grain_730	1.6620	0.8	0.14018	0.6	0.53	0.08132	0.71	1187	59	845	145	988	121	62
LAS395_shot_1055_grain_731	2.0480	1.0	0.18759	0.9	0.61	0.07559	0.82	1072	59	1104	185	1118	133	92
LAS395_shot_1056_grain_732	2.6928	0.8	0.17483	0.7	0.48	0.10332	0.74	1665	58	1037	175	1321	141	87
LAS395_shot_1057_grain_733	4.6536	0.5	0.28821	0.5	0.52	0.10889	0.51	1762	51	1629	263	1753	163	82
LAS395_shot_1058_grain_734	1.3343	1.2	0.12044	0.9	0.79	0.07285	0.78	1015	57	731	126	842	115	84
LAS395_shot_1059_grain_735	13.0133	0.5	0.43466	0.5	0.60	0.20026	0.43	2820	46	2323	355	2675	181	98
LAS395_shot_1060_grain_736	1.0231	2.0	0.09398	1.0	0.23	0.07524	1.98	1294	70	577	101	687	104	85
LAS395_shot_1061_grain_737	2.2803	0.8	0.19355	0.7	0.35	0.07998	0.84	1163	60	1139	190	1194	138	94
LAS395_shot_1062_grain_738	1.2079	0.8	0.11108	0.6	0.34	0.07422	0.85	1027	59	678	117	798	108	50
LAS395_shot_1063_grain_739	1.9248	0.5	0.17212	0.5	0.51	0.07659	0.51	1088	56	1022	172	1087	126	54
LAS395_shot_1064_grain_740	4.6742	1.4	0.20379	1.1	0.92	0.15380	0.55	2368	49	1188	200	1710	164	85
LAS395_shot_1065_grain_741	3.4147	0.8	0.18656	0.7	0.77	0.12748	0.49	2046	49	1101	186	1495	156	80
LAS395_shot_1066_grain_742	2.8501	0.9	0.21535	0.8	0.49	0.09421	0.81	1480	58	1254	209	1357	146	59
LAS395_shot_1073_grain_743	10.3659	1.1	0.40786	1.0	0.91	0.18810	0.48	2715	44	2183	351	2427	206	76
LAS395_shot_1074_grain_744	2.5176	1.2	0.12108	0.6	0.33	0.14957	1.05	2301	54	736	127	1253	130	102
LAS395_shot_1075_grain_745	9.7861	0.8	0.37699	0.8	0.76	0.18863	0.55	2714	47	2052	326	2397	178	95
LAS395_shot_1076_grain_746	2.9155	0.6	0.23941	0.6	0.63	0.08725	0.47	1349	56	1381	228	1383	145	77
LAS395_shot_1077_grain_747	0.5661	0.6	0.06923	0.5	0.44	0.05743	0.56	553	53	432	77	454	71	87
LAS395_shot_1078_grain_748	2.1644	0.6	0.14961	0.5	0.52	0.09960	0.54	1599	54	898	153	1164	132	71
LAS395_shot_1079_grain_749	0.5952	0.6	0.06586	0.5	0.40	0.06135	0.60	668	56	411	73	472	73	77
LAS395_shot_1080_grain_750	8.6918	0.8	0.33271	0.8	0.82	0.17397	0.47	2582	47	1845	298	2286	191	92
LAS395_shot_1081_grain_751	1.7795	1.9	0.12926	1.6	0.89	0.08981	0.89	1389	61	779	136	1001	133	80
LAS395_shot_1083_grain_753	2.0721	1.0	0.16337	0.9	0.81	0.08377	0.57	1265	56	972	167	1122	136	64
LAS395_shot_1084_grain_754	1.7077	0.8	0.15426	0.7	0.51	0.07363	0.74	1009	59	924	157	1003	124	64
LAS395_shot_1085_grain_755	1.7780	0.5	0.15260	0.5	0.60	0.07842	0.43	1143	54	915	155	1035	124	102
LAS395_shot_1086_grain_756	2.3459	0.8	0.16554	0.7	0.74	0.09671	0.53	1546	54	986	167	1212	140	111
LAS395_shot_1093_grain_757	6.1668	1.0	0.28829	0.9	0.86	0.16889	0.51	2534	46	1623	260	1972	167	108
LAS395_shot_1094_grain_758	1.8524	0.7	0.18937	0.7	0.77	0.07662	0.47	1094	56	1116	189	1056	132	99
LAS395_shot_1095_grain_759	0.7800	2.1	0.10141	0.9	0.13	0.06003	2.25	1133	72	621	108	561	90	81
LAS395_shot_1096_grain_760	0.8100	1.2	0.10428	0.7	0.22	0.05934	1.22	810	57	638	111	594	88	98
LAS395_shot_1097_grain_761	1.8679	1.3	0.18020	0.9	0.62	0.07552	0.96	1079	59	1065	183	1043	135	76
LAS395_shot_1098_grain_762	1.0911	1.4	0.09763	0.7	0.60	0.07991	1.09	1149	62	600	104	739	99	102

LAS395_shot_1099_grain_763	13.3418	0.5	0.50441	0.5	0.62	0.18501	0.43	2689	47	2626	396	2697	180	97
LAS395_shot_1100_grain_764	3.4188	1.0	0.22237	0.9	0.72	0.10413	0.65	1693	50	1289	217	1488	153	96
LAS395_shot_1101_grain_765	2.3978	0.7	0.20239	0.6	0.56	0.08006	0.64	1168	58	1187	199	1234	138	92
LAS395_shot_1102_grain_766	0.7774	1.4	0.09007	0.7	0.08	0.05898	1.52	908	62	555	97	573	88	102
LAS395_shot_1103_grain_767	3.2275	0.6	0.23713	0.5	0.40	0.09137	0.65	1420	57	1370	226	1459	148	115
LAS395_shot_1104_grain_768	1.5242	1.1	0.14055	1.0	0.78	0.07303	0.68	992	58	846	146	925	116	115
LAS395_shot_1106_grain_770	1.8061	0.7	0.17183	0.5	0.32	0.07375	0.72	1003	59	1022	174	1042	126	105
LAS395_shot_1113_grain_771	4.9002	0.5	0.38345	0.5	0.48	0.11242	0.52	1818	52	2088	327	1796	162	95
LAS395_shot_1114_grain_772	1.8000	0.7	0.20879	0.5	0.38	0.07602	0.71	1065	59	1220	203	1040	126	58
LAS395_shot_1115_grain_773	1.5656	1.3	0.18129	1.1	0.85	0.07410	0.62	1020	60	1067	182	930	123	111
LAS395_shot_1116_grain_774	1.5962	1.2	0.17743	1.0	0.86	0.07686	0.60	1101	57	1049	179	949	122	109
LAS395_shot_1117_grain_775	5.4137	0.6	0.26530	0.6	0.76	0.17492	0.41	2596	47	1514	246	1879	163	96
LAS395_shot_1118_grain_776	4.8631	0.7	0.36672	0.6	0.39	0.11209	0.69	1805	55	2010	318	1784	163	56
LAS395_shot_1119_grain_777	4.9260	0.8	0.36259	0.7	0.40	0.11427	0.84	1817	57	1987	313	1789	163	113
LAS395_shot_1120_grain_778	1.9926	0.5	0.19928	0.5	0.56	0.08163	0.48	1220	55	1170	196	1109	131	85
LAS395_shot_1121_grain_779	4.6347	0.6	0.23488	0.6	0.70	0.15842	0.43	2425	46	1358	222	1749	160	88
LAS395_shot_1122_grain_780	0.7823	1.9	0.10437	0.9	0.21	0.06097	1.96	1050	66	640	113	567	86	104
LAS395_shot_1123_grain_781	9.7412	0.8	0.41920	0.7	0.82	0.17876	0.45	2631	46	2249	352	2390	185	95
LAS395_shot_1124_grain_782	4.0609	0.9	0.27692	0.8	0.80	0.11107	0.56	1791	51	1569	258	1623	165	72
LAS395_shot_1125_grain_783	5.1888	0.6	0.34428	0.5	0.36	0.11354	0.64	1824	53	1904	304	1843	166	84
LAS395_shot_1126_grain_784	1.7802	0.8	0.17284	0.7	0.77	0.07579	0.46	1074	57	1025	174	1029	130	87
LAS395_shot_1133_grain_785	1.8068	0.5	0.15575	0.5	0.64	0.08466	0.44	1290	54	934	158	1043	126	86
LAS395_shot_1134_grain_786	0.9561	0.6	0.09262	0.6	0.47	0.07576	0.62	1063	59	570	101	679	98	86
LAS395_shot_1135_grain_787	0.5668	1.1	0.06244	0.7	0.66	0.06591	0.79	816	58	390	69	451	70	77
LAS395_shot_1136_grain_788	1.7752	0.6	0.14839	0.5	0.53	0.08754	0.54	1350	55	892	153	1033	126	57
LAS395_shot_1137_grain_789	0.4991	1.3	0.05604	0.9	0.47	0.06529	1.27	806	65	351	63	410	66	56
LAS395_shot_1138_grain_790	1.2786	0.6	0.10423	0.6	0.24	0.08958	0.64	1381	53	639	112	834	111	63
LAS395_shot_1139_grain_791	2.9179	0.7	0.18304	0.6	0.78	0.11610	0.40	1886	50	1082	183	1378	147	45
LAS395_shot_1140_grain_792	6.6481	0.7	0.26420	0.7	0.76	0.18427	0.45	2679	47	1506	244	2054	176	57
LAS395_shot_1141_grain_793	3.7241	0.6	0.21797	0.6	0.48	0.12613	0.58	2026	51	1268	210	1570	154	91
LAS395_shot_1142_grain_794	4.2777	0.6	0.19160	0.6	0.65	0.16441	0.50	2484	47	1128	190	1681	157	89
LAS395_shot_1143_grain_795	5.6030	0.7	0.24978	0.7	0.69	0.16523	0.49	2499	47	1434	231	1906	160	96
LAS395_shot_1144_grain_796	0.9203	1.0	0.09712	0.9	0.58	0.07052	0.87	957	58	596	106	655	97	164
LAS395_shot_1145_grain_797	1.2238	0.7	0.11824	0.7	0.78	0.07633	0.46	1085	56	719	131	805	114	100
LAS395_shot_1146_grain_798	1.4598	0.8	0.14534	0.7	0.71	0.07438	0.55	1026	58	873	159	905	123	110

LAS395_shot_1160_grain_806	6.0677	2.4	0.39530	0.9	0.80	0.11750	1.57	1777	71	2132	367	1854	157	123
LAS395_shot_1161_grain_807	3.2139	0.9	0.33214	0.8	0.06	0.07803	0.65	1124	55	1841	314	1447	153	73
LAS395_shot_1162_grain_808	3.1534	1.1	0.26146	1.0	0.86	0.09374	0.55	1480	54	1487	253	1416	164	104
LAS395_shot_1163_grain_809	0.7682	0.5	0.10387	0.5	0.48	0.05756	0.55	544	55	636	112	577	86	88
LAS395_shot_1164_grain_810	3.1586	0.6	0.28269	0.6	0.49	0.08575	0.61	1303	57	1602	259	1443	150	47
LAS395_shot_1165_grain_811	6.3685	1.0	0.30926	0.9	0.82	0.15344	0.56	2364	49	1727	280	1994	184	97
LAS395_shot_1166_grain_812	3.2892	0.6	0.26424	0.5	0.25	0.09284	0.55	1456	53	1512	241	1471	147	80
LAS395_shot_1173_grain_813	11.3789	0.7	0.43802	0.7	0.74	0.18017	0.46	2642	46	2335	353	2543	179	72
LAS395_shot_1174_grain_814	4.7444	0.5	0.20007	0.5	0.62	0.16373	0.46	2480	47	1174	195	1767	162	105
LAS395_shot_1175_grain_815	0.8394	1.2	0.09556	0.7	0.15	0.06104	1.31	892	60	588	102	609	89	103
LAS395_shot_1176_grain_816	3.4534	0.7	0.23053	0.7	0.71	0.10384	0.53	1673	53	1333	222	1506	153	62
LAS395_shot_1177_grain_817	8.3713	1.2	0.33635	1.1	0.93	0.17067	0.44	2552	46	1850	295	2222	177	58
LAS395_shot_1178_grain_818	2.0826	0.8	0.19214	0.6	0.32	0.07559	0.78	1074	58	1131	190	1132	134	102
LAS395_shot_1179_grain_819	16.0107	0.5	0.56551	0.6	0.60	0.19825	0.50	2794	46	2884	429	2870	187	97
LAS395_shot_1180_grain_820	2.3170	0.6	0.16491	0.6	0.62	0.09900	0.52	1585	52	982	166	1213	139	90
LAS395_shot_1181_grain_821	1.3891	0.9	0.08158	0.5	0.37	0.12061	0.84	1912	56	505	89	877	115	82
LAS395_shot_1182_grain_822	0.8262	1.6	0.09876	0.9	0.22	0.06078	1.65	943	65	606	106	595	91	100
LAS395_shot_1183_grain_823	1.6892	0.5	0.16447	0.5	0.62	0.07378	0.46	1015	57	980	166	1001	124	98
LAS395_shot_1184_grain_824	1.6315	0.6	0.15704	0.6	0.45	0.07527	0.65	1044	58	939	159	977	123	83
LAS395_shot_1185_grain_825	0.7617	1.1	0.07467	0.7	0.27	0.07491	1.12	1086	59	464	81	567	83	99
LAS395_shot_1186_grain_826	2.1323	0.8	0.19598	0.6	0.33	0.07972	0.80	1148	60	1151	192	1150	134	96
LAS395_shot_1193_grain_827	2.0456	0.6	0.19226	0.5	0.45	0.07931	0.60	1150	58	1132	190	1126	131	102
LAS395_shot_1194_grain_828	2.3778	0.6	0.19760	0.6	0.63	0.08933	0.49	1395	54	1162	194	1229	139	95
LAS395_shot_1195_grain_829	1.8538	0.5	0.18122	0.5	0.57	0.07587	0.43	1081	55	1072	181	1062	127	111
LAS395_shot_1196_grain_830	1.3100	1.6	0.13134	1.2	0.81	0.07276	0.86	1016	59	792	138	825	109	101
LAS395_shot_1197_grain_831	0.6531	1.0	0.08365	0.7	0.32	0.05865	1.05	743	54	517	91	506	77	54
LAS395_shot_1198_grain_832	1.2837	1.5	0.12827	1.2	0.76	0.07284	0.91	1011	59	775	134	813	111	98
LAS395_shot_1199_grain_833	2.2195	0.8	0.20920	0.7	0.58	0.07760	0.65	1100	60	1221	203	1175	136	98
LAS395_shot_1200_grain_834	0.8656	1.4	0.10166	0.8	0.22	0.06356	1.49	995	62	623	108	616	93	97
LAS395_shot_1201_grain_835	3.7933	1.1	0.20136	1.0	0.48	0.14363	1.32	2164	57	1175	197	1565	165	95
LAS395_shot_1202_grain_836	5.4204	0.6	0.33689	0.6	0.48	0.11753	0.61	1897	52	1866	296	1880	166	82
LAS395_shot_1203_grain_837	0.5860	1.1	0.07294	0.6	0.19	0.05876	1.11	751	57	453	80	463	73	87
LAS395_shot_1204_grain_838	1.4718	0.5	0.14825	0.5	0.70	0.07193	0.40	969	56	891	152	916	116	94
LAS395_shot_1205_grain_839	2.7057	0.5	0.22233	0.4	0.57	0.08786	0.42	1365	52	1293	214	1327	142	38
LAS395_shot_1206_grain_840	2.0757	1.1	0.17613	1.0	0.86	0.08386	0.55	1269	55	1041	178	1117	138	65

LAS395_shot_1213_grain_841	12.4522	0.8	0.45961	0.8	0.75	0.19617	0.53	2777	47	2426	377	2616	197	93
LAS395_shot_1214_grain_842	1.9701	0.9	0.18235	0.7	0.44	0.07902	0.87	1142	61	1076	181	1092	129	44
LAS395_shot_1215_grain_843	8.3073	0.7	0.14109	0.6	0.76	0.41935	0.54	3966	43	850	145	2252	185	89
LAS395_shot_1216_grain_844	2.2745	1.0	0.16893	0.8	0.80	0.09699	0.57	1550	53	1004	171	1189	136	90
LAS395_shot_1217_grain_845	1.6359	0.6	0.15937	0.5	0.40	0.07454	0.61	1028	59	952	161	980	124	76
LAS395_shot_1218_grain_846	3.6205	0.9	0.17261	0.8	0.84	0.15056	0.49	2341	47	1023	172	1533	150	53
LAS395_shot_1219_grain_847	1.8368	0.9	0.17027	0.6	0.29	0.07826	0.89	1131	60	1011	171	1047	128	55
LAS395_shot_1220_grain_848	0.6775	1.2	0.07532	0.9	0.75	0.06431	0.81	811	54	467	82	519	79	62
LAS395_shot_1221_grain_849	8.8239	1.6	0.35846	1.4	0.91	0.17258	0.62	2562	49	1943	312	2229	198	101
LAS395_shot_1222_grain_850	5.7970	2.5	0.21087	0.8	0.59	0.18545	2.17	2307	93	1230	207	1747	179	99
LAS395_shot_1223_grain_851	3.8059	0.6	0.20076	0.5	0.71	0.13579	0.45	2160	48	1179	197	1586	154	103
LAS395_shot_1224_grain_852	3.3756	1.0	0.20322	0.8	0.72	0.11969	0.72	1920	54	1188	197	1475	151	97
LAS395_shot_1225_grain_853	2.0406	0.7	0.18999	0.6	0.47	0.07773	0.68	1106	59	1119	187	1122	132	62
LAS395_shot_1226_grain_854	13.6296	0.5	0.52157	0.6	0.48	0.19047	0.57	2727	47	2695	400	2720	190	88
LAS395_shot_1233_grain_855	1.9657	0.6	0.19101	0.6	0.42	0.07701	0.65	1092	58	1125	190	1099	129	108
LAS395_shot_1234_grain_856	4.6423	0.5	0.31345	0.6	0.56	0.11141	0.51	1807	52	1753	281	1752	162	80
LAS395_shot_1235_grain_857	1.9139	1.1	0.15275	0.9	0.65	0.09282	0.79	1466	59	915	157	1074	127	91
LAS395_shot_1236_grain_858	0.7896	1.4	0.09110	1.0	0.45	0.06590	1.29	863	59	562	99	582	89	116
LAS395_shot_1237_grain_859	9.7460	0.5	0.42713	0.5	0.66	0.17416	0.42	2586	46	2288	354	2404	181	106
LAS395_shot_1238_grain_860	1.9972	0.6	0.20008	0.5	0.41	0.07670	0.61	1083	58	1175	197	1108	130	101
LAS395_shot_1239_grain_861	1.8828	0.7	0.14181	0.6	0.61	0.10176	0.60	1630	54	854	147	1068	130	103
LAS395_shot_1240_grain_862	2.8862	1.0	0.23597	0.9	0.79	0.09465	0.60	1495	55	1361	227	1359	146	95
LAS395_shot_1241_grain_863	2.3406	0.8	0.22985	0.7	0.53	0.07944	0.75	1146	59	1331	221	1214	139	101
LAS395_shot_1242_grain_864	1.9058	0.6	0.19369	0.5	0.49	0.07625	0.56	1072	57	1141	189	1079	129	91
LAS395_shot_1243_grain_865	1.7958	1.0	0.18534	0.7	0.00	0.07590	1.05	1086	58	1093	183	1027	125	91
LAS395_shot_1244_grain_866	1.3547	1.6	0.14422	1.3	0.72	0.07137	1.02	970	60	863	150	838	114	89
LAS395_shot_1245_grain_867	1.5515	1.2	0.16111	0.9	0.72	0.07302	0.80	1008	57	959	165	929	126	94
LAS395_shot_1246_grain_868	0.6667	0.8	0.08384	0.7	0.53	0.05961	0.69	637	57	519	92	515	79	65
LAS395_shot_1253_grain_869	0.6067	1.1	0.06987	0.6	0.23	0.06241	1.16	816	61	435	76	478	74	108
LAS395_shot_1254_grain_870	1.8022	1.3	0.17625	0.8	0.25	0.07546	1.36	1150	62	1043	176	1025	127	96
LAS395_shot_1255_grain_871	11.6321	0.6	0.45192	0.6	0.74	0.18697	0.41	2705	45	2400	362	2569	179	97
LAS395_shot_1256_grain_872	1.6383	0.5	0.16172	0.4	0.54	0.07384	0.44	1024	57	966	165	983	119	90
LAS395_shot_1257_grain_873	6.6516	1.8	0.28620	1.5	0.73	0.16380	0.60	2465	48	1596	262	1957	184	96
LAS395_shot_1258_grain_874	2.3781	0.8	0.22031	0.7	0.44	0.08125	0.80	1185	59	1280	213	1223	138	87
LAS395_shot_1259_grain_875	2.0601	0.5	0.19341	0.5	0.44	0.08016	0.43	1184	54	1138	190	1132	130	86

LAS395_shot_1260_grain_876	1.6444	0.7	0.16803	0.6	0.66	0.07430	0.56	1029	57	1001	168	982	122	87
LAS395_shot_1261_grain_877	1.8185	0.5	0.17552	0.5	0.12	0.07872	0.43	1151	51	1041	175	1047	118	102
LAS395_shot_1262_grain_878	1.6230	0.6	0.16656	0.5	0.61	0.07460	0.51	1037	57	992	168	975	121	106
LAS395_shot_1263_grain_879	1.0907	0.9	0.10532	0.9	0.81	0.07900	0.55	1146	57	644	112	739	103	89
LAS395_shot_1264_grain_880	2.3252	0.5	0.20062	0.5	0.63	0.08819	0.41	1375	53	1177	196	1216	137	89
LAS395_shot_1265_grain_881	1.9824	0.6	0.18278	0.5	0.55	0.08255	0.52	1240	54	1080	183	1105	131	87
LAS395_shot_1266_grain_882	0.6100	0.7	0.07941	0.6	0.47	0.05816	0.68	601	54	492	86	482	76	89
LAS395_shot_1273_grain_883	2.8762	1.1	0.23324	1.0	0.82	0.08400	0.62	1260	58	1342	226	1343	162	92
LAS395_shot_1274_grain_884	1.2604	0.5	0.12138	0.5	0.61	0.07159	0.48	953	57	738	127	825	111	97
LAS395_shot_1275_grain_885	1.0797	0.9	0.10766	0.7	0.67	0.06923	0.63	883	60	659	115	738	103	90
LAS395_shot_1276_grain_886	11.5732	0.6	0.43673	0.6	0.70	0.18386	0.44	2677	46	2331	361	2564	180	76
LAS395_shot_1277_grain_887	0.9586	1.4	0.09689	1.0	0.84	0.06777	0.75	863	57	595	104	666	95	91
LAS395_shot_1278_grain_888	1.5611	0.5	0.14508	0.5	0.63	0.07614	0.45	1083	55	872	148	952	121	92
LAS395_shot_1279_grain_889	0.5865	0.6	0.07274	0.5	0.46	0.05781	0.57	554	54	453	80	468	72	55
LAS395_shot_1280_grain_890	1.1464	1.1	0.11239	0.8	0.81	0.07242	0.67	970	59	685	118	762	104	86
LAS395_shot_1281_grain_891	2.0409	0.5	0.17049	0.4	0.51	0.08695	0.46	1342	54	1014	172	1125	131	84
LAS395_shot_1282_grain_892	4.7431	0.9	0.30002	0.8	0.41	0.11775	0.95	1858	60	1684	272	1758	162	120
LAS395_shot_1283_grain_893	1.2829	1.6	0.12306	1.4	0.88	0.07660	0.75	1088	59	743	129	809	104	84
LAS395_shot_1284_grain_894	6.7815	1.3	0.26283	1.1	0.85	0.18919	0.67	2718	49	1496	248	2043	183	86
LAS395_shot_1285_grain_895	6.9743	1.3	0.35575	1.2	0.84	0.14410	0.70	2254	52	1937	318	2044	205	86
LAS395_shot_1286_grain_896	1.6378	0.5	0.15785	0.5	0.45	0.07764	0.53	1120	58	943	160	982	122	95
LAS395_shot_1293_grain_897	0.8678	2.4	0.12239	1.6	0.38	0.05435	1.80	846	60	737	127	613	91	92
LAS395_shot_1295_grain_899	0.8284	0.8	0.08204	0.6	0.70	0.07327	0.60	995	59	508	89	607	88	98
LAS395_shot_1296_grain_900	2.5576	0.6	0.20691	0.5	0.54	0.09055	0.54	1411	55	1212	205	1283	139	58
LAS395_shot_1297_grain_901	11.5283	1.0	0.44014	0.9	0.67	0.19154	0.75	2720	50	2335	358	2537	184	80
LAS395_shot_1298_grain_902	3.0227	1.0	0.23811	0.9	0.81	0.09216	0.60	1445	56	1369	230	1387	164	83
LAS395_shot_1299_grain_903	1.3428	0.8	0.13006	0.6	0.79	0.07472	0.50	1042	57	787	135	857	111	98
LAS395_shot_1300_grain_904	0.7352	1.1	0.08714	0.7	0.22	0.06257	1.20	873	57	538	95	551	83	86
LAS395_shot_1301_grain_905	2.4205	1.4	0.11656	0.8	0.35	0.15496	1.39	2249	69	709	123	1213	136	66
LAS395_shot_1302_grain_906	1.4654	1.6	0.11524	1.2	0.86	0.09036	0.88	1398	59	699	123	878	124	90
LAS395_shot_1303_grain_907	1.1952	1.7	0.10605	1.1	0.74	0.08114	1.14	1184	67	648	112	780	107	88
LAS395_shot_1304_grain_908	1.1174	1.4	0.12056	1.1	0.55	0.06850	1.19	969	61	730	126	743	103	97
LAS395_shot_1305_grain_909	10.8286	0.5	0.43002	0.6	0.58	0.18589	0.52	2687	46	2301	355	2501	178	94
LAS395_shot_1306_grain_910	5.3683	3.1	0.24410	2.4	0.97	0.13542	1.18	2045	65	1352	229	1585	176	85
LAS395_shot_1313_grain_911	0.8617	1.2	0.09062	1.0	0.85	0.06813	0.65	857	59	558	98	622	91	103

LAS395_shot_1314_grain_912	4.3039	0.7	0.28057	0.6	0.34	0.11132	0.58	1798	51	1589	257	1682	159	84
LAS395_shot_1315_grain_913	2.0892	0.8	0.19130	0.6	0.32	0.07930	0.84	1162	60	1126	188	1136	135	89
LAS395_shot_1316_grain_914	4.7242	0.6	0.30484	0.6	0.60	0.11228	0.57	1812	52	1713	277	1762	163	92
LAS395_shot_1317_grain_915	1.5287	1.4	0.12939	1.4	0.75	0.08693	1.07	1304	62	778	135	919	118	102
LAS395_shot_1318_grain_916	1.8904	0.7	0.18211	0.6	0.40	0.07536	0.74	1049	60	1076	181	1071	130	83
LAS395_shot_1319_grain_917	2.2493	0.7	0.18798	0.6	0.47	0.08634	0.54	1319	54	1109	188	1189	136	98
LAS395_shot_1320_grain_918	10.8601	0.8	0.43739	0.8	0.77	0.17872	0.51	2623	47	2327	364	2495	184	68
LAS395_shot_1321_grain_919	1.4246	0.7	0.13578	0.6	0.47	0.07509	0.67	1039	61	820	141	893	116	92
LAS395_shot_1322_grain_920	2.2618	0.7	0.20352	0.6	0.39	0.08029	0.71	1167	59	1192	198	1194	137	102
LAS395_shot_1324_grain_922	8.8713	2.0	0.36105	1.7	0.94	0.15989	1.13	2332	76	1928	327	2092	272	99
LAS395_shot_1325_grain_923	1.5888	0.8	0.15848	0.7	0.72	0.07202	0.53	967	58	946	161	957	123	44
LAS395_shot_1326_grain_924	2.8259	0.4	0.19565	0.4	0.56	0.10453	0.38	1692	50	1151	192	1360	141	96
LAS395_shot_1333_grain_925	1.2018	0.6	0.12017	0.6	0.57	0.07658	0.55	1088	55	730	126	797	106	90
LAS395_shot_1334_grain_926	0.5868	1.4	0.07543	0.7	0.11	0.06175	1.51	950	63	468	82	459	73	99
LAS395_shot_1335_grain_927	2.2278	0.6	0.20969	0.5	0.51	0.08287	0.56	1240	57	1226	203	1185	134	92
LAS395_shot_1336_grain_928	3.2541	1.6	0.16846	1.4	0.94	0.14664	0.61	2283	50	995	170	1405	155	100
LAS395_shot_1337_grain_929	1.7080	0.5	0.17667	0.5	0.63	0.07658	0.45	1095	56	1047	176	1007	122	72
LAS395_shot_1338_grain_930	1.3812	0.6	0.15107	0.6	0.36	0.07335	0.52	1003	57	904	149	878	116	95
LAS395_shot_1339_grain_931	4.6540	0.6	0.32816	0.6	0.48	0.11393	0.58	1841	53	1825	293	1751	161	91
LAS395_shot_1340_grain_932	11.8418	0.6	0.48590	0.6	0.66	0.19481	0.49	2773	47	2546	386	2585	181	98
LAS395_shot_1341_grain_933	4.1867	0.6	0.31084	0.6	0.49	0.10823	0.60	1744	54	1743	282	1665	160	79
LAS395_shot_1342_grain_934	2.3668	0.6	0.19166	0.5	0.51	0.09861	0.54	1578	55	1129	188	1227	138	98
LAS395_shot_1343_grain_935	1.0696	0.7	0.11407	0.5	0.46	0.07441	0.61	1021	60	696	121	734	101	87
LAS395_shot_1344_grain_936	15.0513	0.6	0.52835	0.6	0.67	0.22521	0.48	3006	45	2727	406	2812	185	89
LAS395_shot_1345_grain_937	1.8593	0.8	0.18602	0.7	0.41	0.07808	0.81	1123	59	1098	185	1058	131	89
LAS395_shot_1346_grain_938	1.2292	0.7	0.10416	0.5	0.38	0.08972	0.71	1397	56	638	111	809	109	89
LAS395_shot_1353_grain_939	2.1017	0.7	0.18303	0.6	0.46	0.07771	0.68	1106	59	1082	180	1142	133	86
LAS395_shot_1354_grain_940	1.0402	0.6	0.10249	0.5	0.40	0.06859	0.60	863	58	628	109	721	99	94
LAS395_shot_1355_grain_941	12.6643	0.5	0.45514	0.6	0.63	0.18907	0.46	2721	46	2416	366	2650	183	86
LAS395_shot_1356_grain_942	2.0314	0.6	0.17388	0.6	0.39	0.07949	0.61	1164	59	1032	175	1121	130	90
LAS395_shot_1357_grain_943	1.8143	0.6	0.16309	0.6	0.61	0.07650	0.48	1088	57	972	165	1047	127	86
LAS395_shot_1358_grain_944	1.2979	4.1	0.11882	2.5	0.26	0.08175	3.45	1213	52	677	88	807	69	61
LAS395_shot_1359_grain_945	1.6314	0.7	0.15156	0.7	0.61	0.07535	0.57	1055	57	908	154	975	121	92
LAS395_shot_1360_grain_946	4.9346	0.8	0.30777	0.6	0.32	0.11516	0.83	1837	57	1727	280	1795	168	45
LAS395_shot_1361_grain_947	0.6780	1.2	0.07176	0.7	0.28	0.06798	1.25	906	64	446	79	521	80	94

LAS395_shot_1362_grain_948	1.9057	0.5	0.17435	0.5	0.54	0.07881	0.51	1148	57	1035	174	1079	129	84
LAS395_shot_1363_grain_949	2.0317	0.6	0.18000	0.5	0.55	0.08252	0.50	1238	56	1066	180	1123	133	88
LAS395_shot_1364_grain_950	8.0845	0.8	0.30408	0.7	0.85	0.19473	0.42	2772	45	1705	276	2221	185	66
LAS395_shot_1365_grain_951	1.6177	0.7	0.16061	0.6	0.54	0.07480	0.64	1037	59	959	162	974	119	88
LAS395_shot_1366_grain_952	4.7499	3.5	0.17542	2.2	0.96	0.15921	1.58	2244	72	1018	176	1464	162	90
LAS395_shot_1373_grain_953	1.5381	0.7	0.15565	0.5	0.36	0.07303	0.70	991	58	932	159	940	120	61
LAS395_shot_1374_grain_954	1.8882	0.5	0.17108	0.4	0.37	0.08139	0.48	1211	55	1017	172	1074	129	63
LAS395_shot_1375_grain_955	3.6349	0.9	0.25867	0.7	0.78	0.10381	0.55	1672	53	1478	243	1542	158	90
LAS395_shot_1376_grain_956	7.9777	1.1	0.31833	1.1	0.51	0.19135	1.14	2686	57	1773	290	2189	180	88
LAS395_shot_1377_grain_957	1.9875	1.1	0.18470	0.7	0.24	0.08273	1.17	1238	63	1092	186	1098	134	99
LAS395_shot_1378_grain_958	2.0407	0.6	0.18668	0.5	0.52	0.08239	0.58	1230	57	1101	185	1124	131	98
LAS395_shot_1379_grain_959	11.0671	1.4	0.34485	1.4	0.87	0.24376	0.65	3116	47	1896	303	2477	180	91
LAS395_shot_1380_grain_960	2.4236	0.8	0.17705	0.7	0.71	0.10402	0.59	1669	53	1048	177	1240	138	99
LAS395_shot_1381_grain_961	1.3932	0.7	0.13132	0.5	0.50	0.07996	0.64	1161	58	794	136	879	114	79
LAS395_shot_1382_grain_962	1.7587	0.8	0.15032	0.9	0.62	0.09007	0.75	1381	58	900	155	1023	127	86
LAS395_shot_1383_grain_963	0.8412	1.0	0.09835	0.7	0.28	0.06475	0.95	841	56	604	105	611	88	100
LAS395_shot_1384_grain_964	4.7848	0.5	0.31944	0.5	0.46	0.11226	0.54	1816	52	1786	286	1775	164	49
LAS395_shot_1385_grain_965	4.6875	0.6	0.30256	0.6	0.54	0.11551	0.55	1866	51	1700	272	1757	162	87
LAS395_shot_1386_grain_966	0.5722	0.5	0.07297	0.5	0.47	0.05755	0.53	542	53	454	80	458	71	92
LAS395_shot_1393_grain_967	1.7917	0.6	0.13548	0.5	0.30	0.08514	0.67	1279	56	818	140	1037	123	85
LAS395_shot_1394_grain_968	0.7160	0.6	0.07525	0.4	0.31	0.05977	0.59	625	56	468	82	546	80	113
LAS395_shot_1395_grain_969	3.5231	0.6	0.24241	0.6	0.62	0.08981	0.49	1403	53	1399	231	1526	154	71
LAS395_shot_1396_grain_970	4.8352	0.5	0.19545	0.5	0.69	0.15104	0.44	2343	48	1149	192	1785	163	102
LAS395_shot_1397_grain_971	0.9415	3.1	0.09367	1.2	0.25	0.06398	4.16	1221	62	571	97	680	98	76
LAS395_shot_1398_grain_972	0.7113	1.0	0.07554	0.6	0.14	0.05699	1.07	707	56	469	82	541	82	96
LAS395_shot_1399_grain_973	5.7408	0.5	0.30202	0.5	0.54	0.11417	0.44	1854	50	1699	274	1933	170	100
LAS395_shot_1400_grain_974	1.8428	0.7	0.14968	0.7	0.66	0.07420	0.51	1022	56	898	154	1052	129	89
LAS395_shot_1401_grain_975	2.6034	0.8	0.20766	0.7	0.64	0.07620	0.59	1078	58	1215	205	1292	142	84
LAS395_shot_1402_grain_976	1.4572	1.7	0.10208	0.5	0.46	0.08762	1.46	1269	63	626	109	883	95	110
LAS395_shot_1403_grain_977	2.6734	0.5	0.20880	0.5	0.50	0.08087	0.53	1195	57	1220	203	1315	143	81
LAS395_shot_1404_grain_978	3.5706	1.2	0.21978	1.1	0.87	0.10407	0.63	1667	54	1271	213	1501	161	63
LAS395_shot_1405_grain_979	0.8243	1.2	0.09359	0.7	0.25	0.05936	1.17	779	56	576	101	599	89	84
LAS395_shot_1406_grain_980	1.9739	0.9	0.18097	0.7	0.42	0.07580	0.84	1066	58	1071	182	1096	130	41
LAS395_shot_1413_grain_981	2.9653	1.0	0.16545	0.8	0.81	0.14780	0.58	2296	50	985	169	1379	159	90
LAS395_shot_1414_grain_982	5.4385	0.5	0.34047	0.5	0.70	0.13239	0.41	2119	48	1885	299	1886	169	95

LAS395_shot_1415_grain_983	0.9511	0.6	0.09237	0.6	0.53	0.08495	0.58	1288	56	569	100	675	95	79
LAS395_shot_1416_grain_984	1.0572	1.9	0.12828	1.5	0.67	0.06786	1.18	953	61	773	135	701	96	98
LAS395_shot_1417_grain_985	2.0628	0.7	0.18916	0.6	0.81	0.08884	0.43	1384	53	1115	186	1127	133	90
LAS395_shot_1418_grain_986	2.5936	1.3	0.13432	0.9	0.70	0.15490	0.91	2367	54	812	141	1279	141	80
LAS395_shot_1419_grain_987	1.2919	0.7	0.12403	0.7	0.42	0.08449	0.82	1266	57	753	130	839	111	121
LAS395_shot_1420_grain_988	1.1843	1.0	0.10772	0.7	0.64	0.08673	0.75	1323	59	658	114	785	106	108
LAS395_shot_1421_grain_989	3.5639	2.3	0.16105	1.6	0.96	0.15624	1.01	2337	61	953	165	1409	165	88
LAS395_shot_1422_grain_990	1.6566	0.8	0.14733	0.7	0.77	0.08619	0.44	1332	54	884	150	984	121	96
LAS395_shot_1423_grain_991	1.3514	0.9	0.13558	0.8	0.79	0.07652	0.75	1088	60	817	139	857	107	133
LAS395_shot_1424_grain_992	3.2301	0.5	0.23229	0.5	0.60	0.10552	0.44	1714	49	1345	222	1461	149	131
LAS395_shot_1425_grain_993	1.4155	1.2	0.14259	1.0	0.85	0.07336	0.60	997	59	855	147	876	120	119
LAS395_shot_1426_grain_994	0.8794	1.0	0.09262	0.8	0.69	0.06996	0.63	899	57	570	100	632	89	105

LAS396 (20BREM10B)														
Isotopic Ratios								Calculated ages (Ma)						
ID	$^{207}Pb/^{235}U$	2σ	$^{206}Pb/^{238}U$	2σ	Rho	$^{207/206}Pb$	2σ	$^{207/206}Pb$	2σ	$^{206}Pb/^{238}U$	2σ	$^{207}Pb/^{235}U$	2σ	%conc
LAS396_Shot_7_Grain_1	4.3402	0.5	0.30075	0.6	0.55	0.10773	0.50	1753	34	1694	29	1699	20	99.8
LAS396_Shot_8_Grain_2	3.9759	0.5	0.28827	0.5	0.64	0.10219	0.44	1655	34	1633	28	1627	20	100.4
LAS396_Shot_9_Grain_3	3.8876	0.6	0.28534	0.6	0.56	0.10217	0.52	1650	35	1616	28	1608	20	100.5
LAS396_Shot_10_Grain_4	5.5852	0.7	0.26313	0.7	0.64	0.15778	0.61	2423	33	1503	29	1911	22	78.6
LAS396_Shot_11_Grain_5	3.8123	0.5	0.27978	0.5	0.48	0.10245	0.46	1656	33	1588	27	1592	19	99.8
LAS396_Shot_12_Grain_6	3.1318	0.4	0.25031	0.5	0.62	0.09369	0.40	1490	34	1438	24	1437	19	100.1
LAS396_Shot_13_Grain_7	1.8284	0.8	0.17996	0.6	0.32	0.07692	0.82	1082	46	1065	20	1047	18	101.7
LAS396_Shot_14_Grain_8	3.8066	0.5	0.28136	0.5	0.60	0.10163	0.44	1643	34	1596	28	1590	20	100.4
LAS396_Shot_15_Grain_9	4.5457	0.5	0.30500	0.5	0.57	0.11183	0.49	1817	34	1713	29	1739	20	98.5
LAS396_Shot_16_Grain_10	3.2741	0.7	0.26228	0.6	0.37	0.09362	0.69	1474	40	1498	27	1467	20	102.1
LAS396_Shot_17_Grain_11	1.8498	0.6	0.17643	0.5	0.46	0.07893	0.58	1147	39	1047	19	1059	17	98.9
LAS396_Shot_18_Grain_12	1.8193	0.6	0.18089	0.5	0.45	0.07538	0.56	1054	39	1072	19	1050	16	102.1
LAS396_Shot_19_Grain_13	5.0247	0.6	0.33200	0.6	0.56	0.11339	0.54	1843	34	1844	32	1818	21	101.5
LAS396_Shot_20_Grain_14	2.0188	0.6	0.19374	0.5	0.57	0.07817	0.49	1140	37	1141	20	1121	17	101.8
LAS396_Shot_27_Grain_15	11.4904	0.5	0.45568	0.5	0.72	0.18975	0.35	2735	28	2416	39	2557	23	94.5
LAS396_Shot_28_Grain_16	1.7286	0.6	0.16947	0.5	0.19	0.07658	0.51	1087	37	1008	18	1013	16	99.5
LAS396_Shot_29_Grain_17	3.2731	0.7	0.24784	0.6	0.67	0.09869	0.54	1579	37	1426	27	1467	21	97.2
LAS396_Shot_30_Grain_18	2.9582	1.3	0.22250	1.1	0.92	0.09868	0.50	1584	35	1286	32	1360	29	94.5

LAS396_Shot_31_Grain_19	5.2171	0.5	0.33456	0.5	0.57	0.11701	0.42	1901	32	1860	31	1853	21	100.4
LAS396_Shot_32_Grain_20	13.4768	0.5	0.52618	0.5	0.45	0.19303	0.51	2754	30	2720	42	2710	23	100.4
LAS396_Shot_33_Grain_21	2.6489	0.5	0.23004	0.5	0.44	0.08648	0.50	1329	36	1334	23	1311	18	101.7
LAS396_Shot_34_Grain_22	4.0270	0.8	0.26770	0.8	0.64	0.11334	0.64	1822	37	1523	30	1628	22	93.6
LAS396_Shot_35_Grain_23	1.7103	0.5	0.17439	0.6	0.54	0.07356	0.50	1016	38	1035	19	1010	16	102.4
LAS396_Shot_36_Grain_24	4.2487	0.5	0.29640	0.5	0.54	0.10725	0.48	1745	34	1672	28	1682	20	99.4
LAS396_Shot_37_Grain_25	3.3074	1.5	0.23428	1.2	0.62	0.10544	1.06	1674	50	1347	35	1438	30	93.7
LAS396_Shot_38_Grain_26	4.5494	0.6	0.30923	0.6	0.58	0.11009	0.51	1784	36	1735	31	1734	21	100.1
LAS396_Shot_39_Grain_27	1.7258	0.5	0.16432	0.4	0.52	0.07818	0.42	1140	36	980	17	1016	15	96.4
LAS396_Shot_40_Grain_28	3.9626	0.5	0.29193	0.6	0.50	0.10222	0.47	1651	34	1647	29	1622	20	101.6
LAS396_Shot_47_Grain_29	4.6424	0.5	0.31105	0.5	0.55	0.11214	0.48	1825	33	1742	30	1755	21	99.3
LAS396_Shot_48_Grain_30	1.9166	0.6	0.18527	0.5	0.47	0.07753	0.56	1122	38	1094	20	1082	17	101.2
LAS396_Shot_49_Grain_31	3.0149	1.0	0.23590	0.8	0.83	0.09577	0.51	1534	35	1361	29	1396	24	97.5
LAS396_Shot_50_Grain_32	2.8026	0.6	0.23892	0.5	0.52	0.08834	0.48	1381	35	1381	24	1352	19	102.1
LAS396_Shot_51_Grain_33	9.2849	0.6	0.43286	0.7	0.59	0.16105	0.58	2450	33	2313	41	2358	24	98.1
LAS396_Shot_52_Grain_34	2.7412	0.8	0.23053	0.6	0.73	0.08898	0.48	1390	35	1335	24	1329	21	100.4
LAS396_Shot_53_Grain_35	5.2427	0.6	0.33601	0.5	0.26	0.11764	0.48	1906	31	1864	31	1855	21	100.5
LAS396_Shot_54_Grain_36	0.7991	1.0	0.09628	0.7	0.25	0.06291	1.11	820	47	592	12	590	14	100.4
LAS396_Shot_55_Grain_37	4.3916	0.5	0.30568	0.5	0.57	0.10769	0.49	1748	35	1716	29	1706	21	100.6
LAS396_Shot_56_Grain_38	2.2585	0.5	0.20223	0.4	0.45	0.08370	0.48	1267	36	1186	20	1195	17	99.2
LAS396_Shot_57_Grain_39	7.0579	0.7	0.30332	0.7	0.64	0.17451	0.43	2597	30	1706	33	2109	23	80.9
LAS396_Shot_58_Grain_40	4.1222	0.5	0.29331	0.5	0.62	0.10582	0.46	1716	34	1656	28	1657	20	99.9
LAS396_Shot_59_Grain_41	12.4421	0.5	0.49173	0.5	0.66	0.18990	0.38	2736	29	2577	42	2635	24	97.8
LAS396_Shot_60_Grain_42	18.9768	0.6	0.56721	0.6	0.76	0.25184	0.37	3190	28	2889	47	3036	25	95.2
LAS396_Shot_67_Grain_43	3.2115	0.6	0.25757	0.5	0.21	0.09375	0.59	1484	37	1475	26	1456	20	101.3
LAS396_Shot_68_Grain_44	1.8404	1.1	0.17886	0.8	0.24	0.07781	1.19	1159	51	1058	22	1045	22	101.2
LAS396_Shot_69_Grain_45	3.9986	0.8	0.27676	0.6	0.53	0.10908	0.64	1761	36	1572	29	1623	22	96.8
LAS396_Shot_70_Grain_46	2.2837	0.7	0.20657	0.6	0.47	0.08291	0.69	1239	42	1209	22	1200	19	100.8
LAS396_Shot_71_Grain_47	2.9893	0.6	0.24312	0.6	0.52	0.09225	0.51	1458	36	1400	25	1400	19	100.0
LAS396_Shot_72_Grain_48	2.9422	0.5	0.24061	0.5	0.59	0.09131	0.44	1443	34	1388	24	1391	19	99.8
LAS396_Shot_73_Grain_49	1.8494	0.6	0.18203	0.5	0.10	0.07638	0.60	1075	35	1077	19	1059	17	101.8
LAS396_Shot_74_Grain_50	1.7143	0.8	0.17253	0.6	0.18	0.07495	0.80	1028	43	1025	19	1005	18	102.0
LAS396_Shot_75_Grain_51	8.5036	0.6	0.40944	0.5	0.46	0.15606	0.55	2398	33	2209	36	2280	23	96.9
LAS396_Shot_76_Grain_52	6.3671	1.8	0.41369	1.4	0.24	0.12299	2.06	1945	72	2198	61	1952	40	112.6
LAS396_Shot_77_Grain_53	4.9308	0.5	0.32145	0.6	0.55	0.11555	0.50	1872	33	1796	31	1805	21	99.5

LAS396_Shot_78_ Grain_54	5.1820	0.6	0.33989	0.5	0.46	0.11402	0.53	1852	35	1882	32	1845	21	102.0
LAS396_Shot_79_ Grain_55	4.2184	0.5	0.27799	0.4	0.38	0.11326	0.44	1836	33	1579	26	1674	20	94.3
LAS396_Shot_80_ Grain_56	3.6724	0.7	0.22424	0.6	0.59	0.12255	0.54	1979	34	1302	24	1557	21	83.6
LAS396_Shot_87_ Grain_57	1.5667	0.9	0.16503	0.7	0.36	0.07135	0.88	949	46	982	20	951	18	103.3
LAS396_Shot_88_ Grain_58	12.4112	0.6	0.48845	0.6	0.17	0.18975	0.56	2717	30	2560	43	2624	24	97.5
LAS396_Shot_89_ Grain_59	2.7888	0.5	0.23162	0.5	0.55	0.08939	0.47	1399	35	1343	24	1349	18	99.6
LAS396_Shot_90_ Grain_60	4.0771	0.8	0.29557	0.7	0.46	0.10314	0.77	1642	41	1666	32	1638	23	101.7
LAS396_Shot_91_ Grain_61	2.0835	0.5	0.19824	0.5	0.56	0.07862	0.46	1153	35	1165	21	1141	17	102.1
LAS396_Shot_92_ Grain_62	2.8469	0.5	0.23170	0.4	0.56	0.09135	0.43	1439	35	1342	22	1365	18	98.3
LAS396_Shot_93_ Grain_63	4.6798	0.5	0.31188	0.5	0.61	0.11190	0.46	1820	33	1748	30	1762	21	99.2
LAS396_Shot_94_ Grain_64	14.7743	0.5	0.54506	0.6	0.59	0.20311	0.47	2840	30	2797	45	2797	23	100.0
LAS396_Shot_95_ Grain_65	4.1636	0.5	0.29959	0.5	0.59	0.10332	0.41	1675	34	1688	28	1664	20	101.4
LAS396_Shot_96_ Grain_66	13.1888	0.4	0.50762	0.4	0.61	0.19291	0.38	2761	29	2644	40	2692	23	98.2
LAS396_Shot_97_ Grain_67	2.8408	0.5	0.23843	0.5	0.62	0.08902	0.45	1394	35	1377	24	1363	19	101.0
LAS396_Shot_98_ Grain_68	19.6610	0.6	0.60402	0.5	0.49	0.24229	0.50	3119	30	3041	47	3070	23	99.1
LAS396_Shot_99_ Grain_69	2.3648	0.5	0.21102	0.5	0.57	0.08366	0.47	1269	35	1233	22	1230	17	100.2
LAS396_Shot_100_ Grain_70	1.8748	0.7	0.16468	0.5	0.63	0.08509	0.52	1299	38	981	18	1067	17	92.0
LAS396_Shot_107_ Grain_71	3.0400	1.2	0.22219	0.7	0.28	0.10344	1.18	1590	53	1290	25	1394	25	92.5
LAS396_Shot_108_ Grain_72	3.2058	0.6	0.26205	0.6	0.53	0.09221	0.59	1445	34	1498	27	1453	20	103.1
LAS396_Shot_109_ Grain_73	3.1090	0.5	0.25024	0.5	0.58	0.09294	0.45	1476	35	1438	24	1433	19	100.3
LAS396_Shot_110_ Grain_74	16.9335	0.6	0.56019	0.6	0.65	0.22543	0.48	3008	30	2867	48	2925	24	98.0
LAS396_Shot_111_ Grain_75	4.0253	0.7	0.29047	0.6	0.40	0.10390	0.74	1657	41	1640	30	1630	22	100.6
LAS396_Shot_112_ Grain_76	3.9490	0.6	0.28786	0.6	0.50	0.10260	0.59	1653	38	1628	29	1619	21	100.6
LAS396_Shot_113_ Grain_77	2.6283	0.6	0.23065	0.5	0.50	0.08561	0.54	1312	38	1336	24	1307	18	102.3
LAS396_Shot_114_ Grain_78	23.0263	0.6	0.60367	0.5	0.59	0.28691	0.48	3392	29	3038	47	3222	25	94.3
LAS396_Shot_115_ Grain_79	2.0222	0.7	0.19271	0.6	0.39	0.07894	0.69	1135	43	1134	21	1117	18	101.6
LAS396_Shot_116_ Grain_80	4.8693	0.7	0.32886	0.6	0.26	0.11144	0.70	1792	38	1830	32	1786	22	102.5
LAS396_Shot_117_ Grain_81	5.9582	0.6	0.36071	0.6	0.60	0.12441	0.50	2006	34	1980	34	1964	22	100.8
LAS396_Shot_118_ Grain_82	3.0678	0.5	0.24574	0.5	0.53	0.09333	0.50	1481	35	1416	25	1421	19	99.7
LAS396_Shot_119_ Grain_83	4.2628	0.6	0.30900	0.6	0.53	0.10369	0.57	1671	36	1732	31	1683	21	102.9
LAS396_Shot_120_ Grain_84	2.1133	0.7	0.19396	0.6	0.36	0.08162	0.67	1206	41	1141	21	1148	18	99.4
LAS396_Shot_127_ Grain_85	1.8020	0.6	0.18350	0.5	0.54	0.07396	0.52	1018	39	1085	19	1043	17	104.0
LAS396_Shot_128_ Grain_86	2.7291	0.5	0.19484	0.6	0.58	0.10444	0.46	1695	34	1146	21	1333	18	86.0
LAS396_Shot_129_ Grain_87	4.4321	0.5	0.20864	0.6	0.63	0.15832	0.46	2424	31	1219	22	1713	20	71.2
LAS396_Shot_130_ Grain_88	4.0248	0.8	0.27354	0.8	0.74	0.10975	0.56	1767	33	1554	30	1627	22	95.6

LAS396_Shot_131_ Grain_89	4.0494	0.5	0.26704	0.5	0.60	0.11321	0.43	1839	33	1524	26	1639	20	93.0
LAS396_Shot_132_ Grain_90	8.7885	0.6	0.39463	0.6	0.58	0.16618	0.50	2507	32	2142	37	2310	23	92.7
LAS396_Shot_133_ Grain_91	2.2796	0.5	0.20879	0.6	0.62	0.08133	0.51	1216	37	1221	22	1202	18	101.6
LAS396_Shot_134_ Grain_92	4.9266	0.6	0.31805	0.6	0.60	0.11570	0.51	1874	34	1779	31	1802	21	98.7
LAS396_Shot_135_ Grain_93	4.5000	0.7	0.29535	0.7	0.65	0.11400	0.51	1855	34	1662	32	1721	23	96.6
LAS396_Shot_136_ Grain_94	1.1677	0.7	0.11407	0.6	0.52	0.07664	0.63	1087	40	696	13	781	14	89.1
LAS396_Shot_137_ Grain_95	3.3557	0.5	0.22733	0.4	0.37	0.11006	0.50	1784	34	1321	22	1490	19	88.7
LAS396_Shot_138_ Grain_96	5.2853	0.5	0.33535	0.5	0.59	0.11678	0.45	1896	33	1860	31	1865	20	99.8
LAS396_Shot_139_ Grain_97	2.2002	0.5	0.19834	0.5	0.51	0.08318	0.47	1262	36	1166	20	1179	17	98.9
LAS396_Shot_140_ Grain_98	8.8625	0.5	0.43373	0.5	0.48	0.15238	0.41	2366	28	2318	38	2319	22	99.9
LAS396_Shot_147_ Grain_99	16.0464	0.6	0.37398	0.6	0.77	0.31910	0.37	3561	27	2043	36	2869	26	71.2
LAS396_Shot_148_ Grain_100	3.4231	0.6	0.26792	0.6	0.19	0.09557	0.59	1519	35	1526	28	1502	19	101.6
LAS396_Shot_149_ Grain_101	1.7470	0.6	0.17449	0.6	0.46	0.07443	0.63	1032	40	1036	19	1023	17	101.3
LAS396_Shot_150_ Grain_102	1.8909	0.6	0.17735	0.6	0.68	0.07935	0.49	1163	36	1053	20	1073	17	98.1
LAS396_Shot_151_ Grain_103	2.6895	0.6	0.22700	0.6	0.36	0.08906	0.62	1379	37	1316	24	1322	19	99.6
LAS396_Shot_152_ Grain_104	3.9579	0.6	0.28579	0.6	0.55	0.10340	0.54	1671	34	1619	28	1620	20	100.0
LAS396_Shot_153_ Grain_105	12.6385	0.5	0.48776	0.5	0.61	0.19278	0.42	2757	30	2557	41	2650	23	96.5
LAS396_Shot_154_ Grain_106	3.3221	0.5	0.26129	0.6	0.61	0.09478	0.47	1510	35	1493	26	1482	20	100.8
LAS396_Shot_155_ Grain_107	3.2968	0.5	0.26025	0.5	0.55	0.09435	0.47	1500	34	1490	25	1478	19	100.8
LAS396_Shot_156_ Grain_108	4.0072	0.6	0.29531	0.6	0.47	0.10160	0.56	1636	36	1665	29	1633	20	102.0
LAS396_Shot_157_ Grain_109	13.2401	0.6	0.51834	0.6	0.54	0.19096	0.53	2734	32	2688	45	2691	24	99.9
LAS396_Shot_158_ Grain_110	10.7234	0.5	0.44553	0.6	0.59	0.17894	0.46	2634	30	2373	40	2492	23	95.2
LAS396_Shot_159_ Grain_111	1.7516	0.8	0.17578	0.6	0.38	0.07491	0.80	1035	43	1043	20	1021	18	102.1
LAS396_Shot_160_ Grain_112	13.4062	0.5	0.53025	0.5	0.58	0.18900	0.48	2725	30	2739	44	2703	24	101.3
LAS396_Shot_167_ Grain_113	0.7909	1.1	0.09564	0.6	0.14	0.06227	1.10	829	47	589	12	586	14	100.4
LAS396_Shot_168_ Grain_114	2.8473	0.6	0.23840	0.6	0.37	0.08938	0.56	1391	36	1377	25	1361	19	101.1
LAS396_Shot_169_ Grain_115	1.7312	0.5	0.17155	0.4	0.48	0.07490	0.46	1055	37	1020	17	1018	16	100.1
LAS396_Shot_170_ Grain_116	4.4785	1.1	0.27526	0.9	0.05	0.12106	0.82	1936	39	1559	34	1698	28	91.8
LAS396_Shot_171_ Grain_117	2.1257	2.1	0.19424	1.2	0.12	0.08540	2.22	1522	75	1139	30	1096	34	104.0
LAS396_Shot_172_ Grain_118	3.2824	0.5	0.25891	0.5	0.62	0.09378	0.43	1490	35	1483	26	1473	19	100.7
LAS396_Shot_173_ Grain_119	9.4824	1.3	0.42600	0.8	0.78	0.16143	0.82	2441	38	2286	45	2347	29	97.4
LAS396_Shot_174_ Grain_120	10.0124	0.4	0.40421	0.5	0.53	0.18368	0.41	2677	30	2185	35	2432	22	89.9
LAS396_Shot_175_ Grain_121	1.7677	0.7	0.16280	0.5	0.26	0.08038	0.65	1183	40	972	17	1028	17	94.5
LAS396_Shot_176_ Grain_122	2.1560	0.5	0.18332	0.4	0.28	0.08696	0.48	1344	36	1085	18	1164	17	93.2
LAS396_Shot_177_ Grain_123	1.1136	1.3	0.09345	0.5	0.44	0.08748	1.10	1296	53	575	11	744	18	77.4

LAS396_Shot_178_Grain_124	2.5334	0.6	0.21970	0.5	0.58	0.08529	0.48	1305	37	1281	23	1277	19	100.2
LAS396_Shot_179_Grain_125	13.8554	0.6	0.52370	0.6	0.64	0.19528	0.46	2778	31	2708	44	2731	24	99.1
LAS396_Shot_180_Grain_126	1.6698	0.6	0.16670	0.6	0.56	0.07415	0.52	1034	37	993	18	994	16	99.9
LAS396_Shot_187_Grain_127	8.6004	0.7	0.39731	0.7	0.57	0.16209	0.66	2461	36	2155	41	2290	25	94.1
LAS396_Shot_188_Grain_128	5.5136	0.8	0.34662	0.7	0.03	0.11883	0.81	1892	40	1913	36	1885	25	101.4
LAS396_Shot_189_Grain_129	1.9175	0.7	0.18530	0.6	0.47	0.07711	0.63	1096	42	1094	21	1083	18	101.0
LAS396_Shot_190_Grain_130	3.0353	0.5	0.23762	0.5	0.57	0.09410	0.43	1495	34	1373	23	1413	18	97.2
LAS396_Shot_191_Grain_131	8.9963	0.5	0.38471	0.6	0.62	0.17274	0.46	2573	30	2093	36	2334	23	89.7
LAS396_Shot_192_Grain_132	4.2876	0.5	0.29352	0.5	0.38	0.10846	0.46	1760	32	1658	28	1687	19	98.3
LAS396_Shot_193_Grain_133	13.5143	0.5	0.51695	0.6	0.60	0.19340	0.44	2763	30	2687	43	2713	23	99.0
LAS396_Shot_194_Grain_134	1.7792	0.7	0.17691	0.6	0.10	0.07506	0.65	1035	40	1048	19	1031	17	101.7
LAS396_Shot_195_Grain_135	14.3058	0.5	0.53344	0.6	0.60	0.19889	0.50	2804	30	2755	44	2766	23	99.6
LAS396_Shot_196_Grain_136	4.0191	0.6	0.29250	0.5	0.47	0.10242	0.48	1651	34	1652	28	1633	21	101.1
LAS396_Shot_197_Grain_137	2.0878	0.5	0.19677	0.5	0.05	0.07903	0.52	1153	34	1157	20	1141	17	101.3
LAS396_Shot_198_Grain_138	4.0748	0.5	0.29742	0.5	0.48	0.10159	0.46	1641	34	1676	28	1645	20	101.9
LAS396_Shot_199_Grain_139	3.3142	0.7	0.26018	0.6	0.95	0.09524	0.72	1492	40	1491	26	1474	21	101.2
LAS396_Shot_200_Grain_140	12.2897	0.4	0.49133	0.5	0.55	0.18565	0.43	2694	30	2573	41	2624	23	98.1
LAS396_Shot_207_Grain_141	14.7227	0.5	0.53644	0.6	0.54	0.20469	0.50	2854	30	2765	44	2794	23	99.0
LAS396_Shot_208_Grain_142	3.6090	0.5	0.26625	0.5	0.60	0.10050	0.45	1623	35	1521	27	1547	20	98.3
LAS396_Shot_209_Grain_143	5.3997	0.6	0.34316	0.6	0.57	0.11774	0.52	1904	34	1898	33	1879	22	101.0
LAS396_Shot_210_Grain_144	3.9789	0.5	0.29380	0.5	0.57	0.10106	0.46	1626	34	1658	29	1629	20	101.8
LAS396_Shot_211_Grain_145	1.7184	0.6	0.17267	0.5	0.57	0.07411	0.48	1028	37	1026	18	1013	16	101.3
LAS396_Shot_212_Grain_146	2.5485	0.5	0.22098	0.5	0.58	0.08632	0.42	1331	35	1287	22	1282	18	100.4
LAS396_Shot_213_Grain_147	5.6752	0.8	0.35356	0.7	0.47	0.12073	0.61	1951	34	1945	35	1914	23	101.6
LAS396_Shot_214_Grain_148	3.9174	0.5	0.28462	0.6	0.60	0.10292	0.46	1664	33	1611	28	1614	20	99.8
LAS396_Shot_215_Grain_149	1.8784	0.6	0.18332	0.6	0.35	0.07678	0.58	1088	40	1083	20	1070	17	101.3
LAS396_Shot_216_Grain_150	3.7245	0.5	0.25505	0.5	0.41	0.10965	0.50	1779	33	1462	25	1572	20	93.0
LAS396_Shot_217_Grain_151	2.5997	0.5	0.21398	0.4	0.62	0.09070	0.38	1428	34	1250	21	1299	18	96.3
LAS396_Shot_218_Grain_152	3.9532	0.4	0.27910	0.4	0.65	0.10570	0.28	1721	31	1585	25	1622	19	97.7
LAS396_Shot_219_Grain_153	1.4541	0.8	0.14687	0.7	0.77	0.07374	0.47	1020	38	882	17	905	17	97.5
LAS396_Shot_220_Grain_154	2.1454	0.5	0.16681	0.5	0.51	0.09679	0.43	1554	34	993	17	1162	17	85.5
LAS396_Shot_227_Grain_155	10.9183	0.6	0.43772	0.6	0.69	0.18640	0.47	2700	30	2332	40	2507	24	93.0
LAS396_Shot_228_Grain_156	1.5557	0.7	0.14566	0.6	0.43	0.07995	0.68	1165	43	876	16	949	16	92.4
LAS396_Shot_229_Grain_157	4.9843	0.5	0.31991	0.6	0.57	0.11602	0.50	1884	34	1787	31	1812	21	98.6
LAS396_Shot_230_Grain_158	2.0885	0.6	0.19353	0.5	0.55	0.08047	0.56	1185	39	1139	21	1141	18	99.8

LAS396_Shot_231_ Grain_159	3.1989	0.4	0.23913	0.5	0.61	0.09975	0.41	1616	33	1381	23	1456	19	94.8
LAS396_Shot_232_ Grain_160	2.4150	0.7	0.21143	0.6	0.12	0.08573	0.68	1299	40	1234	22	1237	19	99.8
LAS396_Shot_233_ Grain_161	5.2106	0.5	0.33473	0.5	0.49	0.11610	0.49	1882	33	1858	30	1849	21	100.5
LAS396_Shot_234_ Grain_162	2.1431	0.6	0.20255	0.6	0.55	0.07868	0.55	1150	39	1188	22	1158	18	102.6
LAS396_Shot_235_ Grain_163	2.1432	0.7	0.19861	0.6	0.58	0.07999	0.53	1179	39	1166	22	1160	18	100.4
LAS396_Shot_236_ Grain_164	1.5144	0.5	0.14953	0.4	0.57	0.07569	0.37	1077	34	898	15	935	15	96.0
LAS396_Shot_237_ Grain_165	2.3676	0.5	0.21516	0.5	0.58	0.08204	0.48	1236	37	1256	22	1229	18	102.2
LAS396_Shot_238_ Grain_166	2.6159	0.5	0.21430	0.5	0.59	0.09047	0.44	1422	35	1251	22	1302	18	96.1
LAS396_Shot_239_ Grain_167	9.5338	0.9	0.41789	0.7	0.74	0.16815	0.60	2526	33	2240	41	2373	25	94.4
LAS396_Shot_240_ Grain_168	3.9162	0.6	0.27576	0.6	0.63	0.10619	0.46	1725	33	1566	29	1610	21	97.3
LAS396_Shot_247_ Grain_169	12.7443	0.5	0.51496	0.6	0.60	0.18428	0.47	2681	29	2673	42	2659	24	100.5
LAS396_Shot_248_ Grain_170	0.6061	0.5	0.07917	0.5	0.45	0.05714	0.49	513	37	491	9	480	9	102.2
LAS396_Shot_249_ Grain_171	1.8444	1.7	0.18533	1.1	0.16	0.07833	1.94	1314	66	1089	27	1026	27	106.2
LAS396_Shot_250_ Grain_172	4.3884	0.6	0.30120	0.6	0.57	0.10845	0.53	1754	35	1693	30	1703	21	99.4
LAS396_Shot_251_ Grain_173	3.3681	0.5	0.25082	0.5	0.45	0.10000	0.42	1613	32	1442	24	1493	19	96.6
LAS396_Shot_252_ Grain_174	11.3786	0.5	0.45467	0.6	0.52	0.18633	0.54	2695	32	2416	40	2550	23	94.8
LAS396_Shot_253_ Grain_175	1.7295	0.5	0.17238	0.5	0.56	0.07466	0.50	1042	38	1024	19	1017	16	100.7
LAS396_Shot_254_ Grain_176	3.1059	0.5	0.24473	0.5	0.41	0.09454	0.41	1508	32	1411	24	1431	18	98.6
LAS396_Shot_255_ Grain_177	3.6315	0.6	0.27147	0.6	0.49	0.09864	0.58	1581	36	1547	27	1550	20	99.8
LAS396_Shot_256_ Grain_178	3.5076	0.4	0.24504	0.4	0.61	0.10629	0.34	1730	32	1411	23	1526	19	92.5
LAS396_Shot_257_ Grain_179	4.3905	0.6	0.29216	0.6	0.70	0.11154	0.45	1816	33	1649	29	1705	22	96.7
LAS396_Shot_258_ Grain_180	1.8853	0.6	0.18446	0.5	0.44	0.07581	0.57	1069	39	1091	19	1071	17	101.8
LAS396_Shot_259_ Grain_181	2.8459	0.6	0.22190	0.6	0.56	0.09514	0.57	1515	37	1291	24	1362	20	94.8
LAS396_Shot_260_ Grain_182	2.8561	0.6	0.23772	0.6	0.10	0.08900	0.57	1387	36	1373	25	1362	19	100.8
LAS396_Shot_267_ Grain_183	11.1552	0.9	0.44358	0.8	0.89	0.18533	0.39	2692	29	2357	45	2517	29	93.6
LAS396_Shot_268_ Grain_184	6.7839	0.8	0.29555	0.7	0.76	0.17074	0.51	2552	32	1667	32	2072	24	80.5
LAS396_Shot_269_ Grain_185	13.2075	0.5	0.50603	0.5	0.54	0.19383	0.49	2767	30	2634	42	2691	23	97.9
LAS396_Shot_270_ Grain_186	1.8778	1.6	0.18253	0.7	0.08	0.07659	1.21	1063	39	1078	21	1049	14	102.7
LAS396_Shot_271_ Grain_187	5.0746	0.5	0.32333	0.6	0.62	0.11622	0.46	1887	32	1805	31	1830	21	98.6
LAS396_Shot_272_ Grain_188	2.4532	0.5	0.20768	0.5	0.45	0.08719	0.53	1347	37	1216	21	1255	18	96.9
LAS396_Shot_273_ Grain_189	0.5580	0.8	0.07178	0.6	0.19	0.05826	0.88	654	41	447	9	448	10	99.7
LAS396_Shot_274_ Grain_190	4.0650	0.6	0.29726	0.6	0.52	0.10188	0.52	1645	35	1674	29	1644	20	101.8
LAS396_Shot_275_ Grain_191	1.7995	1.0	0.17852	0.7	0.31	0.07630	1.03	1102	48	1056	21	1039	20	101.6
LAS396_Shot_276_ Grain_192	7.0227	0.6	0.36334	0.6	0.52	0.14328	0.57	2251	34	1997	35	2107	23	94.8
LAS396_Shot_277_ Grain_193	4.9023	0.6	0.32026	0.6	0.52	0.11369	0.55	1849	34	1790	32	1796	22	99.7

LAS396_Shot_278_ Grain_194	1.0654	0.6	0.11003	0.6	0.61	0.07199	0.55	960	39	674	13	734	13	91.8
LAS396_Shot_279_ Grain_195	1.7478	0.6	0.16880	0.5	0.39	0.07751	0.65	1100	41	1004	18	1022	17	98.3
LAS396_Shot_280_ Grain_196	2.0893	0.5	0.18941	0.4	0.46	0.08196	0.47	1230	36	1118	19	1143	17	97.8
LAS396_Shot_287_ Grain_197	3.5467	0.7	0.27003	0.7	0.58	0.09788	0.63	1561	38	1540	29	1530	21	100.6
LAS396_Shot_288_ Grain_198	13.1430	0.6	0.51257	0.6	0.17	0.19327	0.51	2756	29	2658	44	2685	23	99.0
LAS396_Shot_289_ Grain_199	2.0026	0.5	0.19259	0.4	0.53	0.07742	0.43	1120	35	1134	19	1115	16	101.7
LAS396_Shot_290_ Grain_200	4.0253	0.6	0.29281	0.6	0.10	0.10254	0.54	1648	34	1654	29	1632	21	101.3
LAS396_Shot_291_ Grain_201	1.3041	1.4	0.13472	1.0	0.75	0.07198	0.86	958	45	811	20	829	20	97.9
LAS396_Shot_292_ Grain_202	3.6210	0.6	0.26421	0.7	0.18	0.10337	0.62	1662	34	1506	28	1546	20	97.4
LAS396_Shot_293_ Grain_203	2.6052	0.8	0.21355	0.7	0.12	0.09112	0.58	1427	37	1244	24	1289	21	96.5
LAS396_Shot_294_ Grain_204	3.0363	0.6	0.23417	0.5	0.38	0.09767	0.58	1559	37	1355	23	1412	19	96.0
LAS396_Shot_295_ Grain_205	13.8428	0.7	0.53054	0.7	0.56	0.19555	0.58	2779	33	2739	47	2733	25	100.2
LAS396_Shot_296_ Grain_206	1.9868	1.4	0.19135	1.1	0.29	0.07781	0.96	1113	48	1120	26	1085	23	103.3
LAS396_Shot_297_ Grain_207	5.4357	0.9	0.25049	0.9	0.79	0.16276	0.55	2473	33	1435	31	1877	26	76.5
LAS396_Shot_298_ Grain_208	6.8523	0.6	0.34895	0.6	0.50	0.14816	0.59	2309	34	1926	34	2086	23	92.3
LAS396_Shot_299_ Grain_209	3.1960	0.6	0.20513	0.6	0.70	0.11624	0.46	1888	33	1201	22	1452	20	82.7
LAS396_Shot_300_ Grain_210	12.1885	0.5	0.46776	0.5	0.62	0.19407	0.39	2772	28	2469	39	2614	23	94.5
LAS396_Shot_307_ Grain_211	1.8341	0.6	0.18077	0.6	0.58	0.07628	0.57	1079	39	1071	20	1055	17	101.5
LAS396_Shot_308_ Grain_212	4.4892	0.6	0.30321	0.7	0.53	0.11112	0.51	1799	34	1703	31	1725	20	98.7
LAS396_Shot_309_ Grain_213	7.0126	0.7	0.29724	0.7	0.74	0.17607	0.49	2605	31	1673	32	2102	23	79.6
LAS396_Shot_310_ Grain_214	12.0336	0.7	0.48015	0.8	0.56	0.18885	0.72	2709	36	2517	47	2596	26	96.9
LAS396_Shot_311_ Grain_215	3.8697	0.6	0.28309	0.6	0.53	0.10231	0.54	1650	35	1605	28	1603	20	100.1
LAS396_Shot_312_ Grain_216	2.0244	0.8	0.18901	0.8	0.46	0.08078	0.83	1174	45	1113	23	1117	19	99.7
LAS396_Shot_313_ Grain_217	3.8296	0.6	0.27219	0.6	0.63	0.10500	0.53	1699	35	1550	28	1594	21	97.2
LAS396_Shot_314_ Grain_218	1.8052	0.6	0.17845	0.6	0.51	0.07608	0.62	1068	41	1057	20	1044	17	101.2
LAS396_Shot_315_ Grain_219	2.9119	0.7	0.16200	0.5	0.64	0.13368	0.52	2129	33	967	17	1376	20	70.3
LAS396_Shot_316_ Grain_220	10.2135	0.6	0.40561	0.6	0.30	0.18803	0.54	2712	31	2193	38	2443	24	89.8
LAS396_Shot_317_ Grain_221	2.6641	0.6	0.20214	0.6	0.46	0.09839	0.51	1583	35	1186	22	1316	18	90.2
LAS396_Shot_318_ Grain_222	4.0281	0.7	0.24401	0.7	0.72	0.12301	0.52	1986	34	1409	27	1631	22	86.4
LAS396_Shot_319_ Grain_223	3.5587	0.8	0.24282	0.8	0.70	0.10998	0.60	1776	36	1396	28	1528	22	91.4
LAS396_Shot_320_ Grain_224	1.4346	0.6	0.14678	0.4	0.45	0.07254	0.54	983	39	882	15	900	15	98.0
LAS396_Shot_327_ Grain_225	3.5536	0.5	0.26927	0.6	0.55	0.09829	0.51	1582	35	1538	27	1536	20	100.1
LAS396_Shot_328_ Grain_226	3.6075	0.5	0.25004	0.5	0.49	0.10708	0.52	1731	35	1437	25	1547	20	92.9
LAS396_Shot_329_ Grain_227	13.8305	0.5	0.52535	0.5	0.55	0.19500	0.50	2773	30	2720	44	2732	23	99.6
LAS396_Shot_330_ Grain_228	13.1523	0.6	0.52385	0.7	0.55	0.18853	0.56	2714	32	2703	46	2682	24	100.8

LAS396_Shot_331_ Grain_229	10.8326	0.6	0.47052	0.6	0.35	0.17104	0.51	2555	30	2484	42	2502	22	99.3
LAS396_Shot_332_ Grain_230	12.1907	0.6	0.49242	0.6	0.69	0.18426	0.50	2678	31	2573	44	2616	24	98.4
LAS396_Shot_333_ Grain_231	1.7688	0.5	0.17403	0.5	0.22	0.07543	0.47	1067	35	1033	18	1031	16	100.2
LAS396_Shot_334_ Grain_232	1.5560	1.7	0.13860	1.2	0.81	0.08132	1.07	1186	50	836	22	921	25	90.8
LAS396_Shot_335_ Grain_233	3.2455	0.8	0.21813	0.7	0.62	0.11087	0.55	1799	33	1269	25	1461	20	86.8
LAS396_Shot_336_ Grain_234	1.8425	0.5	0.18404	0.5	0.61	0.07425	0.44	1042	36	1088	19	1060	16	102.6
LAS396_Shot_337_ Grain_235	1.9597	0.9	0.19379	0.8	0.19	0.07661	0.92	1080	47	1138	23	1095	19	104.0
LAS396_Shot_338_ Grain_236	2.8954	0.6	0.24528	0.6	0.58	0.08871	0.54	1381	37	1411	26	1377	19	102.5
LAS396_Shot_339_ Grain_237	1.8455	0.6	0.17561	0.5	0.21	0.07863	0.57	1139	38	1042	18	1058	16	98.5
LAS396_Shot_340_ Grain_238	7.5435	0.5	0.31912	0.5	0.62	0.17658	0.40	2611	30	1782	29	2175	22	81.9
LAS396_Shot_347_ Grain_239	3.4086	0.6	0.23900	0.6	0.61	0.10726	0.48	1745	33	1378	25	1502	20	91.8
LAS396_Shot_348_ Grain_240	4.5034	0.6	0.31498	0.6	0.62	0.10779	0.51	1748	34	1763	32	1728	21	102.0
LAS396_Shot_349_ Grain_241	4.4793	0.6	0.30353	0.6	0.48	0.11071	0.52	1793	35	1706	29	1724	21	99.0
LAS396_Shot_350_ Grain_242	2.5494	0.6	0.19427	0.6	0.67	0.09826	0.49	1577	35	1143	21	1282	18	89.2
LAS396_Shot_351_ Grain_243	6.1257	0.7	0.26784	0.7	0.78	0.17255	0.44	2573	30	1524	30	1982	24	76.9
LAS396_Shot_352_ Grain_244	9.5148	0.7	0.37693	0.7	0.73	0.19071	0.50	2734	31	2057	38	2376	25	86.6
LAS396_Shot_353_ Grain_245	1.7264	0.7	0.15338	0.7	0.64	0.08488	0.60	1289	39	918	18	1012	17	90.7
LAS396_Shot_354_ Grain_246	1.4349	0.8	0.14360	0.6	0.33	0.07551	0.72	1047	42	864	17	895	17	96.5
LAS396_Shot_355_ Grain_247	4.5374	0.7	0.31118	0.7	0.28	0.11088	0.66	1791	35	1742	32	1727	22	100.9
LAS396_Shot_356_ Grain_248	4.7304	1.1	0.31075	0.9	0.25	0.11869	1.19	1872	53	1736	37	1754	26	99.0
LAS396_Shot_357_ Grain_249	2.8094	0.6	0.23876	0.6	0.48	0.08901	0.60	1379	37	1379	25	1353	19	102.0
LAS396_Shot_358_ Grain_250	8.3127	0.6	0.35464	0.6	0.67	0.17686	0.47	2612	31	1952	35	2258	22	86.5
LAS396_Shot_359_ Grain_251	1.4573	0.9	0.14389	0.7	0.62	0.07693	0.71	1081	42	865	18	906	17	95.5
LAS396_Shot_360_ Grain_252	1.6564	1.3	0.14568	1.0	0.83	0.08483	0.66	1283	41	874	22	969	22	90.1
LAS396_Shot_367_ Grain_253	13.6095	0.6	0.52928	0.7	0.66	0.19561	0.52	2777	31	2728	48	2715	24	100.5
LAS396_Shot_368_ Grain_254	1.5496	0.7	0.15135	0.6	0.61	0.07803	0.62	1121	40	908	17	944	16	96.2
LAS396_Shot_369_ Grain_255	12.0307	0.6	0.48619	0.6	0.59	0.18610	0.47	2698	30	2549	43	2600	24	98.0
LAS396_Shot_370_ Grain_256	4.6579	0.5	0.29270	0.5	0.53	0.12056	0.45	1951	33	1653	28	1755	21	94.2
LAS396_Shot_371_ Grain_257	1.3694	0.5	0.14614	0.5	0.57	0.07112	0.49	946	38	879	16	875	14	100.5
LAS396_Shot_372_ Grain_258	5.1116	0.6	0.32775	0.6	0.59	0.11756	0.52	1904	35	1823	32	1834	21	99.4
LAS396_Shot_373_ Grain_259	3.3421	0.5	0.24815	0.5	0.63	0.10138	0.40	1638	33	1427	24	1491	19	95.7
LAS396_Shot_374_ Grain_260	2.5255	0.7	0.17045	0.6	0.67	0.11104	0.52	1795	34	1013	19	1270	20	79.8
LAS396_Shot_375_ Grain_261	6.3562	0.9	0.37484	0.8	0.40	0.12993	0.93	2044	43	2043	40	2010	25	101.6
LAS396_Shot_376_ Grain_262	1.5531	0.5	0.15684	0.5	0.46	0.07480	0.48	1044	38	938	16	950	15	98.8
LAS396_Shot_377_ Grain_263	3.4526	0.5	0.23551	0.5	0.43	0.10994	0.53	1780	35	1362	23	1510	20	90.2

LAS396_Shot_378_ Grain_264	1.7112	0.8	0.17166	0.7	0.36	0.07515	0.85	1040	46	1020	20	1007	18	101.3
LAS396_Shot_379_ Grain_265	2.8001	1.1	0.21600	1.0	0.67	0.09704	0.60	1545	36	1254	30	1332	25	94.1
LAS396_Shot_380_ Grain_266	12.8958	0.6	0.49513	0.6	0.54	0.19659	0.54	2784	31	2585	43	2663	24	97.1
LAS396_Shot_387_ Grain_267	2.4008	0.7	0.19469	0.6	0.57	0.09315	0.56	1472	36	1146	21	1237	19	92.7
LAS396_Shot_388_ Grain_268	2.8835	0.5	0.23051	0.5	0.60	0.09376	0.49	1490	34	1338	23	1373	19	97.4
LAS396_Shot_389_ Grain_269	1.5336	1.0	0.15736	0.7	0.33	0.07356	1.04	1041	48	941	19	932	19	100.9
LAS396_Shot_390_ Grain_270	2.7553	0.6	0.22677	0.5	0.18	0.09167	0.52	1440	35	1315	23	1337	19	98.4
LAS396_Shot_391_ Grain_271	3.7409	0.5	0.27436	0.5	0.47	0.10258	0.49	1658	35	1561	27	1576	20	99.1
LAS396_Shot_392_ Grain_272	1.6632	0.5	0.16604	0.5	0.57	0.07514	0.47	1056	37	989	18	992	16	99.7
LAS396_Shot_393_ Grain_273	10.1378	0.4	0.41095	0.4	0.62	0.18408	0.35	2684	28	2217	35	2443	22	90.8
LAS396_Shot_394_ Grain_274	10.2239	0.7	0.41092	0.7	0.60	0.18600	0.51	2702	30	2212	39	2452	24	90.2
LAS396_Shot_395_ Grain_275	4.0619	0.7	0.26692	0.7	0.78	0.11407	0.48	1852	34	1521	29	1638	22	92.9
LAS396_Shot_396_ Grain_276	3.5215	1.1	0.25279	1.0	0.74	0.10501	0.78	1701	40	1444	33	1515	26	95.3
LAS396_Shot_397_ Grain_277	9.9775	0.5	0.40217	0.5	0.48	0.18631	0.50	2698	31	2176	36	2427	23	89.7
LAS396_Shot_398_ Grain_278	4.0270	0.5	0.28468	0.5	0.55	0.10610	0.43	1722	33	1614	27	1637	20	98.6
LAS396_Shot_399_ Grain_279	1.8027	0.7	0.17282	0.7	0.53	0.07842	0.64	1132	41	1027	20	1042	17	98.5
LAS396_Shot_400_ Grain_280	2.5482	0.6	0.21977	0.5	0.35	0.08674	0.59	1337	40	1279	22	1281	18	99.8
LAS396_Shot_407_ Grain_281	1.9883	0.6	0.16092	0.5	0.65	0.09269	0.43	1466	35	961	17	1108	17	86.7
LAS396_Shot_408_ Grain_282	9.0232	0.5	0.34517	0.5	0.67	0.19658	0.37	2794	29	1907	32	2333	23	81.8
LAS396_Shot_409_ Grain_283	1.8916	0.6	0.17494	0.4	0.56	0.08118	0.49	1210	36	1039	18	1075	17	96.7
LAS396_Shot_410_ Grain_284	0.7624	1.2	0.08915	0.7	0.07	0.06600	1.32	950	52	551	11	568	14	96.9
LAS396_Shot_411_ Grain_285	2.5155	1.0	0.18277	0.9	0.76	0.10280	0.65	1651	39	1078	23	1260	23	85.6
LAS396_Shot_412_ Grain_286	1.9263	0.5	0.17681	0.4	0.59	0.08191	0.41	1232	35	1048	18	1088	16	96.4
LAS396_Shot_413_ Grain_287	2.8557	0.5	0.23280	0.5	0.62	0.09249	0.44	1464	33	1348	24	1366	19	98.7
LAS396_Shot_414_ Grain_288	5.6336	0.8	0.25846	0.7	0.85	0.16367	0.40	2486	30	1478	28	1906	25	77.6
LAS396_Shot_415_ Grain_289	0.7816	0.6	0.09699	0.4	0.38	0.06080	0.56	635	38	596	10	585	11	101.9
LAS396_Shot_416_ Grain_290	0.5604	0.7	0.07370	0.4	0.09	0.05796	0.74	596	39	458	8	450	9	101.8
LAS396_Shot_417_ Grain_291	9.8257	0.5	0.40362	0.4	0.81	0.18348	0.28	2679	28	2182	34	2412	23	90.5
LAS396_Shot_418_ Grain_292	2.4860	0.5	0.20874	0.5	0.44	0.09027	0.50	1409	36	1222	21	1264	18	96.7
LAS396_Shot_419_ Grain_293	3.8517	0.6	0.26482	0.5	0.55	0.11017	0.51	1784	34	1513	26	1599	20	94.6
LAS396_Shot_420_ Grain_294	1.8068	0.5	0.17229	0.5	0.02	0.07965	0.50	1169	36	1024	18	1044	16	98.1
LAS396_Shot_427_ Grain_295	4.8775	0.5	0.32557	0.5	0.57	0.11305	0.46	1835	33	1813	30	1792	21	101.2
LAS396_Shot_428_ Grain_296	5.1954	0.5	0.33077	0.6	0.64	0.11918	0.45	1933	32	1839	32	1848	22	99.5
LAS396_Shot_429_ Grain_297	4.2926	0.5	0.29565	0.6	0.56	0.10923	0.47	1775	33	1668	29	1687	21	98.9
LAS396_Shot_430_ Grain_298	8.6295	0.7	0.40744	0.7	0.33	0.15978	0.56	2436	31	2201	39	2293	24	96.0

LAS396_Shot_431_Grain_299	4.7469	0.6	0.31426	0.6	0.45	0.11387	0.57	1837	35	1759	31	1771	21	99.3
LAS396_Shot_432_Grain_300	2.1434	0.6	0.20153	0.5	0.28	0.08043	0.52	1192	35	1182	21	1158	18	102.1
LAS396_Shot_433_Grain_301	2.6576	0.5	0.16431	0.5	0.54	0.12171	0.47	1967	33	980	17	1314	18	74.6
LAS396_Shot_434_Grain_302	2.8353	0.8	0.24069	0.6	0.41	0.08941	0.79	1366	43	1389	26	1357	21	102.3
LAS396_Shot_435_Grain_303	1.8845	0.6	0.17890	0.5	0.44	0.07909	0.62	1149	41	1060	19	1071	17	98.9
LAS396_Shot_436_Grain_304	0.9215	0.6	0.09513	0.5	0.38	0.07317	0.60	996	40	585	11	662	12	88.4
LAS396_Shot_437_Grain_305	8.2357	0.8	0.41391	0.8	0.59	0.15075	0.69	2327	37	2225	42	2245	25	99.1
LAS396_Shot_438_Grain_306	2.5076	0.5	0.21193	0.5	0.40	0.08854	0.51	1378	37	1238	21	1271	18	97.4
LAS396_Shot_439_Grain_307	3.5497	0.4	0.25085	0.5	0.70	0.10532	0.33	1713	31	1441	24	1536	19	93.8
LAS396_Shot_440_Grain_308	1.8830	0.8	0.18586	0.6	0.32	0.07566	0.82	1064	45	1098	21	1067	18	102.9
LAS396_Shot_447_Grain_309	2.9983	1.0	0.20925	0.9	0.80	0.10699	0.57	1731	36	1221	27	1396	22	87.5
LAS396_Shot_448_Grain_310	5.9300	0.5	0.25926	0.5	0.61	0.17120	0.45	2555	31	1484	26	1964	22	75.6
LAS396_Shot_449_Grain_311	5.8162	0.6	0.25476	0.6	0.68	0.17036	0.44	2551	30	1459	27	1942	22	75.2
LAS396_Shot_450_Grain_312	4.3834	0.6	0.28861	0.5	0.59	0.11306	0.45	1837	33	1632	28	1706	21	95.7
LAS396_Shot_451_Grain_313	11.1516	0.5	0.44419	0.5	0.67	0.18772	0.44	2712	29	2364	39	2530	23	93.5
LAS396_Shot_452_Grain_314	8.0232	1.0	0.33505	0.8	0.64	0.17853	0.79	2603	38	1858	38	2207	28	84.2
LAS396_Shot_453_Grain_315	6.1464	0.6	0.25966	0.5	0.68	0.17610	0.41	2612	30	1486	26	1989	23	74.7
LAS396_Shot_454_Grain_316	2.5657	0.7	0.19409	0.6	0.58	0.09841	0.59	1572	38	1141	21	1284	19	88.9
LAS396_Shot_455_Grain_317	3.9899	0.5	0.26837	0.5	0.53	0.11060	0.43	1800	33	1531	26	1629	20	94.0
LAS396_Shot_456_Grain_318	2.0315	0.7	0.17665	0.7	0.46	0.08648	0.74	1308	42	1046	20	1118	18	93.6
LAS396_Shot_457_Grain_319	4.0222	0.5	0.28240	0.5	0.51	0.10651	0.47	1730	33	1600	27	1638	20	97.7
LAS396_Shot_458_Grain_320	14.0536	0.6	0.54226	0.6	0.63	0.19419	0.52	2767	30	2787	47	2749	24	101.4
LAS396_Shot_459_Grain_321	2.6474	0.4	0.22398	0.4	0.57	0.08826	0.38	1380	33	1301	22	1313	18	99.1
LAS396_Shot_460_Grain_322	10.0290	0.7	0.38809	0.6	0.81	0.19179	0.39	2752	29	2110	37	2428	25	86.9
LAS396_Shot_467_Grain_323	1.8020	0.8	0.18773	0.7	0.37	0.07231	0.81	978	44	1107	21	1038	18	106.6
LAS396_Shot_468_Grain_324	1.6880	0.7	0.16726	0.6	0.13	0.07552	0.63	1052	39	997	18	997	17	99.9
LAS396_Shot_469_Grain_325	13.2349	0.8	0.52498	0.8	0.47	0.18995	0.81	2704	39	2710	50	2681	27	101.1
LAS396_Shot_470_Grain_326	1.3982	0.5	0.14703	0.4	0.53	0.07070	0.42	940	38	884	15	886	14	99.7
LAS396_Shot_471_Grain_327	4.4095	0.7	0.28309	0.6	0.72	0.11594	0.48	1880	34	1603	29	1706	21	94.0
LAS396_Shot_472_Grain_328	10.1094	1.2	0.39711	1.1	0.84	0.18933	0.66	2712	34	2134	50	2401	35	88.9
LAS396_Shot_473_Grain_329	1.8506	0.7	0.16170	0.6	0.76	0.08534	0.47	1315	35	965	18	1055	18	91.4
LAS396_Shot_474_Grain_330	3.4018	0.6	0.26802	0.6	0.50	0.09534	0.57	1514	37	1528	28	1501	20	101.8
LAS396_Shot_475_Grain_331	1.6641	0.9	0.15619	0.7	0.60	0.07979	0.77	1156	43	933	19	985	19	94.7
LAS396_Shot_476_Grain_332	1.5168	0.5	0.15614	0.5	0.43	0.07271	0.50	989	37	934	16	934	15	100.0
LAS396_Shot_477_Grain_333	1.4640	0.6	0.15105	0.6	0.45	0.07230	0.59	975	40	906	17	912	15	99.3

LAS396_Shot_478_Grain_334	3.4614	0.5	0.25790	0.6	0.60	0.10049	0.48	1618	34	1479	26	1516	19	97.5
LAS396_Shot_479_Grain_335	7.4045	1.4	0.30632	1.3	0.90	0.17797	0.52	2622	31	1713	45	2117	31	80.9
LAS396_Shot_480_Grain_336	1.2489	0.7	0.12736	0.5	0.34	0.07344	0.68	997	42	773	14	819	15	94.3

LAS397 (20BREM13)														
	Isotopic Ratios							Calculated ages (Ma)						
ID	$^{207}Pb/^{235}U$	2σ	$^{206}Pb/^{238}U$	2σ	Rho	$^{207/206}Pb$	2σ	$^{207/206}Pb$	2σ	$^{206}Pb/^{238}U$	2σ	$^{207}Pb/^{235}U$	2σ	%conc
LAS397_Shot_487_Grain_337	0.7217	1.3	0.09032	0.6	0.10	0.06093	1.41	866	54	557	11	543	15	102.4
LAS397_Shot_488_Grain_338	1.8219	0.6	0.17717	0.5	0.38	0.07689	0.58	1094	40	1050	18	1050	17	100.0
LAS397_Shot_489_Grain_339	2.3531	0.7	0.18875	0.5	0.74	0.09228	0.44	1458	35	1113	19	1222	19	91.1
LAS397_Shot_490_Grain_340	13.6150	0.4	0.51725	0.4	0.53	0.19556	0.33	2782	28	2688	40	2722	22	98.8
LAS397_Shot_491_Grain_341	2.8510	0.5	0.23847	0.4	0.45	0.08891	0.44	1390	34	1377	23	1365	18	100.9
LAS397_Shot_492_Grain_342	7.5111	0.7	0.29060	0.6	0.78	0.19122	0.42	2743	29	1640	29	2162	25	75.9
LAS397_Shot_493_Grain_343	3.1221	0.5	0.24718	0.4	0.39	0.09407	0.44	1498	34	1423	23	1435	18	99.1
LAS397_Shot_494_Grain_344	9.9459	0.8	0.40389	0.7	0.86	0.18284	0.36	2671	29	2177	40	2411	26	90.3
LAS397_Shot_495_Grain_345	13.2909	0.4	0.51923	0.4	0.44	0.19109	0.46	2740	29	2692	41	2696	23	99.9
LAS397_Shot_496_Grain_346	2.0963	0.4	0.19550	0.4	0.47	0.07956	0.40	1173	35	1151	19	1145	16	100.5
LAS397_Shot_497_Grain_347	5.8379	0.9	0.32204	0.7	0.19	0.13717	1.09	2122	48	1794	34	1931	26	92.9
LAS397_Shot_498_Grain_348	1.4735	0.5	0.13922	0.4	0.49	0.07849	0.44	1144	36	840	14	918	15	91.5
LAS397_Shot_499_Grain_349	1.6990	0.5	0.16766	0.4	0.34	0.07498	0.51	1049	38	998	17	1005	16	99.3
LAS397_Shot_500_Grain_350	1.8585	0.6	0.17385	0.5	0.50	0.07909	0.55	1158	39	1033	18	1063	17	97.2
LAS397_Shot_507_Grain_351	5.4717	0.9	0.31323	0.8	0.80	0.12942	0.50	2076	33	1752	34	1878	25	93.3
LAS397_Shot_508_Grain_352	2.5151	0.7	0.21157	0.5	0.63	0.08820	0.54	1368	37	1236	21	1267	19	97.5
LAS397_Shot_509_Grain_353	4.3278	1.1	0.26753	0.9	0.85	0.11853	0.57	1916	34	1521	34	1669	29	91.1
LAS397_Shot_510_Grain_354	1.9007	0.8	0.18085	0.6	0.61	0.07857	0.64	1131	40	1070	20	1075	18	99.6
LAS397_Shot_511_Grain_355	9.5206	1.0	0.37953	0.8	0.87	0.18577	0.43	2694	30	2063	41	2364	29	87.3
LAS397_Shot_512_Grain_356	1.6713	1.4	0.15134	1.1	0.79	0.08201	0.78	1198	44	904	23	975	22	92.7
LAS397_Shot_513_Grain_357	9.0161	1.0	0.34853	1.0	0.89	0.19037	0.41	2736	29	1917	42	2307	29	83.1
LAS397_Shot_514_Grain_358	30.4721	0.4	0.67970	0.5	0.64	0.33259	0.36	3625	27	3341	50	3498	24	95.5
LAS397_Shot_515_Grain_359	0.8206	1.2	0.08940	0.8	0.16	0.07135	1.57	1010	52	552	12	600	15	91.9
LAS397_Shot_516_Grain_360	1.8083	0.5	0.17897	0.5	0.48	0.07525	0.52	1058	39	1061	19	1045	16	101.6
LAS397_Shot_517_Grain_361	0.9911	1.3	0.09481	0.7	0.30	0.07828	1.22	1162	53	583	12	687	17	84.9
LAS397_Shot_518_Grain_362	9.3857	0.7	0.38601	0.7	0.76	0.18249	0.44	2669	30	2096	38	2365	24	88.6
LAS397_Shot_519_Grain_363	4.4020	0.4	0.30461	0.5	0.63	0.10767	0.37	1753	32	1712	28	1709	20	100.1

LAS397_Shot_520_ Grain_364	2.1851	0.5	0.19609	0.5	0.58	0.08285	0.45	1253	36	1153	20	1174	17	98.2
LAS397_Shot_527_ Grain_365	13.1283	0.4	0.50506	0.4	0.65	0.19281	0.35	2758	28	2632	40	2685	23	98.0
LAS397_Shot_528_ Grain_366	1.6735	0.5	0.16517	0.4	0.45	0.07585	0.46	1073	37	985	16	997	15	98.8
LAS397_Shot_529_ Grain_367	11.4429	0.5	0.45762	0.4	0.71	0.18540	0.31	2696	28	2426	37	2556	23	94.9
LAS397_Shot_530_ Grain_368	1.6283	0.6	0.16386	0.5	0.51	0.07380	0.56	1011	40	978	17	978	16	100.0
LAS397_Shot_531_ Grain_369	12.8480	0.4	0.49980	0.5	0.49	0.19086	0.43	2738	30	2608	40	2663	23	97.9
LAS397_Shot_532_ Grain_370	12.3149	0.4	0.49988	0.4	0.61	0.18212	0.32	2665	28	2612	38	2626	22	99.4
LAS397_Shot_533_ Grain_371	4.8964	0.4	0.32143	0.4	0.60	0.11271	0.38	1833	31	1794	29	1799	20	99.7
LAS397_Shot_534_ Grain_372	2.7962	0.4	0.23406	0.4	0.50	0.08820	0.38	1377	33	1355	22	1352	18	100.2
LAS397_Shot_535_ Grain_373	2.0117	0.5	0.19680	0.4	0.48	0.07569	0.45	1079	37	1157	19	1117	17	103.6
LAS397_Shot_536_ Grain_374	5.0320	0.4	0.31520	0.4	0.50	0.11783	0.30	1918	30	1764	28	1822	20	96.8
LAS397_Shot_537_ Grain_375	2.7958	0.7	0.22812	0.6	0.80	0.09007	0.40	1415	34	1323	24	1346	20	98.3
LAS397_Shot_538_ Grain_376	5.0750	0.6	0.32731	0.5	0.56	0.11466	0.51	1858	34	1823	31	1826	22	99.9
LAS397_Shot_539_ Grain_377	13.6273	0.4	0.50689	0.4	0.56	0.19767	0.37	2800	29	2639	40	2720	23	97.0
LAS397_Shot_540_ Grain_378	12.2080	0.5	0.47747	0.5	0.64	0.18846	0.42	2717	30	2511	41	2612	24	96.1
LAS397_Shot_547_ Grain_379	11.5818	0.4	0.44973	0.4	0.50	0.19030	0.36	2736	29	2391	36	2568	22	93.1
LAS397_Shot_548_ Grain_380	1.4901	0.7	0.14872	0.5	0.30	0.07420	0.67	1011	41	893	16	922	16	96.9
LAS397_Shot_549_ Grain_381	5.1547	0.5	0.33642	0.4	0.49	0.11304	0.48	1839	33	1867	30	1842	21	101.4
LAS397_Shot_550_ Grain_382	1.0068	0.9	0.11233	0.6	0.32	0.06723	0.92	878	44	686	13	701	15	97.9
LAS397_Shot_551_ Grain_383	3.9805	0.5	0.27195	0.4	0.70	0.10841	0.33	1767	32	1549	26	1626	20	95.2
LAS397_Shot_552_ Grain_384	3.1947	0.3	0.25472	0.3	0.66	0.09230	0.26	1470	31	1462	23	1454	18	100.6
LAS397_Shot_553_ Grain_385	3.0237	0.5	0.24427	0.4	0.64	0.09087	0.41	1435	34	1409	23	1411	19	99.9
LAS397_Shot_554_ Grain_386	1.8261	0.9	0.17726	0.7	0.77	0.07637	0.56	1082	39	1050	21	1047	19	100.3
LAS397_Shot_555_ Grain_387	6.9812	1.5	0.28875	1.2	0.96	0.17536	0.42	2600	30	1618	42	2049	33	79.0
LAS397_Shot_556_ Grain_388	2.1354	0.8	0.18112	0.6	0.62	0.08768	0.60	1344	38	1071	20	1151	19	93.0
LAS397_Shot_557_ Grain_389	4.7141	0.4	0.30098	0.3	0.60	0.11581	0.32	1886	30	1695	26	1767	20	95.9
LAS397_Shot_558_ Grain_390	1.1718	0.8	0.12054	0.6	0.18	0.07326	0.91	1005	46	733	14	782	16	93.8
LAS397_Shot_559_ Grain_391	1.8968	0.7	0.17730	0.6	0.79	0.07924	0.42	1165	35	1051	20	1073	18	97.9
LAS397_Shot_560_ Grain_392	1.7129	0.4	0.17085	0.4	0.51	0.07454	0.36	1046	34	1016	17	1012	15	100.4
LAS397_Shot_567_ Grain_393	2.6141	0.6	0.22673	0.4	0.35	0.08687	0.61	1330	39	1316	22	1298	19	101.3
LAS397_Shot_568_ Grain_394	12.9810	0.4	0.50664	0.4	0.56	0.19157	0.32	2751	28	2640	39	2674	23	98.7
LAS397_Shot_569_ Grain_395	12.5436	0.4	0.50167	0.4	0.52	0.18725	0.37	2709	29	2619	39	2644	22	99.0
LAS397_Shot_570_ Grain_396	3.1698	0.5	0.26218	0.4	0.38	0.09045	0.49	1419	36	1500	25	1446	19	103.7
LAS397_Shot_571_ Grain_397	1.8289	0.9	0.17427	0.6	0.01	0.07916	0.92	1153	43	1034	19	1044	19	99.1
LAS397_Shot_572_ Grain_398	1.6185	0.6	0.16490	0.4	0.03	0.07362	0.68	997	41	983	17	972	16	101.2

LAS397_Shot_573_ Grain_399	9.8352	0.4	0.40529	0.5	0.70	0.18236	0.30	2670	29	2191	34	2416	22	90.7
LAS397_Shot_574_ Grain_400	1.9110	0.5	0.17966	0.4	0.57	0.07949	0.36	1173	34	1065	17	1081	16	98.5
LAS397_Shot_575_ Grain_401	3.7826	0.3	0.26142	0.3	0.54	0.10785	0.29	1757	31	1497	23	1587	19	94.3
LAS397_Shot_576_ Grain_402	2.0423	0.5	0.19304	0.4	0.35	0.07936	0.34	1172	34	1137	19	1126	17	100.9
LAS397_Shot_577_ Grain_403	1.8162	0.7	0.17386	0.5	0.40	0.07863	0.64	1132	39	1033	18	1046	17	98.7
LAS397_Shot_578_ Grain_404	11.1544	0.7	0.45166	0.6	0.85	0.18427	0.34	2684	28	2394	41	2524	26	94.8
LAS397_Shot_579_ Grain_405	1.9146	0.5	0.18271	0.4	0.47	0.07851	0.45	1145	36	1081	18	1083	16	99.8
LAS397_Shot_580_ Grain_406	1.8565	0.6	0.18636	0.4	0.17	0.07534	0.64	1050	42	1101	19	1062	17	103.7
LAS397_Shot_587_ Grain_407	1.9455	0.8	0.17745	0.5	0.19	0.08254	0.89	1216	47	1051	19	1087	19	96.7
LAS397_Shot_588_ Grain_408	3.6130	0.4	0.26390	0.4	0.51	0.10207	0.38	1653	33	1510	24	1549	19	97.4
LAS397_Shot_589_ Grain_409	9.8428	0.6	0.43025	0.6	0.74	0.17077	0.39	2557	30	2304	38	2414	24	95.5
LAS397_Shot_590_ Grain_410	10.6801	0.3	0.43821	0.4	0.57	0.18142	0.31	2659	28	2340	35	2494	21	93.8
LAS397_Shot_591_ Grain_411	11.6626	0.4	0.46627	0.4	0.65	0.18729	0.32	2713	28	2467	36	2576	23	95.8
LAS397_Shot_592_ Grain_412	3.1684	0.5	0.25076	0.5	0.31	0.09496	0.59	1501	38	1441	24	1445	19	99.7
LAS397_Shot_593_ Grain_413	12.5081	0.7	0.52855	0.7	0.66	0.17791	0.56	2613	33	2726	48	2636	25	103.4
LAS397_Shot_594_ Grain_414	3.5621	0.6	0.26294	0.5	0.49	0.10097	0.39	1629	33	1503	26	1537	21	97.8
LAS397_Shot_595_ Grain_415	4.1120	1.9	0.25303	1.6	0.96	0.11430	0.70	1840	39	1432	46	1554	42	92.1
LAS397_Shot_596_ Grain_416	3.4560	0.6	0.25864	0.5	0.67	0.09909	0.42	1594	33	1483	24	1512	20	98.1
LAS397_Shot_597_ Grain_417	2.8661	0.5	0.24176	0.4	0.46	0.08820	0.43	1376	34	1395	23	1372	18	101.7
LAS397_Shot_598_ Grain_418	1.8851	0.6	0.18295	0.4	0.32	0.07675	0.57	1093	39	1082	18	1073	17	100.9
LAS397_Shot_599_ Grain_419	5.2130	0.7	0.23848	0.6	0.81	0.16183	0.35	2469	30	1376	25	1844	23	74.6
LAS397_Shot_600_ Grain_420	4.1789	0.5	0.29479	0.4	0.67	0.10481	0.35	1705	31	1664	27	1665	20	100.0
LAS397_Shot_607_ Grain_421	1.7636	0.6	0.17255	0.5	0.50	0.07594	0.57	1070	40	1026	18	1028	17	99.8
LAS397_Shot_608_ Grain_422	2.7886	1.1	0.21510	0.9	0.90	0.09512	0.45	1517	34	1250	28	1328	26	94.2
LAS397_Shot_609_ Grain_423	10.8294	0.4	0.43228	0.4	0.49	0.18547	0.37	2695	28	2313	35	2506	22	92.3
LAS397_Shot_610_ Grain_424	1.8739	0.8	0.17487	0.7	0.66	0.07940	0.64	1155	40	1037	20	1064	18	97.4
LAS397_Shot_611_ Grain_425	15.3126	0.5	0.54673	0.5	0.54	0.20717	0.46	2871	30	2806	43	2831	23	99.1
LAS397_Shot_612_ Grain_426	12.7810	0.5	0.51234	0.5	0.55	0.18532	0.43	2693	30	2664	41	2659	23	100.2
LAS397_Shot_613_ Grain_427	2.8361	0.6	0.21907	0.5	0.81	0.09563	0.35	1533	33	1277	22	1361	19	93.8
LAS397_Shot_614_ Grain_428	2.0756	0.5	0.15251	0.4	0.55	0.09966	0.39	1611	32	914	16	1138	16	80.4
LAS397_Shot_615_ Grain_429	5.6416	0.9	0.34279	0.7	0.49	0.12339	0.80	1972	40	1895	36	1909	25	99.3
LAS397_Shot_616_ Grain_430	1.9381	1.0	0.17817	0.8	0.67	0.08110	0.75	1182	44	1053	23	1083	20	97.3
LAS397_Shot_617_ Grain_431	1.2848	0.7	0.13006	0.5	0.65	0.07302	0.52	993	39	787	15	836	15	94.2
LAS397_Shot_618_ Grain_432	1.9579	0.8	0.17396	0.6	0.71	0.08329	0.49	1260	37	1032	20	1095	18	94.3
LAS397_Shot_619_ Grain_433	5.1341	0.5	0.33125	0.4	0.56	0.11470	0.39	1865	32	1842	29	1839	20	100.2

LAS397_Shot_620_Grain_434	5.0173	0.6	0.32710	0.5	0.59	0.11335	0.45	1844	33	1822	31	1815	21	100.3
LAS397_Shot_627_Grain_435	9.8284	0.6	0.38599	0.5	0.82	0.18759	0.29	2716	28	2101	34	2411	25	87.2
LAS397_Shot_628_Grain_436	4.9134	1.1	0.22428	0.8	0.87	0.16000	0.49	2440	32	1301	26	1780	25	73.1
LAS397_Shot_629_Grain_437	1.6953	0.5	0.16697	0.4	0.62	0.07484	0.35	1055	35	995	16	1006	15	98.9
LAS397_Shot_630_Grain_438	1.2741	0.7	0.12891	0.5	0.44	0.07276	0.64	979	42	781	14	829	15	94.2
LAS397_Shot_631_Grain_439	1.4890	0.9	0.12242	0.6	0.69	0.08906	0.59	1386	38	743	14	918	17	81.0
LAS397_Shot_632_Grain_440	3.7469	1.2	0.25660	1.0	0.63	0.10914	0.98	1729	45	1464	35	1553	28	94.3
LAS397_Shot_633_Grain_441	8.6135	1.1	0.35121	1.0	0.93	0.17766	0.45	2621	30	1925	44	2248	36	85.7
LAS397_Shot_634_Grain_442	1.2341	0.7	0.12291	0.6	0.30	0.07333	0.77	997	45	747	14	811	15	92.1
LAS397_Shot_635_Grain_443	11.6174	0.7	0.40228	0.6	0.82	0.21229	0.38	2916	28	2172	38	2562	25	84.8
LAS397_Shot_636_Grain_444	3.6261	0.8	0.25287	0.7	0.83	0.10563	0.43	1715	33	1449	28	1542	22	94.0
LAS397_Shot_637_Grain_445	13.2537	0.9	0.48258	0.8	0.91	0.20095	0.34	2828	28	2524	48	2671	30	94.5
LAS397_Shot_638_Grain_446	3.5475	0.5	0.24616	0.5	0.62	0.10642	0.44	1727	34	1417	25	1534	20	92.4
LAS397_Shot_639_Grain_447	7.6889	2.3	0.31908	2.0	0.97	0.16756	0.65	2508	34	1735	65	2034	49	85.3
LAS397_Shot_640_Grain_448	4.0934	0.7	0.27344	0.6	0.73	0.11051	0.49	1790	34	1555	28	1640	22	94.8
LAS397_Shot_647_Grain_449	5.3138	0.4	0.33420	0.4	0.62	0.11739	0.32	1909	30	1857	29	1868	20	99.4
LAS397_Shot_648_Grain_450	1.7308	0.5	0.16995	0.4	0.58	0.07504	0.38	1059	36	1011	17	1017	16	99.4
LAS397_Shot_649_Grain_451	6.6500	0.5	0.28922	0.5	0.69	0.16714	0.38	2524	29	1636	27	2062	22	79.4
LAS397_Shot_650_Grain_452	1.0327	1.1	0.11074	0.9	0.76	0.06834	0.67	855	41	675	15	710	16	95.1
LAS397_Shot_651_Grain_453	8.9556	0.8	0.36813	0.7	0.91	0.17873	0.31	2636	28	2012	38	2311	28	87.1
LAS397_Shot_652_Grain_454	2.2975	0.8	0.19571	0.7	0.88	0.08610	0.35	1332	33	1150	22	1202	20	95.7
LAS397_Shot_653_Grain_455	11.4280	0.6	0.45783	0.5	0.78	0.18317	0.36	2676	29	2432	38	2553	24	95.2
LAS397_Shot_654_Grain_456	35.2470	0.8	0.70200	0.7	0.92	0.36614	0.28	3771	25	3416	58	3632	30	94.1
LAS397_Shot_655_Grain_457	11.8416	0.4	0.47414	0.4	0.62	0.18402	0.31	2685	28	2499	37	2590	22	96.5
LAS397_Shot_656_Grain_458	1.4325	0.7	0.14142	0.5	0.33	0.07575	0.73	1053	43	852	16	897	16	95.0
LAS397_Shot_657_Grain_459	2.0811	0.8	0.18839	0.6	0.36	0.08220	0.80	1209	44	1111	21	1134	19	98.0
LAS397_Shot_658_Grain_460	1.4277	0.4	0.14134	0.4	0.36	0.07468	0.43	1043	36	852	14	900	14	94.7
LAS397_Shot_659_Grain_461	3.9430	0.7	0.26772	0.7	0.87	0.10889	0.38	1770	32	1526	30	1612	23	94.7
LAS397_Shot_660_Grain_462	1.6240	1.0	0.16568	0.8	0.55	0.07307	0.82	991	44	986	21	970	19	101.7
LAS397_Shot_667_Grain_463	1.6214	0.5	0.16071	0.4	0.47	0.07483	0.47	1049	36	960	16	976	15	98.3
LAS397_Shot_668_Grain_464	2.9396	0.7	0.24508	0.5	0.35	0.08917	0.69	1378	41	1411	24	1385	20	101.9
LAS397_Shot_669_Grain_465	12.0162	0.4	0.47662	0.4	0.71	0.18580	0.30	2700	27	2510	37	2602	22	96.5
LAS397_Shot_670_Grain_466	2.5955	0.7	0.21644	0.5	0.76	0.08872	0.37	1388	34	1262	22	1294	20	97.5
LAS397_Shot_671_Grain_467	2.0292	1.1	0.15775	0.6	0.12	0.09609	1.08	1466	50	943	17	1106	21	85.2
LAS397_Shot_672_Grain_468	2.8685	0.5	0.20248	0.5	0.78	0.10448	0.32	1699	31	1188	21	1369	19	86.8

LAS397_Shot_673_Grain_469	3.0389	0.4	0.21310	0.4	0.56	0.10536	0.33	1713	31	1244	20	1415	18	87.9
LAS397_Shot_674_Grain_470	1.2863	0.5	0.13270	0.4	0.52	0.07205	0.41	974	36	803	14	839	14	95.8
LAS397_Shot_675_Grain_471	1.3363	0.7	0.13248	0.6	0.81	0.07480	0.39	1055	35	801	16	857	15	93.5
LAS397_Shot_676_Grain_472	2.8560	0.5	0.22965	0.5	0.54	0.09220	0.38	1461	33	1331	23	1365	19	97.5
LAS397_Shot_677_Grain_473	6.4850	1.3	0.28482	1.1	0.96	0.16490	0.43	2497	30	1602	39	1991	33	80.5
LAS397_Shot_678_Grain_474	1.3752	1.2	0.14052	1.0	0.75	0.07320	0.74	993	43	844	20	866	19	97.5
LAS397_Shot_679_Grain_475	6.3388	1.3	0.29722	1.1	0.91	0.15513	0.53	2395	33	1671	40	2003	31	83.4
LAS397_Shot_680_Grain_476	3.8748	0.4	0.26246	0.4	0.65	0.10901	0.32	1778	31	1501	25	1607	19	93.4
LAS397_Shot_687_Grain_477	1.5407	0.5	0.15579	0.4	0.37	0.07340	0.52	1007	38	933	16	943	15	98.9
LAS397_Shot_688_Grain_478	2.8360	0.4	0.20183	0.4	0.63	0.10399	0.31	1691	32	1184	20	1363	18	86.9
LAS397_Shot_689_Grain_479	4.7035	0.4	0.30642	0.4	0.52	0.11372	0.39	1852	32	1722	27	1766	20	97.5
LAS397_Shot_690_Grain_480	3.8774	0.4	0.27861	0.4	0.30	0.10356	0.35	1679	31	1584	25	1608	18	98.5
LAS397_Shot_691_Grain_481	10.8173	0.4	0.41949	0.4	0.56	0.19097	0.32	2744	28	2256	34	2504	22	90.1
LAS397_Shot_692_Grain_482	17.6182	0.4	0.58558	0.4	0.56	0.22263	0.33	2992	28	2969	43	2967	23	100.1
LAS397_Shot_693_Grain_483	3.2380	0.5	0.25360	0.4	0.44	0.09461	0.46	1505	35	1455	24	1463	19	99.5
LAS397_Shot_694_Grain_484	15.4368	0.4	0.56248	0.4	0.55	0.20355	0.35	2850	29	2873	42	2840	23	101.2
LAS397_Shot_695_Grain_485	19.9291	0.5	0.58843	0.5	0.67	0.25015	0.37	3181	28	2977	45	3082	23	96.6
LAS397_Shot_696_Grain_486	2.7661	0.5	0.19725	0.5	0.74	0.10360	0.37	1681	32	1160	21	1342	18	86.4
LAS397_Shot_697_Grain_487	1.7397	0.4	0.17185	0.4	0.34	0.07507	0.46	1054	36	1022	17	1022	16	100.0
LAS397_Shot_698_Grain_488	1.5990	1.2	0.15457	0.9	0.87	0.07545	0.56	1052	39	923	21	950	21	97.2
LAS397_Shot_699_Grain_489	2.0210	0.6	0.19020	0.5	0.72	0.07879	0.39	1157	35	1121	20	1118	17	100.2
LAS397_Shot_700_Grain_490	5.1877	0.7	0.22800	0.6	0.85	0.16796	0.32	2531	29	1321	24	1840	22	71.8
LAS397_Shot_707_Grain_491	1.9502	1.6	0.15714	1.3	0.93	0.09055	0.57	1414	36	934	26	1070	25	87.3
LAS397_Shot_708_Grain_492	10.4406	0.8	0.41269	0.7	0.83	0.18637	0.43	2702	29	2218	40	2464	26	90.0
LAS397_Shot_709_Grain_493	1.2179	0.6	0.10287	0.5	0.69	0.08744	0.43	1361	35	631	12	806	14	78.2
LAS397_Shot_710_Grain_494	1.7926	0.7	0.17220	0.5	0.27	0.07757	0.74	1097	43	1023	18	1037	17	98.7
LAS397_Shot_711_Grain_495	10.3832	0.7	0.41292	0.6	0.82	0.18277	0.34	2673	28	2223	39	2460	24	90.3
LAS397_Shot_712_Grain_496	5.0514	0.4	0.31842	0.4	0.26	0.11737	0.45	1904	32	1778	28	1824	21	97.5
LAS397_Shot_713_Grain_497	1.1794	1.5	0.12140	1.2	0.74	0.07041	0.77	921	42	735	20	768	20	95.7
LAS397_Shot_714_Grain_498	29.5878	0.5	0.66716	0.6	0.60	0.32859	0.46	3601	28	3289	52	3466	25	94.9
LAS397_Shot_715_Grain_499	12.6668	0.5	0.46688	0.6	0.65	0.19985	0.43	2815	30	2464	40	2648	23	93.1
LAS397_Shot_716_Grain_500	1.7742	0.5	0.17498	0.5	0.49	0.07488	0.48	1054	37	1039	18	1033	16	100.5
LAS397_Shot_717_Grain_501	1.3740	0.5	0.14043	0.4	0.40	0.07185	0.47	969	38	847	14	875	14	96.8
LAS397_Shot_718_Grain_502	4.1271	0.8	0.27142	0.6	0.56	0.11271	0.65	1816	38	1544	28	1647	23	93.7
LAS397_Shot_719_Grain_503	11.9798	0.4	0.46979	0.5	0.60	0.18819	0.37	2719	29	2480	39	2599	23	95.4

LAS397_Shot_720_Grain_504	0.9359	0.9	0.09812	0.6	0.23	0.07087	0.93	961	46	603	11	664	14	90.8
LAS397_Shot_727_Grain_505	2.6503	0.5	0.22496	0.4	0.67	0.08656	0.36	1342	34	1307	22	1310	18	99.8
LAS397_Shot_728_Grain_506	1.5069	0.6	0.15327	0.4	0.24	0.07265	0.62	976	40	919	15	929	15	98.9
LAS397_Shot_729_Grain_507	0.7072	0.9	0.08716	0.5	0.32	0.06001	0.82	681	41	538	10	539	12	99.8
LAS397_Shot_730_Grain_508	1.9276	0.6	0.18835	0.5	0.43	0.07595	0.58	1070	40	1112	19	1086	18	102.4
LAS397_Shot_731_Grain_509	7.1539	1.3	0.31345	1.1	0.96	0.16544	0.39	2504	30	1742	43	2077	33	83.8
LAS397_Shot_732_Grain_510	4.0836	0.4	0.28442	0.4	0.59	0.10598	0.35	1723	31	1613	26	1650	20	97.7
LAS397_Shot_733_Grain_511	5.5255	0.5	0.32943	0.5	0.48	0.12515	0.47	2016	33	1832	30	1900	22	96.5
LAS397_Shot_734_Grain_512	1.6326	0.8	0.16319	0.6	0.44	0.07477	0.72	1040	42	973	18	975	17	99.7
LAS397_Shot_735_Grain_513	3.0233	0.7	0.24401	0.6	0.32	0.09252	0.72	1449	40	1406	25	1407	20	99.9
LAS397_Shot_736_Grain_514	6.1586	1.0	0.26215	0.8	0.84	0.17350	0.50	2575	32	1495	30	1971	27	75.8
LAS397_Shot_737_Grain_515	13.7293	0.5	0.49312	0.4	0.62	0.20712	0.36	2875	28	2581	39	2725	24	94.7
LAS397_Shot_738_Grain_516	3.0567	0.5	0.24679	0.5	0.62	0.09224	0.45	1459	35	1420	24	1416	19	100.3
LAS397_Shot_739_Grain_517	1.5438	0.6	0.15443	0.5	0.64	0.07420	0.46	1030	37	925	16	945	16	97.9
LAS397_Shot_740_Grain_518	1.3473	0.7	0.13797	0.5	0.07	0.07282	0.67	975	41	832	15	861	15	96.7
LAS397_Shot_747_Grain_519	5.0318	0.4	0.32342	0.4	0.51	0.11554	0.34	1881	31	1806	28	1822	20	99.1
LAS397_Shot_748_Grain_520	1.9111	0.5	0.17666	0.4	0.41	0.08077	0.46	1198	36	1048	17	1082	16	96.9
LAS397_Shot_749_Grain_521	0.7477	0.7	0.08353	0.4	0.18	0.06686	0.74	834	42	517	9	565	11	91.6
LAS397_Shot_750_Grain_522	3.5391	1.2	0.15266	0.9	0.84	0.16962	0.66	2528	36	913	20	1505	26	60.7
LAS397_Shot_751_Grain_523	4.2061	0.3	0.27083	0.3	0.42	0.11555	0.32	1881	30	1544	24	1673	19	92.3
LAS397_Shot_752_Grain_524	1.7604	0.8	0.17702	0.7	0.62	0.07446	0.66	1031	42	1049	21	1024	18	102.5
LAS397_Shot_753_Grain_525	1.0590	0.6	0.11012	0.4	0.28	0.07149	0.47	949	38	673	12	730	13	92.2
LAS397_Shot_754_Grain_526	3.9202	0.5	0.27901	0.4	0.46	0.10434	0.48	1690	34	1585	26	1614	20	98.2
LAS397_Shot_755_Grain_527	4.0934	0.9	0.27356	0.8	0.88	0.11069	0.42	1804	32	1553	31	1634	26	95.0
LAS397_Shot_756_Grain_528	1.0191	0.5	0.11036	0.4	0.38	0.06923	0.54	879	40	674	12	712	13	94.7
LAS397_Shot_757_Grain_529	1.8416	0.6	0.18081	0.4	0.37	0.07607	0.58	1070	39	1070	18	1057	17	101.2
LAS397_Shot_758_Grain_530	1.9211	0.5	0.18331	0.4	0.63	0.07780	0.36	1135	34	1085	18	1086	16	99.9
LAS397_Shot_759_Grain_531	5.9741	0.5	0.25721	0.4	0.77	0.17202	0.33	2569	29	1475	24	1967	23	75.0
LAS397_Shot_760_Grain_532	2.9480	0.4	0.21965	0.3	0.48	0.09994	0.29	1617	31	1279	20	1392	18	91.9
LAS397_Shot_767_Grain_533	13.0292	0.4	0.52152	0.4	0.53	0.18507	0.39	2689	29	2701	40	2678	23	100.9
LAS397_Shot_768_Grain_534	2.6940	0.7	0.19283	0.5	0.74	0.10336	0.40	1676	33	1136	20	1319	19	86.1
LAS397_Shot_769_Grain_535	4.2640	1.5	0.20423	1.1	0.95	0.15102	0.48	2341	32	1192	30	1637	31	72.8
LAS397_Shot_770_Grain_536	1.7622	0.4	0.17413	0.4	0.47	0.07514	0.41	1058	36	1034	17	1030	16	100.4
LAS397_Shot_771_Grain_537	3.8339	0.5	0.25995	0.4	0.62	0.10867	0.36	1768	31	1489	24	1597	19	93.2
LAS397_Shot_772_Grain_538	11.1128	0.7	0.42490	0.4	0.74	0.19312	0.40	2758	29	2279	35	2518	25	90.5

LAS397_Shot_773_Grain_539	1.7103	0.4	0.17148	0.4	0.43	0.07408	0.39	1031	35	1020	16	1011	15	100.9
LAS397_Shot_774_Grain_540	1.7456	0.4	0.17035	0.4	0.58	0.07566	0.36	1076	35	1013	17	1023	16	99.0
LAS397_Shot_775_Grain_541	3.6559	0.5	0.24958	0.4	0.75	0.10770	0.30	1755	31	1437	23	1558	19	92.2
LAS397_Shot_776_Grain_542	2.9083	0.4	0.22658	0.4	0.64	0.09521	0.28	1526	31	1316	21	1382	18	95.2
LAS397_Shot_777_Grain_543	9.8332	0.4	0.39620	0.4	0.51	0.18347	0.39	2674	29	2150	33	2416	22	89.0
LAS397_Shot_778_Grain_544	4.0017	0.4	0.29043	0.4	0.41	0.10167	0.43	1641	33	1643	26	1631	19	100.7
LAS397_Shot_779_Grain_545	2.1953	0.5	0.16808	0.4	0.53	0.09685	0.48	1547	35	1001	17	1177	17	85.1
LAS397_Shot_780_Grain_546	2.5215	0.6	0.19570	0.5	0.43	0.09609	0.57	1525	36	1151	20	1275	18	90.3
LAS397_Shot_787_Grain_547	2.9353	0.7	0.23356	0.5	0.63	0.09283	0.47	1474	34	1351	23	1384	20	97.6
LAS397_Shot_788_Grain_548	1.6481	0.5	0.15050	0.4	0.52	0.08098	0.42	1207	35	903	15	986	15	91.6
LAS397_Shot_789_Grain_549	1.6463	1.7	0.14107	1.2	0.70	0.08550	1.03	1285	50	846	23	964	25	87.7
LAS397_Shot_790_Grain_550	6.1322	0.7	0.27966	0.5	0.84	0.16080	0.31	2458	28	1587	28	1987	24	79.9
LAS397_Shot_791_Grain_551	1.2586	1.7	0.12538	1.4	0.36	0.07245	0.68	971	41	756	23	795	23	95.1
LAS397_Shot_792_Grain_552	11.0512	0.5	0.45240	0.4	0.76	0.18012	0.27	2650	28	2403	36	2524	23	95.2
LAS397_Shot_793_Grain_553	1.3894	0.4	0.14042	0.3	0.42	0.07290	0.36	1001	35	847	14	883	14	95.8
LAS397_Shot_794_Grain_554	4.4282	0.5	0.28398	0.4	0.17	0.11466	0.40	1862	32	1610	26	1714	20	93.9
LAS397_Shot_795_Grain_555	7.6910	0.6	0.33095	0.6	0.58	0.17255	0.49	2569	31	1842	32	2189	23	84.1
LAS397_Shot_796_Grain_556	1.5911	0.6	0.15975	0.5	0.70	0.07294	0.42	1000	37	956	17	964	16	99.1
LAS397_Shot_797_Grain_557	1.4137	0.6	0.14148	0.4	0.40	0.07399	0.56	1025	38	853	14	890	15	95.8
LAS397_Shot_798_Grain_558	2.2196	0.5	0.16494	0.4	0.48	0.09945	0.42	1601	34	984	16	1184	17	83.1
LAS397_Shot_799_Grain_559	4.9758	0.5	0.31777	0.5	0.52	0.11547	0.47	1877	34	1777	29	1812	21	98.0
LAS397_Shot_800_Grain_560	1.8903	0.5	0.18258	0.5	0.60	0.07601	0.45	1081	37	1080	19	1076	16	100.4
LAS397_Shot_807_Grain_561	5.1293	0.5	0.32930	0.4	0.48	0.11490	0.45	1867	33	1833	29	1836	21	99.8
LAS397_Shot_808_Grain_562	1.8352	0.4	0.17677	0.4	0.55	0.07638	0.35	1096	34	1049	17	1056	16	99.3
LAS397_Shot_809_Grain_563	3.0957	0.6	0.24562	0.5	0.58	0.09319	0.47	1477	35	1415	24	1425	20	99.3
LAS397_Shot_810_Grain_564	1.4717	0.7	0.11671	0.5	0.58	0.09359	0.58	1475	37	711	13	916	16	77.6
LAS397_Shot_811_Grain_565	1.8220	0.4	0.17669	0.4	0.54	0.07612	0.41	1084	36	1048	18	1052	16	99.7
LAS397_Shot_812_Grain_566	8.4135	0.6	0.35187	0.5	0.44	0.17651	0.30	2614	28	1942	32	2267	24	85.6
LAS397_Shot_813_Grain_567	4.5508	0.4	0.31190	0.5	0.60	0.10809	0.39	1756	33	1748	29	1738	20	100.6
LAS397_Shot_814_Grain_568	9.8699	1.0	0.36769	0.9	0.87	0.19737	0.46	2794	30	2007	41	2393	28	83.9
LAS397_Shot_815_Grain_569	4.7570	0.5	0.31118	0.4	0.43	0.11307	0.48	1835	34	1744	28	1772	21	98.4
LAS397_Shot_816_Grain_570	2.1991	0.8	0.19463	0.6	0.90	0.08296	0.34	1261	33	1144	22	1170	20	97.7
LAS397_Shot_817_Grain_571	2.7694	0.4	0.19088	0.4	0.53	0.10729	0.35	1746	32	1125	18	1345	18	83.7
LAS397_Shot_818_Grain_572	2.4182	0.8	0.20790	0.6	0.86	0.08577	0.38	1324	34	1217	22	1243	20	97.9
LAS397_Shot_819_Grain_573	3.7751	0.5	0.25730	0.4	0.75	0.10816	0.33	1760	31	1475	24	1584	20	93.1

LAS397_Shot_820_Grain_574	3.1510	0.4	0.25037	0.4	0.58	0.09303	0.32	1483	32	1440	23	1444	19	99.7
LAS397_Shot_827_Grain_575	13.9576	0.9	0.49170	0.8	0.85	0.20882	0.44	2887	30	2566	47	2720	30	94.3
LAS397_Shot_828_Grain_576	1.5739	0.5	0.14358	0.4	0.44	0.08090	0.42	1206	35	864	14	958	15	90.3
LAS397_Shot_829_Grain_577	2.1002	0.6	0.19643	0.4	0.49	0.07902	0.53	1149	39	1155	20	1145	17	100.9
LAS397_Shot_830_Grain_578	3.8305	0.4	0.25573	0.3	0.63	0.11041	0.29	1801	30	1467	23	1598	19	91.8
LAS397_Shot_831_Grain_579	7.0117	0.4	0.29480	0.5	0.56	0.17843	0.39	2633	29	1664	28	2111	21	78.8
LAS397_Shot_832_Grain_580	12.5438	0.5	0.49280	0.4	0.73	0.18746	0.33	2715	29	2578	39	2641	23	97.6
LAS397_Shot_833_Grain_581	0.7859	0.6	0.08340	0.5	0.43	0.06941	0.59	895	40	516	9	586	11	88.0
LAS397_Shot_834_Grain_582	1.8625	0.5	0.15379	0.4	0.40	0.08981	0.50	1405	37	922	16	1065	16	86.5
LAS397_Shot_835_Grain_583	1.8979	0.6	0.14799	0.5	0.75	0.09463	0.35	1513	33	889	16	1075	17	82.7
LAS397_Shot_836_Grain_584	8.3945	1.2	0.34821	1.0	0.95	0.17460	0.39	2593	29	1910	44	2224	35	85.9
LAS397_Shot_837_Grain_585	1.0846	0.6	0.11467	0.4	0.67	0.06969	0.40	907	37	699	12	744	13	94.1
LAS397_Shot_838_Grain_586	2.9584	0.6	0.21084	0.4	0.72	0.10311	0.40	1671	33	1232	21	1393	19	88.4
LAS397_Shot_839_Grain_587	4.6687	1.1	0.21240	0.8	0.93	0.15994	0.44	2443	30	1237	26	1730	27	71.5
LAS397_Shot_840_Grain_588	1.1590	0.4	0.12097	0.4	0.50	0.07076	0.39	941	36	736	12	780	13	94.3
LAS397_Shot_847_Grain_589	1.2978	0.5	0.12690	0.3	0.48	0.07548	0.37	1074	35	770	13	843	14	91.3
LAS397_Shot_848_Grain_590	1.4825	0.5	0.12698	0.4	0.71	0.08580	0.37	1324	34	770	13	922	15	83.6
LAS397_Shot_849_Grain_591	4.2205	0.9	0.20501	0.7	0.84	0.15091	0.46	2343	31	1199	24	1661	23	72.2
LAS397_Shot_850_Grain_592	7.5607	1.7	0.28589	1.3	0.97	0.18622	0.59	2685	33	1603	43	2091	39	76.7
LAS397_Shot_851_Grain_593	1.4603	0.5	0.14713	0.4	0.74	0.07288	0.35	1004	34	885	15	912	15	97.0
LAS397_Shot_852_Grain_594	1.2508	0.7	0.12565	0.5	0.22	0.07346	0.73	1003	43	762	13	819	15	93.0
LAS397_Shot_853_Grain_595	2.5487	0.5	0.17783	0.4	0.72	0.10479	0.32	1704	32	1054	18	1283	18	82.1
LAS397_Shot_854_Grain_596	11.8632	0.8	0.47229	0.7	0.88	0.18453	0.36	2685	29	2482	45	2574	28	96.4
LAS397_Shot_855_Grain_597	1.9480	0.6	0.15652	0.5	0.61	0.09148	0.45	1440	35	937	16	1093	17	85.7
LAS397_Shot_856_Grain_598	1.1766	0.5	0.12196	0.4	0.47	0.07077	0.49	938	38	741	13	788	13	94.1
LAS397_Shot_857_Grain_599	3.8398	0.4	0.25747	0.4	0.61	0.10989	0.31	1790	31	1476	23	1599	19	92.3
LAS397_Shot_858_Grain_600	2.1724	0.5	0.14567	0.4	0.66	0.10911	0.33	1779	32	876	15	1169	17	75.0
LAS397_Shot_859_Grain_601	13.3559	0.4	0.51484	0.4	0.51	0.19025	0.37	2737	29	2673	39	2701	23	99.0
LAS397_Shot_860_Grain_602	2.2673	0.5	0.19331	0.5	0.72	0.08609	0.36	1333	34	1138	20	1199	17	94.9
LAS397_Shot_867_Grain_603	2.0717	0.4	0.18475	0.3	0.63	0.08244	0.31	1249	33	1092	18	1138	16	96.0
LAS397_Shot_868_Grain_604	1.9738	0.3	0.18356	0.3	0.48	0.07904	0.33	1166	33	1086	17	1105	16	98.2
LAS397_Shot_869_Grain_605	3.1482	0.6	0.25143	0.5	0.40	0.09227	0.57	1451	37	1444	24	1438	19	100.4
LAS397_Shot_870_Grain_606	2.1205	0.6	0.19780	0.5	0.44	0.07952	0.57	1161	39	1163	20	1150	18	101.1
LAS397_Shot_871_Grain_607	2.8401	2.4	0.18649	1.8	0.98	0.10305	0.77	1632	42	1084	40	1254	40	86.5
LAS397_Shot_872_Grain_608	1.4419	1.3	0.10784	0.8	0.72	0.09674	0.91	1499	47	659	14	884	21	74.6

LAS397_Shot_873_Grain_609	1.1470	0.7	0.11694	0.5	0.43	0.07280	0.66	984	42	713	13	774	14	92.2
LAS397_Shot_874_Grain_610	2.1299	0.4	0.17741	0.4	0.60	0.08825	0.32	1380	33	1053	18	1157	16	91.1
LAS397_Shot_875_Grain_611	3.9688	0.4	0.27404	0.3	0.48	0.10721	0.34	1744	31	1561	25	1626	19	96.0
LAS397_Shot_876_Grain_612	2.8929	0.4	0.19719	0.4	0.43	0.10854	0.42	1766	32	1159	19	1377	18	84.2
LAS397_Shot_877_Grain_613	6.7097	0.8	0.28086	0.7	0.86	0.17637	0.36	2612	29	1592	30	2058	25	77.3
LAS397_Shot_878_Grain_614	4.0826	0.6	0.28299	0.5	0.76	0.10678	0.37	1738	32	1603	28	1649	20	97.2
LAS397_Shot_879_Grain_615	1.5420	0.4	0.15364	0.4	0.62	0.07393	0.31	1033	34	921	15	946	15	97.3
LAS397_Shot_880_Grain_616	1.0488	0.5	0.10887	0.4	0.28	0.07121	0.54	939	40	666	11	726	13	91.7
LAS397_Shot_887_Grain_617	1.5667	1.0	0.16019	0.6	0.20	0.07322	1.11	1022	49	957	18	948	19	100.9
LAS397_Shot_888_Grain_618	3.2874	1.1	0.22217	0.9	0.93	0.10725	0.40	1742	32	1288	28	1453	24	88.6
LAS397_Shot_889_Grain_619	9.0981	0.6	0.36427	0.5	0.79	0.18408	0.37	2682	29	2001	34	2342	23	85.4
LAS397_Shot_890_Grain_620	2.2673	0.6	0.19468	0.5	0.81	0.08552	0.30	1321	33	1145	20	1198	18	95.6
LAS397_Shot_891_Grain_621	1.1664	1.0	0.11840	0.8	0.83	0.07186	0.53	964	38	720	15	776	16	92.8
LAS397_Shot_892_Grain_622	1.2555	0.5	0.12030	0.4	0.35	0.07700	0.53	1103	38	732	13	824	14	88.8
LAS397_Shot_893_Grain_623	3.9590	0.4	0.25819	0.4	0.59	0.11247	0.34	1832	31	1480	24	1623	19	91.2
LAS397_Shot_894_Grain_624	9.8445	1.1	0.38990	0.9	0.92	0.18259	0.41	2666	29	2107	45	2380	34	88.5
LAS397_Shot_895_Grain_625	3.3211	0.4	0.24419	0.3	0.36	0.10024	0.41	1617	33	1407	22	1483	19	94.9
LAS397_Shot_896_Grain_626	2.0500	1.3	0.15170	0.9	0.89	0.09706	0.59	1547	37	907	21	1105	25	82.1
LAS397_Shot_897_Grain_627	7.1319	1.0	0.34098	0.9	0.94	0.15214	0.33	2363	29	1879	41	2093	31	89.7
LAS397_Shot_898_Grain_628	2.4541	0.6	0.19917	0.6	0.69	0.08940	0.45	1406	35	1170	21	1256	18	93.1
LAS397_Shot_899_Grain_629	5.2136	0.9	0.22028	0.7	0.86	0.17213	0.43	2571	29	1280	25	1835	25	69.8
LAS397_Shot_900_Grain_630	3.9060	1.5	0.14428	0.9	0.83	0.19063	1.07	2698	49	866	20	1550	38	55.9
LAS397_Shot_907_Grain_631	2.9353	0.6	0.19612	0.5	0.35	0.10882	0.62	1763	37	1154	20	1388	19	83.2
LAS397_Shot_908_Grain_632	1.2774	0.6	0.12283	0.5	0.66	0.07653	0.44	1093	37	746	13	832	14	89.6
LAS397_Shot_909_Grain_633	2.0726	0.7	0.17495	0.4	0.37	0.08724	0.62	1347	39	1038	18	1135	18	91.5
LAS397_Shot_910_Grain_634	2.1864	1.3	0.17207	0.8	0.12	0.09603	1.41	1477	59	1022	21	1152	24	88.6
LAS397_Shot_911_Grain_635	0.9389	0.9	0.09970	0.6	0.65	0.06903	0.67	878	43	612	12	666	15	91.9
LAS397_Shot_912_Grain_636	0.5092	0.3	0.06519	0.2	0.49	0.05746	0.23	504	36	407	7	418	8	97.5
LAS397_Shot_913_Grain_637	7.8037	0.5	0.34780	0.4	0.79	0.16520	0.27	2506	28	1923	31	2202	23	87.3
LAS397_Shot_914_Grain_638	2.1045	0.4	0.15834	0.4	0.56	0.09819	0.31	1583	32	947	16	1148	16	82.5
LAS397_Shot_915_Grain_639	4.8467	0.5	0.21735	0.4	0.66	0.16295	0.40	2477	30	1267	21	1789	21	70.8
LAS397_Shot_916_Grain_640	10.8435	0.6	0.41682	0.5	0.80	0.19081	0.32	2743	28	2243	36	2504	24	89.5
LAS397_Shot_917_Grain_641	2.0472	0.4	0.17175	0.4	0.63	0.08799	0.35	1372	33	1022	17	1129	16	90.5
LAS397_Shot_918_Grain_642	1.2050	0.4	0.12323	0.3	0.46	0.07217	0.39	978	36	749	12	802	13	93.4
LAS397_Shot_919_Grain_643	1.7440	0.5	0.17101	0.4	0.44	0.07540	0.44	1062	37	1017	17	1022	16	99.5

LAS397_Shot_920_Grain_644	1.2661	0.8	0.11903	0.5	0.26	0.07932	0.84	1143	45	725	13	823	16	88.1
LAS397_Shot_927_Grain_645	3.3547	0.8	0.17143	0.6	0.79	0.14494	0.47	2275	32	1019	20	1481	22	68.8
LAS397_Shot_928_Grain_646	1.9834	0.6	0.18865	0.4	0.36	0.07858	0.56	1139	38	1114	19	1108	17	100.5
LAS397_Shot_929_Grain_647	3.9722	0.7	0.18151	0.5	0.79	0.16155	0.39	2464	30	1074	19	1617	22	66.4
LAS397_Shot_930_Grain_648	6.8084	0.8	0.29924	0.6	0.87	0.16864	0.36	2538	29	1684	30	2069	26	81.4
LAS397_Shot_931_Grain_649	2.1290	0.5	0.18653	0.4	0.57	0.08530	0.39	1310	34	1102	18	1157	17	95.3
LAS397_Shot_932_Grain_650	4.9386	0.7	0.22630	0.6	0.58	0.16053	0.54	2450	33	1314	24	1804	22	72.8
LAS397_Shot_933_Grain_651	1.6436	0.5	0.15678	0.4	0.32	0.07812	0.54	1133	39	939	16	985	15	95.3
LAS397_Shot_934_Grain_652	1.3170	0.5	0.13156	0.4	0.42	0.07481	0.51	1043	38	796	14	851	14	93.6
LAS397_Shot_935_Grain_653	1.2365	1.3	0.12201	1.0	0.89	0.07391	0.59	1012	41	739	18	799	20	92.6
LAS397_Shot_936_Grain_654	3.4598	0.8	0.24239	0.8	0.61	0.10811	0.67	1753	38	1397	29	1514	22	92.3
LAS397_Shot_937_Grain_655	7.5017	1.2	0.33233	1.0	0.92	0.16654	0.46	2512	31	1835	42	2129	31	86.2
LAS397_Shot_938_Grain_656	4.4405	0.4	0.20427	0.4	0.53	0.16235	0.40	2471	30	1198	20	1718	20	69.7
LAS397_Shot_939_Grain_657	1.6098	0.8	0.13081	0.7	0.76	0.09143	0.51	1438	36	792	16	966	17	82.0
LAS397_Shot_940_Grain_658	1.7819	1.1	0.16260	0.7	0.26	0.08257	1.18	1227	53	970	19	1023	21	94.8
LAS397_Shot_947_Grain_659	11.7794	0.8	0.39096	0.8	0.90	0.22418	0.31	3006	27	2116	41	2566	26	82.4
LAS397_Shot_948_Grain_660	1.4480	0.5	0.14322	0.4	0.27	0.07531	0.55	1056	38	863	15	907	15	95.2
LAS397_Shot_949_Grain_661	6.5308	0.7	0.30048	0.6	0.76	0.15911	0.43	2437	31	1691	30	2043	23	82.8
LAS397_Shot_950_Grain_662	1.4731	0.6	0.15279	0.5	0.52	0.07187	0.56	961	39	916	16	916	16	100.0
LAS397_Shot_951_Grain_663	3.0239	0.6	0.21047	0.5	0.66	0.10646	0.42	1728	33	1230	21	1406	20	87.5
LAS397_Shot_952_Grain_664	9.5573	0.5	0.35930	0.4	0.69	0.19657	0.30	2792	28	1977	31	2389	22	82.8
LAS397_Shot_953_Grain_665	2.7348	1.5	0.19664	1.3	0.92	0.10138	0.55	1630	36	1147	32	1293	29	88.8
LAS397_Shot_954_Grain_666	13.0002	0.5	0.51572	0.5	0.59	0.18713	0.43	2709	30	2678	42	2674	23	100.2
LAS397_Shot_955_Grain_667	2.6977	0.5	0.21794	0.4	0.45	0.09181	0.53	1441	36	1270	21	1324	18	96.0
LAS397_Shot_956_Grain_668	2.0486	0.5	0.13204	0.4	0.10	0.11608	0.67	1873	37	799	14	1130	17	70.7
LAS397_Shot_957_Grain_669	29.6511	0.3	0.64403	0.3	0.49	0.33957	0.31	3656	26	3201	44	3472	23	92.2
LAS397_Shot_958_Grain_670	3.1131	0.4	0.21678	0.4	0.33	0.10580	0.42	1722	30	1264	20	1433	18	88.2
LAS397_Shot_959_Grain_671	13.6927	0.5	0.50610	0.5	0.70	0.19894	0.34	2811	28	2634	41	2725	23	96.7
LAS397_Shot_960_Grain_672	2.8609	1.0	0.13394	0.7	0.88	0.15497	0.51	2382	32	809	16	1348	24	60.0
LAS397_Shot_967_Grain_673	10.2311	0.5	0.41276	0.5	0.78	0.18180	0.32	2665	28	2224	35	2452	23	90.7
LAS397_Shot_968_Grain_674	1.3498	0.9	0.13126	0.7	0.67	0.07615	0.64	1070	41	794	16	860	17	92.3
LAS397_Shot_969_Grain_675	10.1005	0.4	0.39118	0.4	0.60	0.19013	0.32	2738	28	2127	33	2441	22	87.1
LAS397_Shot_970_Grain_676	8.7739	0.5	0.35653	0.4	0.74	0.18155	0.30	2661	28	1966	31	2310	23	85.1
LAS397_Shot_971_Grain_677	1.8769	0.5	0.15868	0.4	0.65	0.08752	0.37	1360	33	949	16	1069	16	88.7
LAS397_Shot_972_Grain_678	1.2178	0.9	0.12395	0.6	0.32	0.07336	0.92	1009	47	752	14	803	16	93.6

LAS398 (20BREM15E)														
	Isotopic Ratios							Calculated ages (Ma)						
ID	$^{207}Pb/^{235}U$	2σ	$^{206}Pb/^{238}U$	2σ	Rho	$^{207/206}Pb$	2σ	$^{207/206}Pb$	2σ	$^{206}Pb/^{238}U$	2σ	$^{207}Pb/^{235}U$	2σ	%conc
LAS398_Shot_973_Grain_679	10.6060	0.4	0.42148	0.4	0.66	0.18627	0.31	2706	28	2264	34	2484	22	91.1
LAS398_Shot_974_Grain_680	4.0985	0.5	0.26680	0.4	0.70	0.11349	0.32	1850	31	1523	25	1650	19	92.3
LAS398_Shot_975_Grain_681	5.1603	0.9	0.23317	0.7	0.88	0.16216	0.40	2468	30	1348	26	1829	23	73.7
LAS398_Shot_976_Grain_682	3.0694	1.1	0.15744	0.8	0.91	0.14176	0.56	2227	34	940	20	1398	26	67.2
LAS398_Shot_977_Grain_683	9.9255	0.5	0.38300	0.5	0.87	0.19273	0.26	2761	27	2087	34	2423	22	86.1
LAS398_Shot_978_Grain_684	13.6302	0.4	0.50742	0.3	0.63	0.19891	0.29	2811	27	2642	38	2721	22	97.1
LAS398_Shot_979_Grain_685	4.5142	0.7	0.29151	0.6	0.44	0.11433	0.34	1864	30	1645	29	1723	22	95.5
LAS398_Shot_980_Grain_686	13.0583	0.4	0.49621	0.4	0.53	0.19579	0.31	2785	28	2595	38	2682	22	96.8
LAS398_Shot_987_Grain_687	13.2328	0.4	0.49392	0.4	0.59	0.19986	0.30	2821	28	2585	38	2693	22	96.0
LAS398_Shot_988_Grain_688	1.7568	0.5	0.17595	0.4	0.52	0.07476	0.39	1052	36	1044	17	1029	16	101.5
LAS398_Shot_989_Grain_689	14.2841	0.4	0.53482	0.3	0.55	0.19894	0.32	2813	28	2759	40	2766	22	99.8
LAS398_Shot_990_Grain_690	19.8112	0.3	0.58692	0.4	0.68	0.25132	0.28	3188	26	2975	43	3079	23	96.6
LAS398_Shot_991_Grain_691	9.3600	0.7	0.37120	0.6	0.86	0.18677	0.39	2705	29	2030	35	2361	24	86.0
LAS398_Shot_992_Grain_692	18.7289	0.3	0.52915	0.3	0.68	0.26362	0.23	3265	26	2735	39	3025	23	90.4
LAS398_Shot_993_Grain_693	14.0800	0.5	0.54291	0.4	0.51	0.19442	0.44	2770	29	2794	43	2750	23	101.6
LAS398_Shot_994_Grain_694	11.6022	0.4	0.45213	0.4	0.64	0.19185	0.28	2754	28	2403	36	2569	22	93.6
LAS398_Shot_995_Grain_695	5.0883	0.5	0.33143	0.4	0.34	0.11504	0.46	1866	32	1843	29	1827	21	100.9
LAS398_Shot_996_Grain_696	12.8557	0.3	0.50504	0.3	0.63	0.18967	0.28	2734	28	2633	38	2666	22	98.8
LAS398_Shot_997_Grain_697	12.1861	0.3	0.49007	0.3	0.63	0.18529	0.28	2696	28	2568	37	2617	22	98.1
LAS398_Shot_998_Grain_698	7.2045	1.1	0.29621	1.0	0.94	0.18026	0.34	2652	29	1662	38	2103	28	79.0
LAS398_Shot_999_Grain_699	4.8527	0.4	0.32348	0.4	0.47	0.11233	0.38	1828	32	1805	28	1792	20	100.8
LAS398_Shot_1000_Grain_700	5.0021	0.9	0.26732	0.9	0.88	0.14000	0.41	2219	30	1521	32	1802	24	84.4
LAS398_Shot_1007_Grain_701	4.0363	0.4	0.29225	0.4	0.44	0.10340	0.42	1675	33	1651	26	1637	20	100.9
LAS398_Shot_1008_Grain_702	8.0491	1.8	0.31257	1.4	0.96	0.18617	0.50	2698	31	1730	47	2160	34	80.1
LAS398_Shot_1009_Grain_703	16.0019	0.6	0.51064	0.5	0.76	0.23445	0.38	3074	28	2654	41	2870	24	92.5
LAS398_Shot_1010_Grain_704	12.1205	0.4	0.48138	0.4	0.45	0.18888	0.42	2722	29	2531	38	2609	23	97.0
LAS398_Shot_1011_Grain_705	5.4801	0.8	0.34706	0.6	0.30	0.11968	0.86	1904	43	1917	34	1884	24	101.7
LAS398_Shot_1012_Grain_706	4.9006	0.3	0.31767	0.3	0.50	0.11488	0.32	1869	31	1777	27	1800	20	98.7
LAS398_Shot_1013_Grain_707	11.2776	0.5	0.46603	0.4	0.66	0.18070	0.39	2651	30	2463	38	2542	23	96.9
LAS398_Shot_1014_Grain_708	4.5033	0.4	0.30640	0.3	0.55	0.10989	0.32	1793	31	1721	27	1729	20	99.6

LAS398_Shot_1031_Grain_719	6.1534	0.5	0.27344	0.5	0.76	0.16768	0.31	2528	28	1556	26	1992	22	78.1
LAS398_Shot_1032_Grain_720	3.9039	0.4	0.28582	0.3	0.50	0.10183	0.35	1649	32	1619	25	1613	19	100.4
LAS398_Shot_1033_Grain_721	17.2809	0.5	0.54629	0.4	0.65	0.23592	0.31	3088	27	2808	41	2945	23	95.3
LAS398_Shot_1034_Grain_722	12.7225	0.4	0.47807	0.4	0.55	0.19812	0.36	2803	28	2515	38	2657	22	94.7
LAS398_Shot_1035_Grain_723	13.1790	0.4	0.50737	0.4	0.77	0.19258	0.26	2760	27	2643	39	2690	23	98.3
LAS398_Shot_1036_Grain_724	4.7022	0.6	0.29176	0.4	0.80	0.11906	0.30	1936	31	1649	27	1761	21	93.6
LAS398_Shot_1037_Grain_725	13.6175	0.5	0.52343	0.5	0.42	0.19385	0.50	2760	31	2710	41	2718	23	99.7
LAS398_Shot_1038_Grain_726	15.2418	0.5	0.55009	0.5	0.53	0.20654	0.45	2866	30	2820	43	2825	23	99.8
LAS398_Shot_1039_Grain_727	4.0353	0.4	0.29235	0.4	0.44	0.10205	0.41	1648	33	1653	26	1638	19	100.9
LAS398_Shot_1040_Grain_728	9.0434	0.6	0.38382	0.5	0.85	0.17448	0.28	2596	28	2090	34	2333	24	89.6
LAS398_Shot_1047_Grain_729	11.7086	0.6	0.44518	0.5	0.86	0.19353	0.29	2771	27	2369	38	2579	24	91.9
LAS398_Shot_1048_Grain_730	18.1278	0.5	0.59042	0.5	0.47	0.22775	0.47	3024	29	2988	45	2991	24	99.9
LAS398_Shot_1049_Grain_731	10.9734	0.4	0.39677	0.4	0.83	0.20361	0.27	2850	27	2151	34	2517	22	85.5
LAS398_Shot_1050_Grain_732	2.6244	0.5	0.18784	0.4	0.51	0.10373	0.47	1676	34	1109	19	1303	18	85.1
LAS398_Shot_1051_Grain_733	9.8586	0.7	0.40734	0.6	0.87	0.17794	0.31	2629	28	2196	37	2410	25	91.1
LAS398_Shot_1052_Grain_734	5.4760	0.5	0.34244	0.4	0.40	0.11861	0.46	1922	33	1897	30	1892	21	100.2
LAS398_Shot_1053_Grain_735	11.2627	1.1	0.45528	0.9	0.93	0.18060	0.38	2651	29	2400	50	2504	34	95.9
LAS398_Shot_1054_Grain_736	6.0959	0.3	0.25754	0.3	0.57	0.17510	0.29	2601	28	1477	23	1987	20	74.3
LAS398_Shot_1055_Grain_737	5.0010	0.5	0.33632	0.5	0.69	0.10953	0.37	1785	31	1869	31	1815	21	103.0
LAS398_Shot_1056_Grain_738	9.9207	0.4	0.41014	0.5	0.65	0.17917	0.34	2639	28	2212	35	2428	22	91.1
LAS398_Shot_1057_Grain_739	12.1149	0.4	0.45380	0.4	0.75	0.19630	0.28	2791	28	2411	36	2609	23	92.4
LAS398_Shot_1058_Grain_740	11.9366	0.4	0.48986	0.4	0.60	0.17961	0.33	2642	29	2567	37	2597	22	98.8
LAS398_Shot_1059_Grain_741	5.7195	0.8	0.25423	0.6	0.75	0.16554	0.48	2502	32	1457	27	1918	24	75.9
LAS398_Shot_1060_Grain_742	4.1936	1.0	0.23442	0.7	0.92	0.13009	0.41	2088	31	1353	27	1648	26	82.1
LAS398_Shot_1067_Grain_743	6.3664	0.4	0.27599	0.4	0.66	0.16998	0.28	2554	28	1570	25	2025	21	77.5
LAS398_Shot_1068_Grain_744	5.3147	0.5	0.33800	0.4	0.13	0.11662	0.45	1891	32	1875	29	1866	21	100.5
LAS398_Shot_1069_Grain_745	4.3011	0.5	0.29001	0.4	0.58	0.10964	0.37	1784	31	1641	26	1691	20	97.0
LAS398_Shot_1070_Grain_746	15.8970	0.6	0.50859	0.6	0.18	0.23018	0.34	3048	26	2641	44	2858	25	92.4
LAS398_Shot_1071_Grain_747	5.0067	0.5	0.32912	0.4	0.53	0.11241	0.42	1828	33	1832	29	1816	21	100.9
LAS398_Shot_1072_Grain_748	5.7211	1.4	0.24832	1.2	0.96	0.16635	0.49	2505	32	1417	37	1876	34	75.6
LAS398_Shot_1073_Grain_749	6.1575	0.4	0.36114	0.4	0.45	0.12612	0.38	2034	31	1985	30	1996	21	99.5
LAS398_Shot_1074_Grain_750	9.3080	0.9	0.39126	0.8	0.91	0.17561	0.33	2605	28	2118	40	2348	26	90.2
LAS398_Shot_1075_Grain_751	6.9274	0.6	0.30013	0.5	0.84	0.17031	0.30	2555	28	1689	29	2093	24	80.7
LAS398_Shot_1076_Grain_752	4.5023	0.5	0.30766	0.4	0.45	0.10791	0.44	1754	33	1728	27	1729	20	100.0
LAS398_Shot_1077_Grain_753	1.7602	1.0	0.14112	0.8	0.82	0.09137	0.56	1435	37	849	18	1018	19	83.4

LAS398_Shot_1078_Grain_754	4.3105	0.3	0.28400	0.3	0.46	0.11188	0.31	1824	30	1611	25	1693	19	95.1
LAS398_Shot_1079_Grain_755	5.4073	0.4	0.33920	0.3	0.49	0.11808	0.32	1920	30	1881	28	1884	20	99.9
LAS398_Shot_1080_Grain_756	5.1550	0.6	0.29526	0.5	0.74	0.12893	0.34	2076	30	1665	28	1838	22	90.6
LAS398_Shot_1087_Grain_757	8.0591	0.4	0.32208	0.4	0.55	0.18553	0.33	2696	28	1799	28	2235	21	80.5
LAS398_Shot_1088_Grain_758	11.9020	0.9	0.45257	0.8	0.92	0.19327	0.33	2765	28	2394	45	2572	30	93.1
LAS398_Shot_1089_Grain_759	14.3663	0.4	0.53712	0.3	0.51	0.19774	0.33	2802	28	2768	40	2773	22	99.8
LAS398_Shot_1090_Grain_760	14.9633	0.4	0.53968	0.4	0.60	0.20452	0.35	2858	28	2780	41	2810	23	98.9
LAS398_Shot_1091_Grain_761	6.1539	0.7	0.27837	0.4	0.66	0.16244	0.55	2465	33	1581	26	1985	24	79.7
LAS398_Shot_1092_Grain_762	12.6318	0.4	0.49846	0.4	0.69	0.18743	0.26	2716	28	2604	38	2649	23	98.3
LAS398_Shot_1093_Grain_763	3.2817	0.5	0.25538	0.4	0.56	0.09514	0.43	1520	34	1465	24	1473	20	99.4
LAS398_Shot_1094_Grain_764	4.6358	0.4	0.21547	0.4	0.52	0.15949	0.34	2443	29	1257	21	1753	20	71.7
LAS398_Shot_1095_Grain_765	10.3787	1.0	0.41121	0.9	0.91	0.18481	0.39	2689	29	2207	46	2438	32	90.5
LAS398_Shot_1096_Grain_766	3.9109	0.4	0.26546	0.3	0.65	0.10881	0.28	1775	31	1517	24	1613	19	94.0
LAS398_Shot_1097_Grain_767	14.2431	0.4	0.52843	0.4	0.62	0.19927	0.33	2817	27	2731	40	2762	23	98.9
LAS398_Shot_1098_Grain_768	11.5924	0.4	0.45727	0.4	0.76	0.18832	0.26	2723	27	2424	37	2569	22	94.4
LAS398_Shot_1099_Grain_769	9.9917	0.5	0.35524	0.4	0.83	0.20776	0.24	2885	27	1957	31	2427	23	80.6
LAS398_Shot_1100_Grain_770	3.6308	1.7	0.24962	1.4	0.94	0.10253	0.67	1637	39	1418	43	1474	39	96.2
LAS398_Shot_1107_Grain_771	3.8888	0.4	0.26317	0.3	0.54	0.10923	0.34	1778	31	1505	23	1608	19	93.6
LAS398_Shot_1108_Grain_772	2.9210	0.4	0.24021	0.4	0.69	0.09013	0.29	1422	32	1387	22	1385	18	100.2
LAS398_Shot_1109_Grain_773	6.8568	0.4	0.38526	0.3	0.51	0.13241	0.33	2122	30	2099	32	2091	21	100.4
LAS398_Shot_1110_Grain_774	2.8168	0.4	0.19972	0.3	0.35	0.10437	0.40	1691	33	1173	19	1358	18	86.4
LAS398_Shot_1111_Grain_775	14.8381	0.4	0.54439	0.4	0.58	0.20230	0.32	2838	28	2798	41	2802	23	99.9
LAS398_Shot_1112_Grain_776	4.4878	0.5	0.29295	0.4	0.59	0.11384	0.40	1850	32	1654	26	1724	21	95.9
LAS398_Shot_1113_Grain_777	8.2501	0.4	0.34276	0.4	0.66	0.17814	0.28	2632	28	1899	30	2256	22	84.2
LAS398_Shot_1114_Grain_778	6.5159	0.8	0.27052	0.7	0.93	0.17702	0.30	2621	28	1539	29	2029	25	75.9
LAS398_Shot_1115_Grain_779	4.6172	1.4	0.21740	1.0	0.93	0.15361	0.54	2367	33	1262	30	1703	32	74.1
LAS398_Shot_1116_Grain_780	15.5483	0.5	0.56230	0.5	0.34	0.20414	0.39	2852	29	2872	44	2844	24	101.0
LAS398_Shot_1117_Grain_781	2.8191	0.4	0.23798	0.4	0.41	0.08819	0.43	1374	35	1375	22	1358	18	101.3
LAS398_Shot_1118_Grain_782	4.5053	1.1	0.20905	0.8	0.92	0.15864	0.41	2431	30	1221	25	1709	25	71.4
LAS398_Shot_1119_Grain_783	2.1244	0.9	0.19577	0.5	0.19	0.08204	0.92	1202	47	1151	21	1146	20	100.4
LAS398_Shot_1120_Grain_784	4.5752	0.5	0.30049	0.5	0.55	0.11361	0.45	1850	34	1692	28	1741	21	97.2
LAS398_Shot_1127_Grain_785	5.8510	0.6	0.31429	0.4	0.76	0.13773	0.37	2190	31	1762	28	1946	22	90.5
LAS398_Shot_1128_Grain_786	10.3355	0.3	0.43341	0.3	0.51	0.17800	0.29	2629	28	2323	35	2463	22	94.3
LAS398_Shot_1129_Grain_787	5.1909	0.4	0.33290	0.4	0.65	0.11606	0.34	1890	31	1851	29	1847	21	100.2
LAS398_Shot_1130_Grain_788	5.0079	0.5	0.32585	0.4	0.56	0.11472	0.42	1861	32	1817	29	1817	21	100.0

LAS398_Shot_1131_Grain_789	3.3855	0.4	0.21157	0.4	0.62	0.11964	0.33	1944	30	1237	20	1499	19	82.6
LAS398_Shot_1132_Grain_790	4.5186	0.7	0.30435	0.5	0.67	0.11070	0.48	1798	34	1709	29	1726	22	99.1
LAS398_Shot_1133_Grain_791	6.7688	0.7	0.36058	0.5	0.76	0.13961	0.40	2214	30	1982	33	2074	24	95.6
LAS398_Shot_1134_Grain_792	5.9961	1.0	0.34650	0.7	0.37	0.13158	1.07	2044	50	1912	37	1950	27	98.1
LAS398_Shot_1135_Grain_793	6.7313	0.5	0.28998	0.4	0.81	0.17341	0.27	2587	28	1639	27	2069	22	79.2
LAS398_Shot_1136_Grain_794	2.6255	0.5	0.22874	0.4	0.53	0.08559	0.43	1314	35	1328	22	1304	18	101.8
LAS398_Shot_1137_Grain_795	2.8027	0.6	0.22904	0.4	0.68	0.09090	0.40	1433	34	1328	22	1351	19	98.3
LAS398_Shot_1138_Grain_796	1.7430	0.7	0.17502	0.4	0.32	0.07460	0.61	1027	41	1039	17	1018	17	102.0
LAS398_Shot_1139_Grain_797	4.1654	0.4	0.28732	0.3	0.53	0.10846	0.31	1767	31	1627	25	1665	19	97.7
LAS398_Shot_1140_Grain_798	3.7291	0.8	0.18357	0.6	0.84	0.15121	0.43	2349	31	1085	20	1571	22	69.1
LAS398_Shot_1147_Grain_799	6.3624	0.4	0.37029	0.4	0.50	0.12828	0.40	2064	32	2030	31	2023	21	100.3
LAS398_Shot_1148_Grain_800	10.8878	0.5	0.43216	0.4	0.76	0.18807	0.28	2721	27	2313	36	2508	23	92.2
LAS398_Shot_1149_Grain_801	14.0824	0.4	0.53476	0.3	0.60	0.19619	0.32	2789	27	2758	40	2751	23	100.2
LAS398_Shot_1150_Grain_802	8.9133	1.0	0.32262	0.9	0.96	0.20348	0.29	2849	27	1793	37	2299	27	78.0
LAS398_Shot_1151_Grain_803	12.8547	0.4	0.51826	0.4	0.54	0.18437	0.34	2685	28	2689	39	2665	23	100.9
LAS398_Shot_1152_Grain_804	4.0169	0.6	0.28614	0.5	0.77	0.10389	0.38	1688	32	1620	27	1631	21	99.3
LAS398_Shot_1153_Grain_805	9.3991	2.0	0.34462	1.5	0.98	0.19101	0.62	2727	34	1873	58	2244	48	83.5
LAS398_Shot_1154_Grain_806	14.4171	0.4	0.53422	0.4	0.56	0.20077	0.33	2826	28	2757	40	2775	22	99.3
LAS398_Shot_1155_Grain_807	2.1135	0.6	0.19979	0.4	0.39	0.07873	0.53	1146	39	1173	19	1150	17	102.1
LAS398_Shot_1156_Grain_808	2.0807	0.5	0.19571	0.4	0.37	0.07882	0.49	1150	38	1151	19	1140	17	101.0
LAS398_Shot_1157_Grain_809	4.3579	0.4	0.29416	0.3	0.45	0.10941	0.34	1781	31	1662	25	1702	20	97.7
LAS398_Shot_1158_Grain_810	14.5674	0.5	0.51057	0.4	0.51	0.21219	0.40	2912	29	2654	40	2780	24	95.5
LAS398_Shot_1159_Grain_811	4.7212	1.4	0.26976	1.1	0.95	0.12624	0.47	2033	33	1526	39	1715	34	89.0
LAS398_Shot_1160_Grain_812	4.9874	1.6	0.20462	1.1	0.94	0.17432	0.60	2577	33	1193	29	1760	31	67.8
LAS398_Shot_1167_Grain_813	9.6725	0.4	0.40445	0.4	0.64	0.17666	0.30	2616	28	2188	33	2400	22	91.1
LAS398_Shot_1168_Grain_814	11.2309	0.4	0.48664	0.4	0.65	0.17032	0.33	2556	29	2555	38	2537	23	100.7
LAS398_Shot_1169_Grain_815	9.8664	0.7	0.43844	0.6	0.67	0.16756	0.54	2517	32	2336	39	2410	24	96.9
LAS398_Shot_1170_Grain_816	5.0846	0.6	0.32698	0.5	0.58	0.11549	0.50	1868	34	1821	30	1828	22	99.6
LAS398_Shot_1171_Grain_817	4.6738	0.4	0.30490	0.4	0.48	0.11364	0.40	1848	32	1714	27	1760	20	97.4
LAS398_Shot_1172_Grain_818	12.1111	0.4	0.46790	0.3	0.69	0.19067	0.25	2744	27	2472	36	2610	22	94.7
LAS398_Shot_1173_Grain_819	10.1325	0.5	0.40510	0.5	0.76	0.18457	0.32	2691	28	2188	35	2439	22	89.7
LAS398_Shot_1174_Grain_820	11.8524	0.5	0.47576	0.5	0.41	0.18460	0.51	2682	31	2506	39	2588	23	96.8
LAS398_Shot_1175_Grain_821	4.7070	0.5	0.31598	0.4	0.27	0.11038	0.40	1796	31	1768	28	1764	21	100.2
LAS398_Shot_1176_Grain_822	23.8064	0.5	0.66323	0.5	0.59	0.26576	0.43	3276	28	3273	49	3253	24	100.6
LAS398_Shot_1177_Grain_823	4.6811	2.5	0.23240	1.9	0.98	0.13789	0.96	2130	45	1320	48	1612	47	81.9

LAS398_Shot_1178_Grain_824	1.9527	1.3	0.18573	0.7	0.11	0.08033	1.39	1250	54	1097	22	1080	23	101.5
LAS398_Shot_1179_Grain_825	13.3185	0.5	0.51119	0.4	0.71	0.19319	0.33	2766	27	2657	40	2698	24	98.5
LAS398_Shot_1180_Grain_826	4.6894	0.6	0.30717	0.6	0.79	0.11398	0.38	1853	31	1723	31	1756	22	98.2
LAS398_Shot_1187_Grain_827	15.4799	0.4	0.56176	0.4	0.53	0.20619	0.39	2866	29	2871	41	2840	23	101.1
LAS398_Shot_1188_Grain_828	1.8936	0.4	0.15019	0.4	0.58	0.09433	0.37	1504	33	902	15	1077	16	83.7
LAS398_Shot_1189_Grain_829	19.5518	0.6	0.63001	0.6	0.58	0.23424	0.57	3063	32	3141	50	3060	25	102.7
LAS398_Shot_1190_Grain_830	7.6754	1.2	0.33314	1.1	0.93	0.16880	0.46	2538	30	1837	44	2139	37	85.9
LAS398_Shot_1191_Grain_831	15.1088	0.4	0.51642	0.4	0.68	0.21841	0.30	2965	27	2680	39	2818	23	95.1
LAS398_Shot_1192_Grain_832	12.1305	0.8	0.47942	0.8	0.72	0.19004	0.36	2734	29	2511	47	2594	28	96.8
LAS398_Shot_1193_Grain_833	8.4925	0.6	0.41623	0.5	0.65	0.15334	0.44	2371	32	2240	36	2278	23	98.3
LAS398_Shot_1194_Grain_834	12.7048	0.4	0.50215	0.4	0.38	0.18937	0.33	2729	26	2624	39	2656	21	98.8
LAS398_Shot_1195_Grain_835	4.2789	0.8	0.28345	0.6	0.80	0.11269	0.44	1828	33	1606	29	1683	23	95.4
LAS398_Shot_1196_Grain_836	4.5606	0.4	0.30174	0.5	0.60	0.11392	0.40	1854	31	1699	29	1740	20	97.6
LAS398_Shot_1197_Grain_837	3.2760	1.8	0.22961	1.5	0.97	0.10288	0.53	1655	36	1315	41	1402	35	93.8
LAS398_Shot_1198_Grain_838	5.1077	0.5	0.33685	0.4	0.44	0.11369	0.45	1846	33	1870	29	1832	21	102.1
LAS398_Shot_1199_Grain_839	5.2265	0.5	0.34591	0.5	0.52	0.11408	0.49	1851	34	1912	32	1852	21	103.3
LAS398_Shot_1200_Grain_840	6.7417	0.6	0.26885	0.5	0.81	0.18804	0.31	2720	28	1533	26	2072	23	74.0
LAS398_Shot_1207_Grain_841	7.1772	0.4	0.32794	0.4	0.64	0.16460	0.32	2496	28	1826	29	2131	21	85.7
LAS398_Shot_1208_Grain_842	5.0259	0.4	0.23865	0.4	0.43	0.15954	0.41	2440	30	1379	22	1819	20	75.8
LAS398_Shot_1209_Grain_843	9.4672	0.5	0.37579	0.5	0.71	0.19010	0.33	2736	28	2053	33	2379	23	86.3
LAS398_Shot_1210_Grain_844	5.6461	0.4	0.35100	0.4	0.52	0.12087	0.34	1961	31	1937	30	1922	21	100.8
LAS398_Shot_1211_Grain_845	6.6126	0.5	0.29267	0.5	0.80	0.16936	0.30	2545	28	1652	28	2053	22	80.5
LAS398_Shot_1212_Grain_846	2.5076	0.7	0.17906	0.5	0.74	0.10480	0.41	1700	33	1062	18	1267	20	83.8
LAS398_Shot_1213_Grain_847	12.7965	0.7	0.53044	0.7	0.51	0.18350	0.64	2664	34	2734	46	2656	24	102.9
LAS398_Shot_1214_Grain_848	9.8811	0.7	0.45281	0.8	0.05	0.16511	0.61	2493	30	2391	41	2414	24	99.1
LAS398_Shot_1215_Grain_849	6.9949	0.7	0.31104	0.6	0.76	0.16932	0.41	2544	30	1742	32	2099	24	83.0
LAS398_Shot_1216_Grain_850	3.8413	0.9	0.18894	0.7	0.66	0.15146	0.43	2348	30	1113	23	1583	23	70.3
LAS398_Shot_1217_Grain_851	3.8637	0.4	0.26419	0.4	0.70	0.10900	0.31	1774	31	1510	24	1603	20	94.2
LAS398_Shot_1218_Grain_852	10.7896	0.4	0.42146	0.4	0.53	0.19219	0.35	2753	29	2264	34	2501	23	90.5
LAS398_Shot_1219_Grain_853	3.8978	1.9	0.20402	1.5	0.97	0.13803	0.57	2179	33	1183	37	1540	34	76.8
LAS398_Shot_1220_Grain_854	8.3506	0.4	0.34656	0.3	0.66	0.17937	0.25	2642	27	1917	29	2268	21	84.5
LAS398_Shot_1227_Grain_855	1.1917	0.8	0.12573	0.6	0.42	0.07108	0.54	934	39	762	15	791	15	96.4
LAS398_Shot_1228_Grain_856	5.1047	0.5	0.33220	0.4	0.12	0.11515	0.41	1871	31	1849	29	1834	20	100.8
LAS398_Shot_1229_Grain_857	15.2081	0.4	0.56860	0.4	0.55	0.19893	0.36	2811	28	2901	42	2825	22	102.7
LAS398_Shot_1230_Grain_858	3.5886	1.1	0.24838	0.9	0.91	0.10602	0.43	1721	34	1423	31	1521	26	93.6

LAS398_Shot_1231_Grain_859	5.4284	0.6	0.34690	0.5	0.49	0.11716	0.50	1900	34	1918	31	1885	21	101.7
LAS398_Shot_1232_Grain_860	11.7184	0.7	0.29426	0.6	0.87	0.29541	0.31	3442	27	1659	29	2566	26	64.6
LAS398_Shot_1233_Grain_861	7.5286	0.8	0.32439	0.6	0.87	0.17243	0.35	2574	29	1808	32	2162	25	83.6
LAS398_Shot_1234_Grain_862	12.1866	0.4	0.49008	0.4	0.54	0.18421	0.39	2683	29	2568	39	2617	22	98.1
LAS398_Shot_1235_Grain_863	4.0456	0.4	0.26850	0.4	0.61	0.11236	0.35	1831	31	1531	25	1641	19	93.3
LAS398_Shot_1236_Grain_864	8.5203	0.7	0.35697	0.6	0.79	0.17722	0.37	2619	29	1963	35	2274	24	86.3
LAS398_Shot_1237_Grain_865	23.4451	0.4	0.59187	0.4	0.70	0.29236	0.27	3428	25	2995	42	3243	24	92.4
LAS398_Shot_1238_Grain_866	10.6673	0.5	0.40154	0.4	0.72	0.19695	0.34	2794	28	2173	34	2489	24	87.3
LAS398_Shot_1239_Grain_867	7.6014	0.6	0.28450	0.4	0.72	0.19791	0.35	2803	28	1612	26	2178	23	74.0
LAS398_Shot_1240_Grain_868	1.3641	0.6	0.14579	0.5	0.53	0.06952	0.49	894	39	877	15	870	15	100.7
LAS398_Shot_1247_Grain_869	8.3525	0.5	0.34407	0.5	0.71	0.17982	0.34	2643	29	1903	31	2262	23	84.1
LAS398_Shot_1248_Grain_870	4.6835	0.6	0.29811	0.4	0.76	0.11665	0.32	1898	30	1680	27	1757	22	95.6
LAS398_Shot_1249_Grain_871	2.9356	0.5	0.21087	0.4	0.60	0.10331	0.38	1673	33	1233	21	1388	19	88.8
LAS398_Shot_1250_Grain_872	11.5548	0.4	0.44209	0.4	0.50	0.19421	0.38	2771	28	2357	35	2565	22	91.9
LAS398_Shot_1251_Grain_873	7.6463	0.9	0.32560	0.7	0.93	0.17207	0.34	2572	28	1810	35	2164	29	83.6
LAS398_Shot_1252_Grain_874	0.5928	0.8	0.07470	0.5	0.27	0.05931	0.75	631	40	464	8	470	10	98.7
LAS398_Shot_1253_Grain_875	14.5437	0.4	0.54046	0.4	0.57	0.19979	0.36	2817	28	2782	41	2785	23	99.9
LAS398_Shot_1254_Grain_876	4.8310	0.3	0.31584	0.3	0.61	0.11305	0.28	1844	30	1769	27	1788	20	98.9
LAS398_Shot_1255_Grain_877	13.8928	0.4	0.50896	0.4	0.52	0.20182	0.36	2835	29	2650	39	2738	22	96.8
LAS398_Shot_1256_Grain_878	4.4600	0.4	0.29885	0.4	0.60	0.11093	0.31	1810	31	1687	26	1722	20	98.0
LAS398_Shot_1257_Grain_879	5.1941	0.4	0.33506	0.3	0.59	0.11490	0.29	1873	31	1861	28	1849	20	100.7
LAS398_Shot_1258_Grain_880	14.2377	0.5	0.49487	0.5	0.66	0.21509	0.37	2937	28	2587	40	2762	23	93.7
LAS398_Shot_1259_Grain_881	5.5360	0.5	0.34882	0.4	0.45	0.11792	0.43	1913	33	1928	30	1903	21	101.3
LAS398_Shot_1260_Grain_882	5.0154	0.4	0.32321	0.4	0.46	0.11559	0.36	1881	32	1804	28	1822	19	99.0
LAS398_Shot_1267_Grain_883	7.0848	0.6	0.30312	0.5	0.82	0.17361	0.30	2588	28	1704	28	2113	23	80.6
LAS398_Shot_1268_Grain_884	4.1481	0.5	0.19034	0.5	0.55	0.16245	0.48	2468	31	1122	20	1660	20	67.6
LAS398_Shot_1269_Grain_885	3.0415	0.6	0.16440	0.6	0.25	0.13834	0.53	2193	33	980	18	1413	19	69.3
LAS398_Shot_1270_Grain_886	15.5936	0.5	0.55582	0.5	0.58	0.20968	0.45	2894	29	2844	45	2847	23	99.9
LAS398_Shot_1271_Grain_887	5.3534	0.7	0.34467	0.6	0.53	0.11611	0.62	1880	36	1907	34	1869	23	102.0
LAS398_Shot_1272_Grain_888	13.2449	0.5	0.50884	0.5	0.31	0.19448	0.47	2765	27	2647	42	2694	22	98.2
LAS398_Shot_1273_Grain_889	2.3738	0.9	0.18072	0.7	0.81	0.09727	0.43	1565	34	1068	21	1221	21	87.5
LAS398_Shot_1274_Grain_890	10.5255	1.1	0.42708	0.8	0.92	0.18075	0.39	2651	29	2280	46	2446	32	93.2
LAS398_Shot_1275_Grain_891	6.1182	0.5	0.27659	0.4	0.54	0.16398	0.39	2491	30	1575	25	1992	21	79.0
LAS398_Shot_1276_Grain_892	4.4794	0.6	0.29327	0.6	0.62	0.11311	0.53	1844	34	1654	30	1722	21	96.0
LAS398_Shot_1277_Grain_893	13.2089	0.4	0.48845	0.4	0.67	0.20091	0.30	2827	27	2561	38	2691	22	95.2

LAS398_Shot_1278_Grain_894	15.2152	0.7	0.46928	0.6	0.90	0.23765	0.30	3100	27	2474	41	2821	26	87.7
LAS398_Shot_1279_Grain_895	3.0446	0.4	0.24518	0.3	0.51	0.09201	0.34	1461	32	1413	22	1418	17	99.6
LAS398_Shot_1280_Grain_896	8.3641	0.9	0.33772	0.7	0.90	0.18185	0.37	2663	29	1868	36	2248	29	83.1
LAS398_Shot_1287_Grain_897	3.9467	0.6	0.17978	0.4	0.71	0.16210	0.37	2469	30	1066	18	1616	20	66.0
LAS398_Shot_1288_Grain_898	4.2591	0.5	0.28013	0.4	0.67	0.11253	0.37	1830	31	1590	26	1681	20	94.6
LAS398_Shot_1289_Grain_899	5.8601	1.0	0.27716	0.7	0.86	0.15515	0.47	2388	31	1572	30	1928	28	81.5
LAS398_Shot_1290_Grain_900	3.7589	0.8	0.17918	0.6	0.70	0.15299	0.54	2369	33	1062	20	1579	22	67.3
LAS398_Shot_1291_Grain_901	3.8834	0.8	0.26243	0.6	0.84	0.10954	0.38	1781	32	1499	27	1599	23	93.7
LAS398_Shot_1292_Grain_902	1.6544	0.7	0.16992	0.5	0.33	0.07250	0.70	976	41	1011	18	985	17	102.5
LAS398_Shot_1293_Grain_903	12.3187	0.6	0.46154	0.5	0.78	0.19666	0.35	2793	29	2443	40	2623	24	93.2
LAS398_Shot_1294_Grain_904	4.3220	1.2	0.20161	1.0	0.94	0.15415	0.54	2371	34	1178	28	1653	32	71.2
LAS398_Shot_1295_Grain_905	15.5849	0.4	0.56360	0.5	0.57	0.20460	0.40	2852	29	2877	44	2847	23	101.0
LAS398_Shot_1296_Grain_906	9.0176	0.5	0.36433	0.5	0.68	0.18270	0.35	2671	29	1999	32	2336	22	85.6
LAS398_Shot_1297_Grain_907	13.8846	0.5	0.54291	0.5	0.48	0.19017	0.48	2731	31	2789	42	2735	24	102.0
LAS398_Shot_1298_Grain_908	4.5175	0.9	0.29730	0.7	0.75	0.11195	0.54	1810	35	1672	31	1716	25	97.5
LAS398_Shot_1299_Grain_909	3.2171	0.5	0.17779	0.3	0.53	0.13343	0.39	2133	30	1054	17	1457	19	72.4
LAS398_Shot_1300_Grain_910	4.5701	0.4	0.30174	0.4	0.53	0.11160	0.37	1819	32	1698	27	1742	20	97.5
LAS398_Shot_1307_Grain_911	4.3905	0.4	0.28891	0.3	0.49	0.11237	0.35	1829	31	1635	26	1708	20	95.8
LAS398_Shot_1308_Grain_912	8.8130	0.6	0.40061	0.5	0.66	0.16173	0.44	2465	31	2168	35	2308	24	93.9
LAS398_Shot_1309_Grain_913	11.7864	1.0	0.37884	0.8	0.93	0.22670	0.38	3022	28	2059	42	2553	31	80.6
LAS398_Shot_1310_Grain_914	3.7977	0.6	0.26089	0.5	0.80	0.10765	0.35	1750	31	1492	26	1585	21	94.2
LAS398_Shot_1311_Grain_915	3.4499	0.6	0.19949	0.5	0.67	0.12729	0.43	2049	32	1171	20	1509	21	77.6
LAS398_Shot_1312_Grain_916	3.0461	0.6	0.21072	0.4	0.49	0.10694	0.51	1728	34	1231	21	1414	19	87.1
LAS398_Shot_1313_Grain_917	9.2324	0.4	0.35524	0.4	0.75	0.19036	0.28	2740	28	1961	31	2360	22	83.1
LAS398_Shot_1314_Grain_918	11.0493	0.5	0.41705	0.4	0.83	0.19501	0.28	2780	28	2243	35	2522	24	88.9
LAS398_Shot_1315_Grain_919	5.3002	0.7	0.23955	0.5	0.84	0.16277	0.38	2475	30	1382	25	1856	24	74.4
LAS398_Shot_1316_Grain_920	9.7551	0.3	0.37409	0.4	0.65	0.19229	0.27	2758	27	2046	31	2410	22	84.9
LAS398_Shot_1317_Grain_921	8.8084	0.5	0.36159	0.5	0.77	0.18076	0.29	2655	28	1988	33	2313	22	86.0
LAS398_Shot_1318_Grain_922	11.4871	0.4	0.46660	0.4	0.56	0.18302	0.36	2672	29	2466	37	2560	22	96.3
LAS398_Shot_1319_Grain_923	3.6433	0.4	0.25483	0.4	0.62	0.10580	0.29	1721	31	1463	24	1557	18	94.0
LAS398_Shot_1320_Grain_924	7.3608	0.4	0.29841	0.4	0.58	0.18305	0.31	2675	28	1682	26	2154	21	78.1
LAS398_Shot_1327_Grain_925	17.2429	0.5	0.56937	0.4	0.57	0.22537	0.39	3013	28	2901	43	2942	24	98.6
LAS398_Shot_1328_Grain_926	2.4623	0.7	0.14117	0.5	0.81	0.12843	0.37	2070	30	851	15	1253	20	67.9
LAS398_Shot_1329_Grain_927	9.4686	0.8	0.37667	0.8	0.88	0.18491	0.37	2691	28	2057	40	2367	26	86.9
LAS398_Shot_1330_Grain_928	12.9991	0.8	0.50420	0.7	0.82	0.19133	0.39	2746	30	2622	45	2666	26	98.4

LAS398_Shot_1331_Grain_929	8.4065	1.1	0.34620	0.9	0.93	0.17673	0.43	2614	30	1909	40	2248	29	84.9
LAS398_Shot_1332_Grain_930	9.5147	0.7	0.39598	0.6	0.87	0.17885	0.33	2636	29	2146	37	2376	26	90.3
LAS398_Shot_1333_Grain_931	3.1403	0.9	0.21446	0.7	0.92	0.10807	0.34	1759	32	1249	25	1424	23	87.7
LAS398_Shot_1334_Grain_932	8.8619	0.8	0.35661	0.7	0.75	0.18390	0.31	2686	27	1960	36	2311	28	84.8
LAS398_Shot_1335_Grain_933	13.5650	0.7	0.50718	0.6	0.77	0.19862	0.42	2805	30	2638	44	2709	26	97.4
LAS398_Shot_1336_Grain_934	5.1530	0.5	0.33294	0.4	0.50	0.11564	0.40	1880	32	1850	29	1841	21	100.5
LAS398_Shot_1337_Grain_935	9.5286	0.4	0.39023	0.4	0.59	0.18250	0.32	2670	28	2123	33	2388	21	88.9
LAS398_Shot_1338_Grain_936	12.4993	1.1	0.46498	0.9	0.88	0.19792	0.48	2798	31	2445	50	2601	34	94.0
LAS398_Shot_1339_Grain_937	3.7508	0.5	0.25974	0.4	0.75	0.10739	0.30	1749	31	1488	24	1578	20	94.3
LAS398_Shot_1340_Grain_938	13.4352	0.4	0.52781	0.4	0.49	0.19011	0.43	2736	30	2727	41	2707	23	100.7
LAS398_Shot_1347_Grain_939	6.5611	0.4	0.36776	0.3	0.59	0.13245	0.29	2127	29	2017	31	2051	21	98.3
LAS398_Shot_1348_Grain_940	3.7429	0.9	0.23924	0.7	0.91	0.11496	0.35	1871	32	1379	27	1570	25	87.8
LAS398_Shot_1349_Grain_941	3.9461	0.7	0.19054	0.6	0.83	0.15411	0.36	2382	29	1123	21	1613	21	69.6
LAS398_Shot_1350_Grain_942	1.5306	1.0	0.12931	0.7	0.73	0.08735	0.64	1341	39	782	16	930	19	84.1
LAS398_Shot_1351_Grain_943	4.9544	0.4	0.32190	0.4	0.50	0.11409	0.37	1856	32	1798	28	1811	20	99.3
LAS398_Shot_1352_Grain_944	9.0253	1.7	0.36703	1.4	0.97	0.17604	0.46	2602	31	1981	58	2241	42	88.4
LAS398_Shot_1353_Grain_945	8.9991	1.9	0.38287	1.2	0.95	0.16221	0.92	2417	42	2063	53	2211	47	93.3
LAS398_Shot_1354_Grain_946	3.5292	0.7	0.25819	0.5	0.66	0.10122	0.47	1630	34	1479	26	1527	21	96.8
LAS398_Shot_1355_Grain_947	11.5620	0.3	0.45732	0.3	0.58	0.18678	0.28	2709	27	2427	35	2568	21	94.5
LAS398_Shot_1356_Grain_948	13.9446	0.4	0.42515	0.4	0.63	0.24444	0.32	3143	27	2280	35	2742	23	83.2
LAS398_Shot_1357_Grain_949	6.9886	0.6	0.32122	0.5	0.83	0.16067	0.29	2457	29	1793	30	2102	22	85.3
LAS398_Shot_1358_Grain_950	12.7848	0.4	0.50242	0.4	0.57	0.18842	0.39	2720	29	2621	40	2661	22	98.5
LAS398_Shot_1359_Grain_951	3.5897	0.4	0.26388	0.4	0.61	0.10035	0.33	1624	32	1508	24	1544	19	97.7
LAS398_Shot_1360_Grain_952	4.1852	0.4	0.27709	0.3	0.54	0.11196	0.33	1822	31	1575	25	1668	20	94.5
LAS398_Shot_1367_Grain_953	6.8686	0.9	0.28222	0.7	0.92	0.17897	0.32	2637	28	1596	31	2077	26	76.9
LAS398_Shot_1368_Grain_954	11.0070	1.2	0.44133	1.0	0.93	0.18173	0.40	2662	30	2334	53	2473	36	94.4
LAS398_Shot_1369_Grain_955	14.9219	0.4	0.53752	0.4	0.53	0.20581	0.38	2865	29	2771	41	2806	23	98.7
LAS398_Shot_1370_Grain_956	12.5786	0.4	0.49032	0.4	0.36	0.19010	0.29	2737	27	2569	38	2646	22	97.1
LAS398_Shot_1371_Grain_957	5.3462	0.4	0.33429	0.4	0.54	0.11843	0.33	1924	31	1857	29	1874	20	99.1
LAS398_Shot_1372_Grain_958	5.0607	0.6	0.32859	0.5	0.35	0.11544	0.61	1863	37	1828	30	1824	21	100.3
LAS398_Shot_1373_Grain_959	13.8659	0.8	0.52841	0.7	0.41	0.19798	0.78	2774	37	2724	47	2730	26	99.8
LAS398_Shot_1374_Grain_960	14.8771	0.7	0.51009	0.6	0.87	0.21576	0.31	2943	28	2649	44	2793	27	94.9
LAS398_Shot_1375_Grain_961	10.8783	0.8	0.38079	0.7	0.91	0.21030	0.32	2904	28	2072	38	2491	27	83.2
LAS398_Shot_1376_Grain_962	2.1696	0.5	0.18256	0.4	0.69	0.08838	0.35	1380	33	1081	18	1168	17	92.5
LAS398_Shot_1377_Grain_963	4.4480	0.4	0.28840	0.4	0.67	0.11446	0.32	1867	30	1632	27	1718	20	95.0

LAS398_Shot_1378_Grain_964	4.5945	0.5	0.30858	0.4	0.61	0.11040	0.40	1796	33	1732	28	1742	21	99.4
LAS398_Shot_1379_Grain_965	5.0409	0.4	0.32709	0.4	0.45	0.11502	0.33	1872	31	1823	28	1824	20	100.0
LAS398_Shot_1380_Grain_966	13.6512	0.4	0.49901	0.4	0.68	0.20372	0.30	2852	27	2606	39	2723	23	95.7
LAS398_Shot_1387_Grain_967	14.7719	0.4	0.54337	0.4	0.50	0.20342	0.33	2850	28	2794	40	2797	23	99.9
LAS398_Shot_1388_Grain_968	12.8474	0.4	0.50628	0.3	0.59	0.18997	0.29	2736	28	2638	38	2666	22	98.9
LAS398_Shot_1389_Grain_969	10.2701	0.5	0.40476	0.5	0.75	0.18985	0.33	2734	28	2190	35	2453	23	89.3
LAS398_Shot_1390_Grain_970	12.1830	0.3	0.47535	0.3	0.54	0.19141	0.28	2752	27	2506	36	2616	22	95.8
LAS398_Shot_1391_Grain_971	16.9290	0.6	0.50065	0.6	0.83	0.25262	0.34	3194	27	2610	44	2917	26	89.5
LAS398_Shot_1392_Grain_972	3.9959	0.9	0.26702	0.7	0.92	0.11160	0.32	1818	31	1520	30	1615	25	94.1
LAS398_Shot_1393_Grain_973	11.5046	0.3	0.44397	0.4	0.63	0.19356	0.30	2767	28	2369	36	2564	21	92.4
LAS398_Shot_1394_Grain_974	11.0054	1.4	0.42496	1.2	0.96	0.18981	0.44	2732	30	2253	57	2446	42	92.1
LAS398_Shot_1395_Grain_975	6.7989	0.8	0.29560	0.7	0.86	0.17101	0.37	2560	29	1666	32	2068	26	80.6
LAS398_Shot_1396_Grain_976	12.4028	0.7	0.49460	0.6	0.67	0.18848	0.50	2715	31	2589	43	2624	25	98.7
LAS398_Shot_1397_Grain_977	5.8557	0.8	0.22827	0.7	0.63	0.19340	0.58	2755	31	1323	26	1943	25	68.1
LAS398_Shot_1398_Grain_978	4.9823	0.5	0.32540	0.5	0.60	0.11463	0.46	1865	33	1815	30	1814	21	100.0
LAS398_Shot_1399_Grain_979	10.9356	0.7	0.45208	0.6	0.74	0.18175	0.43	2660	30	2402	40	2510	25	95.7
LAS398_Shot_1400_Grain_980	13.9437	0.5	0.53016	0.5	0.65	0.19788	0.43	2800	29	2735	43	2743	22	99.7
LAS398_Shot_1407_Grain_981	1.9082	0.5	0.18128	0.4	0.67	0.07893	0.35	1161	34	1073	18	1081	16	99.3
LAS398_Shot_1408_Grain_982	3.9817	0.5	0.26469	0.4	0.78	0.11260	0.31	1836	31	1512	25	1625	21	93.1
LAS398_Shot_1409_Grain_983	3.8922	1.0	0.26840	0.8	0.89	0.10800	0.39	1755	32	1526	31	1589	25	96.0
LAS398_Shot_1410_Grain_984	2.1569	2.4	0.16260	1.8	0.97	0.09257	0.78	1426	43	957	35	1078	35	88.8
LAS398_Shot_1411_Grain_985	9.2991	0.9	0.34254	0.7	0.92	0.20198	0.35	2834	28	1897	34	2352	25	80.7
LAS398_Shot_1412_Grain_986	13.6848	0.4	0.53189	0.4	0.43	0.19428	0.40	2771	28	2745	40	2724	23	100.8
LAS398_Shot_1413_Grain_987	12.5544	0.4	0.49529	0.4	0.57	0.19003	0.33	2736	28	2592	38	2644	22	98.0
LAS398_Shot_1414_Grain_988	11.9646	0.5	0.45120	0.4	0.75	0.19918	0.29	2816	27	2398	36	2598	23	92.3
LAS398_Shot_1415_Grain_989	12.4490	0.8	0.46676	0.7	0.90	0.19910	0.31	2814	28	2461	43	2621	28	93.9
LAS398_Shot_1416_Grain_990	5.8219	0.5	0.35576	0.5	0.40	0.12328	0.54	1988	34	1959	32	1942	22	100.8
LAS398_Shot_1417_Grain_991	3.5031	0.4	0.24919	0.3	0.53	0.10541	0.31	1713	31	1433	22	1526	18	93.9
LAS398_Shot_1418_Grain_992	4.8420	0.5	0.31819	0.4	0.57	0.11446	0.36	1862	31	1779	28	1788	20	99.5
LAS398_Shot_1419_Grain_993	4.8994	0.3	0.32487	0.3	0.52	0.11318	0.32	1843	31	1812	28	1801	20	100.6
LAS398_Shot_1420_Grain_994	4.8951	0.5	0.32413	0.4	0.55	0.11292	0.41	1837	32	1808	29	1798	20	100.6
LAS398_Shot_1427_Grain_995	11.9713	0.4	0.46848	0.3	0.49	0.19127	0.35	2746	28	2474	36	2600	22	95.2
LAS398_Shot_1428_Grain_996	1.8159	0.8	0.18047	0.5	0.24	0.07638	0.86	1084	45	1068	19	1044	19	102.3
LAS398_Shot_1429_Grain_997	5.0612	1.1	0.33679	0.8	0.35	0.11381	1.06	1791	50	1867	36	1805	27	103.5
LAS398_Shot_1430_Grain_998	4.1849	0.6	0.28615	0.5	0.31	0.10983	0.62	1768	37	1621	27	1663	21	97.4

LAS398_Shot_1431_Grain_999	1.1546	0.7	0.10814	0.5	0.45	0.07865	0.66	1147	40	662	12	777	15	85.2
LAS398_Shot_1432_Grain_1000	14.9032	0.4	0.54226	0.4	0.59	0.20599	0.35	2867	28	2792	42	2807	23	99.5
LAS398_Shot_1433_Grain_1001	12.9060	0.4	0.50499	0.4	0.63	0.19065	0.33	2742	28	2633	40	2670	22	98.6
LAS398_Shot_1434_Grain_1002	4.8088	0.5	0.31555	0.4	0.10	0.11424	0.44	1854	32	1767	29	1780	21	99.3
LAS398_Shot_1435_Grain_1003	4.1818	0.5	0.29378	0.4	0.52	0.10671	0.43	1731	33	1660	27	1666	20	99.6
LAS398_Shot_1436_Grain_1004	4.6598	0.4	0.31539	0.4	0.58	0.10990	0.37	1791	31	1765	28	1756	20	100.5
LAS398_Shot_1437_Grain_1005	4.5910	0.4	0.30431	0.4	0.62	0.11231	0.35	1829	32	1711	27	1745	20	98.1
LAS398_Shot_1438_Grain_1006	3.2515	0.6	0.24397	0.6	0.80	0.09946	0.37	1608	32	1404	26	1463	20	96.0
LAS398_Shot_1439_Grain_1007	5.1107	0.4	0.22474	0.4	0.19	0.16915	0.39	2539	29	1306	21	1833	20	71.2
LAS398_Shot_1440_Grain_1008	12.7407	0.3	0.47783	0.4	0.57	0.19937	0.31	2814	27	2515	37	2659	21	94.6

LAS399 (20BREM16H)														
Isotopic Ratios								Calculated ages (Ma)						
ID	$^{207}Pb/^{235}U$	2σ	$^{206}Pb/^{238}U$	2σ	Rho	$^{207/206}Pb$	2σ	$^{207/206}Pb$	2σ	$^{206}Pb/^{238}U$	2σ	$^{207}Pb/^{235}U$	2σ	%conc
LAS399_Shot_7_Grain_1	0.7251	1.5	0.08887	0.7	0.24	0.05917	1.50	645	59	549	11	550	13	99.8
LAS399_Shot_8_Grain_2	2.2688	0.5	0.19316	0.5	0.41	0.08522	0.57	1314	33	1139	19	1201	11	94.8
LAS399_Shot_9_Grain_3	3.1989	0.7	0.25211	0.5	-0.22	0.09220	0.72	1458	36	1449	23	1454	14	99.6
LAS399_Shot_10_Grain_4	1.8615	1.8	0.17680	1.1	0.27	0.07721	1.79	1091	73	1048	25	1058	24	99.0
LAS399_Shot_11_Grain_5	2.4413	0.8	0.20803	0.6	0.22	0.08539	0.91	1302	44	1218	21	1253	14	97.2
LAS399_Shot_12_Grain_6	2.7941	1.1	0.14424	1.1	0.87	0.14119	0.52	2235	28	867	22	1349	18	64.3
LAS399_Shot_13_Grain_7	3.0437	1.1	0.24525	0.7	-0.14	0.09029	1.23	1402	53	1415	27	1411	19	100.2
LAS399_Shot_14_Grain_8	2.5904	0.9	0.21425	0.6	0.32	0.08801	0.85	1370	43	1251	21	1296	16	96.5
LAS399_Shot_15_Grain_9	10.2798	0.9	0.27281	0.9	0.86	0.27316	0.48	3323	24	1553	31	2452	21	63.3
LAS399_Shot_16_Grain_10	4.4399	0.6	0.19411	0.7	0.75	0.16598	0.47	2517	27	1144	21	1718	13	66.6
LAS399_Shot_17_Grain_11	2.1360	0.6	0.19442	0.4	0.43	0.07976	0.59	1184	34	1145	17	1159	11	98.8
LAS399_Shot_18_Grain_12	2.0041	0.8	0.16695	0.6	0.35	0.08770	0.79	1359	39	995	17	1114	13	89.3
LAS399_Shot_19_Grain_13	4.2291	0.7	0.30130	0.5	0.38	0.10230	0.72	1653	35	1697	27	1676	15	101.2
LAS399_Shot_20_Grain_14	3.8337	0.6	0.25200	0.6	0.43	0.11076	0.71	1805	36	1448	24	1600	14	90.5
LAS399_Shot_27_Grain_15	10.7304	0.7	0.42208	0.6	0.37	0.18575	0.77	2692	33	2270	36	2495	17	91.0
LAS399_Shot_28_Grain_16	3.2877	0.6	0.22449	0.5	0.36	0.10724	0.66	1742	33	1305	21	1477	13	88.4
LAS399_Shot_29_Grain_17	6.1990	0.6	0.36192	0.5	0.45	0.12522	0.59	2024	30	1990	31	2004	14	99.3
LAS399_Shot_30_Grain_18	14.6535	0.5	0.52980	0.6	0.48	0.20244	0.56	2839	28	2738	42	2790	14	98.1
LAS399_Shot_31_Grain_19	2.7388	1.1	0.15772	0.8	0.26	0.12731	1.15	2039	48	943	19	1333	18	70.8
LAS399_Shot_32_Grain_20	0.4827	0.7	0.06095	0.6	0.57	0.05794	0.64	521	38	381	7	399	6	95.5

LAS399_Shot_33_Grain_21	2.8163	0.6	0.23779	0.5	0.36	0.08657	0.64	1342	35	1375	22	1358	12	101.2
LAS399_Shot_34_Grain_22	1.8598	1.1	0.17785	0.7	-0.02	0.07675	1.21	1078	58	1054	20	1064	17	99.0
LAS399_Shot_35_Grain_23	1.7066	0.7	0.16398	0.6	0.52	0.07594	0.60	1085	35	978	17	1009	11	97.0
LAS399_Shot_36_Grain_24	3.8535	0.7	0.28434	0.6	0.45	0.09935	0.67	1600	34	1612	27	1601	14	100.7
LAS399_Shot_37_Grain_25	2.2389	0.6	0.19126	0.5	0.42	0.08593	0.60	1329	35	1128	18	1192	12	94.6
LAS399_Shot_38_Grain_26	1.8944	0.8	0.15133	0.6	0.44	0.09197	0.84	1455	39	908	15	1076	13	84.4
LAS399_Shot_39_Grain_27	2.6451	0.6	0.21711	0.6	0.44	0.08923	0.61	1402	33	1266	21	1312	11	96.5
LAS399_Shot_40_Grain_28	3.3011	0.7	0.23145	0.6	0.66	0.10451	0.58	1697	31	1341	23	1478	14	90.7
LAS399_Shot_47_Grain_29	5.1974	0.5	0.33536	0.6	0.38	0.11397	0.62	1854	32	1863	30	1851	13	100.7
LAS399_Shot_48_Grain_30	2.4058	0.5	0.20562	0.4	0.33	0.08575	0.59	1325	33	1205	19	1243	11	97.0
LAS399_Shot_49_Grain_31	9.9503	0.5	0.40015	0.6	0.55	0.18251	0.53	2672	26	2168	34	2428	14	89.3
LAS399_Shot_50_Grain_32	1.4257	0.7	0.14182	0.5	-0.24	0.07370	0.85	1016	43	855	14	898	11	95.2
LAS399_Shot_51_Grain_33	4.8649	0.6	0.32343	0.6	0.37	0.11044	0.68	1798	33	1807	30	1793	14	100.8
LAS399_Shot_52_Grain_34	1.9644	0.8	0.18490	0.7	0.64	0.07818	0.63	1140	36	1093	20	1100	13	99.3
LAS399_Shot_53_Grain_35	10.2580	0.5	0.39152	0.5	0.61	0.19245	0.47	2760	25	2129	31	2456	14	86.7
LAS399_Shot_54_Grain_36	1.8592	0.7	0.16387	0.5	0.23	0.08318	0.71	1265	39	978	16	1067	11	91.7
LAS399_Shot_55_Grain_37	1.1885	0.7	0.12225	0.6	0.29	0.07161	0.68	967	38	743	13	794	9	93.6
LAS399_Shot_56_Grain_38	2.6026	0.6	0.22021	0.7	0.69	0.08686	0.50	1352	32	1282	23	1299	12	98.7
LAS399_Shot_57_Grain_39	1.1097	0.7	0.11570	0.7	0.20	0.07052	0.60	935	35	705	14	756	10	93.2
LAS399_Shot_58_Grain_40	3.3979	0.8	0.24068	0.7	0.79	0.10365	0.51	1686	29	1389	26	1501	15	92.5
LAS399_Shot_59_Grain_41	2.6588	0.9	0.21849	0.8	0.77	0.08983	0.58	1413	32	1273	25	1314	15	96.8
LAS399_Shot_60_Grain_42	2.8384	0.6	0.23993	0.5	0.21	0.08720	0.74	1350	37	1386	23	1364	12	101.6
LAS399_Shot_67_Grain_43	2.3977	2.8	0.14184	2.0	0.14	0.12898	2.99	2026	109	855	34	1227	42	69.6
LAS399_Shot_68_Grain_44	1.7859	0.8	0.17619	0.6	0.30	0.07473	0.83	1048	44	1046	18	1039	13	100.7
LAS399_Shot_69_Grain_45	2.3419	0.9	0.20068	0.8	0.37	0.08634	0.96	1321	45	1178	23	1222	15	96.4
LAS399_Shot_70_Grain_46	4.6468	0.6	0.31383	0.5	0.41	0.10891	0.60	1774	32	1759	27	1758	14	100.0
LAS399_Shot_71_Grain_47	2.2789	0.6	0.17076	0.5	0.42	0.09818	0.62	1580	33	1016	16	1205	12	84.3
LAS399_Shot_72_Grain_48	0.5515	1.1	0.07037	0.6	0.25	0.05787	1.12	567	47	438	8	445	9	98.4
LAS399_Shot_73_Grain_49	7.5296	0.6	0.31107	0.5	0.16	0.17713	0.49	2621	26	1747	28	2173	15	80.4
LAS399_Shot_74_Grain_50	2.9280	0.7	0.19725	0.6	0.45	0.10906	0.65	1778	33	1160	20	1388	13	83.6
LAS399_Shot_75_Grain_51	9.3136	0.8	0.37054	0.7	0.65	0.18474	0.62	2690	30	2029	36	2364	17	85.8
LAS399_Shot_76_Grain_52	9.4580	0.6	0.37643	0.5	0.46	0.18446	0.58	2688	29	2058	32	2381	15	86.5
LAS399_Shot_77_Grain_53	1.6826	0.6	0.16452	0.5	0.50	0.07492	0.57	1059	35	981	16	1000	10	98.1
LAS399_Shot_78_Grain_54	3.3245	0.6	0.26144	0.6	0.43	0.09403	0.68	1496	35	1496	25	1484	13	100.8
LAS399_Shot_79_Grain_55	4.4754	0.6	0.28608	0.5	0.48	0.11493	0.59	1872	31	1621	25	1724	14	94.0

LAS399_Shot_80_Grain_56	2.0479	1.2	0.15430	0.8	0.22	0.09785	1.25	1549	54	926	18	1125	17	82.3
LAS399_Shot_87_Grain_57	9.7975	0.6	0.38063	0.6	0.57	0.18864	0.56	2725	28	2080	34	2413	14	86.2
LAS399_Shot_88_Grain_58	1.3302	0.8	0.13201	0.7	0.69	0.07379	0.60	1025	35	799	15	857	12	93.3
LAS399_Shot_89_Grain_59	0.7191	1.1	0.08846	0.7	0.18	0.05967	1.18	629	51	547	10	548	10	99.8
LAS399_Shot_90_Grain_60	12.3784	0.6	0.48415	0.6	0.44	0.18754	0.61	2717	28	2545	40	2631	15	96.8
LAS399_Shot_91_Grain_61	1.9499	0.7	0.18764	0.5	0.30	0.07624	0.72	1100	35	1108	18	1098	11	100.9
LAS399_Shot_92_Grain_62	4.5036	0.5	0.20559	0.5	0.50	0.15956	0.55	2450	29	1205	19	1730	13	69.7
LAS399_Shot_93_Grain_63	5.2470	0.7	0.34519	0.6	0.28	0.11214	0.81	1818	38	1910	31	1859	16	102.7
LAS399_Shot_94_Grain_64	11.7226	0.6	0.47019	0.5	0.50	0.18234	0.55	2669	28	2485	38	2580	14	96.3
LAS399_Shot_95_Grain_65	2.2596	0.9	0.16864	0.7	0.67	0.09788	0.70	1574	35	1004	18	1195	16	84.0
LAS399_Shot_96_Grain_66	1.7452	1.1	0.17988	0.8	0.34	0.07127	1.13	933	53	1065	21	1020	16	104.4
LAS399_Shot_97_Grain_67	9.5741	0.6	0.38194	0.6	0.56	0.18357	0.58	2678	28	2083	34	2391	15	87.1
LAS399_Shot_98_Grain_68	1.5747	0.9	0.15560	0.6	0.33	0.07440	0.95	1026	47	932	17	959	13	97.2
LAS399_Shot_99_Grain_69	1.8669	0.8	0.18190	0.6	0.24	0.07516	0.88	1054	45	1077	19	1066	13	101.0
LAS399_Shot_100_Grain_70	1.8371	1.0	0.17897	0.6	0.27	0.07530	1.02	1056	48	1061	19	1056	15	100.4
LAS399_Shot_107_Grain_71	1.4988	1.8	0.14549	1.0	0.11	0.07677	1.94	1153	71	874	21	922	23	94.8
LAS399_Shot_108_Grain_72	10.2553	0.5	0.45492	0.5	0.59	0.16471	0.48	2499	27	2416	35	2456	14	98.4
LAS399_Shot_109_Grain_73	3.9389	0.6	0.26738	0.5	0.37	0.10740	0.65	1750	33	1527	25	1620	13	94.2
LAS399_Shot_110_Grain_74	12.9113	0.5	0.50887	0.6	0.48	0.18514	0.58	2694	28	2649	41	2671	14	99.2
LAS399_Shot_111_Grain_75	1.2884	1.3	0.12896	0.9	0.29	0.07359	1.34	1010	56	781	17	837	17	93.4
LAS399_Shot_112_Grain_76	2.5243	0.7	0.21514	0.6	0.73	0.08539	0.48	1318	30	1257	22	1278	12	98.4
LAS399_Shot_113_Grain_77	8.5351	0.5	0.34753	0.5	0.38	0.17941	0.49	2644	26	1922	29	2289	13	84.0
LAS399_Shot_114_Grain_78	2.8671	0.5	0.19196	0.5	0.47	0.10896	0.52	1775	30	1132	18	1372	12	82.5
LAS399_Shot_115_Grain_79	0.6416	1.6	0.08181	0.9	0.18	0.05784	1.73	663	60	507	11	500	14	101.2
LAS399_Shot_116_Grain_80	2.1802	0.7	0.18723	0.5	0.59	0.08486	0.56	1306	32	1106	18	1173	12	94.3
LAS399_Shot_117_Grain_81	2.7546	0.6	0.23089	0.5	0.37	0.08710	0.65	1351	35	1338	22	1341	12	99.8
LAS399_Shot_118_Grain_82	1.3662	1.2	0.13491	0.8	0.25	0.07417	1.29	1019	57	815	16	871	16	93.6
LAS399_Shot_119_Grain_83	2.6832	1.3	0.19146	1.0	0.79	0.10151	0.77	1644	37	1128	26	1314	21	85.8
LAS399_Shot_120_Grain_84	2.0287	0.9	0.18476	0.7	0.33	0.08053	0.99	1188	46	1092	21	1122	15	97.3
LAS399_Shot_127_Grain_85	4.0213	2.2	0.26377	1.4	0.18	0.11437	2.41	1774	92	1503	43	1609	38	93.4
LAS399_Shot_128_Grain_86	1.4528	1.1	0.14077	0.7	0.46	0.07561	1.05	1068	48	850	16	909	15	93.5
LAS399_Shot_129_Grain_87	7.0367	0.5	0.30266	0.5	0.63	0.16924	0.42	2546	25	1704	26	2114	13	80.6
LAS399_Shot_130_Grain_88	2.3287	0.5	0.19483	0.4	0.48	0.08703	0.46	1359	29	1147	17	1221	10	94.0
LAS399_Shot_131_Grain_89	2.9506	0.7	0.21332	0.7	0.63	0.10082	0.64	1631	33	1246	23	1394	13	89.3
LAS399_Shot_132_Grain_90	11.2595	0.6	0.44579	0.5	0.51	0.18390	0.54	2684	27	2375	35	2542	15	93.4

LAS399_Shot_133_Grain_91	12.5055	0.7	0.49066	0.7	0.57	0.18535	0.68	2692	31	2570	43	2640	17	97.3
LAS399_Shot_134_Grain_92														
LAS399_Shot_135_Grain_93	1.5041	0.8	0.14652	0.6	0.25	0.07522	0.87	1057	43	881	16	931	12	94.7
LAS399_Shot_136_Grain_94	1.4435	1.0	0.14345	0.8	0.04	0.07349	1.04	1005	51	863	17	904	13	95.5
LAS399_Shot_137_Grain_95	1.6993	1.2	0.12429	0.8	0.18	0.10062	1.25	1601	53	755	15	1003	17	75.3
LAS399_Shot_138_Grain_96	2.5381	0.8	0.20892	0.7	0.58	0.08858	0.68	1385	36	1222	22	1280	14	95.5
LAS399_Shot_139_Grain_97	1.6584	0.8	0.16271	0.6	0.35	0.07489	0.89	1043	44	973	18	991	13	98.1
LAS399_Shot_140_Grain_98	0.7849	1.8	0.07657	1.0	0.29	0.07515	1.83	1052	75	475	11	585	17	81.3
LAS399_Shot_147_Grain_99	1.7808	0.8	0.16712	0.7	0.74	0.07781	0.55	1133	34	996	18	1038	12	95.9
LAS399_Shot_148_Grain_100	4.5798	0.6	0.29876	0.6	0.33	0.11154	0.66	1821	34	1684	27	1745	14	96.5
LAS399_Shot_149_Grain_101	3.9943	4.3	0.17982	3.2	0.97	0.14884	1.78	2257	72	1050	64	1498	76	70.1
LAS399_Shot_150_Grain_102	2.1108	1.3	0.16045	0.6	0.33	0.09637	1.23	1517	52	959	16	1145	19	83.8
LAS399_Shot_151_Grain_103	1.8162	0.6	0.17144	0.5	0.72	0.07700	0.44	1121	30	1020	17	1050	10	97.1
LAS399_Shot_152_Grain_104	3.9941	1.3	0.18459	1.2	0.86	0.15717	0.70	2417	32	1090	29	1621	24	67.2
LAS399_Shot_153_Grain_105	1.7071	0.6	0.16322	0.5	0.33	0.07623	0.68	1091	37	974	16	1009	11	96.5
LAS399_Shot_154_Grain_106	1.6783	0.7	0.16010	0.7	0.69	0.07662	0.54	1103	33	957	17	999	11	95.7
LAS399_Shot_155_Grain_107	1.7609	0.7	0.15670	0.7	0.61	0.08205	0.60	1239	34	938	17	1029	11	91.1
LAS399_Shot_156_Grain_108	2.9247	0.8	0.23497	0.7	-0.13	0.09105	0.98	1423	45	1359	24	1384	15	98.2
LAS399_Shot_157_Grain_109	1.3364	1.5	0.12533	1.0	-0.04	0.07908	1.84	1143	73	760	18	855	19	88.9
LAS399_Shot_158_Grain_110	12.9249	0.9	0.50446	0.7	0.39	0.18678	0.84	2704	36	2629	44	2668	19	98.5
LAS399_Shot_159_Grain_111	1.0542	1.5	0.10366	1.1	0.78	0.07427	0.95	1026	47	635	15	726	17	87.4
LAS399_Shot_160_Grain_112	2.1781	0.7	0.19110	0.6	0.65	0.08300	0.57	1260	33	1127	19	1172	13	96.2
LAS399_Shot_167_Grain_113	9.7482	0.6	0.41289	0.5	0.49	0.17198	0.57	2572	28	2226	34	2409	14	92.4
LAS399_Shot_168_Grain_114														
LAS399_Shot_169_Grain_115	7.4293	1.1	0.29160	1.1	0.74	0.18643	0.77	2704	33	1645	38	2158	24	76.3
LAS399_Shot_170_Grain_116	1.6638	1.0	0.16137	0.6	-0.04	0.07559	1.08	1052	51	964	17	991	14	97.3
LAS399_Shot_171_Grain_117														
LAS399_Shot_172_Grain_118	1.1195	1.0	0.11066	0.7	0.55	0.07360	0.85	1022	42	676	13	762	12	88.7
LAS399_Shot_173_Grain_119	2.3422	2.2	0.08190	2.1	0.19	0.21674	2.74	2822	92	506	22	1201	34	42.1
LAS399_Shot_174_Grain_120	5.3640	0.7	0.26691	0.6	0.50	0.14567	0.65	2291	31	1524	25	1877	14	81.2
LAS399_Shot_175_Grain_121	1.5613	0.9	0.16173	0.6	-0.03	0.07037	0.91	919	46	966	17	952	13	101.5
LAS399_Shot_176_Grain_122	1.4511	0.7	0.14473	0.7	0.73	0.07332	0.53	1014	33	871	16	909	11	95.8
LAS399_Shot_177_Grain_123	5.1511	0.6	0.23330	0.6	0.70	0.16092	0.46	2460	26	1351	22	1842	14	73.4
LAS399_Shot_178_Grain_124	2.3536	1.0	0.21985	0.7	0.59	0.07822	1.03	1128	49	1280	24	1224	16	104.6
LAS399_Shot_179_Grain_125	1.4924	1.0	0.14972	0.6	0.32	0.07270	0.98	987	47	899	16	925	14	97.2

LAS399_Shot_180_Grain_126	6.0753	0.6	0.29686	0.6	0.32	0.14969	0.74	2333	33	1674	28	1983	15	84.4
LAS399_Shot_187_Grain_127	1.8675	0.6	0.17788	0.5	0.39	0.07664	0.59	1102	35	1055	17	1068	10	98.8
LAS399_Shot_188_Grain_128	1.4003	0.9	0.14237	0.8	0.84	0.07169	0.48	974	32	857	17	887	13	96.6
LAS399_Shot_189_Grain_129	3.4079	0.6	0.26409	0.5	0.44	0.09402	0.60	1499	32	1510	24	1504	13	100.4
LAS399_Shot_190_Grain_130	1.7368	1.4	0.17304	0.7	0.27	0.07330	1.37	1004	60	1028	20	1016	19	101.2
LAS399_Shot_191_Grain_131	1.7963	0.6	0.17868	0.5	0.47	0.07326	0.58	1014	34	1059	17	1043	10	101.6
LAS399_Shot_192_Grain_132	2.5110	0.8	0.21636	0.7	0.58	0.08456	0.72	1291	37	1261	23	1273	14	99.1
LAS399_Shot_193_Grain_133	1.8498	0.8	0.17777	0.6	0.32	0.07552	0.83	1070	43	1054	18	1060	13	99.4
LAS399_Shot_194_Grain_134	1.9808	1.5	0.19242	1.1	0.26	0.07693	1.64	1071	68	1133	26	1103	22	102.7
LAS399_Shot_195_Grain_135	1.9523	0.9	0.18660	0.7	0.32	0.07676	0.98	1088	47	1102	20	1097	15	100.5
LAS399_Shot_196_Grain_136	1.8849	0.7	0.18055	0.5	0.40	0.07677	0.66	1102	37	1070	17	1074	11	99.6
LAS399_Shot_197_Grain_137	1.3569	1.0	0.13800	0.7	0.17	0.07227	1.19	959	55	833	16	869	14	95.8
LAS399_Shot_198_Grain_138	1.7568	0.7	0.16160	0.6	0.48	0.07915	0.60	1171	35	965	16	1028	11	93.9
LAS399_Shot_199_Grain_139	0.5701	1.5	0.06908	0.8	0.01	0.06085	1.71	741	64	430	9	455	12	94.6
LAS399_Shot_200_Grain_140	2.3978	0.8	0.19552	0.6	0.21	0.08967	0.90	1398	41	1151	20	1239	14	92.9
LAS399_Shot_207_Grain_141	2.6984	0.5	0.20508	0.4	0.14	0.09610	0.56	1541	31	1202	18	1327	11	90.6
LAS399_Shot_208_Grain_142	2.0006	1.2	0.18821	0.7	0.03	0.07816	1.35	1114	59	1111	21	1109	18	100.1
LAS399_Shot_209_Grain_143	1.3414	1.8	0.09434	1.1	0.06	0.10592	2.03	1668	79	581	15	855	22	67.9
LAS399_Shot_210_Grain_144	2.0388	1.0	0.19945	0.7	0.30	0.07460	1.06	1031	49	1172	21	1123	16	104.3
LAS399_Shot_211_Grain_145	3.1131	0.9	0.24940	0.7	0.32	0.09163	0.93	1437	43	1434	26	1431	16	100.2
LAS399_Shot_212_Grain_146	3.2857	0.8	0.25227	0.6	0.40	0.09544	0.82	1519	40	1449	24	1473	15	98.4
LAS399_Shot_213_Grain_147	3.1410	1.1	0.24976	0.7	0.29	0.09228	1.09	1447	48	1436	26	1437	19	99.9
LAS399_Shot_214_Grain_148	1.7454	0.7	0.17322	0.5	0.20	0.07390	0.83	1019	42	1029	17	1023	12	100.6
LAS399_Shot_215_Grain_149	2.6532	1.0	0.23631	0.7	0.19	0.08226	1.07	1234	48	1368	25	1310	17	104.4
LAS399_Shot_216_Grain_150	10.3850	0.5	0.42775	0.5	0.56	0.17719	0.40	2624	25	2294	33	2469	13	92.9
LAS399_Shot_217_Grain_151	1.9550	0.8	0.18643	0.6	0.12	0.07651	0.84	1096	42	1101	19	1098	13	100.3
LAS399_Shot_218_Grain_152	1.7308	0.9	0.15771	0.6	0.22	0.08034	0.95	1188	45	944	16	1016	14	92.8
LAS399_Shot_219_Grain_153	1.8082	0.7	0.16435	0.6	0.47	0.08025	0.69	1198	38	980	17	1046	11	93.7
LAS399_Shot_220_Grain_154	9.7944	0.5	0.41445	0.5	0.53	0.17307	0.49	2582	27	2234	33	2413	14	92.6
LAS399_Shot_227_Grain_155	3.8143	0.5	0.25286	0.5	0.47	0.11059	0.52	1802	30	1453	23	1595	12	91.1
LAS399_Shot_228_Grain_156	1.6412	0.9	0.15732	0.6	0.60	0.07633	0.70	1092	39	941	17	985	13	95.5
LAS399_Shot_229_Grain_157	11.7988	0.4	0.45368	0.5	0.64	0.19067	0.39	2744	24	2410	35	2587	13	93.2
LAS399_Shot_230_Grain_158	6.0014	0.8	0.25425	0.8	0.67	0.17311	0.63	2581	30	1459	28	1971	17	74.0
LAS399_Shot_231_Grain_159	1.4387	2.1	0.11751	1.3	0.11	0.09178	2.26	1429	89	717	20	891	27	80.4
LAS399_Shot_232_Grain_160	5.1105	0.9	0.32855	0.8	0.30	0.11435	1.02	1853	42	1829	34	1833	18	99.8

LAS399_Shot_233_Grain_161	6.7365	0.5	0.29233	0.5	0.56	0.16922	0.48	2545	26	1652	26	2076	12	79.6
LAS399_Shot_234_Grain_162	4.1880	0.7	0.27556	0.6	0.27	0.11174	0.80	1815	38	1568	26	1668	15	94.0
LAS399_Shot_235_Grain_163	2.3766	1.0	0.17415	0.6	-0.08	0.09982	0.91	1607	41	1034	18	1231	16	84.1
LAS399_Shot_236_Grain_164	1.9965	1.1	0.18377	0.9	0.41	0.08000	1.04	1176	49	1086	23	1109	16	97.9
LAS399_Shot_237_Grain_165	2.0267	0.7	0.19148	0.7	0.45	0.07807	0.71	1143	37	1129	20	1124	13	100.4
LAS399_Shot_238_Grain_166	0.6615	2.9	0.08218	1.5	0.01	0.06121	3.33	993	107	508	16	503	25	101.0
LAS399_Shot_239_Grain_167	1.7737	1.3	0.16926	0.8	0.32	0.07701	1.32	1088	60	1009	21	1028	19	98.1
LAS399_Shot_240_Grain_168	2.3602	0.6	0.20225	0.6	0.61	0.08599	0.56	1329	32	1187	21	1229	11	96.6
LAS399_Shot_247_Grain_169	0.7439	3.3	0.09059	1.6	0.14	0.06207	3.38	1063	104	558	19	549	30	101.5
LAS399_Shot_248_Grain_170	2.1419	0.7	0.19715	0.5	0.35	0.07980	0.68	1182	36	1159	19	1160	12	99.9
LAS399_Shot_249_Grain_171	2.8960	0.7	0.24485	0.6	0.07	0.08662	0.69	1342	37	1411	23	1380	14	102.2
LAS399_Shot_250_Grain_172	1.4216	0.6	0.14332	0.5	0.40	0.07272	0.62	1003	35	863	14	897	10	96.3
LAS399_Shot_251_Grain_173	5.3858	0.6	0.24716	0.6	0.60	0.16000	0.52	2449	28	1423	24	1880	14	75.7
LAS399_Shot_252_Grain_174	2.6413	0.7	0.23149	0.6	0.15	0.08375	0.77	1271	38	1341	23	1309	13	102.4
LAS399_Shot_253_Grain_175	1.9097	0.8	0.17929	0.6	0.30	0.07798	0.82	1131	42	1063	18	1082	13	98.2
LAS399_Shot_254_Grain_176	0.6392	1.3	0.07072	0.9	0.37	0.06667	1.32	818	55	440	10	503	11	87.6
LAS399_Shot_255_Grain_177	1.6504	0.7	0.16444	0.6	0.26	0.07390	0.81	1027	40	981	17	988	12	99.2
LAS399_Shot_256_Grain_178	2.5135	0.6	0.21241	0.6	0.25	0.08708	0.75	1348	37	1241	20	1274	12	97.4
LAS399_Shot_257_Grain_179	11.5263	0.7	0.44537	0.7	0.44	0.19018	0.76	2737	32	2371	41	2564	17	92.5
LAS399_Shot_258_Grain_180	1.9895	0.6	0.19281	0.5	0.43	0.07550	0.60	1074	36	1136	18	1111	11	102.2
LAS399_Shot_259_Grain_181	0.7187	2.1	0.09090	1.0	0.10	0.05891	2.27	811	77	560	13	545	19	102.8
LAS399_Shot_260_Grain_182	4.7110	0.6	0.21859	0.5	0.50	0.15805	0.62	2428	30	1274	20	1766	14	72.1
LAS399_Shot_267_Grain_183	10.4886	0.6	0.42522	0.6	0.51	0.17994	0.57	2647	29	2282	35	2476	15	92.2
LAS399_Shot_268_Grain_184	1.8004	0.7	0.17573	0.5	0.21	0.07527	0.76	1066	39	1043	17	1044	11	100.0
LAS399_Shot_269_Grain_185	2.5888	0.9	0.21806	0.6	0.28	0.08707	0.92	1343	43	1271	22	1293	15	98.3
LAS399_Shot_270_Grain_186	1.4043	1.1	0.14216	0.9	0.43	0.07256	1.05	978	50	856	18	887	14	96.6
LAS399_Shot_271_Grain_187	12.8361	0.5	0.48091	0.5	0.54	0.19504	0.48	2780	26	2529	37	2665	14	94.9
LAS399_Shot_272_Grain_188	3.7649	0.8	0.24291	0.7	0.34	0.11363	0.88	1846	40	1402	26	1582	16	88.6
LAS399_Shot_273_Grain_189	2.6598	0.6	0.18870	0.5	0.48	0.10317	0.57	1673	31	1114	18	1317	12	84.6
LAS399_Shot_274_Grain_190	11.7492	0.5	0.46552	0.5	0.53	0.18416	0.50	2687	27	2462	37	2582	14	95.3
LAS399_Shot_275_Grain_191	2.1695	0.7	0.17235	0.5	0.26	0.09218	0.78	1454	39	1025	17	1172	12	87.4
LAS399_Shot_276_Grain_192	11.3363	0.4	0.45010	0.5	0.49	0.18339	0.46	2682	26	2394	34	2550	13	93.9
LAS399_Shot_277_Grain_193	1.9216	1.2	0.17746	0.7	0.32	0.07923	1.16	1145	52	1052	19	1082	17	97.2
LAS399_Shot_278_Grain_194	9.4262	0.5	0.38247	0.5	0.69	0.17944	0.39	2644	25	2087	31	2378	14	87.7
LAS399_Shot_279_Grain_195	1.9376	1.8	0.18257	1.2	0.08	0.07919	2.03	1177	75	1079	29	1083	24	99.6

LAS399_Shot_280_Grain_196	1.3265	0.8	0.12690	0.6	0.62	0.07649	0.62	1099	35	770	14	857	11	89.8
LAS399_Shot_287_Grain_197	12.9523	0.6	0.48966	0.6	0.44	0.19318	0.62	2761	29	2567	40	2673	15	96.0
LAS399_Shot_288_Grain_198	1.6025	1.1	0.15260	0.7	0.24	0.07579	1.22	1070	55	915	18	966	16	94.7
LAS399_Shot_289_Grain_199	1.9172	0.7	0.17739	0.7	0.68	0.07873	0.53	1159	33	1052	19	1086	12	96.9
LAS399_Shot_290_Grain_200	2.6144	0.7	0.21945	0.6	0.47	0.08665	0.67	1341	35	1278	22	1302	13	98.2
LAS399_Shot_291_Grain_201	1.9587	0.7	0.15165	0.6	0.61	0.09397	0.57	1499	32	910	16	1100	12	82.7
LAS399_Shot_292_Grain_202	4.2625	0.6	0.28015	0.5	0.46	0.11071	0.56	1805	30	1591	24	1684	13	94.5
LAS399_Shot_293_Grain_203	2.4161	0.6	0.20467	0.5	0.13	0.08570	0.56	1325	32	1200	19	1246	11	96.3
LAS399_Shot_294_Grain_204	3.1255	0.5	0.25003	0.5	0.44	0.09088	0.55	1440	32	1439	24	1437	12	100.1
LAS399_Shot_295_Grain_205	1.3807	0.8	0.13631	0.5	0.25	0.07375	0.85	1014	43	824	14	879	11	93.7
LAS399_Shot_296_Grain_206	2.5756	0.5	0.22080	0.4	0.44	0.08486	0.50	1305	31	1287	20	1293	10	99.5
LAS399_Shot_297_Grain_207	3.0062	0.6	0.23830	0.5	0.47	0.09204	0.61	1458	33	1377	22	1408	13	97.8
LAS399_Shot_298_Grain_208	4.2921	0.5	0.24427	0.5	0.67	0.12747	0.43	2060	28	1408	22	1692	13	83.2
LAS399_Shot_299_Grain_209	2.3155	0.7	0.19595	0.6	0.61	0.08629	0.55	1341	31	1153	20	1216	12	94.8
LAS399_Shot_300_Grain_210	2.9521	0.8	0.23889	0.6	0.26	0.09007	0.82	1413	39	1380	23	1392	14	99.1
LAS399_Shot_307_Grain_211	2.8659	0.6	0.24639	0.5	0.38	0.08456	0.63	1297	35	1419	23	1371	12	103.5
LAS399_Shot_308_Grain_212	1.7410	0.8	0.17242	0.6	0.24	0.07348	0.86	1009	44	1025	17	1021	13	100.4
LAS399_Shot_309_Grain_213	2.0813	1.1	0.19277	0.7	0.14	0.07914	1.23	1143	59	1135	21	1140	18	99.6
LAS399_Shot_310_Grain_214	2.5848	0.9	0.19239	0.6	0.37	0.09801	0.94	1564	43	1134	20	1292	16	87.8
LAS399_Shot_311_Grain_215	2.8712	0.5	0.23719	0.4	0.44	0.08799	0.50	1377	30	1373	21	1373	11	100.0
LAS399_Shot_312_Grain_216	3.4135	0.6	0.23646	0.5	0.43	0.10510	0.61	1709	33	1368	22	1505	13	90.9
LAS399_Shot_313_Grain_217	2.2833	1.0	0.19389	0.7	0.29	0.08577	1.03	1316	51	1141	21	1207	17	94.6
LAS399_Shot_314_Grain_218	4.3679	1.9	0.10794	1.8	0.19	0.30337	2.35	3392	79	659	24	1685	33	39.1
LAS399_Shot_315_Grain_219	1.9489	2.5	0.18658	1.3	0.14	0.07787	2.61	1215	86	1100	30	1073	34	102.5
LAS399_Shot_316_Grain_220	2.2146	0.6	0.18761	0.5	0.59	0.08571	0.51	1324	31	1108	18	1184	11	93.6
LAS399_Shot_317_Grain_221	2.6288	0.6	0.20925	0.5	0.58	0.09156	0.50	1453	31	1224	20	1307	11	93.7
LAS399_Shot_318_Grain_222	2.3500	0.7	0.20955	0.6	0.72	0.08160	0.50	1230	32	1226	21	1226	13	100.0
LAS399_Shot_319_Grain_223	2.7899	1.0	0.24131	0.8	0.46	0.08448	0.98	1290	44	1392	28	1348	18	103.2
LAS399_Shot_320_Grain_224	5.5048	0.6	0.34105	0.6	0.50	0.11747	0.58	1912	30	1890	30	1899	14	99.6
LAS399_Shot_327_Grain_225	5.6323	0.7	0.35194	0.6	0.40	0.11692	0.74	1899	34	1942	32	1918	15	101.2
LAS399_Shot_328_Grain_226	4.9149	0.8	0.31737	0.7	0.37	0.11304	0.85	1834	39	1777	31	1805	17	98.5
LAS399_Shot_329_Grain_227	1.4868	2.1	0.06550	1.5	0.06	0.17273	2.74	2455	91	408	13	914	27	44.7
LAS399_Shot_330_Grain_228	1.8690	0.8	0.15522	0.6	0.58	0.08779	0.65	1366	35	930	16	1070	13	86.9
LAS399_Shot_331_Grain_229	3.5209	0.7	0.24202	0.6	0.47	0.10629	0.66	1726	33	1396	23	1530	14	91.3
LAS399_Shot_332_Grain_230	0.7483	2.0	0.08911	1.3	0.15	0.06291	2.26	847	79	550	16	563	18	97.6

LAS399_Shot_333_Grain_231	2.1600	1.1	0.20069	0.7	0.00	0.07874	1.16	1134	52	1178	22	1163	17	101.3
LAS399_Shot_334_Grain_232	0.7512	2.0	0.09105	1.1	0.18	0.06054	2.02	781	72	561	14	562	18	99.9
LAS399_Shot_335_Grain_233	2.5082	0.7	0.20772	0.6	0.48	0.08808	0.66	1372	35	1216	20	1272	12	95.6
LAS399_Shot_336_Grain_234	2.7669	0.7	0.23261	0.6	0.33	0.08659	0.76	1336	38	1347	23	1344	13	100.3
LAS399_Shot_337_Grain_235	9.6325	0.7	0.39815	0.6	0.40	0.17697	0.75	2613	32	2158	35	2396	16	90.1
LAS399_Shot_338_Grain_236	4.2363	0.7	0.28985	0.6	0.43	0.10647	0.67	1729	33	1640	26	1678	14	97.7
LAS399_Shot_339_Grain_237	3.3399	1.0	0.23250	0.8	0.15	0.10534	1.15	1696	49	1346	26	1484	18	90.7
LAS399_Shot_340_Grain_238	3.1620	0.9	0.22365	0.7	0.37	0.10373	0.92	1678	42	1300	24	1444	17	90.0
LAS399_Shot_347_Grain_239	1.6952	0.7	0.15169	0.5	0.38	0.08139	0.69	1226	37	910	15	1005	12	90.6
LAS399_Shot_348_Grain_240	15.1047	0.8	0.54614	0.7	0.40	0.20246	0.83	2841	34	2804	47	2817	19	99.5
LAS399_Shot_349_Grain_241	1.3604	1.3	0.13191	1.0	0.78	0.07521	0.83	1055	42	798	18	868	17	91.9
LAS399_Shot_350_Grain_242	1.9679	0.7	0.18702	0.6	0.15	0.07670	0.85	1100	44	1105	19	1103	13	100.1
LAS399_Shot_351_Grain_243	2.1408	1.0	0.19829	0.7	0.31	0.07879	0.96	1153	46	1165	21	1158	15	100.7
LAS399_Shot_352_Grain_244	2.2438	1.3	0.20389	0.9	0.16	0.08039	1.43	1167	64	1197	26	1189	19	100.7
LAS399_Shot_353_Grain_245	1.5261	0.9	0.14136	0.7	0.37	0.07878	0.89	1145	43	852	16	938	13	90.8
LAS399_Shot_354_Grain_246	3.0780	0.6	0.24360	0.6	0.35	0.09234	0.67	1463	35	1405	23	1426	13	98.5
LAS399_Shot_355_Grain_247	4.3704	1.0	0.22902	0.7	0.36	0.13948	0.98	2204	39	1328	24	1700	18	78.1
LAS399_Shot_356_Grain_248														
LAS399_Shot_357_Grain_249	2.0611	1.7	0.19400	1.0	0.26	0.07816	1.66	1155	67	1141	25	1133	25	100.8
LAS399_Shot_358_Grain_250	0.7538	2.1	0.08946	1.1	0.10	0.06167	2.04	800	75	552	14	562	18	98.1
LAS399_Shot_359_Grain_251	2.3794	0.6	0.21217	0.5	0.45	0.08190	0.59	1233	34	1240	20	1235	11	100.4
LAS399_Shot_360_Grain_252	10.8553	0.6	0.46340	0.6	0.61	0.17018	0.51	2555	28	2452	37	2507	15	97.8
LAS399_Shot_367_Grain_253	2.7447	0.7	0.23743	0.6	0.27	0.08447	0.76	1288	39	1373	23	1340	13	102.4
LAS399_Shot_368_Grain_254	9.7478	3.2	0.18866	3.1	0.27	0.44286	5.12	3457	113	1106	67	2349	63	47.1
LAS399_Shot_369_Grain_255	2.5644	3.5	0.10055	2.4	0.46	0.18839	3.25	2603	109	614	29	1241	51	49.5
LAS399_Shot_370_Grain_256	1.8885	1.3	0.18015	0.9	0.23	0.07641	1.37	1064	61	1067	22	1071	19	99.6
LAS399_Shot_371_Grain_257	1.8269	0.9	0.17684	0.7	0.17	0.07558	1.03	1054	49	1049	19	1052	14	99.7
LAS399_Shot_372_Grain_258	1.8332	0.7	0.17871	0.6	0.40	0.07471	0.70	1053	39	1059	18	1056	11	100.3
LAS399_Shot_373_Grain_259	2.3832	1.1	0.18774	0.6	0.38	0.09192	1.05	1441	47	1110	20	1231	18	90.2
LAS399_Shot_374_Grain_260	1.5942	1.9	0.16063	1.0	0.18	0.07253	1.96	1016	78	959	22	954	24	100.5
LAS399_Shot_375_Grain_261	3.8863	0.7	0.17735	0.7	0.62	0.15910	0.55	2443	29	1052	19	1609	13	65.4
LAS399_Shot_376_Grain_262	1.8751	0.9	0.17852	0.7	0.25	0.07675	0.96	1088	47	1058	19	1071	14	98.8
LAS399_Shot_377_Grain_263	1.9662	1.2	0.18810	0.9	0.07	0.07684	1.33	1100	55	1110	24	1097	18	101.1
LAS399_Shot_378_Grain_264	0.7691	2.5	0.09136	1.4	0.16	0.06193	2.63	901	89	563	17	569	22	98.8
LAS399_Shot_379_Grain_265	12.4250	0.8	0.51789	0.7	0.47	0.17481	0.70	2596	31	2686	45	2632	17	102.1

LAS399_Shot_380_Grain_266	1.8520	0.7	0.18060	0.6	0.39	0.07473	0.72	1047	38	1070	19	1062	11	100.7
LAS399_Shot_387_Grain_267	5.0665	0.6	0.32414	0.5	0.39	0.11362	0.61	1849	32	1809	28	1828	13	98.9
LAS399_Shot_388_Grain_268	2.1018	3.0	0.20129	1.6	0.14	0.07755	3.20	1314	106	1181	39	1117	42	105.7
LAS399_Shot_389_Grain_269	3.8593	0.7	0.25280	0.5	0.28	0.11101	0.72	1803	34	1452	23	1602	14	90.6
LAS399_Shot_390_Grain_270	2.0888	0.7	0.18612	0.6	0.38	0.08162	0.71	1222	38	1100	19	1144	13	96.2
LAS399_Shot_391_Grain_271	1.2571	0.6	0.12583	0.5	0.42	0.07237	0.63	993	38	764	13	826	10	92.5
LAS399_Shot_392_Grain_272	1.1045	0.7	0.11149	0.5	-0.21	0.07198	0.75	969	40	681	12	754	9	90.3
LAS399_Shot_393_Grain_273	13.1983	0.5	0.51519	0.5	0.51	0.18641	0.49	2705	26	2677	38	2692	14	99.4
LAS399_Shot_394_Grain_274	1.8702	1.1	0.18058	0.7	0.15	0.07565	1.21	1054	57	1071	21	1067	16	100.4
LAS399_Shot_395_Grain_275	3.7680	0.7	0.25555	0.6	0.72	0.10680	0.47	1740	29	1466	25	1583	14	92.6
LAS399_Shot_396_Grain_276	1.6670	1.1	0.14912	0.8	0.38	0.08238	1.21	1232	51	895	18	993	16	90.2
LAS399_Shot_397_Grain_277	2.1280	0.6	0.19805	0.5	0.47	0.07803	0.55	1143	33	1164	18	1157	11	100.6
LAS399_Shot_398_Grain_278	8.7833	0.4	0.39268	0.5	0.61	0.16299	0.43	2482	26	2134	32	2315	13	92.2
LAS399_Shot_399_Grain_279	4.4181	0.5	0.28713	0.5	0.54	0.11181	0.49	1825	29	1626	25	1714	12	94.9
LAS399_Shot_400_Grain_280	1.8520	0.9	0.17606	0.7	0.34	0.07654	0.93	1093	45	1045	19	1060	14	98.5
LAS399_Shot_407_Grain_281	12.6899	1.3	0.49365	1.1	0.31	0.18994	1.41	2707	52	2578	54	2642	26	97.6
LAS399_Shot_408_Grain_282	4.0647	0.6	0.27315	0.6	0.27	0.10880	0.72	1767	35	1557	26	1646	13	94.6
LAS399_Shot_409_Grain_283	12.1657	0.5	0.48440	0.5	0.10	0.18348	0.51	2679	27	2545	37	2616	14	97.3
LAS399_Shot_410_Grain_284	4.5430	0.7	0.31058	0.6	0.39	0.10674	0.72	1734	35	1742	28	1737	15	100.3
LAS399_Shot_411_Grain_285	2.1098	0.6	0.19836	0.5	0.44	0.07760	0.57	1127	34	1166	18	1152	11	101.2
LAS399_Shot_412_Grain_286	8.5671	0.6	0.35260	0.5	-0.09	0.17674	0.51	2618	27	1946	30	2290	14	85.0
LAS399_Shot_413_Grain_287	1.5924	0.6	0.15583	0.6	0.70	0.07444	0.49	1052	32	933	16	967	10	96.5
LAS399_Shot_414_Grain_288	7.0578	0.6	0.32430	0.5	0.44	0.15827	0.54	2432	29	1810	28	2116	14	85.5
LAS399_Shot_415_Grain_289	3.1350	0.9	0.24863	0.7	0.43	0.09217	0.87	1454	41	1430	26	1437	16	99.5
LAS399_Shot_416_Grain_290	3.5046	0.9	0.22666	0.8	0.76	0.11292	0.57	1841	30	1316	25	1523	16	86.4
LAS399_Shot_417_Grain_291	1.7144	0.7	0.16806	0.6	0.53	0.07468	0.63	1048	36	1001	17	1013	11	98.8
LAS399_Shot_418_Grain_292	2.6353	0.8	0.20773	0.7	0.38	0.09289	0.81	1469	39	1217	22	1307	14	93.1
LAS399_Shot_419_Grain_293	3.7135	0.7	0.24855	0.6	0.52	0.10911	0.64	1774	33	1430	24	1571	14	91.0
LAS399_Shot_420_Grain_294	2.3288	0.8	0.20795	0.7	0.20	0.08217	0.97	1224	46	1217	22	1217	14	100.0
LAS399_Shot_427_Grain_295	1.5554	0.7	0.14953	0.5	0.03	0.07626	0.83	1082	42	898	14	951	11	94.5
LAS399_Shot_428_Grain_296	11.9227	0.6	0.48178	0.6	0.55	0.18159	0.58	2662	28	2533	39	2595	15	97.6
LAS399_Shot_429_Grain_297	11.9193	0.5	0.46714	0.5	0.47	0.18679	0.50	2710	26	2470	35	2596	14	95.1
LAS399_Shot_430_Grain_298	1.7659	0.6	0.15869	0.5	0.54	0.08162	0.54	1228	32	949	15	1032	11	92.0
LAS399_Shot_431_Grain_299	1.8439	0.9	0.17659	0.7	0.29	0.07651	0.91	1092	46	1048	19	1058	13	99.0
LAS399_Shot_432_Grain_300	1.5354	0.7	0.15155	0.6	0.53	0.07417	0.64	1040	36	909	16	943	11	96.5

LAS399_Shot_433_Grain_301	3.1356	0.5	0.23100	0.5	0.51	0.09965	0.51	1615	30	1339	22	1440	11	93.0
LAS399_Shot_434_Grain_302	2.4594	0.8	0.22094	0.6	0.35	0.08172	0.80	1222	40	1286	22	1258	14	102.2
LAS399_Shot_435_Grain_303	14.9157	0.6	0.54064	0.6	0.51	0.20288	0.62	2842	28	2783	43	2806	16	99.2
LAS399_Shot_436_Grain_304	4.9748	0.7	0.31862	0.5	0.30	0.11449	0.61	1863	32	1782	28	1812	14	98.3
LAS399_Shot_437_Grain_305	1.7391	1.1	0.15948	0.8	0.11	0.07993	1.17	1171	55	953	19	1020	15	93.4
LAS399_Shot_438_Grain_306	9.2056	0.7	0.38356	0.7	0.42	0.17678	0.71	2612	31	2091	35	2355	16	88.8
LAS399_Shot_439_Grain_307	3.8324	0.6	0.25064	0.7	0.59	0.11262	0.59	1833	31	1441	25	1598	14	90.2
LAS399_Shot_440_Grain_308	3.9064	0.8	0.28311	0.8	0.48	0.10132	0.76	1634	37	1605	30	1611	15	99.6
LAS399_Shot_447_Grain_309	1.5105	0.8	0.15814	0.6	0.33	0.07034	0.86	920	45	946	16	932	12	101.5
LAS399_Shot_448_Grain_310	4.6133	0.6	0.30158	0.5	0.49	0.11253	0.53	1835	30	1698	26	1750	13	97.0
LAS399_Shot_449_Grain_311	14.9750	0.5	0.53174	0.6	0.44	0.20684	0.55	2882	26	2746	41	2812	14	97.7
LAS399_Shot_450_Grain_312	1.7809	0.7	0.17813	0.6	0.29	0.07381	0.76	1023	39	1056	18	1037	11	101.9
LAS399_Shot_451_Grain_313	2.3815	1.0	0.21313	0.8	0.24	0.08276	1.09	1246	49	1244	24	1237	16	100.6
LAS399_Shot_452_Grain_314	1.4930	0.9	0.14911	0.6	0.39	0.07390	0.84	1022	43	896	15	926	12	96.7
LAS399_Shot_453_Grain_315	1.6877	0.7	0.16260	0.7	0.41	0.07620	0.76	1087	41	971	18	1002	12	96.9
LAS399_Shot_454_Grain_316	6.0881	1.5	0.23137	1.3	0.92	0.19221	0.57	2756	28	1338	35	1972	27	67.9
LAS399_Shot_455_Grain_317	0.7251	1.9	0.09068	1.0	0.16	0.05922	2.00	728	71	559	14	548	17	101.9
LAS399_Shot_456_Grain_318	13.5463	0.5	0.52239	0.5	0.45	0.19014	0.52	2737	27	2710	40	2716	14	99.7
LAS399_Shot_457_Grain_319	0.7979	2.1	0.09724	1.2	0.00	0.06119	2.33	859	82	597	16	587	19	101.8
LAS399_Shot_458_Grain_320	3.3306	0.7	0.26209	0.6	0.36	0.09394	0.72	1494	36	1500	24	1487	13	100.9
LAS399_Shot_459_Grain_321	3.5943	0.9	0.24496	0.8	0.68	0.10768	0.65	1753	32	1411	28	1543	16	91.4
LAS399_Shot_460_Grain_322	2.3514	0.8	0.22014	0.7	0.58	0.07871	0.67	1152	36	1282	23	1226	13	104.5

LAS400 (20BREM16I)														
	Isotopic Ratios							Calculated ages (Ma)						
ID	$^{207}Pb/^{235}U$	2σ	$^{206}Pb/^{238}U$	2σ	Rho	$^{207/206}Pb$	2σ	$^{207/206}Pb$	2σ	$^{206}Pb/^{238}U$	2σ	$^{207}Pb/^{235}U$	2σ	%conc
LAS400_Shot_467_Grain_323	7.5600	1.3	0.37869	1.2	0.44	0.14928	1.43	2299	53	2063	50	2171	26	95.0
LAS400_Shot_468_Grain_324	1.9676	1.1	0.19197	0.8	0.22	0.07501	1.15	1037	54	1131	23	1098	17	103.0
LAS400_Shot_469_Grain_325	1.8808	1.2	0.17696	0.9	0.18	0.07819	1.31	1118	61	1049	22	1068	18	98.2
LAS400_Shot_470_Grain_326	3.0662	0.8	0.24759	0.8	0.58	0.09138	0.71	1441	36	1425	27	1424	15	100.0
LAS400_Shot_471_Grain_327	1.3480	0.8	0.13725	0.7	0.52	0.07184	0.71	972	38	829	16	865	11	95.8
LAS400_Shot_472_Grain_328	2.7716	0.8	0.22521	0.8	0.41	0.09058	0.86	1418	41	1308	25	1344	15	97.3
LAS400_Shot_473_Grain_329	2.8164	1.7	0.24189	1.2	-0.09	0.08634	1.83	1302	73	1393	34	1342	28	103.8
LAS400_Shot_474_Grain_330	1.6951	0.9	0.13953	0.8	0.38	0.08916	0.92	1401	41	843	17	1003	13	84.0

LAS400_Shot_475_Grain_331	1.1753	1.5	0.12200	1.1	0.47	0.07062	1.30	932	58	741	18	784	18	94.5
LAS400_Shot_476_Grain_332	1.0709	1.0	0.11298	0.8	0.44	0.06964	1.00	897	50	690	14	737	13	93.5
LAS400_Shot_477_Grain_333	4.0466	0.9	0.20216	0.7	0.70	0.14625	0.67	2295	32	1188	23	1638	17	72.5
LAS400_Shot_478_Grain_334	1.3309	1.1	0.11344	0.8	0.21	0.08613	1.15	1324	51	692	14	855	14	80.9
LAS400_Shot_479_Grain_335	11.7716	0.7	0.46101	0.7	0.61	0.18691	0.63	2709	30	2441	41	2582	17	94.5
LAS400_Shot_480_Grain_336	1.7229	1.3	0.17363	1.1	0.49	0.07294	1.17	986	56	1030	25	1013	18	101.7
LAS400_Shot_487_Grain_337	2.8724	0.7	0.19697	0.6	0.57	0.10685	0.60	1737	32	1158	20	1372	13	84.4
LAS400_Shot_488_Grain_338	1.8136	1.4	0.14761	1.0	0.68	0.08969	0.99	1397	47	886	21	1042	19	85.0
LAS400_Shot_489_Grain_339	1.0990	1.3	0.11525	0.8	0.40	0.06978	1.19	886	56	703	15	750	15	93.7
LAS400_Shot_490_Grain_340	1.2780	1.2	0.13076	0.8	0.34	0.07178	1.26	952	54	792	16	831	15	95.3
LAS400_Shot_491_Grain_341	3.5459	1.2	0.24867	1.1	0.79	0.10381	0.76	1681	38	1429	34	1529	22	93.4
LAS400_Shot_492_Grain_342	0.5860	1.3	0.07509	0.7	0.07	0.05735	1.42	608	56	467	9	466	11	100.2
LAS400_Shot_493_Grain_343	5.6729	0.8	0.23460	0.8	0.42	0.17714	0.85	2614	36	1357	27	1922	17	70.6
LAS400_Shot_494_Grain_344	8.1974	0.7	0.33806	0.6	0.38	0.17757	0.73	2622	32	1876	32	2249	15	83.4
LAS400_Shot_495_Grain_345	1.0440	1.1	0.10755	0.8	0.41	0.07101	0.99	937	50	658	13	724	13	90.9
LAS400_Shot_496_Grain_346														
LAS400_Shot_497_Grain_347	3.3942	0.9	0.17919	0.7	0.62	0.13819	0.72	2201	33	1063	21	1498	16	71.0
LAS400_Shot_498_Grain_348	3.1380	0.9	0.16742	0.7	0.50	0.13698	0.82	2177	37	997	19	1439	16	69.3
LAS400_Shot_499_Grain_349	8.0960	0.7	0.34424	0.7	0.63	0.17191	0.64	2570	29	1907	34	2238	16	85.2
LAS400_Shot_500_Grain_350	1.3971	1.6	0.09801	0.9	0.35	0.10391	1.53	1651	62	602	14	879	20	68.5
LAS400_Shot_507_Grain_351	1.7988	0.8	0.17779	0.7	0.46	0.07445	0.80	1035	41	1054	19	1045	13	100.9
LAS400_Shot_508_Grain_352	4.9279	0.8	0.31509	0.7	0.55	0.11475	0.73	1863	34	1764	32	1804	16	97.8
LAS400_Shot_509_Grain_353	0.7992	1.3	0.08568	0.7	0.09	0.06854	1.39	872	58	530	10	593	13	89.3
LAS400_Shot_510_Grain_354	0.6096	1.3	0.07469	0.8	0.13	0.06016	1.44	657	58	464	10	481	11	96.5
LAS400_Shot_511_Grain_355	2.8617	0.7	0.22439	0.7	0.68	0.09343	0.58	1488	32	1304	25	1369	14	95.2
LAS400_Shot_512_Grain_356	4.1459	0.6	0.20570	0.6	0.51	0.14729	0.64	2307	32	1205	21	1662	14	72.5
LAS400_Shot_513_Grain_357	1.7374	0.8	0.16738	0.6	0.05	0.07590	0.79	1078	40	997	18	1021	12	97.7
LAS400_Shot_514_Grain_358	0.7251	2.5	0.07707	1.5	0.25	0.07026	2.67	1028	86	478	15	547	22	87.4
LAS400_Shot_515_Grain_359	1.8532	1.0	0.15397	0.7	0.29	0.08861	1.06	1376	46	923	17	1066	15	86.6
LAS400_Shot_516_Grain_360	2.3119	0.7	0.17948	0.6	0.52	0.09422	0.65	1501	34	1063	19	1213	13	87.7
LAS400_Shot_517_Grain_361	3.3618	0.7	0.23790	0.5	0.35	0.10310	0.68	1677	35	1375	22	1494	13	92.1
LAS400_Shot_518_Grain_362	2.3765	0.8	0.20874	0.6	0.52	0.08301	0.72	1255	37	1223	22	1232	14	99.2
LAS400_Shot_519_Grain_363	11.5576	0.6	0.44651	0.7	0.61	0.18964	0.54	2738	27	2377	40	2570	16	92.5
LAS400_Shot_520_Grain_364	1.5196	1.3	0.13969	0.8	0.29	0.07986	1.31	1148	58	842	16	932	17	90.3
LAS400_Shot_527_Grain_365	0.6254	1.2	0.07020	0.9	0.30	0.06496	1.21	784	55	437	10	491	10	89.0

LAS400_Shot_528_Grain_366	2.0814	1.4	0.12809	1.1	0.84	0.11773	0.75	1914	35	776	19	1135	21	68.4
LAS400_Shot_529_Grain_367	0.8209	1.0	0.07275	0.7	0.32	0.08254	0.99	1240	45	453	9	606	10	74.6
LAS400_Shot_530_Grain_368	1.0464	1.1	0.10499	0.8	0.43	0.07290	1.01	981	50	643	13	724	12	88.8
LAS400_Shot_531_Grain_369	0.6058	0.9	0.07304	0.6	0.24	0.06046	0.95	615	48	454	8	480	8	94.7
LAS400_Shot_532_Grain_370	1.7902	1.3	0.16651	1.1	0.78	0.07814	0.84	1130	42	991	24	1034	19	95.9
LAS400_Shot_533_Grain_371	1.3423	0.8	0.13022	0.7	0.23	0.07578	0.89	1072	43	789	15	862	12	91.5
LAS400_Shot_534_Grain_372	3.9013	0.7	0.26875	0.6	0.60	0.10629	0.60	1730	31	1533	26	1612	14	95.1
LAS400_Shot_535_Grain_373	3.0776	1.0	0.21818	0.9	0.79	0.10270	0.60	1664	32	1273	26	1422	17	89.5
LAS400_Shot_536_Grain_374	4.4744	1.2	0.22614	1.1	0.88	0.14429	0.56	2272	29	1311	31	1717	21	76.4
LAS400_Shot_537_Grain_375	0.7109	1.1	0.07501	0.8	0.37	0.06892	1.06	881	53	466	10	543	10	85.8
LAS400_Shot_538_Grain_376	3.3843	2.7	0.16693	2.1	0.97	0.14407	0.87	2262	38	989	41	1455	43	68.0
LAS400_Shot_539_Grain_377	2.8010	2.2	0.15795	1.5	0.93	0.12683	0.89	2040	39	942	30	1330	33	70.9
LAS400_Shot_540_Grain_378	1.4422	0.7	0.14525	0.6	0.52	0.07242	0.69	989	38	874	16	906	11	96.5
LAS400_Shot_547_Grain_379	1.5366	0.9	0.10401	1.1	0.64	0.10876	0.88	1760	39	637	16	942	13	67.6
LAS400_Shot_548_Grain_380	1.4048	0.9	0.09070	0.8	0.40	0.11308	0.96	1828	41	560	11	890	13	62.9
LAS400_Shot_549_Grain_381	2.0829	0.8	0.19910	0.8	0.38	0.07685	0.88	1100	42	1169	23	1144	12	102.2
LAS400_Shot_550_Grain_382	0.8498	1.1	0.08346	0.8	0.03	0.07397	1.25	1024	58	517	11	622	11	83.2
LAS400_Shot_551_Grain_383	1.3996	0.6	0.14146	0.5	0.43	0.07209	0.59	978	35	853	14	888	10	96.0
LAS400_Shot_552_Grain_384														
LAS400_Shot_553_Grain_385	7.2282	0.7	0.31629	0.7	0.67	0.16657	0.55	2517	28	1770	31	2136	16	82.8
LAS400_Shot_554_Grain_386	0.9896	0.8	0.09934	0.7	0.54	0.07258	0.72	987	39	610	12	697	10	87.6
LAS400_Shot_555_Grain_387	2.0727	1.3	0.19714	0.9	0.28	0.07748	1.34	1083	61	1158	25	1134	19	102.1
LAS400_Shot_556_Grain_388	3.1141	0.7	0.21828	0.7	0.66	0.10380	0.53	1690	30	1272	23	1433	14	88.7
LAS400_Shot_557_Grain_389	10.0019	0.6	0.38880	0.6	0.68	0.18778	0.49	2717	26	2118	34	2433	15	87.1
LAS400_Shot_558_Grain_390	2.0195	1.3	0.19499	1.0	0.33	0.07643	1.30	1076	59	1147	25	1118	19	102.5
LAS400_Shot_559_Grain_391	1.7716	0.5	0.16691	0.5	0.34	0.07733	0.60	1122	35	996	16	1034	10	96.3
LAS400_Shot_560_Grain_392	1.6788	0.7	0.16415	0.6	0.62	0.07450	0.59	1045	35	979	17	999	12	98.0
LAS400_Shot_567_Grain_393	8.9440	0.7	0.35071	0.7	0.51	0.18767	0.67	2714	30	1936	33	2334	16	82.9
LAS400_Shot_568_Grain_394	1.9508	0.9	0.17398	0.8	0.55	0.08199	0.81	1227	41	1033	20	1095	14	94.4
LAS400_Shot_569_Grain_395	1.4164	0.8	0.13287	0.6	0.55	0.07771	0.69	1132	36	804	14	895	11	89.9
LAS400_Shot_570_Grain_396	3.1423	1.2	0.22537	0.9	0.30	0.10287	1.34	1637	56	1308	28	1436	21	91.1
LAS400_Shot_571_Grain_397	0.6908	1.5	0.08568	0.8	0.16	0.05915	1.54	656	60	530	11	531	13	99.8
LAS400_Shot_572_Grain_398	3.5317	1.4	0.17921	1.1	0.86	0.14368	0.66	2262	31	1061	26	1524	23	69.6
LAS400_Shot_573_Grain_399	3.2933	0.7	0.26283	0.8	0.39	0.09210	0.85	1451	40	1503	28	1476	15	101.8
LAS400_Shot_574_Grain_400	11.9138	0.6	0.40974	0.7	0.68	0.21246	0.55	2918	27	2211	36	2594	16	85.2

LAS400_Shot_575_Grain_401	3.3282	0.7	0.23225	0.7	0.16	0.10449	0.62	1701	32	1345	24	1485	14	90.6
LAS400_Shot_576_Grain_402	1.9823	1.0	0.17083	0.8	0.41	0.08458	0.99	1288	46	1016	21	1105	15	91.9
LAS400_Shot_577_Grain_403	4.8661	0.7	0.21935	0.8	0.52	0.16290	0.73	2474	33	1277	24	1792	15	71.3
LAS400_Shot_578_Grain_404	5.5514	0.8	0.35349	0.7	0.05	0.11465	0.83	1858	37	1949	34	1904	17	102.4
LAS400_Shot_579_Grain_405	5.1136	0.7	0.32666	0.7	0.45	0.11482	0.75	1864	35	1820	32	1835	15	99.2
LAS400_Shot_580_Grain_406	1.6596	0.7	0.16346	0.7	0.66	0.07439	0.59	1042	35	975	18	992	12	98.3
LAS400_Shot_587_Grain_407	2.2062	0.9	0.20852	0.7	0.45	0.07772	0.89	1118	44	1222	23	1181	15	103.4
LAS400_Shot_588_Grain_408	2.2274	0.8	0.20663	0.7	0.43	0.07915	0.84	1160	42	1210	22	1187	14	101.9
LAS400_Shot_589_Grain_409	8.5864	0.9	0.35971	0.8	0.73	0.17468	0.64	2596	30	1978	37	2290	20	86.4
LAS400_Shot_590_Grain_410	10.7445	0.7	0.41973	0.7	0.58	0.18836	0.67	2718	30	2256	39	2498	17	90.3
LAS400_Shot_591_Grain_411	2.3236	1.3	0.20929	0.8	0.08	0.08193	1.24	1207	55	1224	25	1210	21	101.1
LAS400_Shot_592_Grain_412	4.2788	0.7	0.29054	0.8	0.53	0.10834	0.76	1766	36	1642	30	1686	15	97.4
LAS400_Shot_593_Grain_413	1.8658	0.8	0.18498	0.7	0.47	0.07425	0.77	1034	41	1093	20	1066	12	102.5
LAS400_Shot_594_Grain_414	10.5188	0.8	0.39968	0.9	0.59	0.19339	0.71	2763	32	2163	42	2478	18	87.3
LAS400_Shot_595_Grain_415	1.9191	0.7	0.18017	0.5	0.33	0.07842	0.74	1142	38	1067	18	1086	12	98.3
LAS400_Shot_596_Grain_416	4.2845	0.7	0.29351	0.6	0.46	0.10702	0.70	1737	34	1658	28	1688	15	98.2
LAS400_Shot_597_Grain_417	1.4871	1.7	0.13106	1.3	0.54	0.08326	1.39	1244	64	792	23	916	22	86.5
LAS400_Shot_598_Grain_418	1.4126	0.9	0.13316	0.5	0.30	0.07801	0.90	1128	45	806	14	893	12	90.3
LAS400_Shot_599_Grain_419	3.6661	0.7	0.26490	0.8	0.61	0.10125	0.70	1638	35	1516	29	1560	15	97.1
LAS400_Shot_600_Grain_420	1.3941	1.2	0.12919	1.0	0.65	0.07941	0.96	1157	46	782	18	883	16	88.7
LAS400_Shot_607_Grain_421	1.9361	1.0	0.19088	0.8	0.43	0.07440	0.93	1038	47	1125	23	1091	15	103.1
LAS400_Shot_608_Grain_422	1.6469	0.6	0.16198	0.5	0.42	0.07434	0.61	1042	36	968	16	987	10	98.1
LAS400_Shot_609_Grain_423	3.0683	0.7	0.24923	0.7	0.48	0.09037	0.72	1422	37	1433	26	1423	13	100.7
LAS400_Shot_610_Grain_424	0.7254	1.7	0.08814	1.1	0.12	0.06176	1.97	770	72	544	14	553	16	98.4
LAS400_Shot_611_Grain_425	2.6660	0.9	0.22115	0.8	0.37	0.08880	0.99	1374	45	1287	25	1314	16	97.9
LAS400_Shot_612_Grain_426	1.8241	0.8	0.17756	0.7	0.48	0.07525	0.77	1065	39	1053	19	1051	13	100.2
LAS400_Shot_613_Grain_427	1.8224	0.9	0.17611	0.7	0.38	0.07583	0.91	1075	45	1045	19	1050	14	99.5
LAS400_Shot_614_Grain_428	2.5837	1.2	0.22229	1.0	0.30	0.08551	1.25	1307	54	1292	28	1288	20	100.3
LAS400_Shot_615_Grain_429	1.2728	1.6	0.12648	1.1	0.32	0.07515	1.70	1062	67	767	19	827	20	92.7
LAS400_Shot_616_Grain_430	2.0715	0.7	0.18169	0.6	0.51	0.08372	0.66	1279	36	1076	19	1138	12	94.5
LAS400_Shot_617_Grain_431	3.0402	0.9	0.23961	0.7	0.49	0.09242	0.78	1463	38	1385	26	1413	15	98.0
LAS400_Shot_618_Grain_432														
LAS400_Shot_619_Grain_433	4.2927	1.0	0.18480	0.9	0.64	0.16939	0.77	2544	35	1092	23	1687	19	64.7
LAS400_Shot_620_Grain_434	2.1152	1.7	0.17821	1.4	0.91	0.08629	0.68	1335	36	1054	32	1140	24	92.4
LAS400_Shot_627_Grain_435	14.3266	0.8	0.53006	0.8	0.61	0.19772	0.71	2797	31	2736	49	2766	18	98.9

LAS400_Shot_628_Grain_436	1.8463	0.8	0.17937	0.8	0.41	0.07554	0.88	1068	43	1063	21	1059	13	100.3
LAS400_Shot_629_Grain_437	2.6218	4.0	0.11339	1.2	0.57	0.16198	3.45	2253	129	691	18	1220	59	56.7
LAS400_Shot_630_Grain_438	0.7028	2.6	0.08525	1.3	0.29	0.06038	2.51	866	85	527	15	529	22	99.6
LAS400_Shot_631_Grain_439	1.6240	1.1	0.15031	0.9	0.39	0.07966	1.10	1159	51	902	19	976	15	92.4
LAS400_Shot_632_Grain_440	3.0416	0.8	0.23937	0.8	0.52	0.09321	0.80	1475	39	1382	27	1414	15	97.7
LAS400_Shot_633_Grain_441	3.2493	0.8	0.22536	0.7	0.83	0.10554	0.75	1710	36	1309	24	1463	15	89.5
LAS400_Shot_634_Grain_442	3.5196	1.3	0.24392	1.0	0.41	0.10661	1.33	1707	52	1404	32	1523	23	92.2
LAS400_Shot_635_Grain_443	2.5410	0.8	0.15874	0.7	0.31	0.11747	0.89	1903	40	949	18	1282	14	74.0
LAS400_Shot_636_Grain_444	2.7621	0.7	0.23591	0.7	0.64	0.08566	0.56	1324	32	1364	24	1345	12	101.4
LAS400_Shot_637_Grain_445	3.8601	0.9	0.26448	0.8	0.73	0.10605	0.65	1730	32	1511	30	1600	17	94.4
LAS400_Shot_638_Grain_446	3.0699	0.7	0.21394	0.6	0.31	0.10471	0.75	1704	35	1250	22	1422	13	87.9
LAS400_Shot_639_Grain_447	2.9078	0.6	0.23216	0.5	0.55	0.09136	0.55	1450	32	1345	22	1383	12	97.3
LAS400_Shot_640_Grain_448	4.1017	0.7	0.29532	0.6	0.48	0.10102	0.61	1641	33	1669	27	1652	14	101.0
LAS400_Shot_647_Grain_449	3.2707	0.8	0.26817	0.7	0.53	0.08899	0.70	1394	36	1530	28	1470	15	104.0
LAS400_Shot_648_Grain_450	2.2936	1.1	0.20004	0.9	0.59	0.08359	0.92	1265	43	1174	24	1204	17	97.5
LAS400_Shot_649_Grain_451	0.7657	1.5	0.09189	0.8	0.34	0.06046	1.43	677	55	566	11	574	14	98.7
LAS400_Shot_650_Grain_452	0.9537	0.8	0.09993	0.6	0.35	0.06960	0.78	899	41	614	11	680	10	90.2
LAS400_Shot_651_Grain_453	2.2168	1.1	0.20199	0.8	0.32	0.08036	1.11	1182	50	1185	24	1181	17	100.3
LAS400_Shot_652_Grain_454	1.0732	1.2	0.11278	0.8	0.30	0.06975	1.23	903	57	688	14	739	13	93.1
LAS400_Shot_653_Grain_455	10.1866	0.6	0.40188	0.7	0.56	0.18522	0.59	2693	28	2175	36	2449	15	88.8
LAS400_Shot_654_Grain_456	3.4049	0.9	0.26530	0.7	0.37	0.09392	0.94	1491	43	1515	28	1502	17	100.9
LAS400_Shot_655_Grain_457	0.6019	0.9	0.07498	0.7	0.41	0.05856	0.87	551	44	466	9	477	8	97.6
LAS400_Shot_656_Grain_458	1.5777	0.8	0.11713	0.7	0.53	0.09823	0.75	1577	36	714	14	959	12	74.4
LAS400_Shot_657_Grain_459	4.0769	0.7	0.27143	0.7	0.59	0.10945	0.62	1781	32	1547	27	1647	15	93.9
LAS400_Shot_658_Grain_460	3.7639	0.7	0.24762	0.6	0.53	0.11042	0.62	1802	32	1425	25	1582	14	90.1
LAS400_Shot_659_Grain_461	1.1259	0.9	0.09903	0.9	0.62	0.08301	0.75	1260	38	608	14	764	11	79.7
LAS400_Shot_660_Grain_462	2.2316	1.7	0.12535	1.0	0.77	0.12866	1.08	2053	45	760	18	1177	24	64.6
LAS400_Shot_667_Grain_463	2.3754	1.0	0.19518	0.8	0.28	0.08832	0.91	1374	43	1148	23	1230	16	93.3
LAS400_Shot_668_Grain_464	1.9130	0.8	0.18036	0.7	0.41	0.07739	0.85	1117	44	1068	20	1084	13	98.6
LAS400_Shot_669_Grain_465	2.3307	1.0	0.19483	0.8	0.54	0.08634	0.85	1337	42	1146	23	1217	16	94.2
LAS400_Shot_670_Grain_466	0.8097	1.2	0.10140	0.8	0.15	0.05834	1.34	599	56	622	13	601	11	103.6
LAS400_Shot_671_Grain_467	8.9845	0.7	0.36931	0.7	0.78	0.17689	0.49	2618	27	2024	35	2332	17	86.8
LAS400_Shot_672_Grain_468	1.6178	0.8	0.16188	0.8	0.70	0.07270	0.62	994	36	966	20	976	11	99.0
LAS400_Shot_673_Grain_469	1.3942	0.6	0.14038	0.5	0.51	0.07215	0.57	983	35	847	14	886	10	95.6
LAS400_Shot_674_Grain_470	4.4356	0.8	0.20513	0.7	0.64	0.15689	0.65	2415	31	1202	23	1716	16	70.0

LAS400_Shot_675_Grain_471	4.4686	0.8	0.29390	0.7	0.44	0.11040	0.80	1796	37	1659	29	1720	16	96.5
LAS400_Shot_676_Grain_472	2.2632	1.2	0.20935	0.9	0.34	0.07909	1.18	1151	53	1224	26	1194	18	102.5
LAS400_Shot_677_Grain_473	4.8362	0.7	0.30705	0.7	0.56	0.11469	0.64	1868	31	1725	30	1788	14	96.4
LAS400_Shot_678_Grain_474	3.1731	0.7	0.22663	0.7	0.56	0.10181	0.67	1646	34	1316	24	1449	14	90.8
LAS400_Shot_679_Grain_475	2.6603	0.8	0.21774	0.8	0.40	0.08877	0.81	1388	40	1269	24	1314	14	96.5
LAS400_Shot_680_Grain_476	0.6099	2.3	0.06818	1.5	0.25	0.06632	2.51	919	89	425	14	477	19	89.0
LAS400_Shot_687_Grain_477	5.3843	0.7	0.28876	0.8	0.69	0.13555	0.63	2164	32	1633	31	1880	16	86.9
LAS400_Shot_688_Grain_478	8.5053	0.6	0.36779	0.7	0.49	0.16847	0.65	2533	30	2017	34	2284	15	88.3
LAS400_Shot_689_Grain_479	12.2371	0.8	0.47674	0.8	0.62	0.18689	0.73	2704	32	2512	46	2620	18	95.9
LAS400_Shot_690_Grain_480	2.2662	1.2	0.20425	0.9	0.39	0.08100	1.18	1189	52	1199	25	1198	18	100.0
LAS400_Shot_691_Grain_481	1.9631	1.1	0.18749	0.9	0.42	0.07608	1.10	1072	52	1108	24	1097	17	101.0
LAS400_Shot_692_Grain_482	1.9688	0.7	0.18568	0.7	0.60	0.07725	0.67	1120	37	1097	21	1103	13	99.4
LAS400_Shot_693_Grain_483	15.7328	0.9	0.55012	0.9	0.57	0.20841	0.77	2887	31	2819	53	2856	19	98.7
LAS400_Shot_694_Grain_484	1.8328	1.0	0.17556	0.8	0.42	0.07585	0.95	1070	47	1042	21	1053	15	98.9
LAS400_Shot_695_Grain_485	2.1602	1.6	0.17334	1.2	0.24	0.09241	1.79	1427	72	1028	27	1162	24	88.5
LAS400_Shot_696_Grain_486	2.9968	0.7	0.24299	0.7	0.60	0.08978	0.62	1410	34	1401	25	1404	13	99.8
LAS400_Shot_697_Grain_487	3.8252	0.7	0.25787	0.8	0.30	0.10827	0.69	1759	34	1477	28	1596	15	92.6
LAS400_Shot_698_Grain_488	5.9049	0.9	0.27539	0.8	0.66	0.15552	0.72	2396	32	1568	31	1956	18	80.2
LAS400_Shot_699_Grain_489	12.1300	0.6	0.48822	0.7	0.47	0.18045	0.66	2650	31	2560	41	2611	16	98.1
LAS400_Shot_700_Grain_490	3.1046	1.2	0.24514	1.0	0.34	0.09283	1.36	1442	58	1411	32	1426	21	98.9
LAS400_Shot_707_Grain_491	1.9255	1.4	0.14923	1.2	0.87	0.09352	0.70	1486	36	895	23	1081	21	82.8
LAS400_Shot_708_Grain_492	4.9373	1.1	0.31586	1.0	0.53	0.11422	1.03	1847	44	1765	39	1800	21	98.1
LAS400_Shot_709_Grain_493	4.2394	0.9	0.20077	0.8	0.72	0.15302	0.65	2378	29	1180	24	1676	17	70.4
LAS400_Shot_710_Grain_494	3.4484	0.8	0.16372	0.9	0.55	0.15329	0.76	2373	34	976	20	1511	15	64.6
LAS400_Shot_711_Grain_495	1.8749	1.0	0.17720	0.8	0.33	0.07691	0.91	1096	44	1052	22	1068	15	98.6
LAS400_Shot_712_Grain_496	5.0344	0.7	0.31594	0.7	0.51	0.11576	0.69	1883	33	1768	31	1822	15	97.0
LAS400_Shot_713_Grain_497	1.1470	0.8	0.12094	0.8	0.59	0.06944	0.79	893	42	735	15	775	11	94.9
LAS400_Shot_714_Grain_498	1.0746	1.0	0.10315	0.7	0.13	0.07621	1.14	1070	52	633	13	738	12	85.7
LAS400_Shot_715_Grain_499	3.8517	1.2	0.23004	1.0	0.51	0.12198	1.06	1963	45	1332	30	1599	20	83.3
LAS400_Shot_716_Grain_500														
LAS400_Shot_717_Grain_501	1.1489	1.2	0.11745	0.8	0.55	0.07102	1.01	941	49	715	15	774	15	92.5
LAS400_Shot_718_Grain_502	3.7949	1.0	0.19437	1.0	0.69	0.14246	0.77	2244	35	1143	25	1589	18	72.0
LAS400_Shot_719_Grain_503	1.3698	0.9	0.13040	0.6	0.29	0.07622	0.92	1081	45	790	14	873	12	90.4
LAS400_Shot_720_Grain_504	1.6516	1.6	0.15828	1.1	0.30	0.07672	1.62	1083	68	946	23	982	21	96.3
LAS400_Shot_727_Grain_505	8.5225	0.7	0.28874	0.6	0.63	0.21392	0.58	2930	28	1636	27	2285	16	71.6

LAS400_Shot_728_Grain_506	4.0634	0.9	0.21582	0.8	0.51	0.13694	0.80	2180	36	1260	24	1642	17	76.8
LAS400_Shot_729_Grain_507	1.1418	1.0	0.11883	0.9	0.63	0.06991	0.82	908	44	723	16	770	12	93.9
LAS400_Shot_730_Grain_508	9.6663	0.8	0.31359	0.9	0.72	0.22351	0.60	3007	29	1756	34	2397	18	73.2
LAS400_Shot_731_Grain_509	5.9608	0.8	0.26587	0.9	0.38	0.16430	0.98	2480	40	1517	32	1967	17	77.1
LAS400_Shot_732_Grain_510	1.0253	1.2	0.09882	0.9	0.31	0.07549	1.20	1049	57	607	13	713	13	85.2
LAS400_Shot_733_Grain_511	1.9899	1.6	0.18954	1.0	0.26	0.07662	1.65	1108	66	1117	25	1102	23	101.4
LAS400_Shot_734_Grain_512	1.6536	0.8	0.16211	0.7	0.37	0.07423	0.81	1032	42	968	18	988	12	97.9
LAS400_Shot_735_Grain_513	2.2931	0.6	0.19213	0.6	0.53	0.08683	0.60	1347	33	1132	19	1208	11	93.7
LAS400_Shot_736_Grain_514	1.4976	1.0	0.14585	0.7	0.28	0.07453	0.99	1036	48	877	16	926	13	94.7
LAS400_Shot_737_Grain_515	4.7666	0.9	0.21817	0.7	0.30	0.15823	0.71	2426	32	1271	24	1773	17	71.7
LAS400_Shot_738_Grain_516	1.3698	1.1	0.12865	0.8	0.27	0.07789	1.15	1111	53	780	15	872	14	89.4
LAS400_Shot_739_Grain_517	1.7600	1.0	0.17048	0.8	0.37	0.07533	1.03	1051	50	1014	20	1026	15	98.8
LAS400_Shot_740_Grain_518	1.9469	1.2	0.17371	0.9	0.27	0.08175	1.26	1206	58	1031	22	1090	18	94.6
LAS400_Shot_747_Grain_519	4.7546	0.7	0.30600	0.8	0.61	0.11318	0.66	1840	33	1719	32	1773	15	96.9
LAS400_Shot_748_Grain_520	0.9947	1.1	0.10091	0.7	-0.07	0.07171	1.20	949	54	619	12	698	13	88.8
LAS400_Shot_749_Grain_521	3.1125	0.9	0.21657	0.8	0.59	0.10456	0.84	1689	38	1262	25	1434	16	88.0
LAS400_Shot_750_Grain_522	4.0928	1.0	0.23545	0.8	0.73	0.12585	0.73	2028	35	1361	27	1647	19	82.6
LAS400_Shot_751_Grain_523	1.6448	0.9	0.15742	0.7	0.51	0.07609	0.86	1081	42	942	18	984	14	95.7
LAS400_Shot_752_Grain_524	3.0850	0.9	0.25322	0.8	0.16	0.08912	0.99	1387	44	1453	29	1426	16	101.9
LAS400_Shot_753_Grain_525	1.5331	1.1	0.14958	0.9	0.60	0.07432	0.91	1030	46	898	19	939	15	95.6
LAS400_Shot_754_Grain_526	1.1139	1.7	0.13187	1.1	0.02	0.06082	1.84	718	69	798	19	754	19	105.8
LAS400_Shot_755_Grain_527	1.0818	1.3	0.11219	1.1	0.71	0.06960	0.94	891	47	685	17	741	15	92.4
LAS400_Shot_756_Grain_528	5.0907	1.0	0.22947	0.9	0.82	0.16054	0.57	2454	29	1330	28	1827	19	72.8
LAS400_Shot_757_Grain_529	3.2737	0.5	0.22173	0.5	0.50	0.10684	0.48	1744	30	1292	21	1473	11	87.7
LAS400_Shot_758_Grain_530	2.4734	1.0	0.21001	0.8	0.28	0.08578	1.06	1313	48	1228	24	1260	17	97.4
LAS400_Shot_759_Grain_531	0.7708	2.3	0.08786	1.2	0.12	0.06443	2.45	897	81	542	14	579	20	93.7
LAS400_Shot_760_Grain_532	1.5719	1.1	0.14402	0.7	-0.01	0.07924	1.11	1154	51	867	16	956	16	90.7
LAS400_Shot_767_Grain_533	1.4184	1.0	0.12842	0.7	0.46	0.07994	0.94	1175	45	778	15	893	14	87.2
LAS400_Shot_768_Grain_534	3.1789	0.7	0.19276	0.6	0.27	0.11943	0.75	1937	36	1137	20	1450	13	78.4
LAS400_Shot_769_Grain_535	3.0524	0.9	0.19114	0.9	0.63	0.11583	0.75	1879	35	1126	24	1418	16	79.4
LAS400_Shot_770_Grain_536	0.9170	1.7	0.09792	1.4	0.50	0.06825	1.52	894	64	601	18	656	17	91.7
LAS400_Shot_771_Grain_537	1.7695	1.0	0.17508	0.8	0.36	0.07335	1.00	1000	48	1039	20	1030	14	100.8
LAS400_Shot_772_Grain_538	5.6874	1.2	0.25524	1.1	0.80	0.16052	0.74	2452	33	1462	35	1920	23	76.1
LAS400_Shot_773_Grain_539	2.2473	1.5	0.20669	1.0	0.32	0.07896	1.54	1135	64	1209	27	1184	23	102.2
LAS400_Shot_774_Grain_540	7.0498	0.8	0.32809	0.8	0.65	0.15569	0.66	2402	32	1827	34	2114	17	86.4

LAS400_Shot_775_ Grain_541	1.7082	0.8	0.15299	0.8	0.46	0.08098	0.84	1211	44	917	18	1011	13	90.7
LAS400_Shot_776_ Grain_542	2.1182	1.4	0.18392	1.0	0.23	0.08353	1.46	1224	64	1087	25	1147	21	94.8
LAS400_Shot_777_ Grain_543	1.4289	1.0	0.13644	0.7	0.26	0.07604	0.98	1083	45	824	15	898	13	91.8
LAS400_Shot_778_ Grain_544	2.9713	0.8	0.14191	0.9	0.63	0.15160	0.75	2354	34	855	19	1396	15	61.2
LAS400_Shot_779_ Grain_545	2.1460	1.2	0.19763	1.1	0.28	0.07827	1.24	1128	53	1166	24	1161	18	100.5
LAS400_Shot_780_ Grain_546	1.5050	1.1	0.13660	1.0	0.65	0.07939	0.91	1166	44	824	20	928	15	88.8
LAS400_Shot_787_ Grain_547	2.0196	0.9	0.18450	0.8	0.45	0.07885	0.84	1159	41	1091	21	1120	13	97.4
LAS400_Shot_788_ Grain_548	5.2640	1.1	0.25222	1.0	0.78	0.15056	0.71	2341	32	1447	32	1856	21	78.0
LAS400_Shot_789_ Grain_549	1.7966	1.0	0.16922	0.8	0.11	0.07613	0.96	1084	47	1009	21	1040	15	97.0
LAS400_Shot_790_ Grain_550	13.8414	0.9	0.54232	1.0	0.73	0.18451	0.73	2683	32	2789	57	2732	21	102.1
LAS400_Shot_791_ Grain_551	4.5285	0.7	0.28015	0.7	0.53	0.11633	0.76	1887	36	1590	29	1732	15	91.8
LAS400_Shot_792_ Grain_552	1.6778	0.6	0.15786	0.6	0.41	0.07660	0.66	1101	36	944	17	999	10	94.6
LAS400_Shot_793_ Grain_553	0.9837	1.6	0.09729	1.1	0.80	0.07218	0.96	969	47	598	15	692	17	86.4
LAS400_Shot_794_ Grain_554	0.6918	1.4	0.07896	0.8	0.14	0.06354	1.50	760	62	490	10	533	12	91.8
LAS400_Shot_795_ Grain_555	1.1889	0.9	0.12292	0.8	0.33	0.06961	1.01	895	49	747	15	795	12	94.0
LAS400_Shot_796_ Grain_556	11.3803	0.7	0.44098	0.7	0.56	0.18556	0.66	2694	30	2352	40	2550	17	92.2
LAS400_Shot_797_ Grain_557	5.2572	0.9	0.32816	0.9	0.56	0.11545	0.82	1874	37	1826	36	1861	17	98.1
LAS400_Shot_798_ Grain_558	2.7974	1.8	0.14709	1.3	0.73	0.13666	1.29	2148	52	883	24	1338	29	66.0
LAS400_Shot_799_ Grain_559	3.5144	0.6	0.24017	0.6	0.42	0.10513	0.63	1709	33	1387	23	1528	12	90.7
LAS400_Shot_800_ Grain_560	0.6745	0.8	0.07596	0.7	0.36	0.06418	0.89	731	46	472	9	523	8	90.2
LAS400_Shot_807_ Grain_561	9.4331	0.7	0.36049	0.6	0.63	0.18781	0.56	2716	27	1983	32	2378	16	83.4
LAS400_Shot_808_ Grain_562	1.6939	0.9	0.15470	0.7	0.01	0.07896	1.04	1150	44	927	17	1003	13	92.4
LAS400_Shot_809_ Grain_563	1.1706	1.1	0.11888	0.8	0.43	0.07092	1.08	932	51	724	15	785	14	92.2
LAS400_Shot_810_ Grain_564	8.3328	0.8	0.34112	0.8	0.61	0.17537	0.67	2602	31	1890	34	2263	17	83.5
LAS400_Shot_811_ Grain_565	8.7314	0.9	0.34411	0.8	0.31	0.18231	0.65	2665	30	1904	36	2304	19	82.6
LAS400_Shot_812_ Grain_566	2.1858	1.2	0.18193	0.9	0.66	0.08634	0.90	1324	43	1076	24	1170	18	92.0
LAS400_Shot_813_ Grain_567	7.5308	0.6	0.31796	0.7	0.64	0.17023	0.57	2555	28	1778	31	2174	14	81.8
LAS400_Shot_814_ Grain_568	1.3391	0.8	0.13028	0.7	0.61	0.07370	0.65	1021	37	789	15	861	11	91.7
LAS400_Shot_815_ Grain_569	8.2910	1.2	0.40087	0.9	0.77	0.14760	0.74	2306	34	2172	44	2251	24	96.5
LAS400_Shot_816_ Grain_570	1.5499	1.0	0.15120	0.7	0.49	0.07342	0.84	1008	45	907	18	947	13	95.8
LAS400_Shot_817_ Grain_571	4.9329	0.9	0.22180	0.8	0.71	0.15979	0.59	2448	29	1290	25	1805	17	71.5
LAS400_Shot_818_ Grain_572	2.5598	0.8	0.18510	0.7	0.43	0.09946	0.85	1599	39	1094	20	1286	14	85.1
LAS400_Shot_819_ Grain_573	2.1905	0.9	0.17353	0.8	0.43	0.09059	0.86	1425	41	1031	20	1174	14	87.8
LAS400_Shot_820_ Grain_574														
LAS400_Shot_827_ Grain_575	1.0992	1.6	0.13151	1.1	0.24	0.06045	1.67	709	63	795	20	745	18	106.7

LAS400_Shot_828_Grain_576	11.2698	0.8	0.44640	0.7	0.54	0.18122	0.72	2653	32	2382	39	2542	18	93.7
LAS400_Shot_829_Grain_577	5.7388	1.1	0.23334	1.0	0.81	0.17583	0.65	2607	31	1350	30	1928	21	70.0
LAS400_Shot_830_Grain_578	1.7929	1.3	0.17050	1.0	0.33	0.07592	1.36	1075	60	1013	24	1039	19	97.6
LAS400_Shot_831_Grain_579	12.3685	0.7	0.49736	0.7	0.61	0.17924	0.64	2637	30	2602	43	2630	17	98.9
LAS400_Shot_832_Grain_580	1.7814	0.8	0.17265	0.8	0.11	0.07390	0.69	1033	38	1026	20	1037	12	98.9
LAS400_Shot_833_Grain_581	5.5393	0.8	0.23527	0.8	0.54	0.16926	0.68	2540	31	1361	26	1902	17	71.5
LAS400_Shot_834_Grain_582	3.9665	0.9	0.26373	0.7	0.47	0.10812	0.86	1757	38	1507	28	1622	17	92.9
LAS400_Shot_835_Grain_583	1.3976	0.9	0.13962	0.8	0.47	0.07224	0.86	971	44	842	17	885	12	95.1
LAS400_Shot_836_Grain_584	2.0925	1.8	0.20160	1.2	0.18	0.07607	2.05	1083	75	1181	30	1133	26	104.3
LAS400_Shot_837_Grain_585	0.9987	1.2	0.09929	0.8	0.37	0.07199	1.11	970	51	610	13	702	12	86.8
LAS400_Shot_838_Grain_586	1.2451	1.4	0.13228	1.1	0.71	0.06771	1.00	838	49	800	20	816	17	98.0
LAS400_Shot_839_Grain_587	0.7353	2.1	0.08911	1.2	-0.03	0.06111	2.43	844	85	550	15	553	19	99.3
LAS400_Shot_840_Grain_588	3.1658	0.9	0.23480	0.7	0.64	0.09677	0.68	1550	35	1358	25	1444	16	94.0
LAS400_Shot_847_Grain_589	5.7095	0.7	0.31541	0.7	0.57	0.13051	0.66	2097	33	1768	31	1930	15	91.6
LAS400_Shot_848_Grain_590	13.6847	0.7	0.52547	0.7	0.64	0.18757	0.59	2713	28	2719	44	2724	16	99.8
LAS400_Shot_849_Grain_591	1.6493	0.7	0.13795	0.7	0.68	0.08636	0.55	1338	32	833	15	988	11	84.2
LAS400_Shot_850_Grain_592	1.0128	1.1	0.10457	0.7	0.12	0.07045	1.24	913	55	641	12	708	13	90.5
LAS400_Shot_851_Grain_593	3.1159	0.8	0.23195	0.7	0.49	0.09673	0.81	1546	38	1345	24	1434	16	93.8
LAS400_Shot_852_Grain_594	1.1324	0.9	0.11864	0.7	0.36	0.06893	0.89	874	45	722	14	767	11	94.2
LAS400_Shot_853_Grain_595	10.4200	0.9	0.41810	0.9	0.70	0.18039	0.68	2646	31	2247	45	2466	20	91.1
LAS400_Shot_854_Grain_596	2.0605	0.8	0.19512	0.8	0.50	0.07654	0.80	1091	41	1148	23	1133	13	101.3
LAS400_Shot_855_Grain_597	1.0515	1.4	0.09380	0.8	0.44	0.08031	1.19	1174	56	578	12	724	15	79.7
LAS400_Shot_856_Grain_598	9.7035	0.9	0.39993	0.9	0.41	0.17503	0.98	2594	40	2171	43	2400	19	90.5
LAS400_Shot_857_Grain_599	1.7898	0.6	0.15426	0.6	0.52	0.08369	0.64	1274	35	924	16	1042	11	88.7
LAS400_Shot_858_Grain_600	1.3412	1.1	0.13068	1.0	0.48	0.07489	1.04	1039	49	791	18	864	15	91.6
LAS400_Shot_859_Grain_601	3.4932	0.7	0.26479	0.7	0.65	0.09499	0.63	1517	34	1513	27	1523	14	99.3
LAS400_Shot_860_Grain_602	0.6702	2.0	0.07597	1.1	0.10	0.06447	2.14	873	75	472	12	519	17	90.9
LAS400_Shot_867_Grain_603	1.7258	0.9	0.16446	0.9	0.74	0.07633	0.67	1093	38	980	22	1016	14	96.5
LAS400_Shot_868_Grain_604	11.4713	0.8	0.44157	0.9	0.70	0.18905	0.66	2725	30	2353	45	2556	18	92.0
LAS400_Shot_869_Grain_605	5.1441	0.9	0.33384	0.9	0.43	0.11213	1.00	1811	42	1854	37	1837	18	100.9
LAS400_Shot_870_Grain_606	3.0867	1.0	0.19880	0.9	0.58	0.11244	0.84	1829	38	1168	24	1423	17	82.0
LAS400_Shot_871_Grain_607	3.3247	1.0	0.26241	0.9	0.44	0.09243	1.03	1450	45	1502	31	1483	18	101.3
LAS400_Shot_872_Grain_608	1.2764	0.9	0.12674	0.8	0.52	0.07296	0.86	994	45	769	15	832	12	92.4
LAS400_Shot_873_Grain_609	1.7950	1.0	0.16909	0.9	0.52	0.07695	0.91	1113	44	1006	21	1041	15	96.7
LAS400_Shot_874_Grain_610	5.5990	0.8	0.35316	0.8	0.60	0.11576	0.76	1881	35	1947	37	1912	17	101.8

LAS400_Shot_875_ Grain_611	2.5828	1.2	0.22129	1.0	0.36	0.08500	1.21	1288	53	1287	28	1290	19	99.8
LAS400_Shot_876_ Grain_612	1.7219	0.8	0.16603	0.7	0.70	0.07517	0.61	1062	35	989	19	1015	12	97.5
LAS400_Shot_877_ Grain_613	10.1132	0.7	0.39511	0.8	0.51	0.18549	0.82	2689	33	2143	39	2440	17	87.8
LAS400_Shot_878_ Grain_614	1.6330	1.2	0.15322	1.2	0.83	0.07729	0.66	1119	37	917	23	978	16	93.9
LAS400_Shot_879_ Grain_615	1.6828	1.1	0.13496	0.9	0.65	0.09040	0.87	1417	42	815	18	997	16	81.8
LAS400_Shot_880_ Grain_616	1.4508	0.8	0.14628	0.9	0.66	0.07224	0.71	978	39	879	18	908	12	96.9
LAS400_Shot_887_ Grain_617	0.7617	2.1	0.09394	1.4	0.23	0.05967	2.20	770	69	578	18	566	20	102.1
LAS400_Shot_888_ Grain_618	1.6327	1.3	0.16557	1.0	0.38	0.07209	1.35	954	61	986	23	978	18	100.9
LAS400_Shot_889_ Grain_619	2.6013	0.9	0.20954	0.7	0.25	0.09053	1.02	1418	46	1225	23	1299	16	94.3
LAS400_Shot_890_ Grain_620	3.5658	1.0	0.23153	0.9	0.76	0.11177	0.65	1823	32	1341	27	1535	18	87.3
LAS400_Shot_891_ Grain_621	2.3147	0.9	0.16643	0.6	0.35	0.10113	0.89	1625	41	992	18	1213	15	81.8
LAS400_Shot_892_ Grain_622	3.5476	0.8	0.24000	0.7	0.37	0.10766	0.87	1742	39	1385	25	1533	16	90.4
LAS400_Shot_893_ Grain_623	2.9799	0.8	0.23203	0.6	0.37	0.09357	0.77	1487	39	1344	23	1399	14	96.1
LAS400_Shot_894_ Grain_624	8.2555	0.7	0.34391	0.7	0.22	0.17422	0.63	2592	30	1903	33	2257	16	84.3
LAS400_Shot_895_ Grain_625	5.5186	1.3	0.26974	1.2	0.88	0.14807	0.61	2317	30	1535	37	1890	25	81.2
LAS400_Shot_896_ Grain_626	0.8687	1.4	0.09210	1.4	0.76	0.06891	0.94	870	47	567	17	631	14	89.9
LAS400_Shot_897_ Grain_627	2.6921	0.7	0.22537	0.7	0.38	0.08686	0.75	1345	39	1309	23	1323	13	98.9
LAS400_Shot_898_ Grain_628	1.6717	0.9	0.13891	0.7	0.36	0.08751	0.90	1351	42	838	15	994	13	84.3
LAS400_Shot_899_ Grain_629	1.7293	0.8	0.11427	0.7	0.26	0.11077	0.94	1796	40	697	13	1018	12	68.5
LAS400_Shot_900_ Grain_630	1.2742	1.4	0.11984	1.0	0.21	0.07776	1.57	1104	65	729	17	829	17	87.9
LAS400_Shot_907_ Grain_631	0.9162	1.2	0.09431	0.7	0.40	0.07084	1.12	926	54	581	11	658	13	88.2
LAS400_Shot_908_ Grain_632	1.8951	0.9	0.17961	0.8	0.39	0.07680	0.97	1090	46	1064	21	1075	14	98.9
LAS400_Shot_909_ Grain_633	2.3898	0.8	0.19422	0.7	0.48	0.08997	0.81	1411	39	1143	22	1237	13	92.4
LAS400_Shot_910_ Grain_634	0.7763	3.1	0.09395	1.5	0.02	0.06049	3.19	967	98	578	18	568	27	101.8
LAS400_Shot_911_ Grain_635	3.9953	0.8	0.18700	0.7	0.54	0.15540	0.73	2394	33	1104	20	1629	16	67.8
LAS400_Shot_912_ Grain_636	1.4534	0.9	0.14482	0.7	0.49	0.07277	0.78	996	41	871	16	910	12	95.8
LAS400_Shot_913_ Grain_637	1.2334	0.8	0.12500	0.6	0.37	0.07164	0.76	962	40	759	13	815	10	93.1
LAS400_Shot_914_ Grain_638	1.4264	1.0	0.13053	0.9	0.71	0.07931	0.70	1166	37	790	17	897	13	88.1
LAS400_Shot_915_ Grain_639	2.4346	1.0	0.20676	0.9	0.55	0.08610	0.94	1317	44	1212	27	1251	16	96.9
LAS400_Shot_916_ Grain_640	1.3528	1.3	0.11446	1.0	0.58	0.08577	1.03	1318	46	698	16	863	17	80.9
LAS400_Shot_917_ Grain_641	1.9663	0.8	0.18971	0.7	0.35	0.07565	0.83	1067	42	1119	20	1101	13	101.6
LAS400_Shot_918_ Grain_642	1.5723	0.9	0.15626	0.9	0.58	0.07358	0.81	1015	41	935	20	956	12	97.8
LAS400_Shot_919_ Grain_643	1.3798	0.8	0.13157	0.6	0.59	0.07592	0.61	1093	35	796	14	878	11	90.7
LAS400_Shot_920_ Grain_644	1.5846	0.7	0.15224	0.7	0.23	0.07540	0.65	1067	36	913	18	962	11	94.9
LAS400_Shot_927_ Grain_645	1.8183	0.8	0.17724	0.8	0.30	0.07506	0.95	1050	45	1051	20	1050	13	100.1

LAS400_Shot_928_ Grain_646	1.2912	0.8	0.13150	0.8	0.69	0.07129	0.60	960	36	796	16	840	11	94.8
LAS400_Shot_929_ Grain_647	2.6694	0.7	0.19187	0.7	0.68	0.10093	0.59	1634	33	1131	21	1317	14	85.8
LAS400_Shot_930_ Grain_648	2.7543	0.9	0.23316	0.7	0.28	0.08623	0.96	1323	44	1350	25	1340	15	100.7
LAS400_Shot_931_ Grain_649	1.6708	0.8	0.16322	0.6	0.13	0.07435	0.97	1032	47	974	17	995	13	97.9
LAS400_Shot_932_ Grain_650	3.8985	0.7	0.27608	0.6	0.35	0.10293	0.73	1670	36	1570	26	1610	14	97.5
LAS400_Shot_933_ Grain_651														
LAS400_Shot_934_ Grain_652	1.1732	1.0	0.12855	0.8	0.54	0.06639	0.84	801	43	779	16	786	12	99.1
LAS400_Shot_935_ Grain_653	1.5590	1.5	0.13015	1.0	0.21	0.08772	1.63	1326	69	789	19	945	20	83.6
LAS400_Shot_936_ Grain_654	6.0407	0.7	0.24928	0.7	0.64	0.17651	0.62	2612	29	1433	27	1978	15	72.5
LAS400_Shot_937_ Grain_655	1.9212	0.8	0.17794	0.7	0.64	0.07829	0.61	1148	36	1055	20	1086	12	97.2
LAS400_Shot_938_ Grain_656	1.3709	1.3	0.13807	1.0	0.32	0.07253	1.38	963	63	833	19	870	17	95.7
LAS400_Shot_939_ Grain_657	2.7523	0.9	0.22898	0.8	0.60	0.08774	0.78	1360	39	1328	27	1341	15	99.0
LAS400_Shot_940_ Grain_658	1.0262	0.9	0.11249	0.7	0.41	0.06655	0.93	802	48	687	13	715	11	96.1
LAS400_Shot_947_ Grain_659	1.1283	1.5	0.08787	1.0	0.86	0.09376	1.43	1458	58	543	12	760	17	71.4
LAS400_Shot_948_ Grain_660	1.7526	0.8	0.17365	0.8	0.67	0.07353	0.67	1016	37	1033	21	1025	13	100.7
LAS400_Shot_949_ Grain_661	0.7892	1.0	0.08899	0.7	0.50	0.06477	0.85	745	45	549	10	589	10	93.3
LAS400_Shot_950_ Grain_662	0.6215	1.0	0.07725	0.7	-0.07	0.05902	1.18	600	50	480	10	489	9	98.0
LAS400_Shot_951_ Grain_663	7.0592	0.9	0.30310	0.9	0.76	0.16911	0.60	2548	30	1704	34	2112	19	80.7
LAS400_Shot_952_ Grain_664	5.1804	0.9	0.24098	0.9	0.72	0.15710	0.64	2418	31	1390	29	1844	18	75.4
LAS400_Shot_953_ Grain_665	2.8405	0.5	0.21034	0.5	0.51	0.09820	0.48	1586	29	1230	19	1365	11	90.1
LAS400_Shot_954_ Grain_666	0.7629	1.2	0.07735	0.7	0.20	0.07225	1.26	974	54	480	9	573	12	83.8
LAS400_Shot_955_ Grain_667	8.8935	0.7	0.37287	0.8	0.56	0.17450	0.72	2593	31	2043	38	2324	17	87.9
LAS400_Shot_956_ Grain_668	2.4919	0.7	0.18056	0.6	0.43	0.10039	0.69	1627	35	1070	18	1267	13	84.4
LAS400_Shot_957_ Grain_669	4.2478	0.7	0.26277	0.6	0.12	0.11810	0.65	1917	32	1503	25	1683	14	89.3
LAS400_Shot_958_ Grain_670	4.5041	0.8	0.19641	0.7	0.63	0.16757	0.74	2522	32	1157	22	1730	16	66.9
LAS400_Shot_959_ Grain_671	1.4767	0.7	0.14362	0.6	0.56	0.07492	0.61	1058	35	866	15	920	11	94.1
LAS400_Shot_960_ Grain_672	1.4091	0.8	0.14460	0.8	0.53	0.07116	0.73	953	39	870	17	891	11	97.7
LAS400_Shot_967_ Grain_673	6.5270	0.7	0.26197	0.7	0.46	0.18216	0.69	2665	31	1499	26	2046	15	73.3
LAS400_Shot_968_ Grain_674	1.6445	1.0	0.16233	0.8	0.54	0.07399	0.93	1021	45	969	19	983	15	98.6
LAS400_Shot_969_ Grain_675	2.4721	1.2	0.13963	1.0	0.77	0.12903	0.74	2072	34	841	20	1256	19	67.0
LAS400_Shot_970_ Grain_676	0.8258	0.9	0.07464	0.7	0.38	0.08056	0.91	1195	46	464	9	609	10	76.1
LAS400_Shot_971_ Grain_677	5.5035	1.0	0.19458	0.8	0.70	0.20617	0.71	2865	31	1145	23	1894	20	60.5
LAS400_Shot_972_ Grain_678	0.5235	1.4	0.05850	0.8	0.15	0.06588	1.56	813	63	366	8	425	11	86.2
LAS400_Shot_973_ Grain_679	1.9646	0.8	0.16808	0.7	0.55	0.08532	0.71	1312	37	1001	19	1101	12	90.9
LAS400_Shot_974_ Grain_680	2.1525	0.7	0.13343	0.6	0.42	0.11830	0.76	1917	36	807	15	1164	13	69.3

LAS400_Shot_975_Grain_681	5.3200	0.6	0.22576	0.6	0.32	0.17267	0.72	2575	33	1311	23	1869	14	70.1
LAS400_Shot_976_Grain_682	0.6799	2.1	0.08066	1.2	0.17	0.06300	2.05	812	69	500	14	527	18	94.8
LAS400_Shot_977_Grain_683	2.5312	0.8	0.21400	0.8	0.62	0.08651	0.65	1343	35	1249	24	1280	14	97.5
LAS400_Shot_978_Grain_684	3.2795	1.1	0.15180	1.1	0.67	0.15751	0.88	2419	37	910	22	1468	19	62.0
LAS400_Shot_979_Grain_685	5.0559	0.7	0.24651	0.7	0.44	0.15015	0.75	2335	33	1419	26	1826	16	77.7
LAS400_Shot_980_Grain_686	2.4636	0.9	0.14887	0.7	0.40	0.12077	0.86	1956	39	894	17	1259	15	71.0
LAS400_Shot_987_Grain_687	0.9958	1.0	0.10705	0.8	0.43	0.06816	0.94	850	49	655	13	699	11	93.7
LAS400_Shot_988_Grain_688	3.7009	0.9	0.17169	0.7	0.46	0.15805	0.83	2422	37	1021	19	1566	17	65.2
LAS400_Shot_989_Grain_689	1.2123	1.0	0.11777	0.6	0.31	0.07515	0.97	1050	47	717	13	803	12	89.3
LAS400_Shot_990_Grain_690	1.9903	0.8	0.15851	0.7	0.51	0.09171	0.70	1451	37	948	17	1109	13	85.4
LAS400_Shot_991_Grain_691	1.4756	0.9	0.14945	0.6	0.42	0.07266	0.85	984	43	899	17	919	12	97.8
LAS400_Shot_992_Grain_692	4.3847	0.7	0.28561	0.6	0.48	0.11193	0.65	1826	33	1618	27	1706	15	94.9
LAS400_Shot_993_Grain_693	0.6248	0.9	0.07774	0.7	0.30	0.05909	0.97	571	47	482	9	492	8	98.2
LAS400_Shot_994_Grain_694	4.7760	0.9	0.30884	0.8	0.45	0.11322	0.93	1835	41	1732	33	1776	18	97.5
LAS400_Shot_995_Grain_695	0.6994	2.5	0.08543	1.5	0.18	0.06097	2.59	854	88	529	17	532	22	99.5
LAS400_Shot_996_Grain_696	2.2426	0.9	0.17636	0.7	0.34	0.09320	0.92	1470	43	1046	19	1190	15	87.9
LAS400_Shot_997_Grain_697	1.5600	0.9	0.15206	0.7	0.49	0.07494	0.84	1050	44	912	18	951	13	95.9
LAS400_Shot_998_Grain_698	3.2376	1.5	0.22950	1.2	0.44	0.10385	1.42	1656	58	1329	33	1452	25	91.5
LAS400_Shot_999_Grain_699	2.7872	0.8	0.19103	0.6	0.24	0.10634	0.85	1720	39	1126	19	1348	14	83.5
LAS400_Shot_1000_Grain_700	6.8761	0.8	0.29900	0.8	0.65	0.16827	0.67	2533	30	1687	30	2090	18	80.7

LAS401 (20BREMS1)														
	Isotopic Ratios							Calculated ages (Ma)						
ID	$^{207}Pb/^{235}U$	2σ	$^{206}Pb/^{238}U$	2σ	Rho	$^{207/206}Pb$	2σ	$^{207/206}Pb$	2σ	$^{206}Pb/^{238}U$	2σ	$^{207}Pb/^{235}U$	2σ	%conc
LAS401_Shot_1007_Grain_701	1.9169	0.6	0.18589	0.6	0.44	0.07531	0.59	1071	35	1099	18	1085	11	101.2
LAS401_Shot_1008_Grain_702														
LAS401_Shot_1009_Grain_703	0.6821	1.7	0.08031	1.0	0.11	0.06279	1.85	797	72	498	12	525	15	94.8
LAS401_Shot_1010_Grain_704	1.2903	1.5	0.09895	1.0	0.31	0.09616	1.53	1523	61	608	14	836	19	72.7
LAS401_Shot_1011_Grain_705	1.6484	1.3	0.15000	0.8	0.28	0.08026	1.31	1161	60	900	18	982	18	91.7
LAS401_Shot_1012_Grain_706	1.6804	1.0	0.15262	0.8	0.34	0.08109	1.07	1202	47	915	19	998	15	91.6
LAS401_Shot_1013_Grain_707	4.0777	1.4	0.24721	0.7	0.51	0.12013	1.25	1926	51	1423	25	1635	26	87.0
LAS401_Shot_1014_Grain_708	2.5424	2.7	0.20210	2.2	0.92	0.08940	0.99	1409	48	1177	50	1245	40	94.6
LAS401_Shot_1015_Grain_709	4.3898	0.6	0.29781	0.6	0.43	0.10794	0.64	1755	33	1679	28	1708	14	98.3
LAS401_Shot_1016_Grain_710	3.3768	0.8	0.24320	0.7	0.55	0.10106	0.67	1635	35	1402	25	1496	14	93.8

LAS401_Shot_1017_Grain_711	1.8821	1.2	0.16115	0.9	-0.07	0.08591	1.27	1294	55	962	21	1068	18	90.1
LAS401_Shot_1018_Grain_712	1.2144	0.8	0.10865	0.6	0.08	0.08207	0.98	1222	46	665	12	805	11	82.6
LAS401_Shot_1019_Grain_713	1.5787	1.2	0.14494	0.9	0.17	0.08016	1.39	1154	63	872	19	957	17	91.1
LAS401_Shot_1020_Grain_714	1.9704	0.7	0.18471	0.6	0.46	0.07805	0.73	1133	38	1092	19	1103	12	99.0
LAS401_Shot_1027_Grain_715	1.7501	0.9	0.16901	0.7	0.45	0.07588	0.85	1071	43	1006	18	1025	13	98.1
LAS401_Shot_1028_Grain_716	1.6168	0.8	0.14796	0.7	0.24	0.07993	0.93	1175	45	889	16	974	13	91.3
LAS401_Shot_1029_Grain_717	1.7347	0.7	0.16981	0.6	0.42	0.07471	0.73	1045	39	1011	18	1019	11	99.1
LAS401_Shot_1030_Grain_718	1.8744	2.0	0.13759	1.1	0.14	0.09926	2.09	1536	87	832	22	1054	27	78.9
LAS401_Shot_1031_Grain_719	1.5194	1.1	0.11985	0.8	0.43	0.09261	1.05	1459	48	729	15	935	16	78.0
LAS401_Shot_1032_Grain_720	1.2816	1.0	0.11912	0.7	0.39	0.07868	0.95	1143	46	725	13	835	13	86.8
LAS401_Shot_1033_Grain_721	2.1828	0.7	0.19377	0.6	0.26	0.08212	0.78	1238	40	1141	19	1173	13	97.3
LAS401_Shot_1034_Grain_722	1.3277	1.4	0.13662	0.9	0.11	0.07103	1.37	927	59	825	18	851	18	96.9
LAS401_Shot_1035_Grain_723	5.0964	0.6	0.32207	0.6	0.38	0.11556	0.67	1878	33	1800	30	1832	14	98.2
LAS401_Shot_1036_Grain_724														
LAS401_Shot_1037_Grain_725	1.7906	0.8	0.16906	0.6	0.36	0.07730	0.84	1113	43	1006	18	1039	13	96.9
LAS401_Shot_1038_Grain_726	1.2334	1.0	0.12685	0.8	0.45	0.07125	0.95	948	44	769	15	814	13	94.5
LAS401_Shot_1039_Grain_727	1.2920	1.2	0.12784	0.9	0.50	0.07361	1.10	1001	52	775	17	837	15	92.5
LAS401_Shot_1040_Grain_728	1.4989	1.9	0.14662	1.4	0.46	0.07577	1.80	1065	69	880	25	921	25	95.6
LAS401_Shot_1047_Grain_729	2.1970	1.4	0.20179	0.8	0.08	0.08013	1.58	1152	67	1184	24	1172	22	101.0
LAS401_Shot_1048_Grain_730	2.8070	0.7	0.24025	0.6	0.52	0.08558	0.66	1319	36	1387	24	1356	13	102.3
LAS401_Shot_1049_Grain_731	2.5349	0.8	0.22230	0.6	0.46	0.08356	0.74	1267	38	1293	23	1280	14	101.0
LAS401_Shot_1050_Grain_732	1.9305	1.1	0.18140	0.8	0.28	0.07852	1.18	1122	54	1074	21	1089	17	98.6
LAS401_Shot_1051_Grain_733	1.5772	0.9	0.15807	0.6	-0.06	0.07314	0.92	993	46	945	17	958	13	98.7
LAS401_Shot_1052_Grain_734	4.0786	1.0	0.22130	1.0	0.39	0.13570	1.11	2146	44	1287	28	1644	20	78.3
LAS401_Shot_1053_Grain_735	0.7860	0.9	0.08361	0.6	0.27	0.06899	0.95	880	47	517	10	589	9	87.9
LAS401_Shot_1054_Grain_736	1.1550	1.4	0.11186	0.9	0.33	0.07552	1.41	1048	64	683	15	774	16	88.3
LAS401_Shot_1055_Grain_737	11.5324	0.7	0.43868	0.9	0.48	0.19324	0.86	2755	35	2344	45	2562	17	91.5
LAS401_Shot_1056_Grain_738														
LAS401_Shot_1057_Grain_739														
LAS401_Shot_1058_Grain_740	12.0265	0.6	0.47835	0.7	0.53	0.18360	0.56	2681	29	2517	41	2603	16	96.7
LAS401_Shot_1059_Grain_741	3.0974	0.9	0.20981	0.8	0.30	0.10796	1.00	1745	44	1227	24	1427	17	86.0
LAS401_Shot_1060_Grain_742	1.7224	0.8	0.17263	0.7	0.31	0.07335	0.92	1000	45	1026	19	1015	13	101.0
LAS401_Shot_1067_Grain_743	3.2799	0.8	0.25712	0.6	0.33	0.09321	0.84	1480	40	1474	25	1474	15	100.0
LAS401_Shot_1068_Grain_744	2.1764	0.8	0.16174	0.7	0.57	0.09826	0.72	1578	36	966	18	1170	14	82.5
LAS401_Shot_1069_Grain_745														

LAS401_Shot_1070_Grain_746	1.7640	0.8	0.15796	0.7	0.30	0.08173	0.83	1223	42	945	17	1030	12	91.8
LAS401_Shot_1071_Grain_747	1.7806	0.9	0.17415	0.7	0.32	0.07488	0.95	1047	48	1036	19	1039	14	99.7
LAS401_Shot_1072_Grain_748	14.2068	0.8	0.51936	0.8	0.57	0.20037	0.74	2818	32	2692	47	2758	18	97.6
LAS401_Shot_1073_Grain_749	12.8905	0.6	0.49745	0.6	0.52	0.18895	0.61	2727	29	2600	41	2670	15	97.4
LAS401_Shot_1074_Grain_750	1.8295	1.0	0.17699	0.7	0.27	0.07594	1.07	1062	50	1050	20	1052	15	99.8
LAS401_Shot_1075_Grain_751	1.5965	1.0	0.15388	0.7	0.26	0.07613	1.12	1068	53	922	17	967	15	95.3
LAS401_Shot_1076_Grain_752	1.3242	1.0	0.13486	0.7	0.29	0.07168	1.07	945	50	815	15	854	13	95.4
LAS401_Shot_1077_Grain_753	1.1922	1.0	0.12812	0.7	0.24	0.06827	1.09	851	52	777	15	795	13	97.7
LAS401_Shot_1078_Grain_754	1.2203	1.1	0.12362	0.7	0.22	0.07230	1.17	976	54	751	14	807	14	93.0
LAS401_Shot_1079_Grain_755	1.5500	1.1	0.15555	0.8	0.40	0.07289	1.07	983	51	931	19	946	15	98.4
LAS401_Shot_1080_Grain_756	4.8716	0.7	0.30646	0.7	0.46	0.11640	0.72	1892	34	1724	30	1795	15	96.0
LAS401_Shot_1087_Grain_757	4.1874	0.7	0.28573	0.6	0.36	0.10737	0.72	1742	36	1619	27	1668	14	97.0
LAS401_Shot_1088_Grain_758	3.6490	0.8	0.25044	0.7	0.09	0.10639	0.79	1723	37	1440	25	1556	15	92.5
LAS401_Shot_1089_Grain_759	1.1844	1.7	0.10809	1.0	0.36	0.07978	1.58	1147	68	662	16	785	19	84.4
LAS401_Shot_1090_Grain_760	1.7726	1.0	0.17429	0.8	0.34	0.07475	1.01	1038	47	1036	21	1033	15	100.4
LAS401_Shot_1091_Grain_761	4.4770	0.5	0.29870	0.6	0.50	0.10945	0.56	1785	30	1684	28	1725	12	97.6
LAS401_Shot_1092_Grain_762	1.5205	0.7	0.15079	0.6	0.32	0.07370	0.77	1016	41	905	16	937	11	96.6
LAS401_Shot_1093_Grain_763	2.9641	0.7	0.21742	0.6	0.49	0.09923	0.69	1597	35	1268	21	1395	14	90.8
LAS401_Shot_1094_Grain_764	2.1041	1.0	0.16188	0.5	0.41	0.09482	0.91	1514	42	967	16	1146	15	84.4
LAS401_Shot_1095_Grain_765	2.6779	0.9	0.20881	0.7	0.45	0.09378	0.85	1488	41	1221	23	1319	15	92.6
LAS401_Shot_1096_Grain_766	1.7028	1.9	0.16539	1.1	0.10	0.07582	2.09	1109	79	987	24	997	26	99.0
LAS401_Shot_1097_Grain_767	12.4550	0.7	0.47642	0.7	0.47	0.19134	0.77	2741	33	2508	43	2637	18	95.1
LAS401_Shot_1098_Grain_768	7.3144	0.5	0.33056	0.6	0.29	0.16152	0.66	2462	31	1840	29	2148	14	85.6
LAS401_Shot_1099_Grain_769	1.7344	0.7	0.16660	0.6	0.45	0.07611	0.71	1084	37	993	17	1021	12	97.2
LAS401_Shot_1100_Grain_770														
LAS401_Shot_1107_Grain_771	1.8176	1.3	0.17937	0.9	0.33	0.07445	1.38	1017	60	1064	23	1046	19	101.7
LAS401_Shot_1108_Grain_772	0.9117	2.1	0.08967	1.3	0.23	0.07588	2.26	1101	83	553	16	650	21	85.1
LAS401_Shot_1109_Grain_773	1.4132	0.9	0.13767	0.6	0.23	0.07526	0.98	1048	47	831	15	893	13	93.1
LAS401_Shot_1110_Grain_774	4.0327	0.9	0.26458	0.7	0.35	0.11157	0.93	1808	42	1512	27	1636	18	92.4
LAS401_Shot_1111_Grain_775														
LAS401_Shot_1112_Grain_776	2.0154	1.8	0.08137	1.0	0.35	0.17895	1.61	2608	59	504	12	1108	25	45.5
LAS401_Shot_1113_Grain_777	4.9617	0.7	0.31518	0.6	0.47	0.11502	0.70	1871	33	1765	29	1812	16	97.4
LAS401_Shot_1114_Grain_778	0.8606	2.0	0.09010	1.1	0.22	0.07061	2.05	987	78	557	14	626	20	89.0
LAS401_Shot_1115_Grain_779	1.6011	0.8	0.15070	0.6	0.34	0.07746	0.86	1113	42	904	16	968	12	93.4
LAS401_Shot_1116_Grain_780	0.6835	2.1	0.07460	1.1	0.09	0.06765	2.23	982	75	463	12	521	18	88.9

LAS401_Shot_1117_Grain_781	2.3294	1.7	0.21283	1.2	0.55	0.07994	1.44	1148	62	1244	32	1209	25	102.9
LAS401_Shot_1118_Grain_782	1.7892	1.4	0.17687	0.9	0.03	0.07501	1.62	1022	67	1049	23	1037	20	101.1
LAS401_Shot_1119_Grain_783	1.4031	0.8	0.13953	0.5	0.16	0.07306	0.85	1010	43	842	14	888	11	94.8
LAS401_Shot_1120_Grain_784	2.3736	0.9	0.16824	0.7	0.30	0.10324	1.02	1662	44	1002	19	1230	16	81.4
LAS401_Shot_1127_Grain_785														
LAS401_Shot_1128_Grain_786	2.5824	0.9	0.18319	0.8	0.54	0.10290	0.85	1662	40	1083	22	1292	16	83.8
LAS401_Shot_1129_Grain_787	1.6101	1.0	0.15668	0.8	0.37	0.07513	1.05	1046	48	938	18	970	14	96.7
LAS401_Shot_1130_Grain_788	7.7676	1.0	0.31188	0.9	0.83	0.18123	0.59	2656	29	1747	35	2197	21	79.5
LAS401_Shot_1131_Grain_789	1.6317	0.9	0.13604	0.7	0.46	0.08723	0.86	1349	42	822	16	982	14	83.7
LAS401_Shot_1132_Grain_790	2.0683	0.9	0.17507	0.7	0.13	0.08630	1.08	1319	49	1039	20	1136	15	91.5
LAS401_Shot_1133_Grain_791	1.8575	0.9	0.17461	0.7	0.33	0.07780	0.95	1117	45	1037	19	1062	14	97.6
LAS401_Shot_1134_Grain_792	1.9978	1.3	0.19320	1.0	0.36	0.07569	1.27	1063	58	1137	26	1109	19	102.5
LAS401_Shot_1135_Grain_793	4.2673	0.6	0.26686	0.6	-0.19	0.11629	0.68	1889	33	1524	25	1684	14	90.5
LAS401_Shot_1136_Grain_794	0.9799	1.7	0.10075	1.1	0.15	0.07091	1.76	993	74	618	15	688	19	89.9
LAS401_Shot_1137_Grain_795	3.8560	0.6	0.23524	0.6	0.24	0.11933	0.81	1933	37	1361	24	1602	14	85.0
LAS401_Shot_1138_Grain_796	1.4314	1.3	0.14523	0.8	0.25	0.07160	1.30	957	59	875	18	896	17	97.6
LAS401_Shot_1139_Grain_797	1.8357	0.9	0.17720	0.6	-0.06	0.07497	0.76	1051	40	1051	18	1052	11	99.9
LAS401_Shot_1140_Grain_798	1.9041	0.9	0.17116	0.7	0.37	0.08160	0.93	1221	43	1018	19	1082	14	94.1
LAS401_Shot_1147_Grain_799	1.7907	1.6	0.17329	0.9	0.21	0.07534	1.72	1057	69	1029	22	1033	23	99.6
LAS401_Shot_1148_Grain_800	2.5893	0.9	0.22300	0.7	0.22	0.08406	0.99	1278	49	1297	24	1294	16	100.2
LAS401_Shot_1149_Grain_801	8.3929	0.7	0.41211	0.7	0.11	0.14768	0.63	2312	31	2222	37	2271	16	97.9
LAS401_Shot_1150_Grain_802	2.9141	0.6	0.23631	0.6	0.55	0.08942	0.55	1407	31	1368	23	1384	12	98.9
LAS401_Shot_1151_Grain_803	1.7473	0.7	0.13129	0.7	0.27	0.09701	0.86	1555	40	795	15	1024	12	77.6
LAS401_Shot_1152_Grain_804	4.3512	1.1	0.24234	0.6	0.35	0.13033	1.03	2082	43	1398	23	1695	20	82.5
LAS401_Shot_1153_Grain_805	14.3208	0.7	0.53879	0.7	0.46	0.19306	0.69	2761	31	2774	45	2767	17	100.3
LAS401_Shot_1154_Grain_806	0.9545	1.3	0.09838	0.8	0.12	0.07070	1.43	946	59	605	13	679	14	89.0
LAS401_Shot_1155_Grain_807	1.8827	0.8	0.17985	0.6	0.18	0.07596	0.90	1074	45	1066	18	1072	13	99.4
LAS401_Shot_1156_Grain_808	1.5887	1.6	0.16348	0.9	0.20	0.07101	1.67	938	67	977	21	956	21	102.2
LAS401_Shot_1157_Grain_809	4.7346	0.6	0.30705	0.6	0.51	0.11185	0.60	1821	31	1725	28	1770	14	97.4
LAS401_Shot_1158_Grain_810	1.7646	0.8	0.17175	0.6	0.47	0.07451	0.76	1042	40	1021	18	1031	13	99.1
LAS401_Shot_1159_Grain_811	0.7959	0.9	0.09481	0.6	0.35	0.06087	0.90	623	46	584	11	594	9	98.3
LAS401_Shot_1160_Grain_812	1.8384	1.5	0.18018	0.9	0.27	0.07449	1.54	1018	64	1067	23	1049	21	101.7
LAS401_Shot_1167_Grain_813	1.7598	0.9	0.17219	0.6	0.29	0.07387	0.87	1023	45	1024	18	1029	13	99.5
LAS401_Shot_1168_Grain_814	2.6162	0.7	0.21572	0.6	0.43	0.08751	0.68	1362	35	1259	21	1303	13	96.6
LAS401_Shot_1169_Grain_815	13.2446	0.6	0.49793	0.6	0.55	0.19199	0.58	2752	28	2602	40	2694	15	96.6

LAS401_Shot_1170_Grain_816														
LAS401_Shot_1171_Grain_817	3.6981	0.6	0.24364	0.5	0.57	0.10992	0.52	1791	29	1405	22	1569	13	89.6
LAS401_Shot_1172_Grain_818	1.9435	1.5	0.18260	1.0	0.20	0.07722	1.61	1092	69	1080	24	1086	22	99.4
LAS401_Shot_1173_Grain_819	1.2485	1.3	0.09258	0.9	0.21	0.09811	1.43	1546	58	570	12	819	16	69.7
LAS401_Shot_1174_Grain_820	1.1966	1.0	0.11199	0.7	0.23	0.07791	1.09	1120	50	684	13	797	13	85.8
LAS401_Shot_1175_Grain_821	13.2647	0.8	0.51761	0.7	0.50	0.18519	0.74	2691	33	2685	45	2693	18	99.7
LAS401_Shot_1176_Grain_822	8.9548	0.6	0.35797	0.6	0.44	0.18083	0.66	2651	31	1971	32	2331	15	84.5
LAS401_Shot_1177_Grain_823	1.5329	1.4	0.14379	0.9	0.15	0.07752	1.57	1094	66	865	19	938	18	92.3
LAS401_Shot_1178_Grain_824	1.8859	0.7	0.18132	0.5	0.38	0.07509	0.67	1063	38	1074	18	1074	11	100.0
LAS401_Shot_1179_Grain_825	1.1299	1.8	0.10654	1.2	0.59	0.07666	1.47	1071	63	653	17	760	21	86.0
LAS401_Shot_1180_Grain_826	0.6150	1.2	0.07281	0.7	0.18	0.06127	1.35	686	56	453	9	484	10	93.5
LAS401_Shot_1187_Grain_827	11.3596	0.4	0.44429	0.5	0.59	0.18430	0.44	2687	25	2368	35	2552	13	92.8
LAS401_Shot_1188_Grain_828	1.6250	1.4	0.15801	0.8	0.26	0.07442	1.46	1016	63	945	19	972	19	97.2
LAS401_Shot_1189_Grain_829	8.8715	1.2	0.42287	0.9	0.56	0.15053	0.79	2338	34	2269	43	2314	23	98.1
LAS401_Shot_1190_Grain_830	2.2104	3.3	0.20772	1.7	0.13	0.07795	3.26	1305	100	1211	40	1137	48	106.5
LAS401_Shot_1191_Grain_831	1.8210	0.8	0.17459	0.5	0.24	0.07521	0.85	1057	42	1037	17	1050	13	98.8
LAS401_Shot_1192_Grain_832	1.8663	1.2	0.18280	0.7	0.34	0.07381	1.18	997	54	1081	21	1063	17	101.7
LAS401_Shot_1193_Grain_833	1.7538	0.8	0.17206	0.6	0.24	0.07396	0.94	1023	45	1023	18	1028	13	99.5
LAS401_Shot_1194_Grain_834	2.2565	0.6	0.19869	0.5	0.48	0.08165	0.56	1228	33	1168	19	1198	11	97.5
LAS401_Shot_1195_Grain_835	6.8876	0.6	0.28514	0.6	0.51	0.17351	0.59	2586	29	1616	27	2094	14	77.2
LAS401_Shot_1196_Grain_836	4.5962	0.8	0.27769	0.7	0.29	0.12005	0.95	1936	41	1578	28	1745	17	90.4
LAS401_Shot_1197_Grain_837	4.6220	0.6	0.28872	0.5	0.47	0.11572	0.62	1882	32	1634	26	1750	14	93.4
LAS401_Shot_1198_Grain_838	1.9122	0.7	0.17804	0.6	-0.04	0.07855	1.41	1122	30	1056	18	1083	12	97.5
LAS401_Shot_1199_Grain_839	5.4363	0.9	0.33883	0.8	0.27	0.11686	1.02	1884	44	1878	36	1888	17	99.5
LAS401_Shot_1200_Grain_840	4.4538	0.7	0.29796	0.6	0.36	0.10797	0.76	1754	37	1680	29	1719	15	97.7
LAS401_Shot_1207_Grain_841	4.6561	0.7	0.30733	0.6	0.35	0.10950	0.72	1784	35	1726	28	1756	15	98.3
LAS401_Shot_1208_Grain_842	1.8535	1.0	0.17865	0.7	0.13	0.07483	1.16	1039	56	1060	20	1061	15	99.9
LAS401_Shot_1209_Grain_843	2.1210	0.7	0.19351	0.7	0.36	0.07961	0.83	1169	41	1140	21	1153	13	98.8
LAS401_Shot_1210_Grain_844	1.5145	1.1	0.15671	0.8	0.20	0.07045	1.20	915	54	938	19	936	15	100.2
LAS401_Shot_1211_Grain_845	1.5113	1.1	0.15422	0.8	0.25	0.07113	1.21	932	56	924	18	930	15	99.3
LAS401_Shot_1212_Grain_846	1.2054	0.9	0.12976	0.8	0.41	0.06741	0.92	834	45	786	15	801	12	98.1
LAS401_Shot_1213_Grain_847	4.4880	0.9	0.29915	0.8	0.36	0.10878	0.96	1760	43	1685	32	1723	18	97.8
LAS401_Shot_1214_Grain_848	1.8383	0.6	0.17631	0.6	0.44	0.07541	0.63	1073	35	1047	18	1058	11	99.0
LAS401_Shot_1215_Grain_849	1.6248	0.7	0.15192	0.6	0.44	0.07757	0.66	1123	36	911	16	978	11	93.2
LAS401_Shot_1216_Grain_850	0.7053	0.8	0.07125	0.6	0.37	0.07197	0.82	977	40	444	8	542	8	81.8

LAS401_Shot_1217_Grain_851	2.4028	1.0	0.17033	0.8	0.15	0.10251	1.17	1644	51	1013	20	1238	17	81.8
LAS401_Shot_1218_Grain_852	1.1670	1.1	0.11921	0.6	0.13	0.07119	1.22	925	57	726	13	782	13	92.9
LAS401_Shot_1219_Grain_853	0.8035	1.2	0.07581	0.6	0.02	0.07697	1.31	1083	61	472	9	597	12	79.0
LAS401_Shot_1220_Grain_854	1.8585	0.8	0.18169	0.7	0.46	0.07419	0.80	1035	40	1075	20	1063	13	101.1
LAS401_Shot_1227_Grain_855	4.0891	1.0	0.29044	0.8	0.28	0.10255	1.05	1652	45	1642	31	1646	18	99.7
LAS401_Shot_1228_Grain_856	4.9984	1.0	0.31678	0.8	0.30	0.11509	1.04	1864	44	1772	33	1814	19	97.7
LAS401_Shot_1229_Grain_857	4.0681	0.8	0.29509	0.6	0.25	0.10021	0.87	1613	39	1666	28	1644	15	101.3
LAS401_Shot_1230_Grain_858	2.6883	0.7	0.22077	0.6	0.49	0.08831	0.64	1381	35	1285	22	1323	13	97.2
LAS401_Shot_1231_Grain_859	1.8891	1.0	0.17876	0.7	0.35	0.07703	1.02	1093	48	1059	20	1075	15	98.5
LAS401_Shot_1232_Grain_860	2.2349	0.7	0.20105	0.6	0.30	0.08064	0.77	1200	39	1180	20	1190	12	99.2
LAS401_Shot_1233_Grain_861	1.6034	1.0	0.15724	0.7	0.20	0.07421	1.15	1016	53	941	18	969	14	97.1
LAS401_Shot_1234_Grain_862	1.7051	0.9	0.17027	0.7	0.30	0.07329	1.01	993	49	1013	19	1008	14	100.5
LAS401_Shot_1235_Grain_863	15.2812	0.6	0.54991	0.6	0.47	0.20208	0.63	2837	30	2821	44	2831	16	99.7
LAS401_Shot_1236_Grain_864	1.9612	1.0	0.18988	0.7	0.31	0.07473	0.96	1047	48	1121	21	1098	15	102.1
LAS401_Shot_1237_Grain_865	1.6634	0.8	0.15730	0.6	0.37	0.07665	0.77	1098	41	941	16	992	12	94.9
LAS401_Shot_1238_Grain_866	3.0098	10.3	0.23531	4.8	-0.99	0.08675	2.55	1255	64	1300	36	1280	23	101.6
LAS401_Shot_1239_Grain_867	2.0184	1.3	0.18639	0.7	0.27	0.07858	1.28	1133	56	1101	21	1114	19	98.8
LAS401_Shot_1240_Grain_868	3.2556	0.8	0.22475	0.7	0.50	0.10518	0.79	1702	37	1306	24	1469	16	88.9
LAS401_Shot_1247_Grain_869	10.3972	0.5	0.43971	0.6	0.58	0.17204	0.52	2573	27	2347	37	2469	14	95.0
LAS401_Shot_1248_Grain_870	1.9273	0.8	0.18129	0.6	0.25	0.07740	0.85	1122	43	1073	18	1089	13	98.6
LAS401_Shot_1249_Grain_871	4.6935	1.0	0.31017	0.9	0.36	0.11086	1.11	1788	47	1739	35	1760	20	98.8
LAS401_Shot_1250_Grain_872	1.9746	1.0	0.17378	0.7	0.43	0.08299	1.03	1240	48	1032	20	1105	16	93.4
LAS401_Shot_1251_Grain_873	11.2157	0.6	0.47033	0.6	0.62	0.17325	0.51	2585	27	2482	39	2538	15	97.8
LAS401_Shot_1252_Grain_874	4.6834	0.9	0.30713	0.8	0.34	0.11138	0.96	1807	42	1724	33	1760	17	97.9
LAS401_Shot_1253_Grain_875	0.7509	3.0	0.09703	1.4	-0.06	0.05813	3.25	936	96	596	18	551	27	108.2
LAS401_Shot_1254_Grain_876	1.8130	1.1	0.17668	0.7	0.16	0.07484	1.17	1026	54	1048	19	1045	16	100.3
LAS401_Shot_1255_Grain_877	1.6542	0.7	0.16384	0.6	0.45	0.07354	0.70	1015	38	978	17	989	12	98.9
LAS401_Shot_1256_Grain_878	1.8905	1.2	0.17052	0.8	0.36	0.08103	1.19	1188	55	1014	21	1073	18	94.5
LAS401_Shot_1257_Grain_879	1.5418	1.0	0.15887	0.6	0.26	0.07076	1.01	926	48	950	17	944	14	100.7
LAS401_Shot_1258_Grain_880	1.1232	1.5	0.12337	1.0	0.13	0.06722	1.68	875	66	749	18	763	17	98.2
LAS401_Shot_1259_Grain_881	2.5796	0.8	0.21077	0.7	0.37	0.08926	0.85	1398	40	1232	22	1294	14	95.2
LAS401_Shot_1260_Grain_882	5.0385	0.6	0.31380	0.6	0.36	0.11705	0.70	1900	34	1758	30	1823	14	96.4
LAS401_Shot_1267_Grain_883	1.5847	0.6	0.15537	0.5	0.33	0.07414	0.68	1034	38	931	15	963	11	96.7
LAS401_Shot_1268_Grain_884	2.3647	1.0	0.21578	0.8	0.57	0.07982	0.86	1172	43	1258	24	1227	16	102.6
LAS401_Shot_1269_Grain_885	1.7946	1.0	0.18011	0.7	0.38	0.07245	0.94	985	47	1067	20	1039	15	102.7

LAS401_Shot_1270_Grain_886	11.8314	0.7	0.47075	0.8	0.11	0.18373	0.75	2680	31	2483	43	2586	17	96.0
LAS401_Shot_1271_Grain_887	2.4607	1.1	0.21152	0.8	0.38	0.08507	1.10	1294	49	1236	24	1258	17	98.3
LAS401_Shot_1272_Grain_888														
LAS401_Shot_1273_Grain_889	1.7155	0.7	0.16959	0.6	0.45	0.07377	0.68	1024	38	1009	18	1012	11	99.7
LAS401_Shot_1274_Grain_890	4.3591	0.6	0.29660	0.6	0.53	0.10706	0.62	1742	33	1673	27	1702	14	98.3
LAS401_Shot_1275_Grain_891	2.0342	0.8	0.19259	0.7	0.41	0.07705	0.79	1105	41	1135	21	1125	13	100.8
LAS401_Shot_1276_Grain_892	9.0973	0.6	0.39288	0.6	0.51	0.16953	0.58	2546	29	2134	34	2346	15	91.0
LAS401_Shot_1277_Grain_893	9.5884	0.7	0.37178	0.7	0.45	0.18938	0.74	2730	32	2035	36	2392	16	85.1
LAS401_Shot_1278_Grain_894	4.8839	0.8	0.31679	0.6	0.42	0.11264	0.74	1832	35	1773	30	1795	16	98.7
LAS401_Shot_1279_Grain_895	1.7835	1.5	0.17282	1.0	0.35	0.07606	1.51	1067	64	1026	24	1032	21	99.5
LAS401_Shot_1280_Grain_896	1.6160	1.2	0.16113	0.8	0.19	0.07389	1.35	1003	61	962	20	972	17	99.0
LAS401_Shot_1287_Grain_897	2.1782	0.7	0.19340	0.6	0.47	0.08267	0.66	1249	36	1139	20	1172	12	97.2
LAS401_Shot_1288_Grain_898	4.7036	0.8	0.31039	0.7	0.36	0.11069	0.78	1799	36	1743	29	1764	16	98.8
LAS401_Shot_1289_Grain_899	1.8490	0.9	0.18365	0.7	0.42	0.07391	0.93	1019	45	1086	20	1059	15	102.6
LAS401_Shot_1290_Grain_900	1.7178	0.9	0.17194	0.7	0.27	0.07322	0.91	1000	46	1022	18	1012	13	101.0
LAS401_Shot_1291_Grain_901	1.7432	0.8	0.16799	0.6	0.43	0.07588	0.78	1077	41	1000	18	1022	13	97.9
LAS401_Shot_1292_Grain_902	1.7730	0.9	0.17120	0.8	0.31	0.07612	0.99	1076	45	1018	20	1033	14	98.5
LAS401_Shot_1293_Grain_903	0.8010	2.1	0.09744	1.2	0.19	0.06107	2.18	752	77	599	16	593	19	101.0
LAS401_Shot_1294_Grain_904	4.9691	1.1	0.33772	0.9	0.27	0.10875	1.18	1749	49	1872	38	1807	21	103.6
LAS401_Shot_1295_Grain_905	3.7578	1.2	0.28347	0.9	0.33	0.09808	1.24	1554	53	1606	34	1579	21	101.7
LAS401_Shot_1296_Grain_906	13.9586	0.7	0.54472	0.7	0.10	0.18795	0.67	2715	31	2799	47	2743	16	102.0
LAS401_Shot_1297_Grain_907														
LAS401_Shot_1298_Grain_908	1.8241	1.1	0.17734	0.7	0.29	0.07550	1.10	1051	53	1052	20	1049	16	100.3
LAS401_Shot_1299_Grain_909	1.6452	0.9	0.16115	0.7	0.49	0.07500	0.81	1050	41	962	18	987	13	97.5
LAS401_Shot_1300_Grain_910	2.1445	0.7	0.19797	0.6	0.54	0.07952	0.60	1177	35	1164	20	1161	12	100.2
LAS401_Shot_1307_Grain_911	9.0862	0.7	0.38913	0.6	0.45	0.17093	0.63	2560	31	2119	34	2344	16	90.4
LAS401_Shot_1308_Grain_912	2.8352	0.9	0.23144	0.8	0.36	0.08997	0.98	1413	44	1343	26	1362	16	98.6
LAS401_Shot_1309_Grain_913	2.1322	0.8	0.19361	0.7	0.27	0.08102	0.96	1197	44	1140	21	1157	14	98.5
LAS401_Shot_1310_Grain_914	2.8609	0.7	0.23766	0.6	0.52	0.08840	0.74	1377	37	1374	24	1369	14	100.4
LAS401_Shot_1311_Grain_915	2.9842	3.8	0.28267	2.3	0.30	0.07942	3.79	1370	119	1587	69	1332	61	119.2
LAS401_Shot_1312_Grain_916	5.7720	1.3	0.30364	1.1	0.43	0.13998	1.28	2200	51	1709	38	1934	25	88.4
LAS401_Shot_1313_Grain_917	1.0024	1.2	0.09472	0.9	0.38	0.07829	1.18	1119	56	583	13	704	14	82.8
LAS401_Shot_1314_Grain_918	7.7582	0.8	0.39802	0.7	0.43	0.14310	0.83	2253	36	2157	37	2198	18	98.1
LAS401_Shot_1315_Grain_919	1.8646	0.8	0.18104	0.6	0.35	0.07535	0.82	1066	41	1072	19	1066	13	100.6
LAS401_Shot_1316_Grain_920	3.3079	0.8	0.25769	0.7	0.39	0.09435	0.82	1501	40	1477	27	1479	15	99.8

LAS401_Shot_1317 _Grain_921	1.8427	0.9	0.18000	0.7	0.42	0.07524	0.87	1054	43	1066	20	1059	14	100.7
LAS401_Shot_1318 _Grain_922	4.6325	0.8	0.30627	0.7	0.37	0.11172	0.83	1811	38	1721	30	1754	15	98.1
LAS401_Shot_1319 _Grain_923	1.8376	1.0	0.17643	0.8	0.28	0.07659	1.08	1082	51	1047	20	1056	16	99.2
LAS401_Shot_1320 _Grain_924	1.7208	1.2	0.16865	0.8	0.23	0.07534	1.29	1041	58	1004	20	1010	17	99.4
LAS401_Shot_1327 _Grain_925	5.0527	1.3	0.33565	1.2	0.38	0.11215	1.45	1795	59	1864	45	1820	25	102.4
LAS401_Shot_1328 _Grain_926	1.4920	1.5	0.15310	0.9	0.09	0.07207	1.62	973	66	917	20	922	20	99.4
LAS401_Shot_1329 _Grain_927	5.1439	0.8	0.33476	0.7	0.39	0.11282	0.83	1835	37	1859	33	1838	17	101.1
LAS401_Shot_1330 _Grain_928	2.1907	1.0	0.20105	0.8	0.26	0.08030	1.05	1183	49	1180	23	1175	16	100.4
LAS401_Shot_1331 _Grain_929	1.8358	0.8	0.18020	0.7	0.25	0.07498	0.89	1046	43	1067	19	1058	13	100.9
LAS401_Shot_1332 _Grain_930	1.5090	0.9	0.15128	0.7	0.34	0.07352	0.95	1006	46	908	17	932	13	97.4
LAS401_Shot_1333 _Grain_931	2.5462	0.7	0.20923	0.6	0.43	0.08900	0.69	1397	37	1224	21	1283	13	95.4
LAS401_Shot_1334 _Grain_932	0.6439	1.2	0.07858	0.8	0.20	0.06046	1.32	664	54	488	10	503	11	97.0
LAS401_Shot_1335 _Grain_933	1.1132	1.2	0.11301	0.9	0.30	0.07231	1.27	976	57	690	15	757	15	91.2
LAS401_Shot_1336 _Grain_934	1.6303	1.2	0.15715	0.8	0.30	0.07612	1.16	1067	52	940	19	976	16	96.3
LAS401_Shot_1337 _Grain_935	0.7329	1.4	0.09133	0.9	0.22	0.05897	1.43	635	58	563	12	555	13	101.5
LAS401_Shot_1338 _Grain_936	0.9637	1.8	0.10703	1.0	0.29	0.06642	1.75	862	66	655	15	677	18	96.7
LAS401_Shot_1339 _Grain_937	0.7313	1.4	0.08707	0.8	0.25	0.06190	1.42	708	58	538	11	554	13	97.2
LAS401_Shot_1340 _Grain_938	10.4724	0.5	0.44233	0.6	0.65	0.17312	0.45	2583	26	2359	36	2476	14	95.3
LAS401_Shot_1347 _Grain_939	1.8074	0.9	0.17524	0.7	0.38	0.07566	0.87	1068	44	1040	20	1045	13	99.5
LAS401_Shot_1348 _Grain_940	1.7192	0.9	0.16770	0.7	0.26	0.07521	0.93	1054	45	999	18	1013	13	98.6
LAS401_Shot_1349 _Grain_941	0.7047	2.6	0.08623	1.4	-0.05	0.06223	2.97	954	93	532	16	534	22	99.8
LAS401_Shot_1350 _Grain_942	4.6401	0.6	0.30020	0.6	-0.14	0.11342	0.70	1843	34	1691	28	1754	14	96.4
LAS401_Shot_1351 _Grain_943	2.9850	0.8	0.24610	0.6	0.39	0.08900	0.78	1388	39	1419	24	1401	15	101.3
LAS401_Shot_1352 _Grain_944	1.8940	0.8	0.18508	0.6	0.36	0.07511	0.81	1053	41	1094	19	1076	13	101.7
LAS401_Shot_1353 _Grain_945	2.6874	0.9	0.22016	0.8	0.33	0.09002	0.99	1405	44	1281	24	1320	16	97.1
LAS401_Shot_1354 _Grain_946	2.1356	1.6	0.17850	0.8	0.26	0.08816	1.60	1318	69	1058	21	1150	23	92.0
LAS401_Shot_1355 _Grain_947	2.0441	0.8	0.19025	0.6	0.42	0.07888	0.77	1156	39	1122	20	1128	13	99.5
LAS401_Shot_1356 _Grain_948	2.6010	0.9	0.21721	0.6	0.45	0.08773	0.79	1363	39	1266	22	1298	15	97.5
LAS401_Shot_1357 _Grain_949														
LAS401_Shot_1358 _Grain_950	1.3233	1.4	0.12208	1.0	0.47	0.07972	1.32	1149	57	742	17	851	17	87.2
LAS401_Shot_1359 _Grain_951	1.8194	0.7	0.17821	0.6	0.06	0.07753	3.32	1055	28	1057	18	1050	11	100.6
LAS401_Shot_1360 _Grain_952	4.0574	0.8	0.29038	0.7	0.23	0.10273	0.94	1653	41	1642	28	1642	15	100.0
LAS401_Shot_1367 _Grain_953	11.7504	0.7	0.45766	0.7	0.55	0.18792	0.68	2716	31	2426	41	2580	17	94.0
LAS401_Shot_1368 _Grain_954	12.9646	0.5	0.49720	0.5	0.56	0.19041	0.47	2746	26	2600	39	2675	14	97.2
LAS401_Shot_1369 _Grain_955														

LAS401_Shot_1370_Grain_956	0.7978	1.3	0.09708	0.8	0.25	0.06036	1.30	661	54	597	12	595	12	100.4
LAS401_Shot_1371_Grain_957	1.8151	0.7	0.17785	0.5	0.38	0.07502	0.72	1057	38	1055	17	1049	12	100.6
LAS401_Shot_1372_Grain_958	4.7406	0.7	0.31566	0.7	0.32	0.11026	0.80	1794	37	1769	31	1773	15	99.8
LAS401_Shot_1373_Grain_959	4.9189	0.7	0.32080	0.6	0.23	0.11252	0.78	1828	37	1792	30	1802	14	99.4
LAS401_Shot_1374_Grain_960	1.8790	1.7	0.18337	1.0	0.17	0.07569	1.82	1096	71	1086	25	1065	24	101.9
LAS401_Shot_1375_Grain_961	1.6885	0.9	0.17220	0.7	0.34	0.07228	0.94	968	46	1024	19	1001	13	102.3
LAS401_Shot_1376_Grain_962	2.7039	0.7	0.22573	0.6	0.32	0.08760	0.79	1360	39	1311	22	1329	14	98.7
LAS401_Shot_1377_Grain_963	1.8394	0.9	0.17766	0.7	0.37	0.07635	0.98	1086	46	1053	20	1057	15	99.7
LAS401_Shot_1378_Grain_964	0.7903	1.5	0.09216	0.8	0.16	0.06310	1.59	746	64	568	12	587	14	96.8
LAS401_Shot_1379_Grain_965	3.0228	0.7	0.24721	0.6	0.38	0.08987	0.72	1409	37	1423	24	1410	13	100.9
LAS401_Shot_1380_Grain_966	1.0385	0.8	0.09662	0.7	0.55	0.07882	0.72	1153	38	594	11	722	10	82.3
LAS401_Shot_1387_Grain_967	9.7350	0.6	0.39462	0.6	0.43	0.18164	0.67	2661	30	2142	35	2408	16	89.0
LAS401_Shot_1388_Grain_968	1.8224	0.7	0.17685	0.6	-0.08	0.07569	0.70	1073	38	1049	18	1051	12	99.8
LAS401_Shot_1389_Grain_969	1.5823	0.7	0.15928	0.7	0.36	0.07314	0.80	1003	41	952	18	961	11	99.1
LAS401_Shot_1390_Grain_970	1.7749	1.1	0.17672	0.8	0.16	0.07415	1.26	1022	54	1048	20	1031	16	101.7
LAS401_Shot_1391_Grain_971	2.0081	1.0	0.19410	0.7	0.30	0.07617	1.06	1068	50	1143	21	1113	16	102.6
LAS401_Shot_1392_Grain_972	14.8277	0.7	0.54653	0.7	0.51	0.19965	0.70	2815	31	2807	46	2800	17	100.2
LAS401_Shot_1393_Grain_973	1.8624	1.7	0.17956	1.1	0.08	0.07664	1.80	1124	74	1063	25	1060	23	100.3
LAS401_Shot_1394_Grain_974	1.9324	0.7	0.18798	0.5	0.34	0.07540	0.70	1072	38	1110	18	1090	12	101.8
LAS401_Shot_1395_Grain_975	0.7049	5.0	0.09554	2.2	0.09	0.05566	5.33	1191	144	586	25	507	44	115.5
LAS401_Shot_1396_Grain_976	2.1752	1.6	0.20423	1.0	0.19	0.07853	1.61	1151	66	1196	27	1166	23	102.6
LAS401_Shot_1397_Grain_977	1.8311	1.0	0.17965	0.7	0.35	0.07497	1.02	1052	48	1064	20	1057	15	100.7
LAS401_Shot_1398_Grain_978	1.8434	0.9	0.17840	0.7	0.37	0.07591	0.90	1073	46	1058	19	1057	14	100.0
LAS401_Shot_1399_Grain_979	1.7253	1.0	0.17277	0.8	0.24	0.07334	1.12	997	54	1026	20	1014	15	101.3
LAS401_Shot_1400_Grain_980	1.9408	0.8	0.18420	0.6	0.50	0.07688	0.69	1104	37	1089	19	1093	12	99.7
LAS401_Shot_1407_Grain_981	1.8615	0.7	0.17954	0.6	0.27	0.07603	0.81	1081	40	1064	18	1065	12	99.9
LAS401_Shot_1408_Grain_982	5.0140	0.8	0.32332	0.7	0.51	0.11401	0.81	1848	37	1804	32	1819	17	99.1
LAS401_Shot_1409_Grain_983	0.7015	1.7	0.07985	1.0	0.09	0.06510	1.88	867	69	495	12	535	15	92.5
LAS401_Shot_1410_Grain_984	0.7908	2.6	0.09513	1.4	0.18	0.06112	2.76	904	92	585	18	580	24	100.8
LAS401_Shot_1411_Grain_985	3.7436	0.8	0.27114	0.7	0.20	0.10106	0.85	1629	40	1545	27	1577	15	98.0
LAS401_Shot_1412_Grain_986	1.7924	1.2	0.17600	0.9	0.27	0.07532	1.32	1043	60	1044	22	1038	18	100.6
LAS401_Shot_1413_Grain_987	2.4262	1.2	0.17825	0.8	0.22	0.09969	1.12	1592	47	1056	21	1243	19	85.0
LAS401_Shot_1414_Grain_988	3.0651	1.0	0.25417	0.8	0.54	0.08833	0.90	1371	44	1458	28	1419	18	102.8
LAS401_Shot_1415_Grain_989	2.0080	0.8	0.18612	0.8	0.32	0.07926	0.92	1159	44	1099	21	1116	13	98.5
LAS401_Shot_1416_Grain_990	1.7462	1.1	0.17389	0.8	0.34	0.07351	1.10	1008	51	1033	21	1021	16	101.2

LAS401_Shot_1417_Grain_991	7.2458	1.2	0.34140	1.0	0.41	0.15508	1.11	2390	44	1889	42	2131	23	88.6
LAS401_Shot_1418_Grain_992	1.3002	1.2	0.13020	0.9	0.35	0.07273	1.18	977	56	788	17	842	15	93.6
LAS401_Shot_1419_Grain_993	1.7049	0.9	0.16431	0.7	0.41	0.07585	0.84	1071	43	980	18	1007	13	97.3
LAS401_Shot_1420_Grain_994	2.0488	0.9	0.19218	0.7	0.24	0.07849	1.03	1135	47	1132	21	1128	14	100.4
LAS401_Shot_1427_Grain_995	3.9668	0.6	0.28810	0.5	0.48	0.10059	0.60	1626	33	1631	26	1626	14	100.3
LAS401_Shot_1428_Grain_996	2.0468	1.6	0.19605	1.0	0.16	0.07699	1.73	1085	71	1152	26	1124	23	102.5
LAS401_Shot_1429_Grain_997	7.8605	0.5	0.34830	0.6	0.58	0.16433	0.49	2495	27	1927	31	2213	13	87.1
LAS401_Shot_1430_Grain_998	1.8573	0.7	0.17056	0.6	0.32	0.07907	0.71	1168	40	1015	17	1064	11	95.4
LAS401_Shot_1431_Grain_999	1.5664	0.7	0.15430	0.6	0.34	0.07377	0.77	1028	41	924	17	955	11	96.8
LAS401_Shot_1432_Grain_1000	1.6573	0.9	0.16194	0.6	0.34	0.07456	0.88	1038	44	968	17	989	13	97.9
LAS401_Shot_1433_Grain_1001	2.5323	0.7	0.21874	0.6	0.62	0.08437	0.68	1297	35	1274	22	1279	13	99.7
LAS401_Shot_1434_Grain_1002	1.9480	1.1	0.18981	0.8	0.28	0.07538	1.23	1041	56	1121	23	1092	17	102.7
LAS401_Shot_1436_Grain_1004	3.0125	1.0	0.20946	0.7	0.29	0.10428	0.98	1685	44	1225	22	1405	17	87.2
LAS401_Shot_1437_Grain_1005	4.4875	0.6	0.29436	0.6	0.56	0.11145	0.57	1815	31	1662	28	1727	14	96.2
LAS401_Shot_1438_Grain_1006	11.1618	0.6	0.44821	0.6	0.63	0.18110	0.52	2657	27	2385	37	2534	15	94.1
LAS401_Shot_1439_Grain_1007	7.3328	1.5	0.41985	1.3	0.31	0.13040	1.72	2051	63	2249	58	2142	30	105.0
LAS401_Shot_1440_Grain_1008	1.9549	1.2	0.18113	0.8	0.37	0.07846	1.19	1133	55	1072	22	1093	18	98.1
LAS401_Shot_1447_Grain_1009	1.6745	1.2	0.16461	0.8	0.11	0.07435	1.41	1014	60	983	20	994	18	98.9
LAS401_Shot_1448_Grain_1010	1.3216	1.1	0.12897	0.7	0.32	0.07491	1.14	1033	55	782	15	854	15	91.6
LAS401_Shot_1449_Grain_1011	5.0694	0.7	0.32110	0.7	0.38	0.11510	0.76	1871	35	1796	30	1829	15	98.2
LAS401_Shot_1450_Grain_1012	4.3535	0.7	0.29195	0.6	0.54	0.10837	0.61	1765	33	1650	27	1702	14	97.0
LAS401_Shot_1451_Grain_1013	1.7317	1.1	0.16803	0.8	0.33	0.07533	1.15	1045	53	1000	20	1015	16	98.5
LAS401_Shot_1452_Grain_1014	1.8101	1.5	0.17500	1.0	0.17	0.07681	1.74	1087	70	1038	23	1043	22	99.6
LAS401_Shot_1453_Grain_1015	6.8440	0.9	0.30692	0.7	0.53	0.16197	0.81	2471	34	1724	31	2084	19	82.7
LAS401_Shot_1454_Grain_1016	2.0733	1.0	0.18985	0.7	0.44	0.07915	0.91	1168	46	1121	21	1135	15	98.8
LAS401_Shot_1455_Grain_1017	2.1483	1.2	0.19721	0.9	0.26	0.07978	1.29	1168	56	1159	24	1159	18	100.0
LAS401_Shot_1456_Grain_1018	1.5966	0.8	0.16208	0.5	0.43	0.07176	0.72	964	39	968	16	967	12	100.1
LAS401_Shot_1457_Grain_1019	1.7868	2.0	0.17564	1.3	0.13	0.07421	2.12	1088	86	1041	28	1023	27	101.7
LAS401_Shot_1458_Grain_1020	1.3674	1.1	0.13692	0.8	0.44	0.07263	1.06	973	49	827	16	871	14	94.9
LAS401_Shot_1459_Grain_1021	1.2749	1.0	0.12090	0.8	0.45	0.07680	0.99	1102	45	735	15	831	13	88.5
LAS401_Shot_1460_Grain_1022	2.3474	0.9	0.20741	0.7	0.25	0.08278	1.02	1240	47	1214	23	1224	15	99.2
LAS401_Shot_1467_Grain_1023	7.0516	0.8	0.28333	0.8	0.44	0.18257	0.80	2663	34	1609	29	2116	17	76.0
LAS401_Shot_1468_Grain_1024	1.7600	0.6	0.17090	0.6	0.45	0.07508	0.68	1057	37	1017	18	1029	11	98.8
LAS401_Shot_1469_Grain_1025	2.5439	0.9	0.21566	0.7	0.44	0.08625	0.91	1321	43	1258	24	1282	15	98.1
LAS401_Shot_1470_Grain_1026	1.8617	1.1	0.17908	0.8	0.24	0.07640	1.15	1075	52	1061	21	1064	16	99.7

LAS401_Shot_1471_Grain_1027	2.8020	1.0	0.17738	0.9	0.22	0.11618	1.19	1865	49	1053	22	1352	18	77.9
LAS401_Shot_1472_Grain_1028	1.8703	0.9	0.17730	0.6	0.32	0.07734	0.96	1105	45	1052	19	1068	14	98.4
LAS401_Shot_1473_Grain_1029	4.8349	0.8	0.31016	0.7	0.51	0.11395	0.73	1851	34	1740	30	1787	16	97.4
LAS401_Shot_1474_Grain_1030	1.8485	0.7	0.17732	0.6	0.32	0.07635	0.80	1086	41	1052	19	1061	12	99.2
LAS401_Shot_1475_Grain_1031	8.5309	1.5	0.24421	0.8	0.70	0.25286	1.08	3187	40	1407	28	2270	29	62.0
LAS401_Shot_1476_Grain_1032	5.2189	0.9	0.33735	0.8	0.44	0.11358	0.93	1840	40	1871	36	1849	18	101.2
LAS401_Shot_1477_Grain_1033	2.1500	1.1	0.21069	0.8	0.24	0.07514	1.23	1051	55	1231	24	1161	17	106.1
LAS401_Shot_1478_Grain_1034	2.7202	0.7	0.22432	0.7	0.38	0.08891	0.76	1387	38	1304	24	1331	13	97.9
LAS401_Shot_1479_Grain_1035	1.4710	1.7	0.14534	1.1	0.48	0.07406	1.59	1012	67	873	22	910	22	96.0
LAS401_Shot_1480_Grain_1036	2.6220	1.0	0.21878	0.8	0.39	0.08744	0.97	1349	46	1274	24	1303	17	97.8

LAS402 (20BREMS2)														
	Isotopic Ratios							Calculated ages (Ma)						
ID	$^{207}Pb/^{235}U$	2σ	$^{206}Pb/^{238}U$	2σ	Rho	$^{207/206}Pb$	2σ	$^{207/206}Pb$	2σ	$^{206}Pb/^{238}U$	2σ	$^{207}Pb/^{235}U$	2σ	%conc
LAS402_shot_7_grain_1	1.9509	0.7	0.12198	0.5	0.43	0.11697	0.65	1886	38	742	9	1094	22	1886
LAS402_shot_8_grain_2	0.6589	1.0	0.08017	0.6	0.52	0.06020	0.83	704	41	497	7	509	14	704
LAS402_shot_9_grain_3	0.6683	0.8	0.07130	0.8	0.38	0.06974	0.79	919	42	443	7	515	14	919
LAS402_shot_10_grain_4	1.0552	2.1	0.11259	1.2	0.22	0.06904	2.24	983	82	688	17	721	26	983
LAS402_shot_11_grain_5	1.0517	0.7	0.11190	0.5	0.48	0.06883	0.61	873	41	683	8	725	17	873
LAS402_shot_12_grain_6	2.3417	0.7	0.16595	0.5	0.67	0.10335	0.49	1667	34	988	12	1218	23	1667
LAS402_shot_13_grain_7	1.0121	0.8	0.11016	0.5	0.53	0.06729	0.65	833	41	673	9	704	17	833
LAS402_shot_14_grain_8	0.9268	3.0	0.09861	1.2	0.08	0.07239	3.23	1588	73	604	15	623	34	1588
LAS402_shot_15_grain_9	3.4623	0.4	0.25285	0.4	0.56	0.10012	0.37	1618	33	1452	15	1515	24	1618
LAS402_shot_16_grain_10	0.8881	0.9	0.09987	0.5	0.44	0.06504	0.78	808	42	613	8	639	16	808
LAS402_shot_17_grain_11	1.1558	0.7	0.12268	0.5	0.50	0.06907	0.61	873	41	746	9	776	17	873
LAS402_shot_18_grain_12	0.5654	0.9	0.07050	0.6	0.41	0.05860	0.82	672	40	439	6	453	12	672
LAS402_shot_19_grain_13	1.3990	1.2	0.13565	0.8	0.38	0.07678	1.12	1127	50	821	14	876	23	1127
LAS402_shot_20_grain_14	0.5692	1.3	0.07219	0.7	0.23	0.05750	1.35	762	47	449	7	456	14	762
LAS402_shot_27_grain_15	1.9715	1.0	0.14632	0.7	0.77	0.09737	0.64	1547	39	878	14	1087	25	1547
LAS402_shot_28_grain_16	0.6743	0.6	0.08196	0.5	0.53	0.06020	0.57	627	37	507	6	520	12	627
LAS402_shot_29_grain_17	0.6987	0.8	0.07929	0.5	0.21	0.06465	0.83	816	42	492	6	535	14	816
LAS402_shot_30_grain_18	0.6814	1.1	0.07508	0.6	0.62	0.06536	0.78	788	44	466	7	523	15	788
LAS402_shot_31_grain_19	1.8629	0.7	0.17260	0.4	0.24	0.07918	0.71	1140	43	1026	11	1061	22	1140
LAS402_shot_32_grain_20	1.6656	0.5	0.16244	0.4	0.37	0.07506	0.52	1047	38	969	11	992	20	1047

LAS402_shot_33_g rain_21	0.7512	0.6	0.08878	0.4	0.42	0.06178	0.55	672	39	548	6	567	14	672
LAS402_shot_34_g rain_22	1.1904	1.0	0.12339	0.6	0.31	0.07108	0.98	998	45	749	10	789	20	998
LAS402_shot_35_g rain_23	1.4144	0.6	0.14254	0.5	0.17	0.07266	0.57	980	41	858	10	892	19	980
LAS402_shot_36_g rain_24	1.4488	0.8	0.14553	0.7	0.71	0.07253	0.55	972	40	874	13	901	20	972
LAS402_shot_37_g rain_25	0.6004	0.8	0.07411	0.5	0.18	0.05901	0.86	669	42	461	6	475	13	669
LAS402_shot_38_g rain_26	0.9173	0.9	0.09784	0.5	0.25	0.06872	0.90	927	43	601	7	654	17	927
LAS402_shot_39_g rain_27	0.7758	0.8	0.09034	0.6	0.35	0.06299	0.82	762	43	557	7	579	15	762
LAS402_shot_40_g rain_28	4.9408	0.5	0.30781	0.5	0.68	0.11697	0.39	1899	32	1727	19	1804	26	1899
LAS402_shot_47_g rain_29	0.9359	0.9	0.09193	0.5	0.25	0.07505	0.90	1073	43	566	7	666	17	1073
LAS402_shot_48_g rain_30	1.2958	0.9	0.13160	0.6	0.65	0.07170	0.70	975	42	796	11	834	20	975
LAS402_shot_49_g rain_31	6.3793	0.5	0.27295	0.5	0.15	0.17286	0.51	2565	32	1553	18	2024	28	2565
LAS402_shot_50_g rain_32	1.8531	1.4	0.12113	0.8	0.72	0.11001	0.88	1741	44	735	13	1039	26	1741
LAS402_shot_51_g rain_33	2.1215	0.5	0.18418	0.4	0.26	0.08451	0.50	1288	37	1089	11	1153	21	1288
LAS402_shot_52_g rain_34	1.1593	2.2	0.09506	1.0	0.75	0.08939	1.98	1560	65	584	12	738	26	1560
LAS402_shot_53_g rain_35	0.6870	0.9	0.08457	0.6	0.53	0.05943	0.77	677	41	523	7	525	14	677
LAS402_shot_54_g rain_36	1.1153	0.9	0.09722	0.6	0.65	0.08401	0.72	1250	44	597	8	752	19	1250
LAS402_shot_55_g rain_37	0.7341	0.7	0.08507	0.5	0.73	0.06323	0.51	700	39	526	7	556	14	700
LAS402_shot_56_g rain_38	4.7631	0.7	0.31306	0.6	0.70	0.11219	0.50	1818	35	1753	22	1767	28	1818
LAS402_shot_57_g rain_39	0.8188	0.6	0.09602	0.5	0.18	0.06288	0.47	686	38	591	7	604	14	686
LAS402_shot_58_g rain_40	1.7020	0.7	0.15665	0.5	0.27	0.08030	0.51	1180	37	937	12	1002	21	1180
LAS402_shot_59_g rain_41	1.0807	0.7	0.11299	0.5	0.24	0.07111	0.73	956	41	690	8	740	17	956
LAS402_shot_60_g rain_42	0.8178	1.0	0.09350	0.5	0.15	0.06512	1.06	886	45	576	8	599	16	886
LAS402_shot_67_g rain_43	2.0710	0.6	0.18079	0.4	0.30	0.08524	0.62	1293	40	1071	12	1133	21	1293
LAS402_shot_68_g rain_44	1.9631	0.8	0.13726	0.5	0.71	0.10558	0.54	1699	37	828	10	1092	23	1699
LAS402_shot_69_g rain_45	6.7023	1.0	0.29032	0.9	0.90	0.16954	0.46	2538	32	1633	28	2036	34	2538
LAS402_shot_70_g rain_46	2.8821	1.8	0.13195	0.5	0.49	0.15931	1.57	2244	61	798	9	1310	33	2244
LAS402_shot_71_g rain_47	1.4294	0.8	0.14338	0.6	0.53	0.07397	0.69	1018	42	863	12	893	20	1018
LAS402_shot_72_g rain_48	5.0748	0.5	0.32083	0.5	0.55	0.11814	0.46	1910	33	1791	20	1826	26	1910
LAS402_shot_73_g rain_49	1.0395	0.8	0.11144	0.6	0.76	0.06914	0.52	886	39	680	10	718	17	886
LAS402_shot_74_g rain_50	0.7532	1.0	0.08996	0.6	0.41	0.06252	0.92	773	43	555	8	564	15	773
LAS402_shot_75_g rain_51	2.2242	0.5	0.18977	0.5	0.75	0.08680	0.33	1346	34	1120	13	1185	22	1346
LAS402_shot_76_g rain_52	2.9827	0.5	0.22627	0.4	0.49	0.09832	0.47	1574	35	1313	14	1398	24	1574
LAS402_shot_77_g rain_53	2.9056	0.6	0.19652	0.5	0.08	0.11024	0.59	1772	34	1156	14	1374	23	1772
LAS402_shot_78_g rain_54	2.6648	0.4	0.21235	0.4	0.23	0.09309	0.36	1482	33	1240	13	1316	22	1482
LAS402_shot_79_g rain_55	1.9466	0.4	0.17919	0.4	0.27	0.08070	0.34	1202	34	1062	11	1094	20	1202

LAS402_shot_80_grain_56	8.2404	0.4	0.41216	0.4	0.39	0.14835	0.35	2317	30	2222	21	2256	27	2317
LAS402_shot_87_grain_57	2.4076	0.7	0.21480	0.5	0.31	0.08281	0.76	1218	44	1253	15	1236	23	1218
LAS402_shot_88_grain_58	0.9508	0.8	0.10452	0.7	0.81	0.06624	0.50	793	40	640	10	672	17	793
LAS402_shot_89_grain_59	0.8091	0.7	0.08873	0.5	0.39	0.06728	0.75	836	42	548	7	598	15	836
LAS402_shot_90_grain_60	0.8517	0.8	0.08783	0.4	0.22	0.07175	0.81	952	44	542	6	621	15	952
LAS402_shot_91_grain_61	1.1536	0.8	0.12056	0.7	0.70	0.06967	0.60	904	40	733	11	774	18	904
LAS402_shot_92_grain_62	0.5769	0.8	0.07003	0.5	0.39	0.06010	0.70	665	36	436	6	460	12	665
LAS402_shot_93_grain_63	3.0546	1.0	0.17072	0.6	0.82	0.12814	0.61	2049	38	1014	14	1396	30	2049
LAS402_shot_94_grain_64	0.7440	1.4	0.07954	0.8	0.75	0.06676	0.97	899	44	493	8	552	17	899
LAS402_shot_95_grain_65	1.2112	0.6	0.12417	0.5	0.64	0.07079	0.49	931	39	755	9	803	18	931
LAS402_shot_96_grain_66	15.3736	2.2	0.23581	1.5	0.98	0.43463	0.88	3960	35	1347	37	2670	48	3960
LAS402_shot_97_grain_67	0.8251	0.8	0.08710	0.5	0.57	0.06850	0.50	859	38	538	7	606	15	859
LAS402_shot_98_grain_68	1.6378	0.7	0.15596	0.4	0.27	0.07627	0.68	1068	42	934	10	978	20	1068
LAS402_shot_99_grain_69	0.5751	0.7	0.07136	0.4	0.21	0.05882	0.73	631	40	444	5	460	12	631
LAS402_shot_100_grain_70	11.6589	0.6	0.46954	0.5	0.44	0.18023	0.41	2644	29	2476	28	2568	29	2644
LAS402_shot_107_grain_71	1.2504	0.6	0.10473	0.4	0.63	0.08660	0.46	1335	36	642	7	820	18	1335
LAS402_shot_108_grain_72	2.6666	0.7	0.22887	0.5	0.48	0.08538	0.80	1274	43	1326	16	1308	24	1274
LAS402_shot_109_grain_73	0.9964	1.2	0.10469	0.9	0.80	0.06821	0.71	874	42	640	12	688	19	874
LAS402_shot_110_grain_74	0.8587	0.8	0.09483	0.5	0.07	0.06590	0.68	786	39	584	7	623	14	786
LAS402_shot_111_grain_75	1.2049	0.5	0.12382	0.3	0.05	0.07092	0.47	934	39	752	8	801	17	934
LAS402_shot_112_grain_76	1.3423	2.1	0.10873	0.8	0.06	0.09119	1.89	1421	53	664	12	824	20	1421
LAS402_shot_113_grain_77	1.5327	0.7	0.13901	0.5	0.60	0.08034	0.57	1179	39	838	11	937	20	1179
LAS402_shot_114_grain_78	1.5362	0.9	0.15712	0.7	0.72	0.07138	0.58	944	41	938	15	934	21	944
LAS402_shot_115_grain_79	0.8228	0.6	0.08683	0.4	0.26	0.06954	0.65	890	41	536	6	607	15	890
LAS402_shot_116_grain_80	1.6262	0.9	0.16717	0.6	0.14	0.07175	0.96	994	44	994	14	968	22	994
LAS402_shot_117_grain_81	1.7785	0.5	0.16703	0.4	0.09	0.07792	0.44	1127	31	995	11	1033	18	1127
LAS402_shot_118_grain_82	3.3214	0.5	0.23462	0.4	0.79	0.10315	0.29	1676	31	1358	14	1481	24	1676
LAS402_shot_119_grain_83	4.2551	0.4	0.29597	0.4	0.74	0.10516	0.31	1709	32	1670	17	1680	25	1709
LAS402_shot_120_grain_84	2.3414	0.4	0.20121	0.3	0.37	0.08538	0.41	1313	35	1181	11	1222	21	1313
LAS402_shot_127_grain_85	0.7290	0.6	0.08346	0.4	0.40	0.06432	0.59	751	39	517	6	554	14	751
LAS402_shot_128_grain_86	1.1486	0.4	0.12053	0.3	0.46	0.06987	0.41	906	38	733	7	775	17	906
LAS402_shot_129_grain_87	1.8460	0.4	0.17990	0.3	0.46	0.07523	0.36	1062	36	1066	10	1060	20	1062
LAS402_shot_130_grain_88	1.2367	0.4	0.12486	0.3	0.30	0.07258	0.40	984	36	758	7	815	17	984
LAS402_shot_131_grain_89	1.9943	0.6	0.19242	0.4	0.11	0.07652	0.63	1070	41	1133	12	1108	21	1070
LAS402_shot_132_grain_90	2.1119	0.6	0.16014	0.4	0.62	0.09629	0.45	1538	35	957	11	1147	22	1538

LAS402_shot_133_grain_91	0.8690	0.9	0.09212	0.6	0.15	0.07007	0.88	923	42	568	8	629	16	923
LAS402_shot_134_grain_92	1.2936	1.1	0.12922	0.9	0.74	0.07282	0.84	1041	38	781	14	830	22	1041
LAS402_shot_135_grain_93	2.8186	0.4	0.23958	0.4	0.41	0.08624	0.42	1329	35	1384	14	1358	23	1329
LAS402_shot_136_grain_94	1.4502	1.0	0.13153	0.7	0.26	0.08263	1.10	1238	49	795	13	900	22	1238
LAS402_shot_137_grain_95	1.6440	0.4	0.15875	0.3	0.18	0.07586	0.42	1073	37	950	9	984	19	1073
LAS402_shot_138_grain_96	1.4816	0.8	0.14136	0.6	0.69	0.07609	0.43	1084	36	851	12	913	21	1084
LAS402_shot_139_grain_97	13.7319	0.4	0.51676	0.4	0.85	0.19462	0.35	2773	29	2681	24	2727	28	2773
LAS402_shot_140_grain_98	1.4057	0.4	0.14329	0.4	0.62	0.07167	0.34	967	36	863	9	890	18	967
LAS402_shot_147_grain_99	0.7826	0.9	0.09081	0.5	0.07	0.06370	0.92	776	43	560	7	580	15	776
LAS402_shot_148_grain_100	1.8867	0.4	0.18234	0.3	0.47	0.07586	0.36	1082	36	1079	10	1074	20	1082
LAS402_shot_149_grain_101	0.6002	0.5	0.07453	0.4	0.36	0.05922	0.52	588	38	463	5	476	12	588
LAS402_shot_150_grain_102	10.7728	0.3	0.41562	0.4	0.64	0.19062	0.29	2742	28	2238	21	2501	28	2742
LAS402_shot_151_grain_103	2.1232	0.5	0.18778	0.4	0.65	0.08301	0.38	1256	35	1109	11	1153	21	1256
LAS402_shot_152_grain_104	1.1309	1.1	0.12326	0.8	0.87	0.06634	0.52	801	40	747	13	755	20	801
LAS402_shot_153_grain_105	3.5355	0.9	0.23540	0.7	0.87	0.10977	0.43	1780	34	1358	20	1516	28	1780
LAS402_shot_154_grain_106	2.6676	0.8	0.21930	0.7	0.74	0.08938	0.55	1386	38	1276	19	1304	25	1386
LAS402_shot_155_grain_107	2.1679	0.4	0.20286	0.3	0.42	0.07880	0.37	1155	35	1190	11	1170	21	1155
LAS402_shot_156_grain_108	1.7258	0.6	0.15318	0.4	0.52	0.08305	0.49	1247	37	918	10	1013	21	1247
LAS402_shot_157_grain_109	1.3018	0.6	0.13081	0.4	0.64	0.07322	0.44	1003	37	792	9	843	18	1003
LAS402_shot_158_grain_110	1.0915	0.4	0.11357	0.4	0.58	0.07088	0.36	940	36	693	7	747	16	940
LAS402_shot_159_grain_111	0.6875	0.5	0.08289	0.4	0.35	0.06120	0.49	643	38	513	5	530	13	643
LAS402_shot_160_grain_112	1.6193	0.5	0.15828	0.5	0.49	0.07571	0.51	1063	39	947	11	974	20	1063
LAS402_shot_167_grain_113	2.4828	0.5	0.20862	0.4	0.55	0.08729	0.41	1351	36	1221	13	1264	22	1351
LAS402_shot_168_grain_114	2.2907	0.7	0.19158	0.5	0.78	0.08758	0.41	1359	35	1128	14	1203	23	1359
LAS402_shot_169_grain_115	0.6471	0.7	0.07853	0.4	0.18	0.06066	0.78	686	40	487	6	503	13	686
LAS402_shot_170_grain_116	1.9027	0.5	0.16100	0.4	0.54	0.08617	0.36	1329	33	961	10	1077	21	1329
LAS402_shot_171_grain_117	2.2523	0.6	0.19235	0.4	0.27	0.08598	0.67	1313	41	1133	12	1192	23	1313
LAS402_shot_172_grain_118	5.5584	0.4	0.34538	0.3	0.57	0.11753	0.31	1910	31	1910	18	1907	26	1910
LAS402_shot_173_grain_119	1.9778	0.7	0.18935	0.5	0.25	0.07658	0.76	1078	44	1116	13	1101	22	1078
LAS402_shot_174_grain_120	1.5188	0.7	0.14570	0.6	0.45	0.07592	0.41	1077	37	875	12	932	20	1077
LAS402_shot_175_grain_121	3.9659	0.4	0.28233	0.4	0.61	0.10242	0.36	1660	33	1602	16	1624	25	1660
LAS402_shot_176_grain_122	1.0867	0.6	0.11549	0.4	0.25	0.06872	0.59	870	40	704	7	744	17	870
LAS402_shot_177_grain_123	3.0562	0.5	0.24744	0.4	0.36	0.08997	0.54	1404	38	1424	15	1417	24	1404
LAS402_shot_178_grain_124	2.0249	0.4	0.17586	0.4	0.30	0.08374	0.43	1274	35	1044	10	1121	21	1274
LAS402_shot_179_grain_125	3.3914	0.3	0.26817	0.3	0.03	0.09190	0.35	1454	33	1531	14	1499	24	1454

LAS402_shot_180_grain_126	1.3468	0.6	0.13824	0.4	0.48	0.07078	0.53	926	40	834	9	862	18	926
LAS402_shot_187_grain_127	1.9001	0.4	0.18198	0.3	0.36	0.07569	0.39	1074	35	1077	10	1080	20	1074
LAS402_shot_188_grain_128	1.3351	0.5	0.13552	0.4	0.46	0.07160	0.51	947	40	819	9	858	18	947
LAS402_shot_189_grain_129	1.2633	0.7	0.12003	0.6	0.78	0.07596	0.46	1072	39	730	10	823	19	1072
LAS402_shot_190_grain_130	1.1900	0.9	0.12103	0.6	0.61	0.07130	0.68	941	42	735	11	787	19	941
LAS402_shot_191_grain_131	2.8376	0.5	0.23463	0.5	0.54	0.08774	0.42	1362	35	1358	15	1362	23	1362
LAS402_shot_192_grain_132	2.9575	0.4	0.23905	0.3	0.43	0.08974	0.39	1408	35	1381	13	1394	23	1408
LAS402_shot_193_grain_133	2.8321	0.4	0.23325	0.3	0.10	0.08799	0.33	1372	33	1351	13	1361	22	1372
LAS402_shot_194_grain_134	2.1282	0.4	0.18145	0.3	0.39	0.08512	0.36	1308	35	1075	10	1156	21	1308
LAS402_shot_195_grain_135	13.0985	0.3	0.50266	0.3	0.60	0.18976	0.27	2737	27	2625	23	2685	28	2737
LAS402_shot_196_grain_136	2.2806	0.5	0.20899	0.4	0.34	0.07932	0.48	1162	38	1224	12	1203	22	1162
LAS402_shot_197_grain_137	4.6082	0.4	0.29241	0.4	0.42	0.11506	0.41	1869	33	1652	16	1747	25	1869
LAS402_shot_198_grain_138	1.7080	0.8	0.17160	0.5	0.33	0.07306	0.76	999	42	1020	13	1004	21	999
LAS402_shot_199_grain_139	1.0433	0.5	0.10933	0.4	0.65	0.06959	0.38	904	37	668	7	724	16	904
LAS402_shot_200_grain_140	1.1147	0.7	0.11741	0.5	0.15	0.06971	0.72	887	41	714	8	755	17	887
LAS402_shot_207_grain_141	1.3725	0.9	0.12544	0.6	0.35	0.08107	0.86	1181	45	761	10	869	20	1181
LAS402_shot_208_grain_142	0.9382	0.9	0.10457	0.7	0.75	0.06532	0.63	783	40	640	10	663	18	783
LAS402_shot_209_grain_143	0.7464	0.6	0.08640	0.4	0.38	0.06361	0.57	728	39	534	6	564	14	728
LAS402_shot_210_grain_144	7.8390	0.5	0.32890	0.5	0.83	0.17510	0.31	2602	29	1832	20	2210	28	2602
LAS402_shot_211_grain_145	4.0329	0.4	0.29123	0.4	0.20	0.10186	0.41	1645	33	1647	16	1636	25	1645
LAS402_shot_212_grain_146	0.7660	1.1	0.09391	0.6	0.06	0.06117	1.25	868	48	578	8	570	17	868
LAS402_shot_213_grain_147	8.3834	1.1	0.34680	0.9	0.90	0.17606	0.46	2603	31	1904	34	2233	34	2603
LAS402_shot_214_grain_148	2.9221	0.5	0.15465	0.4	0.59	0.13887	0.32	2206	30	926	10	1382	23	2206
LAS402_shot_215_grain_149	2.1380	0.4	0.19971	0.3	0.31	0.07896	0.33	1162	34	1173	11	1159	21	1162
LAS402_shot_216_grain_150	1.7585	0.7	0.14419	0.5	0.21	0.08990	0.64	1388	40	868	11	1021	21	1388
LAS402_shot_217_grain_151	2.2615	0.6	0.17804	0.5	0.77	0.09271	0.40	1470	35	1055	12	1194	22	1470
LAS402_shot_218_grain_152	4.4770	0.4	0.30941	0.4	0.49	0.10685	0.38	1735	33	1736	17	1724	25	1735
LAS402_shot_219_grain_153	2.2950	1.0	0.13900	0.7	0.86	0.12017	0.49	1940	34	837	13	1192	25	1940
LAS402_shot_220_grain_154	0.5930	0.4	0.07563	0.3	0.40	0.05794	0.39	526	37	470	5	472	11	526
LAS402_shot_227_grain_155	2.5826	0.4	0.20945	0.3	0.43	0.09083	0.38	1432	34	1226	12	1293	22	1432
LAS402_shot_228_grain_156	2.1618	0.7	0.12037	0.5	0.70	0.13141	0.50	2098	34	732	9	1159	23	2098
LAS402_shot_229_grain_157	3.1884	0.5	0.20887	0.4	0.75	0.11202	0.34	1823	32	1221	13	1449	24	1823
LAS402_shot_230_grain_158	1.5102	0.4	0.15137	0.4	0.56	0.07323	0.37	1007	36	908	9	933	19	1007
LAS402_shot_231_grain_159	2.8615	0.9	0.20599	0.8	0.51	0.10090	0.33	1631	32	1203	19	1352	26	1631
LAS402_shot_232_grain_160	4.3049	0.4	0.21625	0.4	0.65	0.14598	0.36	2292	30	1261	13	1690	26	2292

LAS402_shot_233_grain_161	2.2193	0.5	0.20102	0.4	0.35	0.08103	0.47	1203	38	1180	12	1184	22	1203
LAS402_shot_234_grain_162	1.9368	0.5	0.18547	0.4	0.34	0.07675	0.53	1088	40	1097	12	1090	21	1088
LAS402_shot_235_grain_163	1.4398	0.5	0.14324	0.4	0.74	0.07341	0.38	1011	36	862	10	902	19	1011
LAS402_shot_236_grain_164	0.6530	0.5	0.07698	0.4	0.58	0.06187	0.45	659	39	478	5	509	12	659
LAS402_shot_237_grain_165	1.2030	0.5	0.12088	0.5	0.74	0.07287	0.36	999	36	735	9	799	18	999
LAS402_shot_238_grain_166	11.3364	0.4	0.48207	0.4	0.50	0.17202	0.37	2570	30	2535	23	2548	28	2570
LAS402_shot_239_grain_167	3.8635	0.4	0.27915	0.4	0.43	0.10119	0.40	1633	34	1586	15	1602	24	1633
LAS402_shot_240_grain_168	1.8452	0.3	0.16602	0.3	0.52	0.08109	0.32	1214	34	990	9	1060	20	1214
LAS402_shot_247_grain_169	2.4829	0.6	0.21344	0.4	0.24	0.08537	0.60	1290	39	1246	14	1260	23	1290
LAS402_shot_248_grain_170	3.5559	0.3	0.24712	0.3	0.41	0.10484	0.35	1703	33	1423	13	1538	23	1703
LAS402_shot_249_grain_171	1.2654	0.8	0.13073	0.7	0.82	0.07055	0.48	924	39	790	12	822	19	924
LAS402_shot_250_grain_172	1.5063	0.8	0.15033	0.6	0.67	0.07291	0.62	990	40	902	13	923	20	990
LAS402_shot_251_grain_173	1.5057	0.5	0.14934	0.4	0.44	0.07368	0.48	1012	38	898	9	930	19	1012
LAS402_shot_252_grain_174	2.5982	1.0	0.21334	0.8	0.76	0.08860	0.62	1368	40	1242	20	1280	27	1368
LAS402_shot_253_grain_175	1.1248	0.9	0.11767	0.7	0.69	0.07038	0.63	915	41	716	11	762	18	915
LAS402_shot_254_grain_176	0.9164	0.6	0.10136	0.6	0.57	0.06662	0.52	803	39	622	8	658	15	803
LAS402_shot_255_grain_177	13.6645	0.4	0.51965	0.4	0.65	0.19230	0.32	2756	29	2695	24	2723	29	2756
LAS402_shot_256_grain_178	3.2040	0.6	0.22582	0.5	0.41	0.10368	0.37	1677	33	1310	16	1448	25	1677
LAS402_shot_257_grain_179	1.6492	0.4	0.15501	0.4	0.70	0.07798	0.35	1134	35	928	9	987	19	1134
LAS402_shot_258_grain_180	2.9201	0.5	0.24232	0.4	0.64	0.08812	0.38	1372	35	1398	15	1382	23	1372
LAS402_shot_259_grain_181	8.8337	1.2	0.38207	1.1	0.95	0.16575	0.48	2499	32	2061	43	2248	46	2499
LAS402_shot_260_grain_182	2.2048	0.4	0.19604	0.4	0.41	0.08257	0.41	1248	36	1153	11	1180	21	1248
LAS402_shot_300_grain_210	2.9619	0.5	0.24731	0.4	0.54	0.08852	0.44	1376	36	1423	16	1393	24	1376
LAS402_shot_307_grain_211	1.1402	0.6	0.11928	0.5	0.14	0.07027	0.66	923	42	726	9	769	17	923
LAS402_shot_308_grain_212	0.7667	0.7	0.09559	0.5	0.23	0.05884	0.76	648	40	588	7	574	14	648
LAS402_shot_309_grain_213	4.1659	0.6	0.27538	0.5	0.83	0.11068	0.32	1802	31	1566	18	1660	27	1802
LAS402_shot_310_grain_214	1.4791	0.4	0.15033	0.4	0.58	0.07184	0.36	969	36	902	10	919	18	969
LAS402_shot_311_grain_215	1.6023	0.4	0.15780	0.3	0.41	0.07421	0.41	1031	37	944	9	969	19	1031
LAS402_shot_312_grain_216	2.8555	0.5	0.23054	0.5	0.76	0.09024	0.34	1421	33	1335	15	1366	23	1421
LAS402_shot_313_grain_217	1.3853	1.0	0.11649	0.6	0.84	0.08516	0.55	1297	38	709	10	869	21	1297
LAS402_shot_314_grain_218	3.7664	0.4	0.24875	0.4	0.69	0.10970	0.33	1786	32	1431	14	1583	24	1786
LAS402_shot_315_grain_219	2.9762	0.4	0.24246	0.3	0.45	0.08915	0.38	1397	34	1398	13	1399	23	1397
LAS402_shot_316_grain_220	1.2884	0.7	0.13394	0.5	0.21	0.06995	0.62	900	40	810	10	834	19	900
LAS402_shot_317_grain_221	0.7662	0.7	0.09248	0.5	0.25	0.06037	0.76	679	41	570	7	575	14	679
LAS402_shot_318_grain_222	1.6758	0.5	0.16437	0.4	0.53	0.07416	0.45	1030	37	980	11	997	20	1030

LAS402_shot_319_grain_223	2.5962	0.4	0.21896	0.3	0.52	0.08585	0.34	1323	34	1276	12	1297	22	1323
LAS402_shot_320_grain_224	4.2052	0.4	0.29665	0.4	0.47	0.10296	0.39	1668	32	1673	16	1674	24	1668
LAS402_shot_327_grain_225	2.0357	0.7	0.18701	0.5	0.43	0.07936	0.68	1149	42	1104	14	1119	23	1149
LAS402_shot_328_grain_226	1.8698	0.5	0.17796	0.4	0.39	0.07644	0.48	1084	39	1055	11	1068	20	1084
LAS402_shot_329_grain_227	2.0590	0.5	0.18295	0.4	0.42	0.08176	0.47	1223	37	1082	11	1132	21	1223
LAS402_shot_330_grain_228	3.6901	0.7	0.24148	0.6	0.52	0.11158	0.90	1802	16	1391	18	1558	26	1802
LAS402_shot_331_grain_229	2.0984	0.3	0.19525	0.4	0.59	0.07809	0.32	1140	35	1149	11	1146	21	1140
LAS402_shot_332_grain_230	1.8106	0.7	0.17524	0.5	0.31	0.07546	0.70	1060	42	1039	12	1044	21	1060
LAS402_shot_333_grain_231	1.8772	0.8	0.18073	0.5	0.16	0.07616	0.90	1071	44	1070	13	1063	22	1071
LAS402_shot_334_grain_232	1.8869	0.6	0.18208	0.5	0.27	0.07587	0.67	1064	42	1078	12	1072	21	1064
LAS402_shot_335_grain_233	2.1531	0.4	0.19755	0.4	0.43	0.07943	0.39	1168	35	1161	11	1164	21	1168
LAS402_shot_336_grain_234	2.0327	0.4	0.18893	0.4	0.58	0.07848	0.39	1147	36	1115	12	1124	21	1147
LAS402_shot_337_grain_235	3.0541	0.5	0.24093	0.5	0.20	0.09260	0.40	1462	33	1389	16	1415	24	1462
LAS402_shot_338_grain_236	1.8000	0.4	0.17445	0.3	0.39	0.07533	0.38	1063	35	1036	10	1044	19	1063
LAS402_shot_339_grain_237	1.8007	0.5	0.17612	0.4	0.40	0.07467	0.48	1042	38	1046	11	1043	20	1042
LAS402_shot_340_grain_238	1.7782	0.4	0.17416	0.4	0.44	0.07467	0.42	1043	37	1034	11	1036	20	1043
LAS402_shot_347_grain_239	3.1470	0.4	0.24892	0.4	0.38	0.09268	0.48	1461	36	1431	15	1441	24	1461
LAS402_shot_348_grain_240	1.8879	0.4	0.18178	0.4	0.44	0.07607	0.40	1082	37	1076	11	1074	20	1082
LAS402_shot_349_grain_241	1.9739	0.6	0.19012	0.4	0.10	0.07616	0.63	1063	40	1121	12	1100	21	1063
LAS402_shot_350_grain_242	1.9460	0.4	0.18441	0.4	0.05	0.07738	0.47	1110	37	1090	11	1094	20	1110
LAS402_shot_351_grain_243	1.4469	0.4	0.14426	0.4	0.02	0.07351	0.50	1003	37	868	9	906	18	1003
LAS402_shot_352_grain_244	1.3457	0.5	0.13308	0.4	0.60	0.07389	0.41	1025	37	805	9	863	18	1025
LAS402_shot_353_grain_245	10.7606	0.7	0.41094	0.7	0.88	0.19071	0.35	2742	29	2209	30	2482	32	2742
LAS402_shot_354_grain_246	1.7562	0.5	0.17270	0.4	0.41	0.07432	0.48	1031	38	1027	11	1026	20	1031
LAS402_shot_355_grain_247	1.2723	1.6	0.13033	1.2	0.90	0.06907	0.71	888	42	785	19	801	24	888
LAS402_shot_356_grain_248	2.6576	0.4	0.22060	0.4	0.30	0.08797	0.36	1368	34	1284	13	1314	22	1368
LAS402_shot_357_grain_249	1.2239	0.7	0.12671	0.5	0.56	0.07039	0.44	921	38	768	10	807	18	921
LAS402_shot_358_grain_250	1.6164	0.4	0.15897	0.3	0.32	0.07409	0.33	1032	35	951	9	974	18	1032
LAS402_shot_359_grain_251	1.8833	3.6	0.17726	0.8	0.09	0.07622	1.63	1213	57	1048	17	1006	22	1213
LAS402_shot_360_grain_252	0.7157	0.7	0.08647	0.5	0.39	0.06040	0.68	678	39	535	6	545	14	678
LAS402_shot_367_grain_253	13.0446	0.4	0.50931	0.4	0.19	0.18826	0.37	2716	28	2649	24	2678	29	2716
LAS402_shot_368_grain_254	5.0296	0.4	0.32423	0.4	0.49	0.11361	0.40	1847	33	1809	18	1821	26	1847
LAS402_shot_369_grain_255	1.7911	0.6	0.17551	0.5	0.19	0.07532	0.69	1047	41	1041	12	1037	21	1047
LAS402_shot_370_grain_256	2.4713	0.4	0.21281	0.4	0.52	0.08552	0.41	1313	35	1243	13	1262	22	1313
LAS402_shot_371_grain_257	1.7106	0.6	0.17043	0.5	0.07	0.07561	2.41	1003	26	1014	12	1006	20	1003

LAS402_shot_372_grain_258	1.7510	0.5	0.17338	0.4	0.38	0.07428	0.52	1023	39	1031	11	1025	20	1023
LAS402_shot_373_grain_259	2.9146	0.4	0.23886	0.4	0.41	0.08959	0.44	1402	36	1380	14	1382	23	1402
LAS402_shot_374_grain_260	1.5526	1.0	0.16155	0.6	0.25	0.07127	1.00	992	46	964	13	939	22	992
LAS402_shot_375_grain_261	1.8729	0.5	0.18033	0.4	0.35	0.07650	0.52	1085	38	1069	12	1068	20	1085
LAS402_shot_376_grain_262	4.7114	0.4	0.31237	0.4	0.53	0.11090	0.35	1803	32	1750	17	1767	25	1803
LAS402_shot_377_grain_263	2.0158	0.7	0.18066	0.6	0.84	0.08166	0.38	1225	35	1068	14	1112	22	1225
LAS402_shot_378_grain_264	1.0081	0.7	0.11325	0.5	0.31	0.06586	0.72	808	42	691	8	704	17	808
LAS402_shot_379_grain_265	1.9334	0.6	0.18385	0.5	0.33	0.07757	0.65	1100	42	1087	12	1086	22	1100
LAS402_shot_380_grain_266	2.3062	0.5	0.20082	0.5	0.69	0.08436	0.41	1288	35	1179	14	1210	22	1288
LAS402_shot_387_grain_267	1.7714	0.5	0.17098	0.4	0.35	0.07628	0.57	1077	40	1016	11	1030	20	1077
LAS402_shot_388_grain_268	2.4806	0.4	0.21982	0.4	0.22	0.08258	0.36	1248	30	1281	13	1264	22	1248
LAS402_shot_389_grain_269	1.9227	0.5	0.18798	0.5	0.43	0.07522	0.53	1046	40	1110	12	1085	21	1046
LAS402_shot_390_grain_270	1.8977	0.5	0.18102	0.4	0.13	0.07706	0.52	1097	38	1071	12	1075	21	1097
LAS402_shot_391_grain_271	1.6313	0.4	0.16063	0.3	0.36	0.07427	0.41	1032	37	960	9	981	19	1032
LAS402_shot_392_grain_272	2.0247	0.4	0.18816	0.3	0.17	0.07871	0.35	1154	34	1111	11	1121	21	1154
LAS402_shot_393_grain_273	3.9199	0.4	0.27819	0.4	0.62	0.10297	0.34	1670	32	1582	15	1614	24	1670
LAS402_shot_394_grain_274	1.8263	0.6	0.17546	0.5	0.29	0.07631	0.64	1067	42	1042	12	1048	21	1067
LAS402_shot_395_grain_275	4.4375	0.3	0.29420	0.3	0.60	0.11001	0.31	1793	32	1661	16	1717	25	1793
LAS402_shot_396_grain_276	1.6170	0.6	0.16172	0.5	0.67	0.07294	0.42	995	38	965	11	972	20	995
LAS402_shot_397_grain_277	1.9122	1.0	0.18259	0.6	0.11	0.07755	1.06	1138	49	1080	14	1075	24	1138
LAS402_shot_398_grain_278	2.0789	0.6	0.19150	0.4	0.25	0.07963	0.69	1148	42	1129	12	1134	22	1148
LAS402_shot_399_grain_279	1.7770	0.6	0.17445	0.4	0.07	0.07475	0.61	1029	40	1035	12	1031	21	1029
LAS402_shot_400_grain_280	4.4369	0.5	0.28462	0.4	0.49	0.11419	0.49	1848	35	1613	17	1714	26	1848
LAS402_shot_407_grain_281	0.9604	1.0	0.10669	0.6	0.02	0.06646	0.96	855	44	653	9	674	17	855
LAS402_shot_408_grain_282	0.7404	0.6	0.08663	0.4	0.35	0.06262	0.65	708	40	535	6	560	14	708
LAS402_shot_409_grain_283	1.6892	0.5	0.15278	0.4	0.42	0.08063	0.45	1197	38	916	9	1001	20	1197
LAS402_shot_410_grain_284	4.5068	0.4	0.30432	0.3	0.46	0.10846	0.37	1763	33	1711	16	1729	25	1763
LAS402_shot_411_grain_285	9.2638	0.7	0.35660	0.6	0.87	0.18915	0.34	2728	28	1960	25	2347	30	2728
LAS402_shot_412_grain_286	1.5677	0.5	0.15418	0.4	0.40	0.07452	0.53	1029	40	924	10	953	19	1029
LAS402_shot_413_grain_287	2.0300	0.6	0.19003	0.5	0.19	0.07890	0.60	1135	39	1120	13	1119	22	1135
LAS402_shot_414_grain_288	4.0440	0.4	0.28985	0.4	0.53	0.10249	0.36	1659	33	1640	16	1641	25	1659
LAS402_shot_415_grain_289	2.0918	0.3	0.19607	0.3	0.56	0.07841	0.33	1149	34	1154	11	1145	21	1149
LAS402_shot_416_grain_290	4.7495	0.4	0.30844	0.4	0.58	0.11319	0.39	1839	32	1731	17	1771	26	1839
LAS402_shot_417_grain_291	6.6249	0.4	0.37843	0.5	0.48	0.12932	0.45	2071	30	2066	21	2058	27	2071
LAS402_shot_418_grain_292	1.9687	0.4	0.18311	0.4	0.53	0.07926	0.42	1165	36	1083	12	1102	21	1165

LAS402_shot_419_grain_293	2.9010	0.4	0.23866	0.4	0.48	0.08981	0.44	1406	35	1378	14	1379	23	1406
LAS402_shot_420_grain_294	1.8385	0.4	0.17998	0.3	0.47	0.07538	0.37	1064	36	1067	11	1058	20	1064
LAS402_shot_427_grain_295	1.4733	0.5	0.14656	0.4	0.33	0.07398	0.55	1013	40	881	9	916	19	1013
LAS402_shot_428_grain_296	1.8167	0.7	0.17624	0.6	0.54	0.07600	0.61	1060	42	1045	13	1045	21	1060
LAS402_shot_429_grain_297	0.6655	0.9	0.08175	0.5	0.20	0.05997	0.89	725	41	506	6	514	14	725
LAS402_shot_430_grain_298	2.2559	0.4	0.20165	0.3	0.19	0.08208	0.36	1236	34	1184	11	1196	21	1236
LAS402_shot_431_grain_299	1.7259	0.4	0.17077	0.4	0.46	0.07417	0.37	1037	36	1016	10	1017	19	1037
LAS402_shot_432_grain_300	1.4967	0.6	0.14853	0.5	0.38	0.07408	0.54	1016	39	892	10	925	19	1016
LAS402_shot_433_grain_301	1.5871	0.5	0.15505	0.4	0.53	0.07513	0.46	1054	37	928	10	962	20	1054
LAS402_shot_434_grain_302	1.6826	0.6	0.16827	0.5	0.37	0.07347	0.64	999	43	1002	12	997	21	999
LAS402_shot_435_grain_303	1.8229	0.6	0.17577	0.5	0.82	0.07585	0.63	1066	42	1043	12	1048	21	1066
LAS402_shot_436_grain_304	4.6988	1.6	0.22775	1.2	0.96	0.14510	0.44	2275	31	1314	31	1711	33	2275
LAS402_shot_437_grain_305	1.9727	0.7	0.18987	0.5	0.03	0.07666	0.79	1067	43	1119	14	1097	22	1067
LAS402_shot_438_grain_306	2.7531	0.4	0.22694	0.4	0.56	0.08844	0.41	1377	35	1317	14	1340	23	1377
LAS402_shot_439_grain_307	1.9713	0.7	0.17869	0.5	0.04	0.08122	0.79	1178	43	1058	13	1096	22	1178
LAS402_shot_440_grain_308	3.7243	0.4	0.25445	0.4	0.58	0.10688	0.38	1734	33	1460	15	1575	24	1734
LAS402_shot_447_grain_309	1.8693	0.7	0.18116	0.5	0.03	0.07580	0.73	1045	43	1073	13	1062	21	1045
LAS402_shot_448_grain_310	2.5645	0.5	0.21274	0.4	0.26	0.08818	0.54	1360	36	1242	14	1285	23	1360
LAS402_shot_449_grain_311	2.8340	0.4	0.23404	0.4	0.47	0.08841	0.44	1376	36	1354	14	1361	23	1376
LAS402_shot_450_grain_312	15.3200	0.4	0.54864	0.4	0.71	0.20365	0.32	2849	29	2813	27	2831	29	2849
LAS402_shot_451_grain_313	5.3880	0.5	0.34136	0.5	0.29	0.11532	0.49	1866	33	1889	21	1875	26	1866
LAS402_shot_452_grain_314	1.7595	0.6	0.17154	0.5	0.11	0.07709	1.94	1039	25	1020	12	1024	21	1039
LAS402_shot_453_grain_315	1.8158	1.4	0.14079	0.6	0.33	0.09544	1.36	1458	57	847	12	1029	26	1458
LAS402_shot_454_grain_316	1.8967	0.6	0.18164	0.5	0.30	0.07662	0.63	1074	42	1075	12	1074	21	1074
LAS402_shot_455_grain_317	1.5697	0.6	0.15626	0.5	0.09	0.07379	0.59	1000	40	935	11	953	20	1000
LAS402_shot_456_grain_318	2.0956	0.6	0.19594	0.5	0.01	0.07853	0.62	1130	39	1152	13	1141	22	1130
LAS402_shot_457_grain_319	4.8207	0.4	0.32084	0.4	0.65	0.10985	0.31	1791	32	1795	18	1786	25	1791
LAS402_shot_458_grain_320	2.2736	0.5	0.20078	0.4	0.42	0.08334	0.53	1255	38	1179	13	1201	22	1255
LAS402_shot_459_grain_321	0.6270	0.8	0.07723	0.5	0.21	0.05975	0.86	701	42	479	6	491	13	701
LAS402_shot_460_grain_322	1.7137	0.4	0.16852	0.4	0.45	0.07455	0.45	1040	37	1003	11	1011	20	1040
LAS402_shot_467_grain_323	1.7833	0.9	0.17198	0.6	0.18	0.07728	0.94	1128	46	1022	14	1029	22	1128
LAS402_shot_468_grain_324	1.7902	0.5	0.17412	0.4	0.15	0.07569	0.45	1070	37	1034	11	1038	20	1070
LAS402_shot_469_grain_325	2.6754	0.5	0.21915	0.4	0.36	0.08986	0.52	1403	37	1276	14	1316	23	1403
LAS402_shot_470_grain_326	2.0488	0.6	0.18873	0.5	0.29	0.08029	0.68	1160	43	1114	13	1126	22	1160
LAS402_shot_471_grain_327	1.7448	0.8	0.16686	0.6	0.50	0.07748	0.76	1110	44	994	13	1017	22	1110

LAS402_shot_472_grain_328	15.4190	0.6	0.43492	0.5	0.83	0.25869	0.36	3234	28	2322	27	2832	31	3234
LAS402_shot_473_grain_329	1.8862	0.5	0.18362	0.5	0.46	0.07589	0.50	1074	38	1085	12	1073	21	1074
LAS402_shot_474_grain_330	0.6773	0.5	0.08085	0.4	0.21	0.06166	0.52	654	38	501	6	523	13	654
LAS402_shot_475_grain_331	1.8148	0.7	0.17701	0.5	0.29	0.07544	0.75	1067	43	1049	13	1043	22	1067
LAS402_shot_476_grain_332	2.9263	0.5	0.24213	0.5	0.83	0.08898	0.49	1384	37	1395	15	1382	23	1384
LAS402_shot_477_grain_333	2.1280	0.5	0.19743	0.4	0.16	0.07960	0.54	1157	37	1160	12	1152	21	1157
LAS402_shot_478_grain_334	1.8164	0.6	0.17882	0.5	0.35	0.07496	0.65	1034	42	1060	12	1045	21	1034
LAS402_shot_479_grain_335	3.0519	0.5	0.24557	0.4	0.17	0.09164	0.46	1440	35	1414	15	1416	24	1440
LAS402_shot_480_grain_336	10.9181	0.4	0.41504	0.4	0.32	0.19362	0.32	2765	28	2235	21	2512	28	2765
LAS402_shot_487_grain_337	12.4564	0.4	0.44925	0.4	0.68	0.20384	0.35	2848	29	2388	24	2633	29	2848
LAS402_shot_488_grain_338	2.0404	0.6	0.19071	0.5	0.10	0.07902	0.53	1144	38	1124	13	1124	21	1144
LAS402_shot_489_grain_339	1.8364	0.4	0.17934	0.4	0.56	0.07524	0.35	1065	36	1063	11	1056	20	1065
LAS402_shot_490_grain_340	3.1302	0.4	0.24447	0.4	0.46	0.09449	0.43	1502	34	1408	14	1437	24	1502
LAS402_shot_491_grain_341	1.3232	0.7	0.13632	0.5	0.56	0.07151	0.58	948	41	823	11	851	19	948
LAS402_shot_492_grain_342	1.8074	0.5	0.17533	0.4	0.43	0.07622	0.50	1076	38	1040	11	1044	20	1076
LAS402_shot_493_grain_343	1.5112	0.6	0.15044	0.5	0.25	0.07410	0.58	1012	40	902	11	930	19	1012
LAS402_shot_494_grain_344	10.6996	0.5	0.44445	0.5	0.60	0.17754	0.39	2618	30	2366	25	2491	29	2618
LAS402_shot_495_grain_345	1.8257	0.5	0.17916	0.4	0.11	0.07520	0.52	1047	38	1061	11	1051	20	1047
LAS402_shot_496_grain_346	4.5357	0.4	0.29603	0.4	0.62	0.11285	0.32	1837	31	1670	16	1734	25	1837
LAS402_shot_497_grain_347	1.7700	0.5	0.17292	0.4	0.35	0.07559	0.53	1057	39	1027	11	1031	20	1057
LAS402_shot_498_grain_348	1.6407	0.5	0.16270	0.4	0.13	0.07446	0.56	1025	39	971	10	981	20	1025
LAS402_shot_499_grain_349	2.9599	0.3	0.24719	0.4	0.63	0.08814	0.33	1377	33	1423	14	1396	23	1377
LAS402_shot_500_grain_350	8.8888	0.3	0.41401	0.4	0.57	0.15811	0.33	2427	30	2231	21	2324	27	2427
LAS402_shot_507_grain_351	1.8243	0.4	0.17726	0.4	0.54	0.07588	0.37	1081	36	1052	11	1053	20	1081
LAS402_shot_508_grain_352	4.2964	0.7	0.28908	0.6	0.13	0.10972	0.61	1763	31	1633	21	1677	27	1763
LAS402_shot_509_grain_353	4.6977	0.4	0.30383	0.4	0.59	0.11399	0.36	1854	32	1708	17	1764	26	1854
LAS402_shot_510_grain_354	8.4351	1.4	0.35547	1.2	0.94	0.17111	0.49	2553	32	1936	42	2209	40	2553
LAS402_shot_511_grain_355	0.7390	0.6	0.09179	0.4	0.21	0.05954	0.69	624	40	566	6	560	14	624
LAS402_shot_512_grain_356	1.8364	0.5	0.17849	0.4	0.32	0.07598	0.50	1071	38	1058	11	1055	20	1071
LAS402_shot_513_grain_357	2.2102	0.5	0.19005	0.4	0.14	0.08599	0.54	1315	39	1120	12	1180	22	1315
LAS402_shot_514_grain_358	3.2853	0.4	0.22380	0.4	0.57	0.10815	0.40	1760	33	1300	14	1475	24	1760
LAS402_shot_515_grain_359	3.8021	0.6	0.27444	0.5	0.55	0.10184	0.47	1641	34	1561	18	1585	25	1641
LAS402_shot_516_grain_360	0.9244	0.7	0.10353	0.4	0.04	0.06601	0.77	816	40	635	7	660	16	816
LAS402_shot_517_grain_361	11.3401	0.7	0.44501	0.7	0.86	0.18718	0.36	2707	29	2362	31	2532	32	2707
LAS402_shot_518_grain_362	2.0530	0.4	0.18825	0.3	0.42	0.08053	0.41	1195	36	1111	11	1131	21	1195

LAS402_shot_519_grain_363	1.7565	0.4	0.17142	0.3	0.42	0.07550	0.38	1068	36	1020	10	1028	19	1068
LAS402_shot_520_grain_364	1.8856	0.5	0.18264	0.4	0.25	0.07614	0.57	1079	40	1081	11	1073	21	1079
LAS402_shot_527_grain_365	1.5179	0.9	0.15466	0.7	0.61	0.07262	0.69	969	43	925	13	927	21	969
LAS402_shot_528_grain_366	2.8763	0.5	0.23998	0.4	0.42	0.08882	0.48	1384	36	1386	14	1372	23	1384
LAS402_shot_529_grain_367	4.4387	0.3	0.30541	0.3	0.56	0.10744	0.32	1749	32	1717	16	1717	25	1749
LAS402_shot_530_grain_368	2.5435	0.5	0.21269	0.5	0.29	0.08859	0.44	1377	35	1241	15	1278	23	1377
LAS402_shot_531_grain_369	1.5851	0.9	0.15191	0.7	0.31	0.07662	0.52	1089	38	909	14	952	21	1089
LAS402_shot_532_grain_370	4.7246	0.4	0.30537	0.4	0.73	0.11455	0.31	1867	31	1715	18	1769	26	1867
LAS402_shot_533_grain_371	5.0237	0.4	0.32654	0.4	0.09	0.11426	0.48	1848	34	1820	18	1817	26	1848
LAS402_shot_534_grain_372	3.0457	0.9	0.23820	0.6	0.22	0.09590	0.90	1484	47	1374	18	1403	27	1484
LAS402_shot_535_grain_373	1.6993	0.5	0.16504	0.4	0.09	0.07631	0.46	1082	37	984	10	1004	20	1082
LAS402_shot_536_grain_374	5.1255	0.4	0.33234	0.4	0.27	0.11440	0.39	1856	33	1847	18	1836	25	1856
LAS402_shot_537_grain_375	2.7601	0.7	0.22460	0.6	0.75	0.09094	0.48	1426	36	1303	17	1333	24	1426
LAS402_shot_538_grain_376	1.4574	0.6	0.14457	0.5	0.10	0.07489	0.55	1040	38	870	10	907	19	1040
LAS402_shot_539_grain_377	1.9099	0.7	0.18295	0.5	0.24	0.07789	0.74	1107	43	1082	13	1077	22	1107
LAS402_shot_540_grain_378	1.7537	0.4	0.17521	0.3	0.58	0.07413	0.34	1034	36	1040	10	1026	20	1034
LAS402_shot_547_grain_379	2.7410	0.3	0.23298	0.3	0.56	0.08722	0.31	1357	34	1350	13	1338	22	1357
LAS402_shot_548_grain_380	1.0507	0.6	0.11688	0.5	0.47	0.06700	0.57	825	40	712	9	726	17	825
LAS402_shot_549_grain_381	3.1437	0.4	0.25104	0.4	0.50	0.09306	0.41	1477	34	1443	15	1440	24	1477
LAS402_shot_550_grain_382	2.0080	0.9	0.19040	0.6	0.26	0.07957	1.00	1178	47	1122	15	1107	24	1178
LAS402_shot_551_grain_383	1.7046	0.8	0.16877	0.5	0.24	0.07530	0.83	1058	45	1004	12	1001	21	1058
LAS402_shot_552_grain_384	5.1041	0.4	0.32453	0.4	0.60	0.11636	0.33	1893	31	1810	17	1835	26	1893
LAS402_shot_553_grain_385	10.7214	0.4	0.44008	0.4	0.61	0.18034	0.37	2649	30	2346	23	2495	28	2649
LAS402_shot_554_grain_386	1.7634	0.8	0.17283	0.6	0.25	0.07622	0.80	1064	43	1026	14	1022	22	1064
LAS402_shot_555_grain_387	13.3399	0.4	0.51706	0.4	0.51	0.19114	0.42	2741	30	2683	26	2700	28	2741
LAS402_shot_556_grain_388	1.6673	0.6	0.16506	0.4	0.48	0.07481	0.53	1038	40	984	11	993	20	1038
LAS402_shot_557_grain_389	2.0924	0.6	0.19826	0.4	0.17	0.07931	1.10	1127	28	1165	13	1141	21	1127
LAS402_shot_558_grain_390	1.8219	0.4	0.17884	0.4	0.46	0.07543	0.41	1063	37	1060	11	1051	20	1063
LAS402_shot_559_grain_391	1.7751	0.4	0.17699	0.4	0.62	0.07399	0.31	1032	36	1050	11	1034	19	1032
LAS402_shot_560_grain_392	7.1067	0.9	0.30859	0.8	0.92	0.16856	0.36	2533	30	1724	28	2096	33	2533
LAS402_shot_567_grain_393	0.7035	0.6	0.08681	0.4	0.31	0.05963	0.58	619	38	537	6	539	13	619
LAS402_shot_568_grain_394	1.2503	0.5	0.12979	0.4	0.47	0.07080	0.46	937	38	786	9	821	17	937
LAS402_shot_569_grain_395	2.2283	0.5	0.20238	0.4	0.32	0.08105	0.51	1200	37	1188	12	1187	22	1200
LAS402_shot_570_grain_396	1.8753	0.4	0.18088	0.3	0.40	0.07614	0.37	1086	36	1072	10	1071	20	1086
LAS402_shot_571_grain_397	1.9395	0.4	0.18247	0.4	0.08	0.07814	0.41	1134	36	1080	11	1092	21	1134

LAS402_shot_572_grain_398	14.1497	0.4	0.52125	0.4	0.66	0.19909	0.30	2811	28	2704	24	2757	29	2811
LAS402_shot_573_grain_399	2.1470	0.5	0.19945	0.4	0.34	0.07881	0.49	1148	38	1172	12	1160	21	1148
LAS402_shot_574_grain_400	0.7001	0.9	0.08581	0.5	0.17	0.06006	0.91	725	43	531	7	533	14	725
LAS402_shot_575_grain_401	3.7300	0.7	0.27344	0.6	0.79	0.09957	0.44	1602	35	1557	20	1575	26	1602
LAS402_shot_576_grain_402	2.1267	0.4	0.19445	0.3	0.34	0.08040	0.44	1187	37	1145	11	1156	21	1187
LAS402_shot_577_grain_403	1.8494	0.6	0.17930	0.4	0.25	0.07587	0.67	1052	42	1062	12	1057	21	1052
LAS402_shot_578_grain_404	1.8362	0.6	0.17679	0.4	0.06	0.07631	0.64	1066	40	1048	11	1053	20	1066
LAS402_shot_579_grain_405	3.0570	0.7	0.24702	0.5	0.20	0.09104	0.72	1407	43	1421	16	1414	25	1407
LAS402_shot_580_grain_406	3.3218	0.3	0.25940	0.3	0.54	0.09365	0.31	1496	33	1486	14	1485	23	1496
LAS402_shot_587_grain_407	1.7920	0.6	0.17548	0.5	0.38	0.07526	0.62	1049	41	1041	12	1040	21	1049
LAS402_shot_588_grain_408	2.5372	0.5	0.21665	0.5	0.68	0.08589	0.41	1319	35	1262	15	1278	23	1319
LAS402_shot_589_grain_409	0.7447	1.2	0.08934	0.6	0.09	0.06196	1.31	905	51	551	8	555	16	905
LAS402_shot_590_grain_410	1.8535	0.4	0.18130	0.4	0.44	0.07476	0.42	1048	36	1074	11	1062	20	1048
LAS402_shot_591_grain_411	1.7584	0.4	0.17234	0.3	0.39	0.07465	0.42	1042	36	1024	10	1028	20	1042
LAS402_shot_592_grain_412	3.0845	0.6	0.22479	0.6	0.81	0.10041	0.36	1622	33	1304	17	1423	25	1622
LAS402_shot_593_grain_413	3.4121	0.6	0.22733	0.5	0.57	0.10971	0.31	1786	31	1317	16	1500	24	1786
LAS402_shot_594_grain_414	0.7500	0.6	0.09106	0.4	0.06	0.06050	0.65	647	39	562	6	565	14	647
LAS402_shot_595_grain_415	2.4433	1.0	0.21708	0.6	0.17	0.08339	1.06	1251	49	1264	16	1241	26	1251
LAS402_shot_596_grain_416	1.8370	0.6	0.17468	0.5	0.55	0.07704	0.49	1100	38	1037	12	1054	21	1100
LAS402_shot_597_grain_417	11.2662	0.4	0.48707	0.4	0.46	0.16986	0.37	2545	30	2554	24	2541	28	2545
LAS402_shot_598_grain_418	3.0281	0.4	0.24137	0.4	0.43	0.09186	0.36	1453	33	1393	13	1411	23	1453
LAS402_shot_599_grain_419	2.0924	0.4	0.18961	0.4	0.34	0.08090	0.44	1202	36	1118	11	1144	21	1202
LAS402_shot_600_grain_420	1.7425	0.5	0.17303	0.4	0.69	0.07422	0.57	1018	40	1028	11	1020	20	1018
LAS402_shot_607_grain_421	4.3752	0.3	0.28821	0.4	0.68	0.11126	0.28	1816	31	1631	16	1705	25	1816
LAS402_shot_608_grain_422	1.7647	0.4	0.17193	0.4	0.44	0.07552	0.39	1067	36	1022	10	1031	20	1067
LAS402_shot_609_grain_423	5.2216	0.3	0.32331	0.3	0.55	0.11876	0.30	1930	31	1804	16	1854	26	1930
LAS402_shot_610_grain_424	1.4103	0.8	0.13081	0.6	0.74	0.07905	0.54	1150	38	792	11	884	20	1150
LAS402_shot_611_grain_425	1.4930	0.9	0.15142	0.7	0.59	0.07277	0.68	979	42	907	13	917	21	979
LAS402_shot_612_grain_426	0.3941	0.8	0.05085	0.5	0.20	0.05742	0.82	624	41	320	4	336	9	624
LAS402_shot_613_grain_427	1.7157	0.6	0.16962	0.4	0.21	0.07482	0.59	1039	41	1009	11	1011	20	1039
LAS402_shot_614_grain_428	2.0229	0.4	0.18865	0.4	0.35	0.07921	0.37	1163	35	1113	11	1121	21	1163
LAS402_shot_615_grain_429	1.5621	0.7	0.15757	0.6	0.62	0.07297	0.55	992	40	942	12	949	20	992
LAS402_shot_616_grain_430	1.9131	0.6	0.18877	0.5	0.44	0.07521	0.62	1045	41	1113	14	1081	21	1045
LAS402_shot_617_grain_431	1.8948	0.5	0.18872	0.5	0.61	0.07442	0.42	1037	37	1113	13	1076	20	1037
LAS402_shot_618_grain_432	2.6323	1.0	0.21309	0.8	0.81	0.09072	0.56	1418	39	1240	21	1289	27	1418

LAS402_shot_619_grain_433	4.8368	0.4	0.32080	0.5	0.78	0.11169	0.45	1809	32	1792	19	1786	25	1809
LAS402_shot_620_grain_434	0.7527	0.5	0.09321	0.4	0.49	0.05971	0.47	595	38	574	6	568	14	595
LAS402_shot_627_grain_435	8.7880	1.8	0.35068	1.5	0.95	0.17727	0.58	2602	34	1898	52	2196	46	2602
LAS402_shot_628_grain_436	2.4822	0.7	0.21204	0.6	0.61	0.08647	0.59	1315	39	1237	17	1257	24	1315
LAS402_shot_629_grain_437	1.3277	0.4	0.13504	0.4	0.51	0.07249	0.41	988	36	816	9	856	18	988
LAS402_shot_630_grain_438	1.7959	0.6	0.17712	0.4	0.26	0.07500	0.64	1036	41	1051	12	1039	20	1036
LAS402_shot_631_grain_439	3.0649	0.5	0.24341	0.4	0.40	0.09262	0.51	1461	37	1403	15	1418	24	1461
LAS402_shot_632_grain_440	10.5422	0.4	0.45411	0.4	0.55	0.17071	0.40	2553	30	2409	23	2480	28	2553
LAS402_shot_633_grain_441	4.5338	0.4	0.28680	0.5	0.56	0.11632	0.42	1888	34	1623	18	1734	25	1888
LAS402_shot_634_grain_442	2.2403	0.5	0.19537	0.4	0.83	0.08410	0.37	1282	35	1149	13	1190	21	1282
LAS402_shot_635_grain_443	1.4171	0.5	0.14402	0.4	0.48	0.07237	0.48	976	40	867	10	893	18	976
LAS402_shot_636_grain_444	6.3757	0.4	0.36404	0.4	0.51	0.12860	0.39	2066	32	1999	19	2025	27	2066
LAS402_shot_637_grain_445	13.0672	0.4	0.47384	0.4	0.50	0.20269	0.33	2841	28	2497	24	2682	28	2841
LAS402_shot_638_grain_446	13.0443	0.5	0.51473	0.5	0.17	0.18640	0.47	2695	31	2670	27	2676	29	2695
LAS402_shot_639_grain_447	1.8433	0.7	0.17733	0.6	0.21	0.07725	0.70	1087	42	1050	14	1056	21	1087
LAS402_shot_640_grain_448	1.7489	0.5	0.16742	0.5	0.44	0.07630	0.53	1081	39	997	11	1022	20	1081
LAS402_shot_647_grain_449	6.8593	0.5	0.38408	0.5	0.46	0.13050	0.51	2092	35	2091	23	2087	28	2092
LAS402_shot_648_grain_450	2.5684	0.5	0.21656	0.4	0.43	0.08675	0.46	1334	37	1262	13	1288	23	1334
LAS402_shot_649_grain_451	1.6261	0.8	0.16383	0.6	0.42	0.07301	0.77	989	43	977	13	973	21	989
LAS402_shot_650_grain_452	2.1126	0.7	0.19448	0.5	0.15	0.07993	0.72	1150	42	1144	13	1143	22	1150
LAS402_shot_651_grain_453	2.4454	0.8	0.20896	0.7	0.80	0.08532	0.47	1307	36	1220	17	1243	25	1307
LAS402_shot_652_grain_454	1.7831	0.6	0.17436	0.5	0.11	0.07510	0.46	1050	37	1035	12	1034	20	1050
LAS402_shot_653_grain_455	0.8961	0.8	0.09460	0.5	0.19	0.07082	1.64	917	34	582	7	642	16	917
LAS402_shot_654_grain_456	9.7548	0.7	0.38421	0.6	0.46	0.18557	0.41	2687	29	2089	27	2396	29	2687
LAS402_shot_655_grain_457	2.0249	0.8	0.19141	0.7	0.08	0.07787	0.60	1111	40	1126	17	1112	23	1111
LAS402_shot_656_grain_458	1.7637	0.4	0.17278	0.4	0.43	0.07505	0.44	1050	37	1027	11	1030	20	1050
LAS402_shot_657_grain_459	2.0281	0.4	0.18664	0.4	0.02	0.07987	0.38	1179	34	1102	11	1122	21	1179
LAS402_shot_658_grain_460	1.9091	0.7	0.18659	0.5	0.11	0.07574	0.76	1043	43	1102	13	1076	22	1043
LAS402_shot_659_grain_461	0.9649	1.2	0.10663	0.7	0.27	0.06757	1.21	994	49	652	10	676	19	994
LAS402_shot_660_grain_462	1.8843	0.6	0.18183	0.4	0.31	0.07643	0.60	1075	41	1076	12	1070	21	1075
LAS402_shot_667_grain_463	4.0993	0.4	0.28346	0.4	0.58	0.10661	0.33	1734	32	1608	16	1652	24	1734
LAS402_shot_668_grain_464	6.4380	0.7	0.29136	0.6	0.85	0.16190	0.36	2469	30	1646	22	2022	30	2469
LAS402_shot_669_grain_465	2.2455	0.8	0.17423	0.7	0.78	0.09442	0.53	1492	37	1033	15	1181	24	1492
LAS402_shot_670_grain_466	1.8013	0.8	0.17628	0.6	0.24	0.07609	0.87	1071	45	1045	13	1037	22	1071
LAS402_shot_671_grain_467	3.1925	0.4	0.24203	0.4	0.58	0.09725	0.37	1561	33	1396	14	1451	24	1561

LAS402_shot_672_grain_468	12.8010	0.4	0.50227	0.4	0.22	0.18809	0.38	2716	28	2620	25	2660	28	2716
LAS402_shot_673_grain_469	2.9560	0.5	0.23847	0.4	0.08	0.09179	0.51	1438	36	1377	15	1390	24	1438
LAS402_shot_674_grain_470	0.8956	0.8	0.10286	0.5	0.89	0.06418	0.74	773	42	631	8	644	16	773
LAS402_shot_675_grain_471	1.8073	1.2	0.17839	0.7	0.06	0.07621	1.26	1152	51	1055	16	1029	25	1152
LAS402_shot_676_grain_472	1.6977	0.5	0.16961	0.4	0.40	0.07397	0.51	1021	39	1009	11	1004	20	1021
LAS402_shot_677_grain_473	0.7692	1.1	0.09258	0.6	0.17	0.06204	1.14	836	46	570	8	572	16	836
LAS402_shot_678_grain_474	1.9047	1.3	0.18083	0.7	0.12	0.08008	1.47	1201	55	1068	17	1051	26	1201
LAS402_shot_679_grain_475	4.4916	0.3	0.29930	0.3	0.54	0.11045	0.33	1798	32	1686	16	1727	25	1798
LAS402_shot_680_grain_476	1.6729	0.5	0.16662	0.4	0.40	0.07388	0.46	1020	37	993	10	996	19	1020
LAS402_shot_687_grain_477	0.9847	0.6	0.10283	0.4	0.33	0.07022	0.63	911	42	631	7	693	16	911
LAS402_shot_688_grain_478	1.6313	0.4	0.16059	0.4	0.51	0.07433	0.42	1036	37	960	10	980	19	1036
LAS402_shot_689_grain_479	10.2285	0.7	0.38553	0.7	0.87	0.19373	0.36	2765	29	2095	28	2442	31	2765
LAS402_shot_690_grain_480	1.1901	0.8	0.12198	0.7	0.79	0.07101	0.52	938	39	741	11	788	19	938
LAS402_shot_691_grain_481	5.0090	0.6	0.32119	0.5	0.19	0.11487	0.66	1840	37	1792	21	1811	27	1840
LAS402_shot_692_grain_482	1.7892	0.5	0.17270	0.4	0.46	0.07569	0.49	1069	39	1026	11	1038	20	1069
LAS402_shot_693_grain_483	4.4408	0.4	0.29413	0.5	0.51	0.11009	0.45	1787	34	1659	18	1715	26	1787
LAS402_shot_694_grain_484	1.8124	0.6	0.17632	0.5	0.30	0.07515	0.68	1042	42	1046	12	1044	21	1042
LAS402_shot_695_grain_485	1.6791	1.2	0.15739	1.0	0.75	0.07695	0.59	1094	40	938	18	979	24	1094
LAS402_shot_696_grain_486	2.5721	0.5	0.22113	0.4	0.44	0.08478	0.49	1296	37	1287	14	1288	23	1296
LAS402_shot_697_grain_487	4.3118	0.4	0.28659	0.4	0.50	0.10948	0.36	1781	32	1622	16	1692	25	1781
LAS402_shot_698_grain_488	1.0470	1.0	0.09772	0.6	0.19	0.07893	1.04	1175	47	600	8	719	19	1175
LAS402_shot_699_grain_489	9.3604	0.6	0.43509	0.6	0.35	0.15864	0.69	2406	37	2320	28	2364	30	2406
LAS402_shot_700_grain_490	12.3855	0.4	0.48265	0.4	0.63	0.18676	0.36	2705	30	2533	25	2630	29	2705
LAS402_shot_707_grain_491	1.8049	0.7	0.17368	0.5	0.26	0.07625	0.71	1069	43	1031	12	1042	21	1069
LAS402_shot_708_grain_492	3.0382	0.7	0.24086	0.5	0.34	0.09213	0.68	1441	41	1390	16	1409	25	1441
LAS402_shot_709_grain_493	2.2415	0.5	0.19283	0.4	0.43	0.08508	0.48	1302	36	1136	12	1191	22	1302
LAS402_shot_710_grain_494	12.3576	0.4	0.47890	0.4	0.29	0.18856	0.35	2721	28	2520	23	2627	28	2721
LAS402_shot_711_grain_495	1.7656	0.5	0.17370	0.4	0.36	0.07446	0.51	1035	38	1032	11	1030	20	1035
LAS402_shot_712_grain_496	0.6800	0.7	0.08370	0.5	0.27	0.05959	0.72	656	40	518	6	524	13	656
LAS402_shot_713_grain_497	2.3579	0.7	0.21027	0.5	0.40	0.08239	0.64	1225	42	1228	15	1223	23	1225
LAS402_shot_714_grain_498	1.7331	0.4	0.17027	0.4	0.48	0.07473	0.44	1040	37	1013	11	1019	20	1040
LAS402_shot_715_grain_499	10.9417	1.1	0.43019	1.0	0.93	0.18461	0.44	2685	30	2284	41	2468	38	2685
LAS402_shot_716_grain_500	1.0553	2.1	0.11502	1.4	0.62	0.06687	1.43	987	56	697	19	698	25	987
LAS402_shot_717_grain_501	11.8161	0.4	0.46864	0.4	0.59	0.18550	0.33	2698	29	2475	23	2588	28	2698
LAS402_shot_718_grain_502	4.6314	0.4	0.31002	0.4	0.52	0.11016	0.39	1791	32	1739	17	1753	25	1791

LAS402_shot_719_grain_503	2.3245	0.5	0.19753	0.5	0.64	0.08661	0.39	1341	34	1160	13	1217	22	1341
LAS402_shot_720_grain_504	4.4523	0.4	0.29718	0.4	0.61	0.11036	0.36	1796	32	1676	17	1720	25	1796
LAS402_shot_727_grain_505	1.8705	0.7	0.18147	0.5	0.27	0.07654	0.71	1075	43	1074	13	1064	21	1075
LAS402_shot_728_grain_506	2.6731	0.4	0.19355	0.4	0.66	0.10161	0.38	1642	33	1140	13	1317	23	1642
LAS402_shot_729_grain_507	12.2703	0.4	0.49748	0.4	0.63	0.18190	0.32	2666	29	2600	24	2623	28	2666
LAS402_shot_730_grain_508	2.8708	0.6	0.20414	0.5	0.73	0.10343	0.38	1675	33	1196	14	1367	24	1675
LAS402_shot_731_grain_509	1.7637	0.4	0.17454	0.4	0.45	0.07459	0.42	1041	37	1036	11	1031	20	1041
LAS402_shot_732_grain_510	2.6792	0.4	0.22294	0.4	0.51	0.08812	0.40	1372	35	1296	13	1320	22	1372
LAS402_shot_733_grain_511	4.7953	0.4	0.30999	0.4	0.66	0.11347	0.30	1848	31	1740	17	1781	25	1848
LAS402_shot_734_grain_512	4.2946	1.6	0.17975	0.6	0.67	0.17288	1.18	2499	47	1065	15	1652	32	2499
LAS402_shot_735_grain_513	1.8189	0.7	0.17369	0.5	0.01	0.07718	0.76	1078	42	1031	12	1043	21	1078
LAS402_shot_736_grain_514	1.1682	1.2	0.12109	1.0	0.32	0.07011	0.73	921	41	735	15	767	21	921
LAS402_shot_737_grain_515	2.0235	0.4	0.18768	0.4	0.53	0.07909	0.38	1161	35	1109	11	1122	20	1161
LAS402_shot_738_grain_516	1.8821	0.7	0.18060	0.5	0.22	0.07710	0.81	1090	43	1069	13	1068	22	1090
LAS402_shot_739_grain_517	2.6748	1.2	0.19272	1.0	0.88	0.10085	0.54	1619	36	1130	22	1295	27	1619
LAS402_shot_740_grain_518	0.7791	0.7	0.09343	0.5	0.22	0.06138	0.80	715	41	575	7	582	15	715
LAS402_shot_747_grain_519	2.2736	0.6	0.19380	0.5	0.72	0.08550	0.43	1310	35	1140	14	1197	22	1310
LAS402_shot_748_grain_520	1.6780	0.4	0.16680	0.4	0.51	0.07332	0.38	1008	37	994	10	998	19	1008
LAS402_shot_749_grain_521	1.5726	0.5	0.15510	0.4	0.43	0.07419	0.52	1022	38	929	10	956	19	1022
LAS402_shot_750_grain_522	1.7280	0.6	0.17025	0.4	0.40	0.07408	0.58	1017	39	1013	11	1014	20	1017
LAS402_shot_751_grain_523	1.6459	0.7	0.16295	0.6	0.21	0.07359	0.59	1000	40	972	13	980	21	1000
LAS402_shot_752_grain_524	2.1303	0.6	0.19366	0.5	0.32	0.08044	0.65	1172	42	1140	13	1154	22	1172
LAS402_shot_753_grain_525	2.1232	0.6	0.19521	0.5	0.07	0.07939	0.56	1153	38	1148	14	1150	22	1153
LAS402_shot_754_grain_526	2.7156	0.7	0.22724	0.5	0.25	0.08753	0.78	1321	44	1318	16	1325	24	1321
LAS402_shot_755_grain_527	1.9152	0.6	0.16295	0.5	0.48	0.08558	0.58	1300	40	972	12	1080	21	1300
LAS402_shot_756_grain_528	4.2899	0.5	0.28075	0.5	0.69	0.11105	0.42	1806	33	1592	18	1685	26	1806
LAS402_shot_757_grain_529	1.5481	0.4	0.15726	0.4	0.44	0.07170	0.41	963	37	941	10	948	19	963
LAS402_shot_758_grain_530	3.1849	0.5	0.22409	0.5	0.66	0.10324	0.39	1670	33	1303	15	1451	24	1670
LAS402_shot_759_grain_531	4.9552	0.3	0.31381	0.4	0.48	0.11457	0.36	1864	33	1758	17	1809	25	1864
LAS402_shot_760_grain_532	2.3428	0.6	0.19842	0.5	0.61	0.08597	0.46	1318	36	1165	14	1222	22	1318
LAS402_shot_767_grain_533	1.6565	0.6	0.16341	0.5	0.94	0.07395	0.63	1013	41	975	11	986	20	1013
LAS402_shot_768_grain_534	1.8589	0.5	0.17652	0.4	0.42	0.07656	0.50	1090	38	1047	12	1064	20	1090
LAS402_shot_769_grain_535	1.5112	0.5	0.15111	0.4	0.72	0.07382	1.43	993	21	906	10	931	19	993
LAS402_shot_770_grain_536	1.1545	1.0	0.12263	0.8	0.77	0.06885	0.59	872	41	744	13	771	19	872
LAS402_shot_771_grain_537	2.9786	0.7	0.23484	0.5	0.21	0.09255	0.72	1435	42	1358	15	1394	24	1435

LAS402_shot_772_grain_538	1.2267	0.7	0.12597	0.6	0.64	0.07111	0.54	938	40	764	10	810	18	938
LAS402_shot_773_grain_539	12.5507	0.4	0.48713	0.5	0.58	0.18742	0.43	2707	30	2554	27	2640	29	2707
LAS402_shot_774_grain_540	1.6408	0.8	0.16539	0.6	0.46	0.07268	0.72	977	43	985	13	979	21	977
LAS402_shot_775_grain_541	3.0047	1.4	0.21190	1.2	0.95	0.10031	0.54	1607	37	1228	28	1357	33	1607
LAS402_shot_776_grain_542	4.3629	0.5	0.29288	0.4	0.68	0.10836	0.37	1762	32	1654	18	1700	26	1762
LAS402_shot_777_grain_543	1.4834	0.6	0.13892	0.5	0.64	0.07775	0.50	1119	39	838	11	920	20	1119
LAS402_shot_778_grain_544	2.4678	0.6	0.18432	0.5	0.63	0.09756	0.45	1560	34	1090	12	1257	23	1560
LAS402_shot_779_grain_545	3.6433	0.5	0.26448	0.4	0.40	0.10049	0.51	1615	36	1512	16	1554	25	1615
LAS402_shot_780_grain_546	0.6738	0.9	0.08254	0.5	0.06	0.05984	0.91	654	38	511	7	518	13	654